UNIVERSIDAD COMPLUTENSE DE MADRID
FACULTAD DE CIENCIAS QUÍMICAS
DEPARTAMENTO DE INGENIERÍA QUÍMICA

TESIS DOCTORAL

Procesos verdes para la producción de carbonato de glicerina y solketal

Green processes for the production of glycerol carbonate and solketal

MEMORIA PARA OPTAR AL GRADO DE DOCTOR
PRESENTADA POR

Jesús Esteban Serrano

Director

Félix García-Ochoa Soria

Madrid, 2015

UNIVERSIDAD COMPLUTENSE DE MADRID

Facultad de Ciencias Químicas

Departamento de Ingeniería Química

Procesos verdes para la producción de carbonato de glicerina y solketal / Green processes for the production of glycerol carbonate and solketal

MEMORIA

que para optar al Grado de Doctor por la Universidad Complutense de Madrid en el Programa de Doctorado en Ingeniería Química presenta

Jesús Esteban Serrano

Madrid, 2015

D. FÉLIX GARCÍA-OCHOA SORIA, Catedrático del Departamento de Ingeniería Química de la Facultad de Ciencias Químicas de la Universidad Complutense de Madrid, y D. MIGUEL LADERO GALÁN, Profesor Titular del Departamento del mismo Departamento y Centro CERTIFICAN:

Que el presente trabajo de investigación titulado "Procesos verdes para la producción de carbonato de glicerina y solketal / Green processes for the production of glycerol carbonate and solketal" constituye la memoria que presenta Jesús Esteban Serrano para optar al grado de doctor, y que ha sido realizada en las instalaciones del Departamento de Ingeniería Química de la Universidad Complutense de Madrid bajo su dirección.

Madrid, a 4 de Febrero de 2015

Prof. Dr. Félix García-Ochoa Soria Dr. Miguel Ladero Galán

Jesús Esteban Serrano

After all these years I have reached a finish line, one that at times seemed unreachable, yet here it is. This is the end of a scholar period and, given the uncertainty of circumstances, most likely my life at University. Over these years, I can say that I have acquired a few skills and knowledge on how to do a little bit of science, but most especially I have been capable of identifying my countless limitations and discovering how to capitalize on my very few virtues. However, this is no closure time. If there is something these past five years have made me understand is that life is an ongoing learning process. And I do intend to continue to learn.

It has been a rough time, with far more sadness, disappointments and defeats than victories. I will not deny that. However, all of this has shaped my character and the way I face situations and turned me into what I am today. So here is to the bitterness endured to reach the finish line: somehow you have made me stronger. Notwithstanding, I would not like to make a sad statement in these lines, for this time has also provided me with some moments of glory, which have made me persevere and reach the final destination.

There are quite a few people with whom I have had the honour to cross my path throughout these years at University. I would like to express my deepest gratitude to all of them, for they have granted me with the opportunity to know how things should or should not be done. I would like to acknowledge the following institutions and particularly people, who after all these time possess a piece of my heart and soul. Their teachings, wisdom, advice, support, shoulders to cry on, jokes on bad days and the way they have made me contemplate and appreciate things will remain within my own heart and soul forever.

First, I would like to mention the Complutense University of Madrid, my "alma mater". This has been home for the most part of the past eleven years. It has been a long way in this place at which I have been fortunate to encounter many of the greatest people in my life.

My utmost admiration and gratitude goes to Prof. Dr. Félix García-Ochoa Soria, Full Professor, and Dr. Miguel Ladero Galán, Associate Professor at the Department of Chemical Engineering. Thank you from the bottom of my heart for offering me the opportunity to be a part of this group. I have been blessed with your invaluable trust, advice, support and dedication throughout these past five years. Your wisdom, knowledge and experience have been a true guide.

Félix, you have taught me the true meaning of clarity and determination. Thank you for being the spark that has kept this engine running and for making me see everything clearly.

Miguel, what else could I say but a huge thank you? Thank you for your invaluable time and tireless effort. Thank you for always being willing to get your hands dirty and helping with everything. Thank you for doing your job with such great passion. Thank you for your friendship and humour. Thank you for your inspirational speeches. Thank you for being my academic big brother to watch over me. It has been a pleasure and honour that I will cherish forever.

Von Januar bis April 2014 hatte ich die Ehre beim Lehrstuhl für Technische Chemie an der Technischen Universität Dortmund einen Forschungsaufenthalt durchzuführen. Deshalb möchte ich sehr gern Prof. Dr. rer. nat. Arno Behr und Dr. Andreas J. Vorholt für die Möglichkeit mit ihnen einige Monate zu arbeiten. Außerdem muss ich auch die Hilfe von anderen Kollegen bei TCA anerkennen: Denys, Jonas, Thomas, Tom, Karoline u.v.a.. Vielen Dank für eure Unterstützung!

During my years as an undergraduate I had the chance to study for a year at the University of Texas at Austin. In this outstanding institution not only did I have the opportunity to take courses from prestigious Faculty members, but I also had my first approach to experimental work. For this reason, I would like to thank Dr. K. Sathasivan and Dr. Kerry Kinney for opening their facilities and giving me a first hint of what working in science means.

Back to UCM, I also have to acknowledge the rest of the Faculty with whom I have interacted throughout this period: Dr. Victoria Santos, PI of the first projects in which I was involved, who has always been willing to help and whose tireless scientific and administrative efforts have made my life much easier. Dr. Pedro Yustos, who directed my Undergraduate Final Degree Project and introduced me to Dr. Miguel Ladero and my present group, I probably would not be here were it not for him. Dr. Helena de la Fuente, with whom it was a pleasure to work, for her infinite patience and scientific guidance with the FBRM experiments. Dr. Ángeles Blanco for allowing me to perform experiments in her facilities. Prof. Dr. Carlos Negro, for the opportunity to get involved in ANQUE's events and activities for Young Researchers at the ICCE Congresses.

There are many colleagues with whom I have shared a lot of moments working, some other times putting a smile on each other's faces and some other times doing both things at the same time. Souto (your help was invaluable), Laura and Juanjo, the first batch of lab mates with whom I had the pleasure to work when I joined the group, and whose assistance was invaluable. Kudos to Esther and the rest of the students doing their Final Undergraduate Projects for their experimental effort as well. Marcos and Pablo for letting me reach out to them when I had problems dealing with Aspen and NRTL correlations. Igor, Sebas, Mateusz, Susana and Alberto, the other part of my group, for assisting me in their laboratory. Dr. María González Miquel for her prompt availability conducting countless property estimations and other calculations on her magical COSMO-RS software. Last but not least, Dr. Maribel Guijarro, Dr. José Manuel Toledo, Dr. Sergio Rodríguez, Dr. Eduardo Díez and José Timón for their friendliness, availability and assistance.

Fer and David deserve a special mention. They have helped me on countless occasions with experimental issues and I have had so much fun with them. I would like to thank them for opening up to me and for helping me open up to them and others. This lesson will not be forgotten.

One of the best memories that I will keep from these years is my participation in scientific congresses, during which I have encountered many interesting people. Particularly, I would like to

take this opportunity to highlight the bond that I have established with the students of Prof. Ángel Irabien's and Prof. Inmaculada Ortiz's research groups at the University of Cantabria, particularly Gabriel Zarca and Antía Pérez. Thank you all for your hospitality at the RSEQ's XXXIV Biennial Reunion in your beautiful city.

A few friends have indeed done a great job keeping my sanity within healthy levels in my life out of University, not to mention our adventures all over Spain. Here is to Emilio, Angulo, Alberto and Polo. "May LOL be with you forever, guys!"

Along this path there has been someone who knows from own experience exactly how I have felt at every moment, for better or worse. Unfortunately, the passing of events of life has kept and will keep us separated for far longer than we would like. As difficult as it may seem, it appears that we will have to hang on for a while before we can reunite and walk the path together again. Thank you for the good times: past, present and future.

Por último, y por encima de todos sin duda, queda reconocer a Mamá, Papá y mi hermano. De mis padres, durante toda la vida, no he tenido más que oportunidades, facilidades y apoyo para mi formación. Desde pequeño me han llevado a conocer multitud de lugares y me han transmitido toda su afición por el Arte, Cultura e Historia (aún recuerdo nuestra notaza en Historia estudiando con Mamá para Selectividad). Siempre han tenido en mente que la mejor inversión, que no gasto, que podían hacer era en mi educación, tanto en tiempo como en dinero, e incluso ellos mismos a día de hoy invierten en su propia educación. Tuvieron la visión de llevarme a aprender inglés desde bien pequeñito y luego, con 16 años, me dieron la oportunidad de pasar un año completo estudiando en Tramore, Irlanda, donde la mejora en el idioma fue impresionante y las experiencias que pude vivir me marcaron para siempre. Más tarde, en la Universidad, volvieron a concederme la posibilidad de irme cuando surgió la ocasión de ir a Austin, Texas. Por todo lo brindado y por todo lo que significa ser padres, sin lugar a dudas, este momento es culminación de su obra también. Gracias a los dos. Si algún día llego a ser padre, ojalá pueda hacerlo aunque sólo fuera la mitad de bien que vosotros. Os quiero.

Además, me gustaría agradecer el apoyo del Ministerio de Ciencia e Innovación por la financiación a través de los siguientes proyectos: CTQ2007-60919/PPQ, CTQ2010-15460 y CTQ2011-12725-E. Zuletzt möchte ich dem Deutschen Akademischen Austauschdienst danken, der mir mit seiner finanziellen Unterstützung die Möglichkeit gegeben hat, einen Forschungsaufenthalt an der Technischen Universität Dortmund durchzuführen.

We are functional, we are efficient
We are prepared and self sufficient
And we only destroy for the greater good
So you can be free to consume more as you should
And lead a better life

Where is the line
Between progress and decline?
What is the price to stop ruining life?
Why is functional worth more than sustainability?
Why are we so comfortable in our gullibility?

We are dysfunctional and inefficient
We're unprepared, we are deficient
And we only kill for the bottom line
So you can be free to consume more as you should
And lead a better life

What happened that made us want to be blind?
What is it in us that made us believe in all of the lies?
Spoon fed to us
By the ones who always stand to profit from our loss
Exploiting our misery and selling it back to us for a cost.

"Functional", by **Imperative Reaction**
Minus All (2008) Metropolis Records

The landscape is changing, the landscape is crying
Thousands of acres of forest are dying
Carbon copies from the hills above the forest line
Acid streams are flowing ill across the countryside

'Cause I don't care if you're going nowhere
Just take good care of the world
I don't care if you're going nowhere
Just take good care of the world

Now we're rearranging there's no use denying
Mountains and valleys can't you hear them sighing?
Evolution, the solution, almost certainty
Can you imagine this intrusion of their privacy?

Token gestures, some semblance of intelligence
Can we be blamed for the security of ignorance

"The landscape is changing", by **Depeche Mode**
Construction Time Again (1983) Mute Records

ÍNDICE

ÍNDICE

RESUMEN
SUMMARY

RESUMEN

1. Introducción, alcance y objetivo del trabajo

La intensa demanda energética que precisa la sociedad actual para satisfacer su actividad industrial y económica está llevando a la escasez de recursos energéticos fósiles y, como consecuencia, a un incremento importante de los precios. Por otra parte, el empleo de estos recursos por parte del ser humano ha aumentado preocupantemente las emisiones de gases de efecto invernadero y otros con efectos adversos sobre la salud (IPCC, 2007; IPCC, 2014). Como respuesta internacional a esta preocupación, en 1997 se firmó el Protocolo de Kyoto, que supuso el establecimiento de políticas y marcos regulatorios en el mundo para el fomento del uso de energías renovables.

Entre las energías renovables, los biocarburantes, y más particularmente el biodiesel, ha visto un aumento de su mercado muy significativo durante las últimas décadas, sobre todo en Europa. Como subproducto del proceso se genera glicerina en aproximadamente un 10% en masa respecto al biodiesel producido. Esto ha llevado a saturar el mercado de glicerina, cuyos usos tradicionales no han sido capaces de absorber el exceso producido, desembocando en una marcada caída de los precios y, por consiguiente, de la rentabilidad del proceso de obtención de biodiesel (Lamers y col., 2011).

Por este motivo, surge la necesidad y la oportunidad de encontrar nuevos usos para la glicerina que puedan ayudar a incrementar la demanda de la misma. Para la valorización de este compuesto ha habido un elevado número de estudios para la generación de productos de alto valor añadido (Behr y col., 2008). Considerando el origen biológico de la glicerina y la multitud de productos a los que puede dar lugar, se trata de una molécula de partida o *building block* que podría constituir una materia prima de biorrefinería (Werpy y Petersen, 2004).

Entre los diversos compuestos que surgen como productos a partir de la glicerina destacan dos por sus interesantes aplicaciones: el carbonato de glicerina (Sonnati y col., 2013) y el solketal (García y col., 2014). La obtención de los mismos y el estudio de los fenómenos implicados en los correspondientes procesos: reacciones químicas y equilibrios bifásicos líquido-líquido de los sistemas inertes, así como la transferencia de materia entre fases componen el objeto de estudio de la presente Tesis Doctoral.

2. Resultados y conclusiones

Los resultados de esta Tesis se dividen en tres grandes bloques o sistemas de acuerdo con los tres procesos estudiados. Los sistemas 1 y 2 se centran en la obtención de carbonato de glicerina sin catalizador o con catalizadores homogéneos. El sistema 3 trata de la producción de solketal con resinas sulfónicas de intercambio iónico. Estos resultados han dado lugar a un total de nueve publicaciones en revistas especializadas.

Sistema 1: Producción de carbonato de glicerina por transesterificación de glicerol con carbonato de dimetilo

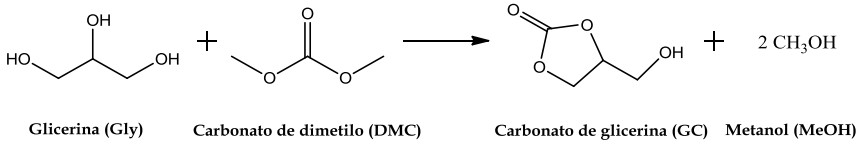

Glicerina (Gly) Carbonato de dimetilo (DMC) Carbonato de glicerina (GC) Metanol (MeOH)

Se estudiaron los equilibrios líquido-líquido existentes en los sistemas ternarios {DMC + MeOH + Gly} y {DMC + GC + Gly} y uno cuaternario {DMC + MeOH + GC + Gly} entre 60 y 70 ºC. La presencia de productos de la reacción de la que forman parte ayudó a la solubilización del sistema en el siguiente orden: GC > GC+ MeOH > MeOH. Por otro lado, la temperatura apenas afectó a los equilibrios. Por ajuste del modelo NRTL a los datos se obtuvieron los parámetros de interacción binaria.

También se llevó a cabo el estudio cinético de la reacción catalizada con catalizadores homogéneos. En primer lugar, se eligieron las condiciones de la reacción: el catalizador (K_2CO_3), el intervalo de temperaturas (66-70 ºC) y la velocidad de agitación (1500 rpm) para asegurar que la transferencia de materia externa no influye en la velocidad del proceso. Con un seguimiento físico y químico de la reacción, se determinó que el cambio de régimen del sistema reaccionante tornaba de bifásico a monofásico a un valor de la conversión de 0,3 independiente de la temperatura o exceso de DMC empleado. Este hecho resultó ser de importancia en la determinación de un modelo cinético, que consta de dos etapas con dos ecuaciones aplicables antes y después de dicho valor de conversión: la primera es de primer orden respecto a la concentración de glicerina y orden cero respecto a la de DMC y la segunda, de primer orden respecto a ambos compuestos. La energía de activación obtenida fue de 179.2 ± 3.7 kJ mol^{-1}.

Además, se estudió la cinética de la reacción con métoxido de potasio como catalizador, con una selectividad prácticamente total al producto. Con las condiciones

de operación seleccionadas se realizaron experimentos cinéticos. En base a las consideraciones fenomenológicas del cambio de dos a una fase antes mencionado, así como atendiendo a la posible desactivación del catalizador, el modelo cinético más representativo plantea dos ecuaciones considerando la irreversibilidad de la reacción y una desactivación de primer orden del metóxido de potasio. La energía de activación fue de 28,4 ± 1,5 kJ·mol^{-1} y la constante de desactivación de 0,03 ± 0,01 min^{-1}. Se observó que la actividad de este catalizador era unas 20 veces superior a la del K_2CO_3.

Sistema 2: Producción de carbonato de glicerina por transesterificación de glicerol con carbonato de etileno

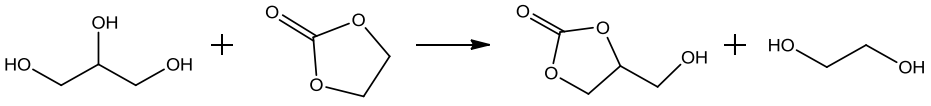

Glicerina (Gly) Carbonato de etileno (EC) Carbonato de glicerina (GC) Etilenglicol (EG)

Se analizan los equilibrios líquido-líquido que se dan en los sistemas {EC + EG + Gly}, {EC + GC + Gly} y {EC + EG + GC + Gly} entre 40 y 50 ºC. Una composición creciente de EG, GC o la mezcla de ambos contribuyen a la transición del sistema bifásico a uno monofásico en el orden: GC > EG > EG+GC. El efecto de la temperatura sobre los equilibrios es poco importante, por lo que todos los datos obtenidos se correlacionaron con el modelo NRTL para la obtención de un conjunto de parámetros de interacción binaria para todo el intervalo estudiado.

Se observó que este sistema constituye un medio monofásico a temperaturas superiores a 80 ºC, y se produce la reacción entre EC y glicerina en ausencia de catalizador. Se realizó un estudio termodinámico de la reacción entre 100 y 140 ºC, en el que se predice la endotermicidad de la reacción y la conversión predicha era prácticamente del 100% y coincidía con la observada experimentalmente en estas condiciones. Además, se estudió la cinética de la reacción, ajustándose mejor que ningún otro un modelo potencial de segundo orden global (primer orden respecto a la concentración de cada reactante) con energía de activación de 61,8 ± 0,8 kJ mol^{-1}. Por último, se vio que la economía atómica y de carbono del proceso son del 100%, el *factor E* nulo, y se comparó la productividad y eficiencia másicas respecto a procesos similares en la literatura que emplean catalizadores, obteniéndose mejores resultados.

El estudio de la cinética también se realizó en condiciones catalíticas, empleando K_2CO_3 como catalizador homogéneo. Se comprobó que el mecanismo propuesto en la

literatura es correcto de acuerdo con la evolución de los compuestos, si bien la alta selectividad observada y el alto grado de cumplimiento de los balances de materia invitan a considerar una reacción simple. Se eligió una agitación de 800 rpm como aquella a la que la transferencia externa de materia no es controlante en la velocidad del proceso. Tras el seguimiento de las especies, así como el físico de la desaparición de la dispersión, se determinó que la transformación en un sistema monofásico se da a una conversión de 0.34. Se propusieron diversos modelos cinéticos basados en dos etapas para considerar el cambio de régimen acontecido en el desarrollo del proceso. Se apreció que el valor de conversión al cual el comportamiento cinético cambia es dependiente de la temperatura y la concentración de catalizador empleada, aunque no de la relación molar entre reactantes; en cualquier caso, el intervalo de valores de estas conversiones es cercano a 0.34. Con esto, se obtuvo el mejor ajuste para un modelo que incluye la posible desactivación del catalizador, así como la presencia de una reacción inversa, al no obtenerse conversión completa en la reacción. Las energías de activación de las constantes de la reacción directa e inversa fueron, respectivamente, de 91.7 ± 2.7 $kJ \cdot mol^{-1}$ y 93.9 ± 15.9 $kJ \cdot mol^{-1}$, y la constante de desactivación de 0.36 ± 0.06 min^{-1}.

Por último, se llevó a cabo la reacción con metóxido de potasio como catalizador, observándose una selectividad casi total hacia el producto. Se realizaron una serie de experimentos cinéticos con condiciones similares a las planteadas con K_2CO_3. Se apreció que el cambio de tendencia de la cinética de los datos varía con la temperatura, concentración de catalizador y exceso molar de carbonato de etileno empleados. El mejor ajuste a los datos se consiguió con un modelo que tiene en cuenta las dos etapas antes mencionadas, así como la reversibilidad de la reacción y la desactivación de primer orden del catalizador. Las energías de activación fueron de 82,3 ± 3,0 $kJ \cdot mol^{-1}$ y 53,5 ± 21,6 $kJ \cdot mol^{-1}$ para las reacciones directa e inversa, respectivamente, y la constante de desactivación de 0.31 ± 0.03 min^{-1}.

Sistema 3: Producción de solketal por acetalización de glicerol con acetona

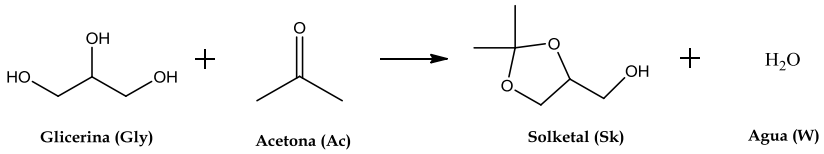

Se evaluó el equilibrio líquido-líquido en el sistema {Ac + Sk + Gly} a 30, 40 y 50 ºC, en el que una concentración cada vez mayor de solketal solubiliza la acetona y la

glicerina y, de nuevo, el efecto de la temperatura es muy limitado. El modelo NRTL se ajustó con éxito a los datos y se determinaron los coeficientes de interacción binaria.

Este proceso es necesario llevarlo a cabo de forma catalítica, eligiendo en este caso catalizadores heterogéneos, para lo cual se realizó una selección entre varias resinas sulfónicas de intercambio iónico comerciales. Se caracterizaron diversos parámetros estructurales de las resinas. El orden de actividad de las resinas fue el siguiente: Lewatit GF101 > Purolite CT275DR > Amberlyst 36dry > Amberlyst 35dry > Amberlyst 15 > Purolite CT276. También se analizó la reutilización de las resinas con y sin regeneración. En este caso, el orden de actividad remanente fue: Purolite CT276 > Amberlyst 36dry > Amberlyst 15 > Purolite CT275DR > Amberlyst 35dry > Lewatit GF101.

Con la resina más activa, Lewatit GF101, se estudió la cinética del proceso. Para ello, se determinaron las condiciones en las que la transferencia de materia no fueran limitantes: agitación de 750 rpm y tamaño de partícula de 190 μm para evitar control por parte de las etapas de difusión externa e interna. Se evaluó el efecto de las variables de operación, apreciándose la alta influencia del exceso molar de acetona a glicerina sobre la posición de equilibrio. Entre los modelos cinéticos que se propusieron, el mejor ajuste se obtuvo con un modelo Eley-Rideal que incluía la reacción inversa: de orden cero respecto a las concentraciones de las especies reactantes y primer orden respecto a la de cada uno de los productos de la reacción. Las constantes adsorción de las especies presentes son nulas, a excepción del agua, con un valor de 128,0 ± 21,4 kJ mol^{-1}. Las energías de activación para la reacción directa e inversa fueron 124,0 ± 12,9 kJ mol^{-1} y 127,3 ± 12,6 kJ mol^{-1}, respectivamente.

3. Referencias citadas

Behr, A., Eilting, J., Irawadi, K., Leschinski, J., Lindner, F. (2008). Improved utilisation of renewable resources: New important derivatives of glycerol. *Green Chem* 10, 1: 13-30.

Garcia, J.I., Garcia-Marin, H., Pires, E. (2014). Glycerol based solvents: synthesis, properties and applications. *Green Chem* 16, 3: 1007-1033.

IPCC (2007). Summary for Policymakers. In Cilmate Change 2007: The Physical Science Basis. Contribution of Working Group I to the fourth assessment report of the International Panel on Climate Change. Cambridge University Press, Cambridge, U.K.

IPCC (2014). Fifth Assessment Synthesis Report. Climate Change 2014. Synthesis Report. Available at http://www.ipcc.ch/.

Lamers, P., Hamelinck, C., Junginger, M., Faaij, A. (2011). International bioenergy trade-A review of past developments in the liquid biofuel market. *Renew Sust Energ Rev* 15, 6: 2655-2676.

Sonnati, M.O., Amigoni, S., de Givenchy, E.P.T., Darmanin, T., Choulet, O., Guittard, F. (2013). Glycerol carbonate as a versatile building block for tomorrow: synthesis, reactivity, properties and applications. *Green Chem* 15, 2: 283-306.

Werpy, T., Petersen, G. (2004). Top value added chemicals from biomass. Volume I - Results of screening for potential candidates from sugars and synthesis gas Pacific Northwest National Laboratory. National Renewable Energy Laboratory. U.S. Department of Energy.

SUMMARY

1. Introduction, scope and aim of the work

The strong energy supply demanded by the current society to fulfill its economic and industrial activity is leading to an impending depletion of fossil resources and, consequently, to significant escalation of prices. Furthermore, the anthropogenic use of such resources has worryingly increased the emissions of greenhouse gases as well as others with adverse effects on health (IPCC, 2007; IPCC, 2014). As an international response to this concern, the so-called Kyoto protocol was signed in 1997, setting a milestone to the establishment of new policies and frameworks to foster the use of renewable energies.

Among renewable energies, biofuels, particularly biodiesel, have seen their market share significantly increased throughout the last decades. Approximately 10% of glycerol with respect to the mass of biodiesel is generated as a by-product of the manufacture process. This has led to a saturation of the existing glycerol market, whose traditional uses have not been capable of absorbing the oversupply, hence causing marked price drops affecting thereby the profitability of biodiesel production processes (Lamers et al, 2011).

For this reason, a need of finding new uses of glycerol has arisen in order to increase its demand. A high number of studies have been reported approaching the valorization of this chemical to high added-value products (Behr et al., 2008). Taking into account the biological origin of glycerol and the wide array of products thereof derived, it can be envisaged as a building block that may constitute feedstock to biorefinery processes (Werpy and Petersen, 2004).

Among the diverse products obtained from glycerol, two can be highlighted owing to their interesting applications, namely: glycerol carbonate (Sonnati y col., 2013) and solketal (García y col., 2014). The aim of the present PhD Thesis is to develop the study of the production of these two chemicals together with the research of the underlying physicochemical phenomena implied in the corresponding chemical reaction kinetics and liquid-liquid equilibria for the inert systems.

2. Results and conclusions

The results presented in this Thesis are divided into three blocks or systems according to the three processes herein studied. Systems 1 and 2 are focused on the production of glycerol carbonate with homogeneous catalysts or in the absence of catalyst in one case. System 3 deals with the production of solketal employing sulfonic ion exchange resins. The results are presented in a total of nine publications.

System 1: Production of glycerol carbonate by transesterification of glycerol with dimethyl carbonate

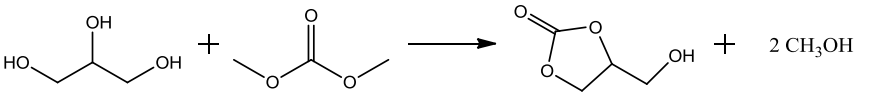

Glycerol (Gly) Dimethyl carbonate (DMC) Glycerol carbonate (GC) Methanol (MeOH)

The liquid-liquid equilibria (LLE) existing in the systems {DMC + MeOH + Gly}, {DMC + GC + Gly} and {DMC+MeOH+GC+Gly} between 60 and 70 ºC were studied. The presence of the products of the reaction increase the solubility of the system in the following order: GC > GC + MeOH > MeOH. Moreover, temperature does not show a significant effect on the equilibria. The NRTL model was successfully correlated to the experimental data, retrieving binary interaction parameters.

The kinetics of the reaction was studied with homogeneous catalysis. First, the reaction conditions were selected: the catalyst (K_2CO_3), the temperature range (66-70 ºC) and the stirring speed (1500 rpm) to ensure non-controlling external mass transfer conditions. Through physical and chemical monitoring of the reaction, it was determined that the reacting system turned from an emulsion-like regime to a single phase liquid at a conversion value of glycerol of 0.3 regardless of temperature and the excess of DMC to glycerol applied. This condition proved significant in the determination of a kinetic model, which consists in two equations applicable in two stages prior and posterior to the aforementioned value of conversion. The first equation is of first order with respect to the concentration of glycerol and zero order to that of DMC; whereas the second equation is of first order with respect to the concentration of both. The activation energy of the constant is 179.2 ± 3.7 kJ mol^{-1}.

Furthermore, the kinetics of the reaction was assessed with potassium methoxide as catalyst, showing a practically complete selectivity to the product. Kinetic

experiments were conducted with the operating previously selected. On the basis of the phenomenological considerations on the switch from two liquid phases to a single phase liquid, together with the consideration of the potential deactivation of the catalyst, the most representative kinetic model contemplates two equations featuring the irreversibility of the reaction and a first-order deactivation of potassium methoxide. The activation energy of the reaction is 28.4 ± 1.5 kJ·mol^{-1} and the deactivation constant has a value of 0.03 ± 0.01 min^{-1}

System 2: Production of glycerol carbonate by transesterification of glycerol with ethylene carbonate

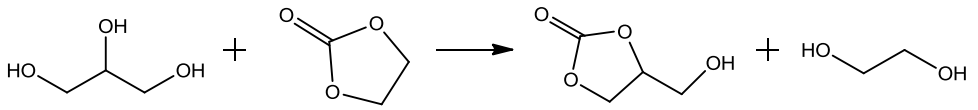

Glycerol (Gly) Ethylene carbonate (EC) Glycerol carbonate (GC) Ethylene glycol (EG)

The LLE pertaining to the systems {EC + EG + Gly},{EC + GC + Gly} and {EC + EG + GC + Gly} between 40 and 50 ºC were analyzed. The increasing presences of EG, GC or a combination of both contribute to the transition from a biphasic liquid-liquid system to a monophasic liquid in the next order: GC > EG > EG+GC. The effect of temperature did not prove remarkable; thus, the NRTL model was fitted to all the experimental data allowing the estimation of the corresponding binary interaction parameters for the range of conditions studied.

It was discovered that this system constitutes a monophasic medium at temperatures above 80 ºC, within which the reaction between EC and glycerol takes place in the absence of catalyst. A thermodynamic study of the reaction was made between 100 and 140 ºC that predicted a virtual completion of the reaction, which was corroborated experimentally. The kinetics of this reaction was studied, fitting an overall second order potential model better than any other with an activation energy of 61,8 ± 0,8 kJ mol^{-1}. Finally, a brief study related to Green Chemistry parameters was made, evaluating the atom and carbon economy (both 100%), the *E-factor* (equal to zero) and the mass productivity and efficiency to other similar processes, obtaining better values of these parameters.

The kinetic study was also made under catalytic conditions, utilizing K_2CO_3 as a homogeneous catalyst. The reaction mechanism proposed in literature was verified

given the observed evolution of the components, yet the high selectivity and compliance of material balances lead to the consideration of a simple chemical reaction. A stirring speed of 800 rpm was selected to operate under non-controlling external mass transfer conditions. From the evolution of the chemical species as well as the extinction of the dispersion, it was determined that the change from a biphasic to a single phase liquid system takes place at a conversion of 0.34. Several kinetic models were proposed on the basis of two stages to account for the phase change regime. The value at which the kinetic behaviour of the process changes was found to be dependent on temperature and concentration of catalyst employed, though not on the molar ratio of reactants; anyhow, all values were sufficiently close to 0.34. The best fit was obtained for a model that appraises the deactivation of the catalyst as well as the presence of a reverse reaction, given that the reaction does not reach completion. The activation energies of the kinetic constants are 91.7 ± 2.7 kJ·mol^{-1} and 93.9 ± 15.9 kJ·mol^{-1} for the direct and reverse reactions, respectively, and the deactivation constant has a value of 0.36 ± 0.06 min^{-1}.

Last, the reaction was performed utilizing potassium methoxide as catalyst, again with a virtually complete selectivity to the product. A series of kinetic experiments were completed under similar conditions to those employed using K_2CO_3. A change in the kinetic behaviour of the data was perceived at conversions of glycerol which varied with temperature, molar excess of ethylene carbonate and concentration of catalyst. The best fit was achieved with a model considering the two mentioned steps as well as the reversibility of the reaction and a first order deactivation of the catalyst. The values of the activation energies are 82.3 ± 3.0 kJ·mol^{-1} and 53.5 ± 21.6 kJ·mol^{-1}, respectively, and that of the deactivation constant is 0.31 ± 0.03 min^{-1}.

System 3: Production of solketal by acetalisation of glycerol with acetone

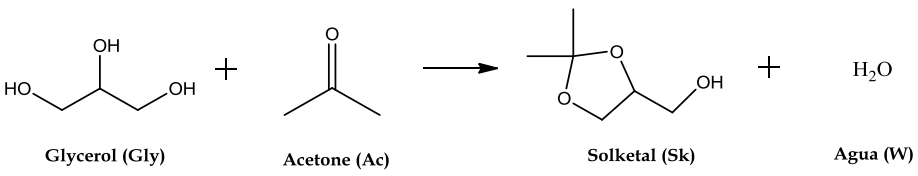

Assessment of the LLE of the system {Ac+Sk+Gly} at 30, 40 y 50 ºC was undertaken, in which an increasing concentration of solketal dissolves acetone and glycerol and the temperature shows a limited effect. The NRTL model was fitted successfully to each set of data and the binary interaction parameters were determined.

This reaction was completed following a heterogeneous catalysis approach, for which different commercially available sulphonic ion exchange resins were screened. Diverse structural parameters of these resins were characterized in relation to its activity, whose order was: Lewatit GF101 > Purolite CT275DR > Amberlyst 36dry > Amberlyst 35dry > Amberlyst 15 > Purolite CT276. Reutilization of the resins with and without generation was also contemplated, being in this case the order of remaining activity as follows: Purolite CT276 > Amberlyst 36dry > Amberlyst 15 > Purolite CT275DR > Amberlyst 35dry > Lewatit GF101.

With the most active resins, Lewatit GF101, the kinetics of this reaction was studied. For this purpose, the conditions under which mass transfer limitations are non-controlling were determined: a stirring speed of 750 rpm and a particle size of 190 μm. The effect of operating variables was assessed, observing a high influence of the molar excess of acetone to glycerol on the equilibrium position. Among the models proposed, the best fitting was obtained with an Eley-Rideal model accounting for a reverse order of zero order with respect to the concentration of the reactant species and first order with respect to that of each of the products. The adsorption constants of the species were zero, except for that of water, whose value was 128.0 ± 21.4 kJ mol^{-1}. The activation energies for the direct and reverse reactions are 124.0 ± 12.9 kJ mol^{-1} and 127.3 ± 12.6 kJ mol^{-1}, respectively.

3. Cited references

Behr, A., Eilting, J., Irawadi, K., Leschinski, J., Lindner, F. (2008). Improved utilisation of renewable resources: New important derivatives of glycerol. *Green Chem* 10, 1: 13-30.

Garcia, J.I., Garcia-Marin, H., Pires, E. (2014). Glycerol based solvents: synthesis, properties and applications. *Green Chem* 16, 3: 1007-1033.

IPCC (2007). Summary for Policymakers. In Cilmate Change 2007: The Physical Science Basis. Contribution of Working Group I to the fourth assessment report of the International Panel on Climate Change. Cambridge University Press, Cambridge, U.K.

IPCC (2014). Fifth Assessment Synthesis Report. Climate Change 2014. Synthesis Report. Available at http://www.ipcc.ch/.

Lamers, P., Hamelinck, C., Junginger, M., Faaij, A. (2011). International bioenergy trade-A review of past developments in the liquid biofuel market. *Renew Sust Energ Rev* 15, 6: 2655-2676.

Sonnati, M.O., Amigoni, S., de Givenchy, E.P.T., Darmanin, T., Choulet, O., Guittard, F. (2013). Glycerol carbonate as a versatile building block for tomorrow: synthesis, reactivity, properties and applications. *Green Chem* 15, 2: 283-306.

Werpy, T., Petersen, G. (2004). Top value added chemicals from biomass. Volume I - Results of screening for potential candidates from sugars and synthesis gas Pacific Northwest National Laboratory. National Renewable Energy Laboratory. U.S. Department of Energy.

1. ALCANCE Y OBJETIVOS
SCOPE AND GOALS

1. ALCANCE Y OBJETIVOS

En las circunstancias actuales y venideras existe una demanda energética que a largo plazo no se podrá satisfacer con las fuentes energéticas tradicionales de origen fósil ante su acuciante escasez y consiguiente elevación de precios. Además, existe una creciente preocupación por la contribución antropogénica de las emisiones de gases de efecto invernadero sobre el calentamiento global y de otras emisiones sobre los ecosistemas y la salud (IPCC, 2014).

Por ello, la Convención Marco de las Naciones Unidas sobre el Cambio Climático estableció el Protocolo de Kyoto en 1997 con una serie de objetivos para la reducción de las emisiones de gases de efecto invernadero. A partir de la firma de este acuerdo, las instituciones a niveles regionales han impulsado el empleo de fuentes de energía renovables desarrollando un marco legislativo a tal efecto. Particularmente, dentro de la Unión Europea las Directivas 2003/30/CE y 2009/28/CE han fijado los objetivos hasta 2010 y 2020, respectivamente, en lo concerniente a la utilización de energías renovables.

Entre las energías renovables, y a consecuencia del mencionando dispositivo jurídico, cabe destacar el auge de la industria del biodiesel, en cuyo proceso de obtención se genera glicerina como subproducto. La creciente producción de glicerina no ha podido ser absorbida por los mercados que tradicionalmente han hecho uso de ella, por lo que el exceso de oferta ha repercutido en una pronunciada caída de sus precios, reduciendo la rentabilidad de los procesos de producción de biodiesel.

Debido a esta tendencia decadente de los precios, se están buscando nuevas aplicaciones y usos de la glicerina. Con esta filosofía, se ha planteado la valorización por medio de un aprovechamiento energético de la misma. Sin embargo, de manera mucho más profusa, en base a sus características fisicoquímicas, la glicerina se ha empleado como materia prima a partir de la cual establecer rutas sintéticas para la obtención de productos de alto valor añadido. En este sentido, si la glicerina viene de un origen biológico, se puede plantear que el glicerol es un compuesto químico base para el planteamiento de una *biorrefinería*, comúnmente denominado como *building block* o también *platform chemical*.

Especialmente a partir del año 2000, el número de trabajos científicos relacionados con la explotación de la glicerina como recurso se ha elevado de manera más que significativa. Se han propuesto un alto número de procesos para la obtención de una amplia variedad de productos, entre los cuales se pueden mencionar: mono, di y tri- ésteres y éteres, así como poliésteres y poliéteres de glicerol o un amplio elenco de productos derivados de su deshidratación, hidrogenolisis y oxidación selectiva. Además de todos los anteriores productos, por distintos procedimientos, se puede obtener carbonato de glicerina y, por último, acetales como el solketal por reacción con una cetona o un aldehído.

Tanto el carbonato de glicerina como el solketal, gracias a sus propiedades físicas y químicas, están demostrando ser útiles en multitud de aplicaciones tanto de una manera directa (disolventes, aditivos, etc) como siendo materia primera para la obtención de otros productos.

Debido al interés que suscitan estos dos productos, el principal objetivo de este trabajo es investigar los aspectos fenomenológicos físicos y químicos subyacentes en los procesos propuestos para su obtención. De este modo, se propone la división de la presente Tesis en tres grandes bloques correspondientes a tres sistemas:

Sistema 1: Producción de carbonato de glicerina por transesterificación de glicerol con carbonato de dimetilo

Sistema 2: Producción de carbonato de glicerina por transesterificación de glicerol con carbonato de etileno

Sistema 3: Producción de solketal por acetalización de glicerol con acetona

Por lo tanto, los dos primeros sistemas están dedicados a la obtención de carbonato de glicerina, la cual se llevará a cabo por vía catalítica homogénea o incluso sin catalizador. El tercer sistema, por su parte, se dedica al estudio de la producción de solketal por vía catalítica heterogénea, concretamente empleando resinas de intercambio iónico sulfónicas comerciales. Para afrontar el análisis de estos procesos se han sugerido una serie de pasos comunes a seguir como metodología del estudio, a saber:

- ***Estudio estequiométrico***

  El balance de elementos químicos se realizó considerando los estudios existentes en literatura al respecto de las reacciones en conjunción con el análisis de las muestras de reacción. En el caso de los Sistemas 1 y 2, el método de análisis se basó en cromatografía en fase líquida de alta presión (HPLC), mientras que en el Sistema 3 se basó en espectroscopía de resonancia magnética nuclear de protón (^{1}H-NMR)

- ***Estudio termodinámico químico téorico y experimental***

  El estudio teórico se basa en la estimación de las constantes de equilibrio a partir de las relaciones termodinámicas, mientras que en el experimental, la constante se estima a partir de la composición en la posición de equilibrio y los coeficientes de actividad de los componentes implicados en el sistema.

- ***Estudio termodinámico de los equilibrios entre fases líquidas***

  Dada la limitada solubilidad entre los reactivos de partida en los tres casos estudiados, se ha planteado el estudio del equilibrio entre las fases líquidas presentes en presencia de codisolventes, en este caso los productos de las respectivas reacciones. Para ello, se adquieren datos de equilibrio variando la composición y la temperatura de los sistemas y se ha realizado el ajuste del modelo termodinámico NRTL para estimar los coeficientes de interacción binaria.

- ***Determinación de las condiciones de reacción***

  Las reacciones aquí planteadas se realizaron en todos los casos en reactores de tipo discontinuo. En este modo de operación, se determinaron las condiciones más favorables mediante la selección de catalizadores y la evaluación del efecto de la variable agitación sobre la transferencia de materia externa (en todos los sistemas) e interna (en el sistema 3 por emplear catálisis heterogénea). El estudio de la influencia sobre la transferencia de materia se lleva a cabo analizando la evolución química de las especies químicas, si bien en el caso concreto de los sistemas 1 y 2, la investigación de la transferencia externa se complementó con una técnica óptica láser (FBRM).

- ***Estudio de la cinética de la reacción química***

  Bajo condiciones en las que la transferencia de materia externa (todos los sistemas) e interna (sistema 3) no es limitante, se realizan una serie de experimentos cinéticos en condiciones diferentes. Con los datos obtenidos, se realiza la proposición de modelos cinéticos para explicar el desarrollo de la reacción, discriminando entre ellos teniendo en cuenta criterios físicos, químicos y estadísticos.

SCOPE AND GOALS

In the current and forthcoming circumstances, the energy demand is very unlikely to be satisfied in the long term with traditional sources of fossil origin, especially considering their growing scarcity and the price increment derived thereof. Moreover, there is an increasing concern about the anthropogenic contribution of green house gases emissions to global warming as well as that of other emissions to ecosystems and health (IPCC, 2014).

For these reasons, the United Nations Framework Convention on Climate Change established the Kyoto Protocol in 1997 aiming at the reduction of green house gas emissions. Upon completion of this agreement, institutions at regional levels have spurred the use of renewable energy sources providing a legislative framework to such effect. Particularly, the European Union has promoted the Directives 2003/30/EC and 2009/28/EC setting goals to the share of use of renewable energies to be used by 2010 and 2020, respectively.

Within the mentioned scenario, the biodiesel industry has experienced a marked boom among the renewable sources, in whose manufacture process glycerine is generated as a by-product. The burgeoning production of glycerine could not be absorbed by the traditional markets, which has led to an oversupply of this product causing prices to drop very significantly, thereby reducing the profitability of biodiesel production process.

Aiming at balancing the declining trend of glycerol prices, new applications and uses of glycerine are being sought after. In this line of work, there have been approaches to its valorisation for energy supply. Nevertheless, given the physicochemical features of the glycerol molecule, its exploitation as feedstock to novel synthetic routes leading to high added-value products has been much more profuse. In this sense, if glycerine stems from a biological source, an approach towards its utilization as a platform chemical may arise to give rise to a so-called biorefinery.

Especially from the year 2000, the reported number of research contributions regarding the use of glycerine as a resource has experienced a significant growth. A high number of processes towards the synthesis of a diverse range of products, among which the following can be mentioned: mono, di and tri-esters and ethers as well as

polyesters and polyethers of glycerol and also a wide array of products derived from the selective dehydration, hydrogenolysis and oxidation of such molecule. In addition to the aforementioned, glycerol carbonate may be obtained through different procedures and, finally, ketals like solketal via the reaction of glycerol with a ketone or aldehyde.

Owing to the properties of glycerol carbonate and solketal, both have proven useful in many direct applications (e.g., solvents and additives) and performing as feedstock to yield further high added-value chemicals.

Considering the interest that these two products attract, the main goal of the present work is to investigate the underlying physicochemical phenomena involved in the chemical reactions proposed for their production.

Distinct approaches will be followed utilizing different reactant species and operating conditions. Hence, the following division into three blocks corresponding to three systems of the present Thesis is proposed:

System 1: Production of glycerol carbonate by transesterification of glycerol with dimethyl carbonate

System 2: Production of glycerol carbonate by transesterification of glycerol with ethylene carbonate

System 3: Production of solketal by acetalisation of glycerol with acetone

Therefore, the first two blocks are devoted to the production of glycerol carbonate, which will be undertaken through a homogeneous catalytic process and even in the absence of catalyst in one case. The third block is dedicated to the study of the production of solketal by means of a hetegeneously catalyzed procedure utilizing commercially available sulphonic ion exchange resins.

In order to undertake the assessment of these processes, a series of steps have been suggested as methodology, namely:

- ***Stoichiometric study***

  Compliance of atom balances was made considering the existing information in the literature regarding the chemical reaction jointly with the analysis of the

reaction samples. In the cases of systems 1 and 2, analysis was based on high performance liquid chromatography (HPLC), whereas in system 3, proton nuclear magnetic resonance spectroscopy was used (^{1}H-NMR).

- ***Study of the experimental and theoretical chemical thermodynamics***

  The theoretical study is based on the estimation of the equilibrium constants from thermodynamic relationships. On the other hand, the experimental constant is determined from the composition at equilibrium and the activity coefficients of the components involved.

- ***Thermodynamic study of the physical liquid-liquid phase***

  Given the limited solubility of the chemicals used as feedstock to the three processes, an assessment of the equilibrium among the liquid phases in the presence of cosolvents was made, being such the products of the reactions proposed. Equilibrium data were acquired varying the composition and temperature of the systems and the non-random two-liquid model (NRTL) was used to fit to such data in order to estimate the binary interaction parameters.

- ***Selection of the reaction conditions***

  The reactions dealt with herein were completed in batch operation. In this type of operation, the most favourable conditions were determined through the screening of catalysts and the evaluation of the effect of the stirring speed on the external (in the three systems) and internal (only in system 3 given the use of heterogeneous catalysis) mass transfer. Such studies were conducted analysing the chemical evolution of the system, though in the particular case of systems 1 and 2, the external mass transfer study could be complemented by an optical laser technique known as Focused Beam Reflectance Measurement (FBRM).

- ***Kinetic modelling***

  Under non-limiting external mass (in the three systems) and internal (system 3) transfer conditions, a series of kinetic runs were completed in varying conditions. With the observed data, proposal of kinetic models to describe the evolution of the reaction and further discrimination and verification accounting for physical, chemical and statistical criteria was made.

2. GLICERINA

2. GLICERINA

Desde hace aproximadamente una década, el descubrimiento de nuevas vías de aprovechamiento de la glicerina está suponiendo un enorme reto debido a la enorme disponibilidad de la misma como consecuencia de los excedentes de la industria del biodiesel, cuyo ciclo se presenta en la Figura 2.1.

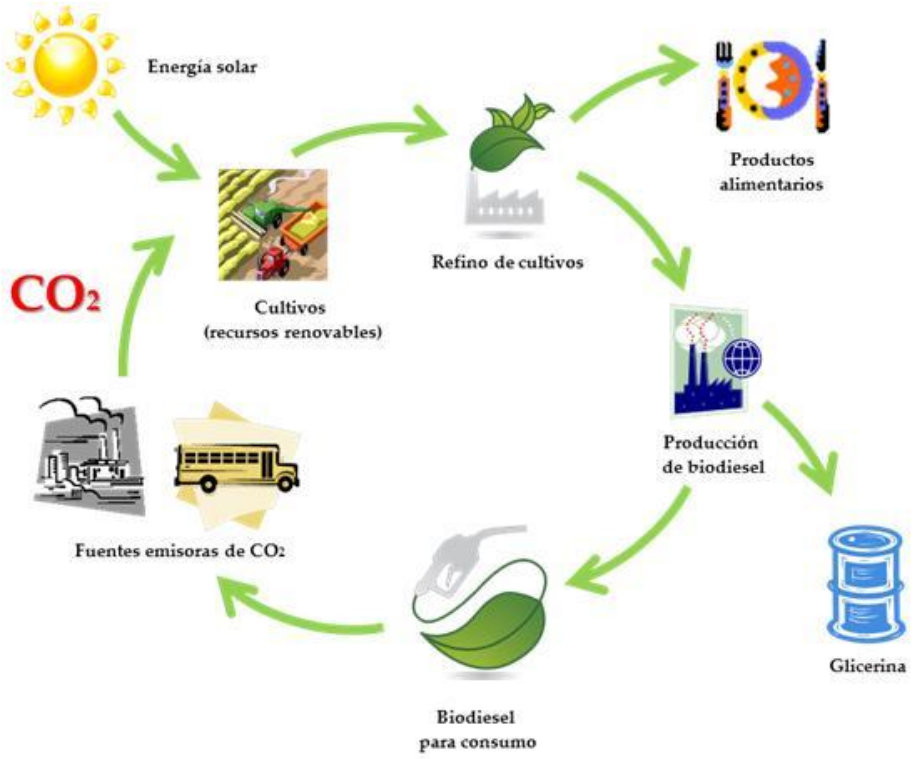

Figura 2.1. El ciclo del biodiesel

2.1. Orígenes del problema de la glicerina.

2.1.1. El marco regulatorio de los biocarburantes

Debido a la creciente demanda energética requerida para el desarrollo de las actividades humanas e industriales actuales, el uso de fuentes energéticas tradicionales de origen fósil ha incidido de manera negativa sobre el medio ambiente causando impacto en el denominado cambio climático, así como efectos en los ecosistemas y la salud asociados a las emisiones generadas. Así mismo, con el paso del tiempo, se hace evidente que la disponibilidad de estos recursos es cada vez más limitada (IPCC, 2007).

Con motivo de estas preocupaciones, la Convención Marco de las Naciones Unidas sobre el Cambio Climático (CMNUCC) estableció el Protocolo de Kyoto en 1997. Dicho protocolo es un acuerdo internacional con el objetivo de reducir entre 2008 y 2012 al menos un 5%, con respecto a 1990, las emisiones de los gases principalmente causantes del efecto invernadero. Dichos gases son: dióxido de carbono, metano, óxido nitroso, así como otros fluorados como el hexafluoruro de azufre (SF_6) y otros correspondientes a las familias de los hidrofluorocarburos (HFC) y perfluorocarbonos (PFC) (UNFCCC, 1997).

A partir de la firma de dicho Protocolo, las instituciones tanto a nivel mundial como regional han venido impulsando el desarrollo de fuentes de energía alternativas. Concretamente, la Unión Europea (UE) ha ido estableciendo y configurando los objetivos y el marco legislativo para el impulso de este tipo de energías. De esta manera, se fueron sucediendo documentos como *El Libro Blanco para una Estrategia y un Plan de Acción Comunitarios. Energía para el futuro: fuentes de energías renovables* (1997), *El libro Blanco para una Política Europea de Transportes de cara al 2010: la hora de la verdad* (2001). En el marco del sector del transporte, debido a sus grandes necesidades energéticas, la UE promulgó en primer lugar la Directiva 2003/30/CE de 8 de mayo de 2003, relativa al fomento del uso de biocarburantes u otros combustibles renovables en dicho sector y más adelante el *Plan de Acción sobre Biomasa* (2005) o la *Estrategia Europea sobre Biocarburantes* (2006).

En España, la transposición de la mencionada Directiva 2003/30/CE a la legislación nacional se hizo mediante el Plan de Energías Renovables para el período 2005-2010. Adicionalmente, la Disposición adicional decimosexta relativa a biocombustibles y biocarburantes de la Ley de Hidrocarburos (Ley 34/1998) establece una serie de objetivos por los cuales se establecía la obligatoriedad de llegar en 2009 al 3,4% y en 2010 al 5,83% de contenido en biocarburantes en relación a los carburantes comercializados. Además, para promocionar la producción de biocarburantes, esta Ley aplicaba un tipo cero en el impuesto de hidrocarburos para el biodiesel (CNE, 1998).

Más recientemente, con el fin de prolongar la acción y establecer nuevos objetivos, la UE aprobó la Directiva 2009/28/CE, que marcaría obligaciones y objetivos para 2020, entre los cuales se incluye el requerimiento de que el 20 % de la energía consumida en la UE sea de fuentes renovables. La transposición de esta última Directiva en nuestro Estados ha resultado en el Plan de Energías Renovables 2011-2020, si bien la

Orden ITC/2877/2008 ya preveía mecanismos para el fomento del uso de biocarburantes y otros combustibles renovables dentro de ese período. El Plan establece como objetivo en 2020 el empleo de 2713 ktep de biocarburantes, de los cuales 2313 ktep se prevén sean biodiesel. Así mismo, se estima la adjudicación de 313 millones de euros en ayudas públicas para actividades de I+D en biocarburantes y aplicaciones térmicas (IDAE, 2011).

2.1.2. El auge del mercado del biodiesel

Con un marco regulatorio que favorece claramente la implantación de los biocarburantes, no es de extrañar el auge que ha sufrido el mercado del biodiesel. Así mismo, se prevé que sea un mercado en continuo aumento, ya que está espoleado por la propia demanda de los carburantes fósiles, pues se trata de un bien sustitutivo de dichos carburantes. En este sentido, los estudios de mercado realizados por Lamers han resultado muy reveladores para observar la coyuntura del mercado de biodiesel a nivel global y europeo (Lamers y col., 2011).

La Figura 2.2 muestra la evolución de la producción global de biodiesel, que creció exponencialmente desde valores menores a 1 Megatonelada en 2000 hasta más de 16 en 2010. Se puede apreciar que la UE es el mayor productor de biodiesel en el mundo, siendo Alemania y luego Francia, Italia y España los países que más aportan a la producción dentro de la UE. Además, los aumentos en la producción observados en los últimos años de la gráfica para Argentina pueden ser atribuidos a las exportaciones realizadas a la UE y quedan por tanto vinculadas al consumo en esta región. En otros casos, como Brasil, este no es el caso por tratarse mayoritariamente de consumo interno (Lamers y col., 2011).

En cuanto a la balanza comercial dentro de la UE (Figura 2.3), el cambio de políticas fiscales en los Estados miembros desde los incentivos iniciales a la imposición posterior ha sido uno de los factores clave para la importación de biodiesel de países como Indonesia o la antes mencionada Argentina. Este ha sido, de hecho, uno de los factores de cierto retroceso en los últimos años de la industria del biodiesel en países como España y Portugal.

En cualquier caso, se puede apreciar que el consumo de biodiesel en la UE queda satisfecho aproximadamente en un 80% por la producción interna desde 2008 en

adelante y que tan solo cantidades residuales de biodiesel se exportan fuera de la Unión. La producción y el consumo de biodiesel en la UE siguen la misma tendencia creciente que la anteriormente comentada para el resto del mundo.

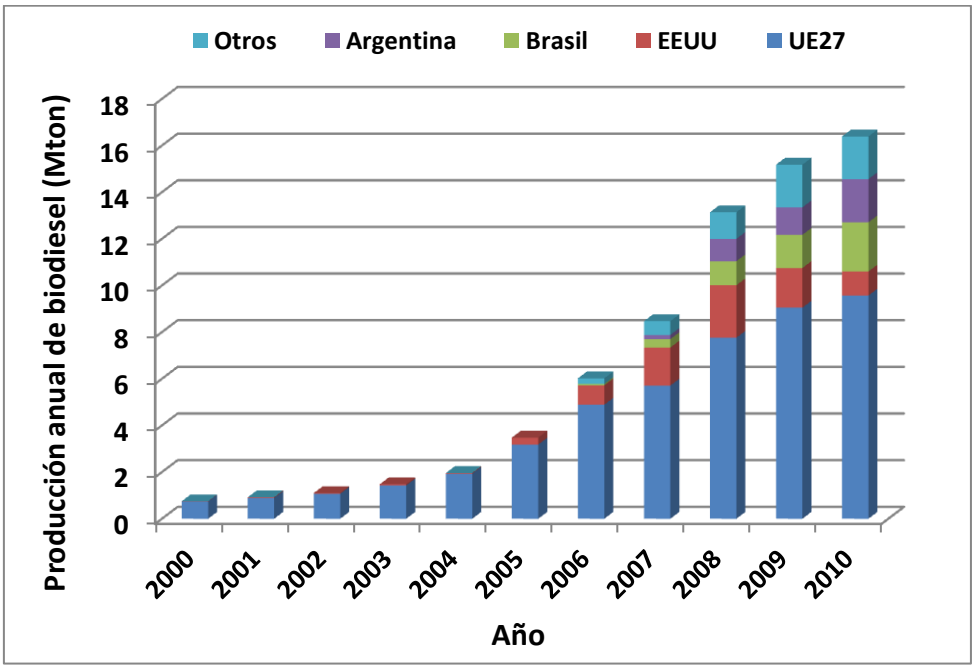

Figura 2.2. Evolución de la producción mundial de biodiesel entre 2000 y 2010. Adaptado (Lamers y col., 2011)

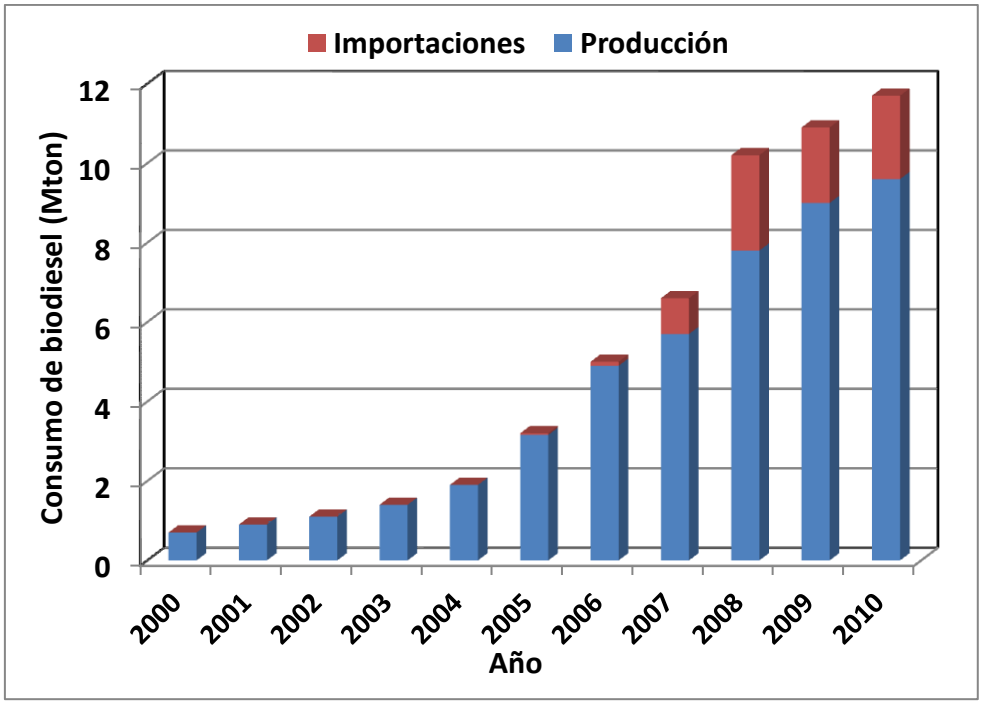

Figura 2.3. Balanza comercial del biodiesel de la UE en el periodo 2000-2010. Adaptado (Lamers y col., 2011)

2.2. Propiedades y calidades de la glicerina

El 1,2,3-propanotriol o glicerol, representado en la Figura 2.4 es el nombre que se le da a la molécula con tres grupos hidroxilo más simple que existe. La Tabla 2.1 recoge algunas propiedades de este compuesto, de entre las cuales se pueden destacar especialmente su alta viscosidad. Así mismo, su punto de ebullición es también remarcablemente elevado, lo cual se puede atribuir a la existencia de puentes de hidrógeno conferidos por los grupos hidroxilo de la molécula.

Tabla 2.1. Propiedades físicas de la glicerina

Propiedad	Valor
Peso molecular ($g \cdot mol^{-1}$)	92,09
Densidad ($g \cdot mL^{-1}$)	1,264
Punto de ebullición (ºC)	290
Punto de fusión (ºC)	17,8
Presión de vapor, 50 ºC (mm Hg)	0,0025
Punto de inflamabilidad (ºC)	177
Viscosidad, 20 ºC (cP)	1499
Tensión superficial ($dina \cdot cm^{-1}$)	63,4
Constante dieléctrica	42,48

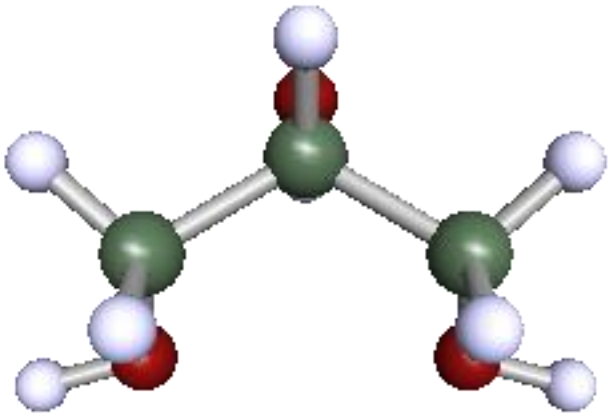

Figura 2.4. Estructura molecular del glicerol

La glicerina se conoce desde el 2800 a.C. en Mesopotomia en la fabricación de jabón calentando grasas mezcladas con cenizas. Sin embargo, se atribuye su descubrimiento a Scheele en 1779, quien consiguió aislar dicho producto tras calentar una mezcla de óxido de plomo con aceite de oliva. Sin embargo, en 1811 Chevrel

patenta por primera vez un método para la obtención de glicerina mediante la reacción de aceites con compuestos alcalinos (Kirk y Othmer, 2007).

Es importante distinguir entre "glicerol" y "glicerina". Si bien se usan frecuentemente indistintamente, el término glicerina normalmente se refiere al producto puro, mientras que glicerol es el término que se refiere a mezclas consistentes en la mayor parte de su composición en dicho alcohol acompañado de impurezas. Y en este sentido, existen varias calidades en función de la pureza que, evidentemente, tiene mucho que ver con el proceso que le ha dado origen.

En contraste con los métodos aludidos con los que se descubrió la glicerina, en la actualidad la mayor parte de la producción de la misma se lleva a cabo principalmente como subproducto de la fabricación de biodiesel; esta reacción química se muestra en la Figura 2.5. En ella, una molécula de triglicérido reacciona con un alcohol para dar lugar a alquilésteres de ácidos grasos (biodiesel) y glicerina como subproducto de la reacción. Los triglicéridos empleados en este proceso suelen proceder de aceites vegetales, si bien en ocasiones se emplean grasas animales; por otro lado, el alcohol más usado es metanol, si bien en lugares como Brasil el etanol es más empleado debido a la disponibilidad del mismo al proceder de la fermentación de azúcares de su avanzada industria del bioetanol. En el proceso global de fabricación de biodiesel se obtiene aproximadamente 1 kg de glicerina por cada 10 kg de biodiesel.

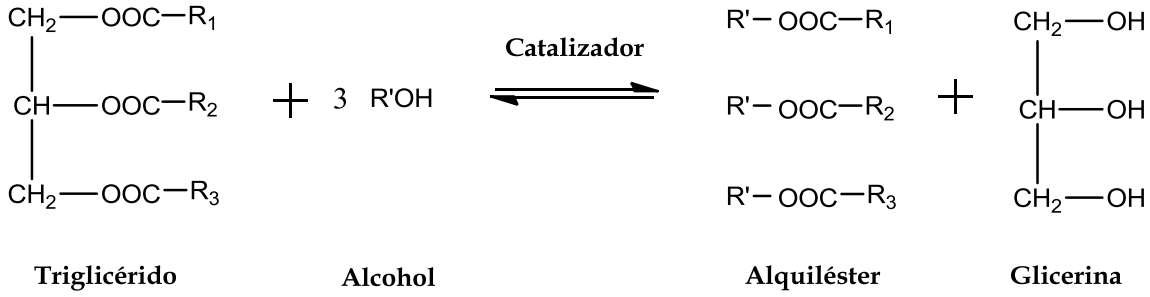

Figura 2.5. Reacción de transesterificación para la producción de biodiesel

Las glicerina es un líquido muy viscoso, altamente higroscópico, inoloro, incoloro y con cierto sabor dulce. La Tabla 2.2 resume la composición de tres calidades de glicerina procedentes de procesos de producción de biodiesel empleando metanol.

Tabla 2.2. Composición de distintos tipos de glicerina. Fuente: (Hazimah y col., 2003)

Característica	Glicerol crudo	Glicerina purificada	Glicerina refinada
Contenido de glicerol (% masa)	60-80	99,1-99,8	99,20-99,98
Contenido de agua (% masa)	1,5-6,5	0,11-0,8	0,14-0,29
Contenido de cenizas (% masa)	1,5-2,5	0,054	<0,002
Contenido de jabón (% masa)	3,0-5,0	0,10-0,16	0,04-0,07
Acidez (pH)	0,7-1,3	0,10-0,16	0,04-0,07
Color (escala APHA)	Oscuro	34-45	1,8-10,3

Se aprecia que no hay grandes diferencias entre la glicerina purificada y la refinada, aunque es clara entre estas dos y la glicerina cruda. En el caso de esta última, se puede apreciar especialmente el mayor contenido en humedad, característica importante que requiere su purificación para muchas actividades. Los procesos de purificación consisten en la eliminación de sales (jabón), el ajuste de pH mediante la eliminación de ácidos grasos libres y la separación de metanol; este compuesto se recupera generalmente por destilación y es reciclado en el propio proceso de producción de biodiesel (Quispe y col., 2013).

La obtención de glicerol crudo de las características indicadas en la Tabla 2.1 suele estar sujeta a procesos de obtención de biodiesel basados en catálisis homogénea, que por otro lado son los más comunes en la industria. Sin embargo, han empezado a implementarse procesos basados en catálisis heterogénea. En 2005, el Instituto Francés del Petróleo puso a punto el proceso Esterfip, en el que se emplea un óxido mixto de zinc y aluminio como catalizador y mediante el que se puede obtener glicerina como subproducto con una pureza de alrededor del 98%. Otro ejemplo es el proceso de Yellowdiesel, una compañía holandesa, que en 2006 desarrolló un método adecuado especialmente a materias primas con alto contenido en ácidos grasos libres tales como aceites empleados en cocina. Este proceso combina reacción y separación en un mismo proceso (destilación reactiva) para desplazar el equilibrio a los productos y reciclar el metanol simplificando el proceso. El proceso de Yellowdiesel puede proporcionar glicerina con una pureza del 99.9% (Pagliaro y Rossi, 2008). Además, se han descrito otros ejemplos en la literatura todavía no implantados industrialmente, como el que describen Bournay y col., que consta de una sección de reacción en la que se incluyen dos lechos fijos en serie en los que se hace reaccionar aceite vegetal y metanol. El

exceso de este último se elimina parcialmente tras cada una de las etapas de reacción por evaporación, mientras que los metilésteres (biodiesel) y la glicerina se separan por decantación, con una pureza de esta última mayores del 98% (Bournay y col., 2005).

Procesos como los mencionados parecen indicar el camino a seguir, ya que sin duda mejorarían la economía del proceso en lo que a purificación de la glicerina respecta para ulteriores aplicaciones en los que se use como materia prima.

2.3. El mercado de la glicerina

Durante aproximadamente los últimos quince años se ha venido apreciando un cambio importante en las fuentes de procedencia de la glicerina disponible en el mercado. Hasta 2003 aproximadamente, se considera que la industria de ácidos grasos es la principal fuente de glicerina seguida por la de producción de jabones. No obstante, a partir de entonces el peso relativo de estas industrias decreció gradualmente, y a partir de 2008 la industria del biodiesel se convirtió en el proveedor mayoritario de este producto (Gholami y col., 2014), lo cual puede explicarse sobre todo si se tiene en cuenta el gran crecimiento sufrido por esta industria, al que se aludió en el apartado 2.1.2. La Figura 2.6 ilustra el cambio sufrido entre 1999 y 2009 respecto a las industrias proveedoras de glicerina. En ella se puede apreciar, además, que la producción de glicerina sintética prácticamente desaparece.

La gran evolución del mercado del biodiesel ha supuesto un incremento en la producción de glicerina muy significativo. La Figura 2.7 muestra la evolución de la producción y los precios de la glicerina refinada y cruda en los Estados Unidos en el período 2001-2011, lo que es ilustrativo de lo que ocurre a nivel mundial. Se puede apreciar, en primer lugar, el aumento continuado de la producción en todo el periodo y la significativa caída de precios de la glicerina desde 2004 ó 2005, especialmente en el caso de la glicerina refinada. Hasta esos momentos, el abastecimiento de glicerol crudo en el mercado había permanecido más o menos estable a pesar del ya observado, aunque aún relativamente pequeño, aumento en la producción de biodiesel (Figura 2.2).

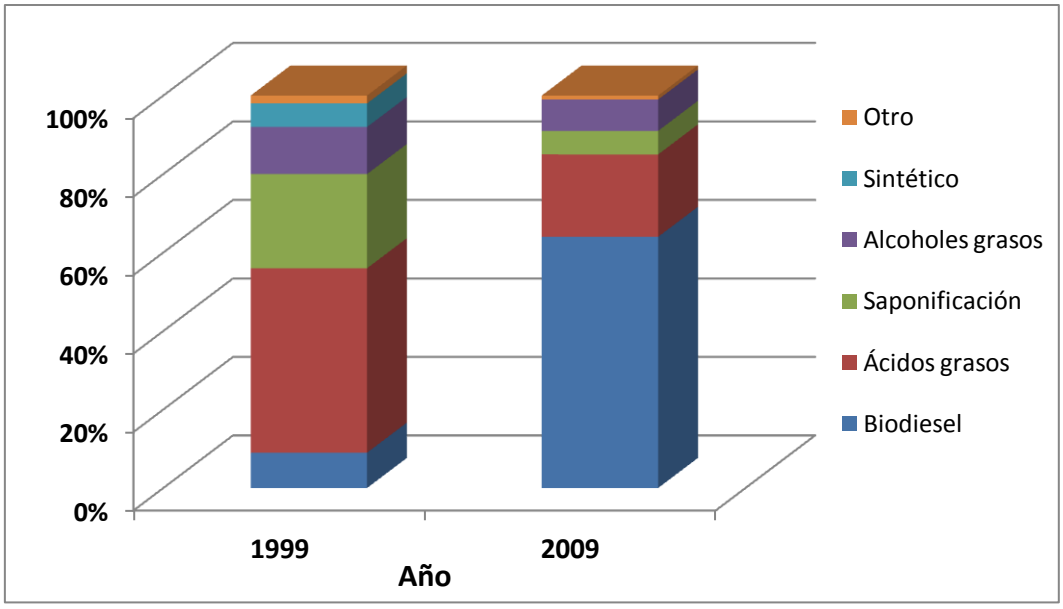

Figura 2.6. Cambio en las fuentes de origen de la glicerina. Fuente: (Bogaart, 2009)

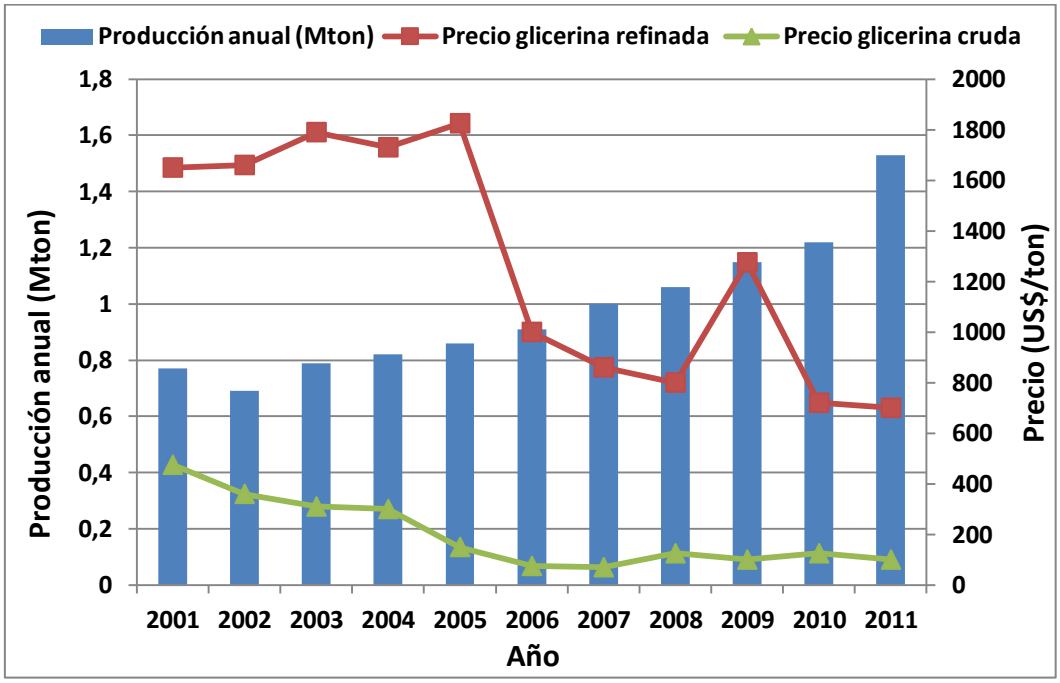

Figura 2.7. Serie histórica de la producción y precios de glicerina Fuente: (Quispe y col., 2013)

De hecho, entre 1980 y 2004, el precio de la glicerina de gran pureza mostró unos precios bastante afianzados variando entre 1200 y 1800 dólares/tonelada debido a que la producción y el mercado eran capaces de regularse con alternativas: cuando los precios de la glicerina eran altos, los demandantes reformulaban su producción en varias aplicaciones recurriendo a alternativas como el sorbitol, y cuando bajaban, se volvía a

emplear glicerina (U.S. Soy Bean Export Council, 2008). Sin embargo, a partir de 2004 la disponibilidad de glicerina creció de manera más notable (obsérvese la tendencia creciente en la Figura 2.7), pero la demanda no sufrió grandes cambios por no surgir mercados diferentes a los tradicionales (Gholami y col., 2014). Esto explicaría la tendencia a la baja de los precios. En 2008, la cantidad de glicerina derivada a aplicaciones industriales se estimó en unas 160.000 toneladas con una previsión de crecimiento interanual de 2.8% (Pagliaro y Rossi, 2008); sin embargo, esto no parece ser suficiente visto los crecimientos interanuales de alrededor del 10% en la producción de glicerina. Por este motivo, la glicerina es considerada una materia prima de interés para diversas aplicaciones, lo cual refuerza su percepción como *platform chemical*.

2.4. Usos y mercados tradicionales de la glicerina

La glicerina se utiliza hasta en 1.500 aplicaciones industriales diferentes, si bien sólo unas cuantas requieren tonelajes significativos de la misma. Gracias a que sus aplicaciones son similares a las de otros polialcoholes, se ha podido incrementar su campo de aplicación, introduciéndose en sectores tradicionalmente ocupados por el sorbitol y el pentaeritritol (Kirk y Othmer, 2007).

La Figura 2.8 muestra la dispersión de los mercados de aplicación de la glicerina, si bien de un modo u otro se han aglutinado en categorías con peso relativo importante.

El principal consumidor de glicerina es la industria de los cosméticos, que incluye los productos de higiene personal. Si a esta industria se le añade la de productos farmacéuticos bajo un nombre común de productos de química fina, casi la mitad de la glicerina va a estas aplicaciones en la industria. Se emplea como ingrediente en la preparación de elixires, anestésicos y jarabes, para la tos por ejemplo, aunque su uso más destacado es como parte de lociones y cremas para la piel, por su alta capacidad humectante, y en dentífricos, por su viscosidad, suavidad y sabor dulce. Algunos de sus derivados son empleados como tranquilizantes (guaiacolato de glicerina) o vasodilatadores (nitroglicerina).

En segundo lugar, con aproximadamente la cuarta parte de las aplicaciones, está el uso en la industria alimentaria, lo cual se puede atribuir a que el glicerol es fácilmente digerible y no es tóxico. Se emplea como disolvente en productos colorantes y

aromatizantes para dar consistencia al producto gracias a su viscosidad. Otros ejemplos son su utilización como agente humectante en siropes, o para retardar la cristalización del azúcar en dulces. También es mencionable la presencia de la glicerina en el procesamiento del tabaco, en el que es una parte importante de la disolución empleada antes de triturar y empaquetar las hojas de tabaco en forma de cigarrillo para evitar que se desmenucen durante el procesamiento. Así mismo, previene la desecación del tabaco y controla la velocidad a la que se consume por el fuego cuando se quema (Kirk y Othmer, 2007). Los polímeros de uretano utilizan óxido de propileno y poliéteres derivados del glicerol como iniciadores de las reacciones para dar espumas de poliuretano rígidas o flexibles, que se emplean en colchones, aislantes industriales o en la construcción. Entre otros usos destacados se incluye su empleo en resinas alquídicas, en materiales de embalaje, lubricantes (especialmente en maquinaria de la industria alimentaria por no ser tóxico) o los explosivos.

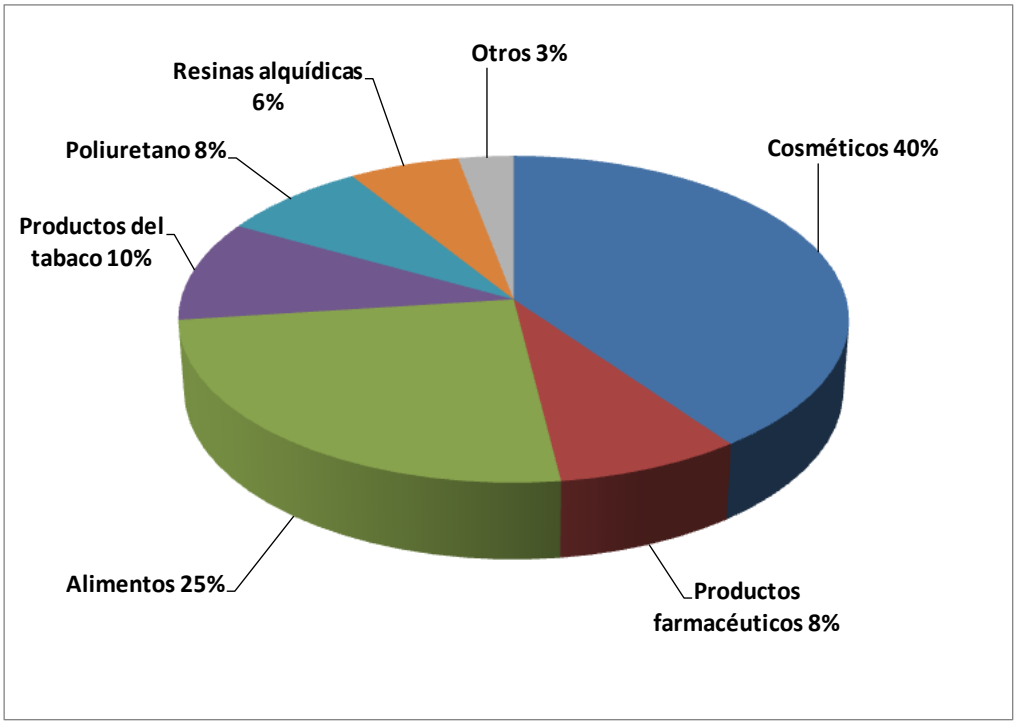

Figura 2.8. Desglose de los usos tradicionales de la glicerina. Fuente: (Stelmachowski, 2011)

2.5. Nuevos usos de la glicerina

Sin embargo, vista la evolución descendente de los precios de la glicerina durante los últimos años, queda claro que los mercados tradicionales de la glicerina no

constituyen una demanda suficiente como para frenar esta caída. Por este motivo, es evidente que surgen nuevas aplicaciones para los que se pudiera constituir en materia prima o *building block*.

En este sentido, se han estado llevando a cabo multitud de nuevas investigaciones para sacar el máximo rendimiento a las propiedades fisicoquímicas de esta sustancia. En los epígrafes siguientes se resumen los procesos más relevantes estudiados durante los últimos años divididos en dos clases: la primera de ellas se centra en la utilización de la glicerina como fuente de energía o como materia prima para la obtención de productos energéticos; en la segunda, mucho más amplia, la revisión distingue algunas de las múltiples rutas sintéticas que emplean glicerina como *building block* para la obtención de productos de alto valor añadido.

2.5.1. Uso energético de la glicerina

Dentro de la intención de mantener un uso completo de las fuentes de triglicéridos para un uso energético, se ha planteado la posibilidad de emplear la glicerina tanto como fuente directa como indirecta de energía.

En primer lugar, se puede contemplar la combustión directa de glicerina como alternativa con el fin de no agravar los problemas de emisiones que producen los combustibles fósiles. La Tabla 2.3 resume las emisiones más relevantes de la combustión de glicerol crudo en una caldera de tubos. La combustión de la glicerina cruda dentro del propio proceso de producción de biodiesel supondría varias ventajas como poder obviar los procesos de purificación y, ante todo, realizar la integración de la energía liberada dentro del propio proceso. Sin embargo, hay varias dificultades de carácter técnico asociadas a la combustión directa. En primer lugar, el poder calorífico de la combustión de la glicerina es bastante moderado, alrededor de 18 MJ/kg, por lo que tiene dificultades para mantener una llama apropiada en una caldera convencional, que además podría verse dañada por el alto contenido en agua y sales, que podrían inhibir la llama. En segundo lugar, su temperatura de autoignición es mucho mayor (370 ºC) que la de la gasolina (280 ºC) o el keroseno (210 ºC). En tercer lugar, su alta viscosidad puede suponer problemas a la hora de atomizarla. Por último, en el proceso de combustión puede generarse acroleína, con el riesgo a la salud que eso puede suponer (Quispe y col., 2013; Thompson y He, 2006).

Tabla 2.3. Emisiones de la combustión de glicerina cruda (Quispe y col., 2013)

Contaminante	Emisión (kg/h)
Partículas	2,27
Óxidos de nitrógeno	1,62
Monóxido de carbono	0,02
Dióxido de azufre	0,42
Compuestos orgánicos volátiles	0,05
Ácido sulfúrico	0,03
Calcio	0,06
Potasio	0,012
Magnesio	0,008
Fósforo	0,045
Ácido clorhídrico	0,015
Cloro	0,002
Acroleína	<0,0036
Acetaldehído	<0,0036

Se ha estudiado también su combustión conjunta con otras fuentes energéticas procedentes de biomasa (Thompson y He, 2006) o bien su incineración por la que, en base a un poder calorífico 18 MJ/kg y precio 0.1 dólar/kg medio asumido, podría suponer un cierto ahorro respecto a la utilización de gas natural (Quispe y col., 2013). Sin embargo, estas estimaciones no cuentan con un análisis profundo de los costes de mantenimiento de los equipos usando uno u otro combustible y, además, está sujeto a que el precio de la glicerina se mantuviera o continuara descendiendo, lo cual no está garantizado.

Por estos motivos, su utilización en este sentido no se prevé que se extienda. No obstante, está en pleno auge la investigación de procesos en los que la glicerina se transforma en productos que se emplean con fines energéticos.

En primer lugar podría mencionarse el reformado en fase acuosa (APR), mediante el cual glicerina en fase acuosa se convierte a CO y H_2 (gas de síntesis o *syngas*). En estos procesos se pueden emplear varios catalizadores para la obtención de mezclas de *syngas* con distinta composición, adecuado para la generación de hidrógeno por un lado o de combustibles de tipo alcanos mediante un proceso combinado de APR con la reacción de Fischer-Tropsch (FT). La Figura 2.9 esquematiza las reacciones de reformado, *water*-gas shift y la reacción de Fischer-Tropsch.

Reformado en fase acuosa	$C_3H_8O_3 + 3\,H_2O \longrightarrow 3\,CO_2 + 7\,H_2$ Glicerina
Water-gas shift	$CO + H_2O \longleftrightarrow H_2 + CO_2$
Síntesis Fischer-Tropsch	$(2n + 1)\,H_2 + n\,CO \longrightarrow C_nH_{(2n+2)} + n\,H_2O$

Figura 2.9. Reformado en fase acuosa, *water-gas shift* y Fischer-Tropsch

En el primero de los casos, se emplea un catalizador de platino a temperaturas moderadas de entre 200 y 250 ºC y presiones entre 16 y 40 bares para la generación del *syngas*. La mezcla obtenida cuando se emplea este catalizador tiene una riqueza mucho mayor en H_2 al favorecerse la reacción conocida como *water-gas shift*, y se puede emplear la corriente que sale del reformado directamente en motores de combustión interna o turbinas de gas. Esta reacción de reformado de vapor en fase acuosa empleando glicerina como materia prima presenta la ventaja de que su consumo energético es menor que el más tradicional reformado de metanol. Además, presenta otras ventajas, como el hecho de que se genera H_2 sin necesidad de evaporar agua, con el consiguiente ahorro energético; a las temperaturas relativamente bajas de operación, se evitan reacciones de descomposición de glicerina y, por otro lado, a las presiones empleadas, la corriente de salida de H_2 se puede purificar mediante adsorción por cambio de presión (Cortright y col., 2002).

También existe la posibilidad de realizar el proceso combinado APR-FT. En esta línea, el objetivo es conseguir realizar la reacción FT a continuación de la obtención de *syngas* en dos lechos catalíticos en serie. Esta reacción se trata de una suerte de oligomerización para dar alcanos de cadena relativamente corta que se puedan usar como combustibles. Para ello, se han utilizado catalizadores de Pt-Re a temperaturas algo superiores al anterior caso (275 ºC) y presión de 17 bares. Con estas condiciones, la selectividad hacia alcanos de cadena más larga de 5 carbonos fue de hasta 0,75. Las ventajas de esta reacción integrada radican en que se evitan los procesos endo y exotérmico que ocurrirían por separado, con las consiguientes necesidades de intercambio de calor, así como la eliminación de la necesidad de condensación de agua

y subproductos hidrocarburos entre los lechos. En la actualidad, el proceso integrado APR-FT se ha visto implantado en la industria, en primer lugar por Virent Energy Systems, Inc., a la que poco más tarde se uniría Madison Gas and Electricity en ese proyecto; posteriormente, Cargill, Shell y Honda se incorporarían como inversores.

Sometiendo la glicerina a pirólisis también se pueden obtener productos para uso energético. La principal diferencia entre estos procesos es que se realizan en total ausencia de oxígeno. Se ha estudiado la pirolisis de glicerina empleando un reactor de flujo laminar a 10 bares y temperaturas entre 680 y 700 ºC obteniéndose C_2H_4 y CH_4 además de gas de síntesis y prácticamente nada de CO_2 como productos (Stein y col., 1983).

La transformación de alcoholes como el etanol o el metanol a olefinas ha sido ampliamente estudiada (Zakaria y col., 2013), aunque esta síntesis también ha empezado a ser estudiada partiendo de glicerina como materia prima del proceso. Las olefinas ligeras tienen una aplicación energética incuestionable, si bien también pueden emplearse para la obtención de polímeros como el polietileno o polipropileno para elaborar fibras con aplicaciones diversas.

El principal reto en este tipo de síntesis es la eliminación de oxígeno de la molécula, culpable de las propiedades hidrófilas, para transformarla en una molécula hidrófoba con capacidad de combustión. Es decir, se busca un producto con una relación H/C lo más alta posible, lo cual en materias primas procedentes de biomasa suele rondar 2/3, mientras que para las que proceden del petróleo está alrededor de 2 en parafinas o de 1 si se trata de aromáticos. Para aumentar dicha relación, se ha utilizado craqueo catalítico, generándose paralelamente H_2 en el proceso, que *a posteriori* se emplea en los propios procesos para aumentar la relación H/C y obtener alcanos y olefinas en reacciones de hidrogenación y deshidratación (Corma y col., 2007). En el caso de la glicerina, las reacciones de deshidratación tienen lugar en centros activos ácidos de los catalizadores, dando lugar a H_2O y compuestos deshidratados (Pathak y col., 2010). Dichas especies deshidratadas pueden reaccionar con H_2 mediante reacciones de transferencia de hidrógeno para dar lugar a olefinas y aromáticos; así mismo, pueden darse reacciones de descarbonilación que darían etileno y CO a partir de la posible acroleína que se pudiera generar por descomposición térmica de la molécula de glicerol. Por último, por reacciones de Diels-Alder o condensación de aldol podrían producirse olefinas y aromáticos de mayor tamaño (Zakaria y col., 2013). La

Tabla 2.4 resume algunos procesos estudiados para la obtención de olefinas cortas, entre los que se puede que la conversión de glicerina es prácticamente completa en todos los casos, aunque con selectividades a los productos no muy elevadas.

Tabla 2.4. Procesos de glicerina a olefinas. Adaptado (Zakaria y col., 2013)

Referencia	Condiciones de operación	Catalizador	Conversión (%)	Selectividad (%)
(Zakaria y col., 2012)	Reactor de lecho fijo. VE=105 h^{-1};T=650 ºC	CuZSM-5	100	16,3
(Barbosa y col., 2009)	Reactor de percolación. VE=0,65 h^{-1}; T=343 ºC; P_{H2}=15,2 MPa	Catalizador macroporoso Ni-W	100	26,6
(Hoang y col., 2007)	Reactor de lecho fijo VE=0,5 h^{-1}; P=0,7 MPa T=300-400 ºC; P=2 MPa	HZSM-5	91 95	18 19
(Corma y col., 2008)	Distintos microrreactores. VE=7 h^{-1}; T=720 ºC; t_{res}=83 s; RCA=6	USY	100	19,4
	VE=30 h^{-1}; T=700 ºC; t_{res}=30 s; RCA=4	ZSM-5	100	32,2

NOTA: VE=velocidad espacial; t_{res}=tiempo de residencia; RCA=relación másica de catalizador a alimentación

Por último, podría hacerse mención al empleo de glicerina en células de combustible. La utilización de glicerina en nuevas tecnologías de células de combustible podría mitigar problemas asociados al uso del hidrógeno (explosivo) o metanol (inflamable). En este sentido, se ha descrito la utilización de glicerina empleando enzimas inmovilizadas en membranas sobre la superficie de un electrodo de carbono sobre una resina de intercambio iónico Nafion modificada con grupos amonio para conseguir un medio más estable para las enzimas. Estos bioánodos de glicerina se han incorporado a una célula de biocombustible glicerol-oxígeno que oxida el glicerol en varias etapas hasta ácido mesoxálico llegando a producir hasta 1.21mW/cm^2 (Arechederra y col., 2007). Esta tecnología ha sido adquirida por la empresa Akermin Inc. y está en fases de desarrollo hacia su implantación comercial, si bien antes deben mejorarse aspectos relativos a la estabilidad de la enzima, clave en el proceso. Además,

el uso de glicerina en estas tecnologías puede producir hasta cuatro veces más energía que con metanol (Pagliaro y col., 2009).

2.5.2. Valorización a productos de alto valor añadido

A pesar de los esfuerzos descritos en lo que al aprovechamiento energético de la glicerina respecta, la gran mayoría de los estudios realizados abogan más bien por emplear la molécula de glicerol como *platform chemical*. Este término viene a significar que, debido a sus destacadas propiedades químicas, esta molécula puede ser especie reactiva en multitud de procesos sintéticos para dar como producto una gran variedad de productos con un potencialmente alto valor añadido (Werpy y Petersen, 2004).

Tal es así que, desde 2007 se han publicado más de una decena de revisiones bibliográficas centradas en recopilar la ingente cantidad de información sobre investigaciones científicas que tratan la explotación de este recurso (Bauer y Hulteberg, 2013; Behr y col., 2008a; Behr y col., 2008b; Behr y Gomes, 2010; Gholami y col., 2014; Kenar, 2007; Len y Luque, 2014; Li y col., 2013; Pagliaro y col., 2009; Pagliaro y Rossi, 2008; Quispe y col., 2013; Zakaria y col., 2013; Zhou y col., 2008). El aprovechamiento de la glicerina como materia prima o *building block* se está estudiando utilizando procesos químicos, con catalizadores clásicos o enzimáticos, así como por transformaciones empleando microorganismos. Las Figuras 2.10 y 2.11 ofrecen esquemas generales de estas vías y los principales productos obtenidos.

En lo que sigue, se ha preferido hacer una descripción de los que se juzgan como principales productos a obtener en las revisiones de aprovechamiento de glicerina antes citadas, con independencia de la vía seguida para su obtención. La Figura 2.12 recoge el esquema con estos productos. Por tratarse del objeto de estudio de la presente Tesis, la obtención de carbonato de glicerina y solketal, un estudio mucho más detallado del estado del arte y aplicaciones de los mismos se llevará a cabo en secciones subsiguientes.

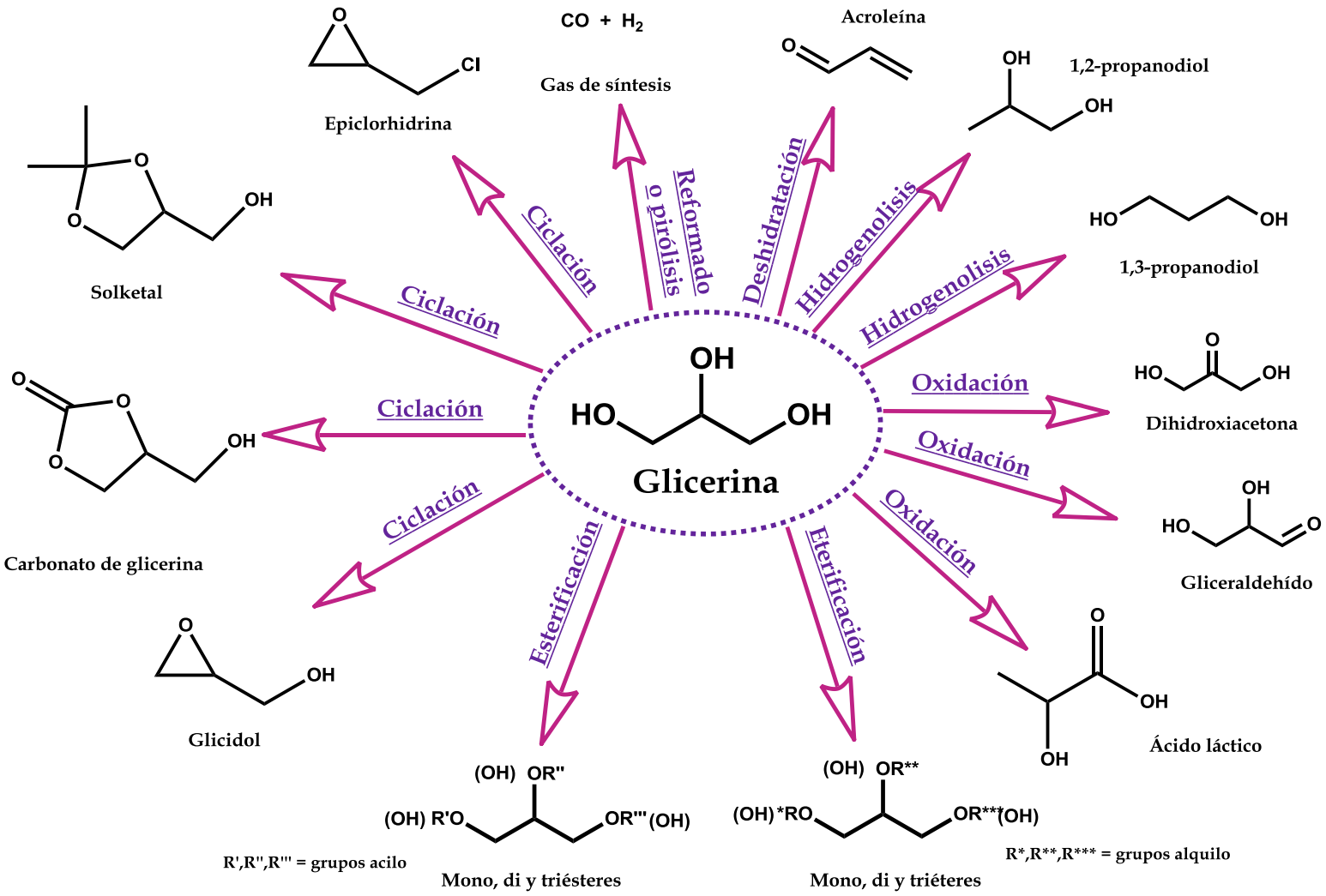

Figura 2.10. Aprovechamiento por vía química de la glicerina

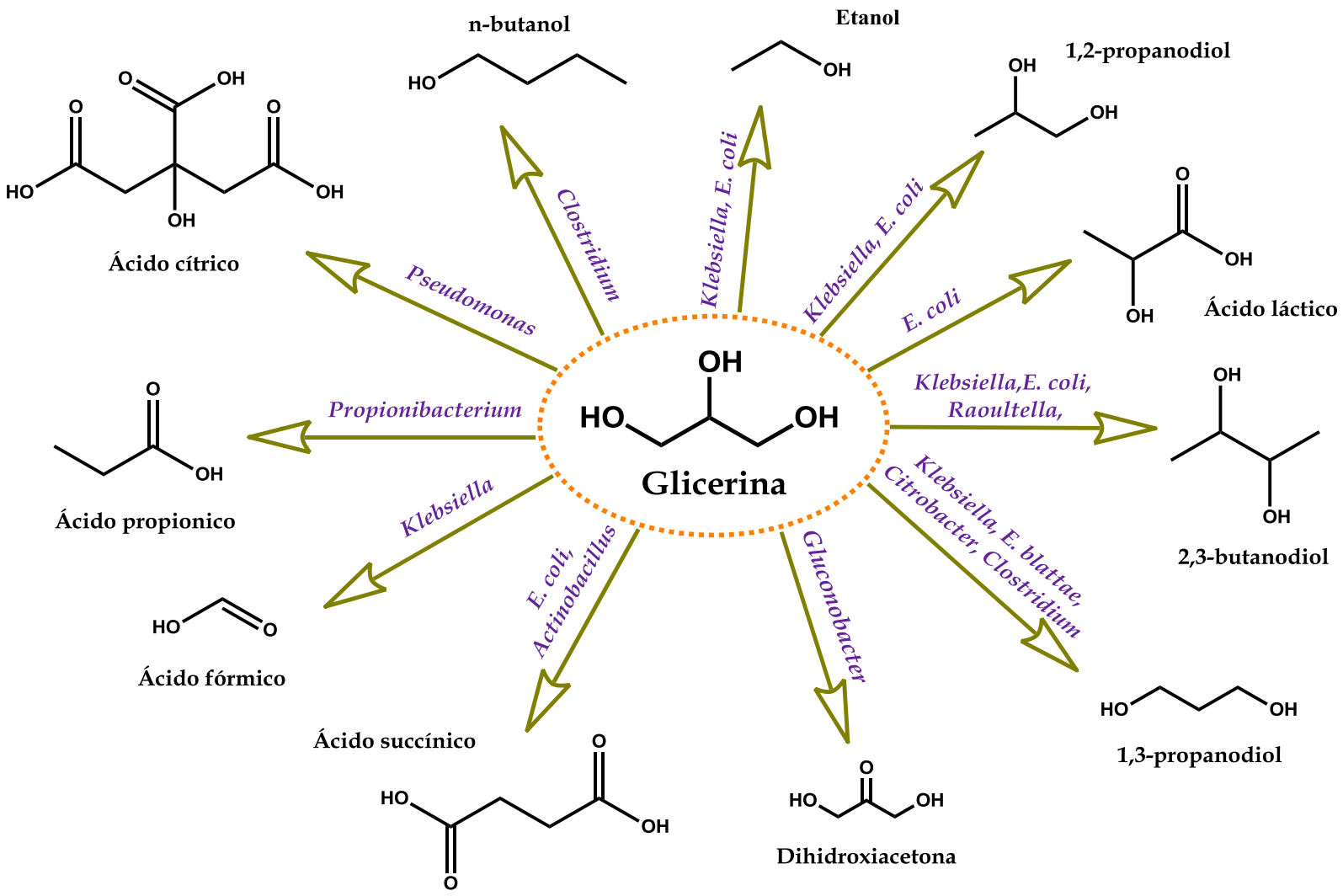

Figura 2.11. Aprovechamiento por vía microbiológica de la glicerina

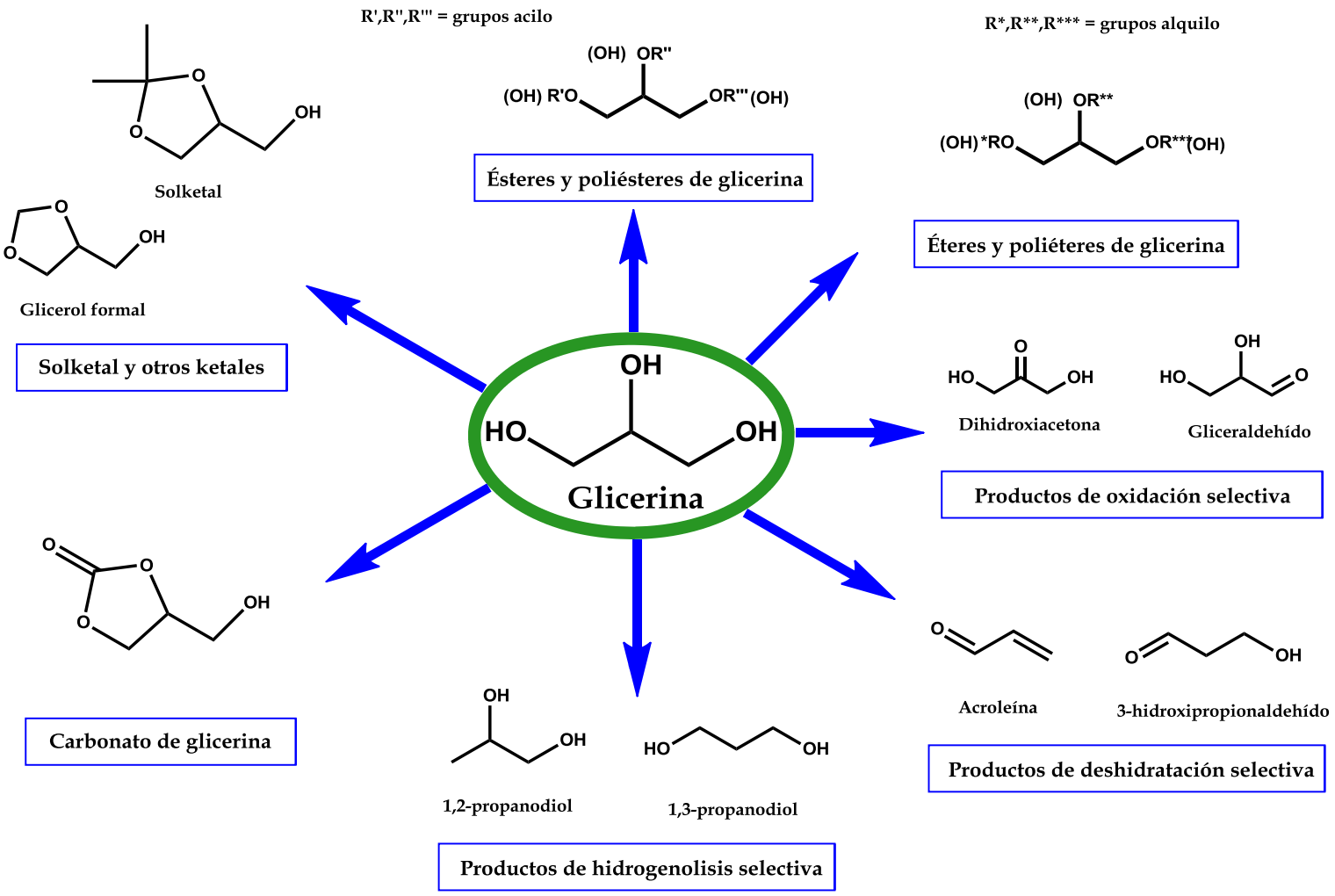

Figura 2.12. Productos surgidos del aprovechamiento de la glicerina

1) Ésteres de glicerol

Estos compuestos tienen reconocidas aplicaciones como emulsionantes en alimentos, cosméticos y productos farmacéuticos debido a su estructura consistente en una cabeza hidrófila y una cola hidrófoba (Kirk y Othmer, 2007). Así mismo, se contempla la posibilidad de su utilización como surfactante biodegradable (Gottlieb y col., 1994).

Los ésteres de monoglicéridos se obtienen generalmente por hidrólisis de triglicéridos, transesterificación de glicerol con metilésteres de ácidos grasos o por esterificación con ácidos grasos. No obstante, debido a que los grupos hidroxilo del glicerol presentan una reactividad muy similar, el producto de las reacciones de esterificación suele ser una mezcla de mono, di, y en ocasiones, triglicéridos, cuya proporción varía en función de las condiciones de reacción y el catalizador empleados (Zhou y col., 2008). Los catalizadores utilizados son mayoritariamente óxidos metálicos o sales soportadas sobre materiales mesoporosos como MCM-41 o materiales de este tipo funcionalizados con grupos organosulfónicos (Bancquart y col., 2001; Barrault y col., 2004a; Perez-Pariente y col., 2003; Pouilloux y col., 2000). No obstante, este tipo de reacciones también se han catalizado enzimáticamente, como la obtención de triglicéridos de ácidos fenilalcanoicos con Novozym 435 (Chang y Wu, 2007) o monoglicéridos por esterificación con ácido benzoico con lipasa B de *Candida antarctica* (Tamayo y col., 2012). También se ha estudiado la esterificación de glicerol con ácidos rosínicos (Ladero y col., 2011; Ladero y col., 2012) o de ácido cinámico y p-metoxicinámico en ausencia de catalizador (Molinero y col., 2013), si bien esta última reacción se puede realizar en condiciones más suaves con la ayuda de un catalizador como PTSA (Molinero y col., 2014).

2) Éteres de glicerol

Los éteres de glicerina pueden verse aplicados principalmente como disolventes oxigenados verdes o aditivos en combustibles con carácter biodegradable. En lo que incumbe a este segundo uso, pueden formarse los éteres terciarios ramificados de glicerol (GTBE), con aplicaciones similares al metil o etil terc-butil éter (Wessendorf, 1995). El GTBE puede aplicarse en la reformulación de mezclas de diesel y biodiesel disminuyendo las emisiones de partículas, hidrocarburos, CO y aldehídos tras su combustión así como aumentar el número de octano (Liotta y col., 2003).

Los alquiléteres de glicerol pueden sintetizarse por la adición de un alqueno al glicerol o bien por la reacción de condensación entre esta molécula y un alcohol alifático con eliminación de agua (Behr y col., 2008b). En la primera de estas reacciones, se han obtenido GTBE a partir de isobuteno en presencia de un catalizador ácido como resinas ácidas o sílices sulfónicas mesoestructuradas, a temperaturas entre 50 y 150 ºC y con relaciones molares de isobuteno a glicerol de 2 a 1 o mayores (Behr y Obendorf, 2001; Melero y col., 2008). Esta reacción también se ha probado en ausencia de disolvente empleando resinas como Amberlyst 35 a 80 ºC, alcanzándose conversiones de glicerina mayores del 92%, si bien se obtenía una mezcla de mono, di y tri terc-butiléter (Karinen y Krause, 2006). En cuanto a la condensación con un alcohol, se ha investigado la reacción con terc-butanol en presencia de catalizadores ácidos como Amberlyst 15 o diversos tipos de zeolitas, con cantidades de catalizador de 8% en peso y una relación equimolar de reactivos (Klepáčová y col., 2003). Más recientemente, se ha estudiado la reutilización de la resina Amberlyst 15 y se ha propuesto y validado un modelo cinético para esta reacción (Pico y col., 2013). Sin embargo, la condensación alcohólica parece obtener rendimientos menores que la adición de un alqueno.

Por otra parte, se han estudiado también procesos para la obtención de oligómeros y polímeros de glicerol. Los oligogliceroles se obtienen empleando catalizadores básicos homogéneos como Na_2CO_3 o NaOH con altas conversiones de glicerol (Charles y col., 2003; Lutz y col., 1998), aunque al igual que en muchas de las reacciones citadas en esta revisión, se tiende al empleo de catálisis heterogénea por la facilidad de separación y reutilización de estos catalizadores, así como por la mayore selectividad observada con zeolitas o resinas de intercambio iónico o metales sobre MCM-41 (Barrault y col., 2004b). Como ejemplo, se puede establecer la comparación entre el empleo de Na_2CO_3, con la que tras 8 horas se obtiene una conversión de glicerol del 80% y selectividad a olígomeros mayores al triglicerol del 41% en total, y un catalizador de Cs-MCM-41, con el que se obtiene una conversión del 95% tras el triple de tiempo, pero con una selectividad a di y triglicerol de casi el 90%. Sin embargo, esta síntesis también se puede llevar a cabo haciendo uso de catalizadores ácidos, y en este sentido se han probado resinas ácidas con mejores resultados en lo que a selectividad respecta, aunque las conversiones han sido menores. Con Amberlyst 16, la conversión ronda el 40%, pero la selectividad a éteres mayores al triglicerol es menor que 1 % y

empleando resinas perfluorosulfónicas Hyflon como H730/MS3030, la conversión alrededor del 50% y selectividad a di y triéteres casi del 99% (Frusteri y col., 2012).

Las reacciones de telomerización son otra clase de polimerización, en este caso de un dieno (como 1,3-butadieno), también conocidas para la obtención de éteres (Behr y Gomes, 2010). Se trata de reacciones catalizadas por complejos que incluyen metales de transición como paladio o níquel, alcanzándose alta selectividad al producto deseado, de hasta el 95% (Behr y col., 2003).

3) Productos de oxidación selectiva

La oxidación del glicerol puede dar lugar a multitud de productos en función de la selectividad de la oxidación; no obstante, suelen tratarse de procesos muy caros, sobre todo por los catalizadores empleados, y su implementación a escala industrial todavía es baja. La Figura 2.9 recoge el esquema de algunos de los procesos y productos más relevantes de estas rutas oxidativas por vía química, enzimática y microbiológica.

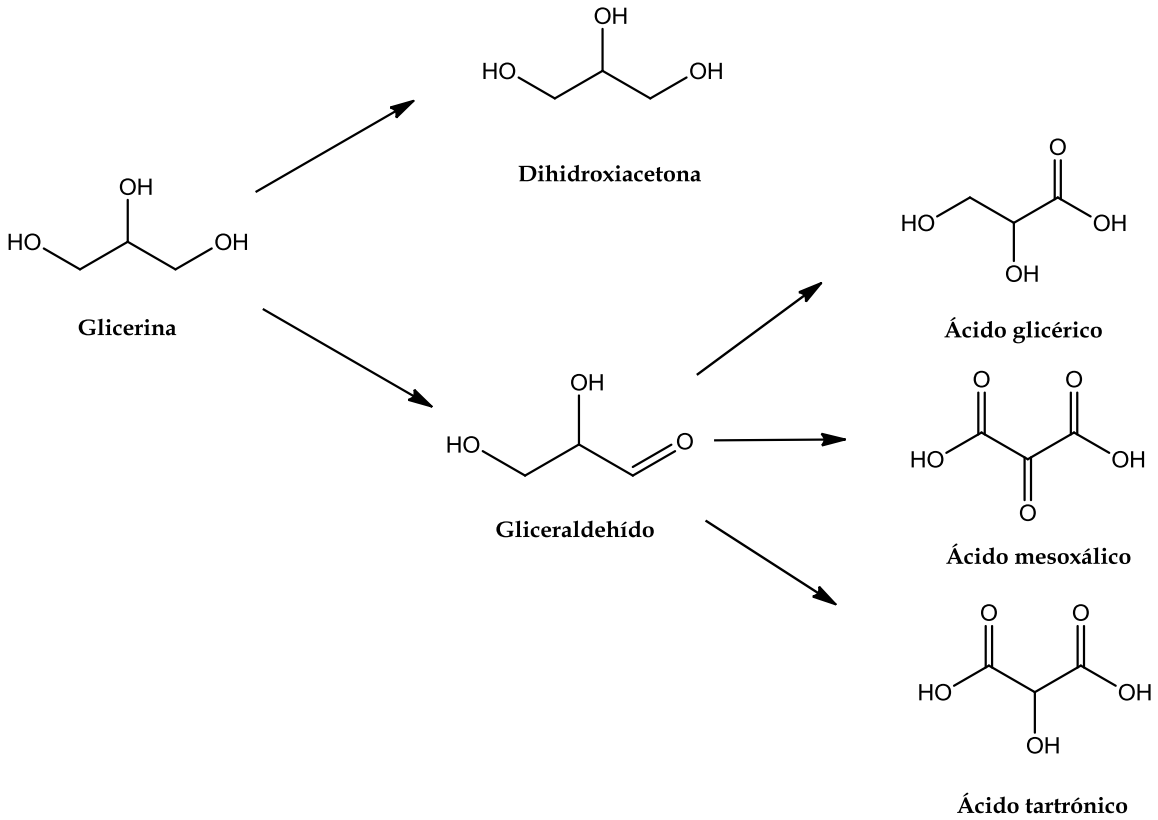

Figura 2.12. Productos de la oxidación selectiva del glicerol

En primer lugar, se puede mencionar la dihidroxiacetona (DHA), cuya aplicación más extendida es la de formar parte de formulaciones para lociones de autobronceado, para la preservación de vino por su capacidad antimicrobiana o bien como monómero para la fabricación de ciertos biomateriales (Eschenbruch y Dittrich, 1986; Pagliaro y Rossi, 2008) A partir de este compuesto, puede producirse ácido hidroxipirúvico o mesoxálico, precursores de productos farmacéuticos (Pagliaro y Rossi, 2008).

El gliceraldehído es otro producto de interés, con un papel destacado como intermedio en el metabolismo de carbohidratos o como molécula de partida para la obtención de ácidos carboxílicos como el glicérico, tartrónico o mesoxálico, que tienen aplicaciones como emulsionantes o para tratamientos de afecciones dermatológicas o anticirrósicas (Stockel, 2007).

El gran reto asociado a las oxidaciones selectivas es el desarrollo de catalizadores para llevarlas a cabo, ya que en general muestran una selectividad bastante platino, oro o paladio (Kwon y col., 2011), que, además de costosos en sí, requieren el uso de bajas presiones de oxígeno para limitar su alta tendencia a la desactivación.

Otra posibilidad es realizar transformaciones microbiológicas, como la dirigida a DHA por vía fermentativa empleando *Gluconobacter oxydans* o *Acetobacter suboxydans* (Li y col., 2013).

4) Productos de deshidratación selectiva

Los principales productos de la deshidratación de la glicerina son la acroleína y el 3-hidroxipropionaldehído (3-HPA).

La acroleína es un producto que puede usarse como herbicida o bien como intermedio en la producción de ácido acrílico, empleado en la fabricación de polímeros absorbentes usados en pañales o para retener agua en la producción de papel. Se ha estudiado la producción de acroleína por deshidratación de glicerina sin necesidad de catalizador en condiciones supercríticas, a temperaturas de 300 ºC y 300 bar, aunque con rendimientos que alcanzan únicamente el 12% (Buhler y col., 2002). Para mejorar el rendimiento hasta el 40%, se ha empleado ácido sulfúrico en concentraciones de 5 mmol/L a temperaturas entre 300 y 350 ºC y 350 bar de presión (Ramayya y col., 1987). Otra opción más reciente ha sido la utilización de catalizadores heterogéneos como óxido de wolframio soportado en óxidos de zirconio, sílice y alúmina en un lecho fijo

empleándose temperaturas de 315 ºC y presión atmosférica y consiguiendo rendimientos cercanos al 60% (Chai y col., 2014).

El 3-HPA es precursor de productos como el ácido acrílico y el 1,3-propanodiol. Su producción se basa en procesos biotecnológicos mediante bacterias como *Klebsiella*, *Citrobacter*, *Enterobacter* o *Clostridium* para las que las condiciones de reacción más comunes son temperatura de 37 ºC y presión atmosférica, con rendimientos del orden del 85% (Pagliaro y Rossi, 2008).

5) Productos de hidrogenolisis selectiva

Los principales productos de la hidrogenación selectiva del glicerol son los glicoles: 1,2-propanodiol (1,2-PD), normalmente conocido como propilenglicol, y 1,3-propanodiol. El primero de ellos tiene aplicaciones similares a las de otro glicol también ampliamente utilizado en la industria, el etilenglicol. Entre los múltiples usos de 1,2-PD se encuentra el de aditivo en productos nutricionales (como disolvente de colorantes y saborizantes), en cosméticos, y como parte de la formulación de lubricantes y anticongelantes o como humectante en tabaco (Kenar, 2007; Zhou y col., 2008). El 1,3-PD, sin embargo, tiene aplicaciones directas más reducidas y tiende a ser material de partida para otros productos de interés. Se emplea para la fabricación de productos con usos como recubrimientos, películas y fibras de poliéster, como los casos de SORONA y HYTREL de DuPont o CORTERRA de Shell (Behr y col., 2008b).

El 1,2-PD se sintetiza actualmente por la hidrólisis de óxido de propileno con agua a temperatura entre 125 y 200 ºC y presiones de 20 bares. En la ruta a partir de glicerol, se han observado selectividades muy cercanas al 100% empleando catalizadores basados mayoritariamente en cobre y zinc. Un par de ejemplos recientes son la hidrogenación, a temperaturas de 200 ºC y presiones de 60 bar, en presencia de cobre soportado sobre óxido de zinc y alúmina (Wang y Liu, 2014) o en condiciones algo más severas, de 240 ºC y 80 bar de H_2 utilizando cobre soportado sobre sílice (Vasiliadou y col., 2014). Las rutas de obtención de 1,2-PD a partir de glicerol están atrayendo el interés de empresas como Dow, Cargill o Huntsman (Kenar, 2007). Así mismo, también hay empresas como Ashland Inc. o Cargill interesadas en la obtención de propilenglicol, para lo cual han optado por transformaciones microbiológicas con *Escherichia coli* o *Thermoanaerobacterium thermosaccharolyticum* (Altaras y Cameron, 1999; Altaras y col., 2001).

Por otro lado, la síntesis de 1,3-PD se lleva a cabo tradicionalmente a partir de de la hidroformilación del óxido de etileno con gas de síntesis (Shell) o por hidratación de acroleína (DuPont) por métodos bastante costosos en términos económicos y de generación de residuos. Las rutas a partir de glicerina para la obtención de 1,3-PD que más atractivas son mayoritariamente microbiológicas; así, se han empleado *Lactobacillus reuteri* (Jolly y col., 2014), *Enterobacter agglomerans* (Barbirato y col., 1996), *Citrobacter freundii* (Seifert y col., 2001) o *Klebsiella pneumoniae* (Galdeano Villegas y col., 2007; Huang y col., 2002). También se están estudiando rutas catalíticas por vía química con catalizadores de rutenio y renio, si bien tienen el inconveniente de no ser excesivamente selectivas hacia 1,3-PD, dando mezclas con bastante presencia de 1,2-PD además de subproductos de menor tamaño molecular (Ma y He, 2009).

3. CARBONATO DE GLICERINA

3. CARBONATO DE GLICERINA

El carbonato de glicerina (GC) constituye un producto con una creciente importancia a nivel de investigación. La Figura 3.1 ilustra el mencionado auge de este producto mostrando la creciente evolución de los resultados de la búsqueda "glycerol carbonate synthesis" en Web of Science.

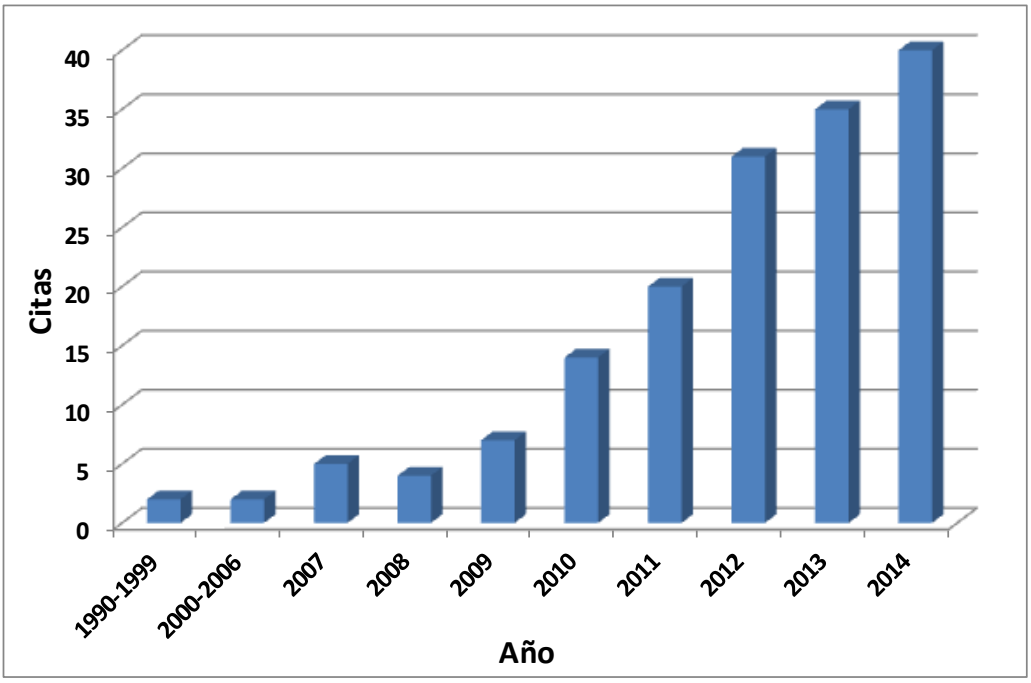

Figura 3.1. Evolución de las publicaciones relacionadas con la síntesis de carbonato de glicerina

Tal es el interés que entre 2012 y 2014 se han publicado hasta tres revisiones exlusivamente dedicadas a este producto (Ochoa-Gomez y col., 2012a; Sonnati y col., 2013; Teng y col., 2014).

Los dos primeros bloques de la presente Tesis están dedicados a la investigación de los aspectos fenomenológicos de carácter físico y químico de la obtención de este producto. A continuación se presentarán los aspectos más relevantes de sus aplicaciones y el estado del arte de su producción.

3.1. Propiedades

La Figura 3.2 representa la molécula 4-(hidroximetil)-1,3-dioxolan-2-ona, también conocida como carbonato de glicerina (CAS: 931-40-8).

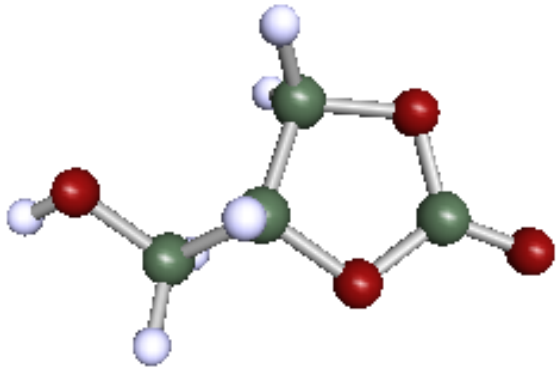

Figura 3.2. Estructura molecular del carbonato de glicerina

La Tabla 3.1 recoge algunos valores relacionados con variables de operación con este compuesto.

Tabla 3.1. Propiedades físicas del carbonato de glicerina

Propiedad	Valor
Peso molecular ($g \cdot mol^{-1}$)	118,09
Densidad, 25 ºC ($g \cdot mL^{-1}$)	1,4
Punto de ebullición, 760 mm (ºC)	353,9
Punto de fusión (ºC)	-69
Presión de vapor, 177 ºC (mm Hg)	0,008
Punto de inflamabilidad (ºC)	190
Viscosidad, 25 ºC (cP)	85,4
Constante dieléctrica, 20 ºC	111,5
LD50 ($g \cdot kg^{-1}$ conejo)	28

El valor de la densidad del carbonato de glicerina es algo superior al de otros carbonatos orgánicos como los carbonatos alquílicos de dimetilo (DMC) o dietilo (DEC) o los carbonatos cíciclos de etileno (EC) o propileno (PC) (ρ_{DMC}=1.07 $g \cdot mL^{-1}$; ρ_{DEC}=0.98 $g \cdot mL^{-1}$; ρ_{EC}=1.33 $g \cdot mL^{-1}$; ρ_{PC}=1.20 $g \cdot mL^{-1}$). Esta diferencia también se aprecia en el punto de ebullición de estas sustancias, que van en un orden parecido (T^{eb}_{DMC}=90 ºC; T^{eb}_{DEC}=127 ºC; T^{eb}_{EC}=248 ºC; T^{eb}_{PC}=242 ºC), lo cual podría atribuirse a la presencia de enlaces de hidrógeno adicionales proporcionados por el grupo hidroxilo de la molécula. Además, su inflamabilidad es bastante baja debido a la estabilidad que le confiere el ciclo de cinco átomos de su estructura, siendo su punto de inflamabilidad muy superior al de carbonatos dialquílicos (T^{flash}_{DMC}=17 ºC). Por otro lado, es reseñable

el hecho de que su viscosidad, aun siendo más de un orden de magnitud menor que la de la glicerina a la misma temperatura (μ_{Gly}= 934 cP a 25 ºC) es también mayor a la de los otros carbonatos cíclicos mencionados.

Si bien la toxicidad del carbonato de glicerina no ha sido todavía estudiada en profundidad, se han realizado estudios de este tipo para PC. Su toxicidad es considerada muy baja (LD_{50}>28 $g \cdot kg^{-1}$ en conejo), con negativos efectos mutagénicos, nula genotoxicidad, muy bajos efectos irritantes sobre la piel humana y, en caso de ingestión, se digieren a glicoles y CO_2. Por la similaridad del compuesto, puede pensarse en GC como un compuesto no tóxico. En lo que a biodegradabilidad respecta, ensayos con PC han demostrado que es muy comparable a la de compuestos como el metanol, etanol y acetona, y que además su hidrólisis da como producto 1,2-PD (propilenglicol), también biodegradable (Sonnati y col., 2013).

Por último, los carbonatos cíclicos son considerados buenos disolventes (Clements, 2003). En el caso del carbonato de glicerina, esto puede corroborarse por el alto valor de su constante dieléctrica y la anteriormente aludida presencia de puentes de hidrógeno por su estructura molecular. Además, el carbonato de glicerina tiene una alta capacidad higroscópica (Kahre y col., 1999).

3.2. Aplicaciones del carbonato de glicerina

A pesar de que la utilización del carbonato de glicerina a nivel comercial todavía se encuentra muy limitada, puede suponer una alternativa de origen biológico muy interesante.

Sus propiedades fisicoquímicas le confieren la posibilidad de ser aplicada directamente en una gran variedad de usos. Por otro lado, la alta reactividad de la molécula por la presencia del grupo carbonato y el hidroxilo le permiten actuar de molécula de partida para la obtención de otros productos.

3.2.1. Utilización directa

La principal aplicación del carbonato de glicerina tiene que ver con sus excelentes propiedades como disolvente, tal como se apuntó en la Sección 3.1. Así, se ha apuntado su potencial en aplicaciones similares a la del carbonato de propileno o etileno (Sonnati y col., 2013). De este modo, podría ser un buen sustituto de estos

compuestos como transportador en cosméticos o medicinas aplicadas por vía tópica (Sun y col., 1999), disolvente en baterías de litio e ion-litio o como transportador de electrolitos (Izutsu y col., 1996).

De manera concreta, se ha estudiado el uso del carbonato de glicerina como disolvente para análisis por resonancia magnética nuclear, donde gracias a su viscosidad se ha podido para alcanzar una buena resolución en el análisis de péptidos con estructuras muy similares entre sí (Lameiras y col., 2011). También se han empleado para sustituir hasta en un 90% el empleo de líquidos iónicos (ILs) en la deshidratación de fructosa a 5-hidroximetilfurfural, suponiendo un potencial ahorro en términos ambientales y sobre todo económicos para procesos en los que pudieran intervenir ILs (Benoit y col., 2010). Así mismo, gracias a la alta constante dieléctrica y a su capacidad de ionizarse y disociarse, se ha visto que la actividad enzimática en disolución con carbonato de glicerina es alta y comparable a la que se da con agua como disolvente y mucho mejor que la de otros disolventes orgánicos en sistemas enzimáticos con CALB y CRL (Ou y col., 2011). Por último, se ha utilizado también en el pretratamiento de bagazo de caña de azúcar, de forma que el carbonato de glicerina o mezclas con glicerol acidificadas con sulfúrico actúan de disolvente en la sacarificación de las fracciones lignocelulósicas a azúcares fermentables (Zhang y col., 2013).

Además del empleo como transportador y disolvente en reacciones químicas, el carbonato de glicerina también se ha utilizado en otros usos diversos. Se ha inmovilizado sobre membranas para la separación de dióxido de carbono y nitrógeno (Kovvali y Sirkar, 2002). También se ha usado para vitalizar plantas en combinación con fertilizantes y agentes quelantes (Nomura y col., 2006). Con aplicación en materiales de construcción, se ha estudiado su utilización como agente curante en matrices puzolánicas mejorando propiedades como la velocidad de endurecimiento o la resistencia a la compresión de aglutinantes de cal y metacaolín (Magniont y col., 2010). Dentro de la industria de los cosméticos, el carbonato de glicerina puede usarse como eliminador de pintauñas (Murase, 1989), como emulsionante en cremas y lociones (Kahre y col., 1999) o agente plastificante en maquillajes, pintalabios o productos para el cabello (Bandres y col., 2012). Por último, su utilización en productos de limpieza ya ha sido probado por Procter & Gamble, que ha patentado su posible inclusión como aditivo en detergentes sólidos (Brooker, 2011) o Henkel (Weuthen y Hees, 1995).

3.2.2. Carbonato de glicerina como materia prima

En lo que concierne a los usos indirectos del carbonato de glicerina, esta molécula ha sido estudiada como *building block* en la producción de otros productos de valor añadido. Este compuesto tiene reactividad nucleófila gracias al grupo hidroxilo y electrófila por el grupo carbonato, lo cual le confiere múltiples posibilidades de reacción. En los siguientes párrafos se resumen algunas de las reacciones más relevantes encontradas en la bibliografía.

A partir de carbonato de glicerina pueden sintetizarse alquil o alquenil oligoglicósidos, que pueden ser empleados como surfactantes no iónicos (Dalelio y Huemmer, 1967); o bien por reacción con sacáridos pueden obtenerse glicósidos útiles como precursores de gliceroglicolípidos o agentes humectantes (Ueno y Mizushima, 2007).

En literatura se pueden encontrar otros surfactantes no iónicos, en este caso ésteres, derivados de la reacción con ácidos grasos como el láurico, oleico o palmítico se pueden obtener α-monoglicéridos con aplicaciones como surfactantes no iónicos (Ghandi y col., 2007). Además, otros ésteres pueden obtenerse por reacciones de acilación en presencia de acilcloruros alifáticos, los cuales poseen además buena resistencia a la oxidación (Mouloungui y Pelet, 2001).

También pueden llevarse a cabo varias reacciones de polimerización con carbonato de glicerina. Así, se pueden encontrar ejemplos como poligliceroles obtenidos por reacción de ésteres de ácidos carboxílicos de sorbitán con carbonato de glicerina para dar también compuestos surfactantes (Bevinakatti y col., 2009); poliéteres hiperramificados por reacción con trimetilolpropano, que podrían ser usados en adhesivos (Rokicki y col., 2005); o policarbonatos con aplicaciones como lubricantes industriales o en motores (Mouloungui y col., 2014). Otras polimerizaciones con heteroátomos recurrentes son la de varias clases de poliuretanos: la obtención de poliuretanos sin isocianato por reacción de carbonato de glicerina con aminas es conocida por mejorar las propiedades como recubrimiento de estos polímeros además de evitar el uso de cianuros (Helou y col., 2011).

Por último, el carbonato de glicerina destaca también para la obtención de glicidol, un intermedio de reacción muy versátil de gran valor. Se obtiene por la contracción del carbonato cíclico a una unidad epoxi cíclica, lo cual puede suceder en

los poros de zeolita A (Pagliaro y col., 2009). Se emplea para la obtención de ésteres, éteres, poligliceroles o, en aplicación directa, en cosméticos, pinturas, productos farmacétuicos o estabilizador.

3.3. Rutas sintéticas para la obtención de carbonato de glicerina

De entre todos los productos derivados de la glicerina comprendidos en la revisión de la anterior sección, el carbonato de glicerina es el que ofrece mayor número de vías para su obtención, que se resumen a continuación.

3.3.1. Fosgenación

Esta primera ruta es, históricamente, la tradicionalmente empleada para la síntesis de este compuesto y otros carbonatos cíclicos a partir de glicoles, cuya patente data de finales del siglo XIX; sin embargo, este proceso ha desaparecido debido al impacto ambiental negativo de los compuestos que emplea, como es el caso del fosgeno. En esta reacción, esquematizada en la Figura 3.3, se operaba a temperaturas de hasta 160 ºC (Nemirowsky, 1885).

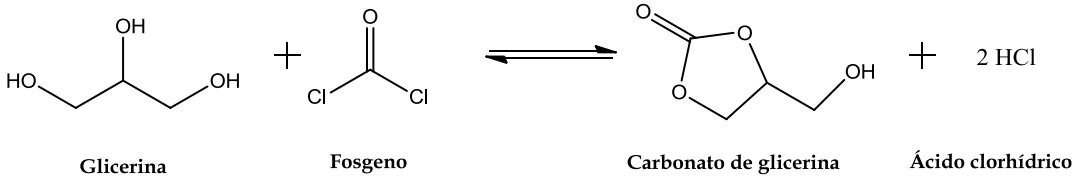

Figura 3.3. Reacción de fosgenación para la obtención de carbonato de glicerina

3.3.2. Adición de CO o CO_2

La adición de formas oxidadas de carbono se lleva a cabo para incluir el grupo carbonato y llevar a cabo la ciclación de la glicerina, como se expone en la Figura 3.4.

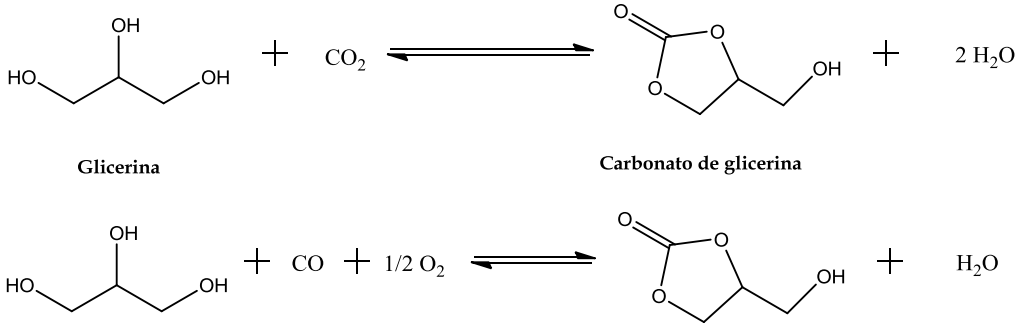

Figura 3.4. Síntesis de carbonato de glicerina por adición de CO o CO_2

En este sentido, se ha experimentado la adición de monóxido de carbono con empleo también de oxígeno en presencia de varios catalizadores. Se ha empleado cloruro de calcio como catalizador en cantidades de 10% molar en presencia y ausencia de disolventes a temperaturas entre 110 y 130 ºC y presiones entre 6 y 8 bar con rendimientos aceptables, si bien los tiempos de reacción oscilaban entre las 20 y 63 horas (Teles y col., 1994). La utilización conjunta de ioduro de potasio y cloruro de paladio con distintos ligandos reducen considerablemente los tiempos de reacción para conseguir altos rendimientos, aunque no eliminan la necesidad de un disolvente (dimetilfurano) y las presiones y temperaturas aplicadas son incluso mayores (Hu y col., 2010). Como principal desventaja de esta ruta está la utilización de CO, que por su toxicidad y dificultad de manejo ofrece pocas posibilidades para un futuro cambio de escala de estos procesos.

Por otro lado, la adición directa de CO_2 evitaría el manejo de un gas tóxico. Hay referencias de procesos de este tipo catalizados con especies basadas en estaño tanto en ausencia como con metanol como disolvente; en este segundo caso, se apreció una disminución significativa de todas las variables de operación para aumentar el rendimiento del proceso en menor tiempo (Aresta y col., 2006; George y col., 2009). Sin embargo, este proceso parece estar termodinámicamente muy poco desplazado hacua los productos, por lo que parece complicado conseguir conversiones elevadas (Li y Wang, 2011a).

3.3.3. Glicerolisis de la urea

En términos generales, más recientemente se ha estudiado la reacción de glicerina con urea, que daría como subproducto además amoniaco, según la Figura 3.5.

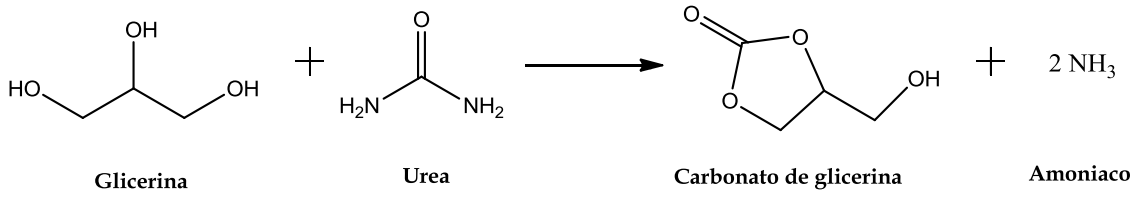

Figura 3.5. Glicerolisis de la urea para obtener carbonato de glicerina y amoniaco

Las condiciones de esta reacción también requieren un consumo energético considerable, sobre todo considerando que para desplazar el equilibrio hacia los productos se debe retirar el amoniaco del medio de reacción. Por otro lado, las temperaturas de operación encontradas en las referencias oscilaban entre 140 y 150 ºC. Como punto a favor, se ha experimentado en todos los casos en ausencia de disolvente. Los catalizadores empleados son de carácter básico por lo general, si bien se ha observado variedad entre ellos: los más habituales son óxidos de metales como zinc, calcio, magnesio, aluminio o incluso lantano (Li y col., 2006; Wang y col., 2011), hidrotalcitas calcinadas (Climent y col., 2010), montmorillonitas (Lee y col., 2014) o catalizadores basados en líquidos iónicos (Kim y col., 2014a; Kim y col., 2014b; Kim y col., 2011)

3.3.4. Transesterificación de glicerina

Esta ruta es la que ha acaparado más interés en la investigación de la síntesis del producto objeto de estudio en los últimos años, en parte porque además se trata de una manera indirecta de llevar a cabo la fijación de CO_2. Esta reacción de transesterificación, sin embargo, se conoce desde hace más de cincuenta años, cuando Huntsman Petrochemical patentó un método para la producción de carbonato de glicerina por esta vía empleando varios carbonatos y bicarbonatos de metales alcalinos (Bell y col., 1959).

La transesterificación con carbonatos orgánicos es una ruta que ofrece la posibilidad de operar a temperaturas moderadas en un medio de reacción exclusivamente líquido, lo cual supone la gran ventaja de poder obviar cualquier necesidad de aplicación de presión o de vacío por la adición de un gas reactivo (como eran los casos del CO y CO_2) o eliminación de un producto (como la eliminación de NH_3 en la glicerolisis de la urea). Por ello, la práctica totalidad de las referencias encontradas operan a presión atmosférica, con la única excepción de algún proceso en condiciones supercríticas.

Los carbonatos empleados son carbonatos de dialquilo o cíclicos, concretamente carbonato de dimetilo (DMC) y de dietilo (DEC) en el primero de los casos, y de etileno (EC) en el segundo. La Figura 3.6 muestra las tres reacciones que se pueden dar con glicerina y estos reactivos, produciéndose en todos los casos alcoholes como subproductos de interés.

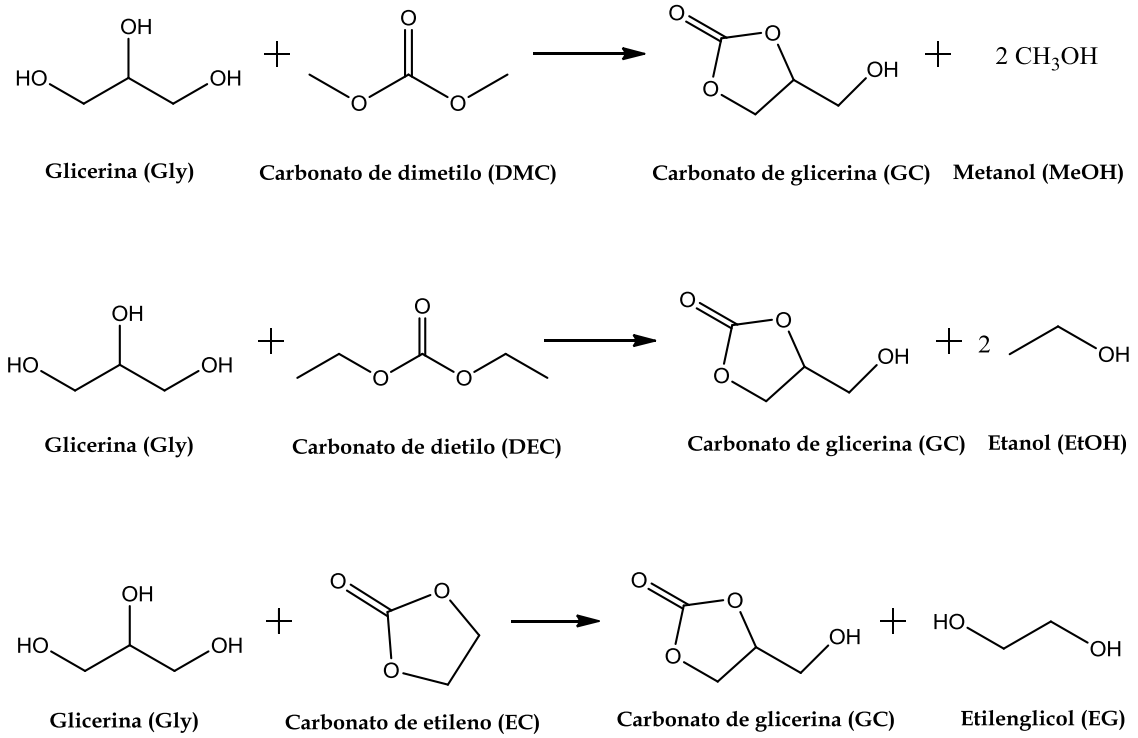

Figura 3.6. Síntesis de carbonato de glicerina por transesterificación de glicerina con carbonatos orgánicos: DMC, DEC y EC

La Tabla 3.2 resume las referencias en la bibliografía encontradas para el estudio de esta reacción, clasificadas en función del carbonato orgánico empleado para la transesterificación.

En primer lugar, se puede destacar el mayor número de referencias existentes en lo que al trabajo con DMC respecta y, en este sentido, cabe destacar la incursión en estudios con catalizadores homogéneos y heterogéneos. Entre los primeros, parecen destacar con muy altos rendimientos el carbonato de potasio y los hidróxidos de metales alcalinos. Entre los heterogéneos, se puede destacar la reiteración en el empleo de óxidos mixtos de diferentes metales como aluminio, calcio o magnesio, hidrotalcitas dopadas con dichos metales en diferentes proporciones y sometidas a distintos tratamientos de calcinación o ciertas resinas de intercambio iónico en algunos casos. También cabe mencionar el empleo de líquidos iónicos, compuestos con una gran variedad de aplicaciones, o ciertas enzimas como la lipasa B de *Candida antarctica* como catalizadores de esta reacción.

Tabla 3.2. Resumen de distintos procesos de obtención de carbonato de glicerina mediante transesterificación con carbonatos orgánicos (continúa)

Referencia	Catalizador[1]	T (ºC)	M[2]	t (h)	cantidad catalizador (% mol o % peso)	Otras condiciones[3] y comentarios	Y_{GC} (%)
Transesterificación con DMC							
(Rokicki y col., 2005)	K_2CO_3	75	3	3	4,5 % peso		97
(Kim y col., 2007)	CALB sobre Novozym 435	60	1	30	54% peso	Catálisis enzimática. Disolvente: tetrahidrofurano	88
(Ochoa-Gomez y col., 2009)	K_2CO_3, KOH, NaOH, H_2SO_4, PTSA, CaO, $CaCO_3$, Amberlyst 131wet, Amberlyst 39wet	75	5	1,5	15% peso	Varios catalizadores homogéneos y heterogéneos básicos y ácidos	100
(Naik y col., 2009)	$[Bmim]_2[CO_2]$	74	3,2	1,33	1% mol	LI[4] como catalizador	100
(Takagaki y col., 2010)	Hidrotalcita Mg-Al	100	5	2	54% peso	Disolvente: dimetilfurano	99
(Bai y col., 2011)	KF/hidroxiapatita	78	2	0,83	3% peso		99
(Malyaadri y col., 2011)	Óxido mixto Mg-Zr-Sr	75	5	1,5	3% peso		100
(Simanjuntak y col., 2011)	Gliceróxido de calcio	75	2	0,5	0,01 % peso		91,4
(Ochoa-Gomez y col., 2012b)	Trietilamina	88	4	2,5	10% mol		98,5
(Chiappe y Rajamani, 2012)	$[Mor\ 1,4][N(CN)_2]$	120	3	13	17% mol	LI como catalizador	95
(Jung y col., 2012)	CALB sobre Novozym 435	60	2	48	75% peso	Catálisis enzimática. Disolvente: acetonitrilo	96,3
(Pan y col., 2012)	Zeolita (NaY)	70	3	4	10% peso	Disolvente: metanol	80
(Gade y col., 2012)	[TMA][OH]	80	3	1,5	1% mol	LI como catalizador	47
(Bai y col., 2013)	$NaOH/\gamma\text{-}Al_2O_3$	78	2	1	3% peso		97
(Simanjuntak y col., 2013)	Óxido mixto Mg-La	85	2	1	5% peso		65
(Khayoon y Hameed, 2013)	Óxido mixto Mg-Ca	70	2	1,5	0,1% peso		100
(Yadav y Chandan, 2014)	Hidrotalcita Mg-Al calcinada	170	3	2,5	15% peso	Disolvente: metanol. P=1,8 MPa	84,7
(Hervert y col., 2014)	Carbenos heterocíclicos con N	25	3,5	0,33	2,6% mol		95,7

Tabla 3.2. Resumen de distintos procesos de obtención de carbonato de glicerina mediante transesterificación con carbonatos orgánicos (finaliza)

Referencia	Catalizador[1]	T (ºC)	M[2]	t (h)	cantidad catalizador (% mol o % peso)	Otras condiciones[3] y comentarios	Y_{GC} (%)
Transesterificación con DEC							
(Alvarez y col., 2010)	Hidrotalcita Mg-Al rehidratada	130	17	10	16% peso		65
(Alvarez y col., 2012)	Hidrotalcita Mg-Al/α-Al_2O_3	130	21	8	216% peso	Sitema continuo. Disolvente: dimetilsulfóxido	84
(Alvarez y col., 2013)	Hidrotalcita Mg-Al/nanofibra de carbono	130	17	2	16% peso		58
(Takagaki y col., 2010)	Hidrotalcita Mg-Al	140	5	3	54% peso	Disolvente: dimetilfurano	77
(Patel y col., 2009)	1,3-diclorodistanoxano	100	5	2	0,5% peso		99
Transesterificación con EC							
(Climent y col., 2010)	Hidrotalcita Al-Ca y Al-MgO, CaO, MgO	35	2	1	0,5% peso		87
(Cho y col., 2010)	Tri-n-butilamina inmovilizada en RNX-MCM41	80	2	1,5	9% peso	LI como catalizador	79
(Vieville y col., 1998)	Purosiv zeolite, Amberlyst A26 OH^-	74	0,63	1	125% peso	Condiciones supercríticas. PCO_2= 13 MPa	32,2

[1]En primer lugar el catalizador con mejores resultados. El resto de condiciones y rendimientos de la tabla se dan empleando dicho catalizador
[2]M=relación molar de carbonato orgánico a glicerina
[3]Reacción a presión atmosférica bajo reflujo a no ser que se indique lo contrario
[4]LI: líquido iónico

Comparando las condiciones recogidas en la tabla para las reacciones, en general se puede apreciar que el empleo de carbonato de etileno y carbonato de dimetilo ofrecen la posibilidad de operar en condiciones suaves. Con el primero de ellos, las temperaturas de operación pueden ser tan bajas como 35 ºC, correspondiente a su punto de fusión mientras que con carbonato de dimetilo se elevan hasta el entorno de los 70 ºC a 80 ºC en la mayor parte de los casos, si bien en ambos casos los excesos molares respecto a glicerina empleados son bastante moderados y se alcanzan rendimientos en el producto en muchos casos prácticamente del 100%. Sin embargo, el empleo de carbonato de dietilo supone elevar la temperatura hasta los 130 ó 140 ºC, a la vez que los excesos molares en glicerina empleados son mucho más elevados, así como las cantidades de catalizador utilizadas, además de que los rendimientos en el producto son mucho más discretos a excepción de una referencia (Patel y col., 2009).

Por último, en lo que a la forma de operación respecta, en ciertos casos se han empleado disolventes orgánicos para conseguir disolver la glicerina y los carbonatos orgánicos, ya que la solubilidad mutua de estos compuestos es muy limitada. Sin embargo, no se ha encontrado mención explícita acerca del propósito de la adición del disolvente en ninguna de las referencias consultadas.

Se ha propuesto un mecanismo en algunas publicaciones para la reacción de glicerina con DEC y DMC (Alvarez y col., 2012; Ochoa-Gomez y col., 2009). La Figura 3.7 presenta este mecanismo, en el que la clave es la presencia de un catalizador básico y transcurre de la siguiente forma:

1) La reacción se inicia a través de la extracción de un protón de un grupo hidroxilo por parte de catalizador básico, generándose un anión gliceróxido.
2) Dicho anión realiza un ataque nucleófilo sobre el grupo carbonato del carbonato orgánico dando lugar a un compuesto intermedio en forma aniónica. En el caso de un carbonato de dialquilo, el enlace marcado en discontinuo no existiría y se produciría en esta etapa la liberación de una molécula de alcohol. Con un carbonato orgánico cíclico, el enlace discontinuo sí existe y el intermedio contiene dicho enlace.
3) El catalizador se regenera dando lugar al compuesto intermedio como tal. Debido a las selectividades a carbonato de glicerina prácticamente del 100% encontradas en las referencias, se puede ver que este intermedio es una especie muy inestable.

4) Por último, se produce la ciclación intramolecular de dicho intermedio para dar lugar a carbonato de glicerina, así como a un alcohol o glicol como subproducto de la reacción. En el caso de un carbonato de dialquilo, es aquí cuando se forma la segunda molécula de alcohol.

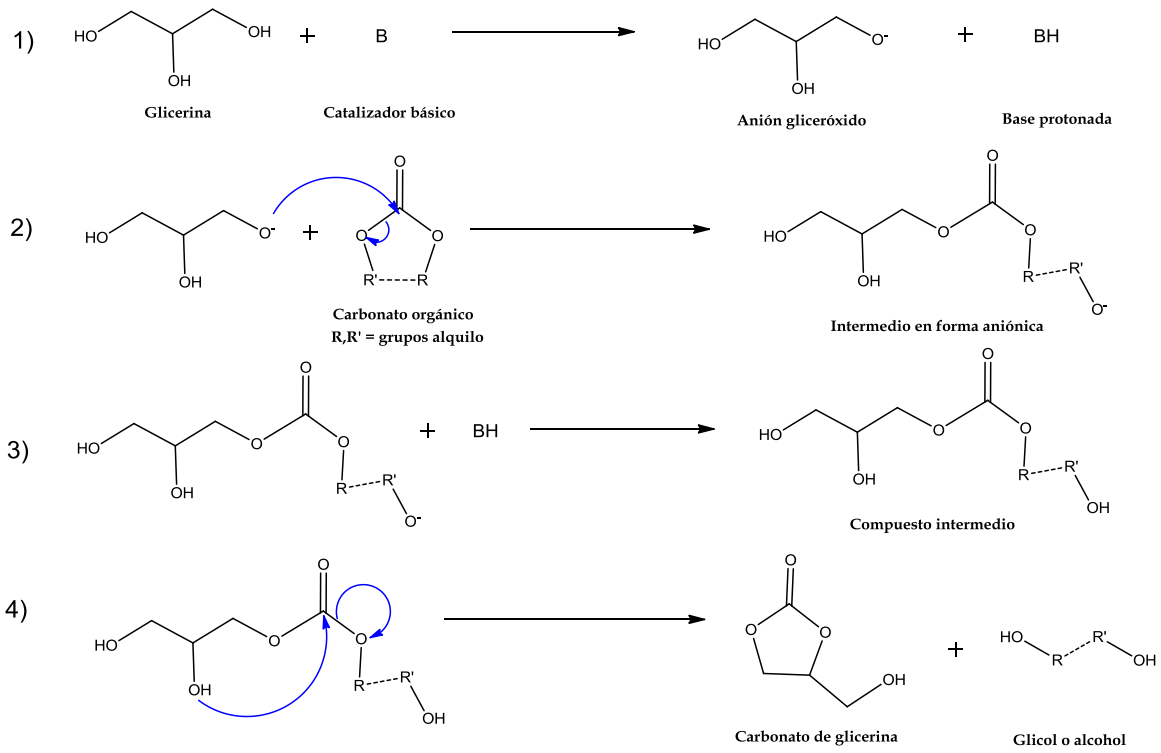

Figura 3.7. Mecanismo de reacción propuesto para la transesterificación de glicerina con carbonatos orgánicos.

A pesar del gran número de referencias encontradas para la síntesis de carbonato de glicerina a través de esta vía, únicamente se ha encontrado una referencia muy reciente que indaga en aspectos cinéticos de esta reacción realizada por catálisis heterogénea empleando hidrotalcitas como catalizador en una operación con disolvente (Yadav y Chandan, 2014).

3.3.5. Otras rutas

Finalmente, se han encontrado también algunas referencias en las cuales se presenta la síntesis de la molécula de carbonato de glicerina, si bien se parte de diferentes materias primas para ello. La naturaleza de estas reacciones es diversa, aunque en ocasiones se pueden asemejar a las síntesis anteriormente expuestas.

Así pues, puede mencionarse la adición de exceso de CO_2 sobre glicidol a 120 ºC y una presión de 40 bar catalizada en presencia de ioduro de potasio y el éter corona 18-crown-6, donde el rendimiento fue de 73% tras 4 horas (Rokicki y col., 1984). El principal inconveniente de esta ruta, además de las severas condiciones de reacción, es el hecho de que el glicidol es un compuesto bastante caro y, de hecho, como ya se apuntó en el apartado 3.2.2, suele emplearse un proceso inverso para obtener glicidol a partir de carbonato de glicerina.

Otro caso con una reacción similar a las vistas empleando glicerina es la transesterificación a partir de aceites vegetales con un carbonato de dialquilo para la obtención conjunta de biodiesel y carbonato de glicerina. Para esta reacción, se ha operado en condiciones supercríticas con excesos de DMC con respecto al aceite del orden de 40 a 1 en ausencia de catalizador (Tan y col., 2010); también se ha completado la reacción con excesos molares del orden de 10 a 1 a presión atmosférica y temperaturas más moderadas (60-90 ºC) con la lipasa Novozym 435 (Min y Lee, 2011) o sales básicas como carbonato de potasio (Dawodu y col., 2014) como catalizadores.

4. SOLKETAL

4. SOLKETAL

Los *ketales* son moléculas con un amplio abanico de aplicaciones que se obtienen a partir de glicoles como el glicerol. De entre todos ellos, el solketal es el producto más estudiado, y se obtiene por la acetalización (o *ketalización*) de la glicerina por reacción con acetona, la cetona más sencilla. Al igual que el carbonato de glicerina, los *ketales* también han visto un notable auge en su investigación durante los últimos años y, aunque aún no hay ninguna revisión exclusivamente dedicada a estos compuestos, se mencionan en una revisión dedicada a disolventes procedentes de transformaciones de glicerina (Garcia y col., 2014). La Figura 4.1 muestra los resultados, filtrados por años, de la búsqueda "glycerol ketalization OR glycerol acetalization OR glycerol acetalisation" en Web of Science.

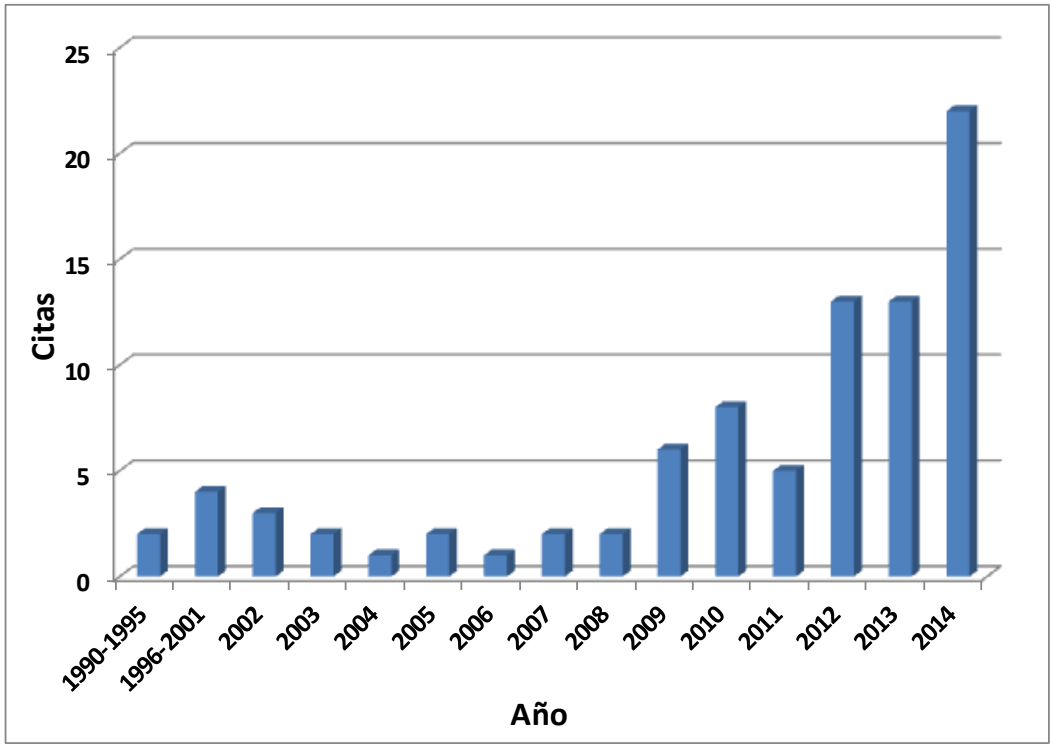

Figura 4.1. Serie histórica de las publicaciones relacionadas con la síntesis de ketales a partir de glicerina.

El tercer y último bloque de esta Tesis se centra en la fenomenología y el estudio fisicoquímico de la síntesis de solketal y, de manera similar a como se hizo con el carbonato de glicerina, en las siguientes páginas se presenta una revisión de las características, aplicaciones y rutas de síntesis de este producto.

4.1. Propiedades.

La Figura 4.2 representa la molécula (2,2-dimetil-1,3-dioxolan-4-il)metanol, también conocida como isopropilidenglicerol o solketal (CAS: 100-79-8), que es una forma protegida del glicerol con un grupo acetal isopropilideno.

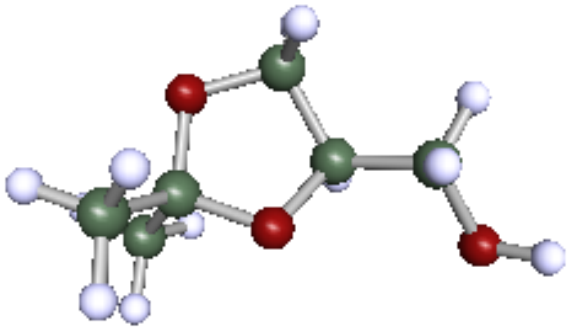

Figura 4.2. Estructura molecular del solketal

El solketal, a presión atmosférica y temperatura ambiente, es un líquido incoloro, soluble en agua e inodoro debido a su relativamente baja presión de vapor. Su estructura molecular y su grupo funcional hidroxilo le confieren la posibilidad de poder establecer puentes de hidrógeno intermoleculares similares a los que podrían establecer los alcoholes alifáticos. Su punto de ebullición, sin embargo, es mucho más alto que el de alcoholes de cadena corta. Además, a pesar de su estructura molecular relativamente similar a la del carbonato de glicerina, su viscosidad es notablemente menor, aunque su toxicidad parece ser un tanto mayor. Estas características físicas y estructurales le proporcionan buenas propiedades como disolvente. La Tabla 4.1 recopila valores numéricos de las propiedades de este compuesto.

Tabla 4.1. Propiedades físicas del solketal

Propiedad	Valor
Peso molecular ($g \cdot mol^{-1}$)	132,16
Densidad, 20 ºC ($g \cdot mL^{-1}$)	1,066
Punto de ebullición, 760 mm (ºC)	188
Punto de fusión (ºC)	-27
Presión de vapor, 25ºC (mm Hg)	107
Punto de inflamabilidad (ºC)	80
Viscosidad, 20 ºC (cP)	11
LD50 ($g \cdot kg^{-1}$ rata)	7

4.2. Aplicaciones del solketal

Gracias a sus características y a su potencial origen biológico, se han venido realizando un creciente número de estudios del solketal relacionados con sus posibles aplicaciones durante los últimos años.

La mayor parte de los estudios encontrados en la literatura de la utilización directa del solketal, así como de otros *ketales*, versan sobre su empleo como aditivos de carburantes y biocarburantes. Esta utilización sin duda tiene que ver con el hecho de tratarse de una molécula oxigenada, ya que con anterioridad determinados éteres como MTBE o ETBE se han empleado como potenciadores de determinadas propiedades de las gasolinas.

Así pues, se ha llevado a cabo la modificación por reacción de cetonas con polioles como el xilitol o la xilosa (Maksimov y col., 2011), con glicerol formal (Hillion y col., 2013) o carbonato de glicerina (Delfort y col., 2004) para proporcionar los correspondientes ketales, así como la reacción de acetona con glicerol para dar solketal (Garcia y col., 2008; Maksimov y col., 2011; Mota y col., 2010). El empleo del solketal ha repercutido en la mejora de determinados parámetros y especificaciones de los carburantes, tales como una reducción en las formación de gomas y mejora del índice de octano empleando volúmenes de hasta el 5% de solketal en gasolinas (Mota y col., 2010). Como aditivo de biodiesel, ha reducido la viscosidad y aumentado la estabilidad a la oxidación cuando se usó como aditivo al tiempo que se logra cumplir con el resto de especificaciones en Europa y Estados Unidos (normas EN 14214 y ASTM D6751) (Garcia y col., 2008). Por otro lado, los productos de ulteriores reacciones de solketal con alcohol bencílico para obtener éteres o la síntesis de metilésteres con carbonatos de dialquilo han sido también estudiados como aditivos (Selva y col., 2012; Suriyaprapadilok y Kitiyanan, 2011).

Aparte de su prometedor uso como aditivo de carburantes, el solketal se ha empleado como disolvente verde en varias aplicaciones. Se ha encontrado en formulaciones de productos tan diversos como pinturas y tintas, refrigerantes, productos de limpieza (Budavari, 1989), pesticidas (Cantero y col., 2010), como agente de suspensión en preparados farmacéuticos o como surfactante (Piasecki y col., 1997). Como medio de reacción, su uso está limitado al empleo de condiciones neutras o básicas debido a la escasa estabilidad del solketal en condiciones ácidas. En un medio

ácido y presencia de agua, tendría lugar la reacción inversa para dar glicerina y acetona. Aun así existen ejemplos, como su uso para modificar la regioselectividad de la lactasa o β-galactosidasa en la producción de ciertos tipos de disacáridos (Perez-Sanchez y col., 2012), para aislar ácidos nucleicos (Bergmann y col., 2009) o como disolvente en cromatografía de columna para la separación de diversos compuestos (Zhou, 2007)

Además de los usos directos mencionados, se puede también utilizar como bloque sintético para la producción de otros productos de interés debido a la reactividad que le confiere su grupo hidroxilo. Así, se ha empleado en la obtención de productos de interés farmacéutico como prostaglandinas, glicerofosfolípidos o β-bloqueantes como el (S)-propranolol, ampliamente utilizado en tratamientos contra la hipertensión y las migrañas (Hof y Kellogg, 1996; Jurczak y col., 1986).

4.3. Reacción de acetalización para la obtención de solketal

La acetalización o ketalización consiste en la reacción de un alcohol con una cetona o aldehído, es decir, compuestos carbonílicos. Si bien esta reacción se ha llevado a cabo con una gran diversidad de compuestos (Showler y Darley, 1967), los esfuerzos en la producción de solketal tienen una creciente importancia por ser una vía de aprovechamiento de la glicerina con acetona. El otro reactivo, la acetona, normalmente procede del proceso de oxidación del cumeno, que se descompone para dar fenol y acetona, lo cual constituye un proceso de origen petroquímico. Sin embargo, la acetona también puede tener un origen biológico, como en el caso del proceso ABE (Acetona, Butanol y Etanol), que emplea residuos de maíz como materia prima (Chiao y Sun, 2007; Ni y Sun, 2009; Zverlov y col., 2006). De esta manera, la producción de solketal podría tener un origen biológico total.

La reacción de acetalización requiere la presencia de un catalizador ácido y transcurre, cuando se parte de glicerol, mediante el mecanismo presentado en la Figura 4.3 (Calvino-Casilda y col., 2014):

1) La reacción se inicia mediante el ataque nucléofilo de un grupo hidroxilo de la glicerina al grupo carbonilo de la acetona.
2) A continuación, el protón procedente del catalizador se agrega al nuevo grupo hidróxilo surgido a raíz del ataque de la etapa anterior.

3) Luego se libera una molécula de agua, dando lugar a una especie intermedia inestable.

4) Por último, se produce la ciclación intramolecular de dicho intermedio, lo cual puede suceder por otro ataque nucleófilo de un grupo hidroxilo, bien desde un hidroxilo en posición 2 (caso a) dando lugar al producto cíclico de 5 átomos (2,2-dimetil-1,3-dioxolan-4-il)metanol, o bien en posición 1 (caso b), obteniéndose el producto cíclico de 6 átomos 2,2-dimetil-1,3-dioxan-5-ol.

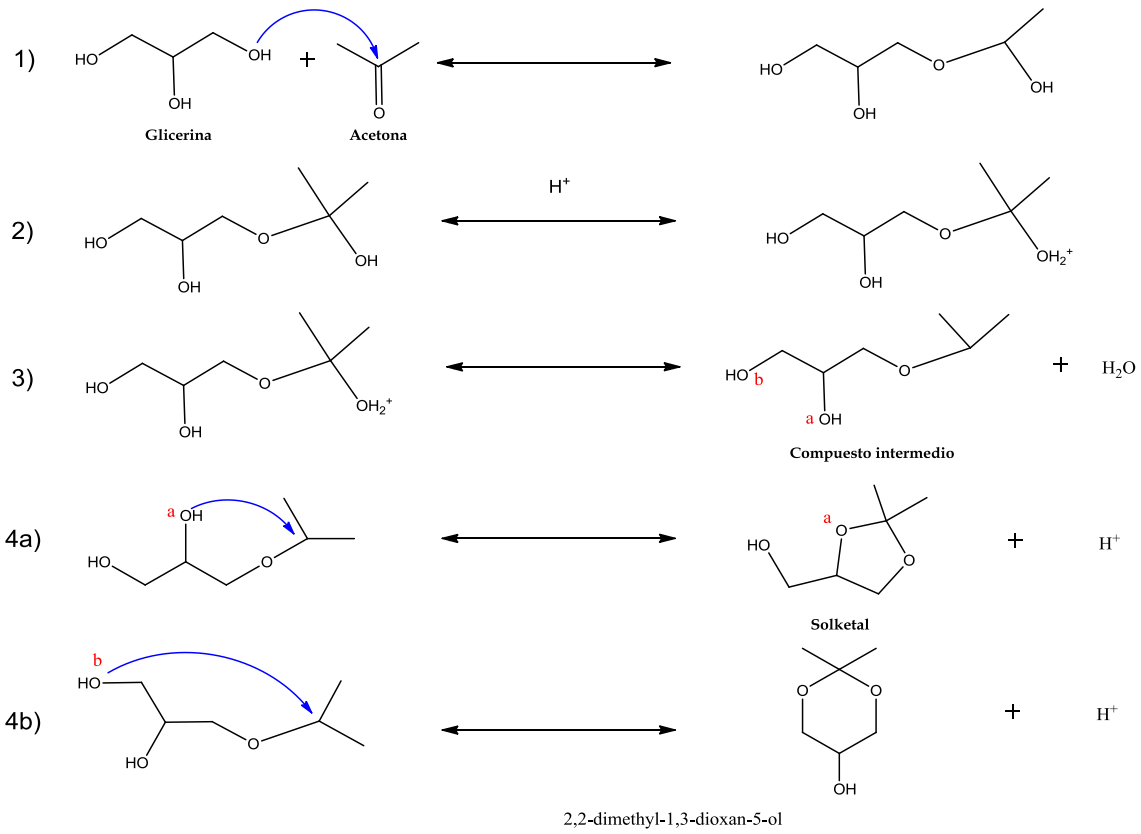

Figura 4.3. Mecanismo de reacción propuesto para la acetalización de glicerol con acetona. Adaptado (Calvino-Casilda y col., 2014)

En relación a la cuarta etapa del mecanismo, como conclusión de la multitud de referencias encontradas con una gran variedad de catalizadores que dan una selectividad prácticamente completa hacia el producto cíclico de 5 átomos, puede decirse que el grupo hidroxilo que inicia el mecanismo está localizado preferentemente en la posición 1 del glicerol y el que cierra el ciclo en la posición 2.

En lo que respecta a estudios cinéticos de esta reacción, aun habiendo varias referencias sobre la producción de solketal, únicamente se ha encontrado un trabajo que

plantea un estudio cinético de la reacción catalizada por una resina de intercambio iónico (Nanda y col., 2014c).

Entre los catalizadores utilizados para esta reacción, puede hablarse de los homogéneos en primer lugar, tales como el ácido p-toluensulfónico, sulfúrico o clorhídrico (Bruchmann y col., 1999a; Garcia y col., 2008; Suriyaprapadilok y Kitiyanan, 2011), aunque los problemas de separación posteriores han hecho que el empleo de catálisis heterogénea haya sido más amplio. Siguiendo esta tendencia, se han realizado estudios con diferentes catalizadores sólidos. Entre ellos hay zeolitas (Clarkson y col., 2001; Deutsch y col., 2007), arcillas (Deutsch y col., 2007), heteropoliácidos inmovilizados (Ferreira y col., 2010a) o silicatos basados en sales de estaño (Li y col., 2012) entre otros, aunque sin duda lo más recurrente ha sido hacer uso de diversos materiales funcionalizados con grupos sulfónicos (Li y col., 2012; Nandan y col., 2013; Vicente y col., 2010), siendo entre ellos los más abundantes las resinas de intercambio iónico basadas en matrices poliméricas de poliestireno-divinil benceno (Clarkson y col., 2001; Chopade, 1999; Deutsch y col., 2007; Kim y col., 2014c; Nanda y col., 2014b; Nanda y col., 2014c).

Por otra parte, se han propuesto diferentes condiciones de reacción y de operación para desplazar la posición de equilibrio que se da en este tipo de reacciones. En este sentido, aunque lo más común es emplear grandes excesos molares de acetona, llegando a ser tan elevados como 20 a 1 respecto a la glicerina (Roldan y col., 2009), también se ha planteado la operación en un proceso consistente en varias etapas en serie, con eliminación intermedia del agua del medio evaporación bajo condiciones de vacío (Vicente y col., 2010), la utilización de membranas para la separación del agua (Roldan y col., 2009) o el empleo de catalizadores con hidrofobicidad modulable para así eliminar el agua de los centros activos, lo cual se ha conseguido con zeolita Beta, más hidrófoba que otras zeolitas como ZSM5 o USY (da Silva y col., 2009).

En cuanto al resto de condiciones, a excepción de un proceso en condiciones supercríticas en ausencia de catalizador (Royon y col., 2011), lo normal es operar a temperatura ambiente o algo superiores (Nanda y col., 2014a, b; Nanda y col., 2014c; Reddy y col., 2011) y en ocasiones con un codisolvente para favorecer la mezcla de acetona y glicerol (Nanda y col., 2014a, b; Nanda y col., 2014c).

La Tabla 4.3 resume la información bibliográfica encontrada concerniente a condiciones y tipo de operación, así como los catalizadores empleados en estos trabajos.

Tabla 4.2. Resumen de distintos procesos de obtención de solketal (continúa)

Referencia	Catalizador[1]	T[2] (ºC)	M[3]	t (h)	cantidad catalizador (% mol o % peso)	Otras condiciones[4] y comentarios	Y_{SK} (%)
(Bruchmann y col., 1999b)	HCl, PTSA, H_2SO_4	20-54	4	9	0,05% mol	Destilación reactiva para desplazamiento del equilibrio	97,6
(Clarkson y col., 2001)	Amberlyst DPT-1	70	3	5	5% peso	Destilación reactiva en columna a contracorriente	98
(Deutsch y col., 2007)	Amberlyst 36	40	1.5	8	1,21% peso	Reflujo con eliminación de agua. Disolvente: diclorometano	88
(Garcia y col., 2008)	PTSA	-	3	16	0,5% mol	Destilación reactiva	90
(Roldan y col., 2009)	Montmorillonita K10	-	20	2	10% peso	Eliminación de agua con membrana de zeolitas	82
(da Silva y col., 2009)	Amberlyst-15, zeolita Beta y ZSM-5, montmorillonita K10, PTSA	70	1.2	1	15% mol		95
(Ferreira y col., 2010b)	Heteropoliácidos sobre sílice: PW_S, SiW_S, PMo_S, SiMo_S	70	6	3	0,72% peso		90
(Vicente y col., 2010)	Sílice mesoestructurada arenosulfónica Ar-SBA-15, Amberlyst 15	70	6	3x0.5	1% peso	3 etapas consecutivas de 30 minutos a reflujo y destilación a vacío	84
(Suriyaprapadilok y Kitiyanan, 2011)	PTSA	-	6	12	1% peso	Reflujo total	81

Tabla 4.2. Resumen de distintos procesos de obtención de solketal (finaliza)

Referencia	Catalizador[1]	T[2] (ºC)	M[3]	t (h)	cantidad catalizador (% mol o % peso)	Otras condiciones[4] y comentarios	Y_{SK} (%)
(Reddy y col., 2011)	Óxidos de zirconio dopados. SO_4^{2-}/ZrO_2, MoO_x/ZrO_2, WO_x/ZrO_2, ZrO_2	25	6	1,5	1% peso		98
(Royon y col., 2011)	Sin catalizador	260	10,8	4	N/A	Condiciones supercríticas. P=8 MPa	22,6
(Li y col., 2012)	Silicatos mesoporos: Hf-TUD1, Zr-TUD1, Al-TUD1	80	2	4	0.07 % peso	Reflujo	65
(Fan y col., 2012)	ZrO_2-SiO_2	70	4	3	2,2% peso	Destilación reactiva	81
(Nandan y col., 2013)	Sílices carbonadas sulfónicas. HSCS, SCS	70	60:10:1[5]	0,5	5% peso	Reflujo. Disolvente: acetonitrilo	78
(Menezes y col., 2013)	$SnCl_2$	60	6	0,5	1% mol	Reflujo	66
(Nanda y col., 2014a)	Amberlyst 36	25	4	N/A	N/A	Operación en lecho fijo. Disolvente: metanol P=3.4 MPa, WHSV=2 h^{-1}	94
(Nanda y col., 2014b)	Amberlyst Wet , Amberlyst Dry, zeolita, sulfato de zirconio, montmorillonita, Polymax	40	6	N/A	N/A	Operación en lecho fijo. Disolvente: metanol P=4,14 MPa, WHSV=4 h^{-1}	88
(Nanda y col., 2014c)	Amberlyst 35	50	2:1:1[5]	4	2% peso	Disolvente: metanol	65
(Shirani y col., 2014)	Purolite PD206	60	3	N/A	1.5 g catalizador	Operación en lecho fijo. P=0.6 MPa. Q_v=0.1 mL·min^{-1}	69

[1]En primer lugar el catalizador con mejores resultados. El resto de condiciones y rendimientos de la tabla se dan empleando dicho catalizador
[2]Valores en blanco de la temperatura implica que no han sido facilitadas en las referencias
[3]M=relación molar de acetona a glicerina
[4]Reacción a presión atmosférica bajo reflujo a no ser que se indique lo contrario
[5]Relación molar de acetona:disolvente:glicerol

5. PARTE EXPERIMENTAL

5. PARTE EXPERIMENTAL

Esta Sección incluye una breve descripción de los materiales y las metodologías experimentales y analíticas seguidas en el desarrollo del trabajo, así como de los procedimientos numéricos con los que se han tratado los datos obtenidos.

5.1. Materiales

Sistema 1

Los compuestos empleados para los experimentos de equilibrio entre fases líquidas y reacciones químicas fueron: glicerol extrapuro (99,88%) de Fischer Chemical; metanol de grado HPLC (99,99%) de Scharlau Chemie; carbonato de glicerina (pureza>99,5%) de Sigma-Aldrich y carbonato de dimetilo (99%), proporcionado por UBE Corporation Europa. Así mismo, se utilizó ácido cítrico (pureza≥99,5%) de Sigma-Aldrich como patrón interno en medidas de HPLC.

Además, para los experimentos cinéticos se emplearon los siguientes compuestos como catalizadores: carbonatos de litio y sodio (pureza>99%) de Aldrich; carbonato de potasio y bicarbonatos de litio, sodio y potasio (pureza>99%) de Alfa Aesar y metóxido de potasio (25% diluido en metanol) de Sigma-Aldrich.

Sistema 2

Para los experimentos de equilibrio y cinéticos los compuestos utilizados fueron: glicerol extrapuro (99,88%) de Fischer Chemical, etilenglicol (99,8% anhidro) de Sigma-Aldrich, carbonato de glicerina (pureza>99,5%) de Sigma-Aldrich y carbonato de etileno (pureza>99%) y ácido cítrico (pureza≥99,5%) de Sigma-Aldrich como patrón interno en HPLC.

Para los experimentos cinéticos se emplearon como catalizadores carbonato de potasio (pureza>99%) de Alfa Aesar y metóxido de potasio (25% disuelto en metanol) de Sigma-Aldrich.

Sistema 3

Los experimentos de equilibrio se realizaron con glicerol extrapuro (99,88%) de Fischer Chemical, solketal (98.1 %) de Aldrich y acetona seca (99,75%) de Acros

Organics. Como patrón interno para cromatografía de gases se empleó dibutiléter (99,1%) y para dilución de muestras isopropanol (99,9%), ambos de Acros.

Los experimentos cinéticos se llevaron a cabo utilizando glicerol extrapuro (99,88%) de Fischer Chemical y acetona de grado HPLC (99,99%) de Romil. La preparación de muestras para ^{1}H-NMR empleó óxido de deuterio (99,8%) de Scharlau Chemie y metanol de grado HPLC (99,99%) como patrón interno. Los catalizadores utilizados fueron: Purolite CT275DR y Purolite CT276, de Purolite; Amberlyst 35dry y Amberlyst 36dry de Rom and Haas y Lewatit GF101 de Lanxess.

Esta Sección incluye una breve descripción de los materiales y las metodologías experimentales y analíticas seguidas en el desarrollo del trabajo, así como de los procedimientos numéricos con los que se han tratado los datos obtenidos.

5.2. Procedimientos experimentales

5.2.1. Obtención de datos de equilibrio líquido-líquido

Para los tres sistemas, el procedimiento fue análogo. Se cargaron matraces de fondo rondo con diferentes composiciones (pesadas en balanza analítica Kern and Sohn ABS-220-4 de 0,0001 g de precisión) cuyo equilibrio se deseaba analizar y se sellaron con septa. Dichos matraces se insertaron en un baño de glicerina en una placa calefactora con temperatura y agitación magnética controlada (IKA Yellow Line TC3).

El procedimiento consiste en someter la mezcla en cada experimento a individual a agitación durante al menos 4 horas para asegurar una transferencia de materia completa llegando, por tanto, al equilibrio. A continuación, se detiene la agitación y se permite la separación de las fases líquidas por decantación, dada la diferencia de densidades entre las fases ricas en glicerina y DMC (sistema 1), EC (sistema 2) o acetona (sistema 3), durante no menos de 3 horas. Posteriormente, se retiran muestras de cada una de las fases ligera y pesada a través de los septa con jeringas con agujas hipodérmicas, lo suficientemente finas para no perturbar la interfase.

En el caso del sistema 2, donde las densidades entre las fases son más similares, se llevó a cabo una centrifugación adicional de las muestras de cada una de las fases para asegurar una total separación. Para ello, se empleó una centrífuga con control de temperatura Sigma4–16 K.

5.2.2. Equipo y procedimiento en experimentos cinéticos

Para llevar a cabo los experimentos con reacción química de cada uno de los tres sistemas, se confeccionaron sistemas experimentales a medida en función de las necesidades del procedimiento. En todos los casos, se trata de dispositivos diseñados para operar por cargas en reactores tipo tanque agitados con tabiques deflectores (volumen aproximado 250 mL); el agitador es de tipo turbina con 6 palas, cuya velocidad se regula con un motor IKA RW20 (250-2000 rpm). El aporte de calor se hace por medio de una resistencia térmica exterior cuya temperatura es contralada por un dispositivo OMRON E5CN PID.

Para el estudio del comportamiento bifásico, se modificó el reactor habilitando una abertura en el fondo para la introducción de una sonda FBRM. Además, se incluyó un sistema de reflujo para evitar la eliminación de DMC y de metanol en su caso. Este diseño, representado en la Figura 5.1, se empleó en el estudio de las reacciones catalíticas en los sistemas 1 y 2 (Publicaciones 2, 5 y 6).

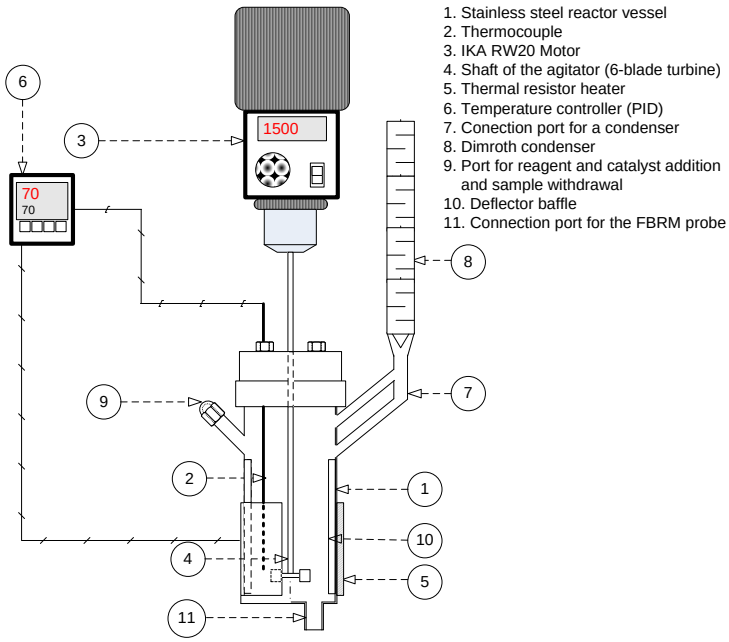

Figura 5.1. Esquema del dispositivo experimental empleado para las reacciones catalíticas de los sistemas 1 y2.

Para la reacción entre EC y glicerina en el caso de la reacción en ausencia de catalizador, entre 100 y 140 ºC, del sistema 2, el aparato incluye un segundo reactor con los mismos accesorios antes descritos para calentar por separado los reactivos. Una vez

alcanzada la temperatura de trabajo en ambos, se agrega desde el segundo recipiente el EC a través de una canalización, tal como se muestra en la Figura 5.2 (Publicación 4)

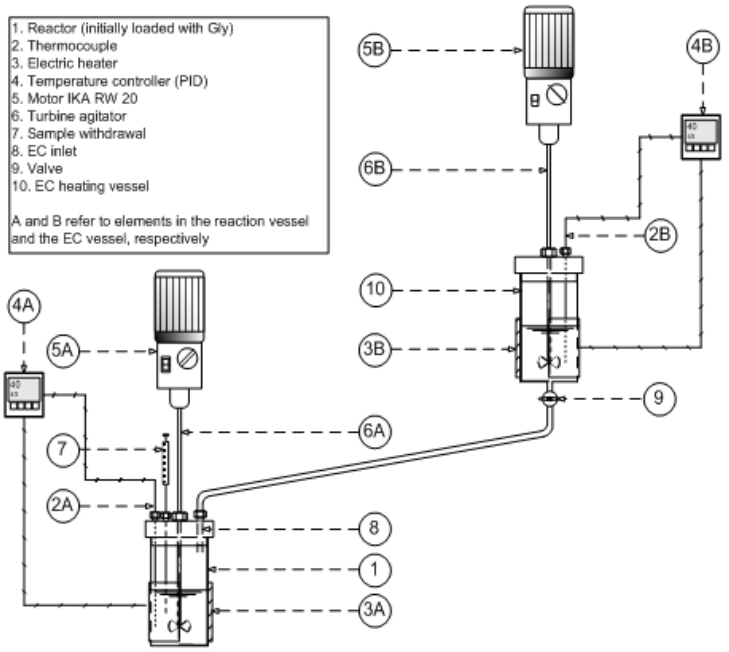

Figura 5.2. Esquema del dispositivo experimental empleado para la reacción en ausencia de catalizador del sistema 2.

El sistema empleado para la reacción en el sistema 3 es el más sencillo y se adapta a lo descrito en el primer párrafo, tal como se muestra en la Figura 5.3 (Publicaciones 8 y 9).

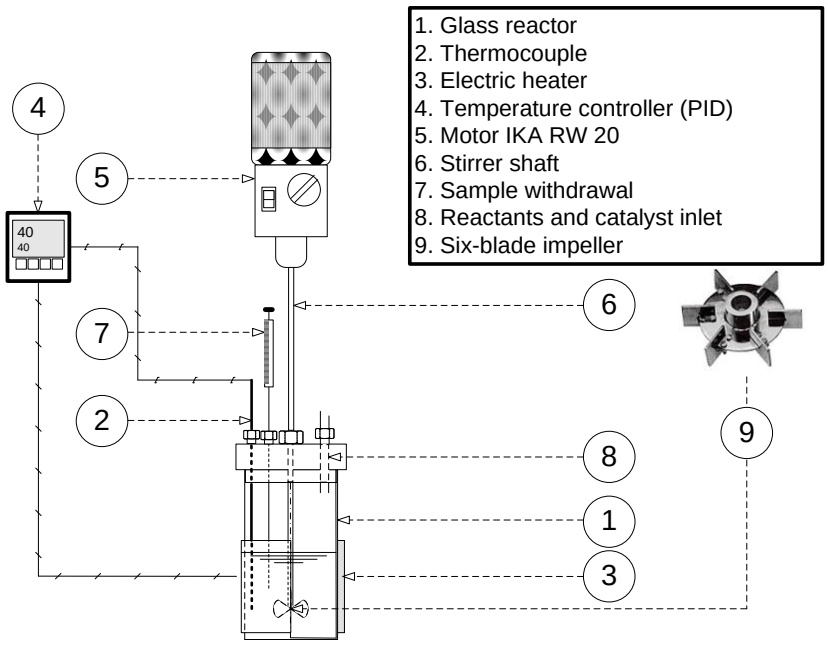

Figura 5.3. Esquema del aparato experimental empleado en el sistema 3.

El procedimiento en los experimentos con adición de un catalizador, dicha adición supone el tiempo cero, una vez alcanzada la temperatura deseada. Posteriormente, en todos los casos, se toman muestras durante el transcurso de la reacción para llevar a cabo el análisis.

5.2.3. Empleo de FBRM para el seguimiento de emulsiones

En los sistemas 1 y 2 se empleó una técnica óptica láser para el seguimiento de la evolución de las dispersiones que se producen. Esta técnica se denomina medida por reflexión de haz enfocado (FBRM en inglés), y permite obtener la distribución de tamaños de cuerda en tiempo real en línea. Se ha empleado con éxito en suspensiones de sólidos en líquidos en sistemas de floculación (Blanco y col., 2002a; Blanco y col., 2002b) o para la determinación de tamaños de partícula en dispersiones líquidas consistentes en aceites minerales y agua (Boxall y col., 2009; Wang y col., 2014; Wang y col., 2013), un caso muy similar al que aquí se trata.

El equipo consta de un sensor, con un generador de un haz de luz láser (λ=791 nm) y un detector conectados a un sistema informático. La lente giratoria que hay en el sensor enfoca el haz en un punto focal, que rota en el seno de la suspensión describiendo una trayectoria circular a alta velocidad (1,9 m/s). Cuando el haz impacta en la superficie de cualquier partícula que pasa por el punto focal, es reflejado y llega al detector, registrándose un pulso de luz de duración determinada, que es traducido en una corriente eléctrica que es amplificada. El producto de la duración del pulso de luz por la velocidad lineal del punto focal es la longitud de cuerda de la partícula detectada. El equipo mide la longitud de las cuerdas de las partículas que atraviesan el punto focal durante un periodo, denominado duración de la medida, obteniendo así una población de longitudes de cuerda de partícula cuya distribución constituye el resultado de la medida (Blanco y col., 2002b).

En el presente trabajo, se empleó un equipo FBRM Lasentec M500LF de Mettler Toledo, Seattle, USA, que se esquematiza en la Figura 5.4.

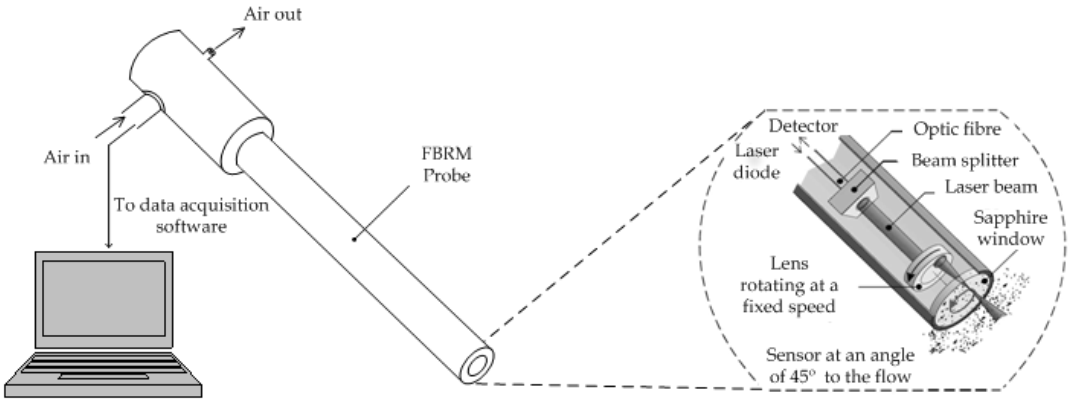

Figura 5.4. Esquema del dispositivo FBRM. Adaptado (Blanco y col., 2002b)

5.3. Métodos de análisis

5.3.1. Sistemas con carbonato de glicerina (Sistemas 1 y 2)

Para la cuantificación de las especies químicas de ambos sistemas, tanto en experimentos de equilibrio como cinéticos, se empleó el mismo método de análisis basado en cromatografía en fase líquida de alta resolución (HPLC). Las muestras se diluyeron 25 veces en una disolución de 8 $g \cdot L^{-1}$ de ácido cítrico en agua MilliQ y se analizan en un equipo JASCO de la serie 2000, con un detector de índice de refracción. La fase estacionaria empleada fue una columna Rezex ROA-Organic acid H^+ (8%) (150 x 7,80 mm) en las siguientes condiciones: caudal constante de 0,5 $mL \cdot min^{-1}$ de agua Milli-Q acidificada (0,005 N H_2SO_4) como fase eluyente y con temperatura de separación de 60 ºC.

5.3.2. Sistema con solketal (Sistema 3)

La cuantificación de los compuestos en el estudio del equilibrio líquido-líquido para este sistema se realiza mediante cromatografía de gases en los laboratorios del grupo Química Técnica A de la Facultad de Ingeniería Química y Bioquímica de la Universidad Técnica de Dortmund.

Las muestras se diluyeron en isopropanol 5 veces empleando 5 $g \cdot L^{-1}$ de dibutiléter como patrón interno. El equipo utilizado fue un Agilent de la serie HP6890 equipado con un detector de conductividad térmica (GC-TCD). La separación de los compuestos se realizó con una columna HP-INNOWax (30 m x 0,25 mm x 0,25 μm) operando con un caudal constante de helio de 1,3 $mL \cdot min^{-1}$. La temperatura del inyector

y el detector fueron 250 ºC y la relación de separación 80:1. La rampa programada fue la siguiente: primeros 6 minutos a 40 ºC, rampa de 40 a 250 ºC a 25 ºC min^{-1}, y 8 minutos a temperatura constante de 250 ºC.

Para los experimentos cinéticos, la cuantificación de solketal se llevó a cabo mediante espectroscopía de resonancia magnética de protón (^{1}H-NMR) en un equipo Bruker DPX 300 MHz BACS60. Las muestras se prepararon en óxido de deuterio usando metanol como patrón interno. Se identificaron señales inequívocas del solketal a desplazamientos de 1,27 y 1,33 ppm.

5.4. Métodos matemáticos

5.4.1. Correlación de los datos de equilibrio con el modelo NRTL

El modelo *non-random two-liquid* (NRTL) correlaciona los coeficientes de actividad de los componentes de mezclas no ideales con la fracción molar en que están presentes. Se ha comprobado que este modelo se ajusta correctamente a los datos obtenidos en múltiples sistemas en equilibrio líquido-líquido (LLE) que incluyen alcoholes (incluidos polioles), carbonatos orgánicos y cetonas (Chafer y col., 2014; Chen y col., 2014; de Azevedo Rocha y col., 2014; Fang y Qian, 2005; Liu y col., 2014; Shin y col., 2013; Wang y Lu, 2012).

En sistemas multicomponentes, la ecuación general para la determinación del coeficiente de actividad de un compuesto i es la siguiente:

$$\ln \gamma_i = \frac{\sum_{j=1}^{n} x_j \tau_{ji} G_{ji}}{\sum_{k=1}^{n} x_k G_{ki}} + \sum_{j=1}^{n} \frac{x_j G_{ij}}{\sum_{k=1}^{n} x_k G_{kj}} \cdot \left(\tau_{ij} - \frac{\sum_{m=1}^{n} x_m \tau_{mj} G_{mj}}{\sum_{k=1}^{n} x_k G_{kj}} \right) \qquad (5.1)$$

donde x_i corresponde a la fracción molar de cada componente y donde G_{ij} denota los parámetros NRTL, calculado como:

$$G_{ij} = \exp(-\alpha_{ij} \cdot \tau_{ij}) \qquad (5.2)$$

en el que α_{ij} es el *non-randomness binary interaction parameter* y τ_{ij} se calcula de acuerdo a:

$$\tau_{ij} = \frac{\Delta g_{ij}}{RT} \qquad (5.3)$$

En la ecuación 5.3, R es la constante de los gases ideales, T es la temperatura y Δg_{ij} son los parámetros de interacción binaria.

Se llevó a cabo, por lo tanto, la correlación del modelo NRTL a los datos de equilibrio líquido-líquido obtenidos en los tres sistemas con el fin de obtener los correspondientes parámetros de interacción binaria, Δg_{ij}, y los *non-randomness binary interaction parameter*, α_{ij}.

Para ello, se empleó el módulo de regresión de datos integrado en Aspen Plus, basado en la obtención de mínimos cuadrados mediante el algoritmo de Britt-Luecke iniciado con el método de Deming de una función objetivo que incluye las composiciones y la temperatura de equilibrio (Britt y Luecke, 1973):

$$OF = \sum_{k=1}^{N}\sum_{j=1}^{2}\sum_{i=1}^{3or4}\left[\frac{\left(T_k^{\exp} - T_k^{est}\right)^2}{\sigma_T^2} + \frac{\left(x_{ijk}^{\exp} - x_{ijk}^{est}\right)^2}{\sigma_x^2}\right] \qquad (5.4)$$

donde los subíndices i, j y k se refieren al componente (hasta i=3 en sistemas ternarios o i=4 en cuaternarios), fase y *tie-line*, respectivamente; N es el número de *tie-lines*; T^{exp} y T^{est} son los valores de temperatura experimentales y estimados; x^{exp} y x^{est}, las fracciones molares experimentales y calculadas por el modelo; y, finalmente, σ_T y σ_x son las desviaciones típicas de la temperatura y fracción molar.

El criterio para valorar la bondad de la regresión de los parámetros de interacción binaria fue el valor de la raíz cuadrada media de la desviación (rmsd en inglés), definida en la ecuación 5.5 para un sistema ternario y en la ecuación 5.6 para uno cuaternario:

$$rmsd = \sqrt{\sum_{k=1}^{N}\sum_{j=1}^{2}\sum_{i=1}^{3}\frac{\left(x_{ijk}^{\exp} - x_{ijk}^{calc}\right)^2}{6N}} \qquad (5.5)$$

$$rmsd = \sqrt{\sum_{k=1}^{N}\sum_{j=1}^{2}\sum_{i=1}^{4}\frac{\left(x_{ijk}^{\exp} - x_{ijk}^{calc}\right)^2}{12N}} \qquad (5.6)$$

5.4.2. Modelización cinética

Los modelos cinéticos propuestos se ajustaron a los datos experimentales obtenidos para cada uno de los casos con el software Aspen Custom Modeler. La regresión se basa en la aplicación del algoritmo de Levenberg-Marquardt en conjunción

con la integración numérica de los modelos a través de un método de Runge-Kutta de cuarto orden. Como metodología general, el ajuste de los modelos se realizó llevando a cabo la correlación individual de cada experimento y, posteriormente, la temperatura se incluyó en el modelo para llevar a cabo el ajuste multivariable.

Además, se han evaluado una serie de criterios estadísticos: el valor de la F de Fischer (F), el error residual medio al cuadrado (RMSE), el porcentaje de variación explicada (VE) y el criterio de información de Akaike. Estos parámetros se definen en las siguientes ecuaciones.

La F de Fischer se basa en una hipótesis nula que dice que el modelo es adecuado a los valores observados de la variable medida. Se define en la ecuación 5.7:

$$F = \frac{\sum_{i=1}^{N} \frac{\left(y_{i,calc}\right)^2}{P}}{\sum_{i=1}^{N} \frac{SQR}{N-P}} \tag{5.7}$$

en la que N es el número de total de datos experimentales; P es el número de parámetros del modelo, SQR la suma de residuos al cuadrado $\left(y_{i,\exp} - y_{i,calc}\right)^2$ donde $y_{i,exp}$ e $y_{i,calc}$ son los valores experimental y calculado de la variable.

RMSE es una medida de la diferencia entre los valores predichos de la variable y los observados. Tiene en cuenta la cantidad de datos y el número de parámetros del modelo, tal como se aprecia en la ecuación 5.8:

$$RMSE = \sqrt{\frac{SQR}{N-P}} \tag{5.8}$$

El porcentaje de variación explicada, VE, viene dado por:

$$VE(\%) = 100 \cdot \left(1 - \frac{\sum_{l=1}^{L} SSQ_l}{\sum_{l=1}^{L} SSQmean_l}\right) \tag{5.9}$$

ecuación en la que SSQ_l y $SSQmean_l$ quedan definidos en las ecuaciones 5.10 y 5.11:

$$SSQ_l = \sum_{i=1}^{N} \frac{(y_{i,\exp} - y_{i,calc})^2}{y_{i,calc}^{\prime\prime}} \tag{5.10}$$

$$SSQmean_j = \sum_{i=1}^{N} \frac{(y_{i,\exp} - \bar{y}_{i,\exp})^2}{y_{i,calc}^{\gamma_j}} \tag{5.11}$$

siendo

$$\bar{y}_{i,\exp} = \frac{\sum_{i=1}^{N} \frac{y_{i,\exp}}{y_{i,calc}^{\gamma_j/2}}}{\sum_{i=1}^{N} \frac{1}{y_{i,calc}^{\gamma_j/2}}} \tag{5.12}$$

En las tres ecuaciones anteriores, γ_j es el llamado parámetro de heteroscedasticidad, circunstancia que se da bajo la suposición de que la varianza de las perturbaciones no es constante a lo largo de las observaciones. Por defecto, Aspen Custom Modeler asigna el valore de este parámetro en 1.

Por último, el criterio de información de Akaike relaciona la cantidad de observaciones experimentales con el número de parámetros del modelo, dando información de la bondad del ajuste penalizando un posible exceso de ajuste debido al aumento del número de parámetros del modelo (Akaike, 1974). Queda definido en la ecuación 5.13:

$$AIC = N \cdot \ln\left(\frac{SQR}{N}\right) + 2 \cdot P \tag{5.13}$$

La bondad y calidad del ajuste de los modelos propuestos aumenta al aumentar el valor de F y VE y al disminuir los valores de RMSE y AIC.

6. RESULTADOS Y DISCUSIÓN

6. RESULTADOS Y DISCUSIÓN

Este capítulo resume los resultados más relevantes, así como las conclusiones obtenidas a lo largo de la realización de esta Tesis, estructurado en tres bloques correspondientes a los tres sistemas estudiados:

Sistema 1: Producción de carbonato de glicerina por transesterificación de glicerol con carbonato de dimetilo: con resultados en las publicaciones 1, 2 y 6.

Sistema 2: Producción de carbonato de glicerina por transesterificación de glicerol con carbonato de etileno: con resultados incluidos en las publicaciones 3, 4, 5 y 6.

Sistema 3: Producción de solketal por acetalización de glicerol con acetona: con resultados en las publicaciones 7, 8 y 9.

Los resultados obtenidos se han publicado o se encuentran en proceso de revisión, y se incluyen en el Anexo de este trabajo. En ellos se incluye información detallada sobre los procedimientos experimentales, analíticos y de cálculo empleados, nomenclatura y la totalidad de los resultados. Las publicaciones son las siguientes:

Publicación 1: Jesús Esteban, Miguel Ladero, Laura Molinero and Félix García-Ochoa. Liquid–liquid equilibria for the ternary systems DMC–methanol–glycerol, DMC–glicerol carbonate–glycerol and the quaternary system DMC–methanol–glycerol carbonate–glycerol at catalytic reacting temperatures. *Chemical Engineering Research and Design* (2014), **92**: 1797-1805.

Publicación 2: Jesús Esteban, Elena Fuente, Ángeles Blanco, Miguel Ladero and Félix García-Ochoa. Phenomenological kinetic model of the synthesis of glycerol carbonate assisted by focused beam reflectance measurements. *Chemical Engineering Journal* (2015), **260**: 434-443.

Publicación 3: Jesús Esteban, Miguel Ladero and Félix García-Ochoa. Liquid–liquid equilibria for the systems ethylene carbonate + ethylene glycol + glycerol; ethylene carbonate + glycerol carbonate + glycerol and ethylene carbonate + ethylene glycol + glycerol carbonate + glycerol at catalytic reacting temperatures. Manuscript in Press *Chemical. Engineering Research and Design* (2014). DOI: 10.1016/j.cherd.2014.08.024.

Publicación 4: Jesús Esteban, Elena Fuente, María González-Miquel, Ángeles Blanco, Miguel Ladero and Félix García-Ochoa. Sustainable joint solventless coproduction of glycerol carbonate and ethylene glycol via thermal transesterification of glycerol. *RSC Advances* (2014), **4**: 53206-53215.

Publicación 5: Jesús Esteban, Miguel Ladero, Elena Fuente, Ángeles Blanco and Félix García-Ochoa. Kinetic modeling of the catalytic coproduction of glycerol carbonate and ethylene glycol from glycerol. Manuscrito enviado a *Journal of Chemical Technology and Biotechnology* en Diciembre de 2014.

Publicación 6: Jesús Esteban, Miguel Ladero and Félix García-Ochoa. Potassium methoxide: a very active catalyst for the production of glycerol carbonate in mild solventless conditions. Manuscrito enviado a *Bioresource Technology* en Enero de 2015.

Publicación 7: Jesús Esteban, Andreas J. Vorholt, Arno Behr, Miguel Ladero and Félix García-Ochoa. Liquid−Liquid Equilibria for the System Acetone + Solketal + Glycerol at (303.2, 313.2, and 323.2) K. *Journal of Chemical and Engineering Data* (2014), **59**: 2850-2855.

Publicación 8: Jesús Esteban, Miguel Ladero and Félix García-Ochoa. Synthesis of solketal with commercially available sulphonic acid based ion exchange resins. Manuscrito enviado a *RSC Advances* en Diciembre de 2014.

Publicación 9: Jesús Esteban, Miguel Ladero and Félix García-Ochoa. Kinetic modeling of the solventless synthesis of solketal with a sulphonic ion exchange resin. Manuscrito reenviado a *Chemical Engineering Journal* tras revisión en Enero de 2015.

6.1. Producción de carbonato de glicerina por transesterificación de glicerina con carbonato de dimetilo

El primero de los sistemas estudiados plantea la reacción de transesterificación de glicerina (Gly) con carbonato de dimetilo (DMC) para obtener carbonato de glicerina (GC) y metanol (MeOH) como subproducto en la reacción según la Figura 6.1:

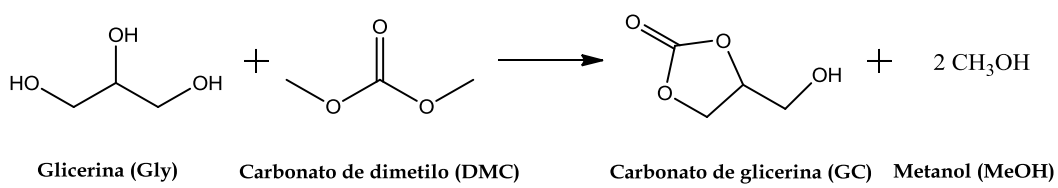

Figura 6.1. Transesterificación de glicerina con carbonato de dimetilo.

Publicación 1

A raíz de la simple observación visual del sistema se aprecia una miscibilidad muy limitada entre DMC y glicerina. Por lo tanto, se procedió a estudiar el equilibrio líquido-líquido existente entre estos compuestos añadiendo concentraciones crecientes de GC, metanol y una combinación de ambos. Los sistemas estudiados fueron, por consiguiente, dos ternarios T1 {DMC + MeOH + Gly} y T2 {DMC + GC + Gly} y uno cuaternario Q {DMC + MeOH + GC + Gly}. Las condiciones elegidas para el estudio fueron temperaturas de 60, 65 y 70 ºC a presión atmosférica, que han demostrado ser de interés en condiciones de reacción (Jung y col., 2012; Khayoon y Hameed, 2013; Kim y col., 2007)

Las cantidades añadidas se calculan en base a la estequiometría para simular composiciones que se darían en el sistema en el caso de que hubiera reacción. Se ha apreciado que la presencia de estos compuestos contribuye a la cosolubilización de DMC y glicerina. Se concluyó que el orden de dicha capacidad solubilizadora fue el siguiente: GC > GC+MeOH >MeOH. Además, tras evaluar los sistemas T1, T2 y Q a las diferentes temperaturas, se apreció que esta variable no tiene un marcado efecto sobre el equilibrio entre las fases en el intervalo estudiado. Los datos de equilibrio obtenidos se recopilan en las Tablas 1, 2 y 3 y, además, en la Figura 2 se realiza la comprobación de los datos del equilibrio del sistema T1 a 60 ºC, experimento del que previamente había información en la literatura (Wang y Lu, 2012).

Se ajustó el modelo NRTL a los datos obtenidos a cada valor de temperatura, de modo que se obtuvieron los parámetros de interacción binaria, recogidos en las Tablas 4, 5 y 6 de la Publicación. Los ajustes se realizaron empleando valores fijos de los parámetros α_{ij} (*non-randomness binary interaction parameter*) en valores indicados recomendados en la bibliografía clásica (Renon y Prausnitz, 1968) y para el sistema T1 en particular (Wang y Lu, 2012) de α_{ij}=0,2 y α_{ij}=0,3. También se realizaron los ajustes liberando los parámetros α_{ij}. A tenor de los valores de la raíz cuadrada media de la desviación (*rmsd*), no se puede optar claramente por un conjunto de valores de los parámetros α_{ij}. En cualquier caso, el modelo NRTL se ajustó con éxito a los datos experimentales, siendo el máximo valor de *rmsd* de 0,0113.

Considerando la necesidad de un medio básico para iniciar el mecanismo de reacción (Alvarez y col., 2012; Ochoa-Gomez y col., 2009), se realizó el estudio cinético empleando dos catalizadores básicos: K_2CO_3 y CH_3OK.

Publicación 2

El estudio cinético de la reacción se realizó en primer lugar empleando como catalizadores una serie de carbonatos y bicarbonatos de metales alcalinos: Li_2CO_3, Na_2CO_3, K_2CO_3, $LiHCO_3$, $NaHCO_3$ y $KHCO_3$. Entre ellos, se eligió K_2CO_3 por ser la especie más activa, al ofrecer una frecuencia de reposición de $6{,}40 \cdot 10^{-2}\ s^{-1}$ (Tabla 1).

En cuanto a la elección de las condiciones de operación, en primer lugar se seleccionó el intervalo entre 66 y 70 ºC, al observar la clara diferencia en la actividad entre 64 y 66 ºC (Figura 2).

La Figura 3 muestra la evolución de los distintos tamaños de las cuerdas de las gotas de la fase dispersa con el tiempo para un experimento concreto seguido con FBRM. Se puede observar que se da un primer aumento del número de cuerdas como consecuencia de que hay una interferencia por parte de las partículas de K_2CO_3, que luego se disuelven; poco después se da un descenso continuado del número de cuentas hasta prácticamente cero, aunque hay un pequeño aumento en el número de cuentas que puede atribuirse a la generación de burbujas de metanol, que además causan un aumento del tamaño medio de las cuerdas. Se evaluó el efecto de la agitación, observándose que el número de cuerdas no varía a partir de las 1500 rpm (Figura 4a) y, además, la evolución de las especies químicas es prácticamente idéntica a esa agitación y valores superiores (Figura 4b). Por lo tanto, a esta agitación puede considerarse que no hay control por parte de la transferencia de materia.

Considerando el estudio realizado en la Publicación 1, se consideró interesante analizar la evolución física del sistema, es decir, de la dispersión y compararla con la evolución química del sistema. La Figura 5a muestra que a una conversión aproximada de 0,3 el número de cuentas es prácticamente nulo, y que este valor no depende del exceso molar de DMC empleado. Puede apreciarse que la composición correspondiente a dicha conversión para las tres relaciones molares es muy cercana a la curva binodal, representada en los diagramas de equilibrio del sistema Q de la Publicación 1, que separa la región bifásica de la monofásica. Al evaluar el efecto de la temperatura (Figura 6) se apreció que, efectivamente, afectaba a la velocidad de la evolución tanto

física como química del sistema, pero sin afectar apenas al valor de conversión al que desaparece la dispersión.

Se realizaron experimentos variando la temperatura (66-70 ºC), la relación molar de reactantes (1,5-3) y la cantidad de catalizador (0,75-1,25 % peso) y se propusieron varios modelos cinéticos para ajustarse a los datos. El estudio termodinámico existente para esta reacción (Li y Wang, 2011a) predice una conversión prácticamente completa de la reacción para la temperatura de 70 ºC, por lo que se proponen modelos sin consideración de la reacción inversa.

Por otro lado, se analizó mediante un test de potasio la presencia de dicho elemento en cada una de las dos fases de las que se compone el sistema de reacción durante los primeros instantes. Se comprobó que este elemento sólo se encuentra en la fase rica en glicerina, de lo que se infiere que la reacción transcurre en dicha fase mientras existen dos fases líquidas.

La Tabla 2 recopila los tres modelos probados, basados en modelos potenciales:

- El primero de ellos de primer orden con respecto a la concentración de la glicerina y orden cero respecto a la de DMC;
- El segundo, de primer orden parcial respecto a la concentración de glicerina y DMC (orden global dos);
- El último se divide en dos etapas, con dos ecuaciones aplicables antes y después de la conversión crítica de 0,3. La primera etapa considera un primer orden parcial respecto a la concentración de glicerina, fase en la cual va introduciéndose DMC, que se mantendría en una concentración constante. En esta primera etapa, el catalizador se encontraría disuelto únicamente en la fase rica en glicerina. La segunda etapa tendría lugar una vez se da la transición de dos a una sola fase, de modo que el catalizador estaría disuelto en todo el volumen de la reacción y, por tanto, con una concentración menor, que afecta a la velocidad de reacción. Esta segunda etapa sería de primer orden parcial respecto a las concentraciones tanto de glicerina como de DMC.

De acuerdo a los criterios estadísticos evaluados expuestos en la Tabla 3, el tercer modelo es el que mejor representa los datos experimentales obtenidos. Si bien la diferencia entre estos parámetros para el segundo y tercer modelo no es muy grande, el tercer modelo contempla aspectos fenomenológicos comprobados experimentalmente.

Publicación 6 (parte 1)

En la literatura existen referencias de la utilización de metóxido de sodio y de potasio en varias reacciones como transesterificaciones y (Kai y col., 2014) y esterificaciones (Zeng y col., 2014). Incluso la reacción que aquí nos ocupa se llevado a cabo de manera heterogénea con metóxido de calcio (Li y Wang, 2011b). En todas estas referencias, se atribuye a los metóxidos una alta actividad catalítica.

En primer lugar, se lleva a cabo el análisis de la evolución de las especies químicas detectadas mediante el análisis HPLC. En dicho análisis se dan dos picos, que se identifican por la evolución de su señal, con un compuesto intermedio y un producto de reacción (Figura 3). La presencia de estos compuestos corroboraría que se sigue el mecanismo propuesto en la literatura (Ochoa-Gomez y col., 2009). Por otro lado, la presencia de estos picos es muy pequeña a lo largo de toda la reacción; tal es así, que el cumplimiento de los balances de materia considerando únicamente DMC, glicerina, carbonato de glicerina y metanol tiene un error, en el peor de los casos, tan sólo del 5,1 %, incluyendo el error experimental por manipulación de muestras y análisis. Por este motivo, se considera que se puede afrontar el estudio de la cinética del proceso mediante la consideración de una reacción simple con error muy poco significativo.

Se realizaron un total de 20 reacciones variando la temperatura (50-70 ºC), exceso molar de DMC a glicerina (1,5-3) y cantidad de catalizador (1000-2500 ppm). Cabe resaltar que empleando este catalizador, se pudo operar a velocidades de reacción considerables por debajo de los 66 ºC, a diferencia de cuando se empleó K_2CO_3. Como es usual, la temperatura y la concentración de catalizador empleados afectaron positivamente a la velocidad de reacción (Figura 5).

Analizando la evolución de los datos cinéticos obtenidos, se aprecia que la tendencia de los datos parece sufrir un cambio a conversiones cercanas a 0,35 en cada una de las reacciones. Esto parece estar de acuerdo con lo observado en la Publicación 2, por lo que se podría atribuir este cambio al cambio de régimen de bifásico a monofásico, como se estudió en la Publicación 1. Por este motivo, se escogió 0,35 como valor de la conversión crítica en los modelos cinéticos.

Los modelos cinéticos propuestos se basan, al igual que en la Publicación 2, en el planteamiento de dos ecuaciones con intervalos de aplicación diferentes: antes y después del valor de conversión crítica.

Por otra parte, empleándose un metóxido como catalizador, puede darse su desactivación. Existe una referencia bibliográfica en la que, en esta misma reacción, se sugiere la desactivación de metóxido de calcio por reacción con CO_2 y H_2O que se genera en el medio por sucesivas reacciones con glicerina y carbonato de glicerina en una red un tanto compleja. La forma de catalizador obtenida sería un carbonato cálcico básico, de fórmula general $Ca_x(OH)_y(CO_3)_z$, con menor actividad que el metóxido original (Li y Wang, 2011b). Este mismo proceso podría sufrirlo el metóxido de potasio.

Así pues, se plantearon cuatro modelos:

- En el primero, se plantea la reacción irreversible, sin considerar desactivación.
- El segundo contempla la reacción reversible, también sin desactivación.
- El tercer modelo tiene en cuenta una reacción irreversible e incluye una desactivación de primer orden del catalizador.
- Por último, el cuarto modelo considera la reversibilidad de la reacción, así como la desactivación mencionada

Los resultados obtenidos en los cuatro casos son muy similares en términos estadísticos, por lo que debe realizarse discriminación en términos fisicoquímicos. Tanto en el primer como en el segundo modelo, los valores obtenidos de la concentración de DMC en la fase rica en glicerina en la primera etapa (C_{DMCsol}) son demasiado altos, por lo que estos modelos quedan excluidos. En el tercero y el cuarto, dichos obtenidos son idénticos entre sí y muy similares a los obtenidos en la Publicación 2. El modelo cuarto, que considera reversibilidad de la reacción, arrojó un valor de la energía de activación inusualmente alto, además de un valor de la F de Fischer algo inferior que el tercero.

Así pues, se selecciona el tercer modelo, que queda validado mediante la Figura 7, en la que se aprecia que por lo general se obtienen diferencias menores a ±15% en la predicción de los valores de conversión respecto a los observados.

Por último, se compara la actividad de CH_3OK con K_2CO_3 para esta reacción, comprobándose que, operando con el mismo exceso de DMC, la frecuencia de reposición del catalizador es 19,89 y 17,31 veces mayor a 66 ºC y 70 ºC, respectivamente.

6.2. Producción de carbonato de glicerina por transesterificación de glicerina con carbonato de etileno

El segundo sistema trata la reacción de transesterificación de glicerina (Gly) con carbonato de etileno (DMC) para la producción simultánea de carbonato de glicerina (GC) y etilenglicol (EG), como muestra la Figura 6.2:

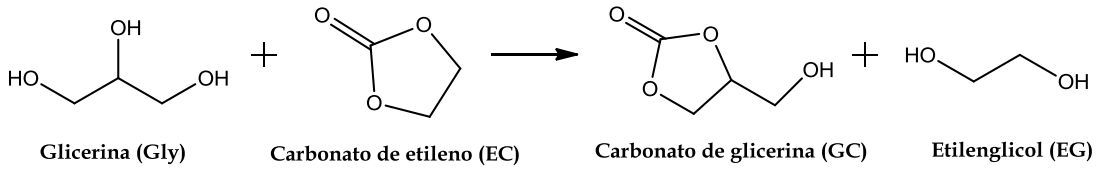

Figura 6.2. Transesterificación de glicerina con carbonato de etileno.

Publicación 3

De una manera similar al Sistema 1, EC y glicerina muestran una solubilidad escasa que se ve favorecida ante la presencia de concentraciones crecientes de GC y EG. Por tanto, los sistemas estudiados fueron los terrnarios T1 {EC + EG + Gly} y T2 {EC + GC + Gly} y el cuaternario Q {EC + EG + GC + Gly}. Las condiciones elegidas del estudio fueron de 40, 45 y 50 ºC de temperatura a presión atmosférica, temperaturas justo por encima del punto de fusión del EC y de interés en condiciones de reacción (Climent y col., 2010).

Realizando una experimentación similar a la explicada en la Publicación 1, se concluyó que el orden de la capacidad de disolución del GC y EG fue en el orden siguiente: GC > EG > EG+GC. Es decir, que la utilización conjunta de EG y GC desfavorece la obtención de un medio monofásico respecto al empleo de ambos por separado. La Figura 5 muestra los coeficientes de reparto de cada uno de estos tres sistemas, en los que se puede ver que el EG tiene una mayor tendencia a permanecer en la fase rica en glicerina, mientras que GC y la mezcla de ambos permanece preferentemente en la fase rica en EC. Además, dentro del intervalo de temperaturas evaluado, esta variable no tuvo un efecto muy alto sobre la solubilización de las fases. La totalidad de los datos experimentales se muestra en las Tablas 1, 2 y 3.

Se comprobó la fiabilidad de los datos con la ecuación de Othmer-Tobias (Othmer y Tobias, 1942). La Tabla 4 muestra la alta correlación existente en los tres casos, indicativo del alto grado del cumplimiento del balance de materia.

Vista la baja influencia de la temperatura, el ajuste del modelo NRTL a los datos se realizó con los datos obtenidos a todas las temperaturas. La Tabla 5 muestra los parámetros de interacción binaria estimados fijando el valor de de los parámetros α_{ij} en 0,2 y 0,3 y sin fijarlos. En este caso, se aprecia que permitiendo flotar los α_{ij}, la correlación mejora en caso de los sistemas T1, donde los valores obtenidos difieren notablemente de los propuestos por Renon y Prausnitz (Renon y Prausnitz, 1968), pero no en el caso de T2 y Q, donde los valores clásicos de estos autores proporcionan el mejor ajuste. El mayor *rmsd* obtenido fue, en cualquier caso, únicamente de 0,0515, un valor muy bajo.

Publicación 4

El mecanismo de la reacción de transesterificación de glicerina con carbonatos orgánicos requiere la presencia de una base para su inicio. Sin embargo, en el trabajo incluido en esta publicación se demuestra que también puede suceder en ausencia de ningún catalizador cuando se aplican unas condiciones de temperatura para las que el sistema es monofásico en todo momento.

En primer lugar se observó mediante FBRM (Figura 1), el descenso del número de cuerdas de la dispersión a medida que la temperatura aumenta, no registrándose ninguna a partir de los 80 ºC.

El estudio termodinámico existente para esta reacción sólo llega hasta los 80 ºC (Li y Wang, 2011a), por lo que en este trabajo se amplía estudiando el intervalo entre 100 y 140 ºC. De este estudio se concluye que la alta constante de equilibrio termodinámico obtenida a partir de las relaciones termodinámicas (Anexo 1) predice una conversión prácticamente completa de la reacción. Esto se demuestra experimentalmente por el cálculo la constante de equilibrio a partir de la composición de la mezcla tras dejar reaccionar el sistema durante 48 horas. En la determinación de esta constante experimental, el cálculo de los coeficientes de actividad (Anexo 2) mediante el software COSMO-RS para la determinación de propiedades termodinámicas de fluidos, basado en métodos químico-cuánticos.

La realización de experimentos cinéticos, incluidos en la Figura 3 y la obtención de datos lleva al planteamiento de cuatro modelos cinéticos potenciales:

- El primero, de primer orden con respecto a la concentración de la EC y orden cero respecto a la glicerina;
- El segundo, de primer orden parcial respecto a la concentración de glicerina y orden cero respecto a la de EC;
- El tercero considera una cinética de segundo orden global con orden uno respecto a las concentraciones de glicerina y EC;
- El último considera un segundo orden global como el tercero, incorporando además la posibilidad de una reacción inversa.

Observando la Tabla 3, a pesar de que el porcentaje de variación explicada del cuarto modelo mejora ligeramente su idoneidad respecto al tercero, el resto de parámetros no dicen lo mismo y, en cualquier caso, el estudio termodinámico realizado proporciona un criterio consistente para despreciar el último modelo en favor del tercero.

En último lugar, se compara la reacción de transesterificación de EC con glicerina en esta publicación con otras referencias en la literatura. Esta comparación se realiza en términos de ciertos parámetros de Química Verde definidos por Constable (Constable y col., 2002). En todos los procesos, incluido el de este trabajo, la economía atómica y de carbono son del 100% si se considera que el subproducto de la reacción, etilenglicol, tiene un alto interés por sus aplicaciones. Además, el *factor E*, indicativo de la cantidad de residuos generados, es nulo. Por último, en la Tabla 4, se compara la productividad másica y la eficiencia másica de reacción, obteniéndose mejores valores en el caso del presente proceso.

Publicación 5

La transesterificación de glicerina con carbonato de etileno se suele realizar empleando catalizadores de carácter básico. Por esta razón, se empleó K_2CO_3, un compuesto barato que ha demostrado ser efectivo en el Sistema 1. Se comprobó que las condiciones a las que se puede operar en este proceso son más moderadas que en el caso del Sistema 1, ya que la reacción transcurre a temperaturas cercanas al punto de fusión del EC (36 ºC) a una velocidad significativa, y las cantidades de K_2CO_3 empleadas se reducen dos órdenes de magnitud respecto al sistema 1.

En la literatura se propone que el mecanismo de la reacción transcurre a través de una especie intermedia y que, además, podría darse un producto derivado de la reacción entre GC y el exceso EC. Por ello, se verificó en primer lugar esta afirmación mediante el seguimiento de la evolución de los compuestos. Además, se observó que la consideración de los dos reactivos (EC y glicerina) y los dos productos mayoritarios (GC y EG), descartando la especie intermedia y el producto antes mencionado, cumplía los balances de materia en todos los análisis con un error inferior al 4%, en el que se incluye el error experimental. Esto lleva a la conclusión de que se puede considerar la reacción sencilla EC + Gly → GC + EG para el planteamiento de modelos cinéticos.

Debido a la presencia de dos fases líquidas al inicio de la reacción, se analizó con FBRM el efecto de la agitación sobre la distribución de tamaño de cuerdas de las gotas de la dispersión de EC y glicerina. El incremento de la agitación aumentó el número total de gotas hasta una velocidad de agitación de 800 rpm, a partir de la cual no se apreció aumento alguno. El valor medio de la longitud de cuerda no sufre apenas variación, aunque el valor modal de la longitud de cuerda se reduce ligeramente con la variable agitación hasta las 800 rpm. Así mismo, se comprueba, completando la reacción química a diferentes valores de agitación, que la velocidad inicial de reacción sigue una tendencia de acuerdo con la evolución del número de cuerdas (Tabla 2). Por otro lado, se evaluó el efecto de la temperatura en la dispersión, observándose una disminución del número de cuerdas según aumenta esta variable con distribuciones similares, lo cual implica un mejor contacto entre fases (Figura 4).

Para completar el análisis con FBRM, se lleva a cabo la evolución física del sistema en condiciones de reacción, acompañando este análisis de la evolución química de los compuestos (Figura 5a). Se observa que el número de cuerdas prácticamente se anula cuando se alcanza una conversión de 0.34, lo cual corresponde a una composición prácticamente coincidente con el límite entre la zona mono y bifásica del equilibrio líquido-líquido del sistema cuaternario, representado en la Figura 4b.

Se realizaron una serie de experimentos cinéticos variando la temperatura (40-50 ºC), el exceso molar de ECa glicerina (2-3) y la concentración de catalizador (125-500 ppm) para la obtención de suficientes datos para llevar a cabo el ajuste de modelos cinéticos. La Figura 6 muestra el efecto positivo de estas variables en lo que a velocidad de reacción respecta y el prácticamente nulo efecto del exceso molar sobre la conversión final obtenida, cercana a 0,95. Además, se evaluó el valor de la conversión

en el cual el comportamiento de la cinética varía, indicada como conversión crítica o X_{crit}. Dicho valor se ve afectado por la temperatura y la cantidad de catalizador empleada, aunque no por el exceso de EC, tal como se aprecia en la Figura 7. Aun así, los valores de X_{crit} obtenidos daban lugar a composiciones en dicho instante de la reacción cercanas a la frontera entre un sistema bifásico y monofásico, según se observa en la Figura 8.

En cuanto a la proposición de modelos cinéticos que pudieran explicar la cinética del proceso, se comprobó en primer lugar la presencia de potasio en la fase rica en glicerina durante la fase de la reacción en la que están presentes dos fases líquidas. Esto conllevó a la consideración de una primera etapa de la reacción que sigue un primer orden parcial respecto a la concentración de glicerina y orden cero respecto a la de EC, cuya concentración se estima constante en un valor EC_{sol}. Por otra parte, tras observar que no se daba conversión completa en la reacción, se consideró la posibilidad de la desactivación del catalizador por la presencia de H_2O y CO_2, dando lugar a $KHCO_3$, especie menos activa que K_2CO_3, por conducir a valores de pH menores. También se tuvo en cuenta la posibilidad de que la reacción inversa tuviera peso. Los modelos propuestos combinando dichas suposiciones se resumen en la Tabla 3:

- El primero considera la reacción directa en la primera etapa y tanto la directa como la inversa en la segunda, sin considerar desactivación.
- El segundo modelo tiene en cuenta la reacción inversa en la segunda etapa, así como la desactivación del catalizador en ambas etapas, con un valor de la energía de activación de la reacción directa igual en ambas etapas.
- El tercer modelo tiene las mismas consideraciones que el segundo, con la salvedad de que considera valores diferentes de la energía de activación de la reacción directa en las dos etapas.
- Por último, el modelo 4 considera la desactivación del catalizador, pero desestima la existencia de reacción inversa en la segunda etapa.

Los valores de los parámetros de ajuste, así como los criterios estadísticos, se muestran en la Tabla 4. Teniendo en cuenta los valores y error de los parámetros, así como el mejor valor de todos los criterios estadísticos considerados, se elige el Modelo 2 como el más representativo de la cinética del proceso.

Publicación 6 (parte 2)

Por último, también se estudia la transesterificación con carbonato de etileno catalizada por metóxido de potasio.

De modo similar a lo expuesto en el comentario de la Publicación 6 (parte 1), se sigue la evolución de las especies detectadas por análisis HPLC, obteniéndose una conclusión análoga: se da la presencia de un compuesto intermedio y otro producto de la reacción en serie de la reacción entre carbonato de glicerina y el exceso de carbonato de etileno que confirman el mecanismo propuesto. Además, debido al escaso error en el cierre de los balances de materia (tan sólo 4,4% como máximo), se considerará una reacción simple en los modelos cinéticos.

Se completaron un total de 16 experimentos variando temperatura (40-50 ºC), concentración de metóxido de potasio (50-150 ppm) y exceso de EC a glicerina (1.5-3) y, apreciándose un efecto positivo sobre la cinética de las dos primeras y un ligero efecto también positivo sobre la posición de equilibrio de la tercera (Figura 6).

Se evaluaron individualmente los experimentos realizados y, de forma similar a lo observado en la Publicación 5, se apreció que el valor de conversión a partir del cual la tendencia de los datos cinéticos varía no permanece constante, como sí sucede en la reacción entre DMC y glicerina. En este caso, el valor de la conversión crítica es creciente con la temperatura y concentración de catalizador, como en la Publicación 5, aunque además también mostró un aumento ligero con el exceso molar empleado (Figura 8).

Los dos modelos cinéticos propuestos se basan, de igual modo, en dos ecuaciones aplicables antes y después de los mencionados valores de la conversión crítica:

- El primer modelo considera la reacción reversible desde los productos sin desactivación del catalizador.
- El segundo modelo tiene en cuenta la reversibilidad, así como una desactivación de primer orden, en base a lo expuesto en la Publicación 6 (parte 1).

En este caso, la bondad del ajuste del segundo modelo es evidentemente mejor que en el primero y, además, se obtienen valores de los parámetros cinéticos de ajuste con pleno significado fisicoquímico. Por ello, se considera como el modelo más

representativo tras su validación, en la que se aprecian que muy pocos valores quedan fuera del límite de ±15% de diferencia entre los valores predichos por el modelo y los experimentales (Figura 9).

Para finalizar, se compara la frecuencia de reposición, indicativa de la actividad del catalizador, de CH_3OK y K_2CO_3 como catalizadores de esta reacción. Bajo el mismo exceso de EC, dicha frecuencia de reposición es 6,57 y 5,36 veces mayor a 40 ºC y 50 ºC, respectivamente, empleando el metóxido.

6.3. Producción de solketal por acetalización de glicerina con acetona

El tercer y último sistema estudia la reacción de acetalización de la glicerina (Gly) con acetona (Ac) con el fin de obtener solketal (Sk) y agua (W), tal como muesta la Figura 6.3:

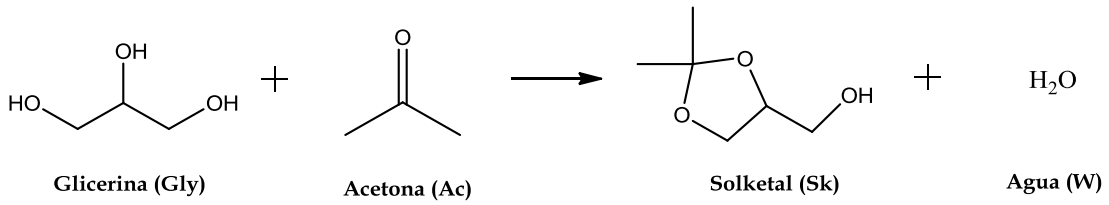

Figura 6.3. Producción de solketal por acetalización de glicerina con acetona.

Publicación 7

En este sistema, a diferencia de los dos primeros, solamente se pudo estudiar un equilibrio ternario, ante la imposibilidad de determinar con fiabilidad la concentración de agua simultáneamente al resto de componentes con el método de análisis disponible. Por lo tanto, el equilibrio evaluado es el correspondiente al sistema {Ac + Sk + Gly} a las temperaturas de 30, 40 y 50 ºC a presión atmosférica, por ser condiciones comunes en la bibliografía para la reacción de acetalización (Deutsch y col., 2007; Nanda y col., 2014a, b; Nanda y col., 2014c; Reddy y col., 2011).

Se obtuvieron los datos de equilibrio, presentados en la Tabla 1, en los se aprecia que una concentración creciente de solketal ayuda a la solubilización de la acetona y la glicerina. Por medio de la Figura 6 se puede comprobar, por un lado, que el solketal es más soluble en la fase rica en acetona y, por otro, el escaso efecto de la temperatura sobre la solubilidad del sistema, en cuanto a que las tres curvas de distribución del

solketal presentan poca diferencia. El bajo efecto de la temperatura puede observarse, además, por la similitud de las Figuras 2, 3 y 4.

La Figura 5 y la Tabla 2 muestran la regresión de los datos con la ecuación de Othmer-Tobias, en la que la correlación es muy alta, indicando una alta fiabilidad de los datos.

Ante el desconocimiento de la combinación de valores de *non-randomness binary interaction parameters,* α_{ij}, de 0,2 y 0,3 a asignar a las interacciones, se procedió como se sugiere en la determinación de la optimización de estos parámetros para el sistema {DMC + MeOH + Gly}(Wang y Lu, 2012). En primer lugar se prueba fijando los valores de α_{ij} en todas sus combinaciones posibles, así como permitiendo flotar estos parámetros en los experimentos a 30 ºC. En la Tabla 3 se puede observar que el mejor ajuste se obtiene permitiendo flotar los parámetros, obteniéndose los valores de α_{12}=0,18, α_{13}=0,29 y α_{23}=0,19. La desviación (*rmsd*) fue muy similar cuando se fijaron los parámetros en α_{12}=0,2, α_{13}=0,3 y α_{23}=0,2, por lo que se decidió tomar estos valores como óptimos para las sucesivos ajustes. Los valores del resto de parámetros de interacción binaria se muestran en la Tabla 4.

Publicación 8

Ante las ventajas que presenta la catálisis heterogénea, se ha afrontado la reacción de producción con catalizadores sólidos. Además, considerando el mecanismo de la reacción de acetalización, la acidez del catalizador es un aspecto clave (Calvino-Casilda y col., 2014), por lo que se ha elegido operar con resinas sulfónicas comerciales de intercambio iónico.

El primer estudio realizado consiste en la selección de una resina sulfónica de intercambio iónico entre varias con aplicaciones de interés. Las resinas analizadas fueron: Purolite CT275DR (CT275DR), con importancia en eterificaciones (Tejero y col., 2001); Purolite CT276 (CT276), para la elimincación de ioduros en tratamientos de aguas (Korzh y col., 2007); Amberlyst 35 dry (A35dry) y Amberlyst 36 (A36dry) para oligomerización de alquenos (Cadenas y col., 2011) y, por último, Lewatit GF101 (GF101), utilizada en la eliminación de ácidos grasos libres en procesos de producción de biodiesel (Ramírez-López y col., 2012). Se caracterizaron varios parámetros estructurales de estas resinas, de interés para su aplicación en catálisis.

En primer lugar, en la Figura 2 se muestran las curvas de intrusión de mercurio para la determinación de la distribución del tamaño de poro. De los datos de esta curva se puede ver que las resinas CT275DR y CT276 tienen una distribución estrecha, prácticamente entre 65 y 80 nm (macroporosas). A35dry y A36dry tienen distribuciones más anchas, con máximos en 35 y 15 nm, respectivamente: en el caso de A35dry la distribución se extiende por encima de 50 nm, por lo que se puede considerar meso y macroporosa, mientras que A36 dry puede decirse que es mesoporosa. Por último, GF101 muestra una distribución bimodal, con un máximo relativo en 12 nm y otro absoluto en 190 nm, aunque la distribución es preponderantemente macroporosa.

El análisis termogravimétrico mostró resultados similares en lo que al comportamiento de las resinas se refiere en los cinco casos, siendo el orden de estabilidad el siguiente: GF101>> CT275DR>CT276> A35dry~ A36dry. Las etapas observadas fueron: una primera, prácticamente despreciable, de eliminación de humedad residual al tratarse de resinas en forma seca; luego una caída del 20-25 % de peso por la degradación de los grupos sulfónicos a 355 ºC; a continuación, otra etapa de de degradación entre 500 y 75'por la degradación de la matriz polimérica; por último, a partir de 750 ºC se da una velocidad de degradación baja y constante.

Por análisis ^{13}C-NMR, cuyo espectro se ve en la Figura 4, se aprecia que la presencia de grupos sulfónicos en posición *para-* (a δ=148 ppm según lo calculado en la Tabla 2) respecto a los átomos de carbono que constituyen la unión del anillo aromático con el esqueleto de vinilbenceno de la matriz. Las resinas en las que se observan picos de mayor tamaño a 148 ppm son GF101 y CT275DR, de lo que se puede inferir que son aquellos en los que los grupos sulfónicos tienen mayor accesibilidad.

El análisis elemental de los sólidos, representado en la Figura 5, muestra composiciones de azufre entre 7 y 15 %, donde CT275DR y GF101 son los que tienen mayor cantidad de este elemento.

Por último, la valoración potenciométrica con n-butilamina de las resinas, en la Figura 6, indica que las resinas tienen sitios ácidos (potencial inicial > 100 mV) y en el siguiente orden: CT275DR > A35dry > GF101 > A36dry > CT276. Sin embargo, el comportamiento de las resinas es muy diferente, dándose en el caso de GF101 la reducción más pronunciada de potencial con la adición de la base, lo cual lleva a pensar que en este catalizador la acidez es más rápidamente disponible que en el resto.

Tras las caracterizaciones, se evaluó la actividad de las resinas llevándose a cabo la reacción en ausencia de disolvente con exceso de acetona. La Figura 7 muestra la actividad de las resinas incluyendo además un experimento adicional realizado con Amberlyst 15 (A15), una referencia clásica de este tipo de resinas. El orden es el siguiente: GF101 > CT275DR > A36dry > A35dry > A15 > CT276, donde la posición de equilibrio de Y_{Sk}=0,48 se alcanza tras 6 horas en el caso de GF101

Por otro lado, se analizó la estabilidad de las resinas evaluando su actividad en sucesivas reutilizaciones de los catalizadores con y sin regeneración del catalizador en la Figura 9. El orden de estabilidad, evaluada en base a la actividad remanente, fue diferente al obtenido para la actividad en las primeras utilizaciones: CT276 > A36dry > A15 > CT275DR > A35dry > GF101. La actividad remanente se define como la actividad en cada reciclo respecto al primero, donde se da la máxima actividad, entendida como la frecuencia de reposición de cada resina.

Publicación 9

Considerando los resultados de la resina Lewatit GF101 en la publicación 8, se seleccionó esta resina para proceder al estudio cinético de la reacción química en un reactor discontinuo.

En primer lugar hay que tener en cuenta que el presente sistema de reacción consta, inicialmente, de tres fases: dos líquidas por la escasa miscibilidad de la acetona y la glicerina a baja extensión de reacción y una sólida, constituida por el catalizador. Por ello, para aislar el estudio de la cinética de la reacción química se lleva a cabo la determinación de aquellas condiciones bajo las cuales las transferencias externa e interna de materia no suponen una etapa controlante.

Para la elección de unas condiciones en las cuales la transferencia de materia externa no es limitante, se evaluó la evolución de la velocidad de reacción empleando diferentes velocidades de agitación. En la Figura 3 pude apreciarse que a partir de 750 rpm el transcurso de la reacción no difiere, por lo que se elige esta agitación para operar en adelante.

La evaluación de la transferencia interna de materia se realiza valorando el efecto del tamaño de partícula de catalizador sobre el progreso de la reacción. Se emplean diferentes tamaños de partícula del catalizador, tras tamizarlo. Además, para

obtener tamaños menores a los disponibles en la muestra comercial, se le somete a trituración. La Figura 5a representa la evolución de la reacción empleando los diferentes tamaños de partícula, mientras que la Figura 5b muestra que someter la resina a stress físico no afecta en su actividad. La Figura 6 muestra el factor de efectividad η, definido como el cociente entre la velocidad del proceso con un tamaño de partícula dado y aquel en el cual se considera que no hay control por la transferencia interna de materia. Puede verse que el valor de η es la unidad para tamaños de partícula de 190 μm y menores, por lo que se selecciona este tamaño para realizar el estudio cinético de la reacción.

A continuación, se realizan una serie de experimentos modificando el valor de las variables que pueden afectar a la cinética de la reacción para la obtención de datos relevantes para la proposición de modelos cinéticos: temperatura (30-40 ºC), cantidad de catalizador (0,5-1 % pesos) y exceso molar de acetona a glicerina (3-12). El cambio del progreso de la reacción con los distintos valores de estas variables puede apreciarse en la Figura 7a, 7b y 7c. En esta última Figura, además, puede verse el notable efecto que la relación molar de acetona a glicerina tiene sobre la posición de equilibrio de la reacción, donde un exceso de 12 a 1 permite alcanzar una conversión cercana al 96%.

Se proponen tres tipos de modelos aplicables a reacciones catalizadas heterogéneamente: modelos pseudohomogéneos (P), modelos basados en Eley-Rideal (ER) y modelos basados en Langmuir-Hinshelwood-Hougen-Watson (LHHW). En las modificaciones propuestas de estos modelos se tiene en cuenta la existencia de la reacción inversa debido a la posición de equilibrio observada pero, además, se consideran hasta cuatro tipos de modificaciones de los modelos variando los órdenes de reacción de los reactivos. Así, se tienen modelos de primer orden respecto a la concentración de la acetona y la glicerina (1), de primer orden respecto a la concentración de la glicerina y nulo para la acetona (2), de primer orden respecto a la acetona y nulo para la glicerina (3) o de orden cero para ambas especies reactantes (4). Las ecuaciones completas de los 12 modelos se presentan en la Tabla 3.

En modelos tipo P, se considera que la adsorción de las especies es nula, y la reacción se daría en la fase líquida. Los modelos ER y LHHW presentan términos de adsorción de los compuestos en el denominador de sus respectivas expresiones. El modelo ER se basa en la suposición que sólo una de las moléculas se adsorbe en el sólido, mientras que la otra reacciona desde la fase fluida, mientras que el LHHW sugiere la reacción por adsorción de las dos moléculas en centros activos adyacentes.

En este caso, los modelos ER y LHHW presentados sólo consideran la constante de adsorción del agua al no conseguirse convergencia de los ajustes incluyendo más constantes de adsorción en las ecuaciones. Por otra parte, en la literatura hay ejemplos de modelos en los que se considera sólo la constante de adsorción del agua operando con resinas sulfónicas debido a la gran apetencia de estos grupos por esta molécula (Lilja y col., 2002; Nanda y col., 2014c).

La Tabla 4 recopila los ajustes obtenidos, con los criterios estadísticos definidos en el Capítulo 5 de esta Tesis. Se aprecia que los modelos ER4 y LHHW4 presentan resultados muy similares entre sí, por lo que podría aceptarse en principio cualquiera de los dos. Sin embargo, se escoge el modelo ER4 como más representativo, ya que parece más probable considerar la reacción por adsorción en un centro de una molécula de acetona dado el exceso molar de esta última con el que se opera, que la reacción en dos centros adyacentes por adsorción de los dos reactivos. En base a estos resultados, se presenta un mecanismo en la Figura 8 basado en las propuestas de Calvino-Casilda (Calvino-Casilda y col., 2014).

7. CONCLUSIONES
CONCLUSIONS

7. CONCLUSIONES

El trabajo experimental y el análisis de los resultados e interpretación de los mismos permiten obtener las siguientes conclusiones acerca de la producción térmica y/o catalítica de carbonato de glicerina y solketal.

Sobre los métodos experimentales empleados

1.- Los métodos experimentales desarrollados para el análisis de los equilibrios líquido-líquido y el seguimiento de los sistemas de reacción son fiables y reproducibles. Las técnicas FBRM y HPLC fueron empleadas en la obtención de carbonato de glicerina para el análisis físico y químico, respectivamente. En el análisis por HPLC, el error en la determinación de la composición en los experimentos de equilibrio se sitúa por debajo del 2%; en el caso de los experimentos cinéticos, los balances de materia de las muestras se cumplen con un error inferior al 5% en todos los casos. Para el estudio de la obtención de solketal, los equilibrios líquido-líquido se analizaron por medio de GC-TCD, con un error inferior al 2%, mientras que los experimentos cinéticos se analizaron por ^{1}H-RMN, cuyo error en la cuantificación de solketal fue inferior al 7%.

Sistema 1: Producción de carbonato de glicerina por transesterificación de glicerol con carbonato de dimetilo

Sobre la fenomenología

2.- El sistema de reacción está constituido inicialmente por dos fases líquidas debido a la escasa miscibilidad entre carbonato de dimetilo (DMC) y glicerina (Gly). Sin embargo, a medida que se generan los productos de reacción, carbonato de glicerina (GC) y metanol (MeOH), la solubilidad de ambos aumenta, y la dispersión inicial se transforma en una única fase líquida; este hecho sucede a partir de una conversión de 0,30 de glicerina.

3.- Se ha estudiado el equilibrio entre fases líquidas para composiciones del sistema correspondientes a valores inferiores a la citada conversión, en condiciones inertes, para los sistemas {DMC + MeOH + Gly}, {DMC + GC + Gly} y {DMC + MeOH + GC + Gly}. Los datos son bien descritos por el modelo termodinámico NRTL con un error mínimo. La temperatura apenas afecta a estos equilibrios.

Sobre las condiciones de operación

4.- La reacción química tiene un mecanismo que se inicia en presencia de catalizadores básicos. Entre varios carbonatos y bicarbonatos de metales alcalinos, se han seleccionado K_2CO_3 como el más adecuado y, por otro lado, también se utilizó CH_3OK. Cuando se empleó K_2CO_3, el intervalo de temperaturas seleccionado para el estudio del proceso fue de 66 a 70 ºC, mientras que el empleo de CH_3OK permitió operar con velocidades de reacción apreciables entre 50 y 70 ºC utilizando concentraciones de catalizador muy inferiores. La selectividad obtenida fue cercana al 100 % con ambos catalizadores en las condiciones de operación mencionadas, lo cual permite plantear el estudio cinético del sistema como una reacción simple, ya que la concentración de otros compuestos fue despreciable.

5.- Se estudiaron los efectos de la transferencia de materia por la presencia inicial de dos fases líquidas. Se determinó que, operando con una velocidad de agitación de 1500 rpm, el proceso está controlado por la reacción química.

Sobre los modelos cinéticos

6.- El modelo cinético de esta reacción hay que formularlo con dos etapas, de acuerdo a la fenomenología observada. Así, se describe la evolución del sistema reaccionante antes y después de la conversión a la que el sistema es monofásico.

7.- Cuando se emplea K_2CO_3 como catalizador, la cinética de la primera etapa es de primer orden respecto a la concentración de glicerina y de orden cero respecto a la de DMC, que reacciona en la fase rica en glicerina con una concentración constante. Este modelo también asume que el catalizador está disuelto sólo en la glicerina. La segunda etapa se describe con una ecuación potencial de segundo orden, primer orden parcial respecto a cada uno de los reaccionantes, DMC y glicerina, considerando que el catalizador está disuelto en todo el volumen de reacción. Las ecuaciones cinéticas, junto con las constantes y sus errores, se expresan a continuación:

$$r_1 = k_1 \cdot C_{cat1} \cdot C_{Gly} \cdot C_{DMCsol} = \left(exp(55.43 \pm 1.31) exp\left(- \frac{(21558 \pm 446)}{T} \right) \right) \cdot \qquad \text{si X} \leq 0{,}30$$
$$\cdot C_{cat1} \cdot C_{Gly} \cdot (3.34 \pm 0.07)$$

$$r_2 = k_1 \cdot C_{cat} \cdot C_{Gly} \cdot C_{DMC} = \left(exp(55.43 \pm 1.31) exp\left(- \frac{(21558 \pm 446)}{T} \right) \right) \cdot C_{cat} \cdot C_{Gly} \cdot C_{DMC} \qquad \text{si X} > 0{,}30$$

8.- Empleando CH_3OK como catalizador, se ha propuesto un modelo que también consta de dos etapas, con consideraciones análogas al anterior, aunque en este caso se considera adicionalmente una desactivación del catalizador de primer orden. Además, se tiene en cuenta un valor de la conversión crítica de 0,35. Las ecuaciones con sus parámetros y error son las siguientes:

$$r_1 = k_1 \cdot C_{cat1} \cdot \left((1-\beta) exp\left(-k_d \cdot t\right) + \beta\right) C_{Gly} \cdot C_{DMCsol} =$$
$$= \left(exp\left(4.84 \pm 0.51\right) exp\left(- \frac{\left(3408 \pm 182\right)}{T} \right) \right) \cdot \qquad \text{si } X \leq 0{,}35$$
$$\cdot C_{cat1} \cdot \left((1-\left(0.32 \pm 0.02\right)) exp\left(-\left(0.03 \pm 0.01\right)\right) + \left(0.32 \pm 0.02\right)\right) C_{Gly} \cdot \left(3.56 \pm 0.68\right)$$

$$r_2 = k_1 \cdot C_{cat} \cdot \beta \cdot C_{Gly} \cdot C_{DMC} =$$
$$= \left(exp\left(4.84 \pm 0.51\right) exp\left(- \frac{\left(3408 \pm 182\right)}{T} \right) \right) \cdot C_{cat} \cdot \left(0.32 \pm 0.02\right) C_{Gly} \cdot C_{DMC} \qquad \text{si } X > 0{,}35$$

Sistema 2: Producción de carbonato de glicerina por transesterificación de glicerol con carbonato de etileno

Sobre la fenomenología

9.- Este sistema presenta inicialmente dos fases líquidas debido a la miscibilidad limitada entre carbonato de etileno (EC) y glicerina (Gly), aunque según progresa la reacción, y se producen carbonato de glicerina (GC) y etilenglicol (EG), el sistema bifásico líquido se transforma en una única fase, lo que sucede para una conversión de glicerina en torno a 0,35.

10.- Se ha estudiado el equilibrio entre fases, cuando el sistema es bifásico, en condiciones inertes para los sistemas {EC + EG + Gly}, {EC + GC + Gly} y {EC + EG + GC + Gly}. Se ajustaron los datos obtenidos con el modelo termodinámico NRTL con errores bajos. De nuevo, se apreció un escaso efecto de la temperatura sobre los citados equilibrios entre fases.

Sobre las condiciones de operación

11.- En primer lugar, el estudio de la reacción se ha llevado a cabo en ausencia de catalizador. En este caso, se requiere la presencia de una única fase líquida (lo que se consigue a temperaturas mayores de 80 ºC), siendo el intervalo de temperatura adecuado entre 100 y 140 ºC. El estudio termodinámico predice una conversión completa en estas condiciones, es decir, la reacción se puede considerar irreversible.

12.- La reacción también puede realizarse en presencia de catalizadores básicos, entre los cuales se seleccionaron K_2CO_3 y CH_3OK. En estas condiciones, el intervalo de temperaturas adecuado se sitúa entre 40 y 50 ºC.

13.- Se estudió la influencia de la agitación en la transferencia de materia externa en los casos de la reacción catalítica, estableciéndose que operando con una agitación de 800 rpm, este fenómeno no controla la velocidad del proceso.

14.- La selectividad del proceso es prácticamente completa, y los balances de materia se cierran con errores despreciables, tanto en presencia como en ausencia de catalizador. De este modo, se puede considerar que el sistema responde a un esquema propio de una reacción simple.

Sobre los modelos cinéticos

15.- La cinética de la reacción en ausencia de catalizador es bien descrita por un modelo potencial de segundo orden global, de acuerdo a la siguiente ecuación:

$$r = k_1 \cdot C_{Gly} \cdot C_{EC} = \left(exp(11.72 \pm 0.25) exp\left(- \frac{(7436 \pm 100)}{T} \right) \right) \cdot C_{Gly} \cdot C_{EC}$$

16.- En presencia de K_2CO_3, el modelo consta de dos etapas, antes y después de un valor de conversión al que se observa un cambio de tendencia en la cinética. Este valor de la conversión es dependiente de la temperatura y la concentración de catalizador empleadas, aunque se sitúa en torno a un valor de 0,35. La primera etapa del modelo considera la reacción directa y la desactivación del catalizador ambas de primer orden parcial respecto a la glicerina y nulo respecto a EC. La segunda etapa tiene en cuenta la reversibilidad de la reacción, así como la desactivación del catalizador. Estas ecuaciones con sus parámetros son las siguientes:

$$r_1 = k_1 \cdot C_{cat1} \cdot ((1-\beta) exp(-k_d \cdot t) + \beta) C_{Gly} \cdot C_{ECsol} = \left(exp(32.71 \pm 1.03) exp\left(- \frac{(11036 \pm 319)}{T} \right) \right) \cdot \text{ si } X \leq X_{crit}$$
$$\cdot C_{cat1} \cdot ((1-(0.08 \pm 0.03)) exp(-(0.36 \pm 0.06) t) + \beta) C_{Gly} \cdot (1.10 \pm 0.46)$$

$$r_2 = k_1 \cdot C_{cat} \cdot \beta \cdot C_{Gly} \cdot C_{EC} =$$
$$= \left(exp(32.71 \pm 1.03) exp\left(- \frac{(11036 \pm 319)}{T} \right) \right) \cdot C_{cat} \cdot (0.08 \pm 0.03) C_{Gly} \cdot C_{EC} \quad \text{si } X > X_{crit}$$

$$r_3 = k_2 \cdot C_{cat} \cdot \beta \cdot C_{GC} \cdot C_{EG} =$$
$$= \left(exp(31.91 \pm 5.95) exp\left(- \frac{(11297 \pm 1911)}{T} \right) \right) \cdot C_{cat} \cdot (0.08 \pm 0.03) C_{Gly} \cdot C_{EC} \quad \text{si } X > X_{crit}$$

17.- Cuando se utiliza CH_3OK como catalizador, el modelo también consta de dos etapas con el mismo fundamento antes descrito, con un valor de conversión límite entre

ambas que varía con la temperatura, concentración de catalizador y exceso molar de carbonato de etileno. En este caso, se considera una desactivación de primer orden del catalizador y la reversibilidad de la reacción. Las ecuaciones y parámetros correspondientes son:

$$r_1 = k_1 \cdot C_{cat1} \cdot \left((1-\beta) \cdot exp(-k_d \cdot t) + \beta \right) C_{Gly} \cdot C_{ECsol} =$$
$$= \left(exp(30.91 \pm 1.11) \cdot exp\left(-\frac{(9897 \pm 361)}{T} \right) \right) \cdot \qquad \text{si } X \leq X_{crit}$$
$$\cdot C_{cat1} \cdot \left((1-(0.020 \pm 0.001)) \cdot exp(-(0.31 \pm 0.03) \cdot t) + (0.020 \pm 0.001) \right) C_{Gly} \cdot (1.11 \pm 0.12)$$

$$r_2 = k_1 \cdot C_{cat} \cdot \beta \cdot C_{Gly} \cdot C_{EC} =$$
$$= \left(exp(30.91 \pm 1.11) \cdot exp\left(-\frac{(9897 \pm 361)}{T} \right) \right) \cdot C_{cat} \cdot (0.020 \pm 0.001) C_{Gly} \cdot C_{EC} \qquad \text{si } X > X_{crit}$$

$$r_3 = k_3 \cdot C_{cat} \cdot \beta \cdot C_{GC} \cdot C_{EG} =$$
$$= \left(exp(14.03 \pm 8.16) \cdot exp\left(-\frac{(6431 \pm 2607)}{T} \right) \right) \cdot C_{cat} \cdot (0.020 \pm 0.001) C_{GC} \cdot C_{EG} \qquad \text{si } X > X_{crit}$$

Sobre la sostenibilidad

18.- Cuando se calculan parámetros aceptados como una medida de la sostenibilidad del proceso en ausencia de catalizador, se obtienen unos valores que indican una economía atómica y de carbono del 100%, un *factor E* nulo y una mayor productividad másica y eficiencia másica que otros procesos similares descritos con anterioridad en la literatura.

Sistema 3: Producción de solketal por acetalización de glicerol con acetona

Sobre la fenomenología

19.- El sistema consta de dos especies reactivas con baja miscibilidad mutua, acetona (Ac) y glicerina (Gly); a medida que reaccionan se produce solketal (Sk) y el sistema bifásico inicial se transforma en un sistema monofásico. La composición a la que ocurre este hecho depende del resto de condiciones de operación que se empleen.

20.- Considerando la naturaleza del sistema, se estudió el equilibrio líquido-líquido en el sistema ternario {Ac + Sk + Gly} en condiciones no reactivas, apreciándose un escaso efecto de la temperatura en el intervalo estudiado. Los datos obtenidos se ajustaron con escaso error al modelo NRTL.

Sobre las condiciones de operación

21.- La reacción precisa de un catalizador ácido para tener lugar en grado apreciable. Se emplearon diferentes resinas sulfónicas de intercambio iónico comerciales en un intervalo de temperatura entre 40 y 50 ºC. En estas condiciones, una variación del exceso molar de acetona sobre glicerina afecta notablemente a la conversión de equilibrio de la reacción, que debe considerarse, en todo caso, reversible.

22.- Se comprobó experimentalmente que no hay control de la velocidad del proceso por parte de las etapas de transferencias externa e interna de materia cuando se emplea una agitación de 750 rpm o mayor y un tamaño de partícula de 190 μm o menor.

23.- Las resinas se caracterizaron por su estructura y composición química y se estudió su actividad, su estabilidad y su regenerabilidad. El orden de actividad de las diferentes resinas estudiadas fue el siguiente: Lewatit GF101 > Purolite CT275DR > Amberlyst 36dry > Amberlyst 35dry > Amberlyst 15 > Purolite CT276, siendo el orden de estabilidad el siguiente: Purolite CT276 > Amberlyst 36dry > Amberlyst 15 > Purolite CT275DR > Amberlyst 35dry > Lewatit GF101.

Sobre el modelo cinético

24.- Operando con Lewatit GF101 se obtuvo un modelo cinético adecuado para describir la evolución del sistema con este catalizador heterogéneo. El modelo es de tipo Eley-Rideal, en el que se considera la reversibilidad de la reacción con primer orden parcial respecto a las concentraciones de los productos, orden cero parcial para cada uno de los reactivos y la constante de adsorción únicamente para el agua. La ecuación cinética y el valor de los parámetros, dentro del intervalo experimental estudiado, es la siguiente:

$$r = \frac{k_1 \cdot C_{cat} - k_2 \cdot C_{cat} \cdot C_{Sk} \cdot C_w}{\left(1 + K_w \cdot C_w\right)^2} =$$

$$= \frac{\left(exp\left(44.14 \pm 5.12\right) exp\left(-\left(14920 \pm 1558\right)/T\right)\right) \cdot C_{cat} - \left(exp\left(45.14 \pm 4.97\right) exp\left(-\left(15318 \pm 1513\right)/T\right)\right) \cdot C_{cat} \cdot C_{Sk} \cdot C_w}{\left(1 + \left(exp\left(51.17 \pm 8.42\right) exp\left(-\left(15938 \pm 2583\right)/T\right) \cdot C_w\right)\right)^2}$$

7. CONCLUSIONS

The experimental work and the analysis and interpretation of the results lead to the following conclusions regarding the thermal and catalytic production of glycerol carbonate and solketal.

On the experimental methods

1.- The experimental methodologies developed to analyse both the liquid-liquid equilibria and monitoring the progress of the reacting systems are reliable and reproducible. FBRM and HPLC were employed in the production of glycerol carbonate to analyse the physical and chemical evolution, respectively. Regarding HPLC, the error associated with the determination of the composition of the equilibrium experiments is below 2%; in the case of the kinetic experiments, quantification of samples complied with material balances with errors below 5% in every case. As for the study of solketal production, liquid-liquid equilibria were measured by means of GC-TCD with an error below 2%, while the kinetic experiments were followed by ^{1}H-RMN, with an error below 7% in the quantification of solketal.

System 1: Production of glycerol carbonate by transesterification of glycerol with dimethyl carbonate

On the phenomenology

2.- This reacting system consists of two liquid phases in its initial stages due to limited miscibility of dimethyl carbonate (DMC) and glycerol (Gly). Nonetheless, as the reaction products generate, i.e. glycerol carbonate (GC) and methanol (MeOH), the solubility of both increases in each other. Thus, the initial dispersion turns into a single phase liquid system, taking place above a value of the conversion of 0.30.

3.- The equilibrium between liquid phases has been studied under inert conditions at compositions of the system corresponding to conversion values below the mentioned value. The systems {DMC + MeOH + Gly}, {DMC + GC + Gly} and {DMC + MeOH + GC + Gly} were analyzed. The data obtained can be well described employing the NRTL thermodynamic model with very low error. Temperature barely affects these equilibria.

On the operating conditions

4.- The mechanism of this chemical reaction is triggered by the presence of basic catalysts. K_2CO_3 was selected as the best catalyst among a series of alkali metal-based carbonates and hydrogen carbonates; additionally, CH_3OK was also employed. The reaction kinetics was studied using both catalysts. When K_2CO_3 was used, the temperature interval selected to study the process was 66 – 70 ºC, while the use of CH_3OK allowed to operate from 50 to 70 ºC at noticeable reaction rates with much lower catalyst concentrations. The selectivity of the process was practically 100% with both catalysts under the mentioned operating conditions, which allows approaching the kinetic study accounting for a simple reaction.

5.- Mass transfer effects were assessed due to the presence of two liquid phases at the early stages of the reaction. A stirring speed of 1500 rpm was determined as that from which the process is controlled by the chemical reaction.

On the kinetic models

6.- According to phenomenology observed, this kinetic model ought to be expressed in two stages. Hence, the evolution of the reacting system is described prior to and after the conversion value at which the system is a single phase liquid.

7.- When K_2CO_3 is employed as catalyst, the kinetics of the first stage is of first order with respect to the concentration of glycerol and zero order to that of DMC, which reacts within the glycerol-rich phase at a constant concentration. This model also assumes that the catalyst is dissolved only in such phase. The second stage is described with a potential law of global second order, being of partial first order with respect to the concentration of both reactants, DMC and glycerol, accounting for the catalyst being dissolved in the entire reacting volume. The kinetic equations featuring the values of the parameters and their errors are the following:

$$r_1 = k_1 \cdot C_{cat1} \cdot C_{Gly} \cdot C_{DMCsol} = \left(exp(55.43 \pm 1.31) exp\left(- \left(21558 \pm 446\right)/T \right) \right) \cdot \quad \text{if X} \leq 0{,}30$$
$$\cdot C_{cat1} \cdot C_{Gly} \cdot (3.34 \pm 0.07)$$

$$r_2 = k_1 \cdot C_{cat} \cdot C_{Gly} \cdot C_{DMC} = \left(exp(55.43 \pm 1.31) exp\left(- \left(21558 \pm 446\right)/T \right) \right) \cdot C_{cat} \cdot C_{Gly} \cdot C_{DMC} \quad \text{if X} > 0{,}30$$

8.- Putting CH_3OK to use as catalyst, an analogous model consisting of two stages is also set forth, though in this case an additional first order deactivation of the catalyst is

accounted for. Moreover, a critical conversion value of 0.35 is taken into consideration. The equations together with their parameters and error are the following:

$$r_1 = k_1 \cdot C_{cat1} \cdot \left((1-\beta) exp(-k_d \cdot t) + \beta \right) C_{Gly} \cdot C_{DMCsol} =$$
$$= \left(exp(4.84 \pm 0.51) exp\left(-\frac{(3408 \pm 182)}{T} \right) \right) \cdot \qquad \text{if } X \leq 0{,}35$$
$$\cdot C_{cat1} \cdot \left((1-(0.32 \pm 0.02)) exp(-(0.03 \pm 0.01) t) + (0.32 \pm 0.02) \right) C_{Gly} \cdot (3.56 \pm 0.68)$$

$$r_2 = k_1 \cdot C_{cat} \cdot \beta \cdot C_{Gly} \cdot C_{DMC} =$$
$$= \left(exp(4.84 \pm 0.51) exp\left(-\frac{(3408 \pm 182)}{T} \right) \right) \cdot C_{cat} \cdot (0.32 \pm 0.02) C_{Gly} \cdot C_{DMC} \qquad \text{if } X > 0{,}35$$

System 2: Production of glycerol carbonate by transesterification of glycerol with ethylene carbonate

On the phenomenology

9.- This system presents at first two liquid phases owing to the restricted miscibility of ethylene carbonate (EC) and glycerol (Gly). As the reaction takes place and glycerol carbonate (GC) and ethylene glycol (EG) are produced, the *ab initio* biphasics system is transformed into a single phase liquid, which takes place at a conversion of glycerol of approximately 0.35.

10.- The liquid-liquid equilibria were evaluated for the systems {EC + EG + Gly}, {EC + GC + Gly} and {EC + EG + GC + Gly} under inert conditions at compositions at which the system is biphasic. The NRTL model was fitted to the observed data with negligible error. In this case, the influence of temperature was not remarkable on the mentioned equilibria.

On the operating conditions

11.- First, the study of the kinetics was undertaken in the absence of catalyst. In this case, the presence of a single liquid phase is required, which is attained at temperatures above 80ºC, being the most adequate temperature interval from 100 to 140 ºC. The thermodynamic study predicts a complete conversion under these conditions; thus, the reaction can be regarded as irreversible.

12.- This reaction can also be performed in the presence of basic catalysts, among which K_2CO_3 and CH_3OK were employed. In this case, the appropriate temperature interval is from 40 to 50 ºC.

13.- The influence of the stirring rate on the external mass transfer in the catalytic reactions was assessed. It was determined that operating at 800 rpm, this phenomenon does not control the overall rate of the process.

14.- The selectivity of the process is virtually complete both in presence and absence of catalysts, with closure of material balances only with negligible errors. Therefore, it can be considered that the system complies with the scheme of a simple reaction.

On the kinetic models

15.- The kinetics of the reaction in absence of any catalyst is well described by means of an overall second order potential model, according to the following equation:

$$r = k_1 \cdot C_{Gly} \cdot C_{EC} = \left(exp(11.72 \pm 0.25) exp\left(- \frac{(7436 \pm 100)}{T} \right) \right) \cdot C_{Gly} \cdot C_{EC}$$

16.- In presence of K_2CO_3, the model consists of two stages, applicable before and after a conversion value at which a trend change in the kinetics of the system is observed. Said conversion value is dependent on temperature and the concentration of catalyst employed, though it is close to the value of 0.35. The first stage of the model considers the direct reaction and deactivation of the catalyst, both of first partial order with respect to the concentration of glycerol and zero order to that of EC. The second stage answers for the reversibility of the reaction as well as the deactivation of the catalyst. These equations and the corresponding parameters are presented in the next equation:

$$r_1 = k_1 \cdot C_{cat1} \cdot ((1-\beta) exp(-k_d \cdot t) + \beta) C_{Gly} \cdot C_{ECsol} = \left(exp(32.71 \pm 1.03) exp\left(- \frac{(11036 \pm 319)}{T} \right) \right) \cdot \text{ if } X \leq X_{crit}$$
$$\cdot C_{cat1} \cdot ((1-(0.08 \pm 0.03)) exp(-(0.36 \pm 0.06) t) + \beta) C_{Gly} \cdot (1.10 \pm 0.46)$$

$$r_2 = k_1 \cdot C_{cat} \cdot \beta \cdot C_{Gly} \cdot C_{EC} =$$
$$= \left(exp(32.71 \pm 1.03) exp\left(- \frac{(11036 \pm 319)}{T} \right) \right) \cdot C_{cat} \cdot (0.08 \pm 0.03) C_{Gly} \cdot C_{EC} \quad \text{if } X > X_{crit}$$

$$r_3 = k_2 \cdot C_{cat} \cdot \beta \cdot C_{GC} \cdot C_{EG} =$$
$$= \left(exp(31.91 \pm 5.95) exp\left(- \frac{(11297 \pm 1911)}{T} \right) \right) \cdot C_{cat} \cdot (0.08 \pm 0.03) C_{Gly} \cdot C_{EC} \quad \text{if } X > X_{crit}$$

17.- When CH_3OK is employed as catalyst, the model also features two stages with the same basis as previously described, where the critical conversion value limiting them varies with temperature, concentration of catalyst and molar excess of ethylene carbonate. In this case, a first order deactivation of the catalyst as well as reversibility of the reaction is contemplated. The equations and the corresponding parameters go as follows:

$$r_1 = k_1 \cdot C_{cat1} \cdot \left((1-\beta) \cdot exp\left(-k_d \cdot t\right) + \beta\right) \cdot C_{Gly} \cdot C_{ECsol} =$$
$$= \left(exp\left(30.91 \pm 1.11\right) \cdot exp\left(- \frac{\left(9897 \pm 361\right)}{T} \right) \right) \cdot \qquad \text{if } X \leq X_{crit}$$
$$\cdot C_{cat1} \cdot \left((1-(0.020 \pm 0.001)) \cdot exp\left(-(0.31 \pm 0.03) \cdot t\right) + (0.020 \pm 0.001)\right) \cdot C_{Gly} \cdot (1.11 \pm 0.12)$$

$$r_2 = k_1 \cdot C_{cat} \cdot \beta \cdot C_{Gly} \cdot C_{EC} =$$
$$= \left(exp\left(30.91 \pm 1.11\right) \cdot exp\left(- \frac{\left(9897 \pm 361\right)}{T} \right) \right) \cdot C_{cat} \cdot (0.020 \pm 0.001) \cdot C_{Gly} \cdot C_{EC} \qquad \text{if } X > X_{crit}$$

$$r_3 = k_3 \cdot C_{cat} \cdot \beta \cdot C_{GC} \cdot C_{EG} =$$
$$= \left(exp\left(14.03 \pm 8.16\right) \cdot exp\left(- \frac{\left(6431 \pm 2607\right)}{T} \right) \right) \cdot C_{cat} \cdot (0.020 \pm 0.001) \cdot C_{GC} \cdot C_{EG} \qquad \text{if } X > X_{crit}$$

On the sustainability

18.- After calculating a series of parameters accepted as a measure of the sustainability of the process in the absence of catalyst, a series of values are obtained indicating values of the atom and carbon economies of 100%, a value of the *E-factor* of zero and higher mass productivity and efficiency than other similar processes previously described in literature.

System 3: Production of solketal by acetalisation of glycerol with acetone

On the phenomenology

19.- The system comprises two reactive species of low mutual miscibility, acetone (Ac) and glicerol (Gly). As they react, solketal (Sk) is produced and initially biphasic system evolves into a monophasic system. The composition at which this occurs depends on the rest of the operating conditions being employed.

20.- Considering the nature of the system, the equilibria existing between the two liquid phases was evaluated in the ternary system {Ac + Sk + Gly}under non-reactive conditions, with temperature proving to have a very low effect on the equilibria. The data were correlated with the NRTL model with a very high degree of agreement.

On the operating conditions

21.- The reaction requires an acid catalyst to take place to a significant degree. Different commercially available sulphonic ion exchange resins were utilized within the temperature range from 40 to 50 ºC. In these conditions, a variation of the molar excess of acetone to glycerol holds a significant effect on the equilibrium conversion of the reaction, which is to be considered reversible, regardless.

22.- It was experimentally verified that the global rate of the process is not controlled by external or internal mass transfer when a stirring speed of 750 rpm and a particle size of 190 μm or lower is put to use.

23.- The resins were characterized in terms of their structure and chemical composition and their activity, stability and regenerability was assessed. The activity order of the resins subject of study was the following: Lewatit GF101 > Purolite CT275DR > Amberlyst 36dry > Amberlyst 35dry > Amberlyst 15 > Purolite CT276, though the stability order differed: Purolite CT276 > Amberlyst 36dry > Amberlyst 15 > Purolite CT275DR > Amberlyst 35dry > Lewatit GF101.

On the kinetic model

24.- Operating with Lewatit GF101, an adequate kinetic model to describe the evolution of the system with this heterogeneous catalyst was obtained It consists in an Eley-Rideal-based model, which considers the reversibility of the reaction with partial first order with respect to the concentration of the products, zero order with respect to that of the reactants and adsorption constant only for water. The kinetic equation and the value of the parameters retrieved within the experimental conditions are featured in the following equation:

$$r = \frac{k_1 \cdot C_{cat} - k_2 \cdot C_{cat} \cdot C_{Sk} \cdot C_w}{\left(1 + K_w \cdot C_w\right)^2} =$$

$$= \frac{\left(exp\left(44.14 \pm 5.12\right) exp\left(-\left(14920 \pm 1558\right)/T\right)\right) \cdot C_{cat} - \left(exp\left(45.14 \pm 4.97\right) exp\left(-\left(15318 \pm 1513\right)/T\right)\right) \cdot C_{cat} \cdot C_{Sk} \cdot C_w}{\left(1 + \left(exp\left(51.17 \pm 8.42\right) exp\left(-\left(15938 \pm 2583\right)/T\right) \cdot C_w\right)\right)^2}$$

BIBLIOGRAFÍA

BIBLIOGRAFÍA

Akaike, H. (1974). A new look at the statistical model identification. *IEEE Transactions on Automatic Control* **19** (6): 716-723.

Altaras, N.E., Cameron, D.C. (1999). Metabolic engineering of a 1,2-propanediol pathway in Escherichia coli. *Applied and Environmental Microbiology* **65** (3): 1180-1185.

Altaras, N.E., Etzel, M.R., Cameron, D.C. (2001). Conversion of sugars to 1,2-propanediol by Thermoanaerobacterium thermosaccharolyticum HG-8. *Biotechnology Progress* **17** (1): 52-56.

Alvarez, M.G., Frey, A.M., Bitter, J.H., Segarra, A.M., de Jong, K.P., Medina, F. (2013). On the role of the activation procedure of supported hydrotalcites for base catalyzed reactions: Glycerol to glycerol carbonate and self-condensation of acetone. *Applied Catalysis B-Environmental* **134** 231-237.

Alvarez, M.G., Pliskova, M., Segarra, A.M., Medina, F., Figueras, F. (2012). Synthesis of glycerol carbonates by transesterification of glycerol in a continuous system using supported hydrotalcites as catalysts. *Applied Catalysis B-Environmental* **113** 212-220.

Alvarez, M.G., Segarra, A.M., Contreras, S., Sueiras, J.E., Medina, F., Figueras, F. (2010). Enhanced use of renewable resources: Transesterification of glycerol catalyzed by hydrotalcite-like compounds. *Chemical Engineering Journal* **161** (3): 340-345.

Arechederra, R.L., Treu, B.L., Minteer, S.D. (2007). Development of glycerol/O-2 biofuel cell. *Journal of Power Sources* **173** (1): 156-161.

Aresta, M., Dibenedetto, A., Nocito, F., Pastore, C. (2006). A study on the carboxylation of glycerol to glycerol carbonate with carbon dioxide: The role of the catalyst, solvent and reaction conditions. *Journal of Molecular Catalysis A: Chemical* **257** (1-2): 149-153.

Bai, R., Wang, S., Mei, F., Li, T., Li, G. (2011). Synthesis of glycerol carbonate from glycerol and dimethyl carbonate catalyzed by KF modified hydroxyapatite. *Journal of Industrial and Engineering Chemistry* **17** (4): 777-781.

Bai, R., Wang, Y., Wang, S., Mei, F., Li, T., Li, G. (2013). Synthesis of glycerol carbonate from glycerol and dimethyl carbonate catalyzed by NaOH/gamma-Al2O3. *Fuel Processing Technology* **106** 209-214.

Bancquart, S., Vanhove, C., Pouilloux, Y., Barrault, J. (2001). Glycerol transesterification with methyl stearate over solid basic catalysts I. Relationship between activity and basicity. *Applied Catalysis A: General* **218** (1-2): 1-11.

Bandres, M., Deswartvaegher, A., De Caro, P., Senet, J.-P., Thiebaud Roux, S. (2012). Plasticizer of natural origin for nail polish. US 08187576.

Barbirato, F., Soucaille, P., Bories, A. (1996). Physiologic mechanisms involved in accumulation of 3-hydroxypropionaldehyde during fermentation of glycerol by Enterobacter agglomerans. *Applied and Environmental Microbiology* **62** (12): 4405-4409.

Barbosa, D.J., Carvalho, D.S.C.D., Marcio, N.P. (2009). Process to transform glicerol and/or biomass into products of greater aggregate value. Patent WO 2009073938 A1.

Barrault, J., Bancquart, S., Pouilloux, Y. (2004a). Selective glycerol transesterification over mesoporous basic catalysts. *Comptes Rendus Chimie* **7** (6-7): 593-599.

Barrault, J., Clacens, J.M., Pouilloux, Y. (2004b). Selective oligomerization of glycerol over mesoporous catalysts. *Topics in Catalysis* **27** (1-4): 137-142.

Bauer, F., Hulteberg, C. (2013). Is there a future in glycerol as a feedstock in the production of biofuels and biochemicals? *Biofuels Bioproducts & Biorefining* **7** (1): 43-51.

Behr, A., Eilting, J., Irawadi, K., Leschinski, J., Lindner, F. (2008a). Improved utilisation of renewable resources: New important derivatives of glycerol. *Green Chemistry* **10** (1): 13-30.

Behr, A., Eilting, J., Irawadi, K., Leschinski, J., Lindner, F. (2008b). New chemical products on the basis of glycerol. *Chimica Oggi-Chemistry Today* **26** (1): 32-36.

Behr, A., Gomes, J.P. (2010). The refinement of renewable resources: New important derivatives of fatty acids and glycerol. *European Journal of Lipid Science and Technology* **112** (1): 31-50.

Behr, A., Obendorf, L. (2001). Process development for acid-catalysed etherification of glycerol with isobutene to form glycerol tertiary butyl ethers. *Chemie Ingenieur Technik* **73** (11): 1463-1467.

Behr, A., Urschey, M., Brehme, V.A. (2003). Aqueous biphasic catalysis as a powerful tool for catalyst recycling in telomerization and hydrogenation chemistry. *Green Chemistry* **5** (2): 198-204.

Bell, J.B., Silver, L., Currier, V.A. (1959). Method for preparing glycerin carbonate. Patent US2915529.

Benoit, M., Brissonnet, Y., Guelou, E., Vigier, K.D.O., Barrault, J., Jerome, F. (2010). Acid-Catalyzed Dehydration of Fructose and Inulin with Glycerol or Glycerol Carbonate as Renewably Sourced Co-Solvent. *Chemsuschem* **3** (11): 1304-1309.

Bergmann, F., Buchberger, B., Donner, H., Lassonczyk, N. (2009). Use of acetals for the isolation of nucleic acids. Patent WO2008071385-A8.

Bevinakatti, H.S., Frank, J., Waite, A.G., Francke, J. (2009). New polyglycerol ether of a sorbitan carboxylic acid ester useful as oil in water or water in oil emulsion, solubilizers, emollients, dispersants, spreading agents and rheology modifiers and dispersants. WO2009016375-A2; WO2009016375-A3; EP2183235-A2; US2010184871-A1; IN201000539-P1; JP2010535183-W; CN102083808-A.

Blanco, A., De la Fuente, E., Negro, C., Monte, M.C., Tijero, J. (2002a). Focused beam reflectant measurement as a tool to measure flocculation. *Tappi Journal* **1** (10): 14-20.

Blanco, A., Fuente, E., Negro, C., Tijero, J. (2002b). Flocculation monitoring: Focused beam reflectance measurement as a measurement tool. *Canadian Journal of Chemical Engineering* **80** (4): 734-740.

Bogaart, V. (2009). Glycerin market brief. Proceedings of the 7th ICIS world oleochemicals conference, Germany.

Bournay, L., Casanave, D., Delfort, B., Hillion, G., Chodorge, J.A. (2005). New heterogeneous process for biodiesel production: A way to improve the quality and the value of the crude glycerin produced by biodiesel plants. *Catal. Today* **106** (1-4): 190-192.

Boxall, J.A., Koh, C.A., Sloan, E.D., Sum, A.K., Wu, D.T. (2009). Measurement and Calibration of Droplet Size Distributions in Water-in-Oil Emulsions by Particle Video Microscope and a Focused Beam Reflectance Method. *Industrial & Engineering Chemistry Research* **49** (3): 1412-1418.

Britt, H.I., Luecke, R.H. (1973). The estimation of parameters in nonlinear, implicit models. . *Technometrics* **15** 233-247.

Brooker, A.T. (2011). Solid detergent composition comprising glycerol carbonate. Patent EP2380958A1.

Bruchmann, B., Haberle, K., Gruner, H., Hirn, M. (1999a). Preparation of cyclic acetals or ketals US Patent 5,917,059.

Bruchmann, B., Haeberle, K., Gruner, H., Hirn, M. (1999b). Preparation of cyclic acetals or ketals, especially isopropylidene glycerin|comprising distilling off some of aldehyde or ketone during reaction with polyol. EP842929-A.

Budavari, S. (1989). Merck Index, 11th edition. Rahway, New Jersey

Buhler, W., Dinjus, E., Ederer, H.J., Kruse, A., Mas, C. (2002). Ionic reactions and pyrolysis of glycerol as competing reaction pathways in near- and supercritical water. *Journal of Supercritical Fluids* **22** (1): 37-53.

Cadenas, M., Bringue, R., Fite, C., Ramirez, E., Cunill, F. (2011). Liquid-Phase Oligomerization of 1-Hexene Catalyzed by Macroporous Ion-Exchange Resins. *Topics in Catalysis* **54** (13-15): 998-1008.

Calvino-Casilda, V., Stawicka, K., Trejda, M., Ziolek, M., Banares, M.A. (2014). Real-Time Raman Monitoring and Control of the Catalytic Acetalization of Glycerol with Acetone over Modified Mesoporous Cellular Foams. *Journal of Physical Chemistry C* **118** (20): 10780-10791.

Cantero, M., Duchamp, G., Gasse, J.J. (2010). NMP-free formulations of neonicotinoids. Patent EP2266400 A1.

Clarkson, J.S., Walker, A.J., Wood, M.A. (2001). Continuous reactor technology for ketal formation: An improved synthesis of solketal. *Organic Process Research & Development* **5** (6): 630-635.

Clements, J. (2003). Reactive applications of cyclic alkylene carbonates for Huntsman Petrochemical Corporation, Austin, TX.

Climent, M.J., Corma, A., De Frutos, P., Iborra, S., Noy, M., Velty, A., Concepción, P. (2010). Chemicals from biomass: Synthesis of glycerol carbonate by transesterification and carbonylation with urea with hydrotalcite catalysts. The role of acid-base pairs. *Journal of Catalysis* **269** (1): 140-149.

CNE (1998). Ley 34/1998 (Ley de Hidrocarburos). 5º edición. BOE núm. 241, de 08/10/1998.

Constable, D.J.C., Curzons, A.D., Cunningham, V.L. (2002). Metrics to 'green' chemistry - which are the best? *Green Chemistry* **4** (6): 521-527.

Corma, A., Huber, G.W., Sauvanaud, L., O'Connor, P. (2007). Processing biomass-derived oxygenates in the oil refinery: Catalytic cracking (FCC) reaction pathways and role of catalyst. *Journal of Catalysis* **247** (2): 307-327.

Corma, A., Huber, G.W., Sauvanauda, L., O'Connor, P. (2008). Biomass to chemicals: Catalytic conversion of glycerol/water mixtures into acrolein, reaction network. *Journal of Catalysis* **257** (1): 163-171.

Cortright, R.D., Davda, R.R., Dumesic, J.A. (2002). Hydrogen from catalytic reforming of biomass-derived hydrocarbons in liquid water. *Nature* **418** (6901): 964-967.

Chafer, A., de la Torre, J., Lladosa, E., Monton, J.B. (2014). Measurements and correlation at different temperatures of liquid-liquid equilibria of 2-butanol or 2-methyl-2-butanol+1,2,3-propanetriol plus water ternary systems. *Fluid Phase Equilibria* **377** 38-44.

Chai, S.-H., Yan, B., Tao, L.-Z., Liang, Y., Xu, B.-Q. (2014). Sustainable production of acrolein: Catalytic gas-phase dehydration of glycerol over dispersed tungsten oxides on alumina, zirconia and silica. *Catal. Today* **234** 215-222.

Chang, C.-S., Wu, P.-L. (2007). Synthesis of triglycerides of phenylalkanoic acids by lipase-catalyzed esterification in a solvent-free system. *Journal of Biotechnology* **127** (4): 694-702.

Charles, G., Clacens, J.M., Pouilloux, Y., Barrault, J. (2003). Preparation of diglycerol and triglycerol via direct polymerisation of glycerol with basic mesoporous catalysators. *Ocl-Oleagineux Corps Gras Lipides* **10** (1): 74-82.

Chen, Y., Wang, Z., Li, L. (2014). Liquid Liquid Equilibria for Ternary Systems: Methyl Butyl Ketone plus Phenol plus Water and Methyl Butyl Ketone plus Hydroquinone + Water at 298.15 K and 323.15 K. *Journal of Chemical and Engineering Data* **59** (9): 2750-2755.

Chiao, J.-s., Sun, Z.-h. (2007). History of the acetone-butanol-ethanol fermentation industry in China: Development of continuous production technology. *Journal of Molecular Microbiology and Biotechnology* **13** (1-3): 12-14.

Chiappe, C., Rajamani, S. (2012). Synthesis of glycerol carbonate from glycerol and dimethyl carbonate in basic ionic liquids. *Pure and Applied Chemistry* **84** (3): 755-762.

Cho, H.-J., Kwon, H.-M., Tharun, J., Park, D.-W. (2010). Synthesis of glycerol carbonate from ethylene carbonate and glycerol using immobilized ionic liquid catalysts. *Journal of Industrial and Engineering Chemistry* **16** (5): 679-683.

Chopade, S.P. (1999). Ion-exchange resin-catalysed ketalization of acetone with 1,4-and 1,2-diols: use of molecular sieve in reactive distillation. *Reactive & Functional Polymers* **42** (3): 201-212.

da Silva, C.X.A., Goncalves, V.L.C., Mota, C.J.A. (2009). Water-tolerant zeolite catalyst for the acetalisation of glycerol. *Green Chemistry* **11** (1): 38-41.

Dalelio, G.F., Huemmer, T. (1967). Preparation and polymerization of some vinyl monomers containig 2-oxo-1,3-dioxolane group. *Journal of Polymer Science Part A1: Polymer Chemistry* **5** (2PA1): 307-341.

Dawodu, F.A., Ayodele, O.O., Xin, J., Zhang, S. (2014). Dimethyl carbonate mediated production of biodiesel at different reaction temperatures. *Renewable Energy* **68** 581-587.

de Azevedo Rocha, E.G., Follegatti-Romero, L.A., Duvoisin, S., Jr., Aznar, M. (2014). Liquid-liquid equilibria for ternary systems containing ethylic palm oil biodiesel plus ethanol plus glycerol/water: Experimental data at 298.15 and 323.15 K and thermodynamic modeling. *Fuel* **128** 356-365.

Delfort, B., Durand, I., Jaecker, A., Lacome, T., Montagne, X., Paille, F. (2004). Reducing air pollution. Patent US20040025417 A1.

Deutsch, J., Martin, A., Lieske, H. (2007). Investigations on heterogeneously catalysed condensations of glycerol to cyclic acetals. *Journal of catalysis* **245** (2): 428-435.

Eschenbruch, B., Dittrich, H.H. (1986). Metabolism of acetic acid bacteria in relation to their importance to wine quality. *Zentralblatt Fur Mikrobiologie* **141** (4): 279-289.

Fan, C., Xu, C., Liu, C., Huang, Z., Liu, J., Ye, Z. (2012). Ketalization of glycerol with acetone to o-heterocyclic compounds over ZrO_2-SiO_2 solid acid catalysts. *Heterocycles* **85** (12): 2977-2986.

Fang, Y.-J., Qian, J.-M. (2005). Isobaric Vapor−Liquid Equilibria of Binary Mixtures Containing the Carbonate Group −OCOO−. *Journal of Chemical & Engineering Data* **50** (2): 340-343.

Ferreira, P., Fonseca, I.M., Ramos, A.M., Vital, J., Castanheiro, J.E. (2010a). Valorisation of glycerol by condensation with acetone over silica-included heteropolyacids. *Applied Catalysis B-Environmental* **98** (1-2): 94-99.

Ferreira, P., Fonseca, I.M., Ramos, A.M., Vital, J., Castanheiro, J.E. (2010b). Valorisation of glycerol by condensation with acetone over silica-included heteropolyacids. *Applied Catalysis B: Environmental* **98** (1-2): 94-99.

Frusteri, F., Frusteri, L., Cannilla, C., Bonura, G. (2012). Catalytic etherification of glycerol to produce biofuels over novel spherical silica supported Hyflon (R) catalysts. *Bioresource Technology* **118** 350-358.

Gade, S.M., Munshi, M.K., Chherawalla, B.M., Rane, V.H., Kelkar, A.A. (2012). Synthesis of glycidol from glycerol and dimethyl carbonate using ionic liquid as a catalyst. *Catalysis Communications* **27** 184-188.

Galdeano Villegas, C., Santos, V.E., Zazo, M., Luis Garcia, J., Garcia-Ochoa, F. (2007). Fermentation of glycerol to 1,3-propanediol by Klebsiella oxytoca NRTL B-199: Study of product inhibition. *Journal of Biotechnology* **131** (2): S102-S102.

Garcia, E., Laca, M., Perez, E., Garrido, A., Peinado, J. (2008). New Class of Acetal Derived from Glycerin as a Biodiesel Fuel Component. *Energy & Fuels* **22** (6): 4274-4280.

Garcia, J.I., Garcia-Marin, H., Pires, E. (2014). Glycerol based solvents: synthesis, properties and applications. *Green Chemistry* **16** (3): 1007-1033.

George, J., Patel, Y., Pillai, S.M., Munshi, P. (2009). Methanol assisted selective formation of 1,2-glycerol carbonate from glycerol and carbon dioxide using (Bu_2SnO)-Bu-n as a catalyst. *Journal of Molecular Catalysis A: Chemical* **304** (1-2): 1-7.

Ghandi, M., Mostashari, A., Karegar, M., Barzegar, M. (2007). Efficient synthesis of alpha-monoglycerides via solventless condensation of fatty acids with glycerol carbonate. *Journal of the American Oil Chemists Society* **84** (7): 681-685.

Gholami, Z., Abdullah, A.Z., Lee, K.-T. (2014). Dealing with the surplus of glycerol production from biodiesel industry through catalytic upgrading to polyglycerols and other value-added products. *Renewable and Sustainable Energy Reviews* **39** (0): 327-341.

Gottlieb, K., Neitsch, H., Wessendorf, R. (1994). Glycerol: A sustainable raw material. *Chemie Ingenieur Technik* **66** (1): 64-66.

Hazimah, A.H., Ooi, T.L., Salmiah, A. (2003). Recovery of glycerol and diglycerol from glycerol pitch. *Journal of Oil Palm Research* **15** (1): 1-5.

Helou, M., Carpentier, J.-F., Guillaume, S.M. (2011). Poly(carbonate-urethane): an isocyanate-free procedure from alpha,omega-di(cyclic carbonate) telechelic poly(trimethylenecarbonate)s. *Green Chemistry* **13** (2): 266-271.

Hervert, B., McCarthy, P.D., Palencia, H. (2014). Room temperature synthesis of glycerol carbonate catalyzed by N-heterocyclic carbenes. *Tetrahedron Letters* **55** (1): 133-136.

Hillion, G., Delfort, B., Durand, I. (2013). Method for producing biofuels, transforming triglycerides into at least two biofuel families: fatty acid monoesters and ethers and/or soluble glycerol acetals. Patent US8419810 B2.

Hoang, T., Danuthai, T., Lobban, L., Resasco, D., Mallinson, R. (2007). Catalytic conversion of glycerol to fuel. *AIChE Annual Meeting*.

Hof, R.P., Kellogg, R.M. (1996). Synthesis and lipase-catalyzed resolution of 5-(hydroxymethyl)-1,3-dioxolan-4-ones: masked glycerol analogs as potential building blocks for pharmaceuticals. *Journal of Organic Chemistry* **61** (10): 3423-3427.

Hu, J., Li, J., Gu, Y., Guan, Z., Mo, W., Ni, Y., Li, T., Li, G. (2010). Oxidative carbonylation of glycerol to glycerol carbonate catalyzed by $PdCl_2$(phen)/KI. *Applied Catalysis A: General* **386** (1-2): 188-193.

Huang, H., Gong, C.S., Tsao, G.T. (2002). Production of 1,3-propanediol by Klebsiella pneumoniae. *Applied Biochemistry and Biotechnology* **98** 687-698.

IDAE (2011). Resumen del Plan de Energías Renovables 2011-2020.

IPCC (2007). Summary for Policymakers. In Cilmate Change 2007: The Physical Science Basis. Contribution of Working Group I to the fourth assessment report of the International Panel on Climate Change. Cambridge University Press, Cambridge, U.K.

IPCC (2014). Fifth Assessment Synthesis Report. Climate Change 2014. Synthesis Report. Available at http://www.ipcc.ch/.

Izutsu, K., Nakamura, T., Miyoshi, K., Kurita, K. (1996). Potentiometric study of complexation and solvation of lithium ions in some solvents related to lithium batteries. *Electrochimica Acta* **41** (16): 2523-2527.

Jolly, J., Hitzmann, B., Ramalingam, S., Ramachandran, K.B. (2014). Biosynthesis of 1,3-propanediol from glycerol with Lactobacillus reuteri: Effect of operating variables. *Journal of Bioscience and Bioengineering* **118** (2): 188-194.

Jung, H., Lee, Y., Kim, D., Han, S.O., Kim, S.W., Lee, J., Kim, Y.H., Park, C. (2012). Enzymatic production of glycerol carbonate from by-product after biodiesel manufacturing process. *Enzyme and Microbial Technology* **51** (3): 143-147.

Jurczak, J., Pikul, S., Bauer, T. (1986). *Tetrahedron* **42** 447-488.

Kahre, J., Loehl, T., Tesmann, H., Hensen, H. (1999). Surface-active compositions, especially cosmetics, containing glycerol carbonate as emulsifier. WO9932216-A; EP1042055-A; DE19756454-C; DE19756454-A; DE19756454-A1; DE19756454-C1; WO9932216-A1; EP1042055-A1; JP2001526106-W.

Kai, T., Mak, G.L., Wada, S., Nakazato, T., Takanashi, H., Uemura, Y. (2014). Production of biodiesel fuel from canola oil with dimethyl carbonate using an active sodium methoxide catalyst prepared by crystallization. *Bioresource Technology* **163** 360-363.

Karinen, R.S., Krause, A.O.I. (2006). New biocomponents from glycerol. *Applied Catalysis A: General* **306** (0): 128-133.

Kenar, J. (2007). Glycerol as a platform chemical: Sweet opportunities on the horizon? *Lipid Technology* **19** (11): 249-253.

Khayoon, M.S., Hameed, B.H. (2013). Mg1+xCa1-xO2 as reusable and efficient heterogeneous catalyst for the synthesis of glycerol carbonate via the transesterification of glycerol with dimethyl carbonate. *Applied Catalysis A: General* **466** 272-281.

Kim, D.-W., Kim, M.-J., Roshith, K., Kim, M.-I., Kwak, J.-Y., Park, D.-W. (2014a). Comparative catalytic activity of supported ZnBr2-containing ionic liquid catalysts for preparation of glycerol carbonate by glycerolysis of urea. *Korean Journal of Chemical Engineering* **31** (6): 972-980.

Kim, D.-W., Park, K.-A., Kim, M.-J., Kang, D.-H., Yang, J.-G., Park, D.-W. (2014b). Synthesis of glycerol carbonate from urea and glycerol using polymer-supported metal containing ionic liquid catalysts. *Applied Catalysis A: General* **473** 31-40.

Kim, D.-W., Park, M.-S., Selvaraj, M., Park, G.-A., Lee, S.-D., Park, D.-W. (2011). Catalytic performance of polymer-supported ionic liquids in the synthesis of glycerol carbonate from glycerol and urea. *Research on Chemical Intermediates* **37** (9): 1305-1312.

Kim, I., Kim, J., Lee, D. (2014c). A comparative study on catalytic properties of solid acid catalysts for glycerol acetylation at low temperatures. *Applied Catalysis B-Environmental* **148** 295-303.

Kim, S.C., Kim, Y.H., Lee, H., Yoon, D.Y., Song, B.K. (2007). Lipase-catalyzed synthesis of glycerol carbonate from renewable glycerol and dimethyl carbonate through transesterification. *Journal of Molecular Catalysis B-Enzymatic* **49** 75-78.

Kirk, R., Othmer, E. (2007). Encyclopedia of Chemical Technology. 5th edition. Sons., J.W. New York

Klepáčová, K., Mravec, D., Hájeková, E., Bajus, M. (2003). Etherification of glycerol. *Petroleum and coal* **45** (1): 54-57.

Korzh, R.V., Bortyshevskii, V.A., Tkachenko, T.V., Evdokimenko, V.A., Boiko, V.V. (2007). Physicochemical properties of membranes based on MSC-H and purolite CT-275 sulfocation-exchange resins. *Russian Journal of Applied Chemistry* **80** (8): 1335-1340.

Kovvali, A.S., Sirkar, K.K. (2002). Carbon dioxide separation with novel solvents as liquid membranes. *Industrial & Engineering Chemistry Research* **41** (9): 2287-2295.

Kwon, Y., Schouten, K.J.P., Koper, M.T.M. (2011). Mechanism of the Catalytic Oxidation of Glycerol on Polycrystalline Gold and Platinum Electrodes. *Chemcatchem* **3** (7): 1176-1185.

Ladero, M., de Gracia, M., Jose Tamayo, J., Lopez de Ahumada, I., Trujillo, F., Garcia-Ochoa, F. (2011). Kinetic modelling of the esterificatiion of rosin and glycerol: Application to industrial operation. *Chemical Engineering Journal* **169** (1-3): 319-328.

Ladero, M., de Gracia, M., Trujillo, F., Garcia-Ochoa, F. (2012). Phenomenological kinetic modelling of the esterification of rosin and polyols. *Chemical Engineering Journal* **197** 387-397.

Lameiras, P., Boudesocque, L., Mouloungui, Z., Renault, J.-H., Wieruszeski, J.-M., Lippens, G., Nuzillard, J.-M. (2011). Glycerol and glycerol carbonate as ultraviscous solvents for mixture analysis by NMR. *Journal of Magnetic Resonance* **212** (1): 161-168.

Lamers, P., Hamelinck, C., Junginger, M., Faaij, A. (2011). International bioenergy trade-A review of past developments in the liquid biofuel market. *Renewable & Sustainable Energy Reviews* **15** (6): 2655-2676.

Lee, S.-D., Park, M.-S., Kim, D.-W., Kim, I., Park, D.-W. (2014). Catalytic performance of ion-exchanged montmorillonite with quaternary ammonium salts for the glycerolysis of urea. *Catal. Today* **232** 127-133.

Len, C., Luque, R. (2014). Continuous flow transformations of glycerol to valuable products: an overview. *Sustainable Chemical Processes* **2** (1): 1-10.

Li, C., Lesnik, K.L., Liu, H. (2013). Microbial Conversion of Waste Glycerol from Biodiesel Production into Value-Added Products. *Energies* **6** (9): 4739-4768.

Li, J., Wang, T. (2011a). Chemical equilibrium of glycerol carbonate synthesis from glycerol. *Journal of Chemical Thermodynamics* **43** (5): 731-736.

Li, J., Wang, T. (2011b). On the deactivation of alkali solid catalysts for the synthesis of glycerol carbonate from glycerol and dimethyl carbonate. *Reaction Kinetics Mechanisms and Catalysis* **102** (1): 113-126.

Li, L., Koranyi, T.I., Sels, B.F., Pescarmona, P.P. (2012). Highly-efficient conversion of glycerol to solketal over heterogeneous Lewis acid catalysts. *Green Chemistry* **14** (6): 1611-1619.

Li, Q.B., Zhang, W.Y., Zhao, N., Wei, W., Sun, Y.H. (2006). Synthesis of cyclic carbonates from urea and diols over metal oxides. *Catal. Today* **115** (1-4): 111-116.

Lilja, J., Murzin, D.Y., Salmi, T., Aumo, J., Arvela, P.M., Sundell, M. (2002). Esterification of different acids over heterogeneous and homogeneous catalysts and correlation with the Taft equation. *Journal of Molecular Catalysis a-Chemical* **182** (1): 555-563.

Liotta, F.J., Kesling, H.S., Karas, L.J. (2003). Transesterifying fat with alcohol and iron oxide or alumina catalyst|comprises diesel fuel hydrocarbon(s) and particulate emission reducing amt. of di: or tri:alkyl glycerol ether. EP641854-A; US5308365-A; EP641854-A1; JP7082576-A; EP641854-B1; DE69415617-E.

Liu, J., Yuan, Y., Pan, Y., Huang, Z., Yang, B. (2014). Liquid-liquid equilibrium for systems of glycerol and glycerol tert-butyl ethers. *Fluid Phase Equilibria* **365** 50-57.

Lutz, J., Gutsche, B., Bunte, R., Jordan, R. (1998). Process for the production of diglycerol. Patent US5710350 A.

Ma, L., He, D. (2009). Hydrogenolysis of Glycerol to Propanediols Over Highly Active Ru-Re Bimetallic Catalysts. *Topics in Catalysis* **52** (6-7): 834-844.

Magniont, C., Escadeillas, G., Oms-Multon, C., De Caro, P. (2010). The benefits of incorporating glycerol carbonate into an innovative pozzolanic matrix. *Cement and Concrete Research* **40** (7): 1072-1080.

Maksimov, A.L., Nekhaev, A.I., Ramazanov, D.N., Arinicheva, Y.A., Dzyubenko, A.A., Khadzhiev, S.N. (2011). Preparation of High-Octane Oxygenate Fuel Components from Plant-Derived Polyols. *Pet. Chem.* **51** (1): 61-69.

Malyaadri, M., Jagadeeswaraiah, K., Prasad, P.S.S., Lingaiah, N. (2011). Synthesis of glycerol carbonate by transesterification of glycerol with dimethyl carbonate over Mg/Al/Zr catalysts. *Applied Catalysis A: General* **401** (1-2): 153-157.

Melero, J.A., Vicente, G., Morales, G., Paniagua, M., Moreno, J.M., Roldan, R., Ezquerro, A., Perez, C. (2008). Acid-catalyzed etherification of bio-glycerol and isobutylene over sulfonic mesostructured silicas. *Applied Catalysis A: General* **346** (1-2): 44-51.

Menezes, F.D.L., Guimaraes, M.D.O., da Silva, M.J. (2013). Highly Selective SnCl2-Catalyzed Solketal Synthesis at Room Ternperature. *Industrial & Engineering Chemistry Research* **52** (47): 16709-16713.

Min, J.Y., Lee, E.Y. (2011). Lipase-catalyzed simultaneous biosynthesis of biodiesel and glycerol carbonate from corn oil in dimethyl carbonate. *Biotechnology Letters* **33** (9): 1789-1796.

Molinero, L., Ladero, M., Tamayo, J.J., Esteban, J., Garcia-Ochoa, F. (2013). Thermal esterification of cinnamic and p-methoxycinnamic acids with glycerol to cinnamate glycerides in solventless media: A kinetic model. *Chemical Engineering Journal* **225** 710-719.

Molinero, L., Ladero, M., Tamayo, J.J., Garcia-Ochoa, F. (2014). Homogeneous catalytic esterification of glycerol with cinnamic and methoxycinnamic acids to cinnamate glycerides in solventless medium: Kinetic modeling. *Chemical Engineering Journal* **247** 174-182.

Mota, C.J.A., da Silva, C.X.A., Rosenbach, N., Jr., Costa, J., da Silva, F. (2010). Glycerin Derivatives as Fuel Additives: The Addition of Glycerol/Acetone Ketal (Solketal) in Gasolines. *Energy & Fuels* **24** 2733-2736.

Mouloungui, Z., Marechal, P., Truong, D.N. (2014). Glycerol polycarbonate, organic compositions containing same and method for obtaining said compositions. Patent CA2576434 C.

Mouloungui, Z., Pelet, S. (2001). Study of the acyl transfer reaction: Structure and properties of glycerol carbonate esters. *European Journal of Lipid Science and Technology* **103** (4): 216-222.

Murase, A. (1989). Nail lacquer remover composition. Patent US4801331A.

Naik, P.U., Petitjean, L., Refes, K., Picquet, M., Plasseraud, L. (2009). Imidazolium-2-Carboxylate as an Efficient, Expeditious and Eco-Friendly Organocatalyst for

Glycerol Carbonate Synthesis. *Advanced Synthesis & Catalysis* **351** (11-12): 1753-1756.

Nanda, M.R., Yuan, Z., Qin, W., Ghaziaskar, H.S., Poirier, M.-A., Xu, C. (2014a). Catalytic conversion of glycerol to oxygenated fuel additive in a continuous flow reactor: Process optimization. *Fuel* **128** 113-119.

Nanda, M.R., Yuan, Z., Qin, W., Ghaziaskar, H.S., Poirier, M.-A., Xu, C. (2014b). A new continuous-flow process for catalytic conversion of glycerol to oxygenated fuel additive: Catalyst screening. *Applied Energy* **123** 75-81.

Nanda, M.R., Yuan, Z., Qin, W., Ghaziaskar, H.S., Poirier, M.-A., Xu, C.C. (2014c). Thermodynamic and kinetic studies of a catalytic process to convert glycerol into solketal as an oxygenated fuel additive. *Fuel* **117** 470-477.

Nandan, D., Sreenivasulu, P., Konathala, L.N.S., Kumar, M., Viswanadham, N. (2013). Acid functionalized carbon-silica composite and its application for solketal production. *Microporous and Mesoporous Materials* **179** 182-190.

Nemirowsky, J. (1885). Über die Einwirkung von Chlorkohlenoxyd auf Glycolchlorhydrin. *Journal für Praktische Chemie* **31** (1): 173-175.

Ni, Y., Sun, Z. (2009). Recent progress on industrial fermentative production of acetone-butanol-ethanol by Clostridium acetobutylicum in China. *Applied Microbiology and Biotechnology* **83** (3): 415-423.

Nomura, T., Hayashi, T., Okutsu, M. (2006). Plant activator used for cultivating plants such as vegetables, fruits, bulbs, flowers, grains and herbs, contains carbonate compound. JP2006182684-A; JP4754210-B2.

Ochoa-Gomez, J.R., Gomez-Jimenez-Aberasturi, O., Maestro-Madurga, B., Pesquera-Rodriguez, A., Ramirez-Lopez, C., Lorenzo-Ibarreta, L., Torrecilla-Soria, J., Villaran-Velasco, M.C. (2009). Synthesis of glycerol carbonate from glycerol and dimethyl carbonate by transesterification: Catalyst screening and reaction optimization. *Applied Catalysis A: General* **366** (2): 315-324.

Ochoa-Gomez, J.R., Gomez-Jimenez-Aberasturi, O., Ramirez-Lopez, C., Belsue, M. (2012a). A Brief Review on Industrial Alternatives for the Manufacturing of Glycerol Carbonate, a Green Chemical. *Organic Process Research & Development* **16** (3): 389-399.

Ochoa-Gomez, J.R., Gomez-Jimenez-Aberasturi, O., Ramirez-Lopez, C., Maestro-Madurga, B. (2012b). Synthesis of glycerol 1,2-carbonate by transesterification

of glycerol with dimethyl carbonate using triethylamine as a facile separable homogeneous catalyst. *Green Chemistry* **14** (12): 3368-3376.

Othmer, D.F., Tobias, P.E. (1942). Toluene and Acetaldehyde Systems, Tie Line Correlation, Partial Pressures of Ternary Liquid Systems and the Prediction of Tie Lines. *Industrial & Engineering Chemistry* **34** 693-696.

Ou, G., He, B., Yuan, Y. (2011). Lipases are soluble and active in glycerol carbonate as a novel biosolvent. *Enzyme and Microbial Technology* **49** (2): 167-170.

Pagliaro, M., Ciriminna, R., Kimura, H., Rossi, M., Della Pina, C. (2009). Recent advances in the conversion of bioglycerol into value-added products. *European Journal of Lipid Science and Technology* **111** (8): 788-799.

Pagliaro, M., Rossi, M. (2008). The Future of Glycerol: New Uses of a Versatile Raw Material. RSC Publishing, Cambridge, UK.

Pan, S., Zheng, L., Nie, R., Xia, S., Chen, P., Hou, Z. (2012). Transesterification of Glycerol with Dimethyl Carbonate to Glycerol Carbonate over Na-Based Zeolites. *Chinese Journal of Catalysis* **33** (11): 1772-1777.

Patel, Y., George, J., Pillai, S.M., Munshi, P. (2009). Effect of liophilicity of catalyst in cyclic carbonate formation by transesterification of polyhydric alcohols. *Green Chemistry* **11** (7): 1056-1060.

Pathak, K., Reddy, K.M., Bakhshi, N.N., Dalai, A.K. (2010). Catalytic conversion of glycerol to value added liquid products. *Applied Catalysis A: General* **372** (2): 224-238.

Perez-Pariente, J., Diaz, I., Mohino, F., Sastre, E. (2003). Selective synthesis of fatty monoglycerides by using functionalised mesoporous catalysts. *Applied Catalysis A: General* **254** (2): 173-188.

Perez-Sanchez, M., Sandoval, M., Hernaiz, M.J. (2012). Bio-solvents change regioselectivity in the synthesis of disaccharides using Biolacta beta-galactosidase. *Tetrahedron* **68** (9): 2141-2145.

Piasecki, A., Sokolowski, A., Burczyk, B., Kotlewska, U. (1997). Chemical structure and surface activity .30. Synthesis and surface properties of chemodegradable anionic surfactants: Sodium (2-n-alkyl-1,3-dioxan-5-yl)sulfates. *Journal of the American Oil Chemists Society* **74** (1): 33-37.

Pico, M.P., Maria Rosas, J., Rodriguez, S., Santos, A., Romero, A. (2013). Glycerol etherification over acid ion exchange resins: effect of catalyst concentration and

reusability. *Journal of Chemical Technology and Biotechnology* **88** (11): 2027-2038.

Pouilloux, Y., Metayer, S., Barrault, J. (2000). Synthesis of glycerol monooctadecanoate from octadecanoic acid and glycerol. Influence of solvent on the catalytic properties of basic oxides. *Comptes Rendus De L Academie Des Sciences Serie Ii Fascicule C-Chimie* **3** (7): 589-594.

Quispe, C.A.G., Coronado, C.J.R., Carvalho, J.A., Jr. (2013). Glycerol: Production, consumption, prices, characterization and new trends in combustion. *Renewable & Sustainable Energy Reviews* **27** 475-493.

Ramayya, S., Brittain, A., Dealmeida, C., Mok, W., Antal, M.J. (1987). Acid-catalyzed dehydration of alcohols in supercritical water. *Fuel* **66** (10): 1364-1371.

Ramírez-López, C., Nieto-Maestre, J., Gómez-Jiménez-Aberasturi, O., Ochoa-Gómez, J.R., Arteche-Calvo, A., Belsue, M., Aragón, J.J., Dobarganes, M.C., Ruiz-Méndez, M.V. (2012). Production of biodiesel from high acidic raw materials. Design and development of an heterogeneous catalytic process, ANQUE International Congress of Chemical Engineering Seville (Spain).

Reddy, P.S., Sudarsanam, P., Mallesham, B., Raju, G., Reddy, B.M. (2011). Acetalisation of glycerol with acetone over zirconia and promoted zirconia catalysts under mild reaction conditions. *Journal of Industrial and Engineering Chemistry* **17** (3): 377-381.

Renon, H., Prausnitz, J.M. (1968). Local Compositions in Thermodynamic Excess Functions for Liquid Mixtures. *AIChE Journal* **14** 135-144.

Rokicki, G., Kuran, W., Pogorzelskamarciniak, B. (1984). Cyclic carbonates from carbon dioxide and oxiranes *Monatshefte Fur Chemie* **115** (2): 205-214.

Rokicki, G., Rakoczy, P., Parzuchowski, P., Sobiecki, M. (2005). Hyperbranched aliphatic polyethers obtained from environmentally benign monomer: glycerol carbonate. *Green Chemistry* **7** (7): 529-539.

Roldan, L., Mallada, R., Fraile, J.M., Mayoral, J.A., Menendez, M. (2009). Glycerol upgrading by ketalization in a zeolite membrane reactor. *Asia-Pacific Journal of Chemical Engineering* **4** (3): 279-284.

Royon, D., Locatelli, S., Gonzo, E.E. (2011). Ketalization of glycerol to solketal in supercritical acetone. *Journal of Supercritical Fluids* **58** (1): 88-92.

Seifert, C., Bowien, S., Gottschalk, G., Daniel, R. (2001). Identification and expression of the genes and purification and characterization of the gene products involved

in reactivation of coenzyme B-12-dependent glycerol dehydratase of Citrobacter freundii. *European Journal of Biochemistry* **268** (8): 2369-2378.

Selva, M., Benedet, V., Fabris, M. (2012). Selective catalytic etherification of glycerol formal and solketal with dialkyl carbonates and K_2CO_3. *Green Chemistry* **14** (1): 188-200.

Shin, S.H., Hwang, I.-C., Park, S.-J., Choi, Y.-Y. (2013). Liquid-liquid equilibria for the pseudo-ternary system {aqueous sulfuric acid solution plus methyl ethyl ketone or methyl isopropyl ketone plus phosphonium-based ionic liquids} at 298.15 K and atmospheric pressure. *Fluid Phase Equilibria* **358** 1-6.

Shirani, M., Ghaziaskar, H.S., Xu, C. (2014). Optimization of glycerol ketalization to produce solketal as biodiesel additive in a continuous reactor with subcritical acetone using Purolite (R) PD206 as catalyst. *Fuel Processing Technology* **124** 206-211.

Showler, A.J., Darley, P.A. (1967). Condensation products of glycerol with aldehydes and ketones. 2-substituted m-dioxan-5-ols and 1,3-dioxolane-4-methanols. *Chemical Reviews* **67** (4): 427-440.

Simanjuntak, F.S.H., Kim, T.K., Lee, S.D., Ahn, B.S., Kim, H.S., Lee, H. (2011). CaO-catalyzed synthesis of glycerol carbonate from glycerol and dimethyl carbonate: Isolation and characterization of an active Ca species. *Applied Catalysis A: General* **401** (1-2): 220-225.

Simanjuntak, F.S.H., Widyaya, V.T., Kim, C.S., Ahn, B.S., Kim, Y.J., Lee, H. (2013). Synthesis of glycerol carbonate from glycerol and dimethyl carbonate using magnesium-lanthanum mixed oxide catalyst. *Chemical Engineering Science* **94** 265-270.

Sonnati, M.O., Amigoni, S., de Givenchy, E.P.T., Darmanin, T., Choulet, O., Guittard, F. (2013). Glycerol carbonate as a versatile building block for tomorrow: synthesis, reactivity, properties and applications. *Green Chemistry* **15** (2): 283-306.

Stein, Y.S., Antal, M.J., Jones, M. (1983). A study of the gas-phase pyrolysis of glycerol. *Journal of Analytical and Applied Pyrolysis* **4** (4): 283-296.

Stelmachowski, M. (2011). Utilization of glycerol, a by-product of the transesterification process of vegetable oils: a review. *Ecological Chemistry and Engineering* **18** (1): 9-30.

Stockel, R. (2007). Method of treating dermatological conditions. Patent US 20070086977 A1.

Sun, Y., Liu, J.C., Kimbleton, E.S., Wang, J.C.T. (1999). Composition base for topical therapeutic and cosmetic preparation. IN9800814-I2.

Suriyaprapadilok, N., Kitiyanan, B. (2011). Synthesis of Solketal from Glycerol and Its Reaction with Benzyl Alcohol. *Energy Procedia* **9** 63-69.

Takagaki, A., Iwatani, K., Nishimura, S., Ebitani, K. (2010). Synthesis of glycerol carbonate from glycerol and dialkyl carbonates using hydrotalcite as a reusable heterogeneous base catalyst. *Green Chemistry* **12** (4): 578-581.

Tamayo, J.J., Ladero, M., Santos, V.E., Garcia-Ochoa, F. (2012). Esterification of benzoic acid and glycerol to alpha-monobenzoate glycerol in solventless media using an industrial free Candida antarctica lipase B. *Process Biochemistry* **47** (2): 243-250.

Tan, K.T., Lee, K.T., Mohamed, A.R. (2010). Optimization of supercritical dimethyl carbonate (SCDMC) technology for the production of biodiesel and value-added glycerol carbonate. *Fuel* **89** (12): 3833-3839.

Tejero, J., Creus, E., Iborra, M., Cunill, F., Izquierdo, J.F., Fite, C. (2001). Comparative study of IPTBE synthesis on HZSM-5 and ion-exchange resin catalysts. *Catal. Today* **65** (2-4): 381-389.

Teles, J.H., Rieber, N., Harder, W. (1994). Glyceryl carbonate and glycidol prodn. from glycerol - by oxidative carbonylation over catalyst, e.g. cuprous chloride and decarboxylation over alkali or alkaline salt, used in polymer prodn. EP582201-A; EP582201-A2; DE4225870-A1; JP6157509-A; US5359094-A; EP582201-A3.

Teng, W.K., Ngoh, G.C., Yusoff, R., Aroua, M.K. (2014). A review on the performance of glycerol carbonate production via catalytic transesterification: Effects of influencing parameters. *Energy Conversion and Management* **88** (0): 484-497.

Thompson, J.C., He, B.B. (2006). Characterization of crude glycerol from biodiesel production from multiple feedstocks. *Applied Engineering in Agriculture* **22** (2): 261-265.

U.S. Soy Bean Export Council, I. (2008). Glycerin market analysis, Indianapolis, United States. ed. ABG Inc.

Ueno, K., Mizushima, H. (2007). New glycerol carbonate glycoside compound for manufacture of glycerol glycoside useful as glyceroglycolipid precursor and

moisturizer. WO2005033122-A1; EP1674476-A1; CN1860126-A; US2007213517-A1; JP2005514465-X; US7351809-B2; CN100415763-C; JP4559362-B2; EP1674476-B1.

UNFCCC (1997). Kyoto Protocol to the United Nations Framework Convention on Climate Change, Kyoto, Japan.

Vasiliadou, E.S., Eggenhuisen, T.M., Munnik, P., de Jongh, P.E., de Jong, K.P., Lemonidou, A.A. (2014). Synthesis and performance of highly dispersed Cu/SiO2 catalysts for the hydrogenolysis of glycerol. *Applied Catalysis B-Environmental* **145** 108-119.

Vicente, G., Melero, J.A., Morales, G., Paniagua, M., Martin, E. (2010). Acetalisation of bio-glycerol with acetone to produce solketal over sulfonic mesostructured silicas. *Green Chemistry* **12** (5): 899-907.

Vieville, C., Yoo, J.W., Pelet, S., Mouloungui, Z. (1998). Synthesis of glycerol carbonate by direct carbonatation of glycerol in supercritical CO_2 in the presence of zeolites and ion exchange resins. *Catalysis Letters* **56** (4): 245-247.

Wang, H., Lu, P. (2012). Liquid–Liquid Equilibria for the System Dimethyl Carbonate + Methanol + Glycerol in the Temperature Range of (303.15 to 333.15) K. *Journal of Chemical & Engineering Data* **57** (2): 582-589.

Wang, L., Ma, Y., Wang, Y., Liu, S., Deng, Y. (2011). Efficient synthesis of glycerol carbonate from glycerol and urea with lanthanum oxide as a solid base catalyst. *Catalysis Communications* **12** (15): 1458-1462.

Wang, S., Liu, H. (2014). Selective hydrogenolysis of glycerol to propylene glycol on hydroxycarbonate-derived Cu-ZnO-Al2O3 catalysts. *Chinese Journal of Catalysis* **35** (5): 631-643.

Wang, W., Cheng, W., Duan, J., Gong, J., Hu, B., Angeli, P. (2014). Effect of dispersed holdup on drop size distribution in oil-water dispersions: Experimental observations and population balance modeling. *Chemical Engineering Science* **105** 22-31.

Wang, W., Liu, J., Wang, P., Duan, J., Gong, J. (2013). Evolution of dispersed drops during the mixing of mineral oil and water phases in a stirringtank. *Chemical Engineering Science* **91** (0): 173-179.

Werpy, T., Petersen, G. (2004). Top value added chemicals from biomass. Volume I - Results of screening for potential candidates from sugars and synthesis gas

Pacific Northwest National Laboratory. National Renewable Energy Laboratory. U.S. Department of Energy.

Wessendorf, R. (1995). Glycerol derivatives as fuel components. *Erdol & Kohle Erdgas Petrochemie* **48** (3): 138-143.

Weuthen, M., Hees, U. (1995). New 2,3-epoxy-propylated glycoside(s)|by reaction of alkyl- and/or alkenyl-oligoglycoside with glycerine carbonate. WO9511250-A; DE4335947-A1; WO9511250-A1.

Yadav, G.D., Chandan, P.A. (2014). A green process for glycerol valorization to glycerol carbonate over heterogeneous hydrotalcite catalyst. *Catal. Today* **237** 47-53.

Zakaria, Z.Y., Amin, N.A.S., Linnekoski, J. (2013). A perspective on catalytic conversion of glycerol to olefins. *Biomass & Bioenergy* **55** 370-385.

Zakaria, Z.Y., Linnekoski, J., Amin, N.A.S. (2012). Catalyst screening for conversion of glycerol to light olefins. *Chemical Engineering Journal* **207** 803-813.

Zeng, D., Li, R., Feng, M., Fang, T. (2014). Continuous Esterification of Free Fatty Acids in Crude Biodiesel by an Integrated Process of Supercritical Methanol and Sodium Methoxide Catalyst. *Applied Biochemistry and Biotechnology* **174** (4): 1484-1495.

Zhang, Z., Rackemann, D.W., Doherty, W.O.S., O'Hara, I.M. (2013). Glycerol carbonate as green solvent for pretreatment of sugarcane bagasse. *Biotechnology for Biofuels* **6**.

Zhou, C., Beltramini, J., Fan, Y., Lu, G. (2008). Chemoselective catalytic conversion of glycerol as a biorenewable source to valuable commodity chemicals. *Chemica1 Society Reviews* **37** (3): 527-549.

Zhou, J.X.H. (2007). Purification by column-chromatography using eluants containing organic solvents. Patent WO2007081906 A2.

Zverlov, V.V., Berezina, O., Velikodvorskaya, G.A., Schwarz, W.H. (2006). Bacterial acetone and butanol production by industrial fermentation in the Soviet Union: use of hydrolyzed agricultural waste for biorefinery. *Applied Microbiology and Biotechnology* **71** (5): 587-597.

ANEXO: PUBLICACIONES
ANNEX: PUBLICATIONS

Publicación 1 / Publication 1

Autores/Authors: Jesús Esteban, Miguel Ladero, Laura Molinero and Félix García-Ochoa

Título/Title: Liquid–liquid equilibria for the ternary systems DMC–methanol–glycerol, DMC–glicerol carbonate–glycerol and the quaternary system DMC–methanol–glycerol carbonate–glycerol at catalytic reacting temperatures

Estado actual/Current status: Chemical Engineering Research and Design (2014), 92: 1797-1805

Índice de impacto / Impact factor 2013: 2.281

Resumen

La reacción entre carbonato de dimetilo (DMC) y glicerina (Gly) para obtener como productos carbonato de glicerina (GC) y metanol (MeOH) ha sido estudiada con relativa profundidad en la bibliografía. Sin embargo, hay poca información sobre el equilibrio entre fases líquidas existente a conversiones bajas de esta reacción a las temperaturas a las que se describen en bibliografía como consecuencia de la limitada solubilidad de las especies reactivas DMC y Gly, así como a su posible repercusión en la descripción cinética del sistema.

Este trabajo presenta una recopilación de datos de equilibrio líquido-líquido obtenidos en ausencia de reacción química para los sistemas involucrados en esta síntesis, a saber:

- El sistema ternario (T1): {DMC + MeOH + Gly}
- El sistema ternario (T2): {DMC + GC + Gly}
- El sistema cuaternario (Q): {DMC + MeOH + GC + Gly}, modelizado como un sistema pseudoternario considerando MeOH y GC como un único componente.

Experimentalmente, se llevó a cabo la agitación de diferentes cargas de cada uno de los sistemas expuestos a las temperaturas de 313.2, 318.2 y 323.2 K. Tras llevar a cabo la separación de las fases líquidas, ambas se analizaron con un método de HPLC para determinar la composición de las mismas.

A medida que aumenta la concentración de MeOH, GC y MeOH + GC en los sistemas T1, T2 y Q, respectivamente, se aprecia un efecto positivo en la solubilización entre las fases líquidas. El efecto solubilizador de cada codisolvente puede clasificarse en el siguiente orden: GC > MeOH + GC > MeOH. El efecto de la temperatura en el intervalo estudiado es despreciable con independencia del codisolvente empleado.

Los datos experimentales obtenidos fueron ajustados con éxito al modelo NRTL, de cuya utilización en sistemas con alcoholes y carbonatos orgánicos hay referencias en bibliografía. Este trabajo incluye los coeficientes de interacción binaria de los sistemas T1, T2 y Q a las temperaturas de 333.2, 338.2 y 343.2 K obtenidos por correlación de dicho modelo termodinámico incluido en el software Aspen Plus.

Contents lists available at ScienceDirect

Chemical Engineering Research and Design

journal homepage: www.elsevier.com/locate/cherd

Liquid–liquid equilibria for the ternary systems DMC–methanol–glycerol, DMC–glycerol carbonate–glycerol and the quaternary system DMC–methanol–glycerol carbonate–glycerol at catalytic reacting temperatures

Jesús Esteban, Miguel Ladero, Laura Molinero, Félix García-Ochoa*

Department of Chemical Engineering, College of Chemical Sciences, Complutense University of Madrid, 28040 Madrid, Spain

A B S T R A C T

Liquid–liquid equilibria of multicomponent systems involved in the synthesis of glycerol carbonate from dimethyl carbonate and glycerol were experimentally measured. Particularly, data for the ternary systems dimethyl carbonate + methanol + glycerol and dimethyl carbonate + glycerol carbonate + glycerol and the quaternary system dimethyl carbonate + methanol + glycerol carbonate + glycerol are provided at 333.2 K, 338.2 K and 343.2 K at atmospheric pressure since these temperatures prove relevant for the synthesis of carbonate glycerol from glycerol and dimethyl carbonate. The experimental data obtained were correlated with a good degree of agreement to the NRTL model in order to obtain the corresponding binary interaction parameters.

Keywords: Glycerol carbonate; Glycerol; Dimethyl carbonate; Methanol; Liquid–liquid equilibria; Green process

1. Introduction

Throughout the last few years, the biodiesel industry has suffered a marked development spurred by the current environmental concerns, leading to an overproduction of glycerol (Gly) as a by-product of the mentioned process (Pagliaro and Rossi, 2008). Consequently, new uses and synthetic routes are being sought after in order to pursue the valorization of the surplus of glycerol that has consequently been produced (Behr et al., 2008; Pagliaro et al., 2009). Among the different products that may be synthesized from glycerol is 4-(hydroxymethyl)-1,3-dioxolan-2-one, also referred to as glycerol carbonate (GC), whose interest as a product as well as its diverse production methodologies have been addressed profusely in literature to the point of becoming the subject of a thorough review (Sonnati et al., 2013). Its applications comprise a wide array of uses, such as a multipurpose green solvent (Lameiras et al., 2011), cosolvent with ionic liquids (Benoit et al., 2010) or a potential additive in Li and Li-ion batteries (Chen et al., 2002) curing agent for pozzolanic matrices (Magniont et al., 2010), assorted uses in the cosmetic industry (lacquer remover, plasticizer or moisturizer) (Sonnati et al., 2013) or as a gas separation membrane component (Kovvali and Sirkar, 2002), to name a few.

Many different synthetic possibilities have been described in literature, including the addition of CO (Hu et al., 2010) or CO_2 (Aresta et al., 2006) to glycerol or the reaction of glycerol with urea (Li et al., 2006). Notwithstanding, transesterification of glycerol with organic carbonates such as dimethylcarbonate (DMC) (Lee et al., 2010; Ochoa-Gomez et al., 2009; Rokicki et al., 2005; Tudorache et al., 2012) or ethylene carbonate (Climent et al., 2010) has proven less demanding in terms of operating

* *Corresponding author*. Tel.: +34 913944164; fax: +34 913944179.
E-mail addresses: mladero@quim.ucm.es, mladerog@ucm.es (M. Ladero).
Received 31 December 2013; Received in revised form 10 May 2014; Accepted 16 May 2014
Available online 4 June 2014
http://dx.doi.org/10.1016/j.cherd.2014.05.026

Nomenclature

HPLC	high-performance liquid chromatography
LLE	liquid–liquid equilibria
NRTL	non-random two-liquid model
OF	objective function
Q	refers to the quaternary system {DMC + MeOH + GC + Gly}
rmsd	root-mean square deviation
T1	refers to the ternary system {DMC + MeOH + Gly}
T2	refers to the ternary system {DMC + GC + Gly}

Greek letters

α_{ij}	non-randomness binary interaction parameter as defined in the NRTL method
Δg_{ij}	binary interaction parameter as defined in the NRTL method

Components

DMC	dimethyl carbonate
GC	glycerol carbonate
Gly	glycerol
MeOH	methanol

Subscripts

I, II	relative to the glycerol-rich and dimethyl carbonate-rich phases

conditions. This strategy requires milder temperatures, atmospheric pressure and solventless systems compared to the operation under pressure and at temperatures higher than 100 °C that the addition of CO and CO_2 requires or the vacuum and temperatures around 150 °C that the glycerolysis of urea demands (Sonnati et al., 2013).

This work focuses on the liquid–liquid equilibria (LLE) of the systems involved in the transesterification of Gly with DMC. While Wang and Lu have previously reported LLE values for the system DMC + methanol (MeOH) + Gly (Wang and Lu, 2012), this study intends to provide further data for the LLE from 333.2 K to 343.2 K of the ternary systems {DMC + MeOH + Gly} (system T1 from this point forward) and {DMC + GC + Gly} (system T2), i.e., each of the initially immiscible reactants with each of the products that generate throughout the process (as indicated in Scheme 1). Moreover, LLE of the entire quaternary system {DMC + MeOH + GC + Gly} (system Q) have been evaluated as a means to assess the influence of the combined presence of both products on the evolution of the biphasic system.

VLE for systems consisting of combinations of glycerol and other alcohols or organic carbonates with alcohols (de la Torre et al., 2006; Shimoyama et al., 2009; Yunhai et al., 2005) as well as LLE for systems with DMC, MeOH and water (Choe and Song, 2002; Katayama et al., 1998) have been studied. To the best of our knowledge, no work on this set of systems within the temperature range herein proposed at atmospheric pressure has previously been reported.

From the mentioned LLE data, correlation with the non-random two-liquid (NRTL) model was performed. Thus, corresponding NRTL binary and non-randomness interaction parameters have thereby been obtained.

2. Materials and methods

2.1. Materials

The following reagents were used throughout the experimental procedure: extra pure Gly (assay grade 99.88%) from Fischer Chemical; MeOH of HPLC grade (assay grade 99.99%) from Scharlau Chemie, Ltd; GC (purity ≥99.5%) from Sigma–Aldrich and DMC (purity 99%), the latter of which was kindly gifted by UBE Corporation, Europe. For HPLC analysis purposes, citric acid ACS reagent (purity ≥99.5%) by Sigma–Aldrich was employed as an internal standard.

2.2. LLE measurements

Magnetically stirred hermetically sealed 25 mL round-bottom flasks were used in order to perform the equilibrium experiments. Appropriate temperature (accuracy ±0.05 K) for each experiment was reached by means of a glycerol bath heated by an IKA Yellow Line TC3 heating and stirring device.

Weighing of the feed samples was performed in a Kern and Sohn ABS-220-4 analytical balance with a precision of 0.0001 g. Then, vigorous stirring of the different test systems was performed for 6 h; afterwards, separation by settling of both the heavy (Gly-rich, I) and light (DMC-rich, II) phases was allowed for not less than 3 h while at the corresponding temperature. In order to avoid phase mixing during the sample withdrawal process, a hypodermic needle was used to retire preliminary volumes of the heavier phase from which samples for analysis would be taken. Data were obtained by performing triplicate experiments.

2.3. Analysis of samples

Dilution of samples in a 5 g/L citric acid (internal standard) solution was performed prior to HPLC analysis. Each component of the two phases was analyzed utilizing a JASCO 2000 series device equipped with a refraction index detector. Acidic Milli-Q water (0.005 N H_2SO_4) was used as mobile phase at a constant flow rate of 0.5 mL/min. Separation of the peaks corresponding to each of the components was realized using a Rezex ROA-Organic Acid H+ (8%) column (150 × 7.80 mm) at 60 °C.

2.4. Data regression and correlation with the NRTL model

Considering previous efforts with these kinds of systems, correlation of the experimental data with the NRTL model has been performed in order to obtain the binary interaction parameters. For this purpose, the data regression module of Aspen Plus provides a useful tool based on least-squares method based on the maximum likelihood principle. As suggested by default by Aspen Plus, the Britt-Luecke (Britt and Luecke, 1973) algorithm was used to obtain the model parameters with the Deming initialization method. The regression convergence tolerance was set to 0.0001. The objective function to be minimized is

$$\mathrm{OF} = \sum_{k=1}^{N}\sum_{j=1}^{2}\sum_{i=1}\left[\frac{\left(T_k^{\mathrm{exp}} - T_k^{\mathrm{calc}}\right)^2}{\sigma_T^2} + \frac{\left(x_{ijk}^{\mathrm{exp}} - x_{ijk}^{\mathrm{calc}}\right)^2}{\sigma_x^2}\right] \quad (1)$$

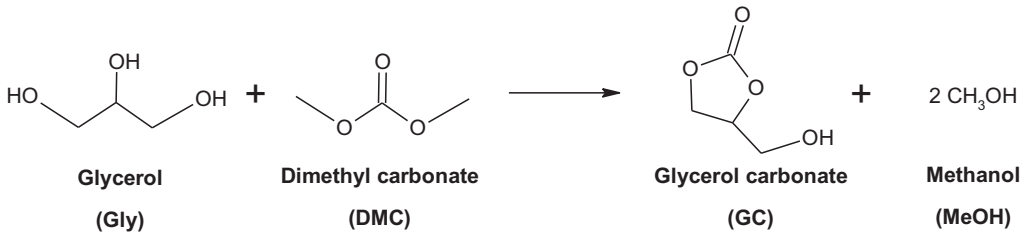

Scheme 1 – Chemical equation of the transesterification reaction of Gly and DMC.

where N stands for the number of tie-lines, T^{exp} and T^{calc} refer to the experimental and calculated values of temperature, respectively, and x^{exp} and x^{calc} denote the experimental and calculated values of mole fraction. The subscripts i, j and k are relative to the component, phase and tie-line, respectively. Finally, σ_T and σ_x are the standard deviation of the temperature and the mole fraction. Their values were taken from the accuracy of the temperature control system ($\sigma_T = 0.05$ K) and the uncertainty of the mole fraction as measured by HPLC ($\sigma_x = 0.0150$).

Regression of the binary interaction parameters as defined by the NRTL method was undertaken considering first a given set of values for the non-randomness parameters α_{ij} regarded as common values; then, optimization of these parameters was also realized. The criterion followed to evaluate the goodness of a set of values of the NRTL parameters was the minimization of the root mean square deviation (rmsd)

$$\text{rmsd} = \sqrt{\sum_{k=1}^{N}\sum_{j=1}^{2}\sum_{i=1}^{2}\frac{\left(x_{ijk}^{exp} - x_{ijk}^{calc}\right)^2}{6N}} \quad (2)$$

3. Results and discussion

3.1. *LLE experimental data*

Prior to measuring the LLE experimental data, a preliminary experiment was run to confirm that no reaction takes place whatsoever in the absence of catalyst. An equimolar feed mixture of Gly and DMC was allowed to mix over a period of 72 h, without any products being present throughout this period according to HPLC analysis. The lack of products observed agrees with the proposed mechanism for this reaction, in which a basic catalyst is necessary to initiate the reaction via a glyceroxide anion (Ochoa-Gomez et al., 2009). Thus, it can be ensured that the results herein presented correspond solely to the LLE among the species.

Tables 1–3 show the LLE data expressed as mole fractions of the ternary systems T1, T2 and the quaternary system Q at each temperature tested (333.2, 338.2 and 343.2 K). Three different equilibrium systems were evaluated, where Gly and DMC are the only common compounds to which cosolvents were added: MeOH (system T1); GC (system T2); and finally, both MeOH and GC (system Q).

Though the present work focuses on a physical equilibrium (thus a non-reacting system), the choice of the composition of the global feed mixtures was made to analyze the potential effect that increasing amounts of the cosolvents would have if the reaction explained by Scheme 1 took place. Each experimental tie-line was obtained from compositions that would take place from a reacting system at increasing conversions of approximately 5% with MeOH, GC and MeOH + GC as products of the reaction, respectively for the systems T1, T2 and Q. While the former two situations are simplifications, the latter describes what in fact occurs throughout the synthesis of GC by means of this procedure.

As stated in Section 1, the system here denoted as T1 had previously been studied at one of the temperatures of interest, particularly at 333.2 K (Wang and Lu, 2012). Fig. 1 is a plot of the data obtained in this work together with the predicted data using the NRTL model at this temperature. It can be seen that both sets of data adjust well to the binodal curve retrieved from the correlation in this work.

In addition to the previous verification, Figs. 2 and 3 depict the tie-lines represented by the data in Tables 1 and 2 and the binodal curves and tie-lines predicted by the NRTL model for the temperature of 343.2 K. Fig. 4 plots the data featured in Table 3 regarding the experiments also at 343.2 K, where a pseudoternary approach has been followed. Accordingly, the compositions of MeOH and GC have been represented together as the summation of both. Likewise, the prediction of the NRTL and binodal curves is also present.

3.2. *Influence of the presence of methanol and glycerol carbonate and temperature in the biphasic system*

It could be seen that MeOH and GC were both soluble in each of the phases, although not to the same extent. MeOH showed

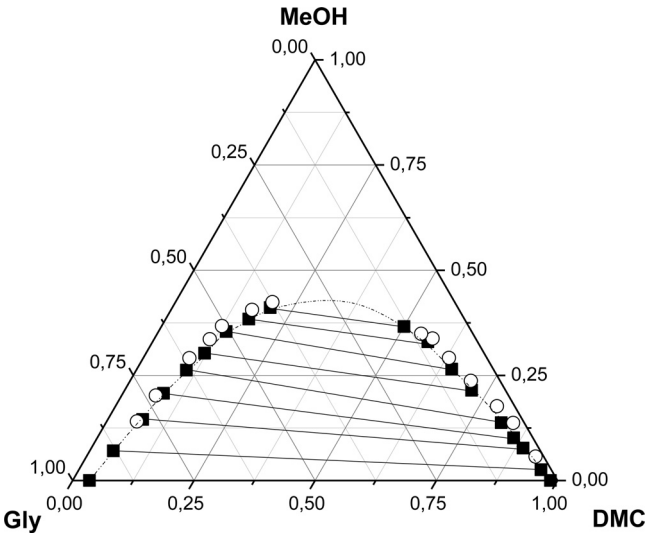

Fig. 1 – Comparison between experimental LLE data for the system T1 {DMC + MeOH + Gly} at 333.2 K. ■ depicts experimental data obtained in the present work, ● represents those obtained by Wang and Lu (2012) and the dashed binodal curve are data calculated with the NRTL model in this work.

Table 1 – Experimental LLE data expressed as mole fractions (x_i) of the ternary system T1 {DMC (1) + MeOH (2) + Gly (3)} at 101.3 kPa.

T (K)	Tie-line	Global composition (feed)			Phase I (Gly-rich) composition			Phase II (DMC-rich) composition		
		x_1	x_2	x_3	x_1	x_2	x_3	x_1	x_2	x_3
333.2	1	0.5053	0.0000	0.4947	0.0350	0.0000	0.9650	0.9857	0.0000	0.0143
	2	0.4696	0.0509	0.4795	0.0487	0.0707	0.8806	0.9534	0.0253	0.0213
	3	0.4468	0.1161	0.4371	0.0722	0.1448	0.7830	0.8905	0.0770	0.0325
	4	0.4209	0.1531	0.4260	0.0837	0.2075	0.7088	0.8592	0.1010	0.0398
	5	0.3922	0.2099	0.3979	0.1037	0.2623	0.6340	0.8153	0.1371	0.0476
	6	0.3648	0.2647	0.3705	0.1338	0.2950	0.5712	0.7162	0.2142	0.0696
	7	0.3428	0.3041	0.3531	0.1514	0.3322	0.5164	0.6498	0.2646	0.0856
	8	0.3250	0.3535	0.3215	0.1722	0.3743	0.4535	0.5577	0.3221	0.1202
	9	0.3057	0.3876	0.3067	0.2029	0.4051	0.3920	0.5008	0.3588	0.1404
338.2	1	0.4985	0.0000	0.5015	0.0379	0.0000	0.9621	0.9836	0.0000	0.0164
	2	0.4679	0.0586	0.4735	0.0502	0.0847	0.8651	0.9525	0.0299	0.0176
	3	0.4516	0.1004	0.4480	0.0792	0.1394	0.7814	0.9079	0.0559	0.0362
	4	0.4151	0.1551	0.4298	0.0998	0.1892	0.7110	0.8559	0.1057	0.0384
	5	0.3945	0.2099	0.3956	0.1036	0.2430	0.6534	0.7590	0.1681	0.0729
	6	0.3647	0.2517	0.3836	0.1211	0.2910	0.5879	0.7267	0.1969	0.0764
	7	0.3534	0.3014	0.3452	0.1456	0.3458	0.5086	0.6687	0.2359	0.0954
	8	0.3252	0.3485	0.3263	0.1637	0.3838	0.4525	0.6017	0.2918	0.1065
	9	0.3025	0.4033	0.2943	0.2326	0.4163	0.3511	0.5085	0.3631	0.1284
343.2	1	0.4991	0.0000	0.5009	0.0438	0.0000	0.9562	0.9781	0.0000	0.0219
	2	0.4709	0.0521	0.4770	0.0680	0.0716	0.8604	0.9345	0.0299	0.0356
	3	0.4532	0.1019	0.4449	0.0887	0.1344	0.7769	0.8993	0.0639	0.0368
	4	0.4249	0.1496	0.4255	0.1077	0.1865	0.7058	0.8503	0.1030	0.0467
	5	0.3946	0.2093	0.3961	0.1269	0.2570	0.6161	0.7982	0.1394	0.0624
	6	0.3738	0.2508	0.3754	0.1391	0.2910	0.5699	0.7455	0.1865	0.0680
	7	0.3548	0.3031	0.3421	0.1726	0.3328	0.4946	0.6400	0.2570	0.1030
	8	0.3168	0.3556	0.3276	0.2033	0.3796	0.4171	0.5695	0.3065	0.1240
	9	0.3094	0.3941	0.2965	0.2571	0.4033	0.3396	0.4816	0.3615	0.1569

Table 2 – Experimental LLE data expressed as mole fractions (x_i) of the ternary system T2 {DMC (1) + GC (2) + Gly (3)} at 101.3 kPa.

T (K)	Tie-line	Global composition (feed)			Phase I (Gly-rich) composition			Phase II (DMC-rich) composition		
		x_1	x_2	x_3	x_1	x_2	x_3	x_1	x_2	x_3
333.2	1	0.4974	0.0000	0.5026	0.0350	0.0000	0.9650	0.9857	0.0000	0.0143
	2	0.4810	0.0272	0.4918	0.0528	0.0188	0.9284	0.9385	0.0352	0.0263
	3	0.4614	0.0521	0.4865	0.0623	0.0379	0.8998	0.8901	0.0690	0.0409
	4	0.4571	0.0796	0.4633	0.0868	0.0613	0.8519	0.8304	0.0977	0.0719
	5	0.4495	0.1072	0.4433	0.1315	0.0847	0.7838	0.7480	0.1318	0.1202
	6	0.4239	0.1461	0.4300	0.1690	0.1238	0.7072	0.6488	0.1578	0.1934
	7	0.4075	0.1788	0.4137	0.2459	0.1682	0.5859	0.5734	0.1865	0.2401
	8	0.3972	0.2119	0.3909	0.3182	0.1996	0.4822	0.4768	0.2126	0.3106
338.2	1	0.5014	0.0000	0.4986	0.0380	0.0000	0.9620	0.9840	0.0000	0.0160
	2	0.4833	0.0272	0.4895	0.0496	0.0163	0.9341	0.9282	0.0379	0.0339
	3	0.4695	0.0548	0.4757	0.0907	0.0438	0.8655	0.8696	0.0690	0.0614
	4	0.4543	0.0853	0.4604	0.1090	0.0666	0.8244	0.7919	0.0977	0.1104
	5	0.4392	0.1155	0.4453	0.1550	0.0962	0.7488	0.6990	0.1344	0.1666
	6	0.4262	0.1460	0.4278	0.2073	0.1187	0.6740	0.5891	0.1673	0.2436
	7	0.4130	0.1679	0.4191	0.2653	0.1474	0.5873	0.5268	0.1762	0.2970
	8	0.4054	0.1984	0.3962	0.3336	0.1852	0.4812	0.4674	0.1996	0.3330
343.2	1	0.4988	0.0000	0.5012	0.0488	0.0000	0.9512	0.9681	0.0000	0.0319
	2	0.4846	0.0246	0.4908	0.0685	0.0163	0.9152	0.9001	0.0352	0.0647
	3	0.4718	0.0548	0.4734	0.1083	0.0465	0.8452	0.8383	0.0640	0.0977
	4	0.4543	0.0853	0.4604	0.1350	0.0690	0.7960	0.7640	0.0951	0.1409
	5	0.4433	0.1072	0.4495	0.1807	0.0950	0.7243	0.6898	0.1214	0.1888
	6	0.4296	0.1347	0.4357	0.2276	0.1187	0.6537	0.6102	0.1448	0.2450
	7	0.4213	0.1513	0.4274	0.2842	0.1501	0.5657	0.5151	0.1631	0.3218
	8	0.4093	0.1805	0.4101	0.3374	0.1655	0.4971	0.4399	0.1735	0.3866

a greater solubility in the phase predominantly consisting of Gly, while GC in the DMC-rich phase, ascribable to the similarity in nature between alcohols and organic carbonates, correspondingly.

As can be seen in Figs. 2–4, the increasing presence of MeOH, GC and MeOH + GC in such feed mixtures (represented by tie-lines located higher along the vertical axis) favoured the solubilization of the initially immiscible system.

Table 3 – Experimental LLE data expressed as mole fractions (x_i) of the quaternary system Q {DMC (1) + MeOH (2) + GC (3) + Gly (4)} at 101.3 kPa.

T (K)	Tie-line	Global composition (feed)				Phase I (Gly-rich) composition				Phase II (DMC-rich) composition			
		x_1	x_2	x_3	x_4	x_1	x_2	x_3	x_4	x_1	x_2	x_3	x_4
333.2	1	0.5020	0.0000	0.0000	0.4980	0.0350	0.0000	0.0000	0.9650	0.9857	0.0000	0.0000	0.0143
	2	0.4609	0.0462	0.0237	0.4692	0.0502	0.0548	0.0299	0.8651	0.9123	0.0169	0.0391	0.0317
	3	0.4274	0.0964	0.0457	0.4305	0.0674	0.0982	0.0649	0.7695	0.8358	0.0431	0.0756	0.0455
	4	0.3910	0.1451	0.0699	0.3940	0.0963	0.1493	0.0920	0.6624	0.7493	0.0631	0.1157	0.0719
	5	0.3605	0.1852	0.0907	0.3636	0.1385	0.1937	0.1077	0.5601	0.6259	0.0956	0.1537	0.1248
	6	0.3327	0.2208	0.1108	0.3357	0.1722	0.2218	0.1344	0.4716	0.5305	0.1039	0.2002	0.1654
	7	0.3044	0.2568	0.1222	0.3166	0.2259	0.2465	0.1437	0.3839	0.4316	0.1529	0.2136	0.2019
338.2	1	0.4966	0.0000	0.0000	0.5034	0.0379	0.0000	0.0000	0.9621	0.9836	0.0000	0.0000	0.0164
	2	0.4609	0.0528	0.0224	0.4639	0.0675	0.0519	0.0428	0.8378	0.9031	0.0207	0.0296	0.0466
	3	0.4218	0.1035	0.0499	0.4248	0.0864	0.1066	0.0663	0.7407	0.8094	0.0526	0.0783	0.0597
	4	0.3944	0.1457	0.0716	0.3883	0.1257	0.1387	0.1094	0.6262	0.7248	0.0753	0.1089	0.0910
	5	0.3605	0.1851	0.0908	0.3636	0.1574	0.2060	0.0895	0.5471	0.6149	0.0986	0.1466	0.1399
	6	0.3337	0.2257	0.1089	0.3317	0.1972	0.2366	0.1146	0.4516	0.5040	0.1154	0.1967	0.1839
	7	0.3044	0.2650	0.1282	0.3024	0.2450	0.2174	0.1788	0.3588	0.4082	0.1342	0.2341	0.2235
343.2	1	0.5039	0.0000	0.0000	0.4961	0.0438	0.0000	0.0000	0.9562	0.9781	0.0000	0.0000	0.0219
	2	0.4640	0.0538	0.0244	0.4578	0.0717	0.0611	0.0396	0.8276	0.8862	0.0284	0.0415	0.0440
	3	0.4250	0.1070	0.0493	0.4187	0.1006	0.1024	0.0758	0.7212	0.7858	0.0513	0.0879	0.0750
	4	0.3868	0.1508	0.0724	0.3900	0.1268	0.1433	0.1078	0.6221	0.7049	0.0756	0.1198	0.0997
	5	0.3574	0.1942	0.0930	0.3554	0.1666	0.2077	0.0990	0.5267	0.5966	0.0960	0.1663	0.1411
	6	0.3337	0.2269	0.1077	0.3317	0.2086	0.2267	0.1304	0.4343	0.4866	0.0946	0.2234	0.1954
	7	0.3142	0.2522	0.1214	0.3122	0.2654	0.2468	0.1322	0.3556	0.4137	0.1080	0.2491	0.2292

Comparison of the individual effects of MeOH and GC (Figs. 2 and 3) evidences that the latter possesses a greater solubilizing action within the system. Up to nine tie-lines were obtained for T1, above which no separation of phases was achievable, with the maxima of the binodal curves ranging from a molar composition of MeOH of 0.40 to 0.42 for the temperatures tested. On the other hand, the system T2 allowed for the acquisition of eight tie-lines, yielding maxima at molar fractions of GC varying from 0.19 to 0.23, which conveys the solubilizing capacity of this compound.

As for the combined solubilizing action of the products, Fig. 4 shows that the system was still biphasic at the seventh tie-line, barely beyond which has the system consisted of a single phase. However, the maxima of the binodal curve correspond to compositions of the summation of MeOH and GC of 0.38 and 0.40, meaning that the combined presence of both barely improves the solubility of the phases compared to the use of MeOH and is far from reaching what GC by itself is capable of in these terms.

According to Wang and Lu's data within the temperature interval assayed, while this variable showed some effect on the miscibility of the phases, the actual impact proved small since only modest decreases in the two-phase regions of the ternary diagrams corresponding to the {DMC + MeOH + Gly} system were observed (Wang and Lu, 2012). Likewise, our data for both ternary systems as well as the quaternary system

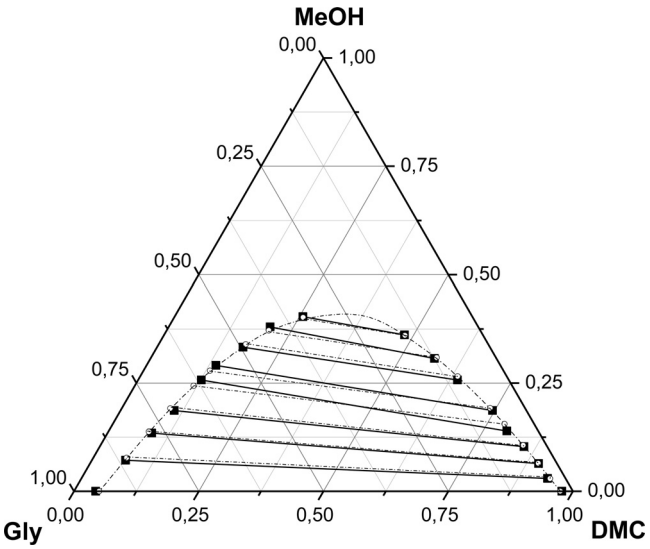

Fig. 2 – Experimental LLE measurements and binodal curve using the NRTL model for the system Q {DMC + MeOH + Gly} at 343.2 K. ■ represents experimental tie-lines and dashed lines are data calculated with the NRTL model.

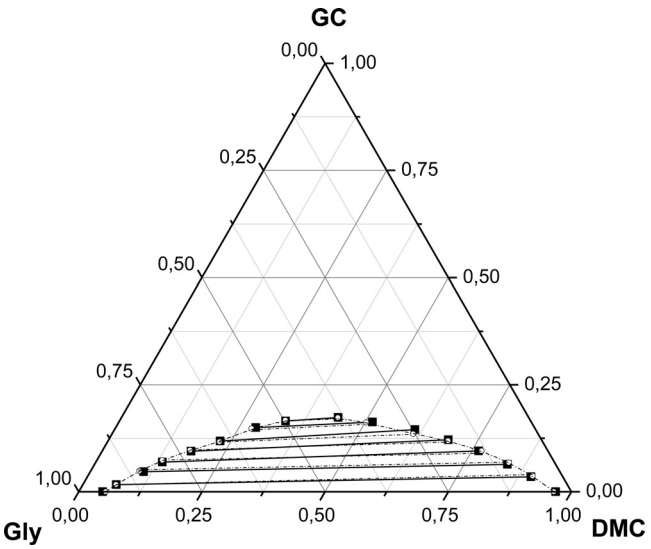

Fig. 3 – Experimental LLE measurements and binodal curve using the NRTL model for the system T2 {DMC + GC + Gly} at 343.2 K. ■ represents experimental tie-lines and dashed lines are data calculated with the NRTL model.

Table 4 – Values of the NRTL binary interaction parameters obtained from the LLE data by regression for the system T1 {DMC (1) + MeOH (2) + Gly (3)}.

T (K)	α_{ij} regression	Components i–j	NRTL parameters			rmsd
			α_{ij}	$(g_{ij} - g_{ii})$ (J mol^{-1})	$(g_{ji} - g_{jj})$ (J mol^{-1})	
333.2	Fixed	1–2	0.2	−29,318.24	2615.67	0.0093
		1–3	0.2	8469.89	5202.32	
		2–3	0.3	−3678.61	−26,369.18	
	Floating	1–2	0.79	−30,023.68	7637.24	0.0079
		1–3	0.07	9655.55	2186.42	
		2–3	0.88	−2011.74	−29,202.84	
338.2	Fixed	1–2	0.2	−32,734.21	2271.30	0.0196
		1–3	0.2	7669.50	5434.20	
		2–3	0.3	−3756.85	−30,187.39	
	Floating	1–2	0.27	−34,499.61	3958.71	0.0143
		1–3	0.31	9374.78	7007.70	
		2–3	0.41	−3145.85	−31,757.57	
343.2	Fixed	1–2	0.2	−30,190.38	2972.84	0.0073
		1–3	0.2	7598.33	4839.41	
		2–3	0.3	−2902.50	−27,817.40	
	Floating	1–2	0.17	−27,054.42	3816.79	0.0057
		1–3	0.31	8309.76	6346.82	
		2–3	0.22	−1902.99	−35,646.61	

Table 5 – Values of the NRTL binary interaction parameters obtained from the LLE data by regression for the system T2 {DMC (1) + GC (2) + Gly (3)}.

T (K)	α_{ij} regression	Components i–j	NRTL parameters			rmsd
			α_{ij}	$(g_{ij} - g_{ii})$ (J mol^{-1})	$(g_{ji} - g_{jj})$ (J mol^{-1})	
333.2	Fixed	1–2	0.2	−38,589.68	−8249.90	0.0055
		1–3	0.2	8884.67	5054.66	
		2–3	0.3	−8131.76	−31,679.33	
	Floating	1–2	0.26	1003.67	650.32	0.0054
		1–3	0.70	2996.37	3595.89	
		2–3	0.12	−82,084.79	10,423.43	
338.2	Fixed	1–2	0.2	−45,414.23	−9760.39	0.0083
		1–3	0.2	8717.15	5017.25	
		2–3	0.3	−9676.08	−35,751.61	
	Floating	1–2	0.20	−6748.81	−37.33	0.0100
		1–3	0.44	3089.98	4544.43	
		2–3	0.25	7707.41	−14,024.64	
343.2	Fixed	1–2	0.2	24,457.04	−8697.03	0.0049
		1–3	0.2	6789.46	4990.40	
		2–3	0.3	−5910.34	19,617.80	
	Floating	1–2	0.81	−12,404.16	−754.83	0.0046
		1–3	0.12	6815.98	4131.81	
		2–3	0.22	−348.19	−11,746.85	

only showed a slight influence of this variable in regards to the solubilization of both phases; no significant decrease of the two-phase area may be observed in the figures.

3.3. *Data correlation and binary interaction parameters*

As described above, the NRTL model was fitted to data were for the three systems considered in this study given that this model had previously been employed for systems containing alcohols and organic carbonates (Fang and Qian, 2005). Accordingly, six binary interaction parameters exist for the ternary systems T1 and T2 and twelve for the quaternary system Q.

Previous work with the system T1 optimized the values of the non-randomness binary interaction parameters α_{ij} at similar temperatures to those being tested throughout the present work (Wang and Lu, 2012). The values reported were $\alpha_{23} = 0.3$ and $\alpha_{12} = \alpha_{13} = 0.2$, which match, respectively, the rules of thumb given for non-polar substances or non-polar with polar non-associated liquids and saturated hydrocarbons with polar non-associated liquids and systems that exhibit liquid–liquid immiscibility (Renon and Prausnitz, 1968).

Given the similar nature of GC, the same set of optimized α_{ij} values were fixed in order to retrieve the rest of the binary interaction parameters $\Delta g_{ij}/R$ after the corresponding fitting of data for the system T2. Tables 4–6 show the values obtained when fitting the data at each temperature tested at the mentioned fixed values of α_{ij}. In the quaternary system,

Table 6 – Values of the NRTL binary interaction parameters obtained from the LLE data by regression for the system Q {DMC (1) + MeOH (2) + MeOH (3) + Gly (4)}.

T (K)	α_{ij} regression	Components i–j	NRTL parameters			rmsd
			α_{ij}	$(g_{ij} - g_{ii})$ (J mol^{-1})	$(g_{ji} - g_{jj})$ (J mol^{-1})	
333.2	Fixed	1–2	0.2	2207.87	1925.52	0.0052
		1–3	0.2	2551.15	−1209.69	
		1–4	0.2	8064.83	5594.99	
		2–3	0.2	3882.22	19,638.92	
		2–4	0.3	−505.08	1442.31	
		3–4	0.3	−2890.53	6027.48	
	Fixed	1–2	0.2	3041.51	1858.93	0.0057
		1–3	0.2	3058.97	−1858.26	
		1–4	0.2	8053.27	5588.17	
		2–3	0.3	5748.22	13,489.80	
		2–4	0.3	−454.69	2249.27	
		3–4	0.3	−2748.69	5346.82	
	Floating	1–2	0.53	5342.58	416.70	0.0049
		1–3	0.00	26,157.42	−20,783.09	
		1–4	0.31	9152.97	7064.07	
		2–3	0.71	623.22	14,453.64	
		2–4	0.14	−10,469.65	20,115.22	
		3–4	0.32	−3556.65	11,664.04	
338.2	Fixed	1–2	0.2	281.01	4199.57	0.0064
		1–3	0.2	−36,757.19	−3005.01	
		1–4	0.2	7818.40	5511.18	
		2–3	0.2	−18,957.00	15,378.57	
		2–4	0.3	−2139.44	2661.81	
		3–4	0.3	−6592.42	−30,956.10	
	Fixed	1–2	0.2	7804.60	1716.92	0.0070
		1–3	0.2	20,397.40	−5265.92	
		1–4	0.2	7407.44	5540.45	
		2–3	0.3	920.53	24,683.27	
		2–4	0.3	−772.70	10,762.22	
		3–4	0.3	−1247.93	22,253.42	
	Floating	1–2	0.19	−552.47	15,506.77	0.0051
		1–3	0.73	52,649.65	6510.53	
		1–4	0.45	12,753.59	13,846.63	
		2–3	0.38	−57,186.19	17,674.90	
		2–4	0.06	4549.01	47,881.99	
		3–4	0.71	7322.56	57,557.57	
343.2	Fixed	1–2	0.2	6951.25	1165.29	0.0113
		1–3	0.2	16,369.35	7495.65	
		1–4	0.2	5322.96	4003.86	
		2–3	0.2	4003.86	32,542.49	
		2–4	0.3	2871.41	3855.45	
		3–4	0.3	−2501.43	13,715.61	
	Fixed	1–2	0.2	7508.54	447.21	0.0108
		1–3	0.2	15,122.75	−4566.55	
		1–4	0.2	7430.89	5366.35	
		2–3	0.3	3703.97	15,142.62	
		2–4	0.3	1897.42	4544.76	
		3–4	0.3	−1925.36	12,180.51	
	Floating	1–2	0.05	45,952.81	−26,799.35	0.0092
		1–3	0.71	685.82	2486.88	
		1–4	0.36	3391.36	4486.48	
		2–3	0.05	29,831.30	−5341.33	
		2–4	0.16	−3304.73	7343.84	
		3–4	0.76	2629.80	2967.02	

fixing the α_{ij} parameter for the interaction between MeOH and GC at 0.2 and 0.3 was tried, resulting in a lower rmsd value when operating with the data at 333.2 and 338.2 K and a higher rmsd at 343.2 K; notwithstanding, the differences were not as remarked as to determine whether the selection of 0.2 or 0.3 is more appropriate.

Furthermore, correlation was also tried floating the non-randomness parameters so as to obtain their optimized values. The rmsd value decreased as a consequence of a higher degree of freedom in the fitting, but no significant differences regarding this criterion were obtained; furthermore, the α_{ij} values in many cases were different to those proposed as standard in literature (Renon and Prausnitz, 1968). Fitting to the NRTL model for the systems T1, T2 and Q proved satisfactory given the small rmsd values retrieved from the correlations.

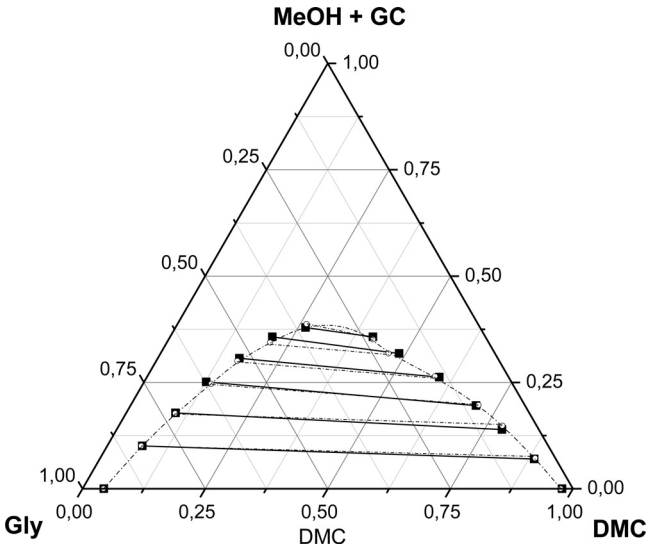

Fig. 4 – Experimental LLE measurements and binodal curve using the NRTL model for the system Q: DMC + (MeOH + GC) + Gly at 343.2 K. ■ represents experimental tie-lines and dashed lines are data calculated with the NRTL model.

4. Conclusions

Ternary systems consisting of {DMC + MeOH + Gly} and {DMC + GC + Gly} and the quaternary system {DMC + MeOH + GC + Gly}, all of which involved in the glycerol carbonate synthesis, were tested for LLE at 333.2, 338.2 and 343.2 K under atmospheric pressure. Assessment of the individual solubilizing effect of MeOH and GC in the ab initio biphasic system showed that the latter enhanced the miscibility of the system significantly more than the former. Simultaneous utilization of MeOH and GC as cosolvents did not favour mutual solubility as much as the single utilization of GC as can be inferred from the figures. However, variation of temperature within the range tested presented no significant effect throughout these assays.

Correlation of the LLE data obtained in this work was performed utilizing the NRTL model. Adequate fitting to data was obtained for each system giving as a result sets of binary interaction parameters utilizing LLE data at each individual temperature as well as for the whole range of this variable.

Acknowledgements

Grateful appreciation goes to the Ministerio de Ciencia e Innovación of the Government of Spain for financial support of the present research through the project CTQ 2010-15460. We would also like to express gratitude to UBE Corporation for kindly supplying dimethyl carbonate for this research.

References

Aresta, M., Dibenedetto, A., Nocito, F., Pastore, C., 2006. A study on the carboxylation of glycerol to glycerol carbonate with carbon dioxide: the role of the catalyst, solvent and reaction conditions. J. Mol. Catal. A: Chem. 257, 149–153.

Behr, A., Eilting, J., Irawadi, K., Leschinski, J., Lindner, F., 2008. Improved utilisation of renewable resources: new important derivatives of glycerol. Green Chem. 10, 13–30.

Benoit, M., Brissonnet, Y., Guélou, E., De Oliveira Vigier, K., Barrault, J., Jérôme, F., 2010. Acid-catalyzed dehydration of fructose and inulin with glycerol or glycerol carbonate as renewably sourced co-solvent. ChemSusChem 3, 1304–1309.

Britt, H.I., Luecke, R.H., 1973. The estimation of parameters in nonlinear implicit models. Technometrics 15, 233–247.

Climent, M.J., Corma, A., De Frutos, P., Iborra, S., Noy, M., Velty, A., Concepción, P., 2010. Chemicals from biomass: synthesis of glycerol carbonate by transesterification and carbonylation with urea with hydrotalcite catalysts. The role of acid–base pairs. J. Catal. 269, 140–149.

Chen, C.-H., Hyung, Y.E., Vissers, D.R., Amine, K., 2002. Lithium ion battery with improved safety, US 7026074 B2.

Choe, J., Song, K.H., 2002. Liquid–liquid equilibrium for the ternary systems nonane + dimethyl carbonate + methanol and decane + dimethyl carbonate + methanol at 298.15 K. J. Chem. Eng. Data 47, 1253–1255.

de la Torre, J., Cháfer, A., Berna, A., Muñoz, R., 2006. Liquid–liquid equlibria of the system dimethyl carbonate + methanol + water at different temperatures. Fluid Phase Equilib. 247, 40–46.

Fang, Y.-J., Qian, J.-M., 2005. Isobaric vapor–liquid equilibria of binary mixtures containing the carbonate group —OCOO—. J. Chem. Eng. Data 50, 340–343.

Hu, J., Li, J., Gu, Y., Guan, Z., Mo, W., Ni, Y., Li, T., Li, G., 2010. Oxidative carbonylation of glycerol to glycerol carbonate catalyzed by $PdCl_2$(phen)/KI. Appl. Catal. A: Gen. 386, 188–193.

Katayama, H., Hayakawa, T., Kobayashi, T., 1998. Liquid–liquid equilibria of three ternary systems: 2-propanone–glycerol–methanol, 2-butanone–glycerol–ethanol, and 2-butanone–glycerol–2-propanol in the range of 283.15 to 303.15 K. Fluid Phase Equilib. 144, 157–167.

Kovvali, A.S., Sirkar, K.K., 2002. Carbon dioxide separation with novel solvents as liquid membranes. Ind. Eng. Chem. Res. 41, 2287–2295.

Lameiras, P., Boudesocque, L., Mouloungui, Z., Renault, J.-H., Wieruszeski, J.-M., Lippens, G., Nuzillard, J.-M., 2011. Glycerol and glycerol carbonate as ultraviscous solvents for mixture analysis by NMR. J. Magn. Reson. 212, 161–168.

Lee, K., Park, C.-H., Lee, E., 2010. Biosynthesis of glycerol carbonate from glycerol by lipase in dimethyl carbonate as the solvent. Bioprocess Biosyst. Eng. 33, 1059–1065.

Li, Q., Zhang, W., Zhao, N., Wei, W., Sun, Y., 2006. Synthesis of cyclic carbonates from urea and diols over metal oxides. Catal. Today 115, 111–116.

Magniont, C., Escadeillas, G., Oms-Multon, C., De Caro, P., 2010. The benefits of incorporating glycerol carbonate into an innovative pozzolanic matrix. Cem. Concr. Res. 40, 1072–1080.

Ochoa-Gomez, J.R., Gomez-Jimenez-Aberasturi, O., Maestro-Madurga, B., Pesquera-Rodriguez, A., Ramirez-Lopez, C., Lorenzo-Ibarreta, L., Torrecilla-Soria, J., Villaran-Velasco, M.C., 2009. Synthesis of glycerol carbonate from glycerol and dimethyl carbonate by transesterification: catalyst screening and reaction optimization. Appl. Catal. A: Gen. 366, 315–324.

Pagliaro, M., Ciriminna, R., Kimura, H., Rossi, M., Della Pina, C., 2009. Recent advances in the conversion of bioglycerol into value-added products. Eur. J. Lipid Sci. Technol. 111, 788–799.

Pagliaro, M., Rossi, M., 2008. The Future of Glycerol. New Uses for a Versatile New Material. RSC Publishing, Cambridge.

Renon, H., Prausnitz, J.M., 1968. Local compositions in thermodynamic excess functions for liquid mixtures. AIChE J. 14, 135–144.

Rokicki, G., Rakoczy, P., Parzuchowski, P., Sobiecki, M., 2005. Hyperbranched aliphatic polyethers obtained from environmentally benign monomer: glycerol carbonate. Green Chem. 7, 529–539.

Shimoyama, Y., Abeta, T., Zhao, L., Iwai, Y., 2009. Measurement and calculation of vapor–liquid equilibria for methanol + glycerol and ethanol + glycerol systems at 493–573 K. Fluid Phase Equilib. 284, 64–69.

Sonnati, M.O., Amigoni, S., de Givenchy, E.P.T., Darmanin, T., Choulet, O., Guittard, F., 2013. Glycerol carbonate as a versatile building block for tomorrow: synthesis, reactivity, properties and applications. Green Chem. 15, 283–306.

Tudorache, M., Protesescu, L., Coman, S., Parvulescu, V.I., 2012. Efficient bio-conversion of glycerol to glycerol carbonate catalyzed by lipase extracted from *Aspergillus niger*. Green Chem. 14, 478–482.

Wang, H., Lu, P., 2012. Liquid–liquid equilibria for the system dimethyl carbonate + methanol + glycerol in the temperature range of (303.15 to 333.15) K. J. Chem. Eng. Data 57, 582–589.

Yunhai, S., Honglai, L., Kun, W., Wende, X., Ying, H., 2005. Measurements of isothermal vapor–liquid equilibrium of binary methanol/dimethyl carbonate system under pressure. Fluid Phase Equilib. 234, 1–10.

Publicación 2 / Publication 2

Autores/Authors: Jesús Esteban, Elena Fuente, Ángeles Blanco, Miguel Ladero and Félix García-Ochoa

Título/Title: Phenomenological kinetic model of the synthesis of glycerol carbonate assisted by focused beam reflectance measurements

Estado actual/Current status: Published. Chemical Engineering Journal (2015), 260: 434-443

Índice de impacto / Impact factor 2013: 4.058

Resumen

En este trabajo se estudia la síntesis de GC a partir de glicerol y DMC en ausencia de disolventes. Primero se planteó la selección de las condiciones de reacción apropiadas. Se eligió K_2CO_3 como catalizador más activo de entre una serie de carbonatos y bicarbonatos de metales alcalinos y se estableció el intervalo de temperaturas en el que operar entre 66 y 70 ºC. Dada la presencia de dos fases líquidas al inicio de la reacción, se estudió mediante una técnica óptica (FBRM) y análisis químico de los compuestos de la reacción el efecto de la agitación, observándose que a 1500 rpm la transferencia externa de materia no supone una etapa limitante de la velocidad global del proceso.

Con estas condiciones seleccionadas, se realizaron una serie de experimentos cinéticos. En ellos, se sigue la desaparición de las dos fases líquidas para dar una sola mediante la disminución de la frecuencia y longitud de las cuerdas de la fase dispersa (glicerina), apreciándose que la variación de la temperatura y la relación molar inicial de DMC a Gly apenas tienen efecto sobre la extensión de reacción a la cual se produce la transición de un sistema líquido bifásico a uno monofásico. Ésta tiene lugar a una conversión de glicerol cercana a 30%, que implica unas composiciones de la mezcla de reacción con un buen grado de coincidencia con la curva que separa las regiones mono y bifásica en los equilibrios líquido-líquido estudiados en la publicación 1.

Ante la escasez de información sobre la cinética de esta reacción, se efectuaron hasta 27 experimentos variando la temperatura, el exceso molar de DMC a glicerol y la cantidad de catalizador. Con los datos obtenidos, se propusieron varios modelos cinéticos, entre los cuales el que mejor se ajustó (con errores inferiores al 6.8%) considera la fenomenología observada en lo que al cambio de fases líquidas respecta. Dicho modelo consta de dos etapas representadas por ecuaciones potenciales aplicables hasta y después de una conversión de reacción del 30%. En la primera, bajo régimen bifásico, la reacción tiene lugar sólo en la fase rica en glicerol y es de primer orden respecto a la glicerina y orden 0 respecto al DMC. En la segunda, se aprecia una caída notable de la velocidad de reacción atribuible a la dilución del catalizador en todo el volumen de la mezcla; esta etapa queda representada por una ecuación potencial de primer orden respecto a las concentraciones tanto de glicerol como de DMC. La energía de activación de la reacción es de 179.2 ± 3.7 kJ mol^{-1}.

Chemical Engineering Journal 260 (2015) 434–443

Contents lists available at ScienceDirect

Chemical Engineering Journal

journal homepage: www.elsevier.com/locate/cej

Phenomenological kinetic model of the synthesis of glycerol carbonate assisted by focused beam reflectance measurements

Jesus Esteban, Elena Fuente, Angeles Blanco, Miguel Ladero *, Felix Garcia-Ochoa

Department of Chemical Engineering, College of Chemical Sciences, Complutense University of Madrid, 28040 Madrid, Spain

HIGHLIGHTS

- Synthesis of glycerol carbonate using inexpensive catalysts was studied.
- The reacting system is a liquid–liquid mixture evolving into a monophasic system.
- The evolution of the dispersion was observed by FBRM.
- The change in the phase regime affects the catalytic behaviour.
- Phenomenological kinetic models were proposed, fitted and verified.

GRAPHICAL ABSTRACT

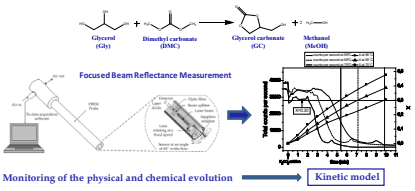

ARTICLE INFO

Article history:
Received 29 July 2014
Received in revised form 9 September 2014
Accepted 10 September 2014
Available online 18 September 2014

Keywords:
Glycerol carbonate
FBRM
Multiphasic reaction
Liquid dispersion
Kinetic model

ABSTRACT

In this paper, the synthesis of glycerol carbonate from glycerol and dimethyl carbonate is studied. First, operating conditions and a catalyst were selected after screening of different alkali metal salts, resulting K_2CO_3 the most active species. Afterwards, given the low degree of miscibility between the reactants, a study of the phase change from a liquid–liquid emulsion to a monophasic sample throughout the reaction was successfully performed with the aid of a focused beam reflectance probe. This change took place at a conversion of approximately 0.30. With the findings of this study, distinct kinetic models were proposed and fitted to the experimental data obtained after the completion of a series of kinetic runs varying temperature (66–70 °C), molar ratio of dimethyl carbonate to glycerol (1.5–3) and catalyst load (0.75–1.25% w/w). A model composed of two potential equations was proposed with activation energy of 179.2 ± 3.7 kJ mol^{-1}. The model was capable of describing the initial biphasic stage and the monophasic regime correlated best to the experimental data, with errors below 6.8%.

1. Introduction

The saturation of the market of glycerol (Gly) following the significant development of the biodiesel industry has lead to a marked price drop of this formerly valuable by-product, considered as a building block from biomass [1]. Thus, research on the synthesis of valuable products derived from glycerol has been a blooming issue as a means of its valorisation. Examples of the processes studied are selective oxidation to dihydroxyacetone, hydrogenation to 1,2-propanediol, ketalization to solketal or even microbiological transformations to 1,3-propanediol and 2,3-butanediol [2,3]. However, currently the synthesis of glycerol carbonate (GC) by carboxylation and transesterification is on the focus of research due to its numerous applications as a multipurpose green solvent as well as a component of gas separation membranes, coating materials and pozzolanic-based building materials. In addition, it has been reported to be a synthon for many different

Abbreviations: DMC, dimethyl carbonate; GC, glycerol carbonate; Gly, glycerol; MeOH, methanol.

* Corresponding author. Tel.: +34 913944164; fax: +34 913944179.
E-mail address: mladero@quim.ucm.es (M. Ladero).

http://dx.doi.org/10.1016/j.cej.2014.09.039
1385-8947/

Nomenclature

AIC	Akaike's information criterion
C	concentration of the components at a given time (mol L^{-1})
E_{ai}/R	ratio of activation energy and the ideal gas constant (K)
F	Fischer's F statistical parameter
FBRM	focused beam reflectance measurement
HPLC	high-performance liquid chromatography
K	number of parameters of a proposed model
M	initial molar ratio of dimethyl carbonate to glycerol
n	total number of components
N	total number of data to which a model is fitted
r	reaction rate (mol L min^{-1})
RMSE	residual mean squared error
SQR	sum of quadratic residues
T	temperature (K)
TOF	turnover frequency (mol converted·mol $catalyst^{-1}$ min^{-1})
X	conversion, as defined by Eq. (8)

Greek letters

γ	heteroscedasticity parameter
v	stoichiometric coefficient of the component i
ω	agitation rate (rpm)

Subscripts

0	relative to the start of the reaction, time equals zero
i	relative to component i
cat	relative to the catalyst
crit	relative to the critical conversion at which the phase regime changes
DMCsol	relative to concentration of DMC dissolved in the glycerol-rich phase

end products, especially polymers used for adhesives and protective coatings or esters obtained by acylation, with good surfactant and oxidation stability features [4].

Synthesis of GC has been researched as a means to valorise glycerol as well as to substitute the traditional environmentally unfriendly production via the phosgene route. Carboxylation with CO_2 under high demanding energy conditions has been achieved, with applied pressures ranging from 3.5 to 10 MPa and temperatures between 80 and 180 °C using zeolites and different metal-based catalysts [5–8]. Vacuum conditions and temperatures around 150 °C with metallic oxides and sulphates have been reported for the glycerolysis of urea as an alternative pathway for the production of GC [9–12]. However, transesterification of glycerol with organic carbonates appears as a methodology with less demanding operating conditions, especially when working with dimethyl carbonate (DMC) or ethylene carbonate. Atmospheric pressure and temperatures from 60 to 75 °C have been reported in the former case [13–16] and around 50 °C in the latter [12,17]. Additionally, solventless syntheses are common practice contrary to the procedures described in the paragraph above and even the catalyst used in some cases are inexpensive, like calcium oxide and potassium carbonate [13,18].

The present study follows the line of the transesterification reaction using DMC as the carbonate source. Initially, in the absence of any catalyst, the reactants Gly and DMC have very low miscibility with each other, which results in an emulsion-like liquid–liquid biphasic system. Nevertheless, as the reaction takes place and products generate, the system evolves into a single phase liquid [19,20]. This type of behaviour has previously been reported for certain esterification [21] transesterification reactions [22].

The mechanism through which the transesterification reaction between glycerol and dialkyl carbonates proceeds requires a basic catalyst. This mechanism basically consists of four steps: (a) formation of a glyceroxide anion by extraction of one of the protons from glycerol by the basic catalyst; (b) attack on the carbonate group by the nucleophile glyceroxide anion releasing a non-cycled unstable reaction intermediate as well as an alkoxide ion; (c) regeneration of the catalyst releasing a proton that combines with the alkoxide ion to form a molecule of alcohol; (d) finally, the unstable intermediate species suffers a rapid cyclation to yield glycerol carbonate and a second molecule of alcohol is also released. [14,23].

The selectivity of the reaction of DMC and Gly to yield has been reported to be above 96% and very close to 100% in many cases using assorted catalysts. Examples of these would be Na_2O [24], KF modified hydroxyapatites, selectivity above 98% [15], Mg–Al hydrotalcites [23], calcined and non-calcined CaO [24] as well as supported on Diatomite, Kaolin and Al_2O_3 [13]. Finally, when potassium carbonate was used the selectivity reported has been 100% for a reaction at very similar conditions to those being tested in this work [14].

The behaviour of distinct phases in multiphasic systems can be measured on-line by different optical techniques like spatial filtering velocimetry, photometric stereo imaging, the patented Eyecon® technology (based on flash imaging), endoscopy or focused beam reflectance measurement (FBRM) [25,26].

Among them, the latter technology has been typically used to determine the particle size distribution of suspensions of solid suspensions in liquid phases, such as in flocculation processes [27,28]. However, more recently it has been employed to monitor the evolution and calculate particle size distributions of the phases of liquid–liquid dispersions consisting of mineral oils and water [29–31]. There is also a reference that reports on the measurement of droplet size distributions by means of a microphotographic system known as bubble-cap tray while the transesterification of Gly with methyl oleate takes place [22].

The performance of the reaction between Gly and DMC under different operating conditions and catalysts has been widely addressed, as already mentioned; however, the kinetic aspects of this process have not been given so much attention. Since a change in the phase regime occurs throughout the conversion to products, it is reasonable to suggest a model that addresses this observation and the potential consequences it can produce on the catalytic behaviour of the system.

Thus, as a means to shed more light on these aspects behind the transesterification of Gly with DMC, the evolution of the initially biphasic system was monitored by FBRM and a set of kinetic runs was completed varying temperature, concentration of catalyst and initial molar ratio of the reactant species.

A series of kinetic models was reasoned and proposed to explain the data observed from a phenomenological standpoint. Discrimination and final selection of a definite phenomenological kinetic model was made on the basis of physicochemical and statistical criteria.

2. Materials and methods

2.1. Materials

Preliminary and kinetic experiments were conducted using extra pure Gly (assay grade 99.88%) from Fischer Chemical and DMC (purity > 99%), kindly donated by UBE Corporation Europe. Lithium carbonate (ACS reagent, purity > 99%), sodium carbonate (ACS reagent, purity > 99%), both from Aldrich, potassium carbonate (purity > 99%), lithium hydrogen carbonate (purity > 99%), sodium hydrogen carbonate (purity > 99%) and potassium hydrogen carbonate (purity > 99%), the latter four from Alfa Aesar, were used as catalysts for the reaction. For analysis purposes, the following chemicals were utilized: citric acid (ACS reagent, purity ⩾ 99.5%) by Sigma–Aldrich was used as an internal standard; HPLC grade methanol (assay grade 99.99%) from Scharlau Chemie and GC (purity ⩾ 99.5%) from Sigma–Aldrich were used for calibration purposes.

2.2. Experimental setup

The device employed throughout the experimentation is outlined in Fig. 1. It is fundamentally a custom made stainless steel stirred tank reactor that includes deflector baffles. The reactor is equipped with a heating mechanism consisting of a thermal resistor surrounding its outer diameter. Temperature is controlled by an OMRON E5CN PID controller linked to the mentioned resistor. The load was stirred by means of a flat six-blade impeller whose speed was regulated by an IKA RW20 motor (250–2000 rpm). A Dimroth condenser was attached to the reactor so as to avoid removal of methanol and DMC as the reaction progressed. Finally, an aperture (item 11) was made to introduce the FBRM for online monitoring of the droplet size. Arrangement of the reactor with the introduction of the FBRM probe was made prior to the beginning of the reactions due to the location of the probe at the bottom of the reactor. This location was selected so as not to interfere in the mixing of the dispersion.

2.3. Droplet size distribution experiments

With Gly being the dispersed phase in all cases given the excess of DMC used in all the experiments, on-line monitoring of the droplet size was made by FBRM. In this work, a Lasentec FBRM M500LF manufactured by Mettler Toledo, Seattle, USA device was used, depicted elsewhere [23].

This technique uses light back scattering effects to obtain the real time chord size distribution of a dispersion without the need to subject it to any type of manipulation. The device consists of a sensor with a laser beam generator (λ = 791 nm) and a detector controlled by a computerized system. The rotating lens inside of the sensor focuses the generated laser beam on a point, which rotates within the dispersion through a circular path of 8 mm of diameter at a high speed of 1.9 m/s. When the laser beam encounters the surface of a droplet of Gly, it is reflected and reaches the detector, which registers a light pulse of a certain duration and is translated into an electrical signal. If the signal acquires an intensity value above the threshold, it is considered to correspond to a certain chord length. The product of the duration of the light pulse multiplied by the lineal velocity of the focal point is the chord length. The FBRM device measures the chord length of the droplets

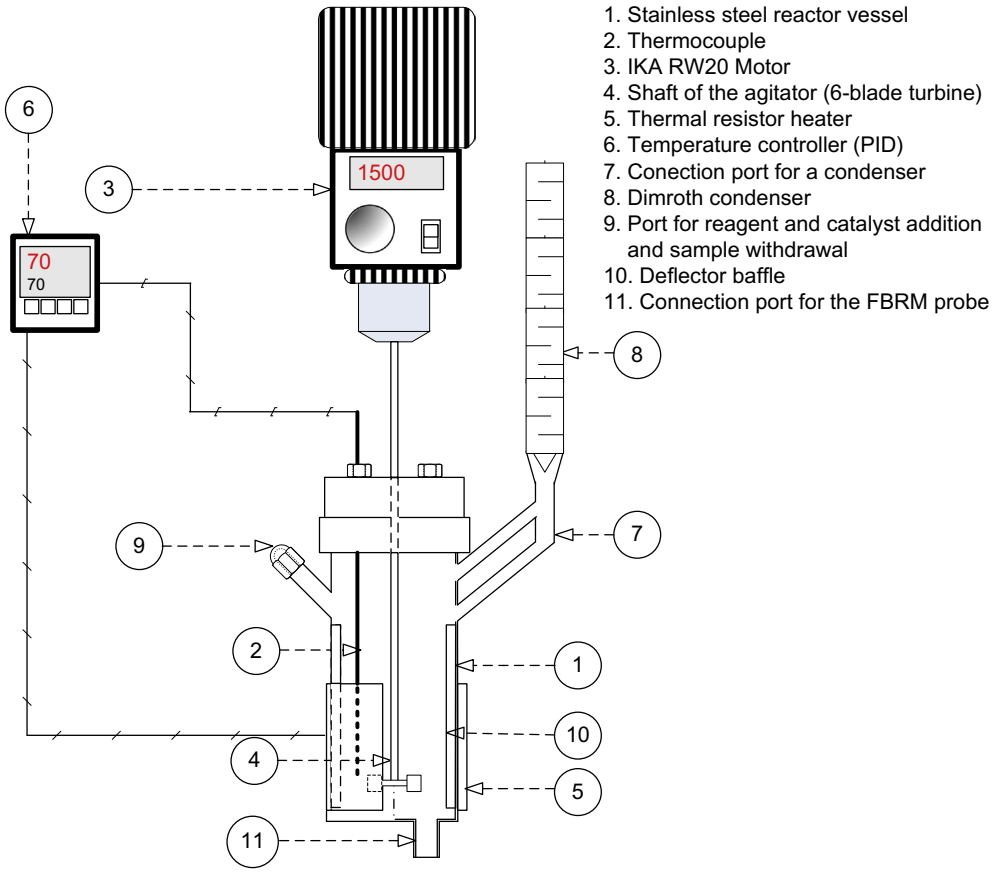

Fig. 1. Experimental device utilized for the kinetic study of the synthesis of glycerol carbonate.

that pass through the focal point during a definite period of time, thereby obtaining a chord length population whose distribution constitutes the end result of the measurement. From the mentioned distribution, statistics like the total count of droplets per unit time or the mean chord length may be computed, whose evolution with time grants interpretation of the changes taking place within the system.

2.4. Methods

2.4.1. Selection of agitation speed

An assessment of this variable was realized while fixing the rest of the operating conditions. Monitoring of the drop size distribution and mean chord length was made at several agitation conditions in the range 750–2000 rpm and the progress of the concentration of the components was also followed.

2.4.2. Batch reactions: selection of catalyst and kinetic studies

Runs were performed in batches, in which the reactor was loaded with glycerol and DMC through port 9 (Fig. 1). After stirring and heating to a point in which the batch was at the desired temperature, catalyst was added and then samples were withdrawn during the course of the reaction and analyzed by HPLC. First, preliminary runs were conducted to select the most adequate catalyst. Then, a set of kinetic runs at a fixed agitation speed were performed varying temperature, catalyst concentration and initial molar ratio of DMC to Gly (M).

2.4.3. Determination of the presence of catalyst in Gly and DMC

For the purpose of the determination of the presence of potassium carbonate in each phase, samples at short times of reaction were withdrawn, while the system was still biphasic. To enhance the separation of phases, a centrifuge (Thermo Scientific Heraeus Pico 17) was used. Then, each phase was analyzed for the presence of potassium with a Quantofix® potassium commercial test, supplied by Macherey–Nagel.

2.5. Analytical methodology

Withdrawn reaction samples were 25-fold diluted in a solution of 8 g/L of citric acid, used as internal standard. Then, a HPLC JASCO 2000 series equipment was employed for sample analysis with the following operating conditions: a constant flow rate of 0.5 mL/min of acid Milli-Q water (0.005 N H_2SO_4) of mobile phase flowing through a Rezex ROA-Organic Acid H+ (8%) column (150 × 7.80 mm) at 60 °C.

2.6. Mathematical methods

The kinetic models were correlated to experimental data with the aid of Aspen Custom Modeler, whose fitting principles are based on the through application of the Levenberg–Marquardt algorithm jointly with the numerical integration of the model via a fourth-order Runge–Kutta method. Initially the models were individually correlated to experimental data at a fixed temperature; afterwards, correlation of all experimental data was made to obtain the multivariable fitting.

Discrimination and selection of models was performed on the basis of physicochemical as well as statistical criteria, including Fischer's F value (F), the residual mean squared error (RMSE), the variation explained (VE) and the Akaike information criterion (AIC) [32].

F is based on a null hypothesis that advocates for the adequacy of the model to the observed values of the measured variable and is defined as Eq. (1) states:

$$F = \frac{\sum_{i=1}^{N} \frac{(y_{i,calc})^2}{P}}{\sum_{i=1}^{N} \frac{SQR}{N-P}} \tag{1}$$

where N is the total number of experimental data, P is the number of parameters of the model, SQR is the sum of quadratic residues, defined as. $(y_{i,exp} - y_{i,calc})^2$, and $y_{i,exp}$ and $y_{i,calc}$ are, respectively, the experimental and calculated values of the variable.

The RMSE is often considered a measure of the difference of the predicted values of the variable and the experimental observations. It takes into account the amount of available data and the number of parameters of the model as its definition indicates [33]:

$$\text{RMSE} = \sqrt{\frac{SQR}{N-P}} \tag{2}$$

The VE, given as a percentage, also quantifies the goodness of fit of the being given by:

$$\text{VE}\ (\%) = 100 \cdot \left(1 - \frac{\sum_{l=1}^{L} SSQ_l}{\sum_{l=1}^{L} SSQmean_l}\right) \tag{3}$$

where SSQ_l and $SSQmean_l$ are defined as follows:

$$SSQ_l = \sum_{i=1}^{N} \frac{(y_{i,exp} - y_{i,calc})^2}{y_{i,calc}^{\gamma l}} \tag{4}$$

$$SSQmean_l = \sum_{i=1}^{N} \frac{(y_{i,exp} - \bar{y}_{i,exp})^2}{y_{i,calc}^{\gamma l}} \tag{5}$$

being

$$\bar{y}_{i,exp} = \frac{\sum_{i=1}^{N} \frac{y_{i,exp}}{y_{i,calc}^{\gamma l/2}}}{\sum_{i=1}^{N} \frac{1}{y_{i,calc}^{\gamma l/2}}} \tag{6}$$

In the three foregoing γ_j is the heteroscedasticity parameter, a measure of the type of error in the measured variable. By default, Aspen Custom Modeler fixes its value at 1.

Finally, AIC relates the amount of experimental data available to the number of parameters of the model. This parameter gives information of the goodness of fit while penalizing model overfitting by increasing the number of parameters of the model [34]. This statistical criterion is defined as:

$$AIC = N \cdot \ln\left(\frac{SQR}{N}\right) + 2 \cdot P \tag{7}$$

As a general rule, the quality of the proposed models to describe the observed data increases with the value of F and VE and as AIC and RMSE decrease.

3. Results and discussion

Throughout the next epigraphs, the variable conversion at each reaction time, denoted as X, will serve as the basis for the comments in terms of performance of the reaction. In this study, defining an average conversion can be performed inasmuch as the four components involved in this transesterification reaction could be adequately measured by means of the analytical procedure described in Section 2.5 and considering that there is a single reaction to be considered. Thus, it will be defined as the average value of the conversions for the reactants Gly and DMC and the yields to GC and MeOH divided by the initial concentration of glycerol, which is the limiting reactant in all cases. Eq. (8) defines this so-called average conversion variable:

$$X = \frac{\sum_{i=1}^{n} \frac{|C_i - C_{i0}|}{\nu_i}}{n} \Big/ C_{Gly0} \tag{8}$$

where C_i, C_{i0} and C_{Gly0} refer to the concentration of each component at the time at which it was measured, at the reaction start and the initial concentration of glycerol, respectively; v_i is the stoichiometric coefficient and n is the total number of components (four in this case). Thereby not only average values can be calculated, but also experimental standard errors for such values.

3.1. Selection of operating conditions

3.1.1. Catalyst screening

As commented in the introduction, general knowledge of the reaction subject of study is that basic conditions are required for the reaction to occur. As far back as in 1959, supply of the necessary basic conditions for the production of GC by transesterification was proposed using alkali metal carbonates and hydrogen carbonates as catalysts [35]. Thus, screening among lithium, sodium and potassium carbonates and hydrogen carbonates was realized at 70 °C, a DMC to Gly molar ratio of 3, a catalyst concentration of 1% w/w and a stirring speed of 1500 rpm.

Table 1 compares the experimental results of the conversion and the turnover frequency (TOF) using different catalysts under the mentioned conditions after one hour of reaction time. It can be inferred that carbonates present a significantly higher activity than hydrogen carbonates, being weaker the basicity of the latter salts. As for the alkali metals, it can be seen that the order of activity for carbonates as well as for hydrogen carbonates was K > Na > Li. Therefore, potassium carbonate was selected for the rest of the experimentation throughout this work.

3.1.2. Selection of temperature

A selection of the operating temperature range was made both on a literature review and experimental operational basis. No reference has been found in bibliography for this reaction at temperatures below 60 °C and, as perceived in Fig. 2, the conversion after 1 h of operation and the TOF value were negligible and the TOF value were negligible at 55 °C. Quantitative yields of GC were obtained using benzene [36] and tetrahydrofurane [37] as reaction media as opposed to the solventless operation approached in this study, in which a conversion of barely 3% was obtained at 60 °C.

Increasing temperature above 60 °C led to better performance as expected; however, a significant leap in the conversion obtained after one hour was observed from 64 to 66 °C. Additionally, operational difficulties were found at atmospheric pressure when operating at temperatures above 70 °C due to the uncontrollable evaporation of methanol as it generated from the reaction. Thus, the temperature interval selected in this work was from 66 to 70 °C.

3.1.3. Assessment of the chord length distribution monitored by FBRM and selection of agitation conditions

In order to evaluate the development and behaviour of the *ab initio* emulsion-like system, a preliminary experiment was conducted at 70 °C, M = 3, 1% w/w of K_2CO_3 and 1500 rpm of stirring speed.

Fig. 3 shows the evolution of the mean chord length and the number of counts in different regions of the chord length distribution. As K_2CO_3 was added to the system (t = 0), the catalyst particles fell on the FBRM window and were detected, as shown

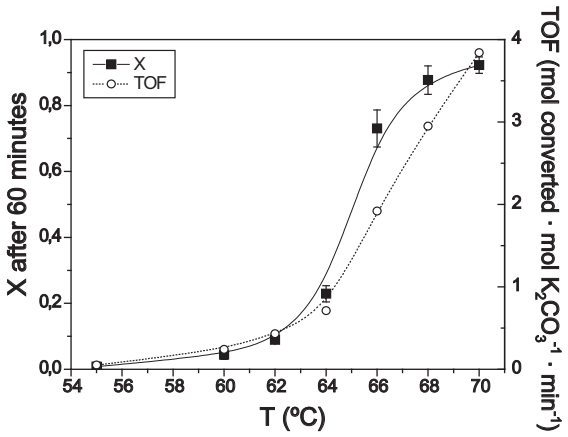

Fig. 2. Conversions observed after 60 min operating at different temperatures. Conditions: M = 3, C_{cat} = 11.3 g/L (1% w/w), ω = 1500 rpm.

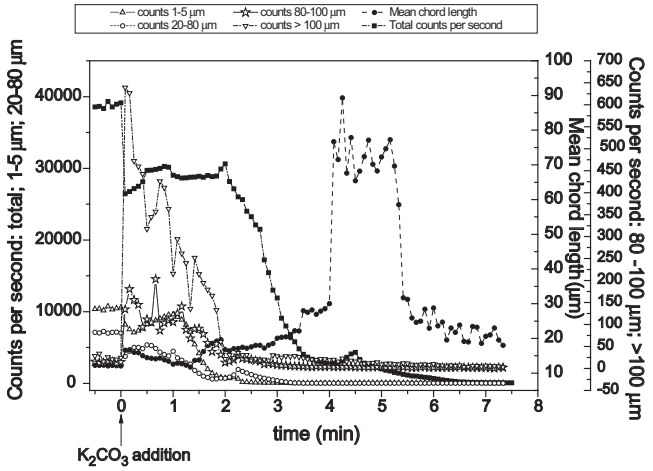

Fig. 3. Evolution of different statistics of the chord length distribution during the reaction. Conditions: T = 70 °C, M = 3, C_{cat} = 11.3 g/L (1% w/w) and ω = 1500 rpm.

by the fast raise of the number of counts over 100 µm. Then, the value of this statistics decreased due to the rapid dispersion and dissolution of the catalyst particles in the Gly-rich phase. The biphasic emulsion evolved towards a homogeneous monophasic system given the fact that the solubility of glycerine on DMC increases with conversion, i.e., as GC and MeOH become present in the mixture [20]. This is proved by the decrease in the total number of counts, which reaches virtually zero when the system becomes homogeneous at a reaction time between 4 and 5 min. Immediately afterwards, a small peak describing an increase of the mean chord length may be observed, ascribable to the detection of methanol bubbles on the surface of the FBRM probe window. Furthermore, throughout the biphasic stage, the formation of methanol increased as the system evolved and encouraged the nucleation of the methanol bubbles. Some large bubbles were formed on the surface of the FBRM probe and, as a result, the mean chord length increased. The high number of small drops of Gly and the decrease in the number of large particles due to the dissolution

Table 1
Performance after 60 min and turnover frequencies attained with each of the catalysts. Conditions: T = 70 °C, M = 3, C_{cat} = 11.3 g/L (1% w/w), ω = 1500 rpm.

Carbonate	X after 60 min	TOF · 10^2 (s^{-1})	Hydrogen carbonate	X after 60 min	TOF · 10^2 (s^{-1})
Li_2CO_3	0.77 ± 0.03	4.82	$LiHCO_3$	0.47 ± 0.01	2.93
Na_2CO_3	0.83 ± 0.03	5.55	$NaHCO_3$	0.54 ± 0.03	3.30
K_2CO_3	0.90 ± 0.01	6.40	$KHCO_3$	0.61 ± 0.02	3.53

of the catalyst moderated the increase of the mean chord length that shows a fast and marked increase of the mean chord size slightly after $t = 4$ min, when the system was starting to become homogeneous.

Given the development of the number of counts of an experiment throughout a catalytic experiment, evaluation of the agitation speed within this heterogeneous system was made with the intention of minimizing the mass transfer phenomena between the liquid phases. Due to the pronounced difference in the densities of DMC (1.07 kg/L at 298.15 K) and Gly (1.26 kg/L at 298.15 K), an increasing agitation rate will eventually compose a well distributed emulsion. By doing this, disregard of mass transfer between phases can be assumed so that the study of the kinetics corresponds solely to the chemical reaction, which would be in turn the limiting step of the process.

Fig. 4(a) depicts the progress of the number of counts below 100 μm while the system was still constituted by an emulsion. This graph provides proof that increasing the stirring speed hardly exerts any influence on the total counts of small chords, which in turn provide the most significant mass transfer surface between phases. As described in the previous section, the chords below 100 μm dismiss practically any particle of catalyst throughout its solubilization period, thus neglecting their presence on the evolution of the number of counts that explains the evolution of the dispersion.

Fig. 4(b) shows the influence of the agitation rate on the progress of the reaction. It can be seen that the evolution of the conversion is hindered by a lack of stirring when operating at 750 and 1000 rpm. However, under 1500 and 2000 rpm, performance of the reaction proved almost identical, which in turn confirms that an optimum agitation speed is reached at which mass transfer could be neglected.

3.2. Effect of temperature and molar ratio of DMC to Gly on the biphasic stage of the reaction

Once the catalyst and agitation conditions have been optimized, influence of temperature and initial molar ratio of reactants was assessed.

Fig. 5 shows the evolution of the dispersion of Gly in the DMC phase represented by the total number of counts per second (left axis) and the evolution of the chemical reaction, represented by the conversion X (right axis). The criterion followed to establish the change from a dispersion to a single phase liquid was to fix it one minute after the maximum of the peak ascribed to the generation of methanol as explained in Section 3.1.3. At this point, it was ensured in all the experiments that the drop of the total counts was at least 98%, so the counts only correspond to eventual air bubbles introduced by the stirring and not to any droplet of Gly. The conversion values observed acquired values of 0.33, 0.31 and 0.30

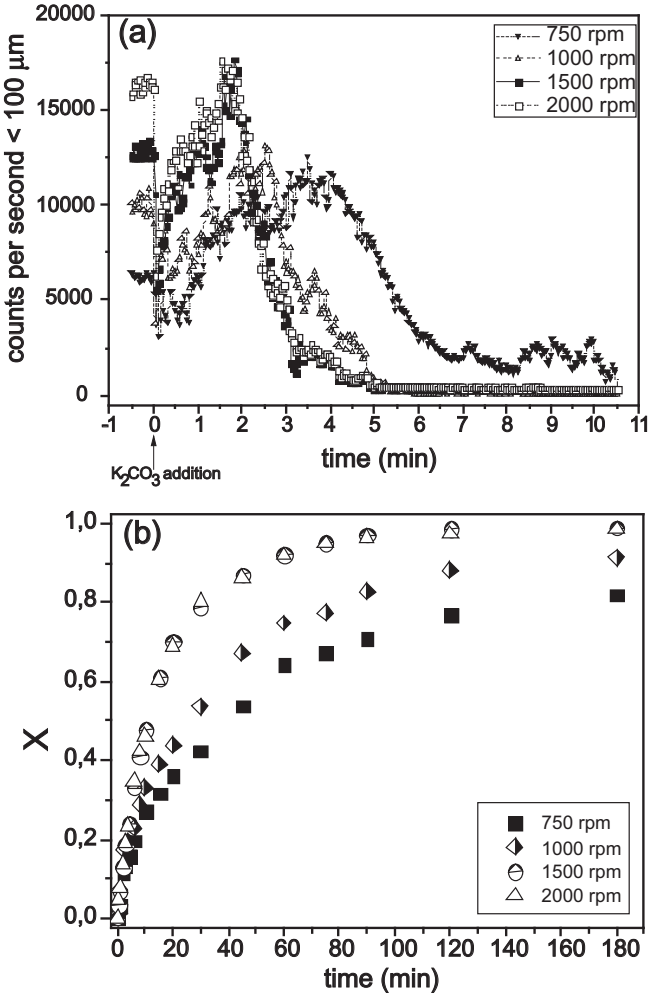

Fig. 4. Evaluation of the influence of the agitation rate (a) on the evolution of the drop counts below 100 μm and (b) on the performance of the transesterification reaction. Conditions: $T = 70$ °C, $M = 3$, $C_{cat} = 11.3$ g/L (1% w/w).

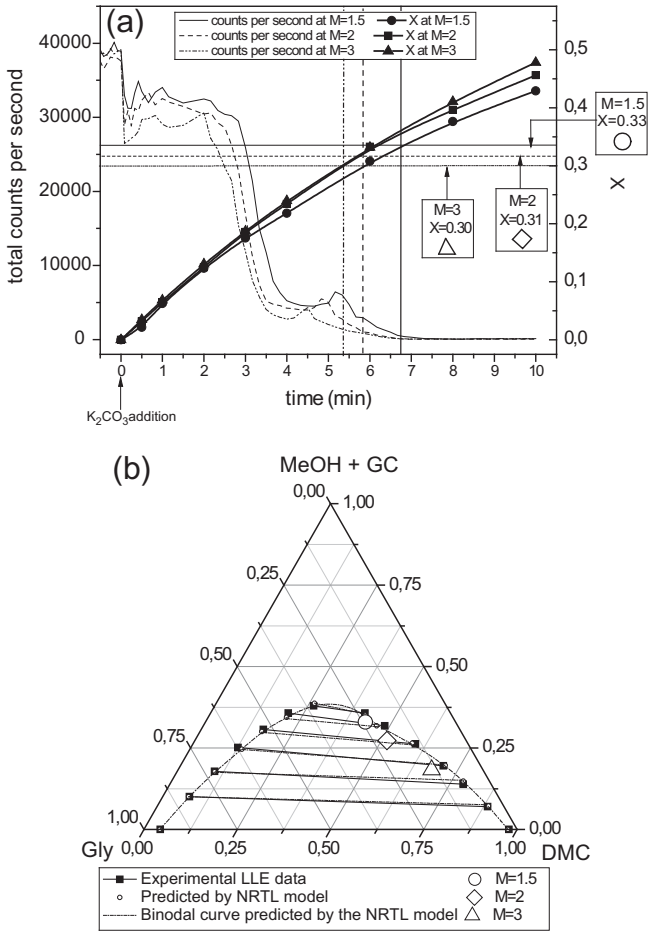

Fig. 5. Evolution of the number of counts and conversion with M (a) and composition of the reacting system at phase change conditions with respect to the liquid–liquid equilibrium [19] (b). Conditions: $T = 70$ °C, $C_{cat} = 11.3$ g/L (1% w/w), $\omega = 1500$ rpm.

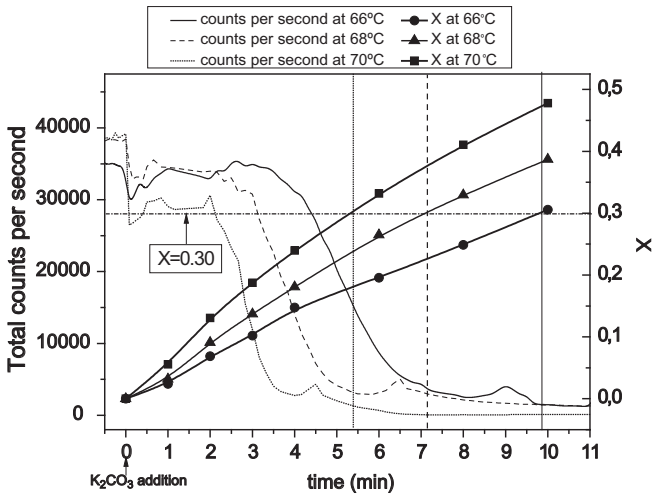

Fig. 6. Evolution of the number of counts per second and conversion with temperature. Conditions: M = 3, C_{cat} = 11.3 g/L (1% w/w), ω = 1500 rpm.

when the initial molar ratios of reactants were 1.5, 2 and 3, respectively. The molar compositions corresponding to such conversions are represented within the liquid–liquid-equilibrium diagram obtained in our previous work [20]. It can be remarked that the composition values at which virtually no counts were observed lie on the binodal curve that separate the biphasic and the monophasic regions, as observed in Fig. 5(b).

On the other hand, Fig. 6 graphs the progression of the number of counts per second and X at different temperatures. While the influence of the molar ratio of DMC to Gly had a somewhat noticeable effect on the critical conversion, temperature did not show such influence. At the temperatures tested, the critical conversion was X_{crit} = 0.3 for all the cases as shown in Fig. 6 following the same criterion as in the paragraph above. The negligible effect of this variable in the phase changing behaviour is not surprising, for it corresponds to what had previously been ascertained from 60 to 70 °C [20] and even in a much wider range of temperatures, from 30 to 60 °C [19].

3.3. Proposal and discrimination of kinetic models

Before proposing kinetic models, it was considered of great importance to determine in which phase the reaction takes place while in the liquid–liquid biphasic stage. For this reason, during the first minutes of the reactions, the Gly-rich and DMC-rich phases were tested for potassium, proving only the former positive for its presence. With all the previous operating conditions and information in mind, 27 kinetic runs varying T, M, and catalyst concentration as indicated in Section 2.4.2 were completed. Fig. 8 represents the evolution of the conversion with respect to time comparing the effect of varying temperature (a), catalyst concentration (b) and M (c).

Table 2 compiles the kinetic models tested to explain the development of this reaction. Model 1 is of potential first order with respect to Gly and zero order with respect to DMC. The polyolic nature of Gly makes it subject to generate an alkali glyceroxide from interaction with the alkali metal carbonates added to the reaction. That is, in the case of adding K_2CO_3, potassium glyceroxide may in turn be the active catalytic species [14].

The second model constitutes another potential kinetic model that considers partial first order for both components, as previously proposed in the literature for a similar transesterification reaction between DMC and ethanol in the presence of sodium ethoxide [38].

Nevertheless, given the experimental observations, a more complex model should be proposed considering that the phase regime could eventually play an important role on the catalytic behaviour of the system. Subsequently, Model 3 suggests a kinetic model with two equations. The first one would correspond to the biphasic regime stage, during which the catalyst is soluble only in the Gly-rich phase, being at a concentration C_{cat1}, and DMC enters that phase and reacts at a concentration of C_{DMCsol}. The second equation describes the situation at values above the critical conversion X_{crit} where the phase regime change takes place, which varies slightly depending on the initial molar ratio of the reactants, as explained throughout Section 3.2. The catalyst becomes then present in the entire batch with a concentration C_{cat}, remarkably lower, given the higher solution volume; thus, a decrease in the reaction rate is observed. Moreover, the concentration of DMC is no longer considered a constant, thereby having this second potential equation a global second order.

To select a model that successfully represents the evolution of the species, the statistical criteria described in Section 2.6 were reckoned for each of the models presented. Table 3 not only summarizes the mentioned statistical parameters, but also includes the kinetic parameters retrieved from correlation. The latter referred to each individual model correspond to the definitions of the models as stated in Table 1 with the additional consideration of the dependence of the kinetic constants k_1 with temperature according to the Arrhenius relationship:

$$\ln\ k_1 = \ln\ k_{10} - \frac{E_{a1}}{R}\cdot\frac{1}{T} \tag{9}$$

where k_{10} and E_{a1}/R are the preexponential factor of the kinetic constant and the ratio between activation energy and the ideal gas constant.

In principle, the values of E_a/R retrieved from correlation agree with the fact that the chemical reaction is the controlling step. In such cases, activation energies usually vary between 40 and 200 kJ/mol. The values obtained for E_{a1} in all the models tested ranged from 152 to 184 kJ/mol. The activation energy for the transesterification reaction of coconut oil with pressurized methanol has been reported to reach values as high as 108 kJ/mol [39]. Additionally, other chemical reactions have activation energies similar to those obtained in this work, such as 133 kJ/mol for the dimers formation in the alkali catalyzed self-condensation of

Table 2
Kinetic models proposed for the transesterification of glycerol to yield glycerol carbonate.

Model number	Rate equations	Observations	Model description
1	$r = k_1 \cdot C_{cat} \cdot C_{Gly}$	Single equation for all X values	Potential model with partial first order for Gly and zero order for DMC
2	$r = k_1 \cdot C_{cat} \cdot C_{Gly}C_{DMC}$		Potential model with partial first orders for both Gly and DMC
3	1st step: $r_1 = k_1 \cdot C_{cat1} \cdot C_{Gly}C_{DMCsol}$ 2nd step: $r_2 = k_1 \cdot C_{cat} \cdot C_{Gly}C_{DMC}$	First step for $X < X_{crit}$ Second step for $X \geqslant X_{crit}$	Two steps considered:(1st) Partial first order potential model with respect to Gly (2nd) Partial first orders for Gly and DMC in the second

Table 3
Kinetic and statistical parameters retrieved for the kinetic models proposed for the transesterification of glycerol and dimethyl carbonate.

Model number	Parameter	Value	±error	*F*	AIC	RMSE	VE (%)
1	$\ln \underline{k}_{10}$	47.81	3.41	15,877	−2523	0.07	95.41
	E_{a1}/R	18,237	1164				
2	$\ln k_{10}$	56.70	1.47	91,463	−3403	0.04	99.20
	E_{a1}/R	21,939	501				
3	$\ln k_{10}$	55.43	1.31	64,168	−3440	0.03	99.27
	E_{a1}/R	21,558	446				
	C_{DMCsol}	3.34	0.07				

cyclohexanone [40] or 161 kJ/mol for sugar degradation in enzymatic lignocelluloses pretreatment [41].

Concerning the agreement between the data and the models proposed, the models presented acceptable goodness of fit. First, following the *F* value criterion, all models reach a significance higher than 0.999, for the values with the number of experimental data obtained and amount of parameters are higher than 999.5 (Models 1 and 2 with 2 parameters), 123.5 (Model 3 with 3 parameters) and 23.8 (Model 4 with 5 parameters). In general, the parameters were estimated with relatively low errors for Models 1 through 3, being the error only as high as 7.1% in the estimation of k_1 in Model 1.

Apart from the error in the estimation of the parameters of the model, differences could be observed as the complexity of the proposed model increased. First, Model 1 was tested and, though it showed a value of the Fischer's *F* much higher than the tabulated for the number of data and parameters of the value (486 and 2, respectively), the percentage of variation of the variable *X* explained by the model was not found entirely satisfactory.

Then Model 2 was regarded, considering an actual influence of the presence of DMC. The values of the four statistical criteria herein considered resulted much more convenient in regards to the fitting of the experimental measurements. The Fischer's *F* value increased noticeably, RMSE decreased by far more than a half with respect to that of Model 1 and AIC also showed an improvement. More markedly, the variation explained by the model improved almost as much as 4%.

Consideration of Model 3 led to even better values of all the criteria except for *F*, improving significantly those obtained with Model 2. Both AIC and RMSE were the lowest obtained with all the models.

Hence, Model 3 was selected as the one that best fits to the experimental data and Fig. 7 shows the fitting of such model to some of the kinetic runs conducted. Finally, in order to further validate the model a comparison of the error in the prediction estimated by the models proposed was made. Fig. 8 depicts how Model 3 keeps the error mostly within the experimental error represented by the dotted line, estimated to have its highest value at

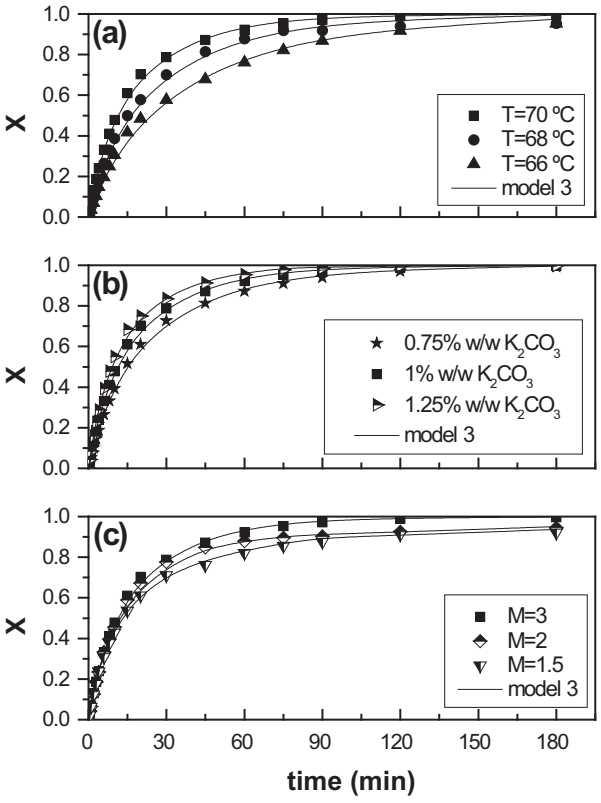

Fig. 7. Evolution of the conversion in kinetic runs comparing the effect of temperature (a), catalyst concentration (b) and molar ratio of reactants (c). Conditions: (a) $M = 3$, $C_{cat} = 11.3$ g/L (1% w/w); (b) $T = 70$ °C, $M = 3$; (c) $T = 70$ °C, $C_{cat} = 11.3$ g/L (1% w/w), all of them at $\omega = 1500$ rpm.

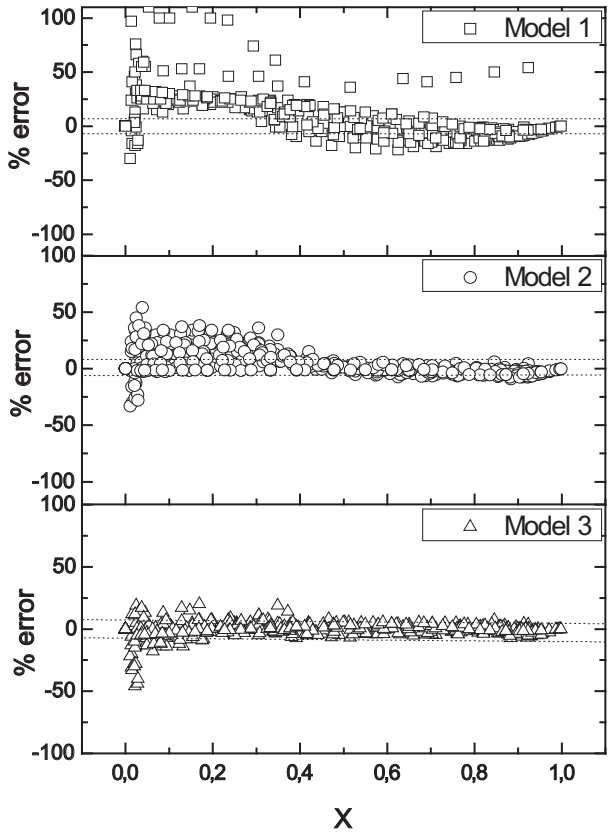

Fig. 8. Relative error of prediction of the three models tested with respect to the observed values.

±6.8%. By contrast, Model 1 showed a marked trend to overestimate the conversion as well as much higher errors, well above the experimental. Finally, Model 2 showed somewhat higher errors than Model 3, though not as high as Model 1; however, it is worthwhile remarking the clear trend in the error that shows that first and overestimation of the conversion and then a slight underestimation are attained with the model.

4. Conclusions

The transesterification of Gly with DMC to yield a valuable product like GC is herein studied and optimized. First, selection of a catalyst and operational conditions was made, resulting K_2CO_3 the most appropriate catalyst and operation between 66 and 70 °C and a stirring speed of 1500 rpm.

Given that the reactants initially form an emulsion, a study of the evolution of the phases throughout the reaction was successfully made by means of FBRM observation. It could be seen that as the products generate, the number of chord counts decreases down to levels close to zero, meaning that the biphasic system disappears. The critical conversion values at which the phase transition occurs according to the FBRM measurements was found to be 0.30, 0.31 and 0.33 when operating with molar excess of DMC to Gly of 3, 2 and 1.5, respectively. The compositions that correspond to such conversions coincide with the binodal curve of the liquid–liquid equilibria existing in the quaternary system under study. Variation of the critical conversion was found negligible with respect to temperature.

A series of kinetic models were proposed to be fitted to kinetic data compiled throughout 27 runs varying temperature, molar ratio of reactants and catalyst load at three levels. The model that fitted best to experimental data consisted of two potential equations: the first describes the events under the biphasic regime, during which the reaction only takes place in the glycerol phase, in which the catalyst was soluble; the second accounts for an irreversible reaction and considers the dilution of the catalyst in the entire reacting volume. Validation of the model and its parameters was successful under statistical and physical criteria with estimation errors below 6.8%.

Acknowledgements

The authors wish to express gratitude to the Spanish Ministry of Science and Innovation (Projects CTQ2007-60919 and CTQ2010-15460) for financial support and UBE Corporation for kindly supplying dimethyl carbonate for this work.

References

[1] T. Werpy, G. Petersen, Top value added chemicals from biomass, Volume I – Results of screening for potential candidates from sugars and synthesis gas, Pacific Northwest National Laboratory, National Renewable Energy Laboratory, 2004.
[2] A. Behr, J. Eilting, K. Irawadi, J. Leschinski, F. Lindner, Improved utilisation of renewable resources: new important derivatives of glycerol, Green Chem. 10 (2008) 13–30.
[3] M. Pagliaro, R. Ciriminna, H. Kimura, M. Rossi, C. Della Pina, Recent advances in the conversion of bioglycerol into value-added products, Eur. J. Lipid Sci. Technol. 111 (2009) 788–799.
[4] M.O. Sonnati, S. Amigoni, E.P.T. de Givenchy, T. Darmanin, O. Choulet, F. Guittard, Glycerol carbonate as a versatile building block for tomorrow: synthesis, reactivity, properties and applications, Green Chem. 15 (2013) 283–306.
[5] M. Aresta, A. Dibenedetto, F. Nocito, C. Pastore, A study on the carboxylation of glycerol to glycerol carbonate with carbon dioxide: the role of the catalyst, solvent and reaction conditions, J. Mol. Catal. A: Chem. 257 (2006) 149–153.
[6] C. Vieville, J.W. Yoo, S. Pelet, Z. Mouloungui, Synthesis of glycerol carbonate by direct carbonatation of glycerol in supercritical CO_2 in the presence of zeolites and ion exchange resins, Catal. Lett. 56 (1998) 245–247.
[7] J. Hu, J. Li, Y. Gu, Z. Guan, W. Mo, Y. Ni, T. Li, G. Li, Oxidative carbonylation of glycerol to glycerol carbonate catalyzed by $PdCl_2$(phen)/KI, Appl. Catal. A 386 (2010) 188–193.
[8] J. George, Y. Patel, S.M. Pillai, P. Munshi, Methanol assisted selective formation of 1,2-glycerol carbonate from glycerol and carbon dioxide using (Bu_2SnO)-Bu-n as a catalyst, J. Mol. Catal. A: Chem. 304 (2009) 1–7.
[9] J.W. Yoo, Z. Mouloungui, Catalytic carbonylation of glycerin by urea in the presence of zinc mesoporous system for the synthesis of glycerol carbonate, Nanotechnol. Mesostruct. Mater. 146 (2003) 757–760.
[10] A. Dibenedetto, A. Angelini, M. Aresta, J. Ethiraj, C. Fragale, F. Nocito, Converting wastes into added value products: from glycerol to glycerol carbonate, glycidol and epichlorohydrin using environmentally friendly synthetic routes, Tetrahedron 67 (2011) 1308–1313.
[11] M. Aresta, A. Dibenedetto, F. Nocito, C. Ferragina, Valorization of bio-glycerol: new catalytic materials for the synthesis of glycerol carbonate via glycerolysis of urea, J. Catal. 268 (2009) 106–114.
[12] M.J. Climent, A. Corma, P. De Frutos, S. Iborra, M. Noy, A. Velty, P. Concepción, Chemicals from biomass: synthesis of glycerol carbonate by transesterification and carbonylation with urea with hydrotalcite catalysts. The role of acid-base pairs, J. Catal. 269 (2010) 140–149.
[13] P. Lu, H. Wang, K. Hu, Synthesis of glycerol carbonate from glycerol and dimethyl carbonate over the extruded CaO-based catalyst, Chem. Eng. J. 228 (2013) 147–154.
[14] J.R. Ochoa-Gomez, O. Gomez-Jimenez-Aberasturi, B. Maestro-Madurga, A. Pesquera-Rodriguez, C. Ramirez-Lopez, L. Lorenzo-Ibarreta, J. Torrecilla-Soria, M.C. Villaran-Velasco, Synthesis of glycerol carbonate from glycerol and dimethyl carbonate by transesterification: catalyst screening and reaction optimization, Appl. Catal. A 366 (2009) 315–324.
[15] R. Bai, Y. Wang, S. Wang, F. Mei, T. Li, G. Li, Synthesis of glycerol carbonate from glycerol and dimethyl carbonate catalyzed by NaOH/gamma-Al_2O_3, Fuel Process. Technol. 106 (2013) 209–214.
[16] M. Malyaadri, K. Jagadeeswaraiah, P.S.S. Prasad, N. Lingaiah, Synthesis of glycerol carbonate by transesterification of glycerol with dimethyl carbonate over Mg/Al/Zr catalysts, Appl. Catal. A-Gen. 401 (2011) 153–157.
[17] H.-J. Cho, H.-M. Kwon, J. Tharun, D.-W. Park, Synthesis of glycerol carbonate from ethylene carbonate and glycerol using immobilized ionic liquid catalysts, J. Ind. Eng. Chem. 16 (2010) 679–683.
[18] G. Rokicki, P. Rakoczy, P. Parzuchowski, M. Sobiecki, Hyperbranched aliphatic polyethers obtained from environmentally benign monomer: glycerol carbonate, Green Chem. 7 (2005) 529–539.
[19] H. Wang, P.Lu. Liquid-Liquid, Equilibria for the system dimethyl carbonate + methanol + glycerol in the temperature range of (303.15 to 333.15) K, J. Chem. Eng. Data 57 (2012) 582–589.
[20] J. Esteban, M. Ladero, L. Molinero, F. Garcia-Ochoa, Liquid-liquid equilibria for the ternary systems DMC-methanol-glycerol; DMC-glycerol carbonate-glycerol and the quaternary system DMC-methanol-glycerol carbonate-glycerol at catalytic reacting temperatures, Chem. Eng. Res. Des. (2014), http://dx.doi.org/10.1016/j.cherd.2014.05.026.
[21] M. Ladero, M. de Gracia, F. Trujillo, F. Garcia-Ochoa, Phenomenological kinetic modelling of the esterification of rosin and polyols, Chem. Eng. J. 197 (2012) 387–397.
[22] D.S. Negi, A. Rochlitz, G. Wozny, R. Schomacker, Drop-size analysis in a two-phase reactive liquid-liquid system on a bubble-cap tray, Ind. Eng. Chem. Res. 44 (2005) 3343–3347.
[23] M.G. Alvarez, M. Pliskova, A.M. Segarra, F. Medina, F. Figueras, Synthesis of glycerol carbonates by transesterification of glycerol in a continuous system using supported hydrotalcites as catalysts, Appl. Catal. B-Environ. 113 (2012) 212–220.
[24] F.S.H. Simanjuntak, T.K. Kim, S.D. Lee, B.S. Ahn, H.S. Kim, H. Lee, CaO-catalyzed synthesis of glycerol carbonate from glycerol and dimethyl carbonate: isolation and characterization of an active Ca species, Appl. Catal. A-Gen. 401 (2011) 220–225.
[25] A.F.T. Silva, A. Burggraeve, Q. Denon, P. Van der Meeren, N. Sandler, T. Van Den Kerkhof, M. Hellings, C. Vervaet, J.P. Remon, J.A. Lopes, T. De Beer, Particle sizing measurements in pharmaceutical applications: comparison of in-process methods versus off-line methods, Eur. J. Pharm. Biopharm. 85 (2013) 1006–1018.
[26] S. Maass, S. Wollny, A. Voigt, M. Kraume, Experimental comparison of measurement techniques for drop size distributions in liquid/liquid dispersions, Exp. Fluids 50 (2011) 259–269.
[27] A. Blanco, E. Fuente, C. Negro, J. Tijero, Flocculation monitoring: focused beam reflectance measurement as a measurement tool, Can. J. Chem. Eng. 80 (2002) 734–740.
[28] A. Blanco, E. De la Fuente, C. Negro, M.C. Monte, J. Tijero, Focused beam reflectant measurement as a tool to measure flocculation, Tappi J. 1 (2002) 14–20.
[29] W. Wang, W. Cheng, J. Duan, J. Gong, B. Hu, P. Angeli, Effect of dispersed holdup on drop size distribution in oil-water dispersions: experimental observations and population balance modeling, Chem. Eng. Sci. 105 (2014) 22–31.
[30] W. Wang, J. Liu, P. Wang, J. Duan, J. Gong, Evolution of dispersed drops during the mixing of mineral oil and water phases in a stirringtank, Chem. Eng. Sci. 91 (2013) 173–179.
[31] J.A. Boxall, C.A. Koh, E.D. Sloan, A.K. Sum, D.T. Wu, Measurement and calibration of droplet size distributions in water-in-oil emulsions by particle

video microscope and a focused beam reflectance method, Ind. Eng. Chem. Res. 49 (2009) 1412–1418.
[32] F. Garcia-Ochoa, A. Romero, J. Querol, Modeling of the thermal normal-octane oxidation in the liquid phase, Ind. Eng. Chem. Res. 28 (1989) 43–48.
[33] M. Ladero, M. de Gracia, J.J. Tamayo, I.L.d. Ahumada, F. Trujillo, F. Garcia-Ochoa, Kinetic modelling of the esterification of rosin and glycerol: application to industrial operation, Chem. Eng. J. 169 (2011) 319–328.
[34] H. Akaike, A new look at the statistical model identification, IEEE Trans. Autom. Control 19 (1974) 716–723.
[35] J.B. Bell, L. Silver, V.A. Currier, Method for preparing glycerin carbonate, Patent US2915529, 1959.
[36] J. Li, T. Wang, On the deactivation of alkali solid catalysts for the synthesis of glycerol carbonate from glycerol and dimethyl carbonate, React. Kinet. Mech. Catal. 102 (2011) 113–126.
[37] S.C. Kim, Y.H. Kim, H. Lee, D.Y. Yoon, B.K. Song, Lipase-catalyzed synthesis of glycerol carbonate from renewable glycerol and dimethyl carbonate through transesterification, J. Mol. Catal. B-Enzym. 49 (2007) 75–78.
[38] T. Keller, J. Holtbruegge, A. Niesbach, A. Górak, Transesterification of dimethyl carbonate with ethanol to form ethyl methyl carbonate and diethyl carbonate: a comprehensive study on chemical equilibrium and reaction kinetics, Ind. Eng. Chem. Res. 50 (2011) 11073–11086.
[39] H.-C. Lin, C.-S. Tan, Continuous transesterification of coconut oil with pressurized methanol in the presence of a heterogeneous catalyst, J. Taiwan Inst. Chem. Eng. 45 (2014) 495–503.
[40] D. Lorenzo, A. Santos, E. Simon, A. Romero, Kinetic of alkali catalyzed self-condensation of cyclohexanone, Ind. Eng. Chem. Res. 52 (2013) 2257–2265.
[41] C. Zhang, C.J. Houtman, J.Y. Zhu, Using low temperature to balance enzymatic saccharification and furan formation during SPORL pretreatment of Douglas-fir, Process Biochem. 49 (2014) 466–473.

Publicación 3 / Publication 3

Autores/Authors: Jesús Esteban, Miguel Ladero and Félix García-Ochoa

Título/Title: Liquid–liquid equilibria for the systems ethylene carbonate + ethylene glycol + glycerol; ethylene carbonate + glycerol carbonate + glycerol and ethylene carbonate + ethylene glycol + glycerol carbonate + glycerol at catalytic reacting temperatures

Estado actual/Current status: Manuscript in Press Chemical. Engineering Research and Design (2014). DOI: 10.1016/j.cherd.2014.08.024

Índice de impacto / Impact factor 2013: 2.281

Resumen

La obtención simultánea de carbonato de glicerina (GC) y etilenglicol (EG) a partir de carbonato de etileno (EC) y glicerina (Gly) es una reacción poco estudiada, mucho menos que la reacción de glicerina y DMC. En este caso, hay una absoluta ausencia de datos de equilibrio entre las fases líquidas que se dan al poner en contacto EC y Gly.

En este trabajo se incluyen datos del equilibrio líquido-líquido físico existente en los dos sistemas ternarios y el cuaternario que incluyen a las especies reactantes de la mencionada reacción con los productos, es decir:

- El sistema ternario (T1): {EC + EG + Gly}
- El sistema ternario (T2): {EC + GC + Gly}
- El sistema cuaternario (Q): {EC + EG + GC + Gly}, modelizado como un sistema pseudoternario considerando conjuntamente EG y GC.

Las temperaturas empleadas para este estudio fueron de 313.2, 318.2 y 323.2 K, a las que se realizaron experimentos de agitación de los sistemas, posterior separación de fases y análisis de las mismas mediante cromatografía líquida.

Se pudo apreciar que la adición de cantidades crecientes de EG, GC o EG+GC, según el caso, ayudaba a la cosolubilización de EC y Gly. El efecto solubilizador de GC y EG utilizados individualmente es mayor que el de la utilización conjunta de ambos, siendo el orden global el siguiente: GC > EG > EG + GC. Se ha comprobado, además, que dentro del intervalo propuesto, la temperatura, aun ayudando a la solubilización, no ejerce un efecto muy significativo sobre el equilibrio. En el caso del sistema cuaternario, la composición de la mezcla a la cual se deja de obtener un sistema bifásico corresponde aproximadamente a la de un sistema de reacción con una conversión del 30% de glicerina.

Los datos de equilibrio se ajustaron al modelo NRTL con desviaciones no superiores a 3% en ninguno de los tres sistemas planteados. En este trabajo se recopilan los coeficientes de interacción binaria correlacionando los datos a todas las temperaturas dada la poca influencia de esta variable.

CHEMICAL ENGINEERING RESEARCH AND DESIGN XXX (2014) XXX–XXX

Contents lists available at ScienceDirect

Chemical Engineering Research and Design

journal homepage: www.elsevier.com/locate/cherd

Liquid–liquid equilibria for the systems ethylene carbonate + ethylene glycol + glycerol; ethylene carbonate + glycerol carbonate + glycerol and ethylene carbonate + ethylene glycol + glycerol carbonate + glycerol at catalytic reacting temperatures

Jesús Esteban, Miguel Ladero, Félix García-Ochoa*

Department of Chemical Engineering, College of Chemical Sciences, Complutense University of Madrid, 28040 Madrid, Spain

ABSTRACT

The measurements of the liquid–liquid equilibria implied in the reaction system to yield glycerol carbonate from ethylene carbonate and glycerol were performed. First, data for the ternary systems consisting of ethylene carbonate + ethylene glycol + glycerol as well as ethylene carbonate + glycerol carbonate + glycerol at 313.2, 318.2 and 323.2 K and atmospheric pressure were acquired. Furthermore, the quaternary equilibrium involving both products of the reaction, i.e., ethylene carbonate + ethylene glycol + glycerol carbonate + glycerol, was evaluated under the same conditions. All the data experimental data were correlated with the NRTL model with root-mean square deviations of about 0.03 for all the systems tested.

Keywords: Glycerol carbonate; Ethylene carbonate; Ethylene glycol; Glycerol; Liquid–liquid equilibrium; NRTL

1. Introduction

The plethora of glycerol available as a consequence of the marked development of the biodiesel industry, particularly throughout the last decade, has provoked the need for the valorization of such formerly profitable by-product of the process. Under such scenario, intensive research has been undertaken in order to obtain valuable products from this promising resource (Pagliaro et al., 2009; Pagliaro and Rossi, 2008). Among the products subject to experimental efforts are solketal, 1,2-propanediol or glycerol carbonate (GC) (Behr et al., 2008; Zhou et al., 2008).

GC, systematically known as 4-(hydroxymethyl)-1,3-dioxolan-2-one has been addressed as a component with potential and promising applications in assorted fields. Among those can be mentioned its utilization as a general purpose solvent (Benoit et al., 2010; Lameiras et al., 2011), electrolyte liquid carrier in Li and Li-ion batteries (Chen et al., 2002), blowing agent in polyurethane foams formation (Gillis et al., 1997) or in gas separation membranes (Kovvali and Sirkar, 2002). Simultaneously, its usefulness as feedstock towards the synthesis of further relevant products has also been reported, particularly polymeric compounds (Iaych et al., 2011; Mouloungui and Pelet, 2001; Rokicki et al., 2005).

Multiple reactions have been reported in literature approaching the generation of GC in substitution of the formerly used phosgenation of glycerol. Pressurized addition of CO (Hu et al., 2010) and CO_2 to glycerol (Ezhova et al., 2012; George et al., 2009) (Gly) or its reaction with urea (Li et al., 2006; Rubio-Marcos et al., 2010) are among the examples. Transesterification of an organic carbonate with glycerol is one of the most followed routes and presents most advantageous operational aspects compared to the aforementioned reactions, for atmospheric pressure suffices and temperatures are significantly lower than those reported for the glycerolysis of urea (Sonnati et al., 2013). Aliphatic

* *Corresponding author*. Tel.: +34 913944164; fax: +34 913944179.
E-mail addresses: mladero@quim.ucm.es, mladerog@ucm.es (M. Ladero).

http://dx.doi.org/10.1016/j.cherd.2014.08.024

Please cite this article in press as: Esteban, J., et al., Liquid–liquid equilibria for the systems ethylene carbonate + ethylene glycol + glycerol; ethylene carbonate + glycerol carbonate + glycerol and ethylene carbonate + ethylene glycol + glycerol carbonate + glycerol at catalytic reacting temperatures. Chem. Eng. Res. Des. (2014), http://dx.doi.org/10.1016/j.cherd.2014.08.024

Nomenclature

Latin characters

HPLC	high-performance liquid chromatography
K	distribution ratio (as defined by Eq. (2))
LLE	liquid–liquid equilibria
NRTL	non-random two-liquid model
OF	objective function
Q	refers to the quaternary system {EC + EG + GC + Gly}
rmsd	root-mean square deviation
T1	refers to the ternary system {EC + EG + Gly}
T2	refers to the ternary system {EC + GC + Gly}

Greek symbols

α_{ij}	non-randomness binary interaction parameter as defined in the NRTL method
Δg_{ij}	binary interaction parameter as defined in the NRTL method

Components

EC	ethylene carbonate
EG	ethylene glycol
GC	glycerol carbonate
Gly	glycerol

Subscripts

I, II	relative to the glycerol-rich and ethylene carbonate-rich phases, respectively
2	in Eq. (2), relative to cosolvents EG (system T1), GC (system T2), EG + GC (system Q)

organic carbonates such as dimethyl carbonate (DMC) (Jiabo and Tao, 2010; Kim et al., 2007; Ochoa-Gomez et al., 2009) or diethyl carbonate (Alvarez et al., 2010; Patel et al., 2009) have been employed to such aim; however, the use of cyclic carbonates, such as ethylene carbonate (EC) has been paid less attention to, despite the by-product of the reaction being ethyleneglycol (EG), widely used as antifreeze to cite only an example (Climent et al., 2010; Cho et al., 2010).

The goal of the present work is to study the liquid–liquid equilibrium (LLE) of the existing systems for the reaction between EC and Gly (represented in Fig. 1), namely: {EC + EG + Gly} (system T1 from this point forward); {EC + GC + Gly} (T2) and the quaternary system {EC + EG + GC + Gly} (Q).

The LLE for similar systems involving the presence of glycerol have already been researched by several authors. First, LLE studies involving its presence as part of the biodiesel production process have been made, covering the equilibria of ternary systems consisting of methylesters of diverse origins + glycerol + methanol (do Carmo et al., 2014; Lee et al., 2010) or ethanol (Basso et al., 2012; de Azevedo Rocha et al., 2014; do Carmo et al., 2014), of importance in the separation of the products of the process. On the other hand, a series of other papers have reported on the LLE existing in systems deriving from processes aimed at the valorization of glycerol. Equilibria among acetone + solketal + glycerol (Esteban et al., 2014a) or acetone + water + glycerol (Krishna et al., 1989) are of interest in the synthesis of solketal, another valuable product from glycerol. Also, ternary equilibria derived from the etherification of glycerol have been described, including different combinations of glycerol and mono-, di- and tri-tert-butylethers (Liu et al., 2014). Wang and Lu studied the system consisting of dimethyl carbonate + methanol + glycerol, also existing in another route to synthesize glycerol carbonate (Wang and Lu, 2012). More recently, this study was profoundly extended to cover the equilibria for the systems comprising dimethyl carbonate + glycerol carbonate + glycerol and the quaternary system dimethyl carbonate + methanol + glycerol carbonate + glycerol (Esteban et al., 2014b), much like it is herein proposed.

The effect of the separate and joint presence of the products will be assessed throughout the reaction initially consisting of an almost immiscible system evolving into a single phase system working with mixtures simulating the development of the reaction. The temperature interval selected for this study was 313.2 K, below which EC is in solid state, and 323.2 K temperature at which this reaction has been reported to take place (Climent et al., 2010). Assays were conducted at atmospheric pressure.

LLE data regression was realized utilizing the non-random two liquid (NRTL) model, common tool for fitting in all of the aforementioned references, with the corresponding binary interaction parameters being retrieved after satisfactory fitting.

2. Materials and methods

2.1. Materials

The following reagents were used throughout the experimental procedure: extra pure Gly (assay grade 99.88%) from Fischer Chemical; EG (99.8%, anhydrous) from Sigma–Aldrich; GC (purity ≥ 99.5%) from Sigma–Aldrich and EC (synthesis grade, purity > 99%), from Scharlau. Citric acid ACS reagent (purity ≥ 99.5%) by Sigma–Aldrich was employed as an internal standard in HPLC analyses.

2.2. Apparatus and procedure

Hermetically sealed 25 mL round-bottom flasks were used to perform LLE experiments. Agitation of the feed mixture was magnetic provided by an IKA Yellow Line TC3 heating and stirring device. Appropriate temperature (bath temperature control oscillation of ±0.05 K) for each experiment was reached by means of a glycerol bath heated.

Feed samples were weighted in a Kern and Sohn ABS-220-4 analytical balance with a precision of 0.0001 g. Energetic stirring of the different feeds was performed for 6 h, enough to ensure total mass transfer between the liquid phases after which separation of the light (Gly-rich, I) and heavy (EC-rich, II) phases was performed. First, settling of the phases was allowed for 3 h. After such period, separation of phases was ensured and even further aided using a thermostatic Sigma 4–16 K centrifuge in order to keep the adequate temperature. Samples were taken from each phase for analysis. Data were obtained by performing triplicate experiments.

2.3. Analytical methodology

Samples from each phase were diluted in a 5 g/L citric acid (internal standard) solution for HPLC analysis. Each component was analyzed with a JASCO 2000 series device, with a refraction index detector. A constant flow rate of 0.5 mL/min of acid Milli-Q water (0.005 N H_2SO_4) was used as mobile phase. Separation was realized using a Rezex ROA-Organic Acid H+ (8%) column (150 × 7.80 mm) at 60 °C.

3. Results and discussion

3.1. LLE experimental data

Tables 1–3 compile the global molar composition of each individual experiment. Three distinct cases were evaluated, namely: EG is the only cosolvent (system T1); only GC is present (system T2); and finally, both EG and GC are used

Please cite this article in press as: Esteban, J., et al., Liquid–liquid equilibria for the systems ethylene carbonate + ethylene glycol + glycerol; ethylene carbonate + glycerol carbonate + glycerol and ethylene carbonate + ethylene glycol + glycerol carbonate + glycerol at catalytic reacting temperatures. Chem. Eng. Res. Des. (2014), http://dx.doi.org/10.1016/j.cherd.2014.08.024

Table 1 – Experimental LLE data expressed as mole fractions (x_i) of the ternary system T1 {EC (1) + EG (2) + Gly (3)} at atmospheric pressure.

T (K)	Global composition (feed)			phase I (Gly-rich) composition			phase II (EC-rich) composition		
	x_1	x_2	x_3	x_1	x_2	x_3	x_1	x_2	x_3
313.2	0.498	0.000	0.502	0.089	0.000	0.911	0.953	0.000	0.047
	0.484	0.025	0.491	0.110	0.034	0.856	0.920	0.017	0.063
	0.468	0.056	0.476	0.130	0.070	0.800	0.874	0.036	0.090
	0.452	0.089	0.459	0.160	0.111	0.729	0.819	0.064	0.117
	0.436	0.120	0.444	0.189	0.137	0.674	0.768	0.089	0.143
	0.425	0.142	0.433	0.207	0.159	0.634	0.726	0.114	0.160
	0.407	0.178	0.415	0.251	0.195	0.554	0.668	0.145	0.187
	0.385	0.212	0.403	0.294	0.226	0.480	0.541	0.190	0.269
318.2	0.501	0.000	0.499	0.101	0.000	0.899	0.939	0.000	0.061
	0.480	0.028	0.492	0.122	0.039	0.839	0.914	0.014	0.072
	0.473	0.056	0.471	0.142	0.075	0.782	0.865	0.034	0.101
	0.459	0.084	0.457	0.178	0.109	0.713	0.800	0.059	0.142
	0.440	0.111	0.449	0.214	0.131	0.656	0.771	0.078	0.151
	0.423	0.145	0.432	0.246	0.162	0.592	0.680	0.120	0.200
	0.408	0.176	0.416	0.300	0.190	0.510	0.579	0.153	0.268
	0.395	0.206	0.399	0.360	0.209	0.431	0.465	0.198	0.338
323.2	0.502	0.000	0.498	0.108	0.000	0.892	0.930	0.000	0.070
	0.481	0.031	0.489	0.132	0.042	0.826	0.898	0.017	0.086
	0.471	0.056	0.474	0.154	0.072	0.774	0.851	0.034	0.115
	0.457	0.084	0.460	0.191	0.103	0.706	0.813	0.056	0.131
	0.441	0.114	0.444	0.232	0.129	0.640	0.725	0.092	0.183
	0.426	0.145	0.429	0.282	0.159	0.560	0.633	0.123	0.245
	0.416	0.165	0.419	0.333	0.173	0.495	0.564	0.148	0.288
	0.405	0.197	0.398	0.367	0.190	0.443	0.493	0.176	0.332

Uncertainty of HPLC analysis ($\sigma_x = 0.018$).

Table 2 – Experimental LLE data expressed as mole fractions (x_i) of the ternary system T2 {EC (1) + GC (2) + Gly (3)} at atmospheric pressure.

T (K)	Global composition (feed)			Phase I (Gly-rich) composition			Phase II (EC-rich) composition		
	x_1	x_2	x_3	x_1	x_2	x_3	x_1	x_2	x_3
313.2	0.502	0.000	0.498	0.089	0.000	0.911	0.953	0.000	0.047
	0.486	0.025	0.489	0.104	0.017	0.879	0.907	0.035	0.058
	0.472	0.059	0.470	0.132	0.043	0.825	0.833	0.074	0.093
	0.458	0.081	0.461	0.152	0.067	0.782	0.793	0.095	0.112
	0.440	0.111	0.449	0.173	0.093	0.735	0.723	0.132	0.145
	0.426	0.145	0.429	0.209	0.119	0.672	0.619	0.168	0.213
	0.412	0.173	0.415	0.262	0.158	0.580	0.558	0.187	0.256
	0.397	0.204	0.400	0.302	0.187	0.511	0.490	0.205	0.306
318.2	0.498	0.000	0.502	0.101	0.000	0.899	0.939	0.000	0.061
	0.482	0.028	0.490	0.117	0.020	0.864	0.878	0.036	0.086
	0.476	0.053	0.470	0.146	0.039	0.815	0.815	0.067	0.118
	0.455	0.081	0.464	0.167	0.064	0.769	0.767	0.095	0.138
	0.451	0.106	0.443	0.200	0.089	0.710	0.691	0.123	0.187
	0.429	0.134	0.437	0.239	0.117	0.644	0.616	0.150	0.234
	0.420	0.162	0.418	0.287	0.148	0.565	0.555	0.176	0.269
	0.405	0.185	0.410	0.365	0.176	0.459	0.484	0.193	0.323
323.2	0.504	0.000	0.496	0.108	0.000	0.892	0.930	0.000	0.070
	0.487	0.028	0.485	0.127	0.020	0.854	0.869	0.036	0.095
	0.474	0.053	0.472	0.161	0.042	0.797	0.799	0.070	0.131
	0.461	0.075	0.463	0.189	0.064	0.747	0.736	0.095	0.170
	0.450	0.106	0.444	0.231	0.092	0.678	0.657	0.123	0.221
	0.434	0.134	0.432	0.278	0.117	0.605	0.585	0.150	0.265
	0.421	0.156	0.423	0.330	0.148	0.522	0.525	0.168	0.307
	0.415	0.173	0.413	0.380	0.170	0.450	0.473	0.181	0.346

Uncertainty of HPLC analysis ($\sigma_x = 0.018$).

Please cite this article in press as: Esteban, J., et al., Liquid–liquid equilibria for the systems ethylene carbonate + ethylene glycol + glycerol; ethylene carbonate + glycerol carbonate + glycerol and ethylene carbonate + ethylene glycol + glycerol carbonate + glycerol at catalytic reacting temperatures. Chem. Eng. Res. Des. (2014), http://dx.doi.org/10.1016/j.cherd.2014.08.024

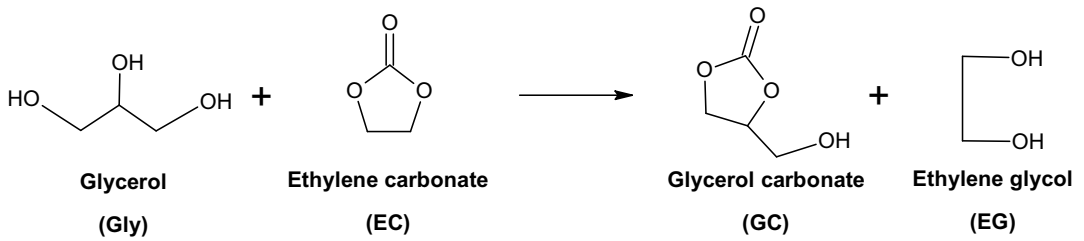

Fig. 1 – Chemical equation of the transesterification reaction of Gly and EC.

Table 3 – Experimental LLE data expressed as mole fractions (x_i) of the system Q {EC (1) + EG (2) + GC (3) + Gly (4)} at atmospheric pressure.

T (K)	Global composition (feed)				Phase I (Gly-rich) composition				Phase II (EC-rich) composition			
	x_1	x_2	x_3	x_4	x_1	x_2	x_3	x_4	x_1	x_2	x_3	x_4
313.2	0.499	0.000	0.000	0.501	0.089	0.000	0.000	0.911	0.953	0.000	0.000	0.047
	0.473	0.026	0.026	0.475	0.105	0.024	0.025	0.847	0.863	0.037	0.027	0.073
	0.450	0.049	0.050	0.451	0.112	0.045	0.043	0.800	0.793	0.058	0.056	0.093
	0.425	0.078	0.077	0.421	0.130	0.066	0.077	0.728	0.709	0.087	0.081	0.123
	0.400	0.100	0.099	0.402	0.155	0.098	0.088	0.658	0.639	0.115	0.095	0.152
	0.375	0.124	0.124	0.377	0.180	0.106	0.130	0.584	0.532	0.140	0.117	0.212
	0.353	0.146	0.146	0.355	0.217	0.134	0.147	0.503	0.434	0.132	0.167	0.268
318.2	0.502	0.000	0.000	0.498	0.101	0.000	0.000	0.899	0.939	0.000	0.000	0.061
	0.472	0.029	0.029	0.470	0.119	0.030	0.025	0.827	0.840	0.031	0.038	0.092
	0.444	0.055	0.054	0.447	0.134	0.056	0.041	0.770	0.764	0.051	0.070	0.115
	0.412	0.084	0.084	0.420	0.168	0.098	0.059	0.675	0.670	0.077	0.101	0.151
	0.394	0.108	0.107	0.392	0.195	0.127	0.076	0.602	0.591	0.096	0.127	0.186
	0.374	0.127	0.127	0.372	0.224	0.154	0.097	0.526	0.480	0.099	0.174	0.247
	0.350	0.151	0.151	0.348	0.256	0.199	0.093	0.453	0.390	0.107	0.202	0.301
323.2	0.501	0.000	0.000	0.499	0.108	0.000	0.000	0.892	0.930	0.000	0.000	0.070
	0.473	0.026	0.026	0.475	0.126	0.025	0.019	0.830	0.844	0.024	0.037	0.096
	0.451	0.054	0.053	0.442	0.143	0.053	0.044	0.761	0.748	0.053	0.071	0.128
	0.424	0.076	0.075	0.425	0.171	0.089	0.051	0.688	0.681	0.073	0.090	0.157
	0.396	0.103	0.104	0.397	0.203	0.119	0.077	0.601	0.580	0.075	0.145	0.200
	0.374	0.126	0.125	0.375	0.236	0.154	0.086	0.524	0.479	0.110	0.154	0.256
	0.353	0.148	0.147	0.352	0.271	0.174	0.107	0.449	0.394	0.098	0.200	0.309

Uncertainty of HPLC analysis ($\sigma_x = 0.018$).

as cosolvents (system Q). The latter scenario describes what actually occurs in the synthesis of GC (as described in Fig. 1), while the former two represent simplifications so as to evaluate the separate effect of EG and GC in the phase equilibria. By doing this, an assessment of the evolution of the composition of the phases within the reacting system is intended. Therefore, an observation of the composition at which the initially biphasic system turns into a monophasic liquid can be made. These tables also include the LLE measurements obtained from experimentation expressed as mole fractions of the systems T1, T2 and Q at 313.2, 318.2 and 323.2 K.

Figs. 2–4 depict the tie-lines represented by the data in Tables 1–3 as well as the binodal curves and tie-lines predicted by the NRTL model.

Verification of the reliability of the experimental LLE results was made making use of the Othmer–Tobias correlation, defined as (Othmer and Tobias, 1942):

$$\left[\log\left(\frac{1-w_{Gly}}{w_{Gly}}\right)\right]_I = a + b\left[\log\left(\frac{1-w_{EC}}{w_{EC}}\right)\right]_{II} \quad (1)$$

in which w_{Gly} and w_{EC} are the mass fractions of Gly in the Gly-rich phase (I) and EC in the EC-rich phase (II), respectively; a and b are the fitting parameters of this linear correlation. Table 4 compiles the values of a and b together with R^2 values close to 1 showing that there is a good correlation in Eq. (1) at the temperatures tested for equilibrium in each system.

Table 4 – Parameters of the Othmer–Tobias correlation (a and b) and correlation coefficients (R^2) for the systems T1 {EC + EG + Gly}; T2 {EC + GC + Gly} and Q {EC + EG + GC + Gly}.

T (K)	a	b	R^2
EC + EG + Gly			
313.2	0.0808	0.8544	0.9971
318.2	0.1092	0.8688	0.9848
323.2	0.0846	0.8624	0.9916
EC + GC + Gly			
313.2	−0.1181	0.7761	0.9791
318.2	−0.0748	0.8695	0.9901
323.2	−0.0359	0.9464	0.9907
EC + EG + GC + Gly			
313.2	−0.1173	0.7422	0.9857
318.2	−0.0808	0.7889	0.9910
323.2	−0.0824	0.8016	0.9913

Please cite this article in press as: Esteban, J., et al., Liquid–liquid equilibria for the systems ethylene carbonate + ethylene glycol + glycerol; ethylene carbonate + glycerol carbonate + glycerol and ethylene carbonate + ethylene glycol + glycerol carbonate + glycerol at catalytic reacting temperatures. Chem. Eng. Res. Des. (2014), http://dx.doi.org/10.1016/j.cherd.2014.08.024

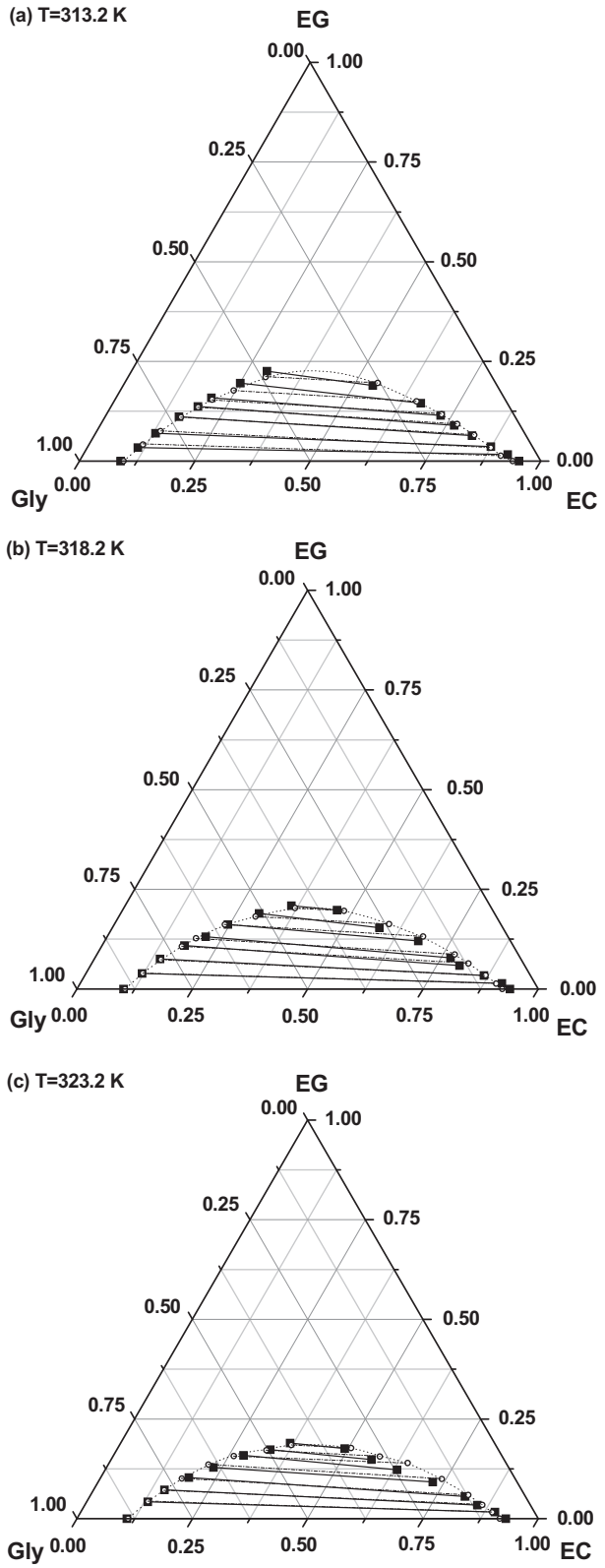

Fig. 2 – Experimental LLE measurements and binodal curve using the NRTL model for the system T1 {EC + EG + Gly} at 313.2 K (a), 318.2 K (b) and 323.2 K (c). Solid squares represent experimental tie-lines and dashed lines data calculated with the NRTL model.

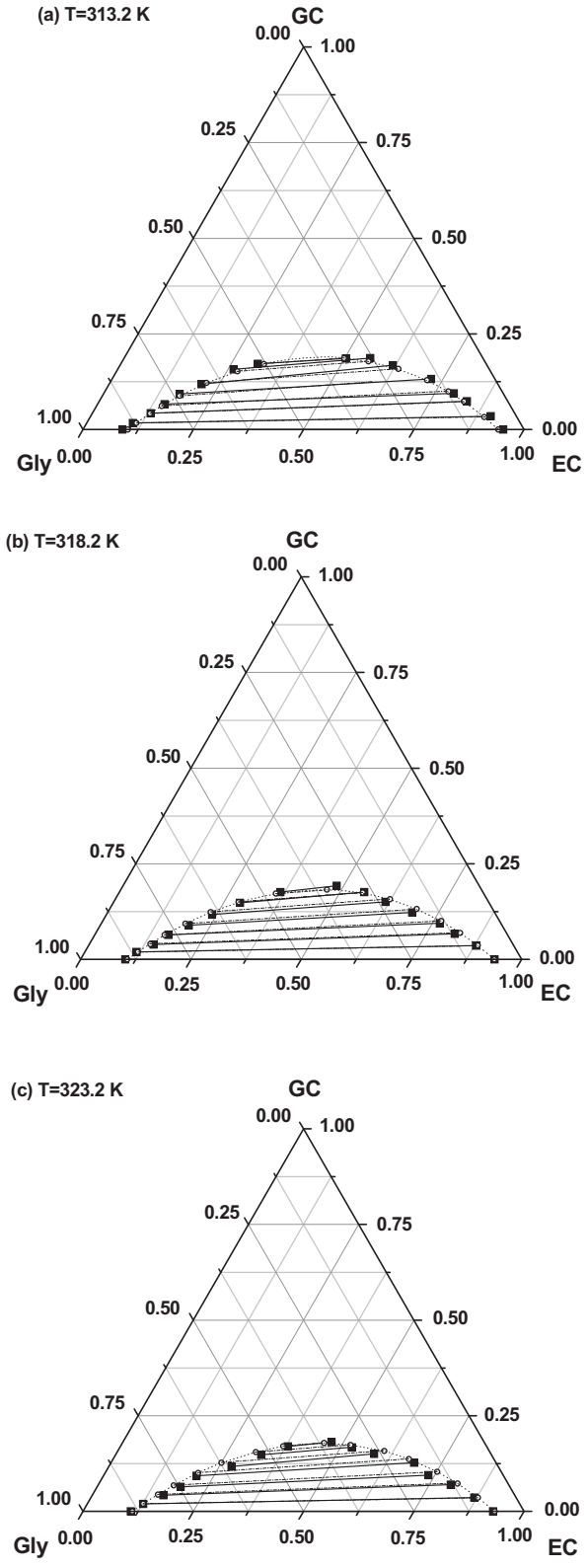

Fig. 3 – Experimental LLE measurements and binodal curve using the NRTL model for the system T2 {EC + GC + Gly} at 313.2 K (a), 318.2 K (b) and 323.2 K (c). Solid squares represent experimental tie-lines and dashed lines data calculated with the NRTL model.

3.2. *Influence of presence of ethylene glycol and glycerol carbonate and temperature in the biphasic system*

EG proved miscible in both phases (Fig. 2), yet the degree of miscibility was higher in the Gly-rich phase, due to the higher similarity between these two polyols. Likewise, GC showed solubility to a higher extent (Fig. 3) in the EC-rich phase rather than in the Gly-rich. In any case, the higher the tie-line along the vertical axis (i.e., the higher the conversion of the simulated reaction), the closer the feed mixture was to reach a monophasic system.

Please cite this article in press as: Esteban, J., et al., Liquid–liquid equilibria for the systems ethylene carbonate + ethylene glycol + glycerol; ethylene carbonate + glycerol carbonate + glycerol and ethylene carbonate + ethylene glycol + glycerol carbonate + glycerol at catalytic reacting temperatures. Chem. Eng. Res. Des. (2014), http://dx.doi.org/10.1016/j.cherd.2014.08.024

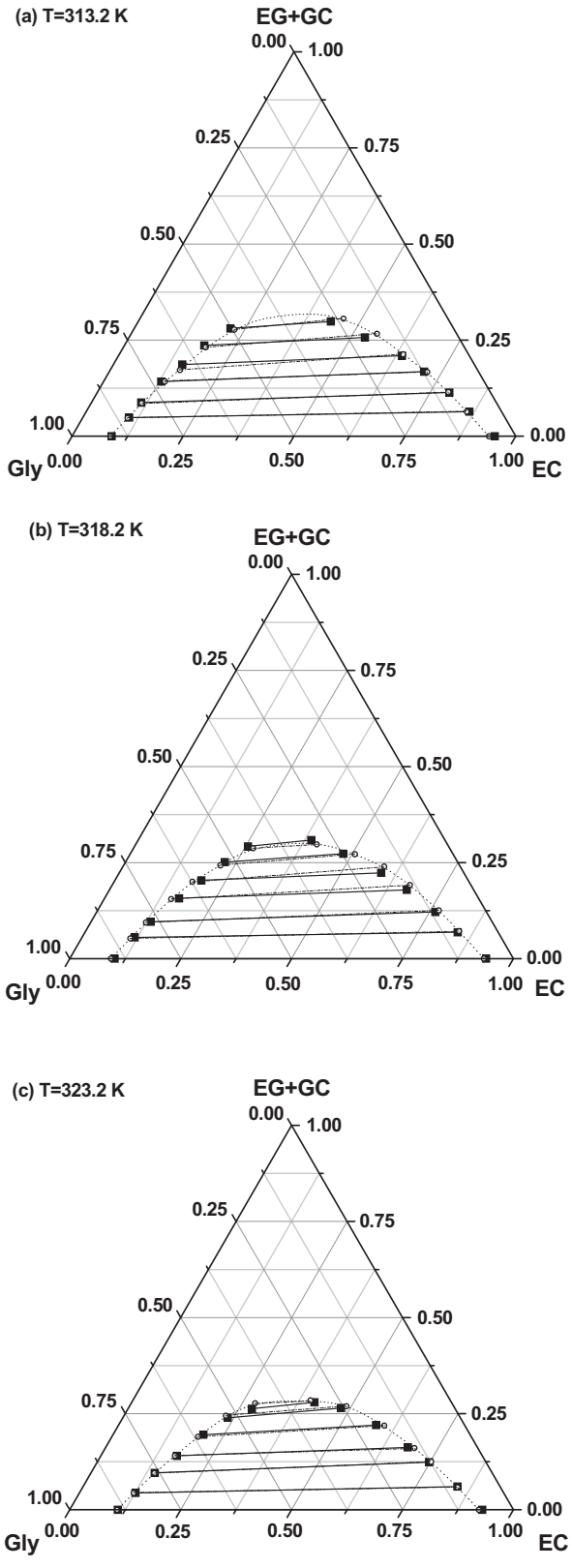

Fig. 4 – Experimental LLE measurements and binodal curve using the NRTL model for the system Q {EC + EG + GC + Gly} at 313.2 K (a), 318.2 K (b) and 323.2 K (c). Solid squares represent experimental tie-lines and dashed lines data calculated with the NRTL model.

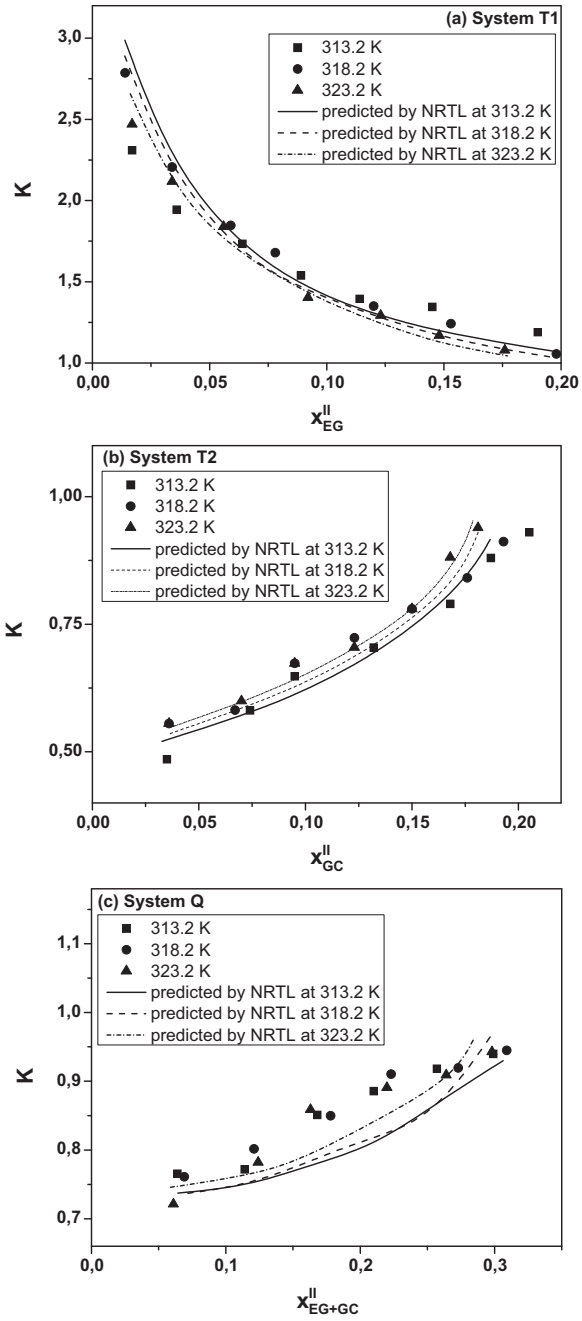

Fig. 5 – Effect of temperature on the experimental and predicted distribution ratios for the systems T1 (a), T2 (b) and Q (c).

Individual comparison of the effect of each cosolvent reflects that GC has a slightly more powerful solubilizing action than EG, due to the fact that the biphasic areas in the ternary diagrams appear somewhat smaller in former case. However, this effect was small considering that the maxima of the binodal curves for the system T1 varied between a molar fraction of EG of 0.20 and 0.22 and that for the system T2 between 0.18 and 0.21 for the temperatures tested. Nevertheless, the joint utilization of EG and GC (system Q) did not show such a positive effect on the solubilizing action, giving worse results than those obtained using them separately. Considering Q as a pseudoternary system, the maxima of the curves at the three temperatures tested lie between values of a joint composition of EG and GC of 0.29 and 0.32.

As for the effect of temperature, an increase of this variable showed practically no perceivable effect in the three systems studied judging from the experimental values of the distribution ratios (*K*) obtained (Fig. 5) with respect to the molar fraction of EG, GC and EG + GC in the EC-rich phase. Only the distribution ratios predicted by the NRTL model showed an

Please cite this article in press as: Esteban, J., et al., Liquid–liquid equilibria for the systems ethylene carbonate + ethylene glycol + glycerol; ethylene carbonate + glycerol carbonate + glycerol and ethylene carbonate + ethylene glycol + glycerol carbonate + glycerol at catalytic reacting temperatures. Chem. Eng. Res. Des. (2014), http://dx.doi.org/10.1016/j.cherd.2014.08.024

Table 5 – Values of the NRTL binary interaction parameters obtained from the LLE data by regression for the systems T1 {EC (1) + EG (2) + Gly (3)}, T2 {EC (1) + GC (2) + Gly (3)} and Q {EC (1) + EG (2) + GC (3) + Gly (4)}.

System	α_{ij} regression	Components i–j	NRTL parameters			rmsd
			α_{ij}	$\Delta g_{ij}/R$ (K)	$\Delta g_{ji}/R$ (K)	
T1	Fixed	1–2	0.2	−2456.00	248.33	0.0301
		1–3	0.2	602.79	453.90	
		2–3	0.3	−525.16	−1951.67	
	Floating	1–2	−1.79	297.97	−69.41	0.0297
		1–3	0.39	810.40	706.15	
		2–3	1.27	−20.60	−111.85	
T2	Fixed	1–2	0.2	−68.06	199.85	0.0300
		1–3	0.2	688.22	416.85	
		2–3	0.3	−200.29	679.07	
	Floating	1–2	0.96	61.94	527.43	0.0515
		1–3	0.36	794.76	643.24	
		2–3	0.85	−14.82	874.12	
Q	Fixed	1–2	0.2	1098.39	62.47	0.0239
		1–3	0.2	977.92	640.39	
		1–4	0.2	470.92	9806.37	
		2–3	0.2	9806.37	8942.80	
		2–4	0.3	190.41	1090.84	
		3–4	0.3	188.33	1128.98	
	Fixed	1–2	0.2	1134.68	86.40	0.0311
		1–3	0.2	1099.56	45.03	
		1–4	0.2	677.37	434.59	
		2–3	0.3	9122.24	9244.16	
		2–4	0.3	229.34	1077.39	
		3–4	0.3	164.72	1162.11	
	Floating	1–2	0.25	242.24	2698.97	0.0247
		1–3	1.37	802.18	77.40	
		1–4	0.19	694.09	435.38	
		2–3	−0.09	844.60	−1025.70	
		2–4	−1.50	193.01	228.51	
		3–4	0.96	−26.59	795.27	

almost negligible positive effect of this variable in system T2. The distribution ratios were computed following Eq. (2):

$$K = \frac{x_2^I}{x_2^{II}} \tag{2}$$

where the subscript 2 refers to the cosolvent, namely: EG (system T1), GC (system T2) and the mixture EG + GC (system Q). *I* is relative to the Gly-rich phase and II to the EC-rich phase, respectively.

3.3. *Data regression and correlation with the NRTL model*

Utilization of the NRTL model has previously been reported for VLE and LLE in multicomponent systems consisting of alcohols and organic carbonates (Fang and Qian, 2005; Wang and Lu, 2012). In order to retrieve the binary interaction parameters corresponding to this model, the data regression module of Aspen Plus was employed. Such tool is based on the least-squares method subject to the maximum likelihood principle. The Britt–Luecke algorithm (Britt and Luecke, 1973) was employed to obtain the parameters using the Deming initialization method. The regression convergence tolerance was set to 0.0001 and the objective function minimized was

$$OF = \sum_{k=1}^{N}\sum_{j=1}^{2}\sum_{i=1}^{3\text{ or }4}\left[\frac{(T_k^{exp} - T_k^{est})^2}{\sigma_T^2} + \frac{(x_{ijk}^{exp} - x_{ijk}^{est})^2}{\sigma_x^2}\right] \tag{3}$$

where the subscripts *i*, *j* and *k* are relative to the component (summation up to $i = 3$ for T1 and T2 and $i = 4$ for Q), phase and tie-line, respectively; *N* is for the number of tie-lines; T^{exp} and T^{est} refer to the experimental and estimated values of temperature, respectively and x^{exp} and x^{est} denote the experimental and calculated values of mole fraction. Finally, σ_T and σ_x are the standard deviation of the temperature and the mole fraction. Their values were taken from the accuracy of the temperature control system ($\sigma_T = 0.05$ K) and the mole fraction ($\sigma_x = 0.018$).

Regression of the binary interaction parameters as defined by the NRTL method was undertaken considering first a given set of values for the non-randomness parameters α_{ij} regarded as common values; then, optimization of these parameters was also realized. The criterion followed to evaluate the goodness of a set of values of said parameters was the minimization of the root mean square deviation (rmsd), which is defined by Eq. (3) for the ternary systems T1 and T2 and Eq. (4) for the quaternary system Q

$$\text{rmsd} = \sqrt{\sum_{k=1}^{N}\sum_{j=1}^{2}\sum_{i=1}^{3}\frac{(x_{ijk}^{exp} - x_{ijk}^{calc})^2}{6N}} \tag{4}$$

$$\text{rmsd} = \sqrt{\sum_{k=1}^{N}\sum_{j=1}^{2}\sum_{i=1}^{4}\frac{(x_{ijk}^{exp} - x_{ijk}^{calc})^2}{12N}} \tag{5}$$

Please cite this article in press as: Esteban, J., et al., Liquid–liquid equilibria for the systems ethylene carbonate + ethylene glycol + glycerol; ethylene carbonate + glycerol carbonate + glycerol and ethylene carbonate + ethylene glycol + glycerol carbonate + glycerol at catalytic reacting temperatures. Chem. Eng. Res. Des. (2014), http://dx.doi.org/10.1016/j.cherd.2014.08.024

3.4. Data correlation and binary interaction parameters

The NRTL model was fitted to data for the three systems considered in this study. Consequently, six binary interaction parameters exist for each of the ternary systems T1 and T2 and twelve for the quaternary system Q.

Prior works with organic carbonates and alcohols optimized the values of the non-randomness binary interaction parameters, α_{ij} (Wang and Lu, 2012). The values reported were $\alpha_{23} = 0.3$ and $\alpha_{12} = \alpha_{13} = 0.2$, which agree with those suggested for non-polar substances or non-polar with polar non-associated liquids and saturated hydrocarbons with polar non-associated liquids and systems that exhibit liquid–liquid limited miscibility (Renon and Prausnitz, 1968).

Table 5 compiles the values of the binary interaction parameters $\Delta g_{ij}/R$ retrieved from correlation of the entire set of data at the three temperatures tested given the mild effect of this variable on the equilibria as discussed in Section 3.2. First, regression was made keeping the α_{ij} constant at the values previously indicated for the ternary systems. Regarding system Q, two sets of α_{ij} values were used, with the only difference being keeping α_{ij} constant during the fitting procedure for the interaction between EG and GC. Said values were fixed at $\alpha_{23} = 0.2$ and $\alpha_{23} = 0.3$, respectively, for the two regressions. Additionally, simultaneous correlation of all the binary interaction parameters was also completed without keeping constant any of the non-randomness parameters to obtain their optimized values.

As can be seen in Table 5, regression with $\alpha_{23} = 0.2$ gave very similar values of the rmsd values for the system T1 to those obtained when floating all the parameters. In the case of system T2, the rmsd retrieved was lower. Finally, system Q, the best results in terms of rmsd value were obtained using $\alpha_{23} = 0.2$. Floating all the parameters yielded a very similar result, but not better in any case. In light of the results obtained after correlation of the three systems studied, it can be said that a set of standard values proposed by Renon and Prausnitz are optimal.

4. Conclusions

Acquisition of data of the LLE systems involved in the synthesis of GC through the reaction of Gly and EC was performed. Thus, the ternary systems comprising {EC + EG + Gly} and {EC + GC + Gly} in addition to the quaternary system {EC + EG + GC + Gly} were analyzed at 313.2, 318.2 and 323.2 K at atmospheric pressure. The individual and joint effects of EG and GC on the biphasic system that EC and Gly represent was assessed, proving that GC was more effective in solubilizing the immiscible components than the former. The joint action of EG + GC did not show such a positive effect on the solubilizing action, being the results better when using them individually. The effect of temperature within this range was also evaluated through the distribution ratio of the cosolvent, leading to conclude that its effect can be considered negligible.

Correlation of all the available LLE data acquired with the NRTL model was made so as to obtain a set of optimal binary interaction parameters valid at all the temperatures tested. Correlation with conventional non-random binary interaction parameters as obtained in classical references was optimal leading to the best prediction of the model.

Acknowledgements

The authors would like to express their grateful appreciation to the Ministerio de Ciencia e Innovación of the Government of Spain for financial support of this research through the project CTQ 2010-15460.

References

Alvarez, M.G., Segarra, A.M., Contreras, S., Sueiras, J.E., Medina, F., Figueras, F., 2010. Enhanced use of renewable resources: transesterification of glycerol catalyzed by hydrotalcite-like compounds. Chem. Eng. J. 161, 340–345.

Basso, R.C., de Almeida Meirelles, A.J., Caldas Batista, E.A., 2012. Liquid–liquid equilibrium of pseudoternary systems containing glycerol plus ethanol plus ethylic biodiesel from crambe oil (Crambe abyssinica) at T/K = (298.2,318.2,338.2) and thermodynamic modeling. Fluid Phase Equilib. 333, 55–62.

Behr, A., Eilting, J., Irawadi, K., Leschinski, J., Lindner, F., 2008. Improved utilisation of renewable resources: new important derivatives of glycerol. Green Chem. 10, 13–30.

Benoit, M., Brissonnet, Y., Guélou, E., De Oliveira Vigier, K., Barrault, J., Jérôme, F., 2010. Acid-catalyzed dehydration of fructose and inulin with glycerol or glycerol carbonate as renewably sourced co-solvent. ChemSusChem 3, 1304–1309.

Britt, H.I., Luecke, R.H., 1973. The estimation of parameters in nonlinear, implicit models. Technometrics 15, 233–247.

Climent, M.J., Corma, A., De Frutos, P., Iborra, S., Noy, M., Velty, A., Concepción, P., 2010. Chemicals from biomass: synthesis of glycerol carbonate by transesterification and carbonylation with urea with hydrotalcite catalysts. The role of acid–base pairs. J. Catal. 269, 140–149.

Chen, C.-H., Hyung, Y.E., Vissers, D.R., Amine, K., 2002. Lithium ion battery with improved safety, (Patent US 7026074 B2).

Cho, H.-J., Kwon, H.-M., Tharun, J., Park, D.-W., 2010. Synthesis of glycerol carbonate from ethylene carbonate and glycerol using immobilized ionic liquid catalysts. J. Ind. Eng. Chem. 16, 679–683.

de Azevedo Rocha, E.G., Follegatti-Romero, L.A., Duvoisin Jr., S., Aznar, M., 2014. Liquid–liquid equilibria for ternary systems containing ethylic palm oil biodiesel plus ethanol plus glycerol/water: experimental data at 298.15 and 323.15 K and thermodynamic modeling. Fuel 128, 356–365.

do Carmo, F.R., Evangelista, N.S., de Santiago-Aguiar, R.S., Fernandes, F.A.N., de Sant'Ana, H.B., 2014. Evaluation of optimal activity coefficient models for modeling and simulation of liquid–liquid equilibrium of biodiesel plus glycerol plus alcohol systems. Fuel 125, 57–65.

Esteban, J., Vorholt, A.J., Behr, A., Ladero, M., Garcia-Ochoa, F., 2014a. Liquid–liquid equilibria for the system acetone + solketal + glycerol at 303.2, 313.2 and 323.2 K. J. Chem. Eng. Data, http://dx.doi.org/10.1021/je500469a (in press).

Esteban, J., Ladero, M., Molinero, L., Garcia-Ochoa, F., 2014b. Liquid–liquid equilibria for the ternary systems DMC–methanol–glycerol; DMC–glycerol carbonate–glycerol and the quaternary system DMC–methanol–glycerol carbonate–glycerol at catalytic reacting temperatures. Chem. Eng. Res. Des., http://dx.doi.org/10.1016/j.cherd.2014.05.026 (in press).

Ezhova, N.N., Korosteleva, I.G., Kolesnichenko, N.V., Kuz'min, A.E., Khadzhiev, S.N., Vasil'eva, M.A., Voronina, Z.D., 2012. Glycerol carboxylation to glycerol carbonate in the presence of rhodium complexes with phosphine ligands. Pet. Chem. 52, 91–96.

Fang, Y.-J., Qian, J.-M., 2005. Isobaric vapor–liquid equilibria of binary mixtures containing the carbonate group —OCOO—. J. Chem. Eng. Data 50, 340–343.

George, J., Patel, Y., Pillai, S.M., Munshi, P., 2009. Methanol assisted selective formation of 1,2-glycerol carbonate from

glycerol and carbon dioxide using (Bu_2SnO)-Bu-n as a catalyst. J. Mol. Catal. A: Chem. 304, 1–7.
Gillis, H.R., Stanssens, D., De Vos, R., Postema, A.R., Randall, D., 1997. Polymeric foams, (Patent US5703136 A).
Hu, J., Li, J., Gu, Y., Guan, Z., Mo, W., Ni, Y., Li, T., Li, G., 2010. Oxidative carbonylation of glycerol to glycerol carbonate catalyzed by $PdCl_2$(phen)/KI. Appl Catal. A: Gen. 386, 188–193.
Iaych, K., Dumarçay, S., Fredon, E., Gérardin, C., Lemor, A., Gérardin, P., 2011. Microwave-assisted synthesis of polyglycerol from glycerol carbonate. J. Appl. Polym. Sci. 120, 2354–2360.
Jiabo, L., Tao, W., 2010. Coupling reaction and azeotropic distillation for the synthesis of glycerol carbonate from glycerol and dimethyl carbonate. Chem. Eng. Process. 49.
Kim, S.C., Kim, Y.H., Lee, H., Yoon, D.Y., Song, B.K., 2007. Lipase-catalyzed synthesis of glycerol carbonate from renewable glycerol and dimethyl carbonate through transesterification. J. Mol. Catal. B: Enzym. 49, 75–78.
Kovvali, A.S., Sirkar, K.K., 2002. Carbon dioxide separation with novel solvents as liquid membranes. Ind. Eng. Chem. Res. 41, 2287–2295.
Krishna, R., Low, C.Y., Newsham, D.M.T., Oliverafuentes, C.G., Paybarah, A., 1989. Liquid–liquid equilibrium in the system glycerol–water–acetone at 25 °C. Fluid Phase Equilib. 45, 115–120.
Lameiras, P., Boudesocque, L., Mouloungui, Z., Renault, J.-H., Wieruszeski, J.-M., Lippens, G., Nuzillard, J.-M., 2011. Glycerol and glycerol carbonate as ultraviscous solvents for mixture analysis by NMR. J. Magn. Reson. 212, 161–168.
Lee, M.-J., Lo, Y.-C., Lin, H.-M., 2010. Liquid–liquid equilibria for mixtures containing water, methanol, fatty acid methyl esters, and glycerol. Fluid Phase Equilib. 299, 180–190.
Li, Q., Zhang, W., Zhao, N., Wei, W., Sun, Y., 2006. Synthesis of cyclic carbonates from urea and diols over metal oxides. Catal. Today 115, 111–116.
Liu, J., Yuan, Y., Pan, Y., Huang, Z., Yang, B., 2014. Liquid–liquid equilibrium for systems of glycerol and glycerol tert-butyl ethers. Fluid Phase Equilib. 365, 50–57.
Mouloungui, Z., Pelet, S., 2001. Study of the acyl transfer reaction: structure and properties of glycerol carbonate esters. Eur. J. Lipid Sci. Technol. 103, 216–222.
Ochoa-Gomez, J.R., Gomez-Jimenez-Aberasturi, O., Maestro-Madurga, B., Pesquera-Rodriguez, A., Ramirez-Lopez, C., Lorenzo-Ibarreta, L., Torrecilla-Soria, J., Villaran-Velasco, M.C., 2009. Synthesis of glycerol carbonate from glycerol and dimethyl carbonate by transesterification: catalyst screening and reaction optimization. Appl. Catal. A: Gen. 366, 315–324.
Othmer, D.F., Tobias, P.E., 1942. Toluene and acetaldehyde systems, tie line correlation, partial pressures of ternary liquid systems and the prediction of tie lines. Ind. Eng. Chem. 34, 693–696.
Pagliaro, M., Ciriminna, R., Kimura, H., Rossi, M., Della Pina, C., 2009. Recent advances in the conversion of bioglycerol into value-added products. Eur. J. Lipid Sci. Technol. 111, 788–799.
Pagliaro, M., Rossi, M., 2008. The Future of Glycerol. New Uses for a Versatile New Material. Cambridge, RSC Publishing.
Patel, Y., George, J., Pillai, S.M., Munshi, P., 2009. Effect of liophilicity of catalyst in cyclic carbonate formation by transesterification of polyhydric alcohols. Green Chem. 11, 1056–1060.
Renon, H., Prausnitz, J.M., 1968. Local compositions in thermodynamic excess functions for liquid mixtures. AIChE J. 14, 135–144.
Rokicki, G., Rakoczy, P., Parzuchowski, P., Sobiecki, M., 2005. Hyperbranched aliphatic polyethers obtained from environmentally benign monomer: glycerol carbonate. Green Chem. 7, 529–539.
Rubio-Marcos, F., Calvino-Casilda, V., Banares, M.A., Fernandez, J.F., 2010. Novel hierarchical Co_3O_4/ZnO mixtures by dry nanodispersion and their catalytic application in the carbonylation of glycerol. J. Catal. 275, 288–293.
Sonnati, M.O., Amigoni, S., de Givenchy, E.P.T., Darmanin, T., Choulet, O., Guittard, F., 2013. Glycerol carbonate as a versatile building block for tomorrow: synthesis, reactivity, properties and applications. Green Chem. 15, 283–306.
Wang, H., Lu, P., 2012. Liquid–liquid equilibria for the system dimethyl carbonate + methanol + glycerol in the temperature range of (303.15–333.15) K. J. Chem. Eng. Data 57, 582–589.
Zhou, C., Beltramini, J., Fan, Y., Lu, G., 2008. Chemoselective catalytic conversion of glycerol as a biorenewable source to valuable commodity chemicals. Chem. Soc. Rev. 37, 527–549.

Please cite this article in press as: Esteban, J., et al., Liquid–liquid equilibria for the systems ethylene carbonate + ethylene glycol + glycerol; ethylene carbonate + glycerol carbonate + glycerol and ethylene carbonate + ethylene glycol + glycerol carbonate + glycerol at catalytic reacting temperatures. Chem. Eng. Res. Des. (2014), http://dx.doi.org/10.1016/j.cherd.2014.08.024

Publicación 4 / Publication 4

Autores/Authors: Jesús Esteban, Elena Fuente, María González-Miquel, Ángeles Blanco, Miguel Ladero and Félix García-Ochoa

Título/Title: Sustainable joint solventless coproduction of glycerol carbonate and ethylene glycol via thermal transesterification of glycerol

Estado actual/Current status: RSC Advances (2014), 4: 53206-53215

Índice de impacto / Impact factor 2013: 3.708

Resumen

Este artículo presenta la síntesis conjunta de GC y EG por transesterificación de glicerina y EC en una reacción que presenta como novedad la ausencia de catalizador, a diferencia de otros trabajos anteriores en la literatura.

En primer lugar se estudió, mediante la técnica FBRM, la influencia de la temperatura en la emulsión constituida por los reactivos EC y glicerina y se observó que las fases iban solubilizándose entre sí hasta que la emulsión desaparece a partir de 80 ºC. Así mismo, se comprobó que en el sistema no hay reacción en ausencia de catalizador en el intervalo de temperaturas en el cual es una emulsión y, sin embargo, hay reacción química en condiciones en las que el sistema es monofásico.

A pesar de haber un estudio de la termodinámica de la reacción publicado, este estudio no incluye las temperaturas a las que se ha operado en el presente trabajo, por lo que se amplió dicho análisis. En el intervalo estudiado, se predice una conversión prácticamente total de la reacción, coincidiendo en este sentido con los resultados experimentales, además de concluirse que la reacción es endotérmica.

A continuación, se realizaron un total de diez experimentos cinéticos entre 100 y 140 ºC empleando relaciones molares iniciales de EC a glicerina de 2 y 3 y se propusieron un total de cuatro modelos cinéticos para ajustarse a los datos experimentales. Se llevó a cabo la discriminación entre dichos modelos siguiendo criterios estadísticos así como el estudio termodinámico realizado. El modelo elegido como representativo de la cinética de la reacción contempla la reacción directa obviando la posible reacción inversa y propone una ecuación potencial de primer orden parcial respecto a las concentraciones de glicerina y EC (de segundo orden global, por tanto), siendo la energía de activación de 61.82 ± 0.83 kJ·mol^{-1}.

Por último, se realizó un estudio comparativo de esta reacción con otras referencias en la literatura en las que se empleaban catalizadores en términos de *Parámetros de Química Verde* relacionados con la utilización de recursos materiales para llevarla a cabo. En este sentido, la reacción aquí propuesta presenta una productividad másica y una eficiencia másica de reacción mayores a los otros procesos descritos en la bibliografía. Además, la eficiencia atómica y la de carbono son del 100% y el valor del factor-E, que considera la generación de residuos, es nulo.

RSC Advances

PAPER

View Article Online
View Journal | View Issue

Cite this: *RSC Adv.*, 2014, **4**, 53206

Sustainable joint solventless coproduction of glycerol carbonate and ethylene glycol *via* thermal transesterification of glycerol†

Jesús Esteban,[a] Elena Fuente,[a] María González-Miquel,[b] Ángeles Blanco,[a] Miguel Ladero*[a] and Félix García-Ochoa[a]

Received 28th July 2014
Accepted 7th October 2014

DOI: 10.1039/c4ra11209a

www.rsc.org/advances

This study focuses on the thermal reaction between glycerol and ethylene carbonate to obtain glycerol carbonate and ethylene glycol under solventless homogeneous operation, the process being a transcarbonation of glycerol or a glycerolysis of ethylene carbonate. As the two reagents constitute an immiscible system at 40 °C evolving into a single phase at 80 °C, the evolution of phases with temperature was studied by focused beam reflectance measurement. As the biphasic system was inert, runs were completed under a monophasic regime from 100 to 140 °C with molar ratios of ethylene carbonate to glycerol of 2 and 3, achieving quantitative conversion of glycerol, as corroborated by a thermodynamic study. Second order potential kinetic models were proposed and fitted to the data. Finally, a comparison with analogous catalytic approaches was made, showing that this process performs better material-wise.

Introduction

Due to the high production of glycerol (Gly) from biodiesel processes, its valorisation has been the subject of a thorough study.[1] Many valuable products have been obtained based on syntheses from glycerol, among which are solketal, 1,3-propanediol, dihydroxyacetone and glycerol carbonate (GlyCarb).[2]

GlyCarb has received increasing interest as a potential bio-based product.[3] It has shown outstanding properties in many applications as surfactant and solvent.[4] Its use as a green-based solvent has been credited in Li-ion batteries,[5] analytical applications,[6] cosolvent with ionic liquids[7] or as a solvent in immobilized liquid membranes for selective carbon dioxide separation from CO_2/N_2 mixtures.[8] Moreover, its inclusion in building materials has proven effective for rapid hardening, reducing shrinkage of the material and improving compressive strength.[9]

Moreover, GlyCarb can also be regarded as a building block. Atom transfer radical polymerization initiators can be synthesized to yield polymers with end-functional five-membered cyclic carbonate groups for application as coatings, macromolecular surfactants and adhesives.[10] GlyCarb has substituted the less environmentally friendly glycidol in the synthesis of hyperbranched polyethers.[11] By acylation of GlyCarb, several esters have been obtained with surfactant features as well as thermal and oxidation stability.[12] Secondary amines also react with it to produce alkyl glycerol carbamates used as thickeners in surface-active preparations.[13]

Traditional production of GlyCarb used to be accomplished with phosgene. Nevertheless, this hazardous method has been substituted by alternative procedures. Reaction of glycerol with urea at 140 to 150 °C under vacuum conditions and catalysts like rare earth metal oxides, La_2O_3, Zn and Mn sulphates or calcined Zn hydrotalcites yields 86% GlyCarb in the best case scenario.[14–19] Direct addition of CO_2 was tested with tin-based catalysts under solventless conditions at 180 °C and 5 MPa;[20] in the presence of methanol as solvent, conditions were lowered to 80 °C and 3.5 MPa improving the yield of the process.[21] Even supercritical conditions (40 °C, 10 MPa) with basic ion exchange resins and zeolites[22] were tried. In none of these cases the yields achieved were higher than 35%.[21] Similarly, carbonylation *via* the addition of CO and O_2 mixtures with a palladium-based catalyst has been undertaken with a yield as high as 92% and almost total selectivity.[23]

However, the most followed trend is the use of organic carbonates to perform the transesterification of glycerol, known for over fifty years,[24] due to the high yield obtained at low temperature. Particularly, transesterification to GlyCarb with dialkyl carbonates has been much more widely covered[11,25–31] than that with ethylene carbonate (EtCarb), with fewer references being found until the present date.[19,22,32,33] As presented in Scheme 1, an additional advantage of the latter reaction is that

[a]*Department of Chemical Engineering, Complutense University of Madrid, Avda. Complutense s/n. 28040, Madrid, Spain. E-mail: mladero@quim.ucm.es; Fax: +34-913944179; Tel: +34-913944164*

[b]*School of Chemical Engineering and Analytical Science, The University of Manchester, The Mill Sackville Street, M139PL, Manchester, UK*

† Electronic supplementary information (ESI) available. See DOI: 10.1039/c4ra11209a

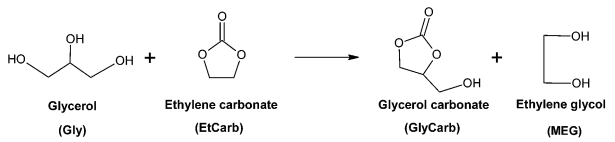

Scheme 1 Transesterification reaction of Gly and EtCarb.

ethylene glycol (MEG) is obtained as well, being this a product extensively used as antifreeze and other applications. This substance is obtained by hydrolysis of ethylene oxide (EO), giving MEG and oligoglycols. The best procedure seems to be Shell's OMEGA process, in which EO is carbonated and subsequently hydrated to yield 99.5% MEG, a further effort to reach the most valuable product and the maximum achievable exploitation of feedstock.[34–37]

At temperatures above the melting point of EtCarb (36 °C), the two reactants of the proposed reaction constitute a liquid–liquid dispersion up to a certain temperature. In order to study heterogeneous systems, focused beam reflectance measurement (FBRM) has been successfully applied. This technique has been used to measure particle and droplet sizes in suspensions of solids in liquids,[38] flocculation processes[39] and liquid–liquid dispersions.[40,41] An *in situ* monitoring of the evolution of the dispersion with temperature is herein proposed to determine the phase changing behaviour of the system.

According to literature, thus far, GlyCarb synthesis has only been pursued through catalytic procedures, with the concomitant need for removing the catalyst from the final product and/or regenerating it after a certain operation time. Hence, the aim of this work is to develop a novel and more sustainable solventless thermal process at atmospheric pressure and low to moderate temperatures. A thermodynamic study of the reaction at the conditions tested is presented together with a kinetic model for this thermal reaction.

Results and discussion

Assessment of the miscibility of the liquid phases

Prior to experimentation aimed at obtaining the kinetic model, experiments were performed to monitor the evolution of the biphasic system with temperature. Assessment of the evolution of the *ab initio* biphasic system was made following a variable that gives an idea of the decrease of the size of the droplets within the emulsion. Said variable was the mean chord length of the droplets and the number of counts per second, parameters whose value decrease as temperature increases from 40 to 80 °C, as shown in Fig. 1.

Values of the mean chord length at 40 °C are in the millimetre range, while at temperatures equal or higher than 75 °C they are in the micrometer range. At 80 °C, the mean chord length was negligible, indicating that the size of the droplets was smaller than the detection limit of the FBRM (1 μm), so it can be inferred that EtCarb and Gly gradually dissolved in each other so that the dispersion system evolved into a single phase above 80 °C. This is confirmed by the exponential reduction of

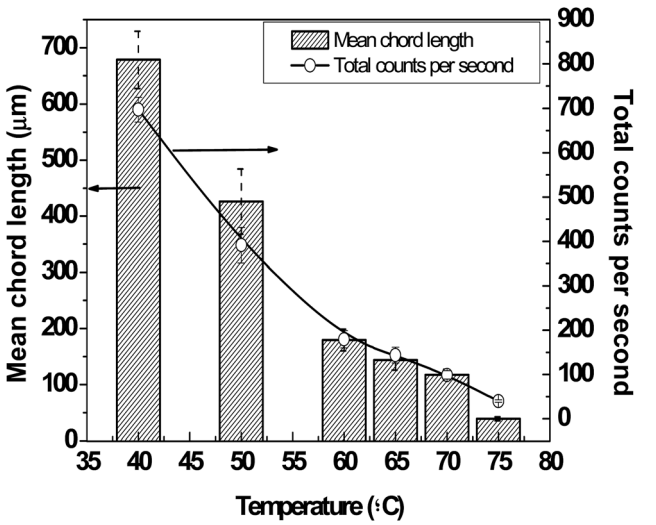

Fig. 1 Evolution of the mean chord length and droplet count per second with temperature. Conditions: stirring speed (SS) of 750 rpm and Gly at a EtCarb to Gly molar ratio (*M*) of 3.

the number of counts or events per second detected by the FBRM.

To observe the influence of the number of phases in the reacting system and the temperature, some preliminary runs were conducted at different temperatures allowing batches of the reagents (molar ratio of EtCarb to Gly equal to 2) to interact under agitation for 24 hours (data not shown). No products were detected while operating at temperatures within which the system showed liquid–liquid biphasic behaviour, at 75 °C and lower temperatures. Only the presence of products was observable when operating at 80 °C, though the conversion *X* only amounted to 9.3% after the mentioned period of time. Thus, it can be said that the system was almost inert while in a liquid–liquid biphasic state and the thermal reaction only took place at appreciable rate under homogeneous conditions and temperature equal to or higher than 100 °C. At atmospheric pressure and 140 °C, some evaporation phenomena were observed, thus being this the highest temperature selected for further studies.

Thermodynamic study

The purpose of this study was to determine whether the thermodynamic equilibrium constant value was high enough to predict that the behaviour of the reaction was shifted towards the products as well as to assess its endo- or exothermicity. A thermodynamic study of this type has previously been reported, yet the calculations were made at lower temperatures than those investigated in the present paper. However, the methodology presented therein served as a basis to develop a thermodynamic evaluation for the scenarios approached in this study.[42]

Application of the well-known Kirchhoff laws for reaction enthalpy and entropy as functions of temperature leads to values of these thermodynamic functions at 80 to 140 °C. Gibb's free energy values have been estimated from the mentioned

functions and the equilibrium constants from Gibbs free energy at the temperature values were also computed (Appendix 1). For the mentioned calculations to be performed, several literature references were consulted.[43–49] The main results are summarized in Table 1. It can be seen from the value of the equilibrium constant at temperatures equal to or higher than 100 °C that the global reaction is shifted towards the products, while reaction enthalpies imply endothermicity. The influence of the entropy in the equilibrium is decisive, being the most influential term in Gibb's free energy, with a higher impact as temperature rises. For this system, the following equations relate the thermodynamic functions and the equilibrium constant with temperature:

$$\Delta H_r^0 = 166.21 - 0.1556T[\mathrm{K}] \quad (1)$$

$$\Delta S_r^0 = -9193 + 30.49T[\mathrm{K}] \quad (2)$$

$$\Delta G_r^0 = 4862 - 14.93T[\mathrm{K}] \quad (3)$$

$$K = 10^{-5}\, e^{0.037T[\mathrm{K}]} \quad (4)$$

Runs for 48 hours were performed at temperatures in the 100 to 140 °C interval and at EtCarb to Gly molar ratios of 2 and 3, in order to reach equilibrium conditions in the relevant operational range. In parallel, calculation of values of conversion at equilibrium was performed from the equilibrium constant at each temperature using eqn (5).

$$K_{eq} = \frac{\left(\gamma_{GlyCarb}(X_{eq})\cdot x_{GlyCarb}(X_{eq})\right)^{\upsilon_{GlyCarb}}\cdot\left(\gamma_{MEG}(X_{eq})\cdot x_{MEG}(X_{eq})\right)^{\upsilon_{MEG}}}{\left(\gamma_{Gly}(X_{eq})\cdot x_{Gly}(X_{eq})\right)^{\upsilon_{Gly}}\cdot\left(\gamma_{EtCarb}(X_{eq})\cdot x_{EtCarb}(X_{eq})\right)^{\upsilon_{EtCarb}}} \quad (5)$$

where x_i, ν_i and γ_i refer to the molar fraction, stoichiometric coefficient and activity coefficient, respectively. The activity coefficients depend on the composition of the mixture, *i.e.*, the molar fraction of each component, and they can be related to the conversion X. Thus, the conversion at equilibrium can be computed. Two scenarios were contemplated, namely: ideal and real thermodynamic behaviour. In the former, γ_i were considered equal to one, while in the second these parameters were calculated for all compositions, temperatures and EtCarb to Gly molar ratios by applying a COSMO-RS (COnductor like Screening MOdel for Real Solvents) approach using the software COSMOtherm version C3.0 Release 12.01 with its implicit parameterization BP_TZVP_C30_01201. Activity coefficients are displayed in tables in Appendix 2.

Table 1 Enthalpy, entropy standard Gibbs free energy of reaction and chemical equilibrium constant of the transesterification of EtCarb and Gly at the temperatures tested in this work

Temperature (°C)	ΔH_r^0 (kJ mol^{-1})	ΔS_r^0 (J mol^{-1} K^{-1})	ΔG_r^0 (kJ mol^{-1})	K
100	108.26	2186.66	−707.37	14.42
110	106.53	2487.25	−846.08	20.78
120	104.91	2790.85	−991.89	30.04
130	103.41	3097.22	−1144.77	43.55
140	102.04	3406.11	−1304.69	63.29

Experimental conversion values for Gly, with their absolute errors, are shown in Fig. 2, together with the computed conversions for the ideal and real liquid approaches. It can be inferred that the system approaches total conversion as the temperature rises and the EtCarb to Gly molar ratio increases, in agreement with the equilibrium constant values. At the same time, although activity coefficients are far from the unit, especially in the case of glycerol and glycerol carbonate, the effect of the high concentration of reagents and products in solution is almost negligible. Moreover, computed values for conversion at equilibrium are in agreement with experimental values, given the absolute error intervals for the latter.

Transesterification runs

Once the FBRM study allowed for the determination of the operational range in which the system is homogeneous, a series of experiments were completed in order to study the kinetics of the reaction. A total of 10 experiments were conducted at a fixed agitation speed of 750 rpm with temperature ranging between 100 and 140 °C (in intervals of 10 °C) and initial molar ratios of EtCarb to Gly of 2 and 3. Fig. 3 shows the evolution of the conversion in the kinetic runs and fitting of the selected kinetic model.

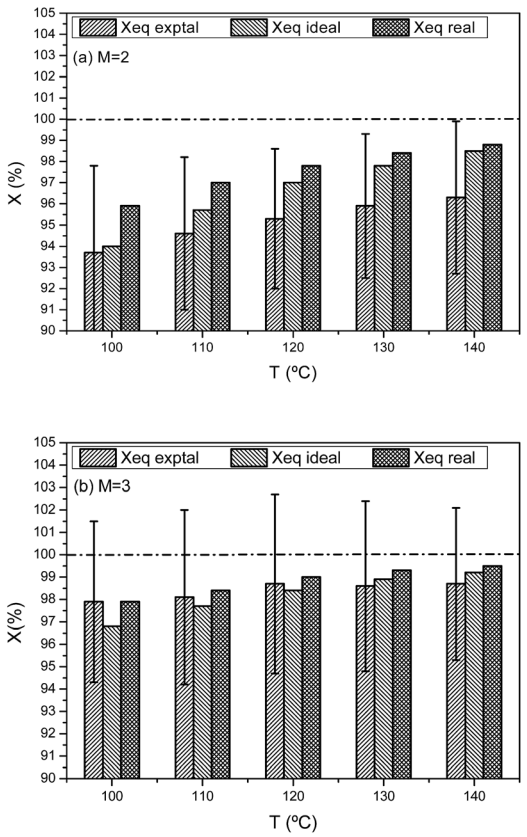

Fig. 2 Experimental and calculated conversion of Gly at initial molar ratios of EtCarb to Gly of 2 (a) and 3 (b).

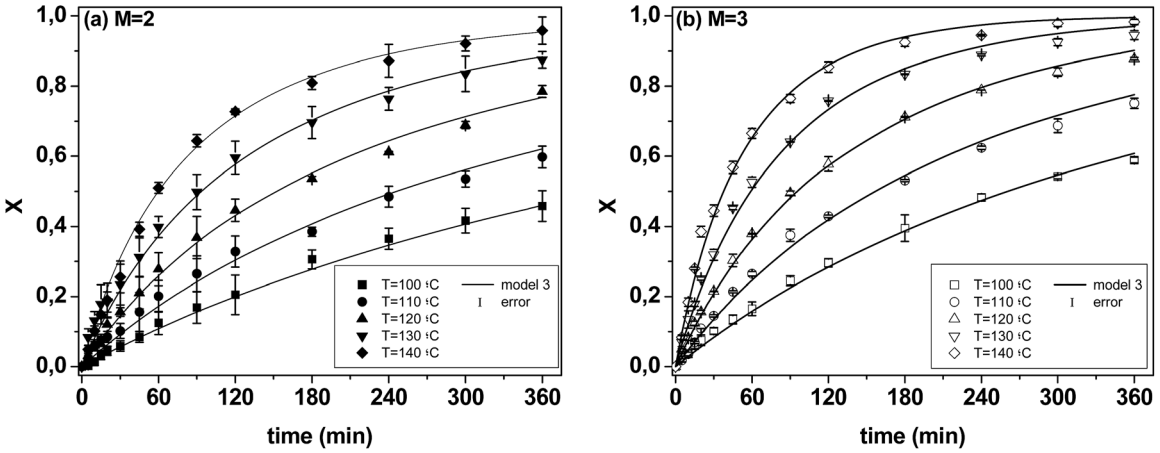

Fig. 3 Experimental results of the kinetic runs of the heat-driven transesterification of EtCarb and Gly and prediction using Model 3. Conditions: Temperature varied from 100 to 140 °C using (a) $M = 2$ and (b) $M = 3$ and agitation was kept constant at 800 rpm.

For kinetic model fitting purposes, the software Aspen Custom Modeler was employed. In this program, an algorithm for non-linear regression based on the Levenberg–Marquardt method was applied simultaneously with the numerical integration of the proposed kinetic equation corresponding to each model through a fourth-order Runge–Kutta method.

Initially, correlation of each model was realized at individual temperatures. After obtaining the value of the kinetic constant (or constants) at each temperature, estimates of E_a/R parameters were retrieved, from which simultaneous correlation or each kinetic model to all data at all temperatures was performed to obtain the multivariable fitting parameters.

Table 2 compiles the diverse kinetic models utilized to fit to the experimental data gathered that were proposed in this work. Model 1 was defined as a potential model of first order with respect to EtCarb, keeping the concentration of Gly constant, and a part of the apparent kinetic constant thereof obtained. Model 2 considered an analogous situation, in which only the concentration of Gly was regarded as influential to the kinetic model, becoming the concentration of EtCarb a part of the apparent constant. These models imply that one of the reagents is the main component of the phase were the reaction takes place; the other phase is mainly composed by the other reagent. The dispersed phase droplets would be forming a nano-emulsion, so an FBRM analysis would be not able to detect it (The FBRM herein employed had a lower limit of 1 μm for the diameter of the detected particle).

Model 3 describes an overall second order potential kinetic model, with partial first orders with respect to the concentrations of the reactants. Successful fitting of this type of model for the transesterification of dimethyl carbonate and ethanol has been reported.[50] Likewise, second order potential kinetic models have been applied to esterification reactions.[51,52] Finally, Model 4 still considers a reversible second order potential model. Said situation would be described with a reverse reaction from the products to the reactants. The latter model was tested after some results from the equilibrium runs suggested a conversion slightly lower than one for EtCarb to Gly molar ratio of 2 and temperature varying from 100 to 120 °C.

To select one of the proposed models, statistical criteria defined in the experimental section were used, as well as physicochemical criteria as the value of activation energies.

Table 3 compiles the statistical and fitting parameters calculated after multivariable correlation of all data. Regarding the parameters of the models, a definition of the dependence of the kinetic constants k_j with temperature was made following a

Table 2 Summary of the kinetic models assessed to fit to experimental data obtained from the thermal transesterification of EtCarb and Gly

Model number	Rate equations
1	$r = k_1 C_{EtCarb} = k_1 C_{EtCarb0}(M - X)$
2	$r = k_2 C_{Gly} = k_2 C_{Gly0}(1 - X)$
3	$r = k_3 C_{Gly} C_{EtCarb} = k_3 {C_{Gly0}}^2 (1 - X)(M - X)$
4	$r = k_4 C_{Gly} C_{EtCarb} - k_5 C_{MEG} C_{GlyCarb} = k_4 {C_{Gly0}}^2 (1 - X)(M - X) - k_5 (C_{Gly0} X)^2$

Table 3 Kinetic and statistical parameters obtained for each kinetic model for the thermal transesterification of glycerol and ethylene carbonate

Model	Parameter	Value	±Error	F_{95}	AIC	RMSE	VE (%)
1	$\ln k_{10}$	2.64	0.98	718	−3.90	0.14	77.61
	E_{a1}/R	3656	388				
2	$\ln k_{10}$	13.04	0.67	4407	−5.62	0.06	96.01
	E_{a1}/R	7154	263				
3	$\ln k_{10}$	11.72	0.25	34426	−7.69	0.02	99.50
	E_{a1}/R	7436	100				
4	$\ln k_{10}$	11.22	0.29	25335	−8.08	0.02	99.67
	E_{a1}/R	7217	116				
	$\ln k_{20}$	21.64	3.73				
	E_{a2}/R	5143	1472				

modified Arrhenius equation suitable for computational purposes:

$$k_j = \exp\left(\ln k_{j0} - \frac{E_{aj}}{R}\frac{1}{T}\right) \quad (6)$$

where k_{j0} and E_{aj}/R are the preexponential factors of the kinetic constants and the ratio between activation energy and the ideal gas constant, respectively.

The activation energies range from 30 kJ mol^{-1} to around 60 kJ mol^{-1}. The activation energies of processes controlled by the chemical reaction step usually acquire values between 40 and 200 kJ mol^{-1}. These figures can be expected for a homogeneous reacting system.

Due to the value of E_{a1}/R being below this interval and the poor degree of fitting shown, especially concerning the variation explained (VE), Model 1 was dismissed. Model 2 showed better agreement between experimental and predicted values, increasing significantly the adjusted Fischer parameter (F) and VE. Correlation of Models 3 and 4 lead to a further marked enhancement of all statistical criteria. Nevertheless, as inferred from the results in Table 3, there is no clear evidence that Model 3 is better than Model 4 or *vice versa*: while F is higher for Model 3 and RMSE has a similar value, VE and AIC show both slightly worse values in terms of goodness of agreement than those obtained for Model 4. In any case, as stated, second order models had been proposed in literature to describe comparable chemical reactions,[50–52] and these results further probes the observations in the FBRM studies: the system is homogeneous.

Nonetheless, taking into account results from the thermodynamic studies, it can be said that only the direct reaction takes place when the molar ratio of EtCarb to Gly is equal or higher than 3, while at lower values, the influence of the reverse reaction is considerable, mainly at temperatures of 120 °C or lower. This leads to select Model 3 as the most adequate to represent the transesterification of glycerol and ethylene carbonate in the more common situation of $M \geq 3$, and to select Model 4 as the most precise for lower values of the reagent's molar ratio. In Fig. 3, the reasonable fitting of Model 3 to experimental results can be observed.

Finally, Fig. 4 shows the evolution of the relative error of the prediction for Model 3, with a positive value implying an underestimation of such model with respect to the observed data. While the relative error is higher at short times than afterwards, partly due to the absolute values of the variable X being much smaller, no clear trend in regards of an under or overestimation can be observed for the two sets of experiments; thus, this is further proof for the validation of the model, acceptable even for $M = 2$ if experimental error bars showed in Fig. 3 are taken into account.

Metrics to green chemistry of the process

Given the more and more important view on the sustainability of chemical processes, the advantages of this process have been evaluated with a metrics to green chemistry approach. For this purpose, certain sustainability parameters as described by Constable *et al.* (2002)[34] have been computed for this work as well as for the other references found in literature.

First, it can be said that the atom economy and the carbon efficiency, as defined in the experimental section of this work (eqn (14) through (16)) of the transesterification of Gly and EtCarb to give GlyCarb and MEG are virtually 100%, and the E-factor value is equal to zero in all cases if only the synthetic process herein studied is considered. None of the references cited the use of any solvents and the catalysts employed, where applicable, could be subject to reutilization. The process studied is a one-step solventless reacting system in all cases.

Regarding the comparison between the thermal process herein reported and the catalytic ones found in literature, mass productivity (MP) and reaction mass efficiency (RME) were computed on the basis of a reference experiment (at 100 °C and a molar ratio of EtCarb to Gly of 2). The same parameters were

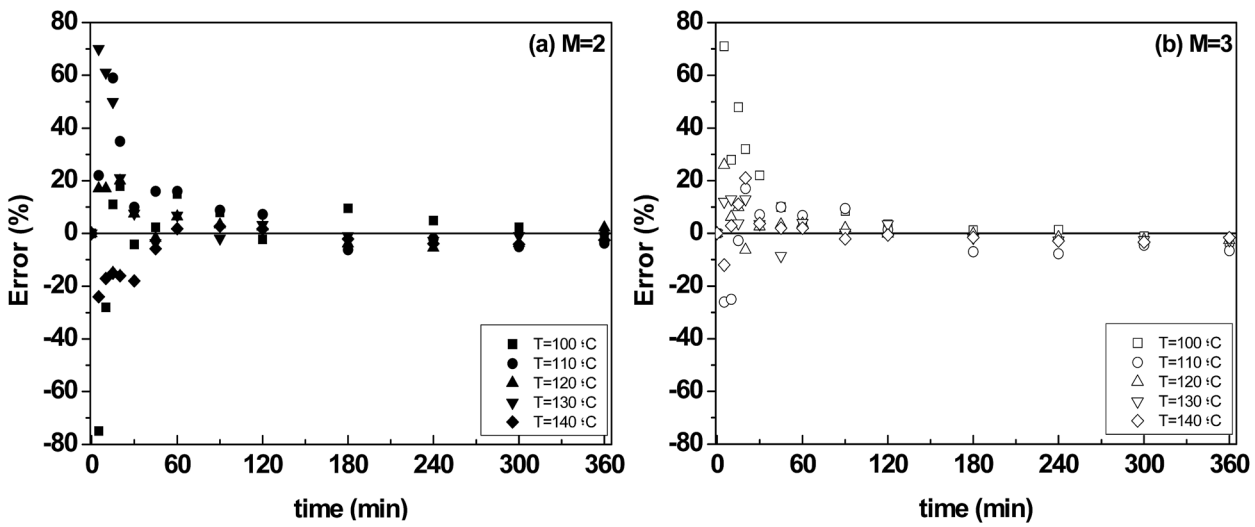

Fig. 4 Evolution of the error of prediction of Model 3 with respect to the experimental measures operating with (a) $M = 2$ and (b) $M = 3$ Conditions: fixed agitation speed of 750 rpm.

Table 4 Comparative study of the mass productivity and reaction mass efficiency for various transesterifications of EtCarb and Gly performed in batches

Reference	Y_{GC} (%)	Catalyst	Reaction conditions	MP (%)	RME (%)
19	91.0	Al–Mg mixed oxide derived from hydrotalcite with Al/Mg molar ratio of 0.25	$T = 50$ °C; $M = 2$; 7 wt% of catalyst with respect to the total weight of reactants[a]	45.92	61.80
22	32.2	Purosiv zeolite	$P = 13$ MPa; $T = 74$ °C; $M = 0.63$; 125% wt% of catalyst with respect to total weight of reactants[b]	11.70	24.68
33	83.8	Tri-*n*-butylamine supported on MCM-41 molecular sieve	$T = 80$ °C; $M = 2$; 3.1% wt% of catalyst with respect to the total weight of reactants[a]	44.92	56.29
This work	96.9	None: thermal reaction	$T = 140$ °C; $M = 2$[a]	50.26	66.37

[a] At atmospheric pressure except otherwise specified. [b] Supercritical conditions.

calculated for the experiments that achieved the best yields to products in the other references.

Table 4 compiles the mentioned calculations along with the operating conditions and catalysts described in the other references. The values of MP and RME show that the process herein proposed performs better than the rest. This can be ascribable to the fact that no catalyst was used and virtually total conversion was achieved. When catalysts were used, yields to the products were lower given the activity limitations to the completion of the reaction; whereas in the thermal process, the final yield to product (equal, being this an elemental reaction, to the conversion of glycerol in percentage) is only restricted by thermodynamic considerations, not by mass transfer or deactivation of the catalyst. Also, the values of MP and RME herein obtained apply to batch processes, where no recycling of the molar excess of EtCarb used in is contemplated. Should this excess be recycled, the values of these sustainability parameters could be further improved in all cases.

Experimental section

Materials

The following materials were utilized throughout the present study: extra pure glycerol (assay grade 99.88%) from Fischer Chemical and ethylene carbonate (synthesis grade, purity > 99%), from Scharlau. Citric acid ACS reagent (purity ≥ 99.5%) by Sigma-Aldrich was employed as an internal standard in HPLC analysis. Ethylene glycol (99.8%, anhydrous) and glycerol carbonate (purity ≥ 99.5%), both from Sigma-Aldrich, were used for calibration purposes.

Preliminary studies of the immiscible liquid–liquid system by means of FBRM

A commercially available FBRM system (Lasentec FBRM M500LF) was used for this purpose, whose operating principle is based on scanning a highly focused laser beam at a fixed speed across a non-continuous phase in a fluid phase and measuring the time duration of the backscattered light. The product of the duration of the reflection from each droplet and the velocity of the scanning laser, which is known, determines the chord length. Multiple measurements are retrieved per unit time and are classified in intervals of size according to the length. A schematic outline of this device may be found elsewhere.[39]

Procedure for performing kinetic runs

To carry out runs to obtain kinetic data for the system in study, reaction conditions regarding agitation speed and temperature were set and controlled in the apparatus depicted in Fig. 5. This device consists of two vessels, each with their individual agitation and heating systems controlled by PID controllers. The presence of the two vessels was a measure to ensure a constant temperature during addition of reagents and reaction. Thus, reagents were heated to the desired temperature in different vessels rather than jointly so as to initiate the thermal reaction at the exact temperature of the experiment instead of having it started by the time the set temperature was reached. When both

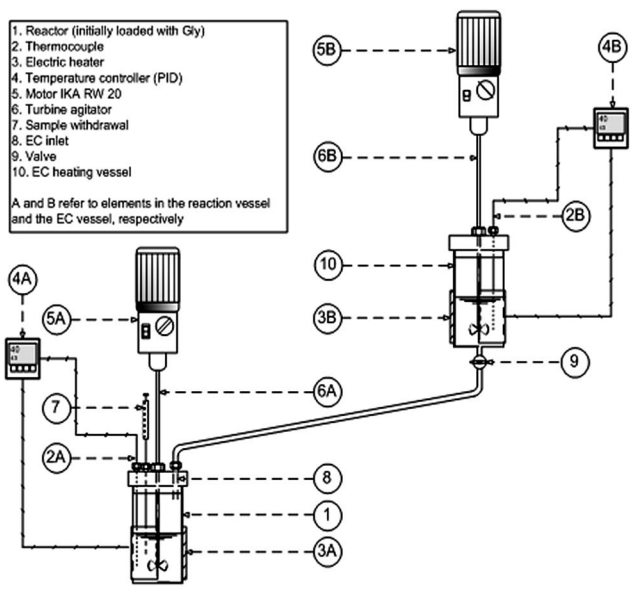

Fig. 5 Schematic representation of the device employed for the kinetic experiments.

reached the desired temperature, EtCarb was added to the vessel in which Gly was being heated in order to avoid any loss of reagent given its viscosity. Samples were acquired at several time values throughout experimentation.

Analytical methods

Samples were diluted in a 5 g L^{-1} citric acid (internal standard) solution for HPLC analysis in a JASCO 2000 series device, equipped with a refraction index detector. A constant flow rate of 0.5 mL min^{-1} of acid Milli-Q water (0.005 N H_2SO_4) was used as mobile phase. Separation was realized using a Rezex ROA-Organic Acid H^+ (8%) column (150 × 7.80 mm) at 60 °C.

Mathematical analysis

Comparison of models and the final selection of the most appropriate were made following physical and statistical criteria. The main physical criterion when fitting models to all experimental data was an adequate value for each activation energy. Statistical criteria include narrow error intervals for the model constants computed and reasonable values for information and goodness-of-fit criteria.

Fischer's F is based on a null hypothesis which accounts for the adequacy of the model to the observed values of the variable compared to given values of F at 95% confidence (or other). It is defined according to the following equation

$$F = \frac{\sum_{i=1}^{N} \frac{\left(y_{i,\mathrm{calc}}\right)^2}{P}}{\sum_{i=1}^{N} \frac{\mathrm{SQR}}{N-P}} \tag{7}$$

in which N is the total number of data, P is the number of parameters, SQR is the sum of quadratic residues, defined as $(y_{i,\mathrm{exp}} - y_{i,\mathrm{calc}})^2$, and $y_{i,\mathrm{exp}}$ and $y_{i,\mathrm{calc}}$ refer to the experimental and calculated values of the fitted variable, respectively. When defined as in eqn (7), this parameter reflects goodness-of-fit at the lowest number of predictors or constants of the model possible, being better when its value is high.

Furthermore, the Akaike's information criterion (AIC) has been regarded given that it has previously been applied as a standard of judgment for kinetic model discrimination.[53,54] This parameter relates the amount of experimental data available to the number of parameters of the model proposed and is defined following eqn (8), being the model better when the AIC value, always negative, is lower:[55]

$$\mathrm{AIC} = N \ln\left(\frac{\mathrm{SQR}}{N}\right) + 2P \tag{8}$$

In addition to the F and AIC, the residual mean squared error (RMSE) has been regarded as measure of the difference of the values of the variable being evaluated predicted by the model to those obtained experimentally considering, once again, the number of data available together with the parameters.[54] As this parameter is related to the sum of variances, the better the model fits to data, the lower the value of RMSE is:

$$\mathrm{RMSE} = \sqrt{\frac{\mathrm{SQR}}{N-P}} \tag{9}$$

Finally, if the variation between adjacent data is considered, the percentage of variation explained (VE) also gives information of the quality of fit for each measured variable, being best when all experimental trends are well explained by the tested model (a value near or equal to 100%). It is quantified using eqn (10):

$$\mathrm{VE}(\%) = 100 \times \left(1 - \frac{\sum_{j=1}^{J} \mathrm{SSQ}_l}{\sum_{j=1}^{J} \mathrm{SSQ}_{\mathrm{mean}l}}\right) \tag{10}$$

where SSQ_j and $\mathrm{SSQ}_{\mathrm{mean}j}$ are defined according to eqn (11) and (12), respectively:

$$\mathrm{SSQ}_j = \sum_{i=1}^{N} \frac{\left(y_{i,\mathrm{exp}} - y_{i,\mathrm{calc}}\right)^2}{{y_{i,\mathrm{calc}}}^{\zeta_j}} \tag{11}$$

$$\mathrm{SSQ}_{\mathrm{mean}j} = \sum_{i=1}^{N} \frac{\left(y_{i,\mathrm{exp}} - \overline{y}_{i,\mathrm{exp}}\right)^2}{{y_{i,\mathrm{calc}}}^{\zeta_l}} \tag{12}$$

and

$$\overline{y}_{i,\mathrm{exp}} = \frac{\sum_{i=1}^{N} \frac{y_{i,\mathrm{exp}}}{{y_{i,\mathrm{calc}}}^{\zeta_j/2}}}{\sum_{i=1}^{N} \frac{1}{{y_{i,\mathrm{calc}}}^{\zeta_j/2}}} \tag{13}$$

In eqn (11) through (13), ζ_l is the heteroscedasticity parameter, which is a measure of the type of error in the measured variable. When the value of this parameter is not fixed, as such was the case, Aspen Custom Modeler considers $\zeta_l = 1$ by default.

Definitions

Conversion (X): The explanation of the results obtained was based on the conversion X defined as follows rather than the concentrations of the components given that only one key component is necessary when the reacting system considered consists of one reaction. This variable can be defined given that all the reactants and products of the transesterification reaction can be quantified by the analytical method presented above. Subsequently, the conversion is defined as the ratio of the average of the extents of reaction of the reactants and products related to the initial concentration of Gly, which is always the limiting reactant.

$$X(\%) = \frac{\sum_{i=1}^{n} \frac{C_i - C_{i0}}{\nu_i}}{\frac{n}{C_{\mathrm{Gly0}}}} \times 100 \tag{14}$$

in which C_i, C_{i0} denote the concentration of each component at a definite time and initially, C_{Gly0} is the initial concentration of

Gly, ν_i refers to the stoichiometric coefficient and n is the total number of components.

Green metrics parameters

The following definitions adapted from Constable *et al.* (2002)[34] were followed as a means to measure the degree of sustainability of the process under study as well as those found in literature.

The atom economy (AE) is defined as the ratio of the summation of the molecular weights of the desired products to that of the reagents utilized.

$$\mathrm{AE}(\%) = \frac{\sum \mathrm{MW}_{\mathrm{products}}}{\sum \mathrm{MW}_{\mathrm{reagents}}} \times 100 \quad (15)$$

The *E*-factor computes the mass of waste generate per unit mass of the products.

$$E\text{-factor}(\%) = \frac{M_{\mathrm{waste}}}{M_{\mathrm{product}}} \times 100 \quad (16)$$

The carbon efficiency (CE) regards the amount of carbon that transits from the reactants to the desired end products.

$$\mathrm{CE}(\%) = \frac{\sum C_{\mathrm{products}}}{\sum C_{\mathrm{reagents}}} \times 100 \quad (17)$$

The mass productivity (MP) accounts for the mass of the actual product in relation to the total mass of material utilized in the process.

$$\mathrm{MP}(\%) = \frac{M_{\mathrm{product}}}{M_{\mathrm{process}}} \times 100 \quad (18)$$

Finally, the reaction mass efficiency (RME) considers the total actual mass of the products to the mass of reagents used.

$$\mathrm{RME}(\%) = \frac{\sum M_{\mathrm{product}}}{\sum M_{\mathrm{reagents}}} \times 100 \quad (19)$$

Conclusions

Simultaneous synthesis of glycerol carbonate and ethylene glycol was found to take place in the absence of any catalyst at temperatures higher than 80 °C, though significant reactivity exists only at 100 °C or higher temperature. This process can be envisaged as a glycerol transcarbonation with an organic carbonate or as an ethylene carbonate glycerolysis.

It was observed by means of a FBRM probe that the system constituted a dispersion-like liquid–liquid biphasic system from 25 °C to 80 °C, decreasing the droplet size and number as temperature increased, till it was monophasic.

A thermodynamic study determined that the reaction was almost irreversible at 100 °C or higher temperature. A kinetic study served to determine by statistical means that an overall second order potential model, accounting only for the direct reaction, represents adequately the transesterification of ethylene carbonate and glycerol in these conditions.

Finally, a comparative study with other references found in literature regarding the sustainability of the process was conducted; proving that the thermal process herein studied could play an attractive role when taking into account the sustainability of the process, according to common green metric parameters.

Nomenclature

Components

EtCarb	Ethylene carbonate
MEG	Ethylene glycol
GlyCarb	Glycerol carbonate
Gly	Glycerol

Nomenclature

AE	Atom economy (eqn (15))
AIC	Akaike's information criterion
C	Concentration of the components at a given time (mol L^{-1})
CE	Carbon efficiency (eqn (17))
C_p	Specific heat capacity (J mol^{-1} K^{-1})
E_{aj}/R	Ratio of activation energy and the ideal gas constant (K)
F	Fischer's F statistical parameter at 95% confidence
FBRM	Focused beam reflectance measurement
H	Enthalpy (kJ mol^{-1})
HPLC	High-performance liquid chromatography
K	Thermodynamic constant of equilibrium
$k_{1\ldots5}$	Kinetic constants for the tested models
k_{j0}	Preexponential factor of the kinetic constant
l	Referenced individual variable in eqn (11)–(13).
M	Initial molar ratio of dimethyl carbonate to glycerol
MP	Mass productivity (eqn (17))
N	Total number of components
N	Total number of data to which a model is fitted
P	Number of parameters of a proposed model
r	Reaction rate (mol L^{-1} min^{-1})
R	Ideal gas constant (J mol^{-1} K^{-1})
RME	Reaction mass efficiency
RMSE	Residual mean squared error
S	Entropy (J mol^{-1} K^{-1})
SQR	Sum of quadratic residues
SS	Stirring speed (rpm)
T	Temperature (K)
VE	Variation explained (%)
x	Molar fraction
X	Conversion, as defined by eqn (14)

Greek letters

γ	Activity coefficient
δ	Variation
ζ	Heteroscedasticity parameter
ν	Stoichiometric coefficient of the component i
ω	Agitation rate (rpm)

Subscripts

0	Relative to the start of the reaction, time equals zero
cat	Relative to the catalyst
f	Relative to formation (enthalpy)
i	Relative to component i
j	Relative to reaction j ($j = 1$, direct reaction; $j = 2$, reverse reaction)
r	Relative to reaction (enthalpy and entropy)

Superscripts

0	Relative to standard conditions

Acknowledgements

The authors would like to express their gratitude to the Ministerio de Ciencia e Innovación of the Government of Spain for financial support of the project CTQ 2010-15460.

References

1 M. Pagliaro and M. Rossi, *The future of glycerol. New uses for a versatile new material*, RSC Publishing, Cambridge, 2008.
2 A. Behr, J. Eilting, K. Irawadi, J. Leschinski and F. Lindner, *Green Chem.*, 2008, **10**, 13–30.
3 M. O. Sonnati, S. Amigoni, E. P. T. de Givenchy, T. Darmanin, O. Choulet and F. Guittard, *Green Chem.*, 2013, **15**, 283–306.
4 H. Hensen, T. Loehl, H. Tesmann and J. Kahre, Patent DE19756454, 1999.
5 C.-H. Chen, Y. E. Hyung, D. R. Vissers and K. Amine, US20030157413 A1, 2002.
6 P. Lameiras, L. Boudesocque, Z. Mouloungui, J.-H. Renault, J.-M. Wieruszeski, G. Lippens and J.-M. Nuzillard, *J. Magn. Reson.*, 2011, **212**, 161–168.
7 M. Benoit, Y. Brissonnet, E. Guélou, K. De Oliveira Vigier, J. Barrault and F. Jérôme, *ChemSusChem*, 2010, **3**, 1304–1309.
8 A. S. Kovvali and K. K. Sirkar, *Ind. Eng. Chem. Res.*, 2002, **41**, 2287–2295.
9 C. Magniont, G. Escadeillas, C. Oms-Multon and P. De Caro, *Cem. Concr. Res.*, 2010, **40**, 1072–1080.
10 D. V. Palaskar, P. S. Sane and P. P. Wadgaonkar, *React. Funct. Polym.*, 2010, **70**, 931–937.
11 G. Rokicki, P. Rakoczy, P. Parzuchowski and M. Sobiecki, *Green Chem.*, 2005, **7**, 529–539.
12 Z. Mouloungui and S. Pelet, *Eur. J. Lipid Sci. Technol.*, 2001, **103**, 216–222.
13 D. Herault, A. Eggers, A. Strube and J. Reinhardt, Patent DE10110855-A1, 2003.
14 J. W. Yoo and Z. Mouloungui, *Nanotechnology in Mesostructured Materials*, 2003, vol. 146, pp. 757–760.
15 A. Dibenedetto, A. Angelini, M. Aresta, J. Ethiraj, C. Fragale and F. Nocito, *Tetrahedron*, 2011, **67**, 1308–1313.
16 V. Calvino-Casilda, G. Mul, J. F. Fernandez, F. Rubio-Marcos and M. A. Banares, *Appl. Catal., A*, 2011, **409**, 106–112.
17 F. Rubio-Marcos, V. Calvino-Casilda, M. A. Banares and J. F. Fernandez, *J. Catal.*, 2010, **275**, 288–293.
18 M. Aresta, A. Dibenedetto, F. Nocito and C. Ferragina, *J. Catal.*, 2009, **268**, 106–114.
19 M. J. Climent, A. Corma, P. De Frutos, S. Iborra, M. Noy, A. Velty and P. Concepción, *J. Catal.*, 2010, **269**, 140–149.
20 M. Aresta, A. Dibenedetto, F. Nocito and C. Pastore, *J. Mol. Catal. A: Chem.*, 2006, **257**, 149–153.
21 J. George, Y. Patel, S. M. Pillai and P. Munshi, *J. Mol. Catal. A: Chem.*, 2009, **304**, 1–7.
22 C. Vieville, J. W. Yoo, S. Pelet and Z. Mouloungui, *Catal. Lett.*, 1998, **56**, 245–247.
23 J. Hu, J. Li, Y. Gu, Z. Guan, W. Mo, Y. Ni, T. Li and G. Li, *Appl. Catal., A*, 2010, **386**, 188–193.
24 J. B. Bell, L. Silver and V. A. Currier, Patent US2915529, 1959.
25 J. Li and T. Wang, *React. Kinet., Mech. Catal.*, 2011, **102**, 113–126.
26 J. R. Ochoa-Gomez, O. Gomez-Jimenez-Aberasturi, B. Maestro-Madurga, A. Pesquera-Rodriguez, C. Ramirez-Lopez, L. Lorenzo-Ibarreta, J. Torrecilla-Soria and M. C. Villaran-Velasco, *Appl. Catal., A*, 2009, **366**, 315–324.
27 A. Takagaki, K. Iwatani, S. Nishimura and K. Ebitani, *Green Chem.*, 2010, **12**, 578–581.
28 M. G. Alvarez, A. M. Segarra, S. Contreras, J. E. Sueiras, F. Medina and F. Figueras, *Chem. Eng. J.*, 2010, **161**, 340–345.
29 Y. Patel, J. George, S. M. Pillai and P. Munshi, *Green Chem.*, 2009, **11**, 1056–1060.
30 M. G. Álvarez, A. M. Frey, J. H. Bitter, A. M. Segarra, K. P. de Jong and F. Medina, *Appl. Catal., B*, 2013, **134–135**, 231–237.
31 M. G. Álvarez, M. Plíšková, A. M. Segarra, F. Medina and F. Figueras, *Appl. Catal., B*, 2012, **113–114**, 212–220.
32 Z. Mouloungui, J. Yoo, C. Gachen, A. Gaset, G. Vermeersch and J. W. Yoo, FR2733232-A, EP739888-A, EP739888-A1, FR2733232-A1, 2000.
33 H.-J. Cho, H.-M. Kwon, J. Tharun and D.-W. Park, *J. Ind. Eng. Chem.*, 2010, **16**, 679–683.
34 D. J. C. Constable, A. D. Curzons and V. L. Cunningham, *Green Chem.*, 2002, **4**, 521–527.
35 J. W. van Hal, J. S. Ledford and X. Zhang, *Catal. Today*, 2007, **123**, 310–315.
36 K. M. C. C. Kawabe, EP 1125915 A1, 2005.
37 K. M. C. C. Kawabe, US 09/271,435, 2000.
38 A. R. Heath, P. A. Bahri, P. D. Fawell and J. B. Farrow, *AIChE J.*, 2006, **52**, 1987–1994.

39 A. Blanco, E. Fuente, C. Negro and J. Tijero, *Can. J. Chem. Eng.*, 2002, **80**, 734–740.
40 J. A. Boxall, C. A. Koh, E. D. Sloan, A. K. Sum and D. T. Wu, *Ind. Eng. Chem. Res.*, 2009, **49**, 1412–1418.
41 W. Wang, J. Liu, P. Wang, J. Duan and J. Gong, *Chem. Eng. Sci.*, 2013, **91**, 173–179.
42 J. Li and T. Wang, *J. Chem. Thermodyn.*, 2011, **43**, 731–736.
43 J. Dean, *Lange's Handbook of Chemistry*, New York, 1999.
44 S. P. Verevkin, V. N. Emel'yanenko, A. V. Toktonov, Y. Chernyak, B. Schaeffner and A. Boerner, *J. Chem. Thermodyn.*, 2008, **40**, 1428–1432.
45 S. P. Verevkin, A. V. Toktonov, Y. Chernyak, B. Schaeffner and A. Boerner, *Fluid Phase Equilib.*, 2008, **268**, 1–6.
46 I. Vasilev and A. Korkhov, *Transactions on Chemistry and Chemical Technology*, 1974, **36**, 103–105.
47 N. N. Ezhova, I. G. Korosteleva, N. V. Kolesnichenko, A. E. Kuz'min, S. N. Khadzhiev, M. A. Vasil'eva and Z. D. Voronina, *Pet. Chem.*, 2012, **52**, 91–96.
48 B. Poling, J. Prausnitz and J. O'Connell, *The properties of gases and liquids*, New York, 2001.
49 V. Ruzicka and E. S. Domalski, *J. Phys. Chem. Ref. Data*, 1993, **22**, 619–657.
50 T. Keller, J. Holtbruegge, A. Niesbach and A. Górak, *Ind. Eng. Chem. Res.*, 2011, **50**, 11073–11086.
51 R. Alenezi, G. A. Leeke, J. M. Winterbottom, R. C. D. Santos and A. R. Khan, *Energy Convers. Manage.*, 2010, **51**, 1055–1059.
52 A. T. Williamson and C. N. Hinshelwood, *Trans. Faraday Soc.*, 1934, **30**, 1145–1148.
53 J. J. Knol, J. P. H. Linssen and M. A. J. S. van Boekel, *Food Chem.*, 2010, **120**, 1047–1057.
54 M. Ladero, M. de Gracia, J. J. Tamayo, I. L. d. Ahumada, F. Trujillo and F. Garcia-Ochoa, *Chem. Eng. J.*, 2011, **169**, 319–328.
55 H. Akaike, *IEEE Trans. Autom. Control*, 1974, **19**, 716–723.

Electronic supplementary information

Appendix 1: Kirchoff's laws applied to the glycerol-ethylene carbonate system

The equilibrium constant can be related to the Gibbs enthalpy of reaction with the following relationship:

$$\ln K = -\frac{\Delta G_r^0}{R \cdot T} \quad (1)$$

in which R is the ideal gas constant, T is the temperature, and ΔG^0_r is the standard Gibbs free energy, which can further be defined by Equation 2:

$$\Delta G_r^0 = \Delta H_r^0 - T \cdot \Delta S_r^0 \quad (2)$$

where ΔH^0_r and ΔS^0_r are the enthalpy and entropy of reaction, respectively. Both can be defined taking into account the stoichiometric coefficients νi of the reaction (positive for reaction products and negative for reactants), the enthalpies of formation ($\Delta H^0_{f,i}$) and entropies (S^0_i) along with the contribution to the enthalpy and entropy from the standard temperature (298 K) to the temperature considered in each case, for which the specific heat capacity as a function of temperature, $C_p(T)$, must be considered:

$$\Delta H_r^0 = \sum_i \upsilon_i \cdot \Delta H_{f,i}^0 + \sum_i \nu_i \cdot \int_{298}^{T} C_{p,i}(T)\,dT \quad (3)$$

$$\Delta S_r^0 = \sum_i \upsilon_i \cdot S_i^0 + \sum_i \nu_i \cdot \int_{298}^{T} \frac{C_{p,i}(T)}{T}\,dT \quad (4)$$

Tables A1.1, A1.2 and A1.3 summarize the calculations and bibliographic information related to the thermodynamic study presented in equations 1 through 4. Specifically, Table 3 compiles the equilibrium constants calculated at the temperatures at which the reactions were performed, and their values were high enough to consider that the reaction is shifted towards the products (with observed experimental equilibrium conversions virtually reaching completion in all cases).

Table A1.1 Enthalpies of formation and entropies of the components taking part in the transesterification of EtCarb and Gly.

Component	ΔH_0^f (kJ·mol^{-1})	Reference	Observations	S_0 (J·mol^{-1}·K^{-1})	Reference	Observations
Gly	-668.52	43		206.30	43	
EtCarb	-573.50[a]	44 and 45	$\Delta H^0_{f,g}$=-510.7 kJ·mol^{-1} λ_v=62.8 kJ·mol^{-1}	107.60[b]	46	S^0_g=132.54 J·mol^{-1}·K^{-1} T_{eb}= 533.8 K
GlyCarb	-784.90[a]	44 and 45	$\Delta H^0_{f,g}$=-699 kJ·mol^{-1} λ_v=85.9 kJ·mol^{-1}	230.11[b]	47	S^0_g=386.20 J·mol^{-1}·K^{-1} T_{eb}= 550.3 K
MEG	-455.30	43		163.20	43	

[a] The standard enthalpy of formation in liquid state was calculated as the difference between the standard molar enthalpy of formation in gas phase and the standard latent heat of vaporization: $\Delta H^0_{f,l} = \Delta H^0_{f,g} - \lambda^0_v$.
[b] The standard entropy in liquid state was calculated as the difference between the standard molar entropy in gas phase and the ratio between the latent heat and temperature: $S^0_l = S^0_g - \lambda^0_v/T$.

Table A1.2 Specific heat capacity correlations and parameters as a function of temperature found in literature for the components involved in the transesterification of EtCarb and Gly

Component	Equation and parameters				Reference
	$C_p\left(J \cdot mol^{-1} \cdot K^{-1}\right) = R\left[A + B\frac{T}{100} + C\left(\frac{T}{100}\right)^2\right]$				
	A	B	C		
Gly	5.1401	1.4964	0.1523		47
EtCarb	-34.3637	0.1359	0		48
	$C_p(J \cdot mol^{-1} \cdot K^{-1}) = a + b \cdot T + c \cdot T^{-2} + d \cdot T^3$				
	a	b	c·10^3		
GlyCarb	-108.9200	-1.7968	4.4743		49
MEG	75.8780	0.6418	-1.6493	1.6940	49

Table A1.3 Enthalpy, entropy standard Gibbs free energy of reaction and chemical equilibrium constant of the transesterification of EtCarb and Gly at the temperatures tested in this work

Temperature (ºC)	ΔH^0_r (kJ·mol^{-1})	ΔS^0_r (J·mol^{-1}·K^{-1})	ΔG^0_r (kJ·mol^{-1})	K
100	108.26	2186.66	-707.37	14.42
110	106.53	2487.25	-846.08	20.78
120	104.91	2790.85	-991.89	30.04
130	103.41	3097.22	-1144.77	43.55
140	102.04	3406.11	-1304.69	63.29

Appendix 2: Activity coefficients calculated by means of COSMO-RS

COSMO-RS (COnductor like Screening Model for Real Solvents) is a quantum-chemical computer-based method developed by Klamt and co-workers to predict the thermodynamic equilibrium properties of fluids and liquid mixtures [A2.1]. This methodology processes the screening charge densities on the surface of molecules from quantum chemical calculations, and subsequently introduces a statistical thermodynamic procedure for the molecular surface interactions to estimate the chemical potentials of the species in solution, which are the basis for the calculation of the thermodynamic equilibrium properties [A2.2]. A feature of this prediction method is that only structural information of the compounds is required to perform the thermodynamic estimations. Thus far, different publications have supported the general suitability of COSMO-RS to estimate the thermodynamic properties of a broad variety of systems, including the activity coefficients of fluid mixtures [A2.3]

The activity coefficients were computed at 100, 110, 120, 130 and 140 ºC and different composition of the mixtures within the range of variation of the composition interval given the initial molar ratios of ethylene carbonate to glycerol,. Table A2.1 compiles the average values obtained from computing these activity coefficients.

Table A2.1 Average activity coefficients for each component at the temperatures experimentally tested obtained from calculations by COSMO-RS

Temperature	Molar ratio of EtCarb to Gly =2				Molar ratio of EtCarb to Gly =3			
(ºC)	γ_{Gly}	γ_{EC}	γ_{GC}	γ_{MEG}	γ_{Gly}	γ_{EC}	γ_{GC}	γ_{MEG}
100	1.464	1.201	0.887	1.317	1.767	1.122	0.865	1.488
110	1.425	1.179	0.898	1.286	1.692	1.108	0.878	1.437
120	1.388	1.160	0.908	1.257	1.624	1.096	0.890	1.391
130	1.354	1.142	0.917	1.231	1.561	1.085	0.900	1.350
140	1.322	1.126	0.924	1.207	1.504	1.075	0.908	1.312

References

A2.1 A. Klamt, in *COSMO-RS: From quantum chemistry to fluid phase thermodynamics and drug design*, Elsevier Science Ltd., Amsterdam, 2005.

A2.2 A. Klamt, F. Eckert, A. Wolfgang. *Annual Review of Chemical and Biomolecular Engineering.* 2010, **1**, 101-122

A2.3 M. Gonzalez-Miquel, J. Palomar, F. Rodriguez. *The Journal of Physical Chemistry B.* 2013, **117**, 296-306

Publicación 5 / Publication 5

Autores/Authors: Jesús Esteban, Miguel Ladero, Elena Fuente, Ángeles Blanco and Félix García-Ochoa

Título/Title: Kinetic modeling of the catalytic coproduction of glycerol carbonate and ethylene glycol from glycerol

Estado actual/Current status: Manuscript submitted to Journal of Chemical Technology and Biotechnology as of November 2014

Índice de impacto / Impact factor 2013: 2.494

Resumen

Se estudia la producción de carbonato de glicerina y etilenglicol por reacción de glicerina con carbonato de etileno con K_2CO_3, que no había sido empleado aún para esta reacción. La ventaja de este proceso es que permite trabajar a temperaturas y cantidades de catalizador inferiores a la reacción entre carbonato de dimetilo y glicerina.

En primer lugar, se verifica por medio del análisis de las muestras de reacción el mecanismo propuesto en la literatura para esta reacción. Así mismo, debido a la presencia insignificante de un compuesto intermedio y otro producto ulterior de reacción, junto al alto grado de cumplimiento de los balances de materia (error inferior al 4 %), se puede considerar una reacción simple.

Dada la naturaleza bifásica de los reactivos, se analizó con FBRM el efecto de la agitación sobre la distribución del tamaño de cuerda de la dispersión del sistema inerte. Se determinó que a velocidades de agitación superiores a 800 rpm, la distribución no cambia. Además, se realizó también la reacción química, apreciándose que, efectivamente, a agitaciones mayores a dicho valor, la velocidad del proceso no cambia, por lo que se puede considerar que la transferencia de materia no controla el proceso en estas condiciones. Para completar el análisis con FBRM, observó la evolución física del sistema en reacción, junto a la evolución química de los compuestos, y se observa que el número de cuerdas se anula a una conversión de 0.34, que corresponde a una composición casi coincidente con el límite del equilibrio líquido-líquido del sistema.

Se realizaron experimentos variando la temperatura (40-50 ºC), el exceso molar de EC a glicerina (2-3) y la concentración de catalizador (125-500 ppm). Con los datos obtenidos, se evaluó el valor de la conversión al que la cinética varía (conversión crítica). Dicho valor depende de la temperatura y la cantidad de catalizador empleada, si bien las composiciones a las que corresponden son cercanas a 0.34. Se propusieron varios modelos cinéticos para la reacción, siendo el más adecuado uno de dos etapas, antes y después de la conversión crítica. En la primera, se da primer orden parcial respecto a la concentración de glicerina y orden cero respecto a la de EC; en la segunda, hay reacción inversa y primer orden respecto a todos los compuestos. Además, hay desactivación del catalizador. Los valores de las energías de activación fueron de 91.7 ± 2.7 $kJ \cdot mol^{-1}$ y 93.9 ± 15.9 $kJ \cdot mol^{-1}$ para la reacción directa e inversa, respectivamente, y la constante de desactivación de 0.36 ± 0.06 s^{-1}.

Kinetic modeling of the catalytic coproduction of glycerol carbonate and ethylene glycol from glycerol

Jesús Esteban, Miguel Ladero*, Elena Fuente, Ángeles Blanco, Félix García-Ochoa
Department of Chemical Engineering. College of Chemical Sciences. Complutense University of Madrid. 28040. Madrid. Spain.
*Corresponding author: mladero@quim.ucm.es. (Phone: +34-913944164/fax: +34-913944179)

Abstract

BACKGROUND: This work approaches the valorization of glycerol with ethylene carbonate to yield glycerol carbonate and ethylene glycol simultaneously. In comparison to other processes to obtain glycerol carbonate, this method allows for the utilization of milder operating conditions. Due to the limited miscibility of the reactant species before products generate, a study of the evolution of the phases is made using focused beam reflectance measurements (FBRM). With the information provided, kinetic modeling is undertaken.

RESULTS: A stirring speed of 800 rpm was found to be sufficient for mass transfer not to be a rate-controlling step. A change from biphasic into a single phase liquid system took place at an approximate conversion of glycerol of 0.34. Completion of kinetic runs varying temperature, molar ratio of reactants and catalyst concentration supplied enough data to propose a kinetic model.

CONCLUSION: The models proposed consisted of two differentiated stages with equations applicable before and after a critical value of the conversion of glycerol after the observation of the FBRM results. The model with the best correlation considered the reverse reaction from the products and deactivation of the catalyst, being the activation energies of the direct and reverse reactions 91.7 ± 2.7 kJ·mol^{-1} and 93.9 ± 15.9 kJ·mol^{-1}, respectively, and the deactivation constant had a value of 0.36 ± 0.06 s^{-1}.

Keywords: glycerol carbonate, ethylene glycol, kinetic model, solventless synthesis, FBRM

INTRODUCTION

The philosophy of Green Chemistry is based on a series of pillars aimed at acting on the source to prevent pollution and misuse of resources. Among these principles can be mentioned the emphasis on waste prevention, maximization of atom economy, use of safer solvents if any, employing catalysts and utilizing renewable feedstock. [1]

Policies aimed at increasing gradually the share of use of energy based on renewable sources have been promoted especially in the European Union, especially since the early years of the present century. Subsequently, a boom of the biodiesel industry has taken place, which has had an oversaturation of the glycerol (Gly) market and a price drop as a consequence. [2] After awareness of this situation, multiple efforts to research on the possibilities of this by-product of biodiesel have been undertaken as a combined manner of attempting to improve the economics of the process as well as approaching the principle of Green Chemistry of preventing waste generation. The chemical features of glycerol have made it subject to very diverse transformations to obtain many interesting products; up to this point, a significant number of thorough reviews on very assorted synthetic routes have been published. [3-6]

Many examples of valuable products have been obtained from reactions involving glycerol as a raw material. [7, 8] A product that has received increasing attention is 4-(hydroxymethyl)-1,3-dioxolan-2-one, commonly known as glycerol carbonate (GC), to the point that it has been subject of three recent reviews. [9-11] It has proven a valuable product with positive features towards its application as a solvent for mixture analysis by nuclear magnetic resonance [12], cosolvent with ionic liquids for dehydration reactions [13], a potential additive in Li and Li-ion batteries [14], curing agent for pozzolanic matrices [15], a gas separation membrane component [16]. More recently, the use of acidified GC and mixtures consisting of GC and glycerol have been applied as green solvents in the pretreatment of sugarcane bagasse aiming at the saccharification of lignocellulosic biomass to yield fermentable sugars.[17] The latter application demonstrates the importance of this product from a Green Chemistry standpoint, for it can be produced from renewable resources and it can also play a role in the production of other products from renewable resources.

Originally, the synthesis of this organic carbonate implied the utilization of phosgene, in a process that dates as far back as the 19th century and has therefore been substituted [18]. Much more recently, the glycerolysis of urea has been proposed as a route to obtain GC under vacuum conditions and temperature around 150 ºC. Metallic oxides and sulphates have been employed as catalysts for this reaction pathway. [19-22]. A different approach to the synthesis has been followed using this reaction as a means to fix CO_2 directly; nevertheless, application of pressures well above 1 atm (3.5 – 10 MPa) together with temperatures ranging from 80 to 180 ºC have been reported catalysts [23-26].

Nonetheless, the development of reaction pathways using organic carbonates has been receiving a great deal of attention for over a decade since they present the advantage of being an indirect manner of CO_2 fixation. The transesterification of glycerol with these reactants has been achieved using milder conditions than those reported for the aforementioned procedures. Operation with dimethyl carbonate (DMC) at atmospheric pressure from 60 to 75ºC has been described with quantitative yield to product. [27-31] Likewise, synthesis with diethyl carbonate has been performed with positive results, though the reaction conditions were somewhat more severe: while operation at atmospheric pressure was still conducted, large molar excesses of diethyl carbonate to Gly have been used (17:1 to 21:1) and use of temperatures of 130 ºC have been described using different types of hydrotalcites as catalysts.[32, 33] On the other hand, alternative reactant ethylene carbonate (EC) has been put to use in this reaction with remarkably less demanding conditions, with temperatures of 50 to 80 ºC being employed with molar excess of EC to Gly of 2 to 1 The latter reaction has been catalysed by Mg/Al hydrotalcites and MCM41 based materials [22, 34].

The reaction mechanism of this type of reaction has been covered in detail [28, 32], being the key aspect the presence of a basic catalyst to initiate the reaction through a glyceroxide anion. Furthermore, the selectivity of the reaction with several different catalysts has been reported to be almost complete despite the mechanism implying the presence of an intermediate species, which is in turn highly unstable allowing for its immediate cyclation to the final product GC. [28, 29, 32]

The aim of this work is the study of the transesterification of EC with Gly, which presents the additional advantage of producing monoethylene glycol (EG) as a by-product, broadly used in the formulation of antifreeze or dye inks. EG stems from the hydrolysis of ethylene oxide (EO), giving EG and oligoglycols. Currently, the best

industrial approach towards its synthesis appears to Shell's OMEGA process, in which EO is carbonated and subsequently hydrated to yield 99.5% MEG, a further effort to reach the most valuable product and the maximum achievable exploitation of feedstock[35-38]. In addition, in terms of biodegradability of the components that this route involves, EG has been labeled as "readily biodegradable" (World Health Organization (http://www.who.int/ipcs/publications/cicad/en/cicad22.pdf)) and EC has been said to have a biodegrade up to 80.8% after 9 days (OECD 301B analysis) (Environmental Protection Agency (http://epa.gov/hpv/pubs/summaries/ethlcarb/c15859.pdf)). In contrast, in the most followed route in literature, DMC biodegrades 90% after as many as 28 days [39] and the by-product methanol only 50% after 18 days.[40]

Our approach to this reaction is to use inexpensive potassium carbonate as the base catalyst. Considering the lack of information on the kinetics of the catalytic synthesis of GC through this route available in the literature, the objective of the present work is to obtain a kinetic model as a necessary stage towards process development and reactor design. An assessment of whether a relationship with the evolution of the emulsion-like system exists is in this work undertaken, with confirmation of this hypothesis being made following physicochemical as well as statistical criteria.

MATERIALS AND METHODS

Materials

During the course of the experimental work, the next chemicals were utilized: extra pure glycerol (assay grade, 99.88 %, Fischer Chemical) and ethylene carbonate (synthesis grade, purity>99%, Scharlau) as the reactant species; potassium carbonate (purity>99%, Alfa Aesar) as a catalyst; finally, ethylene glycol (99.8%, anhydrous, Sigma-Aldrich), glycerol carbonate (purity≥99.5%, Sigma-Aldrich) and citric acid ACS reagent (purity ≥99.5%, Sigma-Aldrich) for calibration and as internal standard for HPLC anlaysis purposes.

Experimental device

A scheme of the apparatus with all the main components labelled is displayed in Figure 1. The main piece is a bespoke stainless steel tank reactor (1) featuring deflector baffles wherein the reaction takes place (2). This vessel is provided with a heating resistor surrounding the outer diameter (3) connected to an OMRON E5CN PID

temperature controller (4). The reacting mixture is stirred by a six-blade impeller (6) regulated by an IKA RW20 motor (200-2000 rpm) (7). An opening (8) on the bottom of the vessel was made to allow for the introduction of the FBRM probe (9) and avoidance on any interference on the online droplet size distribution measurements. Additionally, a series of ports are located on the upper part of the reactor for insertion of a thermocouple (5) and for introduction of the reactants and catalyst as well as for sample withdrawal (10).

Droplet size distribution experiments

Throughout this work, a Lasentec FBRM M500LF (Mettler Toledo, Seattle, USA) equipment was employed to assess the droplet size distribution of the dispersed liquid glycerol within the continuous phase EC. This system has already been employed for the determination of particle or droplet size distributions in the study of flocculation processes [41, 42] or liquid-liquid dispersions of similar nature to the one herein studied. [40, 41 31]

FBRM is an optical technique based upon the use of light back scattering effects that allows for the online retrieval of chord size distributions of a phase dispersed in another. The probe possesses a sensor with a laser beam generator at a wavelength of 791 nm coupled with a computer controlled detector that allows for the retrieval of real time measurements. The rotating lens in the sensor focuses the laser beam on a focal point, which revolves in circles of 8 mm of diameter within the dispersion at a speed of 1.9 m/s. As the beam hits the surface of a droplet that flows through the focal point, it is reflected and reaches the detector causing a pulse of light, which is in turn translated into an electric signal. The chord length of the droplet is calculated as the product of the duration of the pulse by the lineal velocity of the focal point. A chord length distribution can be determined, from which changes in the nature of the poliphasic system can be observed. This laser technique can detect droplets, bubbles or particles down to a threshold of 1 μm. A detailed scheme of this apparatus is shown elsewhere.[41, 42]

Methods

Study of the influence of temperature and stirring speed on the emulsion

The reactants glycerol and EC have very limited miscibility, giving rise to a dispersion at the temperatures above the melting point (36 ºC); however, as the reaction

proceeds and products appear, the *ab initio* liquid-liquid biphasic system transforms into a single phase liquid. [43]

The effect of agitation speed was evaluated under non reactive conditions, i.e., in the absence of catalyst. For this purpose, the droplet size distribution of glycerol was tracked varying the stirring at several values. Likewise, the behaviour of the chord length distribution was assessed with temperature at a fixed agitation rate taking into consideration that the system must be kept at a minimum temperature of 40 ºC to avoid solidification of EC, which was found to take place at 35-37 ºC.

Kinetic studies

With the optimal stirring conditions, kinetic runs were completed varying temperature, initial molar ratio of EC to Gly (*M*) and catalyst concentration. Table 1 compiles the experimental program.

The procedure consisted in loading the reactor initially with Gly and allowing to heat to a minimum temperature of 40ºC, slightly above the melting point of EC. Then, EC in liquid state (kept in an oven for such purpose) can be added while keeping the total load under continuous agitation. Once the whole batch reaches the set temperature, potassium carbonate is added to start the reaction. Throughout the course of the reaction, samples are withdrawn for analysis of the chemicals by HPLC.

Methods of analysis

Analysis of samples was made by a JASCO 2000 series HPLC device equipped with a refraction index detector, which presents the advantage of being a universal detector. Quantification of the species involved in the reaction was made employing a constant flow rate of 0.5 mL/min of Milli-Q water (acidified with a solution of 0.005 N H_2SO_4) as eluent flowing through a Phenomenex Rezex ROA-Organic Acid H+ (8%) column (150x7.80 mm) at 60 ºC. Samples directly taken from the reaction medium were prepared by diluting 50-fold in a solution of 5 g/L of citric acid.

Presence of potassium was tested with a Quantofix® potassium test (Macherey-Nagel). While the system still consisted of a biphasic liquid-liquid emulsion (i.e., at short times of reaction), settling of the phases was aided by a Thermo Scientific Heraeus Pico 17 for 1 minute. Then, the light (Gly-rich) and the heavy phases (EC-rich) were analysed separately dipping a test stick. Last, pH value was measured utilizing a Eutech Instruments series 700 pH-meter.

Numerical methods

Aspen Custom Modeler (ACM) was the software used for kinetic model correlation. Fitting of the proposed models is based upon the application of the Levenberg-Marquardt algorithm together with its numerical integration by means of a fourth-order Runge-Kutta method. The methodology followed was to correlate the models at a fixed temperature in the first place, the purpose being to obtain an initial guess of the activation energy and preexponential factor from the values of the kinetic constants retrieved thereof. These estimates are used as initial values for multivariable fitting of the entire set of experimental data at all temperatures.

Suggestion of plausible kinetic models was made on the basis of acquired physicochemical knowledge of similar systems, whereas appropriate discrimination among kinetic models was judged on statistical criteria. Fischer's F value (*F*), variation explained (*VE*), residual mean squared error (*RMSE*) and the Akaike Information Criterion (*AIC*) were used as the key statistical indicators for good correlation of the models [44].

F is based on a null hypothesis that supports the adequacy of the goodness of the correlation of the model to the experimental values of the measured variable. It is defined as follows

$$F = \frac{\sum_{i=1}^{N} \frac{\left(y_{i,calc}\right)^2}{P}}{\sum_{i=1}^{N} \frac{SQR}{N-P}} \qquad (1)$$

where N is the amount of experimental data collected, P is the number of parameters featured in the model, SQR stands for the sum of quadratic residues, defined as $\left(y_{i,\exp} - y_{i,calc}\right)^2$, and $y_{i,exp}$ and $y_{i,calc}$ are the experimental and calculated values of the variable, respectively.

VE is a parameter calculated by ACM that also quantifies how well the model represents the data. It is expressed as a percentage by the following definitions:

$$VE(\%) = 100 \cdot \left(1 - \frac{\sum_{l=1}^{L} SSQ_l}{\sum_{l=1}^{L} SSQav_l} \right) \qquad (2)$$

where SSQ_l and $SSQav_l$ are defined by

$$SSQ_l = \sum_{i=1}^{N} \frac{(y_{i,\exp} - y_{i,calc})^2}{y_{i,calc}^{\gamma_l}} \tag{3}$$

$$SSQav_l = \sum_{i=1}^{N} \frac{(y_{i,\exp} - \bar{y}_{i,\exp})^2}{y_{i,calc}^{\gamma_l}} \tag{4}$$

being

$$\bar{y}_{i,\exp} = \frac{\sum_{i=1}^{N} \frac{y_{i,\exp}}{y_{i,calc}^{\gamma_l / 2}}}{\sum_{i=1}^{N} \frac{1}{y_{i,calc}^{\gamma_l / 2}}} \tag{5}$$

In equations 3 through 5, γ_j is the so-called heteroscedasticity parameter, a measure of the type of error in the measured variable. By default, ACM uses a fixed value of 1.

RMSE manifests the difference between the values of the variable predicted by the model and the experimental observations. The total amount of available data and the number of parameters of the model are factored in [45]:

$$RMSE = \sqrt{\frac{SQR}{N - P}} \tag{6}$$

Finally, *AIC* gives an insight on the goodness of fit while considering possible overfitting of the model due to an excess of parameters being therein. AIC is defined by equation 7:

$$AIC = N \cdot \ln\left(\frac{SQR}{N}\right) + 2 \cdot P \tag{7}$$

The goodness of fit of the proposed models improves as the value of *F* and *VE* increase and *AIC* and *RMSE* decrease.

RESULTS AND DISCUSSION

Mass balance and selectivity

The reaction mechanism proposed for the transesterification of Gly with organic carbonates suggests that the reaction takes place through an unstable intermediate, as appointed in the introduction. Figure 2 shows the plausible structure of this reaction

intermediate A, which appears from the attack of the glyceroxide anion on the carbon of the carbonate group. In addition, further reaction of GC with excess EC can take place as the former generates and compound B can also be produced. [46]

Figure 3a depicts a chromatogram of a sample withdrawn from the reaction, in which the peaks corresponding to each species is labeled correspondingly. In addition to the reactants EC and Gly and products GC and EG, the reaction intermediate A and the further product of reaction B could be assigned to other two minor peaks of the chromatogram following the evolution of the signals with time, as depicted in Figure 3b.

Anyhow, despite the presence of these two peaks, mass balance of the samples withdrawn considering the major components Gly, EC, GC and EG could be closed at any time with a maximal error of 3.1%. This amount would eventually include not only the presence of the mentioned compounds A and B, but also errors in experimental data acquisition, including sample manipulation and HPLC analysis. Previously, selectivity to GC as high as 96% was reported for this reaction using magnesium oxide supported on hydrotalcites. [22]

Owing to the virtually complete selectivity towards GC, the conversion *X* will be considered henceforth. In this piece of work, a definition of an average conversion can be established insomuch as our analysis allows for an accurate quantification of the main four components of the reaction. For this reason, *X* is herein defined following equation 8:

$$X = \frac{\sum_{i=1}^{n} \frac{|C_i - C_{i0}|}{\nu_i}}{\frac{n}{C_{Gly0}}} \qquad (8)$$

in which C_i, C_{i0} and C_{Gly0} refer to the concentration of each component at a given time, at the start of the reaction and the initial concentration of glycerol, respectively; ν_i stands for the stoichiometric coefficient and *n* accounts for the total number of components considered (here n=4). This definition can be envisaged as an average of the conversion of Gly and EC and the yield to GC and EG.

Assessment of the influence of agitation and temperature

Binary systems consisting of glycerol and organic carbonates have been reported to have limited miscibility, giving rise to a liquid-liquid biphasic system. [43, 47, 48] Owing to the excess of organic carbonate phase usually applied in this type of reacting systems, they constitute an emulsion in which glycerol behaves as the dispersed phase within the continuous organic carbonate phase.

FBRM measurements serve the purpose of monitoring this behaviour counting the number and length of chords of the dispersed phase. In addition, due to the FBRM providing the information of a distribution, the modal value of the chord size is given.

Table 2 shows the effect of stirring binary mixtures of EC and glycerol at a fixed temperature of 40 ºC and a molar excess of EC to glycerol of 3 on the mean chord size, modal value and total counts per second (TCS), i.e., the chord length distribution. These assays were made over the course of 10 minutes to acquire a significant amount of data, hence the values of the standard deviations. It can be seen that as stirring increases, so does TCS: up to a stirring speed of 300 rpm, the power input is still not very significant and only slight differences in the chord size distribution can be noticed; from 400 rpm onwards, TCS increases noticeably up to a value of approximately 700 counts per second at 800 and 1000 rpm. The mean chord length, for its part shows a practically constant value of 13 μm from 400 rpm, while the modal chord length can be seen to decline slightly as stirring increases, being practically identical at 800 and 1000 rpm. In general, it can be seen that beyond 800 rpm, further efforts in agitation do not prove successful in varying much the distribution, that is, in producing a larger amount of smaller droplets which could potentially provide a greater surface area with which the biphasic system could react.

This is further verified conducting the chemical reaction by adding catalyst to the dispersion. From differentiation of the data obtained, it could be seen that the initial rate of reaction increases with stirring, except for 800 and 1000 rpm, in which the value is virtually the same.

For these reasons, 800 rpm has been selected as the agitation value with which the rest of the experimentation will be performed. In this manner, it can be contemplated that mass transfer between phases is not a limiting step and, thus, further kinetic studies correspond to the chemical reaction step.

Similarly, the influence of temperature has also been evaluated, fixing the stirring at the optimal value of 800 rpm. The range selected was from 40 ºC, practically the minimum temperature at which the load of the reactor was in a well defined liquid state, and 50 ºC, at which the reaction has been reported to take place using as much as 7% w/w of catalyst with a molar ratio of EC to Gly of 2. [22] Figure 4 depicts the effect of this variable on the distribution, demonstrating that an augmentation of temperature leads to a contraction in the frequency of chords counted, meaning that the liquid-phases interact more with each other, with its corresponding kinetic implications.

Evolution from a biphasic liquid-liquid emulsion into a single liquid phase

With the stirring speed selected on the basis of the observed chord length distribution of the emulsion, the development of the reacting system was analyzed considering the progress of the emulsion while it still exists as well as the chemical evolution of the species.

Figure 5a depicts the evolution of a kinetic experiment (T=40 ºC, M=3 and C_{cat}=500 ppm) during the first ten minutes, within which the first stage of the reaction is included, i.e., when the reacting system still consists of two liquid phases. The diminution of the total number of chord counts (left Y-axis) is presented with the increase of the conversion X (right Y-axis). It can be seen that the number of counts approaches zero (a drop of 98% of TCS with respect to the initial value) slightly after 4 minutes, moment at which the extent of the reaction is at a value of X of 0.34. The corresponding molar composition of the reacting mixture would be of x_{EC}=0.665, x_{Gly}=0.165 and x_{GC+EG}=0.170. The mentioned composition is plotted in Figure 5b, a ternary diagram that also represents the liquid-liquid equilibrium at 40 ºC determined for the quaternary system herein involved. [43] As may be seen, the composition at which the phase change behaviour takes place lies very close to the binodal curve separating the mono and biphasic regions of this equilibrium.

Influence of the operating variables on the development of the reaction

The influence of the variables that affect the progress of the chemical reaction was assessed for the entire reaction period. Figure 6 reflects the impact of the variation of temperature (40-50 ºC) (a), molar excess of EC to glycerol (2 – 3) (b) and catalyst load (125-500 ppm) (c). From the graphs it can be inferred that the three variables have a positive effect on the kinetic behaviour of the reaction inasmuch as development of

the reaction took place more rapidly under increasing values of the mentioned variables. It can be seen how a different molar excess of EC barely affects the conversion at equilibrium.

Proposal and discrimination of the kinetic model of the reaction

Taking into account the initial biphasic nature of this reacting system and the homogeneous catalysis approach followed, determination of which phase dissolved the catalyst was an additional piece of information to be regarded. For this purpose, samples were withdrawn from the reaction medium at short times of reaction and, after separation of the heavy (EC-rich) and light (Gly-rich) phases, they were tested for the presence of the potassium cation (Quantofix ® potassium test). Potassium was present mostly in the Gly-rich phase, which in turn ascertains the mechanism proposed for this reaction, which initiates through a glyceroxide anion [28, 32].

Table 3 features the kinetic models suggested to be fitted to the observed values of conversion. All of these models are based on the assumption that this reaction proceeds in two distinct stages according to the observations of phase regime change. On these grounds, the models are composed of different equations to be applied before and after a critical conversion value, X_{crit}.

The rate equations corresponding to the first step are envisaged to describe the reaction taking place exclusively in the Gly-rich phase due to the catalyst being soluble therein (at a concentration C_{cat1}) while EC progressively enters this phase to react with glycerol being its concentration C_{ECsol}, assumed as a constant value. Consequently, these equations are of first order with respect to the concentration of glycerol and zero order with respect to that of EC. Additionally, no reverse reaction is being accounted for in this stage, for the concentration of the products is still not sufficient for it to be considered.

The equations corresponding to the second step are of first order with respect to the concentrations of glycerol and EC, making them of global second order. Throughout this stage, the catalyst is dissolved in the entire reacting mixture with a concentration C_{cat} lower than $C_{cat1,}$ since it corresponds to the catalyst diluted in the total volume of reaction. For this reason, the reaction makes progress at a remarkably lower rate during this second part.

The four models herein suggested contemplate variations of the general description of the equations mentioned above:

Model 1 considers the direct reaction in the first step and also the reverse reaction from the GC and EG during the second step. This model does not account for the deactivation of the catalyst.

Nevertheless, the species used herein as catalyst, K_2CO_3, may react with H_2O and CO_2 through the following reaction, which can occur at a significant rate [49]:

$$CO_2 + H_2O + K_2CO_3 \leftrightarrow 2\,KHCO_3 \qquad (9)$$

Operating with a non-inert atmosphere, as is the case, the concentration of H_2O and CO_2 can be sufficient to significantly reduce the concentration of K_2CO_3 to yield the less active $KHCO_3$ species. Considering the low concentrations of catalyst herein used, ranging from as little as 125 to 500 ppm, the amount of $KHCO_3$ produced can be high enough to reduce the pKa value of the CO_3^{2-} ion. Consequently, the pH value of the reacting system was measured (data not shown), reaching a value of approximately 9.6 after 30 minutes, while the pK_a value of the CO_3^{2-} ion is 10.33.

For this reason, the remaining three models (Models 2, 3 and 4) account for the possibility that a first-order deactivation of the catalyst may be taking place throughout the course of the transesterification reaction. In the first stage, the following equation is used:

$$r_1 = k_1 \cdot C_{cat1} \cdot \left((1-\beta) \cdot \exp\left(-k_d \cdot t\right) + \beta \right) C_{Gly} C_{ECsol} \qquad (10)$$

where β is the remaining catalytic activity of the final catalytic species with respect to the initial. Additionally, the term $(1-\beta)\cdot\exp\left(-k_d \cdot t\right)$ corresponds to the partial deactivation, in which k_d stands for the deactivation constant and t is time.

In addition to these considerations regarding the three latter models, the following particular assumptions are made. Model 2 considers the reversibility of the reaction and equal constants for the direct reaction in both stages. Model 3 also reflects a reversible reaction, yet the kinetic constants k_1 and k_2 for the direct reaction are different for the two stages, leading to different activation energies. Finally, Model 4 disregards the existence of the reversible reaction, thus accounting only for the deactivation of the catalyst.

Multivariable fitting of the experiments was made considering initially a constant value of X_{crit}. Said value was fixed at 0.34 on the grounds of the observations made with the FBRM system (Figure 5) leading to poor results (not shown). In our previous work regarding the reaction between DMC and glycerol, a change of trend of the experimental data was observed at a constant value of X_{crit}, coincidental with compositions at which the transition from a biphasic to a monophasic system occurred [31]. Notwithstanding, in this case, the critical conversion value at which the tendency of the experimental data changed varied with temperature and amount of catalyst, while no variation was found with respect to the molar excess of EC used. Figure 7, valid for M=2 and M=3, depicts such variation of X_{crit} which ranges from 0,2 and 0,6 and is seen to increase with temperature and catalyst concentration.

Figure 8 shows the composition of the 18 corresponding reacting systems, detailed in Table 1, at the critical conversion values. It can be seen that, while not all the compositions lie on the binodal curve, the composition of the systems are relatively close to the border between a biphasic and single liquid phase system. This in turn signifies that the change in the trend of the kinetics is closely related to the phase change transition

Table 4 compiles the values of the parameters considered in each of the models with their estimation errors. These parameters are all included in the definition of the rate equations in Table 3, with the additional consideration of the Arrhenius equation to reflect the dependence of the kinetic constants with respect to temperature.

$$\ln k_i = \ln k_{i0} - \frac{E_{ai}}{R}.\frac{1}{T} \qquad (11)$$

where k_{i0} is the preexponential factor and E_{ai}/R stands for the activation energy to the ideal gas constant ratio.

Values obtained for the activation energies after correlation ranged from 72 to 92 kJ·mol^{-1} for the direct reaction, while that of the reverse reaction, where considered, varied from 83 to 107 kJ·mol^{-1}. These values are similar to those observed in another reaction using glycerol as feedstock, as is its hydrogenolysis to yield propanediol, with an activation energy value of 97 kJ·mol^{-1} [50].

The values retrieved of the deactivation constant in Models 2, 3 and 4, they are all around 0,30, being the values of the relative activity β below 0,10.

Finally, regarding the concentration of EC estimated to react in the glycerol-rich phase during the first step, Model 1 estimates a concentration as high as 10.31 $mol \cdot L^{-1}$. This value is excessively high considering that pure EC has a concentration of 14.98 $mol \cdot L^{-1}$; thus, it would imply, in turn, an EC-rich phase rather than a glycerol-rich. While Models 2, 3 and 4 retrieve much lower values, the error in the estimation is higher than the actual value for Model 4 and, more especially, Model 3, thus leaving C_{ECsol}=1,10 $mol \cdot L^{-1}$ as the only reasonable value.

Table 4 also features the computed values of the statistical criteria defined in the Numerical Methods section. From this standpoint, given the values of F, AIC, RMSE and VE acquired, it becomes clear that Model 2 outperforms the rest of the models. While Model 3 also shows adequate performance and values of the mentioned criteria similar to those of Model 2, the high error in the estimation C_{ECsol} becomes a further consideration towards its dismissal.

Figure 6 shows the fitting of Model 2 to the selected experiments to illustrate the evolution of the reaction with varying conditions. Finally, Figure 9 shows the validation of this model, where errors below 15% can be seen for the vast majority of the experimental data.

CONCLUSIONS

Simultaneous production of glycerol and ethylene carbonate can be effectively attained from the transesterification of glycerol with ethylene carbonate. For this purpose, inexpensive K_2CO_3 was used as catalyst in a solventless operation using mild temperatures and low amounts of catalyst.

The reactants initially constitute a liquid-liquid biphasic system that turns into a single phase liquid when enough products generate. The influence of stirring was studied with the aid of FBRM to determine the chord length distribution of the mixture of ethylene carbonate and glycerol as well as conducting the chemical reaction, becoming clear that above 800 rpm, the influence of this variable is not important.

The evolution of the reacting dispersion was followed by FBRM and it was observed that it turned into a single phase liquid at an approximate conversion value of 0.34, which corresponds to a composition lying very close to the boundary between the

biphasic and monophasic regions, as determined by liquid-liquid equilibria (LLE) studies performed prior to this work.

A total of 18 kinetic runs were completed varying temperature, molar excess of ethylene carbonate (M) and catalyst concentration. Different critical conversion values, X_{crit}, were established from the observation of individual experiments, considered as those at which the observed trend of the kinetic data showed a change. While variable with temperature and concentration of catalyst employed and not with M, they showed resemblance to 0.34.

Finally, a series of kinetic models were proposed to fit to the experimental data, all of which were based on the division of the model into different equations, applicable at conversion values smaller and greater than X_{crit}. The first equation is based on a potential model of partial first order with respect to the concentration of glycerol and zero order with respect to ethylene carbonate, while the second accounts for partial first orders with respect to both. After discrimination based on physicochemical and statistical criteria, the model that showed the best performance contemplated the presence of the reverse reaction from the products and deactivation of the catalyst, where the activation energy of the direct and reverse reactions are, respectively, 91.7 ± 2.7 $kJ \cdot mol^{-1}$ and 93.9 ± 15.9 $kJ \cdot mol^{-1}$and the deactivation constant had a value of 0.36 ± 0.06 s^{-1}.

Acknowledgements

The authors wish to express gratitude to the Spanish Ministry of Science and Innovation (Projects CTQ2007-60919 and CTQ2010-15460) for financial support.

List of abbreviations

Components

DMC	Dimethyl carbonate
EC	Ethylene carbonate
EG	Ethylene glycol
GC	Glycerol carbonate
Gly	Glycerol

Nomenclature

AIC	Akaike's information criterion
C	Concentration of the components at a given time ($mol \cdot L^{-1}$)
d	chord length (μm)
E_{ai}/R	Ratio of activation energy and the ideal gas constant (K)
F	Fischer's F statistical parameter
FBRM	Focused Beam Reflectance Measurement
HPLC	High-performance liquid chromatography
ISTD	Internal standard
k_d	Deactivation constant (s^{-1})
k_i	kinetic constant ($L^2 \cdot gcat^{-1} \cdot mol^{-1} \cdot min^{-1}$)
K	Number of parameters of a proposed model
M	Initial molar ratio of ethylene carbonate to glycerol
n	Total number of components
N	Total number of data to which a model is fitted
r	reaction rate ($mol \cdot L \cdot min^{-1}$)
RMSE	Residual mean squared error
SQR	Sum of quadratic residues
t	time (min)
T	Temperature (K)
TCS	Total counts per second, as provided by FBRM
TOF	Turnover frequency (mol converted·mol $catalyst^{-1} \cdot min^{-1}$)
X	Average conversion, as defined by equation (8)

Greek letters

β	Remaining catalytic activity
γ	Heteroscedasticity parameter
ν	Stoichiometric coefficient of the component i

ρ	Density ($g \cdot mL^{-1}$)
ω	Agitation rate (rpm)

Subscripts

0	Relative to the start of the reaction, time equals zero
i	Relative to component i
calc	Relative to a calculated value
cat	Relative to the catalyst
crit	Relative to the critical conversion value
exp	Relative to experimental values or the exponential function
d	Relative to deactivation of the catalyst
ECsol	Relative to concentration of EC dissolved in the glycerol-rich phase

References

1. Anastas P and Warner J, Green Chemistry Theory and Practice. Oxford University Press, New York (2008).
2. Pagliaro M and Rossi M, The Future of Glycerol: New Uses of a Versatile Raw Material, in RSC Green Chemistry Book Series, ed by Publishing R. RSC Publishing, Cambridge, UK (2008).
3. Behr A, Eilting J, Irawadi K, Leschinski J and Lindner F, Improved utilisation of renewable resources: New important derivatives of glycerol. *Green Chemistry* **10**: 13-30 (2008).
4. Beltran-Prieto JC, Kolomaznik K and Pecha J, A Review of Catalytic Systems for Glycerol Oxidation: Alternatives for Waste Valorization. *Australian Journal of Chemistry* **66**: 511-521 (2013).
5. Tan HW, Aziz ARA and Aroua MK, Glycerol production and its applications as a raw material: A review. *Renewable & Sustainable Energy Reviews* **27**: 118-127 (2013).

6. Zhou C-H, Beltramini JN, Fan Y-X and Lu GQ, Chemoselective catalytic conversion of glycerol as a biorenewable source to valuable commodity chemicals. *Chem Soc Rev* **37**: 527-549 (2008).
7. Gómez-Jiménez-Aberasturi O, Ochoa-Gómez JR, Pesquera-Rodríguez A, Ramírez-López C, Alonso-Vicario A and Torrecilla-Soria J, Solvent-free synthesis of glycerol carbonate and glycidol from 3-chloro-1,2-propanediol and potassium (hydrogen) carbonate. *Journal of Chemical Technology & Biotechnology* **85**: 1663-1670 (2010).
8. Tamura M, Honda M, Nakagawa Y and Tomishige K, Direct conversion of CO2 with diols, aminoalcohols and diamines to cyclic carbonates, cyclic carbamates and cyclic ureas using heterogeneous catalysts. *Journal of Chemical Technology and Biotechnology* **89**: 19-33 (2014).
9. Teng WK, Ngoh GC, Yusoff R and Aroua MK, A review on the performance of glycerol carbonate production via catalytic transesterification: Effects of influencing parameters. *Energy Conversion and Management* **88**: 484-497 (2014).
10. Sonnati MO, Amigoni S, de Givenchy EPT, Darmanin T, Choulet O and Guittard F, Glycerol carbonate as a versatile building block for tomorrow: synthesis, reactivity, properties and applications. *Green Chemistry* **15**: 283-306 (2013).
11. Ochoa-Gomez JR, Gomez-Jimenez-Aberasturi O, Ramirez-Lopez C and Belsue M, A Brief Review on Industrial Alternatives for the Manufacturing of Glycerol Carbonate, a Green Chemical. *Organic Process Research & Development* **16**: 389-399 (2012).
12. Lameiras P, Boudesocque L, Mouloungui Z, Renault J-H, Wieruszeski J-M, Lippens G and Nuzillard J-M, Glycerol and glycerol carbonate as ultraviscous solvents for mixture analysis by NMR. *Journal of Magnetic Resonance* **212**: 161-168 (2011).
13. Benoit M, Brissonnet Y, Guélou E, De Oliveira Vigier K, Barrault J and Jérôme F, Acid-Catalyzed Dehydration of Fructose and Inulin with Glycerol or Glycerol Carbonate as Renewably Sourced Co-Solvent. *ChemSusChem* **3**: 1304-1309 (2010).
14. Chen C-H, Hyung YE, Vissers DR and Amine K, Lithium ion battery with improved safety.Patent US20030157413 A1 (2002).

15. Magniont C, Escadeillas G, Oms-Multon C and De Caro P, The benefits of incorporating glycerol carbonate into an innovative pozzolanic matrix. *Cement and Concrete Research* **40**: 1072-1080 (2010).
16. Kovvali AS and Sirkar KK, Carbon dioxide separation with novel solvents as liquid membranes. *Industrial & Engineering Chemistry Research* **41**: 2287-2295 (2002).
17. Zhang Z, Rackemann DW, Doherty WOS and O'Hara IM, Glycerol carbonate as green solvent for pretreatment of sugarcane bagasse. *Biotechnology for Biofuels* **6** (2013).
18. Nemirowsky J, Über die Einwirkung von Chlorkohlenoxyd auf Glycolchlorhydrin. *Journal für Praktische Chemie* **31**: 173-175 (1885).
19. Yoo JW and Mouloungui Z, Catalytic carbonylation of glycerin by urea in the presence of zinc mesoporous system for the synthesis of glycerol carbonate. *Nanotechnology in Mesostructured Materials* **146**: 757-760 (2003).
20. Dibenedetto A, Angelini A, Aresta M, Ethiraj J, Fragale C and Nocito F, Converting wastes into added value products: from glycerol to glycerol carbonate, glycidol and epichlorohydrin using environmentally friendly synthetic routes. *Tetrahedron* **67**: 1308-1313 (2011).
21. Aresta M, Dibenedetto A, Nocito F and Ferragina C, Valorization of bio-glycerol: New catalytic materials for the synthesis of glycerol carbonate via glycerolysis of urea. *Journal of catalysis* **268**: 106-114 (2009).
22. Climent MJ, Corma A, De Frutos P, Iborra S, Noy M, Velty A and Concepción P, Chemicals from biomass: Synthesis of glycerol carbonate by transesterification and carbonylation with urea with hydrotalcite catalysts. The role of acid-base pairs. *Journal of Catalysis* **269**: 140-149 (2010).
23. Aresta M, Dibenedetto A, Nocito F and Pastore C, A study on the carboxylation of glycerol to glycerol carbonate with carbon dioxide: The role of the catalyst, solvent and reaction conditions. *Journal of Molecular Catalysis A: Chemical* **257**: 149-153 (2006).
24. Vieville C, Yoo JW, Pelet S and Mouloungui Z, Synthesis of glycerol carbonate by direct carbonatation of glycerol in supercritical CO_2 in the presence of zeolites and ion exchange resins. *Catalysis Letters* **56**: 245-247 (1998).

25. Hu J, Li J, Gu Y, Guan Z, Mo W, Ni Y, Li T and Li G, Oxidative carbonylation of glycerol to glycerol carbonate catalyzed by $PdCl_2$(phen)/KI. *Applied Catalysis A: General* **386**: 188-193 (2010).
26. George J, Patel Y, Pillai SM and Munshi P, Methanol assisted selective formation of 1,2-glycerol carbonate from glycerol and carbon dioxide using (Bu_2SnO)-Bu-n as a catalyst. *Journal of Molecular Catalysis A: Chemical* **304**: 1-7 (2009).
27. Lu P, Wang H and Hu K, Synthesis of glycerol carbonate from glycerol and dimethyl carbonate over the extruded CaO-based catalyst. *Chemical Engineering Journal* **228**: 147-154 (2013).
28. Ochoa-Gomez JR, Gomez-Jimenez-Aberasturi O, Maestro-Madurga B, Pesquera-Rodriguez A, Ramirez-Lopez C, Lorenzo-Ibarreta L, Torrecilla-Soria J and Villaran-Velasco MC, Synthesis of glycerol carbonate from glycerol and dimethyl carbonate by transesterification: Catalyst screening and reaction optimization. *Applied Catalysis A: General* **366**: 315-324 (2009).
29. Bai R, Wang Y, Wang S, Mei F, Li T and Li G, Synthesis of glycerol carbonate from glycerol and dimethyl carbonate catalyzed by NaOH/gamma-Al2O3. *Fuel Processing Technology* **106**: 209-214 (2013).
30. Malyaadri M, Jagadeeswaraiah K, Prasad PSS and Lingaiah N, Synthesis of glycerol carbonate by transesterification of glycerol with dimethyl carbonate over Mg/Al/Zr catalysts. *Applied Catalysis A: General* **401**: 153-157 (2011).
31. Esteban J, Fuente E, Blanco A, Ladero M and Garcia-Ochoa F, Phenomenological kinetic model of the synthesis of glycerol carbonate assisted by focused beam reflectance measurements. *Chemical Engineering Journal* **260**: 434-443 (2015).
32. Alvarez MG, Pliskova M, Segarra AM, Medina F and Figueras F, Synthesis of glycerol carbonates by transesterification of glycerol in a continuous system using supported hydrotalcites as catalysts. *Applied Catalysis B-Environmental* **113**: 212-220 (2012).
33. Alvarez MG, Segarra AM, Contreras S, Sueiras JE, Medina F and Figueras F, Enhanced use of renewable resources: Transesterification of glycerol catalyzed by hydrotalcite-like compounds. *Chemical Engineering Journal* **161**: 340-345 (2010).

34. Cho H-J, Kwon H-M, Tharun J and Park D-W, Synthesis of glycerol carbonate from ethylene carbonate and glycerol using immobilized ionic liquid catalysts. *Journal of Industrial and Engineering Chemistry* **16**: 679-683 (2010).
35. Constable DJC, Curzons AD and Cunningham VL, Metrics to 'green' chemistry - which are the best? *Green Chemistry* **4**: 521-527 (2002).
36. van Hal JW, Ledford JS and Zhang X, Investigation of three types of catalysts for the hydration of ethylene oxide (EO) to monoethylene glycol (MEG). *Catal Today* **123**: 310-315 (2007).
37. Kawabe KMCC, Process for simultaneous production of ethylene glycol and carbonate esterEP 1125915 A1 (2005).
38. Kawabe KMCC, Method for producing monoethylene glycolUS 09/271,435 (2000).
39. Tundo P and Selva M, The chemistry of dimethyl carbonate. *Accounts of Chemical Research* **35**: 706-716 (2002).
40. Dawodu FA, Ayodele OO, Xin J and Zhang S, Dimethyl carbonate mediated production of biodiesel at different reaction temperatures. *Renewable Energy* **68**: 581-587 (2014).
41. Blanco A, Fuente E, Negro C and Tijero J, Flocculation monitoring: Focused beam reflectance measurement as a measurement tool. *Canadian Journal of Chemical Engineering* **80**: 734-740 (2002).
42. Blanco A, De la Fuente E, Negro C, Monte MC and Tijero J, Focused beam reflectant measurement as a tool to measure flocculation. *Tappi Journal* **1**: 14-20 (2002).
43. Esteban J, Ladero M and Garcia-Ochoa F, Liquid-liquid equilibria for the ternary systems ethylene carbonate-ethylene glycol-glycerol; ethylene carbonate-glycerol carbonate-glycerol and the quaternary system ethylene carbonate-ethylene glycol-glycerol carbonate-glycerol at catalytic reacting temperatures. *Chemical Engineering Research and Design DOI: doi:101016/jcherd201408024* (2014).
44. Garcia-Ochoa F, Romero A and Querol J, Modeling of the thermal normal-octane oxidation in the liquid phase. *Industrial & Engineering Chemistry Research* **28**: 43-48 (1989).

45. Ladero M, de Gracia M, Tamayo JJ, Ahumada ILd, Trujillo F and Garcia-Ochoa F, Kinetic modelling of the esterification of rosin and glycerol: Application to industrial operation. *Chemical Engineering Journal* **169**: 319-328 (2011).
46. Rokicki G, Rakoczy P, Parzuchowski P and Sobiecki M, Hyperbranched aliphatic polyethers obtained from environmentally benign monomer: glycerol carbonate. *Green Chemistry* **7**: 529-539 (2005).
47. Esteban J, Ladero M, Molinero L and Garcia-Ochoa F, Liquid-liquid equilibria for the ternary systems DMC-methanol-glycerol; DMC-glycerol carbonate-glycerol and the quaternary system DMC-methanol-glycerol carbonate-glycerol at catalytic reacting temperatures. *Chemical Engineering Research and Design* **92**: 1797-1805 (2014).
48. Wang H and Lu P, Liquid–Liquid Equilibria for the System Dimethyl Carbonate + Methanol + Glycerol in the Temperature Range of (303.15 to 333.15) K. *Journal of Chemical & Engineering Data* **57**: 582-589 (2012).
49. Ye X and Lu Y, Kinetics of CO2 absorption into uncatalyzed potassium carbonate-bicarbonate solutions: Effects of CO2 loading and ionic strength in the solutions. *Chemical Engineering Science* **116**: 657-667 (2014).
50. Vasiliadou ES and Lemonidou AA, Kinetic study of liquid-phase glycerol hydrogenolysis over Cu/SiO2 catalyst. *Chemical Engineering Journal* **231**: 103-112 (2013).

Table 1. Summary of the experimental program.

Run	Temperature (ºC)	M	C_{cat} (ppm)
1	40	2	125
2			250
3			500
4		3	125
5			250
6			500
7	45	2	125
8			250
9			500
10		3	125
11			250
12			500
13	50	2	125
14			250
15			500
16		3	125
17			250
18			500

Table 2. Effect of the stirring speed on the chord length distribution of the emulsion composed by EC and Gly. Conditions: T=40 ºC and M=3.

ω (rpm)	$\overline{d_p} \pm \sigma_{\overline{dp}}$ (µm)	$d_p^{mode} \pm \sigma_{d_p^{mode}}$ (µm)	TCS ± σ_{TCS}	r_0 ($mol_{conv} \cdot L^{-1} \cdot min^{-1}$)*
100	18.33 ± 3.99	17.16 ± 15.44	85.84 ± 24.79	0.08
200	16.62 ± 1.77	11.95 ± 5.02	49.16 ± 4.41	0.13
300	22.52 ± 9.79	13.59 ± 6.58	114.38 ± 18.43	0.16
400	12.44 ± 2.18	12.09 ± 6.50	406.47± 69.66	0.29
500	13.13 ± 0.41	9.62 ± 1.23	422.21 ± 25.97	0.35
600	12.39 ± 0.79	9.08 ± 1.19	495.83 ± 23.17	0.42
800	12.97 ± 0.64	8.38 ± 0.97	701.12± 20.85	0.52
1000	13.04 ± 0.63	8.51 ± 1.07	697.53 ± 28.23	0.53

* Obtained by differentiation of the kinetic data obtained adding 500 ppm of K_2CO_3

Table 3. Kinetic models proposed for the transesterification of glycerol with ethylene carbonate to simultaneously yield glycerol carbonate and ethylene glycol.

Model number	Rate equations	
1	$r_1 = k_1 \cdot C_{cat1} \cdot C_{Gly} \cdot C_{ECsol}$	if $X \leq X_{crit}$
	$r_2 = k_1 \cdot C_{cat} \cdot C_{Gly} \cdot C_{EC}$ $r_3 = k_3 \cdot C_{cat} \cdot C_{GC} \cdot C_{EC}$	if $X > X_{crit}$
2	$r_1 = k_1 \cdot C_{cat1} \cdot \left((1-\beta) \cdot \exp(-k_d \cdot t) + \beta \right) C_{Gly} C_{ECsol}$	if $X \leq X_{crit}$
	$r_2 = k_1 \cdot C_{cat} \cdot \beta \cdot C_{Gly} \cdot C_{EC}$ $r_3 = k_3 \cdot C_{cat} \cdot \beta \cdot C_{GC} \cdot C_{EG}$	if $X > X_{crit}$
3	$r_1 = k_1 \cdot C_{cat1} \cdot \left((1-\beta) \cdot \exp(-k_d \cdot t) + \beta \right) C_{Gly} C_{ECsol}$	if $X \leq X_{crit}$
	$r_2 = k_2 \cdot C_{cat} \cdot \beta \cdot C_{Gly} \cdot C_{EC}$ $r_3 = k_3 \cdot C_{cat} \cdot \beta \cdot C_{GC} \cdot C_{EG}$	if $X > X_{crit}$
4	$r_1 = k_1 \cdot C_{cat1} \cdot \left((1-\beta) \cdot \exp(-k_d \cdot t) + \beta \right) C_{Gly} C_{ECsol}$	if $X \leq X_{crit}$
	$r_2 = k_1 \cdot C_{cat} \cdot \beta \cdot \exp(-k_{d2} \cdot t) C_{Gly} C_{EC}$	if $X > X_{crit}$

Table 4. Summary of the kinetic parameters and statistical criteria retrieved from multivariable correlation of the proposed models to all the available data.

Model	Parameter	Value	±error	F	AIC	RMSE	Variation explained (%)
1	$\ln k_{10}$	29.88	1.19	8334	-1631	0.0486	95.48
	E_{a1}/R	10943	376				
	$\ln k_{30}$	34.36	7.62				
	E_{a3}/R	12897	2444				
	C_{ECsol}	10.31	0.55				
2	$\ln k_{10}$	32.71	1.03	8598	-1954	0.0401	98.45
	E_{a1}/R	11036	319				
	$\ln k_{30}$	31.91	5.95				
	E_{a3}/R	11297	1911				
	k_d	0.36	0.06				
	β	0.08	0.03				
	C_{ECsol}	1.10	0.46				
3	$\ln k_{10}$	31.62	2.50	7220	-1941	0.0409	98.38
	E_{a1}/R	10981	469				
	E_{a2}/R	10624	798				
	$\ln k_{30}$	28.15	6.97				
	E_{a3}/R	10012	2237				
	k_d	0.34	0.05				
	β	0.07	0.03				
	C_{ECsol}	2.77	9.25				
4	$\ln k_{10}$	26.47	2.08	4224	-1717	0.0591	96.63
	E_{a1}/R	8831	356				
	k_d	0.28	0.07				
	k_{d2}	0.01	0.00				
	β	0.04	0.07				
	C_{ECsol}	0.55	0.91				

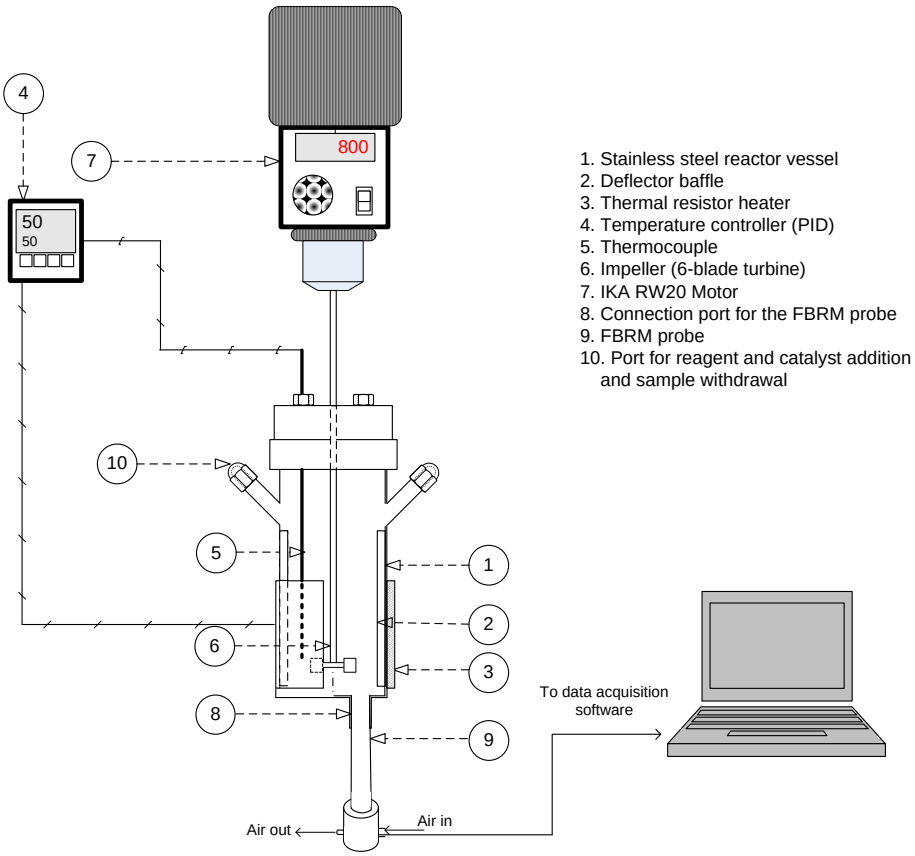

Figure 1. Experimental set used for the kinetic and droplet size distribution studies of the synthesis of glycerol carbonate

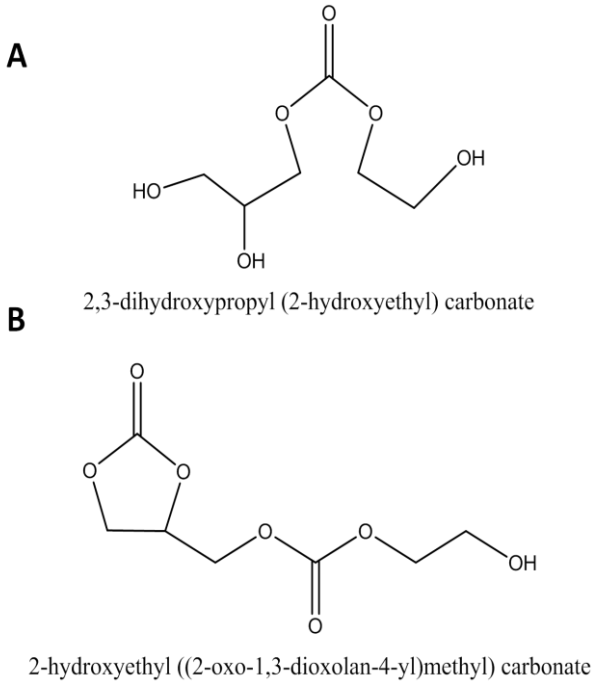

Figure 2. Chemical structure of the plausible reaction intermediate (species A) and product of the reaction between GC and EC (species B)

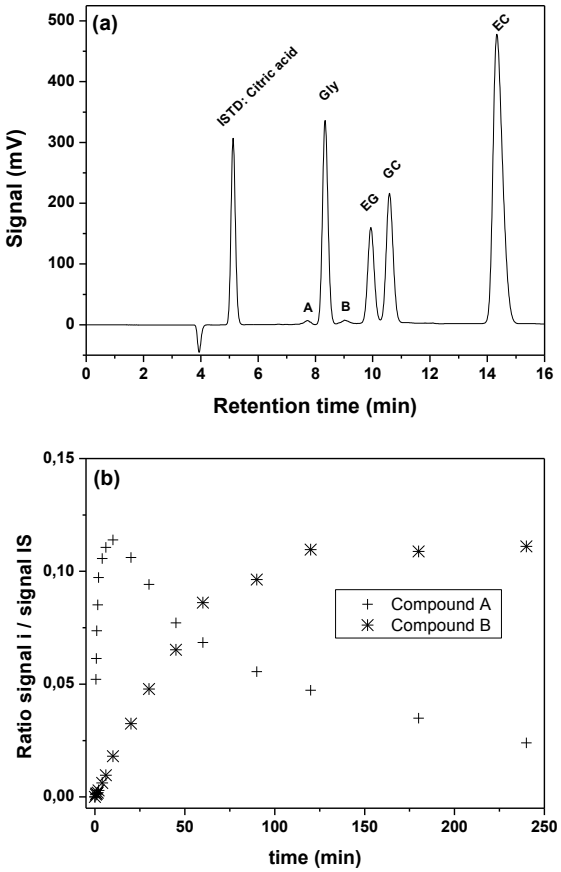

Figure 3. Sample chromatogram of the reaction with all the species identified (a) and evolution of the signal of species A and B (b)

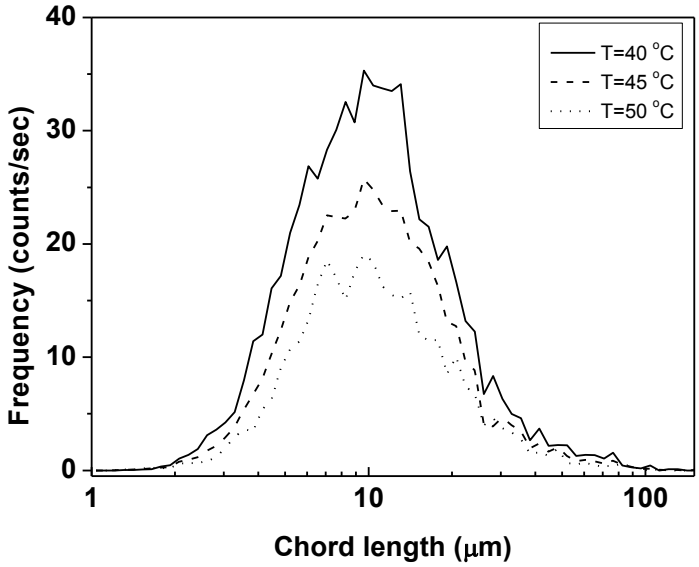

Figure 4. Effect of the stirring speed on the droplet size distribution of the emulsion composed by EC and Gly. Conditions: M=3 and ω=800 rpm.

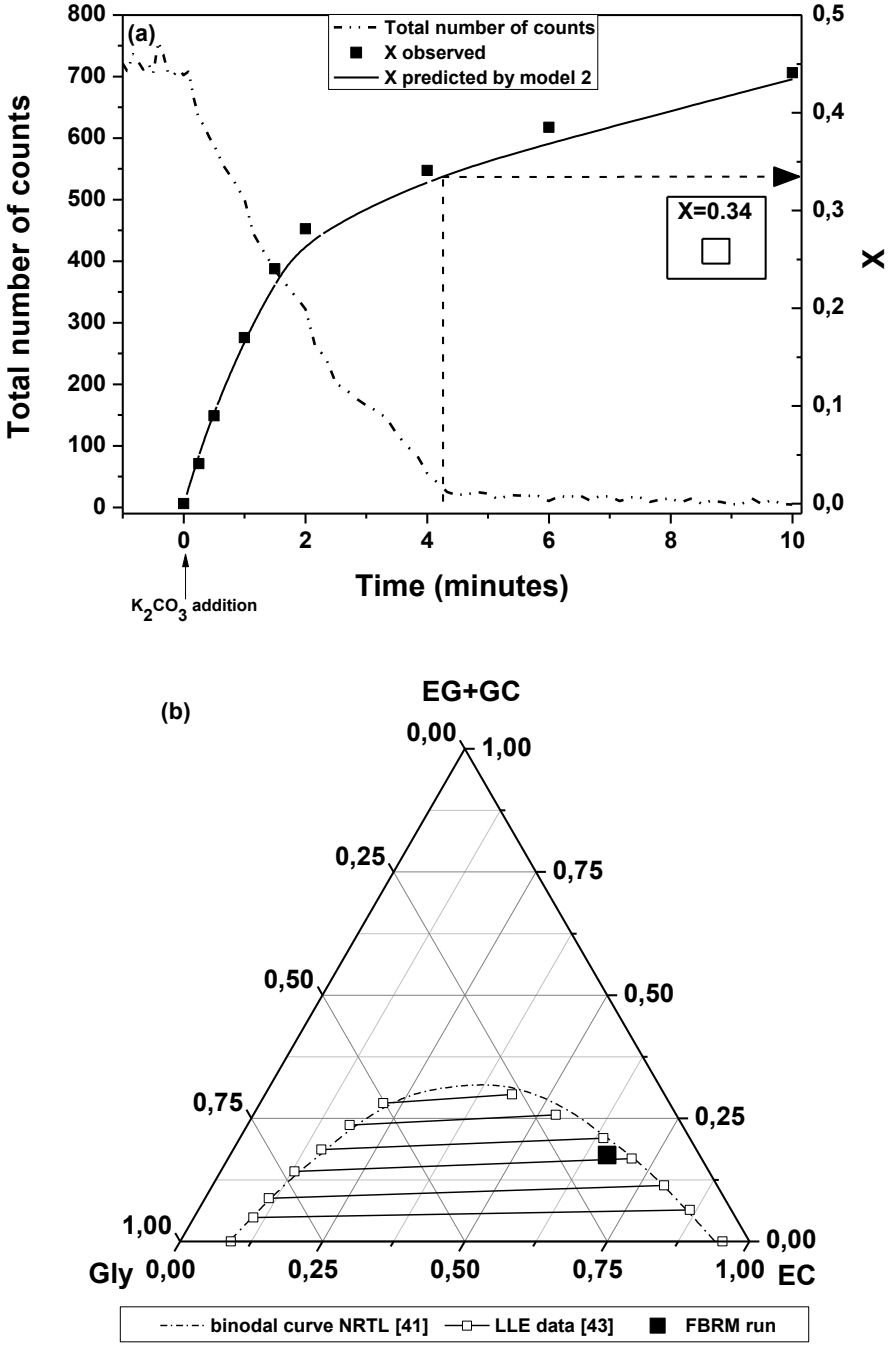

Figure 5. Evolution of the number of counts and conversion (a) and composition of the reacting system at phase change conditions with respect to the liquid-liquid equilibrium [43] (b). Conditions of FBRM run: T=40 ºC, M=3, C_{cat}= 500 ppm, ω=800 rpm.

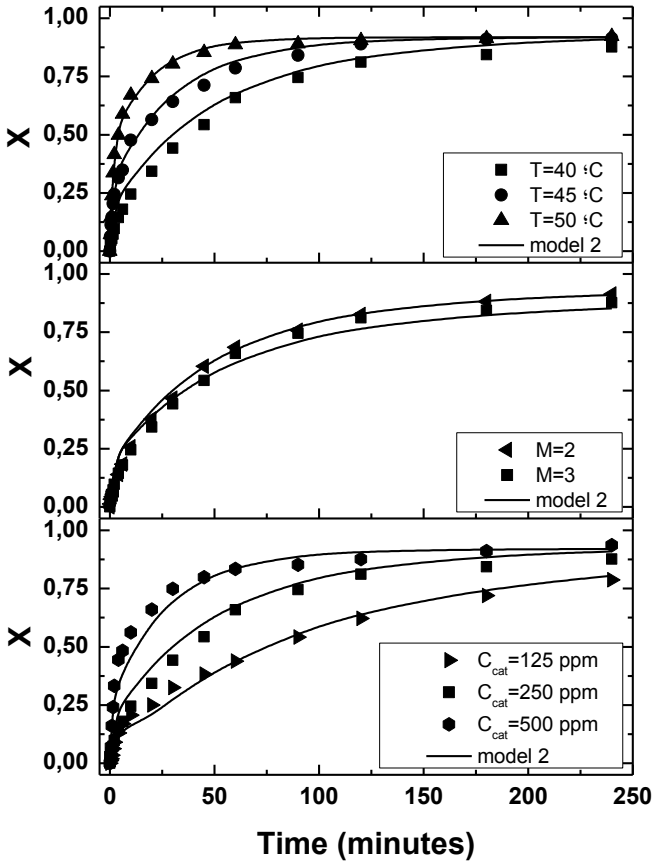

Figure 6. Evolution of the reaction comparing the effect of temperature (a), molar ratio of reactants (b) and catalyst concentration (c). Conditions: (a) M=3, C_{cat}= 250 ppm; (b) T=40ºC, C_{cat}= 250 ppm and (c) T=40ºC, M=3. Every kinetic run at ω=800 rpm.

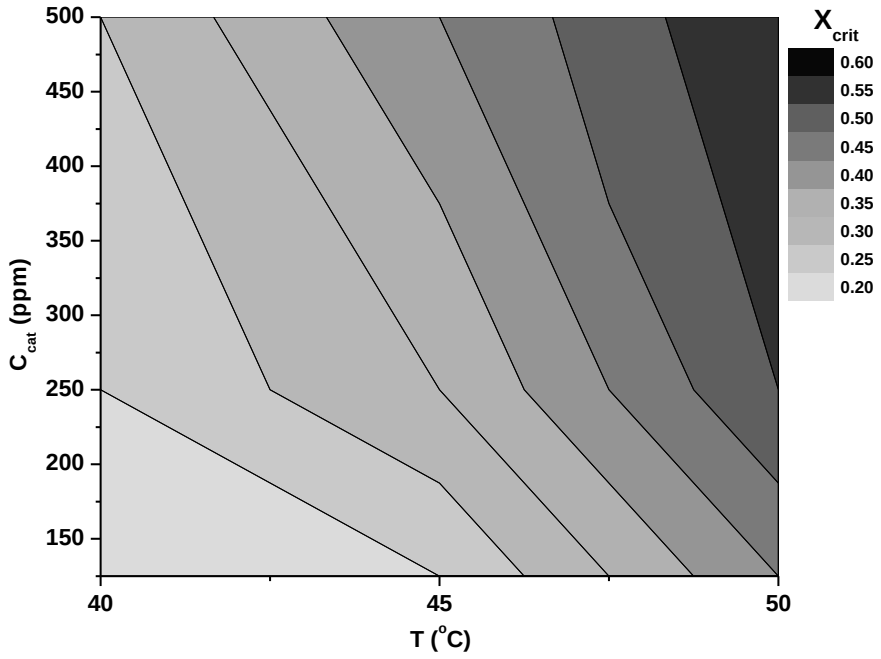

Figure 7. Dependence of the critical conversion with respect to temperature and catalyst concentration.

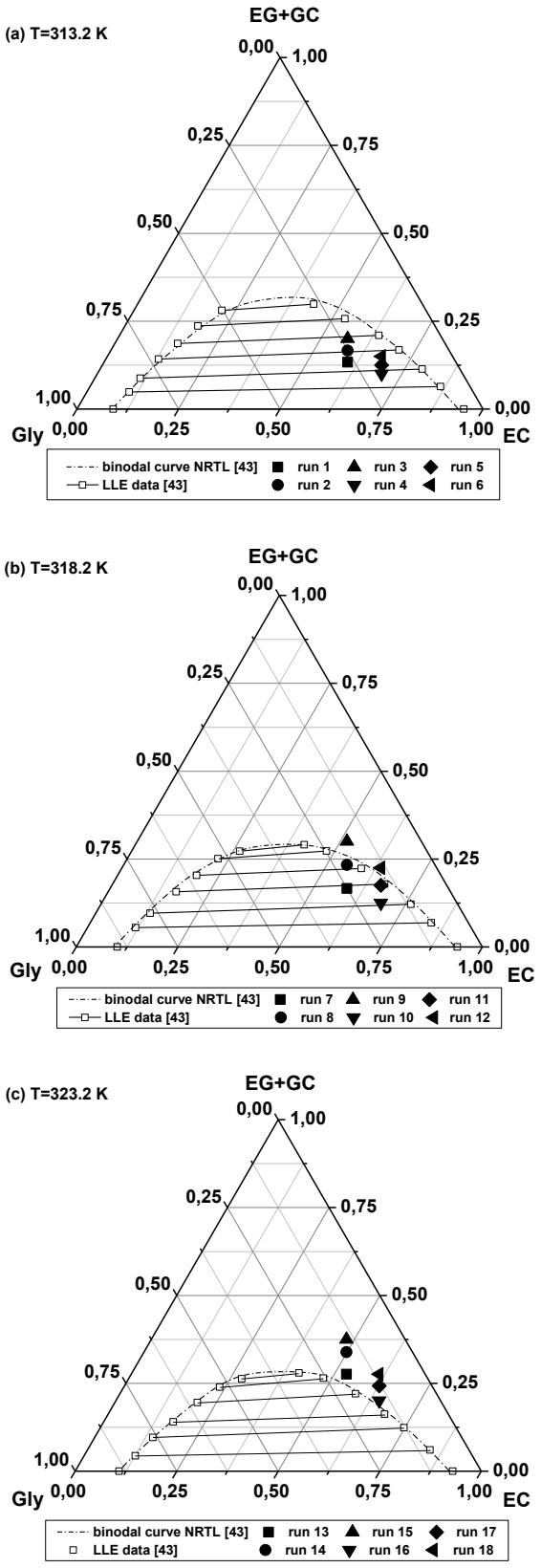

Figure 8. Comparison of the LLE of the system {EC + EG + GC + Gly} and the composition of the 18 reacting systems tested at the critical conversion values estimated by multivariable fitting at T=40 ºC (a), T=45 ºC (b) and T=50 ºC (c). Adapted from [43]

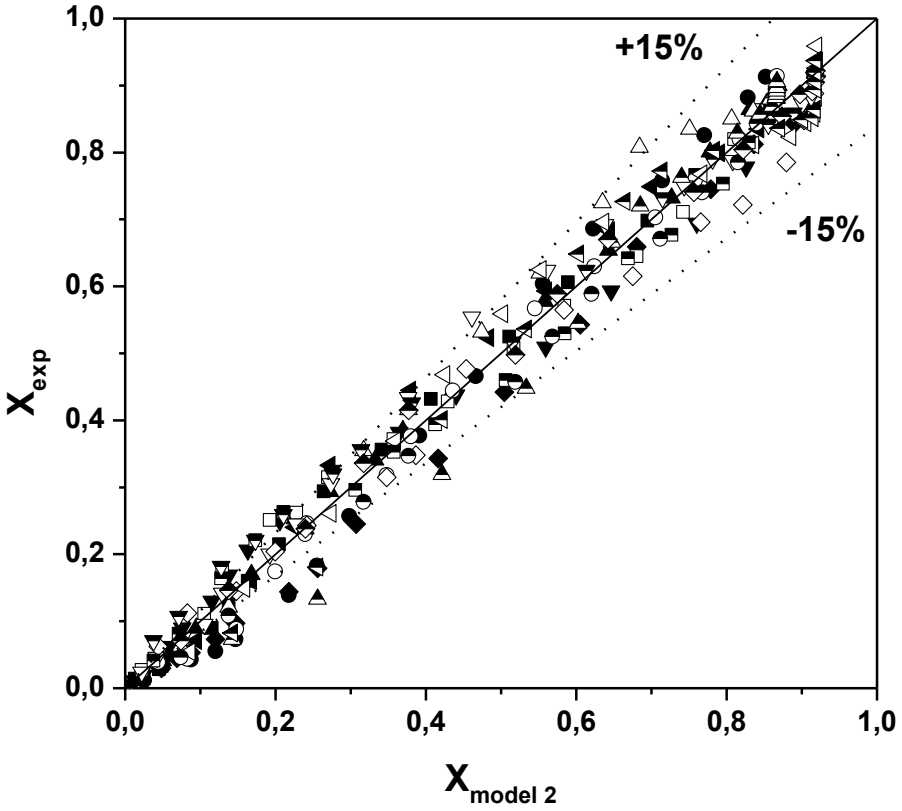

Figure 9. Validation of Model 2 with all the available experimental data.

Publicación 6 / Publication 6

Autores/Authors: Jesús Esteban, Miguel Ladero and Félix García-Ochoa

Título/Title: Potassium methoxide: a very active catalyst for the production of glycerol carbonate in mild solventless conditions

Estado actual/Current status: Manuscript submitted to Bioresource Technology as of January 2015

Índice de impacto / Impact factor 2013: 5.039

Resumen

Se plantea la producción de carbonato de glicerina por dos reacciones de transesterificación de glicerina empleando carbonato de dimetilo (DMC) y carbonato de etileno (EC) utilizando metóxido de potasio como catalizador.

Se analiza la evolución de las especies químicas, comprobándose que se corresponde con lo que predice el mecanismo propuesto en la literatura. Además, el cumplimiento de los balances de materia es prácticamente total (errores máximos de 5,1% y 4,4% incluido el error experimental para la reacción con DMC y EC, respectivamente) por la alta selectividad de este catalizador. Por ello, los estudios cinéticos se pueden aproximar a reacciones simples con bajo error.

Se llevaron a cabo una serie de experimentos cinéticos variando temperatura (50-70 ºC con DMC; 40-50 ºC con EC), exceso molar de carbonato a glicerina (1.5-3) y concentración de catalizador (1000-2500 ppm con DMC; 50-150 ppm con EC).

En la reacción con DMC, se aprecia que la tendencia de los datos cinéticos cambia a una conversión cercana a 0,35. Por ello, se elige este valor como crítico para la aplicación de los modelos cinéticos basados en dos ecuaciones, de acuerdo a la fenomenología observada de cambio de régimen de bifásico a monofásico. En el caso de la reacción con EC, el valor crítico varió entre 0,25 y 0,75, aumentando con las tres variables analizadas.

Para la reacción con DMC, el modelo que mejor ajusta considera dos etapas, además de reacción irreversible con desactivación del catalizador de primer orden ante la posibilidad de desactivación del metóxido contemplada en la literatura. La energía de activación de este modelo fue de 28.4 ± 1.5 $kJ \cdot mol^{-1}$, con una constante de desactivación de 0.03 ± 0.01 min^{-1}. En la reacción con EC, el modelo contempla desactivación, con constante 0.31 ± 0.03 min^{-1} y reacción reversible con energías de activación 82.3 ± 3.0 $kJ \cdot mol^{-1}$ y 53.5 ± 21.6 $kJ \cdot mol^{-1}$ para las reacciones directa e inversa, respectivamente.

Por último, se compara la actividad de CH_3OK con K_2CO_3, previamente utilizado en las dos reacciones. Se comprueba que la actividad del primero, evaluada mediante la frecuencia de reposición en condiciones similares de reacción, es aproximadamente 20 veces mayor que la del último en el caso de la reacción con DMC y unas 6 veces mayor en el caso de la reacción con EC.

Potassium methoxide: a very active catalyst for the production of glycerol carbonate in mild solventless operational conditions

Jesús Esteban, Miguel Ladero*, Félix Garcia-Ochoa

Department of Chemical Engineering. College of Chemical Sciences. Complutense University of Madrid. 28040. Madrid. Spain.

*Corresponding author: mladero@quim.ucm.es. (Phone: +34-913944164/fax: +34-913944179)

Abstract

The production of glycerol carbonate is approached through the transesterification of glycerol with dimethyl carbonate (DMC) and ethylene carbonate (EC), using potassium methoxide as catalyst, with virtually complete selectivity to glycerol carbonate. Kinetic runs were conducted under mild reaction conditions: temperature (50- 70 ºC using DMC; 40-50 ºC using EC), low molar excess of organic carbonate to glycerol (1.5-3) and moderate to low catalyst load (1000-2500 ppm for DMC; 50-150 ppm for EC). With both reactive systems, kinetic models were proposed, fitted and verified. These considered the transition from a biphasic to a single phase liquid system as well as a first order deactivation of the catalyst. In the reaction with DMC, a model was proposed contemplating an irreversible reaction with an activation energy of 28.4 ± 1.5 kJ·mol^{-1} and a deactivation constant of 0.03 ± 0.01 min^{-1}. Using EC, a reversible model with activation energies of 82.3 ± 3.0 kJ·mol^{-1} and 53.5 ± 21.6 kJ·mol^{-1} for the direct and reverse reactions, respectively, and a deactivation constant of 0.31 ± 0.03 min^{-1} was verified. This catalyst has demonstrated a much higher activity for these two paradigmatic reactions than that achieved using other catalysts reported in the literature.

Keywords: glycerol carbonate, potassium methoxide, kinetic model, solventless synthesis, high activity

1. Introduction

Since approximately the year 2000, a marked development of the biodiesel industry has taken place due to successive regulations to increase the share of renewable energy use. This scenario has given rise to an oversupply of glycerol, a by-product of the biodiesel manufacture process, with subsequent price drops that make the profitability of the process lower and lower (Lamers et al., 2011; Quispe et al., 2013).

Given the necessity and the opportunity derived from this situation, glycerol has been considered as one of the key *building blocks* from biomass (Werpy & Petersen, 2004) and a series of reviews covering the wide spectrum of the exploitation of this compound have followed (Behr et al., 2008; Pagliaro & Rossi, 2008; Zakaria et al., 2013). In this sense, many processes have been studied, such as the production of biopolyols, potential feedstock for polyurethane manufacture (Luo et al., 2013), the synthesis of oxygenate biofuel additives by means of acetylation (Khayoon & Hameed, 2011) or etherification reactions (Ayoub et al., 2012) or the esterification of glycerol to yield bioadditives for applications like cosmetics (Zhu et al., 2013).

A product that has awakened much interest is glycerol carbonate (GC) (Garcia et al., 2014; Ochoa-Gomez et al., 2012; Sonnati et al., 2013; Teng et al., 2014). Thanks to its features, it has proven useful in direct applications. To cite a few examples, its use has been reported as solvent in the ^{1}H-NMR resolution of peptides (Lameiras et al., 2011), the dehydration of fructose to 5-hydroxymethylfurfural substituting ionic liquids (Benoit et al., 2010) or to improve the enzymatic activity of systems featuring CALB or CRL with respect to water or other organic solvents (Ou et al., 2011). Apart from its use as a solvent, it has been immobilized in membranes to enhance the separation of CO_2 and N_2 (Kovvali & Sirkar, 2002), used to revitalize plants (Nomura et al., 2006), as a curing agent in puzzolanic matrices (Magniont et al., 2010) or as an additive in solid detergents (Brooker, 2011). Additionally, given its chemical functionality, it can further react to yield other products of interest; among them, α-monoglycerides with applications as surfactants (Ghandi et al., 2007) can be mentioned.

While the first-ever synthetic route studied for the production of GC involved the use of highly toxic phosgene (Nemirowsky, 1885), several novel methods have appeared to substitute such obsolete process. Throughout the years, an array of chemical reactions have been reported, including: direct addition of CO (Hu et al., 2010) and CO_2 to glycerol (Aresta et al., 2006; George et al., 2009), addition of CO_2 to glycidol (Rokicki et al., 1984), glycerolysis of urea (Kim et al., 2014; Lee et al., 2014) or the transesterification of vegetable oils with dimethyl carbonate to yield simultaneously fatty acid methylesters, i.e. biodiesel, and glycerol carbonate through enzymatic and other catalytic processes (Dawodu et al., 2014; Jo et al., 2014; Kai et al., 2014).

Without the shadow of a doubt, the procedure that has drawn the most attention is the transesterification of glycerol with organic carbonates, especially owing to the

fact that the reaction conditions are milder than those used in the aforementioned processes (Teng et al., 2014). The key aspect of this process appears to be the presence of a basic medium within which the reaction mechanism is triggered (Alvarez et al., 2012; Ochoa-Gomez et al., 2009). In this line, several authors have tried to approach this reaction with dialkyl carbonates like dimethyl carbonate (DMC) using K_2CO_3 (Rokicki et al., 2005), CaO (Simanjuntak et al., 2011) or Al-Mg based hydrotalcites supported on hexagonal silica (Yadav & Chandan, 2014) as catalysts. On the other hand, the synthesis of GC can be completed employing a cyclic carbonate like ethylene carbonate (EC), for which Al-Ca hydrotalcites (Climent et al., 2010) or ionic liquids supported on mesoporous MCM-41 (Cho et al., 2010) have been employed. Figure 1 represents these two reactions.

With a low presence of the products of reactions {a} and {b}, glycerol has proven to have a limited miscibility with DMC and EC. When GC generates together with methanol, in the former case, and ethylene glycol, in the latter, the system becomes entirely miscible with a transition from a biphasic liquid-liquid system to a single-phase liquid taking place (Esteban et al., 2014a; Esteban et al., 2014b). In turn, this feature has proven of importance when determining a kinetic model for reaction {a} using K_2CO_3 as catalyst (Esteban et al., 2015).

The use of methoxides as catalysts has been reported in literature by way of a few examples. For instance, sodium methoxide has been employed to conduct the transesterification of canola oil with dimethyl carbonate, with the authors claiming that this catalyst is highly active (Kai et al., 2014) or to achieve the esterification of free fatty acids of crude biodiesel (Zeng et al., 2014)[bmim][Br] to achieve the electrochemical valorisation of CO_2 giving DMC as a productThe work presented herein deals with the solventless synthesis of GC approached via the transesterification of glycerol using DMC and EC catalyzed using potassium methoxide. The aim of this study is to analyse the evolution of said reactions and supply more kinetic information on these processes considering the scarcity of this type of studies in literature.

2. Materials and Methods

2.1. Materials

Experiments were completed using the following chemicals: extra pure glycerol (assay grade 99.88%) from Fischer Chemical; dimethyl carbonate (purity>99%), kindly

donated by UBE Corporation Europe and ethylene carbonate (synthesis grade, purity>99%) from Scharlau as the reactant species. Potassium methoxide (diluted in methanol 25% v/v) from Sigma-Aldrich and potassium carbonate (purity>99%) from Alfa Aesar were used as catalysts. For the calibration of the HPLC analysis, the following were used: glycerol carbonate (purity≥99.5%) from Sigma-Aldrich, HPLC grade methanol (assay grade, 99.99%) from Scharlau Chemie and anhydrous ethylene glycol (purity>99.8%) from Sigma-Aldrich; finally, citric acid ACS reagent (purity ≥99.5%) from Sigma-Aldrich was used as internal standard.

2.2. Experimental setup, procedure and analysis

The experimental device has been explained in detail elsewhere (Esteban et al., 2015). It basically consists of a setup conceived to perform the reaction in batch operation.

After loading the reactor with the corresponding amounts of glycerol and DMC or EC, depending on the case, the reactants were stirred and heated to the desired temperatures. Once the temperature set point was reached, different amounts of potassium methoxide were added to conduct reactions throughout which samples are withdrawn and analysed.

Samples were analysed making use of HPLC. The particular details of the analytical methodology pertaining to this work have also previously been described (Esteban et al., 2015). It is worthwhile remarking that the same analytical procedure provides adequate resolution of the peaks corresponding to the components existing in reactions {a} and {b}. Thus, appropriate identification and quantification of the chemical species could be made.

In addition to the quantification of the components present in each sample during the course of the reaction, presence of potassium was determined during the first stages of the reaction with a Quantofix® potassium commercial test, supplied by Macherey-Nagel. To ease the separation of phases, samples were centrifuged with Thermo Scientific Heraeus Pico 17.

2.3. Mathematical methods

Multiple data from the evolution of the components with time were collected, and several kinetic models were proposed and correlated to these experimental observations. These models were fitted using the software Aspen Custom Modeler,

which implements a Levenberg-Marquardt algorithm coupled with a fourth order Runge-Kutta numerical integration in order to perform the correlation. The models were first correlated separately to experimental data at a fixed temperature to obtain a first estimate of the activation energy. Then, multivariable regression of all the data simultaneously at various conditions for each of the systems herein studied was made.

Models were proposed based on physicochemical assumptions, though models were finally selected following certain statistical criteria related to the goodness of fit. The next parameters were evaluated: Fischer's F (*F*), residual mean squared error (*RMSE*), variation explained (*VE*) and the Akaike information criterion (*AIC*) (Akaike, 1974; Garcia-Ochoa et al., 1989). All of these parameters are adequately defined elsewhere (Esteban et al., 2015; Molinero et al., 2013) and have previously been used successfully for kinetic modeling discrimination purposes (Garcia-Ochoa et al., 1989; Molinero et al., 2014). As a general rule, the goodness of fit of the proposed models improves with an increasing value of *F* and *VE* and with a decreasing value of *AIC* and *RMSE*.

3. Results and discussion

3.1 Selectivity of the catalyst

Considering that there are no records of publications of any of the two reactions herein approached using potassium methoxide, it is considered of interest to analyse the selectivity to the product as well as the degree of compliance of material balances.

The reaction of transesterification of glycerol with organic carbonates has been described to take place via a mechanism through an intermediate species resulting from the attack of the glyceroxide anion on the carbon of the carbonate group. This intermediate will eventually cycle and give glycerol carbonate as a final product (Alvarez et al., 2012; Climent et al., 2010; Ochoa-Gomez et al., 2009). In the case of reactions {a} and {b}, the intermediate compounds would be A1 and B1, as depicted in Figure 2. In addition, these processes are usually conducted in excess of organic carbonate. Thus, the reaction could further proceed between glycerol carbonate and the excess of the mentioned reactants; in this line, Rokicki observed the presence of the product from the reaction between DMC and GC when using a 10-fold excess of the former (Rokicki et al., 2005). The potential products from the described reactions with DMC and EC are shown in Figure 2 as A2 and B2, respectively.

Figure 3a shows the chromatogram from a sample withdrawn from the reaction medium of reaction {a}. It features the internal standard as well as the two reactant species, DMC and glycerol, and the products GC and methanol, all of them identified adequately. In addition, given that no standards were available for the species A1 and A2, the two minor peaks appearing at retention times of 7.2 and 9.6 min, respectively, could be identified following the evolution of their signals with respect to that of the internal standard, as shown in Figure 3b. It can be seen that the progress of the signals throughout time corresponds to those typical of an intermediate species in the case of A1 and a product of a further reaction in-series in the case of A2.

Likewise, Figure 4a features all the components present in reaction {b}, in which identification of the species B1 and B2 was made on the basis of the evolution observed in Figure 4b.

In spite of the mentioned species being present in the two reactions, the compliance of the material balances considering the major components of each reaction could be achieved to satisfaction in both cases. In the case of reaction {a}, the maximal error in closing the balance was only as high as 5.1%, while that of reaction {b} was 4.4%. It is worthwhile remarking that these figures include the presence of A1 and A2 as well B1 and B2 together with any experimental error derived from sample manipulation and analysis.

This almost entirely complete selectivity to GC observed in reactions {a} and {b} allow for the consideration of a simple reaction rather than a system of various in-series reactions. In addition, the variable conversion X is defined in equation 1 and will be considered in the discussion of the results. It basically computes an average value of the conversion as obtained from the quantification of the major components of each reaction in light of the accuracy of the analysis is high and single reactions are being considered.

$$X = \frac{\sum_{i=1}^{n} \frac{|C_i - C_{i0}|}{\nu_i}}{\frac{n}{C_{Gly0}}} \qquad (1)$$

where C_i and C_{i0} refer to the concentration of each component at a certain time and at the start of the reaction, respectively; C_{Gly0} stands for the initial concentration of

glycerol; v_i is the stoichiometric coefficient of each component and, finally, n is the total number of components consider (n=4 for both reactions).

3.2. Description of the development of the reactions

As appointed in the introduction, both reacting systems initially constitute liquid-liquid biphasic systems owing to the limited miscibility between DMC and Gly in the case of reaction {a} and EC and Gly in reaction {b} that evolves into single phase liquid systems. In a previous work, we followed the progress of the chemical species of reaction {a} together with the physical evolution of the system by monitoring the chord length of the existing dispersion as it disappeared during the course of the reaction. It was found that no chords, and thus no droplets of dispersed phase, were counted after a time span at which the conversion was 0.30 (Esteban et al., 2015). This value corresponds to a composition of the reacting system agreeing with the curve separating the biphasic and monophasic liquid regions measured in the liquid-liquid equilibria of the quaternary system comprising {DMC + MeOH + GC + Gly} (Esteban et al., 2014b).

3.3. Influence of the operating variables

First, considering potential mass transfer limitation problems due to the presence of two liquid phases at the initial stages of the reaction, the stirring speeds were fixed at 1500 rpm for reaction {a} (Esteban et al., 2015) and 800 rpm for reaction {b}. Under those stirring conditions, the variables that typically show an effect on the kinetics and conversion at equilibrium were evaluated for both reactions.

Figure 5 depicts the evolution of reaction {a} showing the influence of temperature (50-70 ºC) (a), molar excess of DMC to glycerol (1.5-3) (b) and concentration of catalyst (1000-2500 ppm) (c). From the plots, it can be easily seen that temperature and the amount of catalyst have a positive effect on the kinetics, though the effect of the molar excess does not appear to be so clear.

Likewise, Figure 6 shows the evolution of selected kinetic runs performed for reaction {b} varying the same variables as above within other levels: temperature (40-50 ºC) (a), molar excess of EC to glycerol (1.5-3) (b) and concentration of CH_3OK (50-150 ppm) (c). The selection of 40 ºC as the lowest value of the temperature interval holds significance due to EC solidifying at approximately 37 ºC.

It is remarkable that despite the conversion of glycerol achieving very high values, it did not reach 100% in any of the two reactions, meaning that either chemical equilibrium is being reached or the catalyst undergoes deactivation.

3.4. Kinetic modeling

According to the development of the reaction described above, a phenomenological kinetic model was proposed and verified for reaction {a} using K_2CO_3 as catalyst. This model consisted on the utilization of two equations before and after a value of the conversion defined as critical conversion, X_{crit}, and these equations were based on potential laws in which different concentrations of catalyst were contemplated. The first describes the progress under the biphasic regime, during which the reaction only takes place in the glycerol-rich phase, where the catalyst is soluble at a concentration of C_{cat}'; hence, a first order was assumed with respect to the concentration of glycerol and a zero order to that of DMC, which reacts within this phase at a constant concentration C_{DMCsol}. The second equation, for its part, accounts for the single phase stage and considers that the catalyst is dissolved in the entire reaction medium at C_{cat}; during this second part, first order was assumed with respect to the concentrations of both reactants. (Esteban et al., 2015)

The utilization of potassium methoxide should trigger the reaction mechanism by the formation of a glyceroxide anion, thus being potassium present only in the glycerol-phase (Alvarez et al., 2012; Ochoa-Gomez et al., 2009). As a means to confirm this end, the presence of potassium was tested in the two phases after removing samples at 30 seconds in experiments of both reactions and separating phases (conditions for reaction {a}: T=50 ºC; M=3; C_{cat}=2500 ppm; conditions for reaction {b}: T=40 ºC; M=3; C_{cat}=150 ppm). As expected, potassium was detected solely in the glycerol-rich phase.

Seeing that the phase change regime has an evident effect on the kinetic behaviour of this type of systems due to the catalyst performing at different effective concentrations, a number of models is presented for reactions {a} and {b} using potassium methoxide on this basis.

3.4.1. Kinetics of reaction {a}: transesterification of glycerol with dimethyl carbonate

A total of 20 kinetic runs were conducted to obtain enough experimental data to perform a reliable fitting of the models. First, the data collected were observed, realising

that there was a change of trend of the data at conversion values between 0.30 and 0.35, which is in accordance with was observed for the reaction catalyzed by K_2CO_3. For this reason, X_{crit} will be set as 0.30 (Esteban et al., 2015).

Table 1 gathers the four kinetic models proposed to describe the reaction. Model {a}1 presents two equations representing an irreversible reaction, while Model {a}2, on the other hand, proposes that the reaction is indeed reversible.

However, more complex models were contemplated considering the nature of the catalyst and its potential deactivation. The utilization of calcium methoxide had already been investigated for the transesterification of DMC and glycerol and it was observed that this catalyst suffered from deactivation. Such deactivation process takes place through a complex reaction network in which calcium methoxide is eventually transformed into basic calcium carbonate, represented by the formula $Ca_x(OH)_y(CO_3)_z$, whose basic strength is much lower than the original $Ca(CH_3O)_2$ or calcium diglyceroxide, which is the species initiating the reaction mechanism for reaction {a} (Li & Wang, 2011). Subsequently, Models {a}3 and {a}4 are herein presented to take into account a first order catalyst deactivation in which an analogous basic potassium carbonate species would be formed. Of these two, the former advocates for an irreversible reaction and the latter for a reversible one.

In addition to the equations compiled in Table 1, further consideration of the Arrhenius equation to account for temperature as a variable, as stated in equation 2, is considered:

$$ln\, k_{\{a\}i} = ln\, k_{\{a\}i0} - \frac{E_{a\{a\}i}}{R} \cdot \frac{1}{T} \qquad (2)$$

in which $k_{\{a\}i}$ is each of the $_i$ kinetic constants of reaction {a}, $k_{\{a\}i0}$ is the preexponential factor, $E_{a\{a\}i}$ stands for the activation energy and finally R is the ideal gas constant.

Table 2 summarizes the kinetic parameters retrieved from multivariable correlation as well as the statistical criteria computed for comparison purposes. One of the first things that may strike attention is the high degree of similarity among the statistical criteria, especially *AIC*, *RMSE* and *VE*. In principle, this would leave *F* as the criterion to decide which one would be the most adequate in statistical terms. Following that logic, Model {a}1 should be selected.

Notwithstanding, statistical criteria by themselves should not be fully relied on and further physicochemical criteria must be contemplated. First, the value of C_{DMCsol} obtained for Models {a}1 and {a}2, 10.56 and 9.05 mol·L^{-1}, are too high considering that it represents the concentration of DMC in the glycerol-rich phase during the first part of the reaction. Also, the identical values attained for Models {a}3 and {a}4, 3.56 mol·L^{-1} are in good agreement for those observed when K_2CO_3 was employed, 3.34 mol·L^{-1} (Esteban et al., 2015).

Additionally, from the discussion above on the possible deactivation of the catalyst, it appears obvious that this process can be taking place to a noticeable extent, especially because small concentrations of catalyst (1000-2500 ppm) are used in this work. This would leave Models {a}3 and {a}4 from which to decide in the end. However, the unusually high value of the activation energy estimated for the reverse reaction and its remarkably high error, 305.7 ± 68.5 kJ·mol^{-1}, together with a much lower value of the *F* renders Model {a}4 statistically less significant. Consequently, Model {a}3, with an activation energy of 28.4 ± 1.5 kJ·mol^{-1}, is selected as the most representative.

Finally, Figure 7 validates Model {a}3, in which it can be seen that the predicted values rarely differ more than ±15% with respect to observed data.

3.4.2. Kinetics of reaction {b}: transesterification of glycerol with ethylene carbonate

In this case, 16 batch experiments were undertaken to acquire sufficient experimental data. After individual analysis of each of the experiments, yet again a change in the kinetic trend was identified; nevertheless, unlike in the case of reaction {a}, where X_{crit} remained virtually constant under the varying conditions tested, the value of X_{crit} showed certain degree of dependence with respect to the three variables tested. Figure 8a, 8b and 8c show that X_{crit} increases as temperature and concentration of catalyst rise. The effect of the molar excess of EC also appears positive if the three graphs are compared, though to a lesser extent. For this reason, distinct values of the critical conversion will be considered individually when fitting the models to the data.

Table 3 shows the two models regarded for this reaction, both of which consider the reversible reaction seeing that after as many as 7 hours of reaction, total conversion of glycerol was not achieved in any of the experiments performed (see Figure 6 for a few runs). Model {b}1 considers no deactivation, while Model {b}2 accounts for a first

order deactivation again on the basis of the same situation taking place as described before.

Table 4 compiles the kinetic parameters and statistical criteria after fitting the models to the experimental data. In this case, it is much more evident to see that a model accounting for the deactivation of the catalyst yields much better results than one ignoring it. All the statistical criteria evaluated point in that direction and the values of the parameters considering physicochemical criteria do not say otherwise. A C_{ECsol} value of 1.11 $mol \cdot L^{-1}$ is achieved, which appears very reasonable, and the activation energies for the direct and reverse reactions are 82.3 ± 3.0 $kJ \cdot mol^{-1}$ and 53.5 ± 21.6 $kJ \cdot mol^{-1}$, respectively.

Similarly, Figure 9 validates the Model {b}2 with errors of estimation of data below ±15% compared to the experimental values.

3.5. Comparison of the use of K_2CO_3 and CH_3OK as catalysts

The search for the mildest operating conditions in pursuance of sustainability is one of the main objectives of the development of the so-called Green Processes (Anastas & Warner, 2008). For this reason, it was considered of significance to compare the use of potassium methoxide with potassium carbonate in each of the reactions.

First, for reaction {a}, it was found that using CH_3OK, the interval could be increased significantly to operate with acceptable performance with respect to the utilization of K_2CO_3, whose activity below 66 ºC was found to be very low, probably due to solubilisation issues below this temperature (Esteban et al., 2015). For comparison purposes, data obtained at 66 and 70 ºC will be used herein. As for reaction {b}, in addition to the kinetic experiments completed with CH_3OK to deduce a kinetic model, two additional experiments were completed using K_2CO_3 as catalyst at 40 and 50 ºC, the lowest and highest temperatures of the interval previously tested.

Table 5 summarizes the conditions of temperature and molar excess of organic carbonate to glycerol utilized to perform these analogous reactions. As a basis to compare the performance of the catalysts under the same conditions, the turnover frequency (TOF) was computed according to:

$$TOF = \frac{r_0}{C_{cat}} \tag{3}$$

where r_0 stands for the initial rate of reaction and C_{cat} is the concentration of catalyst, the former being computed from the differentiation of the kinetic data for each run (curves not shown).

As can be seen from the values of all the runs conducted, comparing one reaction to the other, the catalysts acquire much higher TOF values in reaction {b}, even operating at lower temperatures. Comparing individually reaction {a}, it can be observed from the runs at the same temperature, that the use of CH_3OK increases the TOF as much as 19.89 times at 66 ºC (runs 1 and 2) and 17.31 at 70 ºC (runs 3 and 4). On the other hand, in the case of reaction {b}, employing CH_3OK also increased the performance, though not as much as in the other reaction, being the relative increase of the TOF 6.57 and 5.36 at 40 (runs 7 and 8) and 50 ºC (runs 9 and 10), respectively.

Finally, Table 5 also includes a comparison with TOF values computed for other references from which sufficient kinetic data were available to obtain a value of the initial rate of reaction. In the case of reaction {a}, it can be seen that a TOF value above 8 (Run 5) was reached utilizing Al-Mg-based calcined hydrotalcites, though the reaction conditions were much more demanding than in our case and methanol was used as a solvent (Yadav & Chandan, 2014). On the other hand, when calcium oxide was employed as catalyst (Run 6) under similar conditions to those tested in Runs 1 through 4, the TOF value was 0.41(Simanjuntak et al., 2011), which is comparable yet still lower than that achieved using K_2CO_3. For reaction {b}, the computed TOF value employing an ionic liquid-based catalyst (Run 11) (Cho et al., 2010) was of approximately one and two orders of magnitude lower than those using K_2CO_3 and CH_3OK, respectively, even operating at a higher temperature. Finally, Run 12 shows the activity of magnesium oxide at 50 ºC (Climent et al., 2010), which compared to Runs 9 and 10, at the same temperature, shows an activity of a thousand times less than that of CH_3OK and about two hundred times lower than K_2CO_3, respectively.

4. Conclusions

The synthesis of glycerol carbonate via the transesterification of glycerol with dimethyl carbonate and ethylene carbonate using CH_3OK as catalyst was investigated. This catalyst proved to have a virtually complete selectivity to the desired product in both reactions.

A series of kinetic runs were completed under mild conditions and kinetic models were proposed, describing the progress before and after the transition from biphasic to single phase reacting liquid systems. In addition, these models took into account first order deactivation of the catalyst.

Finally, the use of CH_3OK was compared to other catalysts, proving that it is far more active than other examples in the literature.

Acknowledgements

The authors wish to express gratitude to the Spanish Ministry of Science and Innovation (Projects CTQ2007-60919 and CTQ2010-15460) for financial support and UBE Corporation for kindly supplying dimethyl carbonate for this work.

List of abbreviations

Components

A1	2,3-dihydroxypropyl methyl carbonate
A2	Methyl ((2-oxo-1,3-dioxolan-4-yl)methyl) carbonate
B1	2,3-dihydroxypropyl (2-hydroxyethyl) carbonate
B2	(2-oxo-1,3-dioxolan-4-yl)methyl propyl carbonate
DMC	Dimethyl carbonate
EC	Ethylene carbonate
EG	Ethylene glycol
GC	Glycerol carbonate
Gly	Glycerol
MeOH	Methanol

Nomenclature

{a}	Refers to the transesterification of glycerol with DMC
AIC	Akaike's information criterion
{b}	Refers to the transesterification of glycerol with EC
C	Concentration ($mol \cdot L^{-1}$)

E_{ai}/R	Ratio of activation energy and the ideal gas constant (K)
F	Fischer's F statistical parameter
HPLC	High-performance liquid chromatography
k	Kinetic constant
M	Initial molar ratio of dimethyl carbonate to glycerol
n	Total number of components
r	reaction rate ($mol \cdot L \cdot min^{-1}$)
RMSE	Residual mean squared error
T	Temperature (K)
TOF	Turnover frequency, defined in equation 3 (mol converted·mol $catalyst^{-1} \cdot min^{-1}$)
VE	Variation explained (%)
X	Conversion, as defined by equation (1)

Greek letters

v	Stoichiometric coefficient of the component i

Subscripts

0	Relative to the start of the reaction, time equals zero
i	Relative to component i
cat	Relative to the catalyst
crit	Relative to the critical conversion at which the kinetic behaviour changes
DMCsol	Relative to concentration of DMC dissolved in the glycerol-rich phase
ECsol	Relative to concentration of EC dissolved in the glycerol-rich phase

Superscripts

'	Refers to the concentration of catalyst throughout the first stage of the reaction

References

Akaike, H. 1974. A new look at the statistical model identification. *IEEE Transactions on Automatic Control*, **19**(6), 716-723.

Alvarez, M.G., Pliskova, M., Segarra, A.M., Medina, F., Figueras, F. 2012. Synthesis of glycerol carbonates by transesterification of glycerol in a continuous system using supported hydrotalcites as catalysts. *Applied Catalysis B-Environmental*, **113**, 212-220.

Anastas, P., Warner, J. 2008. *Green Chemistry Theory and Practice.* Oxford University Press, New York.

Aresta, M., Dibenedetto, A., Nocito, F., Pastore, C. 2006. A study on the carboxylation of glycerol to glycerol carbonate with carbon dioxide: The role of the catalyst, solvent and reaction conditions. *Journal of Molecular Catalysis A: Chemical*, **257**(1-2), 149-153.

Ayoub, M., Khayoon, M.S., Abdullah, A.Z. 2012. Synthesis of oxygenated fuel additives via the solventless etherification of glycerol. *Bioresource Technology*, **112**, 308-312.

Behr, A., Eilting, J., Irawadi, K., Leschinski, J., Lindner, F. 2008. Improved utilisation of renewable resources: New important derivatives of glycerol. *Green Chemistry*, **10**(1), 13-30.

Benoit, M., Brissonnet, Y., Guélou, E., De Oliveira Vigier, K., Barrault, J., Jérôme, F. 2010. Acid-Catalyzed Dehydration of Fructose and Inulin with Glycerol or Glycerol Carbonate as Renewably Sourced Co-Solvent. *ChemSusChem*, **3**(11), 1304-1309.

Brooker, A.T. 2011. Solid detergent composition comprising glycerol carbonate, Procter & Gamble.

Casas, A., Jesus Ramos, M., Perez, A. 2011. Kinetics of chemical interesterification of sunflower oil with methyl acetate for biodiesel and triacetin production. *Chemical Engineering Journal*, **171**(3), 1324-1332.

Climent, M.J., Corma, A., De Frutos, P., Iborra, S., Noy, M., Velty, A., Concepción, P. 2010. Chemicals from biomass: Synthesis of glycerol carbonate by transesterification and carbonylation with urea with hydrotalcite catalysts. The role of acid-base pairs. *Journal of Catalysis*, **269**(1), 140-149.

Cho, H.-J., Kwon, H.-M., Tharun, J., Park, D.-W. 2010. Synthesis of glycerol carbonate from ethylene carbonate and glycerol using immobilized ionic liquid catalysts. *Journal of Industrial and Engineering Chemistry*, **16**(5), 679-683.

Dawodu, F.A., Ayodele, O.O., Xin, J., Zhang, S. 2014. Dimethyl carbonate mediated production of biodiesel at different reaction temperatures. *Renewable Energy*, **68**, 581-587.

Esteban, J., Fuente, E., Blanco, A., Ladero, M., Garcia-Ochoa, F. 2015. Phenomenological kinetic model of the synthesis of glycerol carbonate assisted by focused beam reflectance measurements. *Chemical Engineering Journal*, **260**, 434-443.

Esteban, J., Ladero, M., Garcia-Ochoa, F. 2014a. Liquid-liquid equilibria for the ternary systems ethylene carbonate-ethylene glycol-glycerol; ethylene carbonate-glycerol carbonate-glycerol and the quaternary system ethylene carbonate-ethylene glycol-glycerol carbonate-glycerol at catalytic reacting temperatures.

Chemical Engineering Research and Design. DOI: doi:10.1016/j.cherd.2014.08.024.

Esteban, J., Ladero, M., Molinero, L., Garcia-Ochoa, F. 2014b. Liquid-liquid equilibria for the ternary systems DMC-methanol-glycerol; DMC-glycerol carbonate-glycerol and the quaternary system DMC-methanol-glycerol carbonate-glycerol at catalytic reacting temperatures. *Chemical Engineering Research and Design.*, **92**, 1797-1805.

Garcia-Herrero, I., Alvarez-Guerra, M., Irabien, A. 2014. Electrosynthesis of dimethyl carbonate from methanol and CO_2 using potassium methoxide and the ionic liquid [bmim][Br] in a filter-press cell: a study of the influence of cell configuration. *Journal of Chemical Technology & Biotechnology. DOI: 10.1002/jctb.4605.*

Garcia-Ochoa, F., Romero, A., Querol, J. 1989. Modeling of the thermal normal-octane oxidation in the liquid phase. *Industrial & Engineering Chemistry Research*, **28**(1), 43-48.

Garcia, J.I., Garcia-Marin, H., Pires, E. 2014. Glycerol based solvents: synthesis, properties and applications. *Green Chemistry*, **16**(3), 1007-1033.

George, J., Patel, Y., Pillai, S.M., Munshi, P. 2009. Methanol assisted selective formation of 1,2-glycerol carbonate from glycerol and carbon dioxide using (Bu_2SnO)-Bu-n as a catalyst. *Journal of Molecular Catalysis A: Chemical*, **304**(1-2), 1-7.

Ghandi, M., Mostashari, A., Karegar, M., Barzegar, M. 2007. Efficient synthesis of alpha-monoglycerides via solventless condensation of fatty acids with glycerol carbonate. *Journal of the American Oil Chemists Society*, **84**(7), 681-685.

Hu, J., Li, J., Gu, Y., Guan, Z., Mo, W., Ni, Y., Li, T., Li, G. 2010. Oxidative carbonylation of glycerol to glycerol carbonate catalyzed by $PdCl_2$(phen)/KI. *Applied Catalysis A: General*, **386**(1-2), 188-193.

Jo, Y.J., Lee, O.K., Lee, E.Y. 2014. Dimethyl carbonate-mediated lipid extraction and lipase-catalyzed in situ transesterification for simultaneous preparation of fatty acid methyl esters and glycerol carbonate from Chlorella sp KR-1 biomass. *Bioresource Technology*, **158**, 105-110.

Jogunola, O., Salmi, T., Kangas, M., Mikkola, J.P. 2012. Determination of the kinetics and mechanism of methyl formate synthesis in the presence of a homogeneous catalyst. *Chemical Engineering Journal*, **203**, 469-479.

Kai, T., Mak, G.L., Wada, S., Nakazato, T., Takanashi, H., Uemura, Y. 2014. Production of biodiesel fuel from canola oil with dimethyl carbonate using an active sodium methoxide catalyst prepared by crystallization. *Bioresource Technology*, **163**, 360-363.

Khayoon, M.S., Hameed, B.H. 2011. Acetylation of glycerol to biofuel additives over sulfated activated carbon catalyst. *Bioresource Technology*, **102**(19), 9229-9235.

Kim, D.-W., Park, K.-A., Kim, M.-J., Kang, D.-H., Yang, J.-G., Park, D.-W. 2014. Synthesis of glycerol carbonate from urea and glycerol using polymer-supported metal containing ionic liquid catalysts. *Applied Catalysis A: General*, **473**, 31-40.

Kovvali, A.S., Sirkar, K.K. 2002. Carbon dioxide separation with novel solvents as liquid membranes. *Industrial & Engineering Chemistry Research*, **41**(9), 2287-2295.

Lameiras, P., Boudesocque, L., Mouloungui, Z., Renault, J.-H., Wieruszeski, J.-M., Lippens, G., Nuzillard, J.-M. 2011. Glycerol and glycerol carbonate as

ultraviscous solvents for mixture analysis by NMR. *Journal of Magnetic Resonance*, **212**(1), 161-168.
Lamers, P., Hamelinck, C., Junginger, M., Faaij, A. 2011. International bioenergy trade-A review of past developments in the liquid biofuel market. *Renewable & Sustainable Energy Reviews*, **15**(6), 2655-2676.
Lee, S.-D., Park, M.-S., Kim, D.-W., Kim, I., Park, D.-W. 2014. Catalytic performance of ion-exchanged montmorillonite with quaternary ammonium salts for the glycerolysis of urea. *Catalysis Today*, **232**, 127-133.
Li, J., Wang, T. 2011. On the deactivation of alkali solid catalysts for the synthesis of glycerol carbonate from glycerol and dimethyl carbonate. *Reaction Kinetics Mechanisms and Catalysis*, **102**(1), 113-126.
Luo, X., Hu, S., Zhang, X., Li, Y. 2013. Thermochemical conversion of crude glycerol to biopolyols for the production of polyurethane foams. *Bioresource Technology*, **139**, 323-329.
Magniont, C., Escadeillas, G., Oms-Multon, C., De Caro, P. 2010. The benefits of incorporating glycerol carbonate into an innovative pozzolanic matrix. *Cement and Concrete Research*, **40**(7), 1072-1080.
Molinero, L., Ladero, M., Tamayo, J.J., Esteban, J., Garcia-Ochoa, F. 2013. Thermal esterification of cinnamic and p-methoxycinnamic acids with glycerol to cinnamate glycerides in solventless media: A kinetic model. *Chemical Engineering Journal*, **225**, 710-719.
Molinero, L., Ladero, M., Tamayo, J.J., Garcia-Ochoa, F. 2014. Homogeneous catalytic esterification of glycerol with cinnamic and methoxycinnamic acids to cinnamate glycerides in solventless medium: Kinetic modeling. *Chemical Engineering Journal*, **247**, 174-182.
Nemirowsky, J. 1885. Über die Einwirkung von Chlorkohlenoxyd auf Glycolchlorhydrin. *Journal für Praktische Chemie*, **31**(1), 173-175.
Nomura, T., Hayashi, T., Okutsu, M. 2006. Plant activator used for cultivating plants such as vegetables, fruits, bulbs, flowers, grains and herbs, contains carbonate compound, Kao Corp.
Ochoa-Gomez, J.R., Gomez-Jimenez-Aberasturi, O., Maestro-Madurga, B., Pesquera-Rodriguez, A., Ramirez-Lopez, C., Lorenzo-Ibarreta, L., Torrecilla-Soria, J., Villaran-Velasco, M.C. 2009. Synthesis of glycerol carbonate from glycerol and dimethyl carbonate by transesterification: Catalyst screening and reaction optimization. *Applied Catalysis A: General*, **366**(2), 315-324.
Ochoa-Gomez, J.R., Gomez-Jimenez-Aberasturi, O., Ramirez-Lopez, C., Belsue, M. 2012. A Brief Review on Industrial Alternatives for the Manufacturing of Glycerol Carbonate, a Green Chemical. *Organic Process Research & Development*, **16**(3), 389-399.
Ou, G., He, B., Yuan, Y. 2011. Lipases are soluble and active in glycerol carbonate as a novel biosolvent. *Enzyme and Microbial Technology*, **49**(2), 167-170.
Pagliaro, M., Rossi, M. 2008. *The future of glycerol. New uses for a versatile new material*. RSC Publishing, Cambridge.
Quispe, C.A.G., Coronado, C.J.R., Carvalho, J.A., Jr. 2013. Glycerol: Production, consumption, prices, characterization and new trends in combustion. *Renewable & Sustainable Energy Reviews*, **27**, 475-493.
Rokicki, G., Kuran, W., Pogorzelskamarciniak, B. 1984. Cyclic carbonates from carbon dioxide and oxiranes *Monatshefte Fur Chemie*, **115**(2), 205-214.

Rokicki, G., Rakoczy, P., Parzuchowski, P., Sobiecki, M. 2005. Hyperbranched aliphatic polyethers obtained from environmentally benign monomer: glycerol carbonate. *Green Chemistry*, **7**(7), 529-539.

Simanjuntak, F.S.H., Kim, T.K., Lee, S.D., Ahn, B.S., Kim, H.S., Lee, H. 2011. CaO-catalyzed synthesis of glycerol carbonate from glycerol and dimethyl carbonate: Isolation and characterization of an active Ca species. *Applied Catalysis A: General*, **401**(1-2), 220-225.

Sonnati, M.O., Amigoni, S., de Givenchy, E.P.T., Darmanin, T., Choulet, O., Guittard, F. 2013. Glycerol carbonate as a versatile building block for tomorrow: synthesis, reactivity, properties and applications. *Green Chemistry*, **15**(2), 283-306.

Teng, W.K., Ngoh, G.C., Yusoff, R., Aroua, M.K. 2014. A review on the performance of glycerol carbonate production via catalytic transesterification: Effects of influencing parameters. *Energy Conversion and Management*, **88**, 484-497.

Werpy, T., Petersen, G. 2004. Top value added chemicals from biomass. Volume I - Results of screening for potential candidates from sugars and synthesis gas Pacific Northwest National Laboratory. National Renewable Energy Laboratory. U.S. Department of Energy.

Yadav, G.D., Chandan, P.A. 2014. A green process for glycerol valorization to glycerol carbonate over heterogeneous hydrotalcite catalyst. *Catalysis Today*, **237**, 47-53.

Zakaria, Z.Y., Amin, N.A.S., Linnekoski, J. 2013. A perspective on catalytic conversion of glycerol to olefins. *Biomass & Bioenergy*, **55**, 370-385.

Zeng, D., Li, R., Feng, M., Fang, T. 2014. Continuous Esterification of Free Fatty Acids in Crude Biodiesel by an Integrated Process of Supercritical Methanol and Sodium Methoxide Catalyst. *Applied Biochemistry and Biotechnology*, **174**(4), 1484-1495.

Zhu, S., Zhu, Y., Gao, X., Mo, T., Zhu, Y., Li, Y. 2013. Production of bioadditives from glycerol esterification over zirconia supported heteropolyacids. *Bioresource Technology*, **130**, 45-51.

Table 1. Kinetic models proposed for the transesterification of glycerol with DMC

Model number	Rate equations	
{a}1	$r_{\{a\}1} = k_{\{a\}1} \cdot C'_{cat\{a\}} \cdot C_{Gly} \cdot C_{DMCsol}$	if $X \le X_{crit}$
	$r_{\{a\}2} = k_{\{a\}1} \cdot C'_{cat\{a\}} \cdot C_{Gly} \cdot C_{DMC}$	if $X > X_{crit}$
{a}2	$r_{\{a\}1} = k_{\{a\}1} \cdot C'_{cat\{a\}} \cdot C_{Gly} \cdot C_{DMCsol}$	if $X \le X_{crit}$
	$r_{\{a\}2} = k_{\{a\}1} \cdot C'_{cat\{a\}} \cdot C_{Gly} \cdot C_{DMC}$ $r_{\{a\}3} = k_{\{a\}3} \cdot C'_{cat\{a\}} \cdot C_{GC} \cdot C_{MeOH}$	if $X > X_{crit}$
{a}3	$r_{\{a\}1} = k_{\{a\}1} \cdot C'_{cat\{a\}} \cdot \left(\left(1-\beta_{\{a\}}\right)\exp\left(-k_{\{a\}d} \cdot t\right)+\beta_{\{a\}}\right) C_{Gly} \cdot C_{DMCsol}$	if $X \le X_{crit}$
	$r_{\{a\}2} = k_{\{a\}1} \cdot C'_{cat\{a\}} \cdot \beta_{\{a\}} \cdot C_{Gly} \cdot C_{DMC}$	if $X > X_{crit}$
{a}4	$r_{\{a\}1} = k_{\{a\}1} \cdot C'_{cat\{a\}} \cdot \left(\left(1-\beta_{\{a\}}\right)\exp\left(-k_{\{a\}d} \cdot t\right)+\beta_{\{a\}}\right) C_{Gly} \cdot C_{DMCsol}$	if $X \le X_{crit}$
	$r_{\{a\}2} = k_{\{a\}1} \cdot C'_{cat\{a\}} \cdot \beta_{\{a\}} \cdot C_{Gly} \cdot C_{DMC}$ $r_{\{a\}3} = k_{\{a\}3} \cdot C'_{cat\{a\}} \cdot \beta_{\{a\}} \cdot C_{GC} \cdot C_{MeOH}$	if $X > X_{crit}$

Table 2. Kinetic and statistical parameters retrieved for the kinetic models proposed for the transesterification of glycerol and DMC catalyzed with potassium methoxide

Model	Parameter	Value	±error	F	AIC	RMSE	Variation explained (%)
{a}1	$\ln k_{\{a\}10}$	4.34	0.46	18198	-2250	0.0517	97.12
	$E_{a\{a\}1}/R$	3618	152				
	C_{DMCsol}	10.56	0.41				
{a}2	$\ln k_{\{a\}10}$	5.87	0.48	11860	-2285	0.0484	97.31
	$E_{a\{a\}1}/R$	4100	159				
	$\ln k_{\{a\}30}$	81.28	37.63				
	$E_{a\{a\}3}/R$	30662	12812				
	C_{DMCsol}	9.05	0.39				
{a}3	$\ln k_{\{a\}10}$	4.84	0.51	10455	-2247	0.0500	97.16
	$E_{a\{a\}1}/R$	3408	182				
	$k_{\{a\}d}$	0.03	0.01				
	$\beta_{\{a\}}$	0.32	0.02				
	C_{DMCsol}	3.56	0.68				
{a}4	$\ln k_{\{a\}10}$	6.68	0.56	7895	-2286	0.0489	97.13
	$E_{a\{a\}1}/R$	4028	196				
	$\ln k_{\{a\}20}$	99.27	21.56				
	$E_{a\{a\}2}/R$	36764	8235				
	$k_{\{a\}d}$	0.03	0.01				
	$\beta_{\{a\}}$	0.36	0.05				
	C_{DMCsol}	3.56	0.72				

Table 3. Kinetic models proposed for the transesterification of glycerol with EC

Model number	Rate equations	
{b}1	$r_{\{b\}1} = k_{\{b\}1} \cdot C'_{cat\{b\}} \cdot C_{Gly} \cdot C_{ECsol}$	if $X \leq X_{crit}$
	$r_{\{b\}2} = k_{\{b\}1} \cdot C'_{cat\{b\}} \cdot C_{Gly} \cdot C_{EC}$ $r_{\{b\}3} = k_{\{b\}3} \cdot C'_{cat\{b\}} \cdot C_{GC} \cdot C_{EG}$	if $X > X_{crit}$
{b}2	$r_{\{b\}1} = k_{\{b\}1} \cdot C'_{cat\{b\}} \cdot \left(\left(1 - \beta_{\{b\}} \right) \exp\left(- k_{\{b\}d} \cdot t \right) + \beta_{\{b\}} \right) C_{Gly} \cdot C_{ECsol}$	if $X \leq X_{crit}$
	$r_{\{b\}2} = k_{\{b\}1} \cdot C'_{cat\{b\}} \cdot \beta_{\{b\}} \cdot C_{Gly} \cdot C_{EC}$ $r_{\{b\}3} = k_{\{b\}3} \cdot C'_{cat\{b\}} \cdot \beta_{\{b\}} \cdot C_{GC} \cdot C_{EG}$	if $X > X_{crit}$

Table 4. Kinetic and statistical parameters of the kinetic models proposed for the transesterification of glycerol and EC

Model	Parameter	Value	±error	F	AIC	RMSE	Variation explained (%)
{b}1	$\ln k_{\{b\}10}$	38.45	5.08	1263	-986	139	79.14
	$E_{a\{b\}1}/R$	12404	1618				
	$\ln k_{\{b\}30}$	21.49	8.46				
	$E_{a\{b\}3}/R$	7129	2690				
	C_{ECsol}	3.17	0.72				
{b}2	$\ln k_{\{b\}10}$	30.91	1.11	9479	-1588	0.042	98.16
	$E_{a\{b\}1}/R$	9897	361				
	$\ln k_{\{b\}30}$	14.03	8.16				
	$E_{a\{b\}3}/R$	6431	2607				
	$k_{\{b\}d}$	0.31	0.03				
	$\beta_{\{b\}}$	0.020	0.001				
	C_{ECsol}	1.11	0.12				

Table 5. Comparison of TOF using K_2CO_3 and CH_3OK with other catalysts reported in literature for the two reactions herein studied

Reaction {a}: DMC + Gly → GC + 2 MeOH					
Run	**Conditions**				**TOF[a]**
	Catalyst	**T (ºC)**	**M**	**C_{cat} (g/L)**	**(mol converted·mol catalyst^{-1}·min^{-1})**
1	CH_3OK	66	3	2.78	11.77
2[b]	K_2CO_3	66	3	14.12	0.59
3	CH_3OK	70	3	2.78	19.10
4[b]	K_2CO_3	70	3	14.12	1.10
5[c]	Al:Mg hydrotalcite[d]	180[e]	3	2	8.34
6[f]	CaO	75	2	11.31	0.41
Reaction {b}: EC + Gly → GC + EG					
Run	**Conditions**				**TOF[a]**
	Catalyst	**T (ºC)**	**M**	**C_{cat} (g/L)**	**(mol converted·mol catalyst^{-1}·min^{-1})**
7	CH_3OK	40	3	0.24	118.00
8	K_2CO_3	40	3	0.79	17.96
9	CH_3OK	50	3	0.24	273.31
10	K_2CO_3	50	3	0.79	50.91
11[g]	RNX-MCM41	80	2	40.35	2.92
12[h]	MgO	50	2	90.91	0.24

[a]computed on the basis of the active species of the catalyst when not a pure chemical
[b](Esteban et al., 2015)
[c](Yadav & Chandan, 2014)
[d]Al:Mg (1:2) calcined hydrotalcita supported on hexagonal silica
[e]Methanol as solvent. P=17 atm
[f](Simanjuntak et al., 2011)
[g](Cho et al., 2010)
[h](Climent et al., 2010)

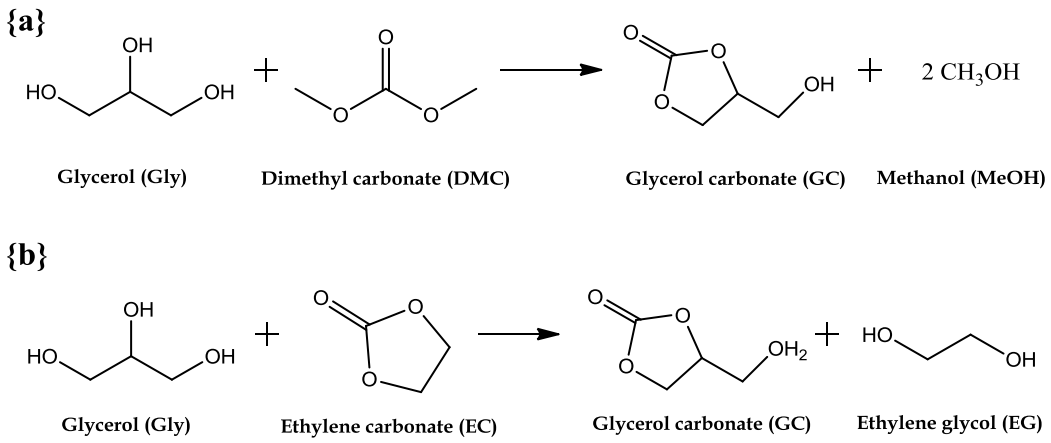

Figure 1. Transesterification of glycerol with (a) dimethyl carbonate to yield glycerol carbonate and methanol and (b) ethylene carbonate to yield glycerol carbonate and ethylene glycol.

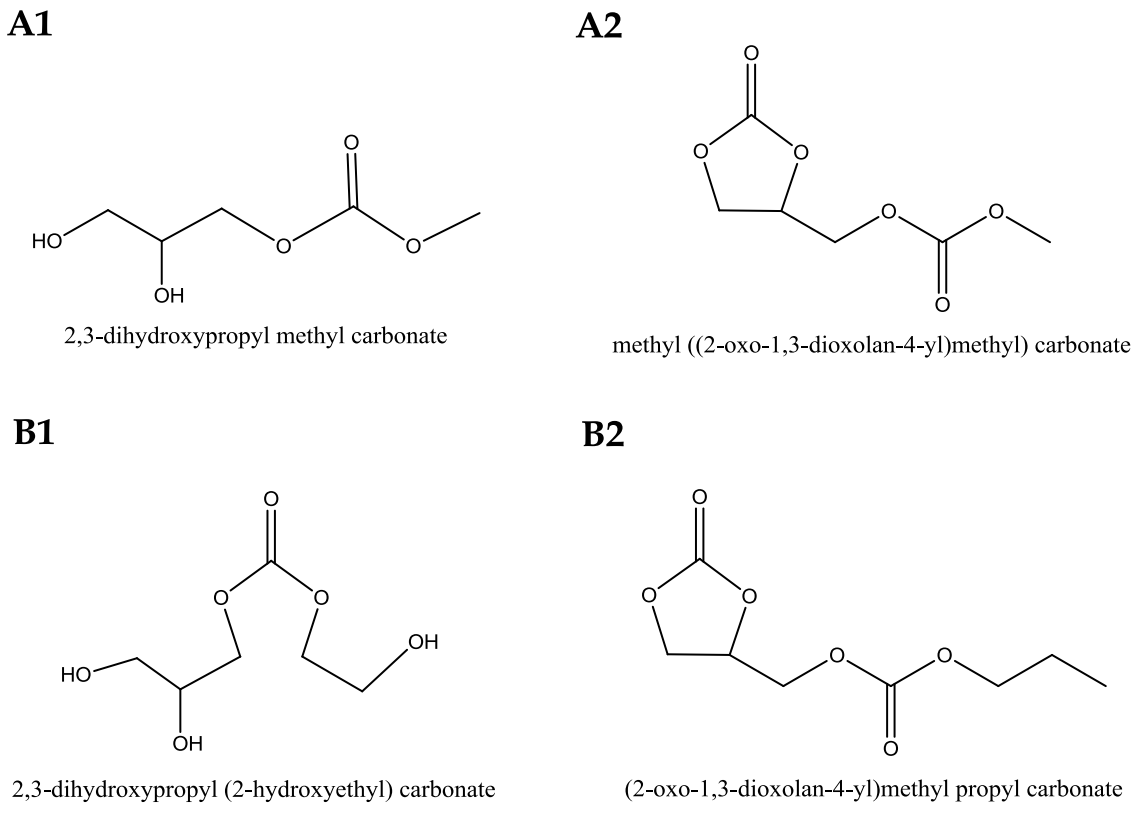

Figure 2. Possible reaction intermediates (A1 and B1) and products derived from the reaction of GC with the excess of DMC and EC, respectively (A2 and B2)

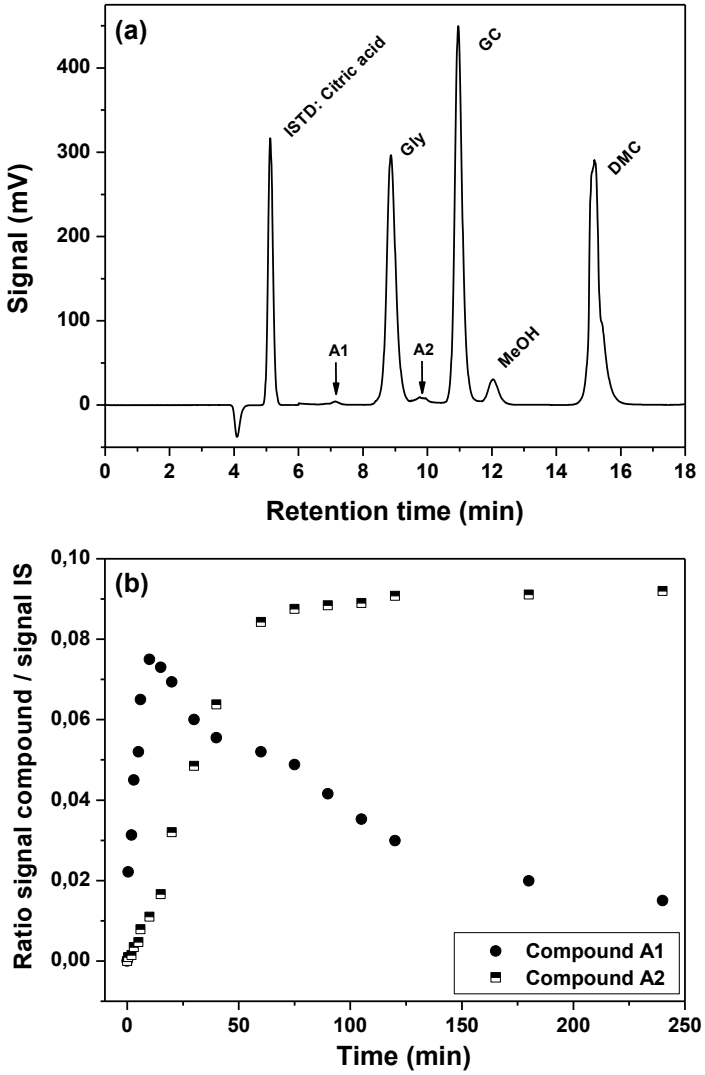

Figure 3. Chromatogram of the reaction between DMC and Gly (a) and evolution of the signal of species A1 and A2 (b)

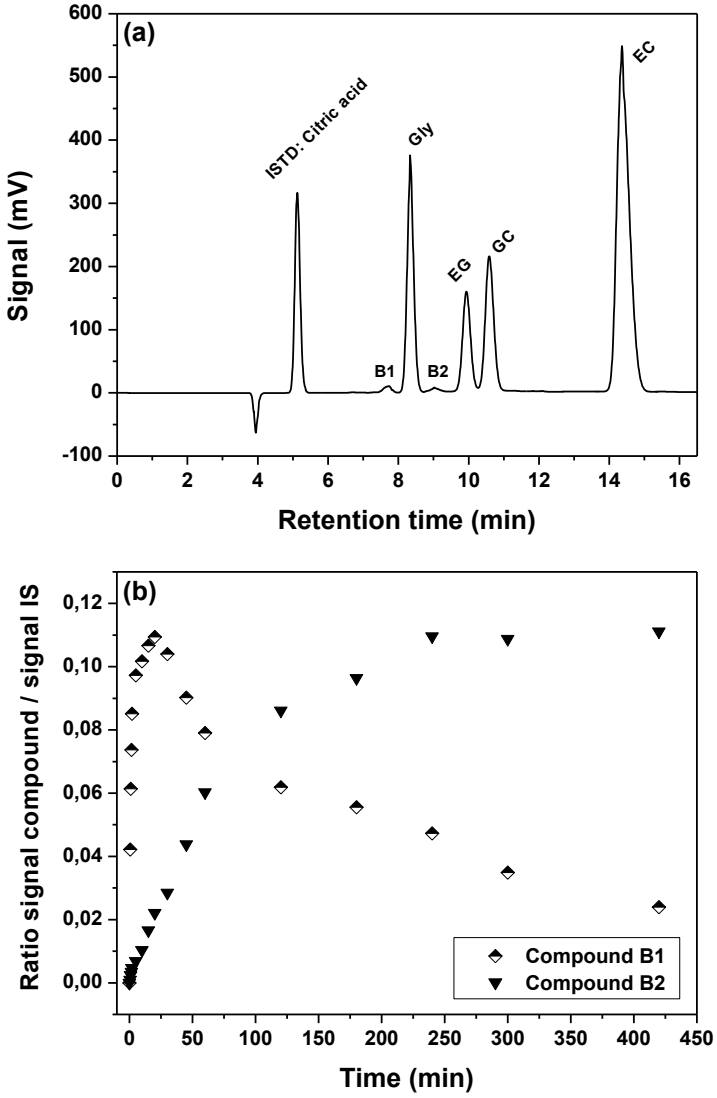

Figure 4. Sample chromatogram of the reaction between EC and Gly (a) and progress of the signal of species B1 and B2 with time (b)

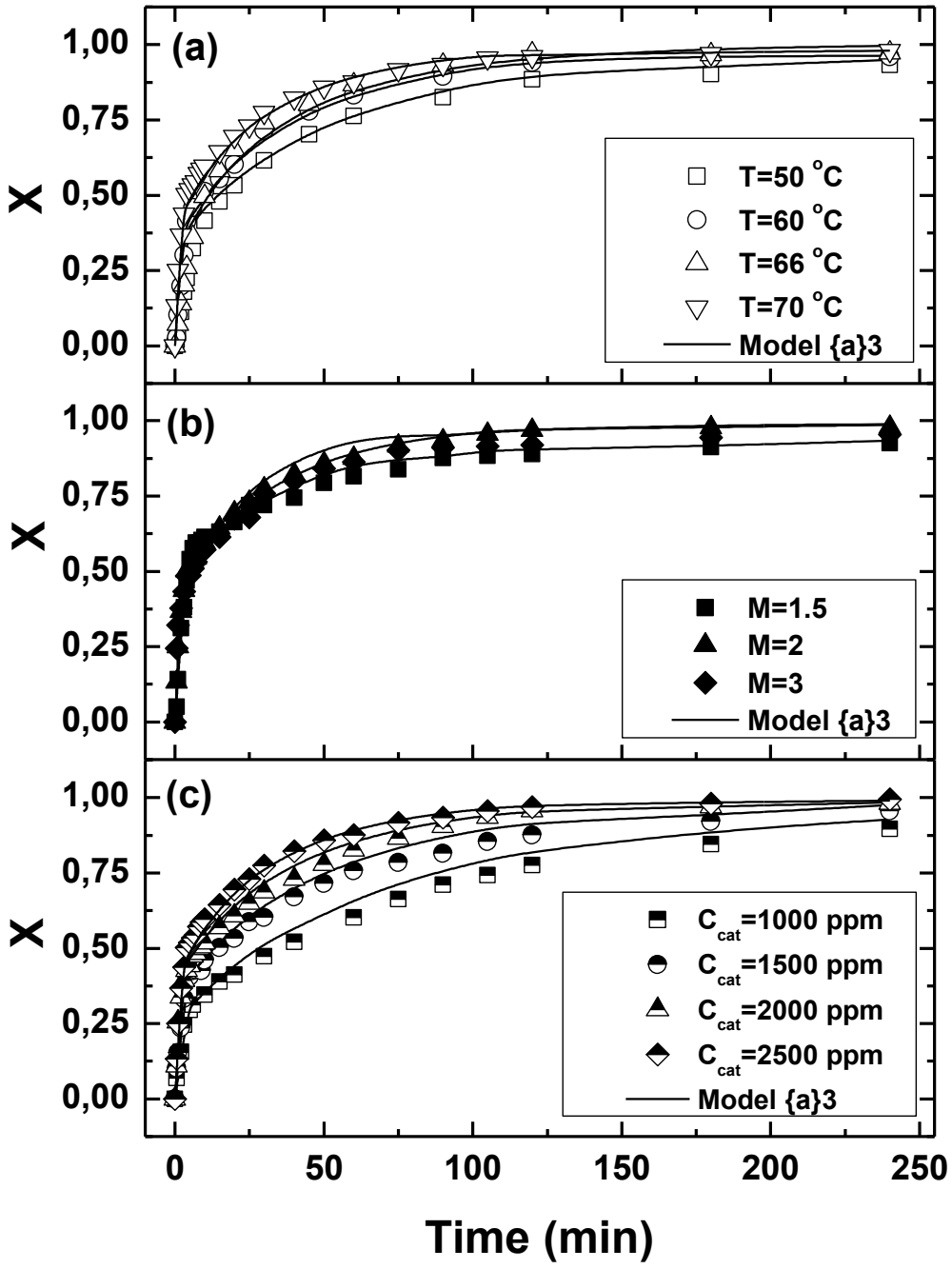

Figure 5. Evolution of kinetic runs for the reaction between DMC and glycerol comparing the effect of temperature (a), molar excess of DMC (b) and concentration of potassium methoxide (c). Conditions: (a) M=2, C_{cat}= 2500 ppm; (b) T=70ºC, C_{cat}= 2500 ppm; (c) T=70ºC, M=2. Agitation speed was kept at 1500 rpm.

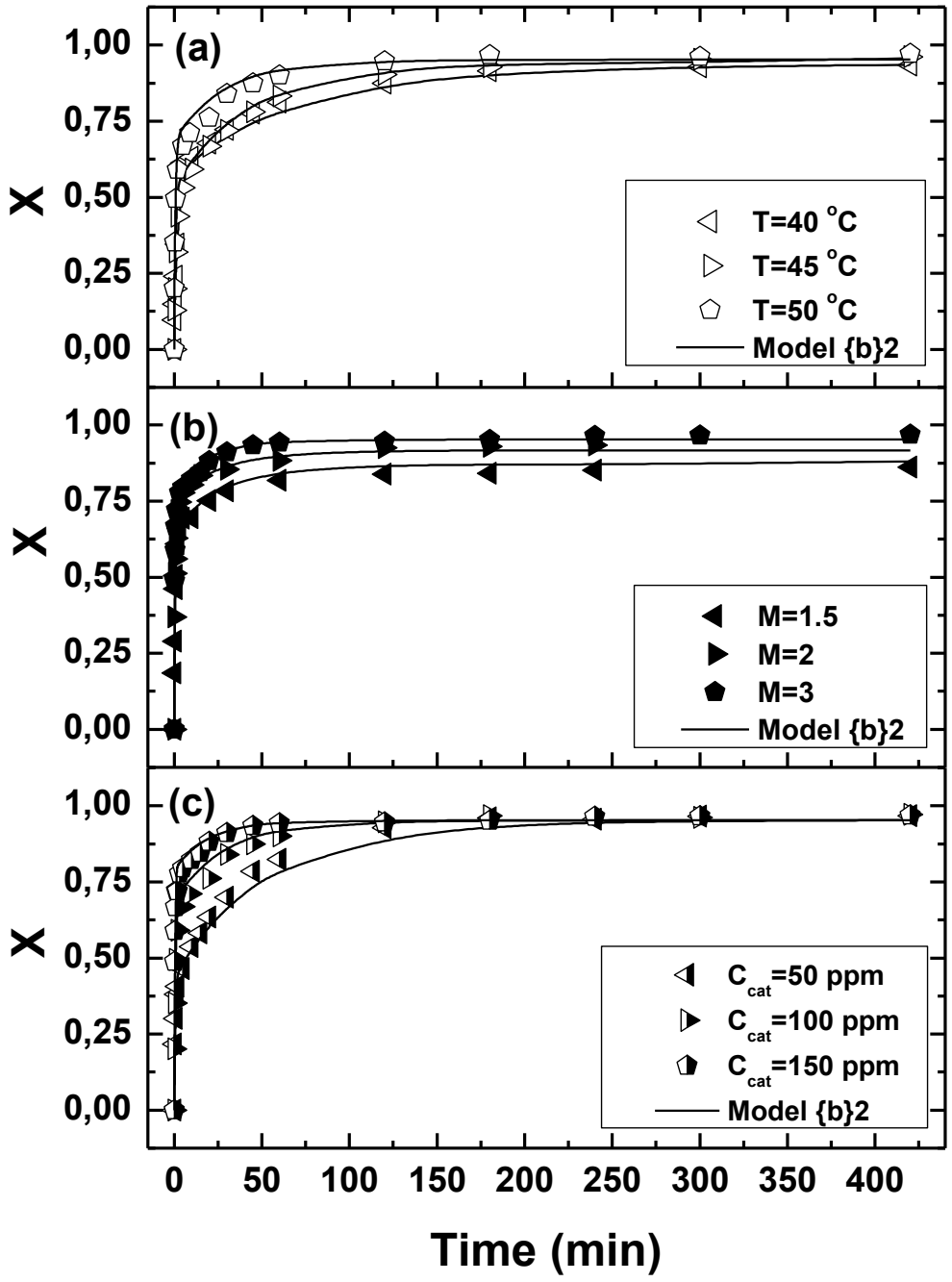

Figure 6. Evolution of kinetic runs for the reaction between EC and glycerol varying temperature (a), molar excess of EC (b) and concentration of potassium methoxide (c). Conditions: (a) M=3, C_{cat}= 100 ppm; (b) T=50ºC, C_{cat}= 150 ppm; (c) T=50ºC, M=4. Stirring speed was kept constant at all times at 800 rpm.

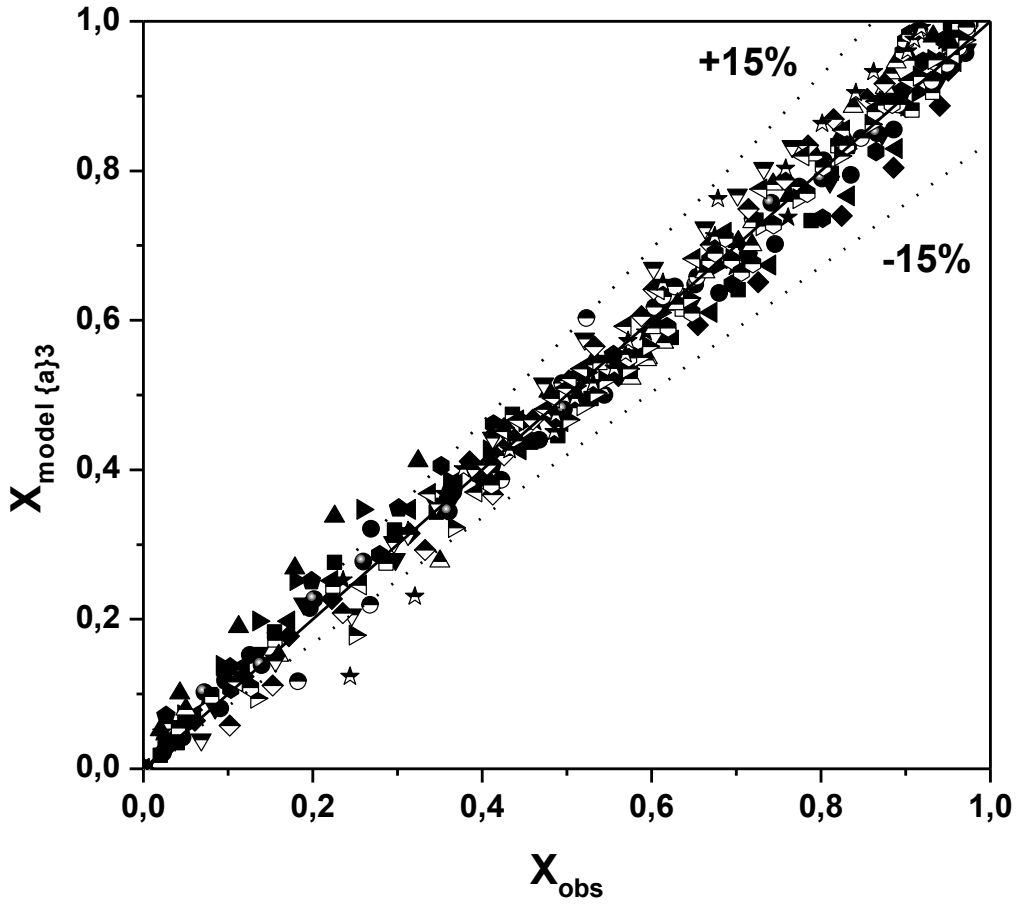

Figure 7. Verification of the values predicted by Model {a}3 against the observed values for the transesterification of glycerol using DMC.

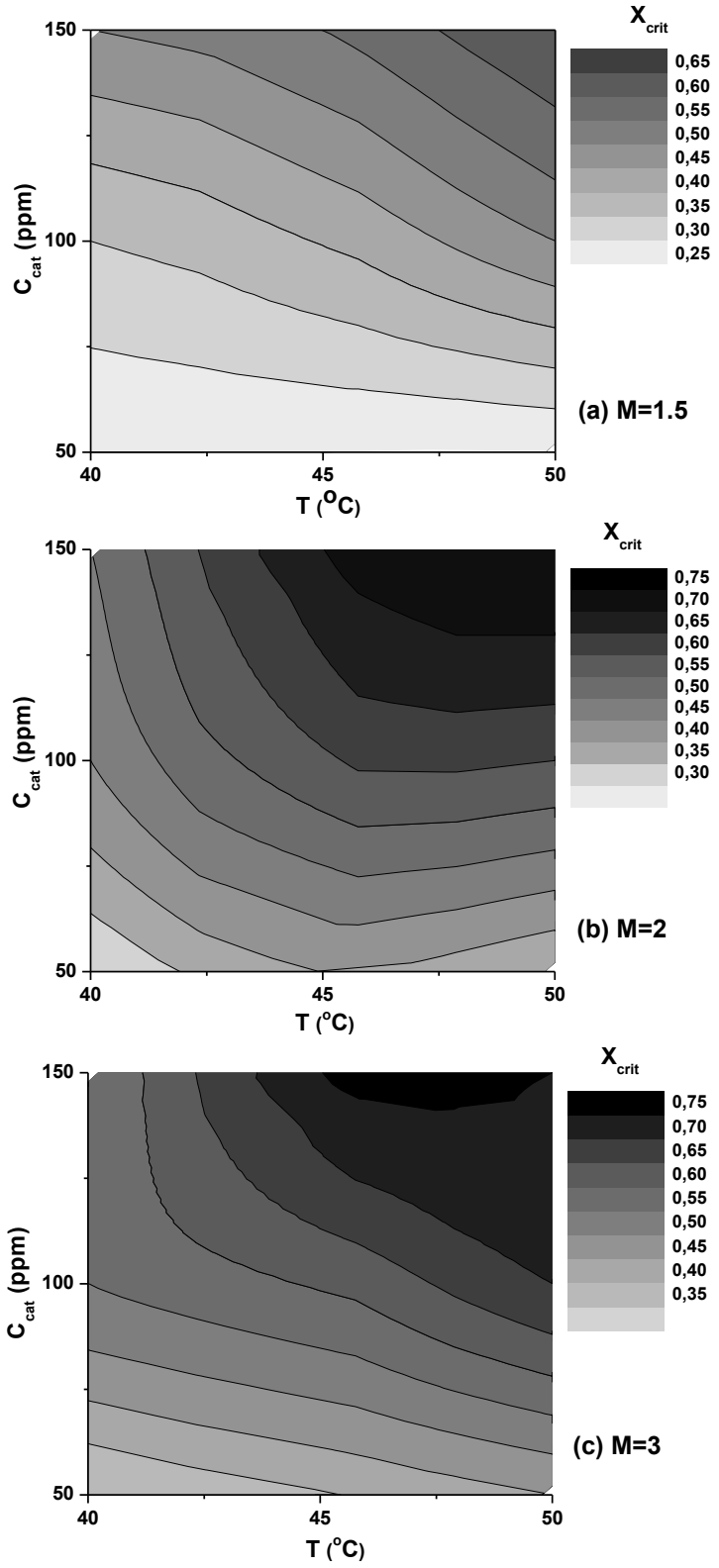

Figure 8. Variation of the critical conversion in the transesterification of glycerol with EC with respect to temperature and catalyst concentration using molar excesses of EC of M=1.5 (a), M=2 (b) and M=3 (c).

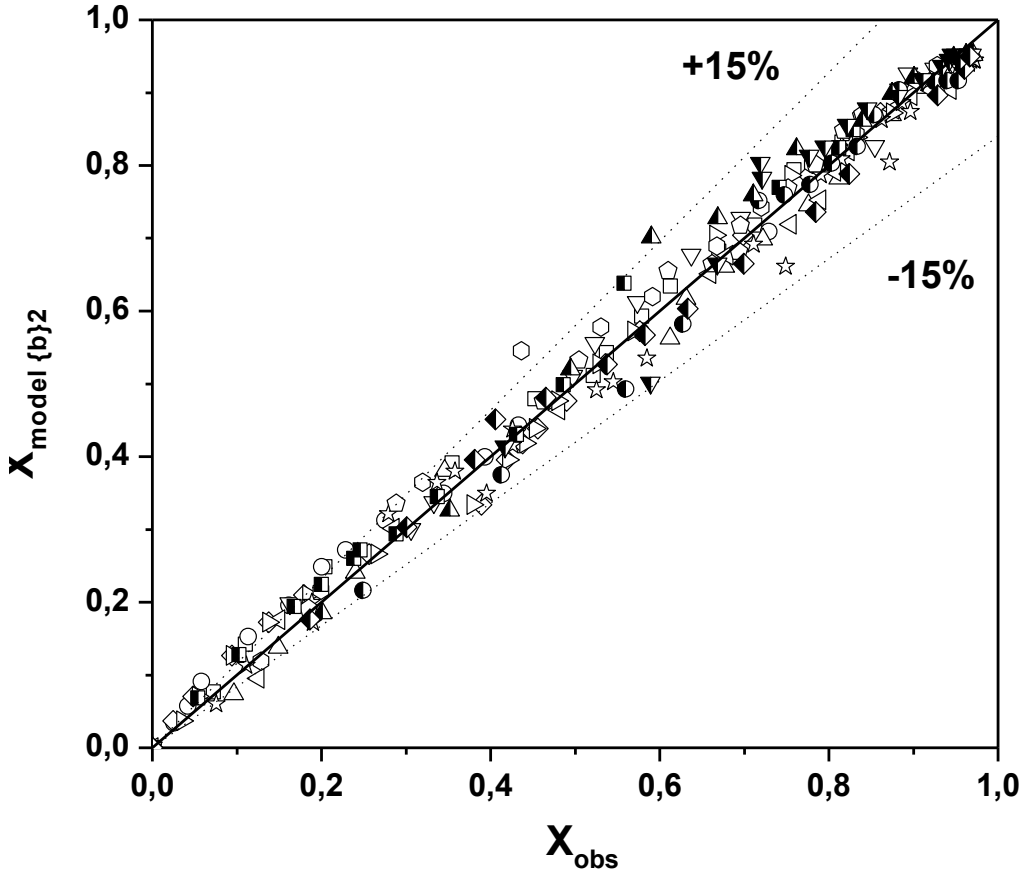

Figure 9. Validation plot of the predicted values using Model {b}2 versus the experimental values for the transesterification of glycerol using EC

Publicación 7 / Publication 7

Autores/Authors: Jesús Esteban, Andreas J. Vorholt, Arno Behr, Miguel Ladero and Félix García-Ochoa

Título/Title: Liquid−Liquid Equilibria for the System Acetone + Solketal + Glycerol at (303.2, 313.2, and 323.2) K

Estado actual/Current status: Journal of Chemical and Engineering Data (2014), 59: 2850-2855

Índice de impacto / Impact factor 2013: 2.045

Resumen

La reacción de acetalización entre la glicerina (Gly) y la acetona (Ac) da como producto principal solketal (Sk) y, además, agua como subproducto. A pesar del reciente interés que esta reacción ha despertado, no existen estudios relativos al equilibrio ternario entre las dos especies reactantes y el principal producto de la reacción.

Ac y Gly muestran una solubilidad muy limitada entre sí y, por tanto, constituyen un sistema bifásico líquido-líquido. Sin embargo, a medida que aumenta la concentración de Sk, la emulsión desaparece para dar lugar a un sistema monofásico. En este artículo se recogen datos del equilibrio mencionado, en ausencia de reacción química, a las temperaturas de 303.2, 313.2 y 323.2 K.

Para la experimentación, se configuraron diferentes recipientes cargados con cantidades variables de los tres compuestos y equipados con un sistema de control de temperatura y velocidad de agitación. Después de un periodo de separación de fases, se tomaron muestras de cada una de ellas y se analizaron por cromatografía de gases para determinar la composición de las mismas, con lo que se determinaron las diferentes *tie-lines* del equilibrio, verificándose la fiabilidad de los datos obtenidos mediante la correlación de Othmer-Tobias

Se evaluó el efecto de la temperatura, observándose que en el intervalo ensayado esta variable no afecta de manera importante al equilibrio de fases.

Por último, con la ayuda del software Aspen Plus, se llevó a cabo la correlación de los datos experimentales con el modelo NRTL, que se había empleado en otras referencias bibliográficas en sistemas que incluían glicerina. Se optimizaron los parámetros de interacción binaria no aleatoria, coincidiendo con valores clásicos ofrecidos en la literatura (valores de α_{ij} de 0.2 y 0.3) y se obtuvieron con un buen grado de ajuste (desviaciones menores a 0.0050) el resto de parámetros de interacción binaria a cada una de las temperaturas ensayadas

Journal of chemical & engineering data

Article

pubs.acs.org/jced

Liquid−Liquid Equilibria for the System Acetone + Solketal + Glycerol at (303.2, 313.2, and 323.2) K

Jesus Esteban,[†] Andreas J. Vorholt,[‡] Arno Behr,[‡] Miguel Ladero,[†,*] and Felix Garcia-Ochoa[†]

[†]Department of Chemical Engineering. College of Chemical Sciences, Complutense University of Madrid, 28040, Madrid, Spain
[‡]Department of Bio- and Chemical Engineering, Technical University of Dortmund, 44227, Dortmund, Germany

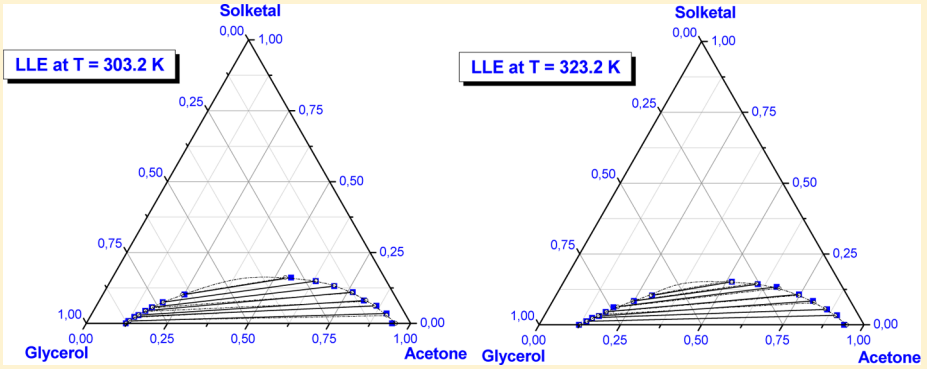

ABSTRACT: Experimental measurements of the liquid−liquid equilibrium of the ternary system consisting of acetone + solketal + glycerol were made. The conditions selected for this study were (303.2, 313.2, and 323.2) K at 101.3 kPa, relevant for the synthesis of solketal from glycerol and acetone through a ketalization reaction. The data obtained were correlated to the nonrandom two liquid (NRTL) model, and the binary interaction parameters of the ternary system were retrieved after the optimization of the nonrandomness binary interaction parameters. The liquid−liquid equilibrium data predicted by the NRTL model agreed adequately with the experimental results.

1. INTRODUCTION

Despite the fact that glycerol (Gly) has been widely utilized throughout history in countless applications, the development of the biodiesel industry in the early years of this century has given rise to an overabundance that has caused its price to decline.[1] Subsequently, capitalization on its outstanding chemical properties has been made as a means to valorize it. The study of several syntheses using glycerol as a building block to yield value-added products has been undertaken.[2,3]

Among them, the production of 1,2-isopropylideneglycerol (solketal, Sk) has received increasing attention in the past few years. This compound has been put to use as a plasticizer, a green solvent, and stabilizing agent in pharmaceutical and food preparations.[4] Additionally, the oxygenate nature of Sk has led to its use as a fuel additive. Certain performance parameters were enhanced in biodiesel formulations, where solketal has been reported to improve viscosity, flash point, and oxidation stability.[5] In gasoline, the inclusion of this ketal has upgraded the octane index and reduced gum formation.[6] In addition, derivatives of solketal have been synthesized and studied as potential additives to fuels, such as ethers and methylesters.[7,8] Additionally, the use of this compound as feedstock to further reactions has been explored, leading to chemicals of appreciated value in the pharmaceutical industry such as prostaglandins or certain β-blockers.[9,10]

Cyclic ketals are obtained by the ketalization reaction between polyols and carbonylic compounds. In this case, solketal is synthesized via the ketalization of glycerol and acetone, as schemed in Figure 1. What appears to be the key of this type of reaction is the presence of an acidic medium that can initialize the mechanism. Therefore, several acidic homogeneous catalysts like *p*-toluenesulfonic, sulfuric, or hydrochloric acid have been utilized.[5,8,11] Additionally, acid-functionalized solid catalysts have also been used to study this transformation, such as ion exchange resins,[12] heteropolyacids immobilized on silica,[13] and sulfonic acidified silicas.[14] Several articles report on very assorted conditions under which this reaction was completed, ranging from temperatures above the boiling point of acetone[12,14] to milder temperatures close to or slightly above 20−25 °C at atmospheric pressure.[11,13,15,16]

While some work has already been published regarding kinetic and thermodynamic aspects of the synthesis of solketal,[17] no efforts have been made concerning the physical equilibrium between glycerol, acetone, and solketal. Thus, herein, we developed a study of the liquid−liquid equilibrium (LLE) existing in the ternary system featuring {Ac + Sk + Gly} at mild conditions that have proven of interest for the reaction

Received: May 26, 2014
Accepted: August 7, 2014
Published: August 14, 2014

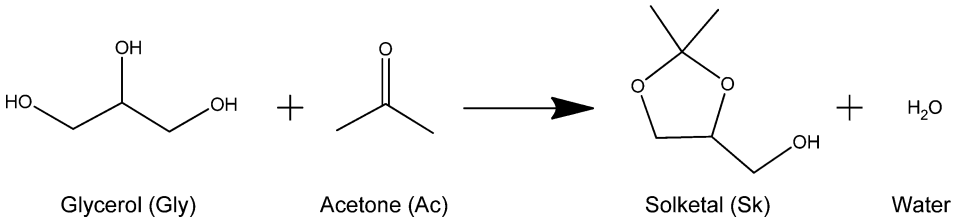

Figure 1. Scheme of the ketalization reaction of glycerol and acetone.

to take place: atmospheric pressure and temperatures of (303.2, 313.2, and 323.2) K.

Additionally, once the LLE experimental data had been acquired, fitting to the nonrandom two-liquid model (NRTL) was successfully realized and the corresponding binary interaction parameters were retrieved.

2. EXPERIMENTAL SECTION

2.1. Materials. The following chemicals were employed during the experimental process: extra pure glycerol (assay grade 99.88 %, purity checked by ^{1}H NMR analysis = 99.88 %) from Fischer Chemical; solketal (purity ≥ 98 %, purity checked by GC analysis = 98.1 %) from Aldrich; and acetone dry (purity ≥ 99.5 %, purity checked by GC = 99.75 %) from Acros Organics. Additionally, dibutyl ether (99 + % extra pure, purity checked by GC = 99.1 %) supplied by Acros was used as an internal standard for GC analysis and isopropyl alcohol (99.9 % pure, purity checked by GC = 99.9 %), also by Acros, for sample dilution.

2.2. Liquid−Liquid Equilibria Measurements. The experimental apparatus put to use throughout the experimentation comprises sealed round-bottom flasks of 50 mL of volume into which the appropriate amounts of the chemicals were added for each individual experiment. The adequate weight of the chemicals to be added was made with a Kern and Sohn ABS-220-4 precision balance with an accuracy of 0.0001 g. Mixing of the content of the flasks was achieved by magnetic stirring and heating with a temperature controlled glycerol bath. A temperature-controlled IKA Yellow Line TC3 device was used for the mentioned heating and stirring purposes.

The procedure consists of putting the feeds of each individual experiment to stir for 4 h to ensure a good mass transfer between the liquid phases until reaching phase equilibrium conditions. At that point, stirring was stopped and no less than 3 h were allowed for settling of the phases. Separation by decantation given the difference of density of the Gly-rich (I) and Ac-rich (II) phases was easily achievable and no turbidity was observed within any of the phases. Afterward, cautious sample withdrawal through the septa with syringes with fine hypodermic needles was performed. Samples from the Ac-rich phase were taken from the top of the upper phase. As for the heavy phase (Gly-rich), special care to avoid mixing between phases was taken because the needle had to poke through the interphase between the liquid phases. The Gly-rich sample was taken from the very bottom of the flask to prevent proximity with the interphase. Samples withdrawn from each phase were of at least 0.3 mL to ensure that 0.1500 g would be available to prepare the sample for analysis. Temperature was kept constant during the sample withdrawal process. Experimental data from triplicate experiments were procured.

2.3. Analytical Methods. Samples were diluted in isopropyl alcohol using dibutyl ether as internal standard prior to gas chromatography (GC) analysis. The components of the samples from the two phases were analyzed in an Agilent HP6890 Series GC system equipped with a thermal conductivity detector (TCD). Separation of the components was achieved using a HP-INNOWax capillary column (30 m × 0.25 mm i.d. × 0.25 μm) operating at a constant flow of 1.3 mL/min of helium as the carrier gas. The temperatures of the injector and detector were both 250 °C and the split ratio used was 80:1. The programmed temperature ramp for the oven was as follows: an initial hold of 6 min at 40 °C, then a ramp from 40 to 250 °C at 25 °C·min^{-1}, and finally a 8 min hold at 250 °C.

2.4. Data Regression and Correlation with the NRTL Model. Fitting of the experimental data was made using the NRTL model. The tool used to obtain the binary interaction parameters was the data regression module implemented in Aspen Plus, which used a least-squares method based upon the maximum likelihood principle. To retrieve the parameters, the Britt-Luecke[18] algorithm was used along with the Deming initialization method while setting the regression convergence tolerance at 0.0001. The objective function that the regression procedure minimizes is

$$\mathrm{OF} = \sum_{k=1}^{N}\sum_{j=1}^{2}\sum_{i=1}^{3}\left[\frac{(T_k^{\mathrm{exp}} - T_k^{\mathrm{calc}})^2}{\sigma_T^2} + \frac{(x_{ijk}^{\mathrm{exp}} - x_{ijk}^{\mathrm{calc}})^2}{\sigma_x^2}\right] \quad (1)$$

where T^{exp} and T^{calc} denote the experimental and calculated values of temperature, respectively; x^{exp} and x^{calc} denote the experimental and calculated values of mole fraction; the subscripts i, j, and k refer to the component, phase, and tie-line, respectively, and N is the number of experimental tie-lines obtained. Finally, σ_T and σ_x are the standard deviations of temperature and the molar fraction, whose values were fixed from the accuracy of the temperature control system (σ_T = 0.05 K) and the uncertainty of the GC-TCD analysis (σ_x = 0.019).

Fitting to the NRTL was first completed fixing various sets of values of the nonrandomness binary interaction parameters α_{ij}. Comparison of the goodness of fit with the results obtained from optimizing the α_{ij} was also made, and then a certain set of the parameters was fixed for the rest of the regressions. The goodness-of-fit of the parameters was decided on the basis of the minimization of the root-mean-square deviation (rmsd), defined as follows:

$$\mathrm{rmsd} = \sqrt{\sum_{k=1}^{N}\sum_{j=1}^{2}\sum_{i=1}\frac{(x_{ijk}^{\mathrm{exp}} - x_{ijk}^{\mathrm{calc}})^2}{6N}} \quad (2)$$

3. RESULTS AND DISCUSSION

3.1. LLE Experimental Data. First, a preliminary experiment was undertaken to ensure that the reaction between Ac and Gly did not take place in the absence of catalyst. For this

dx.doi.org/10.1021/je500469a | J. Chem. Eng. Data 2014, 59, 2850−2855

Table 1. Experimental LLE Data Expressed as Mole Fractions (x_i) of the Ternary System {Ac + Sk + Gly} at 101.3 kPa

	global composition (feed)			phase I (Gly-rich) composition			phase II (Ac-rich) composition		
T/K	x_{Ac}	x_{Sk}	x_{Gly}	x_{Ac}	x_{Sk}	x_{Gly}	x_{Ac}	x_{Sk}	x_{Gly}
303.2	0.499	0.000	0.501	0.121	0.000	0.879	0.943	0.000	0.057
	0.493	0.016	0.491	0.125	0.008	0.867	0.908	0.035	0.057
	0.482	0.036	0.482	0.136	0.023	0.841	0.863	0.062	0.075
	0.474	0.052	0.474	0.146	0.029	0.825	0.815	0.081	0.104
	0.464	0.071	0.465	0.159	0.044	0.796	0.767	0.110	0.123
	0.455	0.091	0.454	0.174	0.057	0.769	0.698	0.132	0.170
	0.444	0.113	0.443	0.198	0.075	0.727	0.633	0.149	0.218
	0.432	0.135	0.433	0.251	0.102	0.647	0.551	0.162	0.288
313.2	0.501	0.000	0.499	0.123	0.000	0.877	0.939	0.000	0.061
	0.492	0.017	0.491	0.139	0.013	0.848	0.901	0.034	0.066
	0.481	0.034	0.485	0.151	0.025	0.824	0.860	0.054	0.086
	0.475	0.053	0.472	0.169	0.031	0.801	0.801	0.084	0.115
	0.463	0.072	0.465	0.182	0.045	0.773	0.747	0.107	0.147
	0.455	0.092	0.453	0.198	0.062	0.740	0.664	0.134	0.202
	0.445	0.111	0.444	0.250	0.084	0.666	0.601	0.143	0.255
	0.432	0.132	0.436	0.296	0.104	0.600	0.517	0.152	0.331
323.2	0.499	0.000	0.501	0.145	0.000	0.856	0.938	0.000	0.062
	0.490	0.017	0.493	0.148	0.014	0.838	0.880	0.039	0.081
	0.480	0.036	0.484	0.160	0.023	0.817	0.842	0.053	0.105
	0.471	0.055	0.474	0.180	0.035	0.786	0.777	0.084	0.139
	0.465	0.070	0.465	0.202	0.053	0.745	0.727	0.101	0.172
	0.455	0.091	0.454	0.215	0.074	0.711	0.647	0.132	0.222
	0.443	0.113	0.444	0.247	0.098	0.655	0.589	0.146	0.264
	0.428	0.140	0.431	0.288	0.120	0.592	0.510	0.159	0.331

Standard uncertainties: $u(T)$ = 0.1 K and $u(x)$ = 0.019.

purpose, an equimolar mixture of Ac and Gly was kept under stirring conditions at 40 °C for 72 h. After that period, two liquid phases were still present and the analysis of both proved that no Sk was present at all. This absence of product agrees with the fact that an acid catalyst is needed to initiate the ketalization mechanism. Hence, it was confirmed that the following results correspond only to the LLE of the ternary system presented.

Table 1 compiles the experimental LLE data expressed as molar fractions obtained for the system {Ac + Sk + Gly} at (303.2, 313.2, and 323.2) K and 101.3 kPa. This system would correspond to the reactants of the reaction described in Figure 1 and the main product of the reaction, Sk, which helps the phases to dissolve in each other. Additionally, the global compositions of the feeds of each batch are included.

Despite this work focusing on the physical equilibrium between the liquid phases, the feeds were designed so as to acquire tie-lines that come from simulating the production of Sk in the progress of the chemical reaction. Particularly, each batch was loaded considering compositions that come from increasing assumed conversions of 3.3 % from an initial equimolar amount of Ac and Gly to yield only Sk as a product.

Figures 2, 3 and 4 represent the tie-lines according to the data shown in Table 1 at (303.2, 313.2, and 323.2) K, respectively. Together with the experimental data, the mentioned figures include the tie-lines and the binodal curve as predicted by the NRTL model.

Verification of the reliability of the experimental LLE results was made applying the Othmer−Tobias correlation,[19] which is defined as follows:

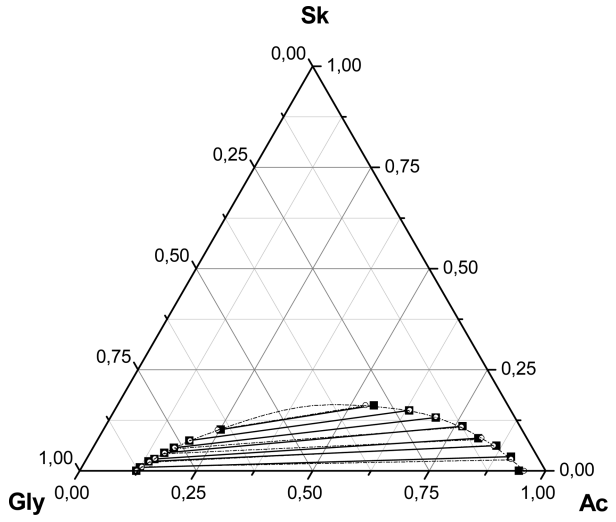

Figure 2. Experimental LLE data and binodal curve using the NRTL model for the system {Ac + Sk + Gly} at 303.2 K and 101.3 kPa: ■, experimental tie-lines; ---, data calculated with the NRTL model.

$$\left[\log\left(\frac{1-w_{Gly}}{w_{Gly}}\right)\right]_{I} = a + b\left[\log\left(\frac{1-w_{Ac}}{w_{Ac}}\right)\right]_{II} \quad (3)$$

in which w_{Gly} is the mass fraction of Gly in the Gly-rich phase (I); w_{Ac} accounts for the mass fraction of Ac in the Ac-rich phase (II); and a and b are the fitting parameters of this linear correlation. Figure 5 is a plot of the correlation in eq 3 at the three temperatures tested for equilibrium, while Table 2 summarizes the values of a and b along with R^2 values close to 1, proving the goodness of fit.

dx.doi.org/10.1021/je500469a | J. Chem. Eng. Data 2014, 59, 2850−2855

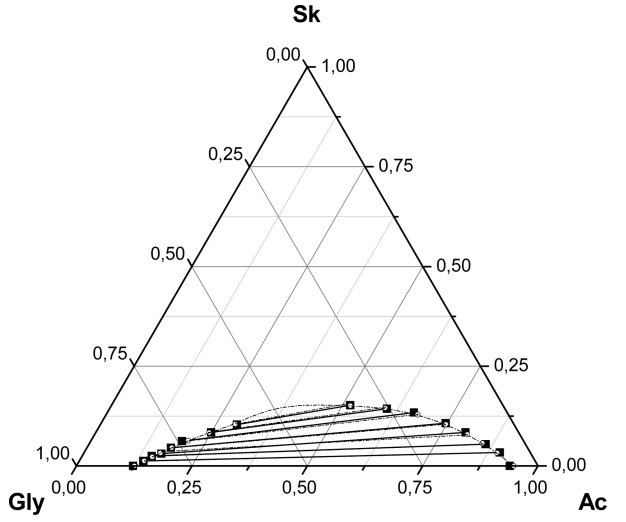

Figure 3. Experimental LLE data and binodal curve using the NRTL model for the system {Ac + Sk + Gly} at 313.2 K and 101.3 kPa: ■, experimental tie-lines; ---, data calculated with the NRTL model.

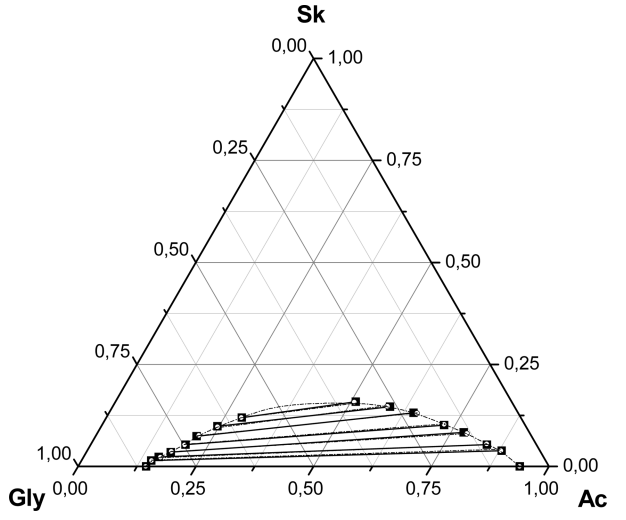

Figure 4. Experimental LLE data and binodal curve using the NRTL model for the system {Ac + Sk + Gly} at 323.2 K and 101.3 kPa: ■, experimental tie-lines; ---, data calculated with the NRTL model.

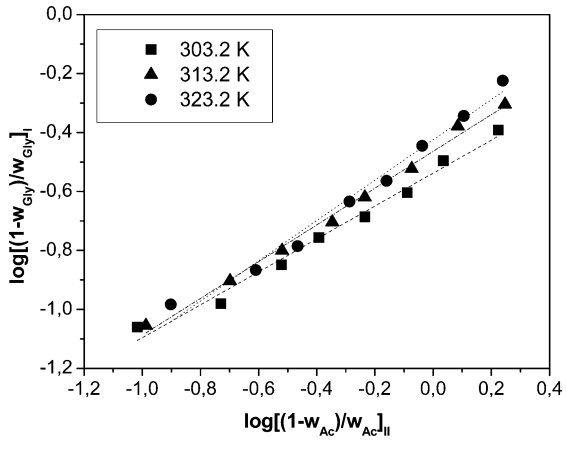

Figure 5. Othmer–Tobias graphs for the system {Ac + Sk + Gly} at the temperatures tested.

Table 2. Parameters of the Othmer–Tobias Correlation (a and b) and Correlation Coefficients (R^2) for the System {Ac + Sk + Gly}

T/K	a	b	R^2
303.2	−0.5376	0.5587	0.9858
313.2	−0.4639	0.6237	0.9941
323.2	−0.4250	0.6835	0.9901

3.2. Influence of the Presence of Solketal and Temperature in the Miscibility of the Biphasic System. It could be assessed that Sk was soluble both in the phase mainly consisting of Gly and that composed of Ac. The presence of increasing amounts of Sk helped the solubilization of one phase into the other, so it can be said that acts somehow as a cosolvent. Notwithstanding, the tendency of Sk to dissolve in each phase was not the same. As can be inferred from the data in Table 1 and Figure 6, Sk is more soluble in the Ac-rich phase (II) than in the Gly-rich phase (I).

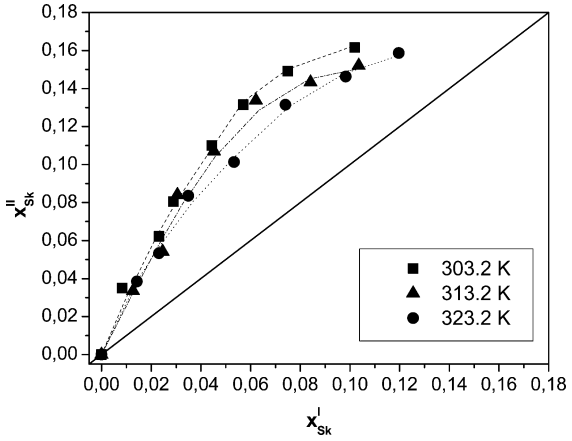

Figure 6. Effect of temperature on the distribution of Sk in the Ac and Gly-rich phases. Symbols represent experimental data, and broken lines represent the prediction of the NRTL model.

Similar situations have been observed in other systems aimed at the valorization of glycerol, in which the initial reactants are not fully miscible in each other and the growing presence of the products leads the system to turn monophasic. Examples of such behavior would be the synthesis of glycerol carbonate from glycerol and dimethyl carbonate or the esterification of rosin and glycerol.[20−22]

The effect of temperature was also evaluated. The representation in Figure 6 shows that this variable has a very slight effect on the distribution of Sk: the lower is the temperature, the more Sk tends to remain in the Ac-rich phase. As temperature rises, the distribution tends to become a little more even between the two phases, though at 323.2 K it is still far from being equal. Additionally, from the ternary diagrams in Figures 2, 3 and 4, it can be remarked that the area below the binodal curve (i.e., the biphasic region) barely decreased as the temperature increased. Subsequently, temperature does not play a major role in the LLE of the system under study.

3.3. Data Fitting to the NRTL Model and Retrieval of Binary Interaction Parameters. The NRTL was used to correlate the experimental data for the ternary system. Fitting of the model with three components leads to three nonrandom binary interaction parameters, α_{ij} ($\alpha_{ij} = \alpha_{ji}$), and six binary interaction parameters, Δg_{ij} and Δg_{ji}.

dx.doi.org/10.1021/je500469a | J. Chem. Eng. Data 2014, 59, 2850−2855

Optimization of the α_{ij} was made by giving fixed data at 303.2 K. For this purpose, first the three nonrandom binary interaction parameters were fixed at 0.2 and 0.3. These values are the rule of thumb proposed in literature for nonpolar substances or nonpolar with polar nonassociated liquids and saturated hydrocarbons with polar nonassociated liquids and systems that exhibit liquid−liquid immiscibility.[23] Table 3 shows the goodness of fit, described by the root of the mean squares deviation or rmsd, both after fitting the data with the eight possible combinations, fixing the α_{ij} parameters, and leaving the mentioned parameters floating. When these parameters were floating, it was observed that the retrieved values were α_{12} = 0.18, α_{13} = 0.29, and α_{23} = 0.19, which are very similar to the rule of thumb mentioned above. Moreover, the rmsd value was virtually the same as that obtained when fixing the values at α_{12} = 0.2, α_{13} = 0.3 and α_{23} = 0.2. Thus, the latter set of values for these parameters was used for subsequent correlations.

Table 3. Optimization of the Nonrandom Binary Interaction Parameters α_{ij} at 303.2 K

α_{ij} regression	α_{12}	α_{13}	α_{23}	rmsd
fixed	0.20	0.20	0.30	0.0078
	0.20	0.30	0.30	0.0068
	0.20	0.30	0.20	0.0050
	0.30	0.20	0.20	0.0057
	0.30	0.30	0.20	0.0069
	0.30	0.30	0.30	0.0056
	0.20	0.20	0.20	0.0075
	0.30	0.20	0.30	0.0056
floating	0.18	0.29	0.19	0.0048

Finally, Table 4 compiles the values calculated for the binary interaction parameters at the temperatures tested together with the *rmsd* values computed from the NRTL model. The low values of such deviations confirm that the NRTL model can describe the behavior observed for this LLE appropriately.

Table 4. Values of the NRTL Binary Interaction Parameters Obtained from the LLE Data by Regression for the System {Ac + Sk + Gly}

		NRTL parameters			
T/K	components *i*−*j*	α_{ij}	Δg_{ij} (J·mol^{-1})	Δg_{ji} (J·mol^{-1})	rmsd
303.2	1−2	0.2	3933.58	9652.28	0.0050
	1−3	0.3	11131.17	5578.47	
	2−3	0.2	−1017.30	13864.14	
313.2	1−2	0.2	9025.11	−6041.48	0.0047
	1−3	0.3	11050.19	5668.88	
	2−3	0.2	4748.62	244.37	
323.2	1−2	0.2	−2842.21	−2318.73	0.0029
	1−3	0.3	10901.35	5512.20	
	2−3	0.2	−1207.11	4.82	

4. CONCLUSIONS

The LLE of ternary system formed by {Ac + Sk + Gly} was assessed at (303.2, 313.2, and 323.2) K given its importance in a process to valorize glycerol. It could be seen that Sk plays a role as a solubilizing agent for Ac and Gly, being a little more prone to dissolve in the Ac-rich phase rather than in the Gly-rich. Within the temperature range studied, the effect of temperature was limited concerning the distribution of Sk in each of the phases as well as the global solubilization of both phases.

The LLE experimental data obtained throughout this work fit satisfactorily to the NRTL model. After correlation of the data, sets of binary interaction parameters were retrieved at each temperature.

AUTHOR INFORMATION

Corresponding Author

*E-mail: mladero@quim.ucm.es. Tel.: +34-913944164. Fax: +34-913944179.

Funding

This work is a collaboration thanks to the financial support of the German Academic Exchange Service (DAAD), which made possible Mr. Esteban's research stay at the Chair of Technical Chemistry at the Technical University of Dortmund.

Notes

The authors declare no competing financial interest.

REFERENCES

(1) Pagliaro, M.; Rossi, M. *The Future of Glycerol. New Uses for a Versatile New Material.*; RSC Publishing: Cambridge, 2008.

(2) Behr, A.; Eilting, J.; Irawadi, K.; Leschinski, J.; Lindner, F. Improved utilisation of renewable resources: New important derivatives of glycerol. *Green Chem.* **2008**, *10*, 13−30.

(3) Zhou, C.; Beltramini, J.; Fan, Y.; Lu, G. Chemoselective catalytic conversion of glycerol as a biorenewable source to valuable commodity chemicals. *Chem. Soc. Rev.* **2008**, *37*, 527−549.

(4) *Merck Index*, 11th ed.; Merck & Co. Inc.: Rahway, NJ, 1989.

(5) Garcia, E.; Laca, M.; Perez, E.; Garrido, A.; Peinado, J. New Class of Acetal Derived from Glycerin as a Biodiesel Fuel Component. *Energy Fuels* **2008**, *22*, 4274−4280.

(6) Mota, C. J. A.; da Silva, C. X. A.; Rosenbach, N., Jr.; Costa, J.; da Silva, F. Glycerin derivatives as fuel additives: The addition of glycerol/acetone ketal (solketal) in gasolines. *Energy Fuels* **2010**, *24*, 2733−2736.

(7) Selva, M.; Benedet, V.; Fabris, M. Selective catalytic etherification of glycerol formal and solketal with dialkyl carbonates and K_2CO_3. *Green Chem.* **2012**, *14*, 188−200.

(8) Suriyaprapadilok, N.; Kitiyanan, B. Synthesis of solketal from glycerol and its reaction with benzyl alcohol. *Energy Procedia* **2011**, *9*, 63−69.

(9) Hof, R. P.; Kellogg, R. M. Synthesis and lipase-catalyzed resolution of 5-(hydroxymethyl)-1,3-dioxolan-4-ones: Masked glycerol analogs as potential building blocks for pharmaceuticals. *J. Org. Chem.* **1996**, *61*, 3423−3427.

(10) Jurczak, J.; Pikul, S.; Bauer, T. (*R*)-2,3-*o*-isopropylideneglyceraldehyde and (*S*)-2,3-*o*-isopropylideneglyceraldehyde in stereoselective organic synthesis. *Tetrahedron* **1986**, *42*, 447−488.

(11) Bruchmann, B.; Haeberle, K.; Gruner, H.; Hirn, M. Preparation of cyclic acetals or ketals, especially isopropylidene glycerin|comprising distilling off some of aldehyde or ketone during reaction with polyol. Patent EP842929-A, 1999.

(12) Clarkson, J. S.; Walker, A. J.; Wood, M. A. Continuous reactor technology for ketal formation: An improved synthesis of solketal. *Org. Process Res. Dev.* **2001**, *5*, 630−635.

(13) Ferreira, P.; Fonseca, I. M.; Ramos, A. M.; Vital, J.; Castanheiro, J. E. Valorisation of glycerol by condensation with acetone over silica-included heteropolyacids. *Appl. Catal., B* **2010**, *98*, 94−99.

(14) Vicente, G.; Melero, J. A.; Morales, G.; Paniagua, M.; Martin, E. Acetalisation of bio-glycerol with acetone to produce solketal over sulfonic mesostructured silicas. *Green Chem.* **2010**, *12*, 899−907.

(15) Reddy, P. S.; Sudarsanam, P.; Mallesham, B.; Raju, G.; Reddy, B. M. Acetalisation of glycerol with acetone over zirconia and promoted

zirconia catalysts under mild reaction conditions. *J. Ind. Eng. Chem.* **2011**, *17*, 377−381.
(16) Matsushita, H.; Shibagaki, M.; Takahashi, K.; Kuno, H. Acetal or ketal preparation from aldehyde or ketone using as catalyst a hydrous oxide of an element of gp = IV of the periodic table. Patent EP271091-A1, 1989.
(17) Nanda, M. R.; Yuan, Z.; Qin, W.; Ghaziaskar, H. S.; Poirier, M.-A.; Xu, C. C. Thermodynamic and kinetic studies of a catalytic process to convert glycerol into solketal as an oxygenated fuel additive. *Fuel* **2014**, *117*, 470−477.
(18) Britt, H. I.; Luecke, R. H. The estimation of parameters in nonlinear, implicit models. *Technometrics* **1973**, *15*, 233−247.
(19) Othmer, D. F.; Tobias, P. E. Toluene and acetaldehyde systems, tie line correlation, partial pressures of ternary liquid systems and the prediction of tie lines. *Ind. Eng. Chem.* **1942**, *34*, 693−696.
(20) Esteban, J.; Ladero, M.; Molinero, L.; Garcia-Ochoa, F. Liquid−liquid equilibria for the ternary systems DMC−methanol−glycerol; DMC−glycerol carbonate−glycerol and the quaternary system DMC−methanol−glycerol carbonate−glycerol at catalytic reacting temperatures. *Chem. Eng. Res. Des.* **2014**, DOI: 10.1016/j.cherd.2014.05.026.
(21) Wang, H.; Lu, P. Liquid−liquid equilibria for the system dimethyl carbonate + methanol + glycerol in the temperature range of (303.15 to 333.15) K. *J. Chem. Eng. Data* **2012**, *57*, 582−589.
(22) Ladero, M.; de Gracia, M.; Trujillo, F.; Garcia-Ochoa, F. Phenomenological kinetic modelling of the esterification of rosin and polyols. *Chem. Eng. J.* **2012**, *197*, 387−397.
(23) Renon, H.; Prausnitz, J. M. Local compositions in thermodynamic excess functions for liquid mixtures. *AIChE J.* **1968**, *14*, 135−144.

Publicación 8 / Publication 8

Autores/Authors: Jesús Esteban, Miguel Ladero and Félix García-Ochoa

Título/Title: Synthesis of solketal with commercially available sulphonic acid based ion exchange resins

Estado actual/Current status: Manuscript submitted to RSC Advances as of January 2015

Índice de impacto / Impact factor 2013: 3.708

Resumen

Como alternativa para la valorización de glicerina se presenta la reacción de acetalización (o ketalización), consistente en este caso en la reacción de glicerina con acetona para dar como productos solketal y agua. La reacción tiene una extensión apreciable si se emplea catálisis heterogénea bajo condiciones de reacción suaves (presión atmosférica y temperatura de 40 ºC) en ausencia de disolventes. En concreto, se utilizan 5 resinas sulfónicas de intercambio iónico disponibles comercialmente: Amberlyst 35dry, Amberlyst 36dry, Purolite CT275DR, Purolite CT276 y Lewatit GF101.

En primer lugar, se realizó una profunda caracterización de estas resinas, evaluándose su acidez, así como su composición elemental, curvas termogravimétricas, espectros de resonancia magnética nuclear de carbono 13 y la superficie específica y distribución de poros por porosimetría de mercurio. Mediante estas caracterizaciones, se apreció que Lewatit GF101 seguida de Purolite CT275DR, aun no siendo las resinas con mayor superficie específica, poseen una acidez alta y los mayores contenidos de azufre, y además los grupos sulfónicos parecen estar en una posición más accesible dentro de los centros activos.

Estas caracterizaciones explican el orden de actividad observado para estos sólidos. El orden fue el siguiente, incluyendo además la resina Amberlyst 15, una referencia clásica: Lewatit GF101 > Purolite CT275DR > Amberlyst 36dry > Amberlyst 35dry > Amberlyst 15 > Purolite CT276.

Además, se llevó a cabo la reutilización de las resinas, teniendo en cuenta que una de las grandes ventajas de plantear el empleo de catálisis heterogénea es la posibilidad de reciclar los catalizadores. Se observó la caída de la actividad remanente, definida como la frecuencia de reposición con los sucesivos ciclos respecto a la observada para el primer uso. Se apreció, por un lado, que una regeneración del catalizador repercutía en una menor estabilidad del mismo con el paso de los usos y, por otro, que el orden de estabilidad observado para las resinas era bastante diferente al resultante anteriormente para la actividad. El orden de estabilidad fue, concretamente: Purolite CT276 > Amberlyst 36dry > Amberlyst 15 > Purolite CT275DR > Amberlyst 35dry > Lewatit GF101.

RSC Advances

RSCPublishing

ARTICLE

Solventless synthesis of solketal with commercially available sulfonic acid based ion exchange resins

Cite this: DOI: 10.1039/x0xx00000x

Jesús Esteban, Miguel Ladero and Félix García-Ochoa

Received 00th January 2015,
Accepted 00th January 2015

DOI: 10.1039/x0xx00000x

www.rsc.org/

As a means to valorise glycerol, the synthesis of solketal through a ketalization reaction with acetone was performed. Solventless operation at 40 ºC and a molar excess of acetone to glycerol of 4.5 to 1 were the conditions selected to test the activity of different commercially available sulfonic ion exchange resins that had already been used for other applications, namely: Amberlyst 35dry, Amberlyst 36dry, Purolite CT275DR, Purolite CT276 and Lewatit GF101. Thorough characterization of the resins is herein provided and discussed, including acidity, elemental analysis, thermogravimetric, ^{13}C-NMR, surface area and pore distribution measurements. Lewatit GF101 showed the best performance reaching a yield to solketal of 47% after 6 hours of operation, being the availability of active centres as well as the ease of access to them a key aspect to explain the observed activity. Additionally, reutilization of the resins was performed up to five cycles, showing that Purolite CT276 had the lowest relative drop of its maximum activity despite being the least active in each of the cycles.

Introduction

The philosophy of Green Chemistry is based on principles aimed at acting on the source to prevent pollution and misuse of resources. Thus, emphasis is put on waste prevention, use of safer solvents if any, employing catalysts and utilization of renewable feedstock [1].

Under a scenario in which glycerol is overabundant due to the current situation of the biodiesel market, new applications of this chemical have been searched for. Owing to its chemical structure and functionality, assorted valuable chemicals have been obtained[2-4]. Among them, the following can be mentioned: glycerol carbonate [5] or 1,3-propanediol [6], to name a couple.

1,2-isopropylideneglycerol, also referred to as solketal (Sk), is one of such products. As a final product, it is put to use as a plasticizer, a green solvent and suspending agent, especially in pharmaceutical preparations [7]. Moreover, its chemical reactivity makes it a feedstock to other chemicals of pharmaceutical interest like diglycerides, prostaglandins, glycerophospholipids or β-blockers like (S)-propranolol, extensively used for hypertension, migraine and other medical treatments [8, 9].

Undoubtedly, one of the most explored features of oxygenate derivatives from glycerol has been its use as fuel additives[10-13]. In this context, solketal has proven to enhance certain performance parameters and specifications. Reduced gum formation and improvement of the octane index was observed when using up to 5% volume of solketal to gasoline [14], while addition of said ketal to biodiesel not only improved its viscosity, but also complied with the flash point and oxidation stability specifications as enacted by European and American Standards (EN 14214 and ASTM D6751) [15]. Even further reactions of solketal have been explored to yield new potential additives, namely: its upgrade to benzyl alcohol ether [16] or the synthesis of solketal o-methylesters through the reaction with dialkyl carbonates under basic conditions [17].

While the synthesis of ketals has been pursued throughout the years, an increasing number of efforts have been made more recently. Ketalization consists in the reaction of an alcohol with ketones or aldehydes in an acidic medium; more specifically, cyclic ketals (like solketal) may be obtained through the reaction of polyols (like glycerol) with said carbonyl moiety-containing compounds.

Experimental conditions and operating procedures of very different nature have been employed to undertake the production of solketal. Table 1 compiles a brief review of some works focused on these aspects. It can be seen that different experimental approaches have been followed to shift the equilibrium existing in this reaction towards the products. The most followed operation modes are reactive distillation [15, 18-20] and other different strategies to remove water from the reaction medium, some of which are explicitly mentioned in the corresponding references [21-23], though some others can be inferred from the results reported [24-27]. Other operation methodologies include reflux operating at temperatures above the boiling point of acetone (56 ºC)[16, 28-30] or the use of a fixed bed through which the reacting mixture flows[31-33]. Additionally, it should be remarked that some studies, among which some of the aforementioned are included, have made use of solvents to avoid the initial liquid system with limited miscibility[21, 30-32, 34]. As a general rule, molar excesses of acetone to glycerol as high as 20 to 1 [22] have been employed. As for the values of temperature, they have usually been moderate, ranging from room temperature to 80 ºC, with the only exception of a process operated under supercritical conditions in the absence of any catalyst[35].

Sulphonic-based ion exchange resins can provide the acidic medium necessary for the reaction subject of study to occur.

Table 1 Overview of different processes to yield solketal present in literature

Ref.	Catalyst[a]	T (ºC)[b]	M[c]	t (h)	Catalyst load	Other conditions[d]	Y_{sk} (%)
15	PTSA	-	3	16	0.5% mol	Reactive distillation to shift equilibrium	90
16	PTSA	-	6	12	1% w/w	Reflux	81
18	HCl, PTSA, H_2SO_4	20-56	4	9	0.05% mol	Reactive distillation	97.6
19	Amberlyst DPT-1	70	3	5	5% w/w	Counter-current reaction distillation column	98
20	ZrO_2-SiO_2	70	4	3	2.2% w/w	Reactive distillation	81
21	Amberlyst 36	40	2.7:1.8:1[e]	8	1.21% w/w	Water removal. Solvent: dichloromethane	88
22	Montmorillonite K10	-	20	2	10% w/w	Water removal by means of a zeolite-based membrane	82
23	Arenesulfonic mesostructured silica Ar-SBA-15, Amberlyst 15	70	6	3x0.5	1% w/w	3 consecutive 2-step batches of 30 min under reflux and then evaporation under vacuum	84
24	Amberlyst-15, zeolite Beta, ZSM-5, montmorillonite K10, PTSA	70	1.2	1	15% mol	water removal by unknown method to shift equilibrium[f]	95
25	Amberlyst-15, zeolite Beta	70	2	1	3.18 % w/w	water removal by unknown method to shift equilibrium[f]	95
26	Heteropolyacids supported on silica: PW_S, SiW_S, PMo_S, SiMo_S	70	6	3	0.72% w/w	water removal by unknown method to shift equilibrium[f]	90
27	Promoted zirconia: SO_4^{2-}/ZrO_2, MoO_x/ZrO_2, WO_x/ZrO_2, ZrO_2	25	6	1.5	1% w/w	water removal by unknown method to shift equilibrium[f]	98
28	Mesoporous silicates: Hf-TUD1, Zr-TUD1, Al-TUD1	80	2	4	0.07 % w/w	Reflux	65
29	Sulphonated carbon silica meso composites. HSCS, SCS	70	6	0.5	5% w/w	Reflux	78
30	$SnCl_2$	60	60:10:1[e]	0.5	1% mol	Reflux Solvent: acetonitrile	66
31	Amberlyst 36	25	1:4:1[e]	N/A	N/A	Operation in fixed bed. Solvent: ethanol P=3.4 MPa, WHSV[g]=2 h^{-1}	94
32	Amberlyst Wet , Amberlyst Dry, zeolite, $ZrSO_4$, montmorillonite, Polymax	40	1:6:1[e]	N/A	N/A	Operation in fixed bed. Solvent: methanol P=4,14 MPa, WHSV[g]=4 h^{-1}	88
34	Amberlyst 35	50	1:2:1[e]	4	2% w/w	Solvent: methanol	65
33	Purolite PD206	60	3	N/A	1.5 g_{cat}	Operation in fixed bed. P=0.6 MPa. Q_v=0.1 mL·min^{-1}	69
35	No catalyst	260	10.8	4	N/A	Supercritical conditions: P=8 MPa	22.6

[a] First is the catalyst showing the best results. The rest of the conditions and yields compiled in this table apply to such catalyst. [b] - Indicates that the temperature was not mentioned in the corresponding reference. [c] M=acetone to glycerol molar ratio. [d] Reactions conducted at atmospheric pressure unless otherwise stated. [e] Molar ratio solvent:acetone:glycerol. [f] These conditions are not explicitly described in the references; however, they can be inferred from the results due to the existing chemical equilibrium. [g] WHSV: weight hourly space velocity.

As appointed in Table 1, some works have reported on the use of these materials as catalysts for this reaction. In this work, other resins that have proven of research interest will be tested. Purolite CT275 has been used for the synthesis of isopropyl tert-butylether from isopropanol and isobutene by means of an etherification reaction [36] or in membranes for the purification and drying of alcohols [37]. Purolite CT276 has been employed in water treatments for the removal of iodides together with Purolite CT275 [38]. The two mentioned Purolite resins along with Amberlyst 35 and Amberlyst 36 have been used in other reactions like the oligomerization of 1-hexene [39] and etherifications and dehydrations from alcohols [40]. Lewatit GF101 has only been reported thus far in the removal of free fatty acids in biodiesel manufacture processes and is, therefore, the one that lacks the most information [41].

Even more interestingly, the Amberlyst 35 and 36 resins have been found to be used in reactions involving the transformation of glycerol as a means to pursue its valorization. Amberlyst 35 has proven useful in etherification [42] and the production of triacetylglycerol by esterification and acetylation of glycerol [43] or even in the ketalization of glycerol to solketal in a solvent-based operation [34]. On the other hand, the use of Amberlyst 36 has been reported for acetylation to yield products like mono or polyacetates used in biodegradable polymers and products in the cosmetic and food industry [44].

The general aim of this work is to continue the studies of glycerol valorization at moderate temperature avoiding the use of solvents and cosolvents, following the premises of Green Chemistry. More precisely, this work deals with the solventless synthesis of solketal through the reaction of glycerol with acetone (Ac) using commercially available sulfonic acid-based ion exchange resins at temperatures below the boiling point of acetone. Thus, a screening among the five aforementioned resins was undertaken through evaluation of performance, characterization and reutilization, comparing their functionality among them and to the classical acid resin Amberlyst 15.

Experimental section

Materials

Chemicals. Experiments were performed with extra pure glycerol (99%) (Scharlau Chemie, Ltd) and acetone (HPLC grade) (Romil, Ltd). Preparation of samples required methanol (HPLC grade) (Fisher Scientific UK, Ltd.) as internal standard and deuterium oxide (99.8%, NMR spectroscopy grade) (Scharlau Chemie, Ltd.) as solvent.

Catalysts. The following acidic ion exchange resins were employed: Purolite CT275DR, Purolite CT276 (Purolite, Ltd.); Amberlyst 35dry, Amberlyst 36dry (Rom and Haas France SAS) and Lewatit GF101 (Lanxess Deutschland GmbH), all of which were kindly supplied by each manufacturer. Amberlyst 15, used for functional comparison purposes, was purchased to Sigma-Aldrich. While all the

catalyst were supplied in their dry form, additional overnight drying at 373 K in a Heraeus Series 6000 vacuum oven was conducted in order to ensure complete dryness prior to catalytic experiments.

Catalyst characterization

BET surface area of the resins was determined using the N_2 adsorption-desorption technique at 196 K performed by a Beckman Coultier SA3100 analyzer. Prior to the measurements, samples were degassed at 100 ºC during 120 minutes.

Porosimetry by mercury extrusion was completed for an approximate sample mass of 0.25 g of each resin in a Thermo Electron Pascal 440 series device to quantify for meso and macropores. The calculation of the pore diameter was made using the Washburn cylindrical pore model, where the surface tension of mercury and the mercury contact angle were taken as 0.484 N/cm and 141º, respectively.

Thermogravimetric analyses (TGA) were made in a Mettler Toledo 851e TGA/SDTA instrument. Temperature was increased from 333 to 833 K at a heating rate of 10 K/min under a nitrogen flow of 20 mL/min so as to keep an inert atmosphere. Each sample weighed approximately 10 mg. The curves obtained for the thermal decomposition of each catalyst was the average of three experiments. Solid state ^{13}C-NMR spectroscopy of the catalysts was performed at 400 scans in a Bruker DSX300 MHz BACS60 device with an automatic sampler.

Elemental microanalysis was performed in a LECO CHNS-932 equipment. Prior to the analysis of the resins, samples of 3 mg were dried overnight at 373 K to avoid errors due to the residual moisture. For the potentiometric titration of the catalysts, a suspension of 25 mg of the resin in 40 mL of acetonitrile was prepared and kept under stirring for 24 hours prior to the addition of a solution of N-butylamine in acetonitrile (0.005 N) at a constant flow rate of 0.4 mL/min. Potential was measured with an Eutech Instruments pH 700 pH-meter.

Additionally, Brönsted acidity of the resins was suspending overnight 10 mg of the resins in a solution of 7.5 g/L of KCl in water. The acid capacity was determined from measuring the pH value.

Table 2 compiles the physical and chemical properties of the resins determined from the aforementioned methods or as specified by the suppliers.

Apparatus and methodology

The experimental setup consists of a glass reactor heated by means of a thermal resistor placed surrounding its outer walls with temperature being controlled by an OMRON E5CN PID controller linked to the resistor. Stirring of the system was regulated by a flat six-blade impeller on an IKA RW20 motor (250 to 2500 rpm). Sample withdrawal was performed with a syringe with a wide-bore needle piercing a Teflon lid tightly fitted to the upper part of the reactor.

The operational procedure followed in all the experiments started by loading the reactants glycerol and acetone into the glass reactor. Catalyst was added when the set temperature was reached and samples were withdrawn thenceforth.

For the catalyst recycling experiments, up to four repetitions of the assay under the same conditions were completed. From experiment to experiment, the catalyst was filtered out of the reaction mixture, washed with methanol and dried at 373 K overnight. For catalyst regeneration, consecutive methanol washing, vacuum drying and treatment with 10 mL of a solution containing perchloric acid (1 N) per gram of resin was completed.

Analysis of samples

Analysis of samples was performed by ^{1}H NMR spectroscopy with a BRUKER DPX 300MHz BACS60 device using methanol as an internal standard for quantification purposes and deuterium oxide as solvent for the samples.

Solketal was the chemical species followed, whose signal was quantified and related to the concentration present in the reaction sample using methanol as an internal standard. Figure 1 shows a representative spectrum of the reaction, with the peaks corresponding to the protons of every compound present in the sample properly identified.

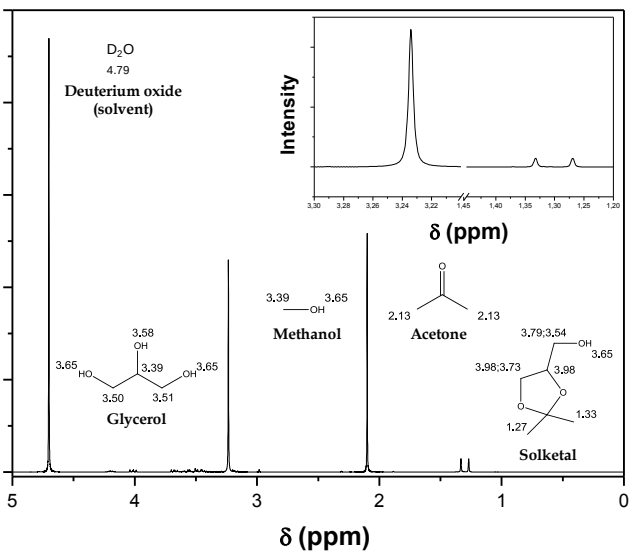

Fig. 1 Representative 1H NMR spectrum 300 MHz spectra of a sample of the reaction with all the protons identified.

Table 2 Properties of the sulfonated ion exchange resins used for the synthesis of solketal

Sample	Appearance	Maximum operating temperature (K)[a]	Acid capacity (eq H^+ kg^{-1})[b]	BET surface area (m^2 g^{-1})[c]	Pore volume (cm^3 g^{-1})[d]	Surface area (m^2 g^{-1})[d]	Bulk density (g cm^{-3})[d]	Apparent density (g cm^{-3})[d]
GF101	beige opaque solid	403	5.11	28	0.270	48	1.15	1.67
CT275DR	brown opaque solid	453	4.98	29	0.434	45	1.00	1.77
CT276	brown opaque solid	403	4.90	26	0.411	45	1.10	2.01
A35dry	gray opaque solid	423	5.25	30	0.336	78	1.10	1.75
A36dry	gray opaque solid	423	5.42	31	0.128	40	1.54	1.92

[a] from supplier. [b] obtained from ion exchange with NaCl. [c] obtained from BET. [d] from mercury porosimetry

Results and discussion

Characterization of ion exchange resins

Figure 2 plots the mercury intrusion curves (a) and its differentiated curve (b) performed for the determination of the pore size distribution. It can be observed that CT275DR and CT276 behave very similarly in the intrusion curve, with a maximum slope of the decrease of mercury volume intruded at a pore diameter between 65 and 80 nm, with a very narrow distribution and both can be said to be macroporous resins. A35dry and A36dry, on the other hand, show their drop at much lower pore diameters, reaching the maxima at approximately 35 and 15 nm, respectively, though with much wider pore size distributions than those observed for both Purolite resins. In the particular case of A35dry, there is an appreciable amount of pores above 50 nm, which means that this resin can be regarded as meso and macroporous; on the contrary, the pore size distribution size of A36dry barely stretches beyond 43 nm, so it can be said that it is mainly a mesoporous resin. Finally, GF101 shows a somewhat different trend, with a bimodal pore size distribution with a relative maximum at 12 nm and an absolute maximum at 190 nm. Nevertheless, the preponderant fraction of pores ranges from slightly below 100 nm to 1000 nm; therefore, it can mostly be considered macroporous.

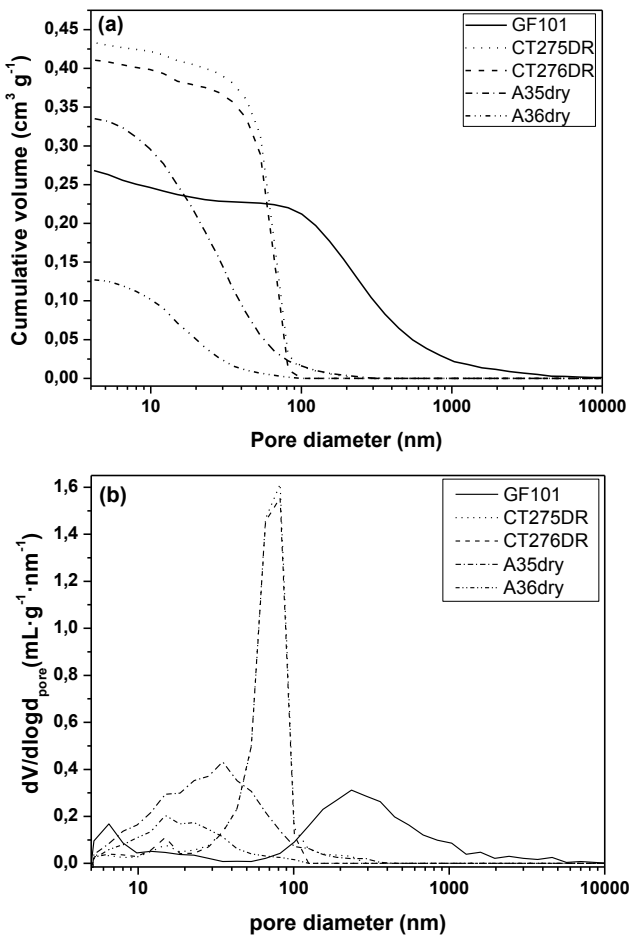

Fig. 2. Mercury intrusion curves for the ion exchange resins (a) and pore size distribution derived from the intrusion curves (b)

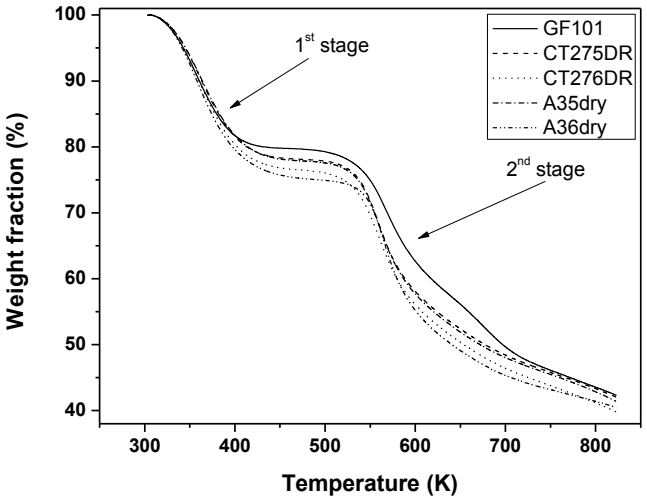

Fig. 3. Thermal decomposition curves of the resins from 333 to 823 K

Thermograms of the ion exchange resins are plotted in Figure 3. Despite the similar behaviour of the presented curves for all the resins, the weight drop intervals vary from resin to resin. At temperatures up to 200 ºC, there is a typical slight weight loss due to the removal of moisture within the matrix of samples. However, in this case, due to the dryness of these particular resins, these curves practically do not show this removal (not higher than 1-2% regardless of the resin considered). Neglecting this residual moisture removal interval, the curves exhibit a two-stage decay behaviour with a middle step in which the weight remains almost constant. The first stage corresponds to a weight loss of 20-25 %, ascribable to the degradation of sulfonic acids, being the resin GF101 the one with a lower quantity of sulfonic acids and similar sulfurized groups. Maximum degradation rate in this temperature interval is attained at 355 ºC in all cases. The second stage weight drop can be attributed to the degradation of resin polymeric matrices, as described in several references 43, 44. In resin GF101, as depicted in Figure 2b, there are two weight loss zones within the 500-800 ºC temperature interval in GF101, indicating two different polymeric matrices in this resin, one of them slightly less stable than the other. In Figure 2b, maximal degradation rates of the polymeric supports are observed at 555 ºC for Purolite resins, at 266 ºC for Amberlyst resins, and at 266 and 677 ºC for the Lewatit GF101. Judging from these temperatures and the maximal degradation rates of the polymers, whose order is A36dry > A35dry > CT276 > CT275DR >> GF101, the thermal stability of the polymer in GF101 appears to be somewhat higher than the rest. At temperatures higher than 750 ºC, a low and constant degradation rate, similar for all resins, is observed.

Solid ^{13}C-NMR was performed to acquire a deeper knowledge on the presence of sulfonic groups within the structure of the resins. Figure 4 compiles the spectra obtained for the solid samples, where a series of representative signals can be seen. First, secondary and tertiary aliphatic carbons can be identified at a shift of about 42.5 ppm, being these carbons accountable for the constitution of the backbone of the divinylbenzene structure [45]. Also, a signal whose maximum is at 127 ppm is observed, which corresponds to the overlapping of the signals of aromatic carbon atoms at *ortho*- and *meta*-positions with respect to the carbon to which the sulfonic group is attached, which range between 123.0 and 129.4 ppm as calculated in Table 3 considering the different carbons to which the sulfonic group can be attached [45, 46]. Finally, the peak at

Table 3. Estimated ^{13}C-NMR shifts for the carbon atoms of vinylbenzene sulphonated at *ortho-*, *meta-* and *para-* positions [45, 46]

Sulphonated vinylbenzene	Carbon atom	z_i [a] (alkyl chain)	δ (ppm)	z_i [a] (SO3H)	δ (ppm)	δ_{total} (ppm)[a]
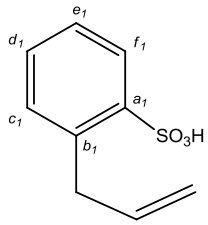	a_1	z_2	-0.6	z_1	15.0	142.9
	b_1	z_1	15.7	z_2	-2.2	142.0
	c_1	z_2	-0.6	z_3	1.3	129.2
	d_1	z_3	-0.1	z_4	3.8	132.2
	e_1	z_4	-2.8	z_3	1.3	127.0
	f_1	z_3	-0.1	z_2	-2.2	126.3
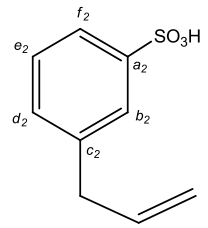	a_2	z_3	-0.1	z_1	15.0	143.4
	b_2	z_2	-0.6	z_2	-2.2	125.7
	c_2	z_1	15.7	z_3	1.3	145.5
	d_2	z_2	-0.6	z_4	3.8	131.7
	e_2	z_3	1.3	z_3	-0.1	129.7
	f_2	z_4	-2.8	z_2	-2.2	123.5
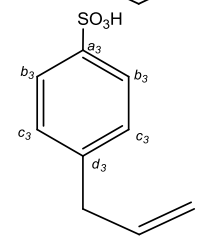	a_3	z_4	-2.8	z_1	15.0	140.7
	b_3	z_3	-0.1	z_2	-2.2	126.2
	c_3	z_2	-0.6	z_3	1.3	129.4
	d_3	z_1	15.7	z_4	3.8	148

[a] Total shift was calculated according to $\delta_{total} = 128.5 + \sum_i z_i$, where 128.5 is the shift corresponding to any carbon atom in the benzene ring and z_i is the shift due to the presence of a substituent in the position $_i$.

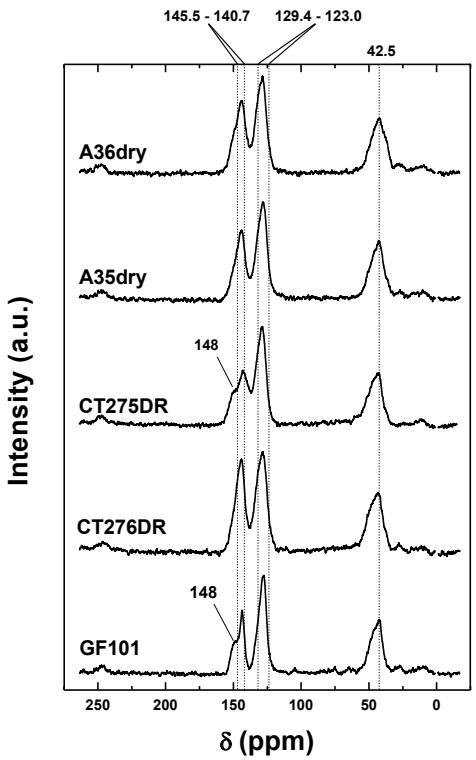

Fig. 4. ^{13}C-NMR spectra of the sulfonic resins with identifying guidelines (detailed in the text and Table 2).

140.7-145.5 ppm can be ascribed to directly alkylated or sulphonated carbon atoms, as estimated for the atoms a_1, b_1, a_2, c_2 and a_3 in Table 3; nevertheless, in the cases of CT275DR and GF101 a shoulder at 148 ppm appears. Detections at this value correspond to directly alkylated aromatic carbons at a *para-*position with respect to the sulphonated carbon atom, i.e., carbon atoms labeled as d_3 in Table 3. These signals at shifts very similar to the one reported herein corresponding to such type of carbon atoms in sulphonated solids have previously been reported [47, 48]. The greater the presence of these atoms, which appears to be more predominant in the mentioned resins, the more available the sulfonic group is owing to lower steric effects.

The elemental analysis of solids can also shed light on the presence of sulfonic groups. Figure 5 shows the elemental microanalysis performed for the resin samples, whose oxygen weight fraction has been determined as the difference of the summation of the weight fraction of carbon, hydrogen, nitrogen and sulfur to 100%. The presence of sulfur ranges among 7 and 15 %, being CT275DR the solid containing most sulfur closely followed by GF101; A35dry and A36dry have similar sulfur content of 11.5% and 10.5%, respectively; finally, CT276 possesses the lowest content.

Finally, Figure 6 depicts the potentiometric titration of the five resins. According to Pizzio's classification, all of the resins have very strong sites given that the initial potential values are above 100 mV [49] and the order of strength would be as follows: CT275DR > A35dry > GF101 > A36dry > CT276. However, it is worthwhile mentioning the fact that the curves exhibit different behaviours. CT276, CT275DR and A35dry show a relatively slight reduction of the potential at the beginning of the titration and then a steep decrease; A36dry presents a

similar curve, though the drop is not as pronounced as in the previous three cases. On the other hand, GF101 shows a marked decline of the potential practically from the beginning. This can lead to think that the acidity of the latter catalyst becomes available more quickly than the others and, thus, can be associated to a highest strength and catalytic activity.

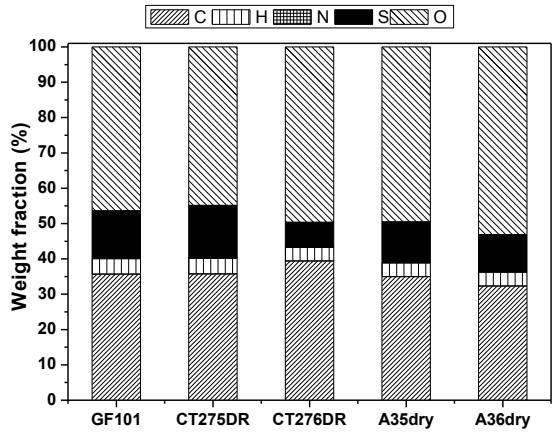

Fig. 5. Elemental microanalysis of the ion exchange resins

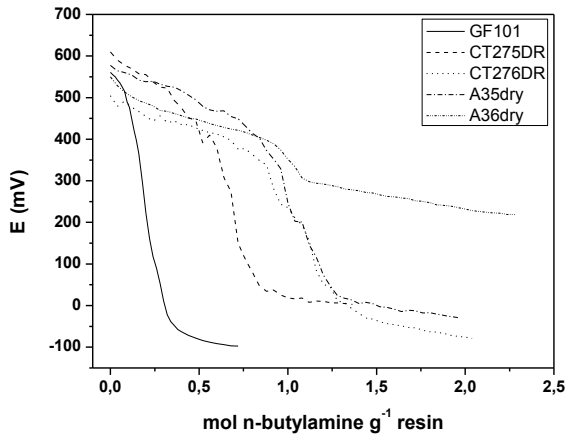

Fig. 6. Potentiometric titration of the sulfonic acid-based ion exchange resins

Catalytic experiments

The ionic exchange resins were tested for activity in the synthesis of solketal under solventless operation at a temperature of 40 ºC and a molar excess of acetone to glycerol with a catalyst load of 0.5 % w/w of each resin. It is worthwhile remarking the fact that at these temperature and composition conditions, acetone and glycerol are immiscible to a high extent. As the products of the reaction generate, solketal and water, the system turns into a single phase liquid. [50]

Figure 7 shows the evolution of the yield to solketal obtained throughout assays with each of the resins, with yield being defined as the percentage of the ratio of the concentration of solketal at each moment to the initial concentration of glycerol. In addition to the five resins herein tested, Amberlyst 15 (A15) has been used as a reference. It is a well-known classic cation exchange resin existing for over 50 years which has been characterized [51] and used in the acetylation of glycerol, a relatively similar reaction [44]. From the plot it can be seen that the reaction reaches its equilibrium position at approximately 5 hours only when GF101 is used; however, after 6 hours, equilibrium is still not reached in the cases of CT275DR, A35dry, A36dry and A15, which exhibited similar performance, and CT276.

Figure 7 shows the evolution of the yield to solketal obtained throughout assays with each of the resins, with yield being defined as the percentage of the ratio of the concentration of solketal at each moment to the initial concentration of glycerol. From the plot it can be seen that the reaction reaches its equilibrium position at approximately 5 hours only when GF101 is used; however, after 6 hours, equilibrium is still not reached in the rest of the cases. CT275DR, A35dry and A36dry exhibited similar performance, while A15 and CT276 had slightly less catalytic activity.

The inset graph of Figure 7 shows the progress of the reaction within the first hour of the reaction. The shapes of the curves are typical of those obtained using heterogeneous catalysts. It can be seen that, from the very beginning of the reaction, the performance observed for GF101 is better than the rest. This observation could be explained given the features described for this throughout Section 3.1. As shown by mercury porosimetry, this resin exhibits a bimodal pore distribution size curve, with an absolute maximum at 190 nm yet with a distribution around this size which spreads well across the macroporous region. At short times of reaction there is still a liquid-liquid biphasic system due to the limited miscibility between the two reactant species; therefore, the viscosity of glycerol plays an important role. GF101 possesses a much wider macroporous region, which in turn facilitates the access of glycerol into the pores. In addition, the solid ^{13}C-NMR analysis showed that the presence of sulfonic groups in para-positions with respect to the vinyl matrix is significant in GF101 as well as in CT275DR, the resin with the second best performance. These results also agree with the results obtained from the elemental microanalysis, in which the presence of sulfur was the highest for these two resins and the lowest for CT276, the least active catalyst. Moreover, the potentiometric titration and the acid capacity of the resins also show that GF101 have a greater acidity. In summation, the availability of the active acid sites appears to be the key aspect to explain the performance of these catalysts, despite the fact that the two most active resins do not possess the highest pore volume or surface area within their structures (see Table 2).

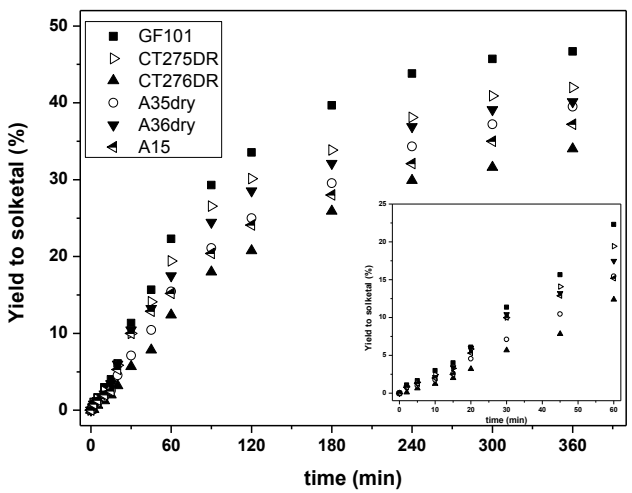

Fig. 7. Yield to solketal obtained for each of the tested catalysts at 313 K, a molar excess of acetone to glycerol of 4.5 and a catalyst load of 0.5 % w/v

Additionally, the effect that the presence of water generated as a byproduct may exert on the catalyst has to be taken into account. Resins based on sulfonic acids, like Amberlyst 15, Amberlyst 16 and Dowex Wx8, have been tested for deactivation in the presence of water[52-56], reaching the conclusion that there is a high affinity of sulfonic acids for water. This fact, coupled to cation exchange, could explain the deactivation of the catalyst with time as well as the fact that the equilibrium conversion is difficult to shift towards the products and only reaches approximately 47%.

Reutilization of the catalyst

A series of recycling assays were performed in order to assess the stability of the resins to deactivation throughout consecutive experiments. The activity of the resins was considered as the turnover frequency (TOF) observed for each resin at each cycle, established as

$$TOF = \frac{r_{max}}{C_{cat}} \quad (1)$$

where r_{max} is the maximum reaction rate ($mol \cdot L^{-1} \cdot min^{-1}$) and C_{cat} the equivalent concentration of protons ($mol \cdot L^{-1}$), obtained from the acid capacity of the resins (Table 2).

After observing the evolution of the yield to solketal in the inset of Figure 7, the evolution of the concentration of solketal with respect to time was fitted making use of the Hoerl curve [57] to the kinetic data obtained in successive recycling experiments, as defined by eq. (2):

$$C_{Sk} = A \cdot B^t \cdot t^C \quad (2)$$

where C_{sk} is the concentration of solketal ($mol \cdot L^{-1}$), t is time and A, B and C are the fitting parameters of the equation. From the differentiation of eq. (2), the reaction rate as a function of time is obtained, whose maximum value is herein considered as rmax to be used in equation 1.

Figure 8 depicts the evolution of the TOF of each resin vs. the number of recycling experiments. It can be observed that GF101 has the highest activity in practically all the cycles followed by CT275DR as already addressed. Nonetheless, it is worthwhile mentioning that as the reutilization of the catalysts progresses, the activity of these two resins approaches similar values to those obtained by the rest of the catalysts.

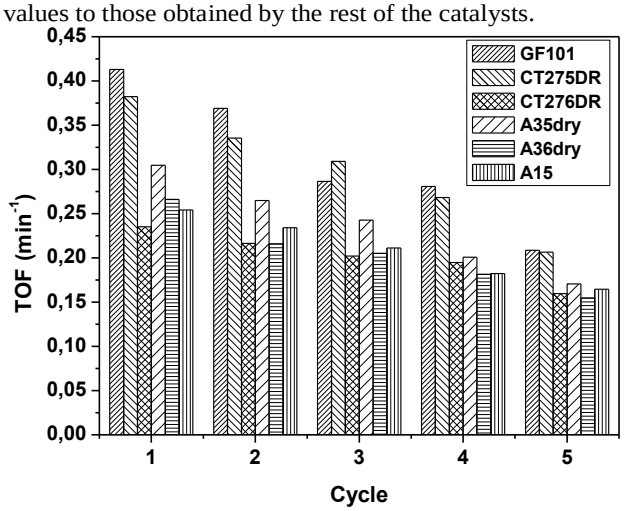

Fig. 8. Evolution of TOF of the resins with recycling experiments at 313 K, M=4.5 and catalyst load of 0.5 % w/w

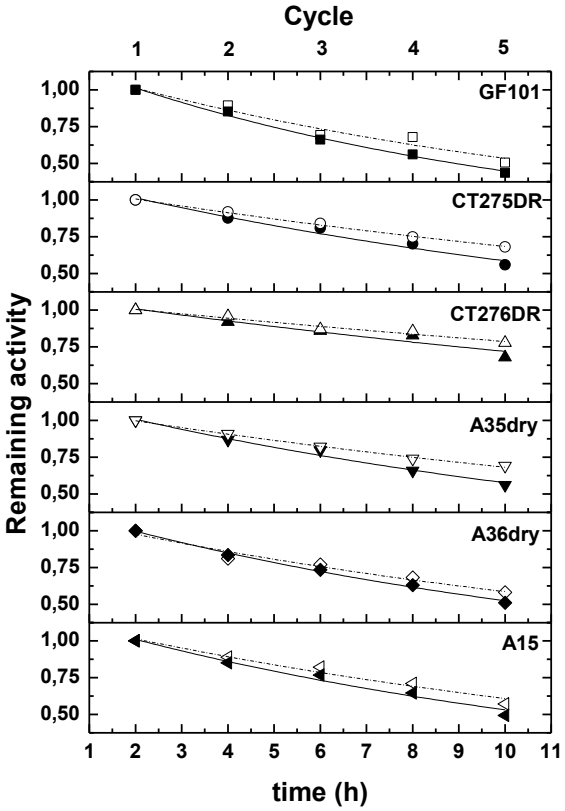

Fig. 9. Progress of the experimental and fitted remaining activity with total operating time and number of recycles of the catalysts. Solid markers correspond to regenerated catalysts, open markers correspond to non-regenerated.

Figure 9 deepens on these findings. This graph plots the remaining activities referred to the first use of each resin as a function of the total operating time. Each cycle was performed for two hours in these reutilization experiments. It can be seen that a regeneration of the catalyst with perchloric acid improves to some extent the remaining activity with respect to the non-regenerated catalyst. The remaining activities of the non-regenerated and regenerated resins have been fitted relatively well to an exponential decay model of the following type

$$a_r = A \cdot exp(-k_d \cdot t) \quad (3)$$

in which a_r is the remaining activity, t refers to the total operating time of the resin and A and k_d are the amplitude and the decay constant, i.e., the fitting parameters of the curve.

Table 4 compiles the values of the mentioned parameters as well as the half-life period. This value corresponds to the number of cycle at which the model predicts that the remaining activity will be equal to 0.5.

Both in Figure 9 and from the half-life value in Table 4 it can be inferred that GF101 suffers the highest decrease in activity despite showing the best performance in all the cycles. CT275DR, A35dry, A36dry and A15 have all similar half-life values of around 6 cycles. Curiously, the least active species in this work, i.e., CT276, showed the lowest decay in activity with only a loss of 18% after the first four cycles when no regeneration was made and 24% when such procedure was performed, reaching lower though somewhat similar values to those obtained silica-included heteropolyacids, where the activity drop was estimated to be between up to 13% after the same number of recycles[26].

Table 4. Summary of the parameters used for the remaining activity exponential decay model (eq. 3) and half-life period for the fresh and regenerated catalysts, with their TOF values

Catalyst state	Catalyst	A ± error	k_d ± error	r^2	$t_{1/2}$ (h)	TOF (min^{-1})
First use	GF101	1.19 ± 0.07	0.08 ± 0.01	0.94	10.82	0.42 ± 0.041
	CT275DR	1.16 ±0.05	0.07± 0.01	0.95	12.32	0.37 ± 0.034
	CT276	1.10 ±0.04	0.04± 0.01	0.91	18.58	0.23 ± 0.033
	A35dry	1.16 ±0.03	0.07± 0.02	0.98	12.03	0.30 ± 0.039
	A36dry	1.11 ±0.04	0.07± 0.01	0.96	12.49	0.27 ± 0.028
	A15	1.15 ± 0.05	0.07 ± 0.02	0.96	12.36	0.25 ± 0.032
Regenerated	GF101	1.24 ±0.03	0.10±0.01	0.99	8.93	0.41 ± 0.036
	CT275DR	1.19 ±0.04	0.08±0.02	0.98	10.28	0.36 ± 0.034
	CT276	1.13 ±0.03	0.06±0.01	0.97	14.37	0.24 ± 0.038
	A35dry	1.20 ±0.03	0.08±0.01	0.99	10.51	0.31 ± 0.042
	A36dry	1.17 ±0.02	0.08±0.01	0.99	10.62	0.27 ± 0.035
	A15	1.19 ± 0.04	0.08 ± 0.02	0.98	10.55	0.24 ± 0.042

Regeneration of the resins and further use for solketal synthesis proved, according to Table 4, that the procedure was successful at least once in all cases, taking into account the TOF values attained.

Conclusions

A series of commercially available sulfonic ion exchange resins have been employed to convert glycerol and acetone to solketal through a reaction that at short time of reaction consists of a liquid-liquid biphasic system. The six resins herein tested showed accepted performance in completing the reaction.

Thorough characterization of five of those resins was conducted, revealing that Lewatit GF101 followed by Purolite CT275DR had the highest sulfur content and provided the best accessibility and availability of sulfonic active sites despite not showing the highest surface area among the resins tested. The order of activity of the resins observed could be explained by such mentioned features of the resins. The order of activity goes as follows including the traditional resin Amberlyst 15: Lewatit GF101 > Purolite CT275DR > Amberlyst 35dry > Amberlyst 36dry > Amberlyst 15 > Purolite CT276.

Reutilization of the catalysts was also performed through an assessment of the decrease of the TOF after successive recycles with and without regeneration of the catalyst. In this case, evaluation of the half-life of the remaining activity of the fresh and regenerated catalysts revealed that the order of stability was very different to the performance, namely: Purolite CT276 > Amberlyst 36dry > Amberlyst 15 > Purolite CT275DR > Amberlyst 35dry > Lewatit GF101.

Acknowledgements

The authors wish to acknowledge the financial support received from the Spanish Ministry of Science and Innovation through Projects CTQ2007-60919 and CTQ2010-15460.

Contact information

[a]Department of Chemical Engineering, Complutense University of Madrid, Avda. Complutense s/n. 28040, Madrid, Spain. E-mail: mladero@quim.ucm.es; Fax: +34- 913944179; Tel: +34-913944164

1. P. Anastas and J. Warner, *Green Chemistry Theory and Practice.*, Oxford University Press, New York, 2008.
2. C.-H. Zhou, J. N. Beltramini, Y.-X. Fan and G. Q. Lu, *Chem. Soc. Rev.*, 2008, **37**, 527-549.
3. A. Behr, J. Eilting, K. Irawadi, J. Leschinski and F. Lindner, *Green Chemistry*, 2008, **10**, 13-30.
4. M. Pagliaro and M. Rossi, *The Future of Glycerol: New Uses of a Versatile Raw Material*, RSC Publishing, Cambridge, UK, 2008.
5. J. Esteban, M. Ladero, E. Fuente, A. Blanco and F. García-Ochoa, *RSC Advances*, 2014, **4:**, 53206-53215.
6. Y. Li, H. Liu, L. Ma and D. He, *Rsc Advances*, 2014, **4**, 5503-5512.
7. S. Budavari, Merck & Co. Inc., Rahway, New Jersey, 1989.
8. J. Jurczak, S. Pikul and T. Bauer, *Tetrahedron*, 1986, **42**, 447-488.
9. R. P. Hof and R. M. Kellogg, *Journal of Organic Chemistry*, 1996, **61**, 3423-3427.
10. R. S. Karinen and A. O. I. Krause, *Applied Catalysis A: General*, 2006, **306**, 128-133.
11. K. Klepáčová, D. Mravec, A. Kaszonyi and M. Bajus, *Applied Catalysis A: General*, 2007, **328**, 1-13.
12. J. A. Melero, R. van Grieken, G. Morales and M. Paniagua, *Energy & Fuels*, 2007, **21**, 1782-1791.
13. N. Rahmat, A. Z. Abdullah and A. R. Mohamed, *Renewable & Sustainable Energy Reviews*, 2010, **14**, 987-1000.
14. C. J. A. Mota, C. X. A. da Silva, N. Rosenbach, Jr., J. Costa and F. da Silva, *Energy & Fuels*, 2010, **24**, 2733-2736.
15. E. Garcia, M. Laca, E. Perez, A. Garrido and J. Peinado, *Energy & Fuels*, 2008, **22**, 4274-4280.
16. N. Suriyaprapadilok and B. Kitiyanan, *Energy Procedia*, 2011, **9**, 63-69.
17. M. Selva, V. Benedet and M. Fabris, *Green Chemistry*, 2012, **14**, 188-200.
18. B. Bruchmann, K. Haeberle, H. Gruner and M. Hirn. EP842929-A, 1999.
19. J. S. Clarkson, A. J. Walker and M. A. Wood, *Organic Process Research & Development*, 2001, **5**, 630-635.
20. C. Fan, C. Xu, C. Liu, Z. Huang, J. Liu and Z. Ye, *Heterocycles*, 2012, **85**, 2977-2986.
21. J. Deutsch, A. Martin and H. Lieske, *Journal of catalysis*, 2007, **245**, 428-435.
22. L. Roldan, R. Mallada, J. M. Fraile, J. A. Mayoral and M. Menendez, *Asia-Pacific Journal of Chemical Engineering*, 2009, **4**, 279-284.
23. G. Vicente, J. A. Melero, G. Morales, M. Paniagua and E. Martin, *Green Chemistry*, 2010, **12**, 899-907.
24. C. X. A. da Silva, V. L. C. Goncalves and C. J. A. Mota, *Green Chemistry*, 2009, **11**, 38-41.
25. C. X. A. da Silva and C. J. A. Mota, *Biomass & Bioenergy*, 2011, **35**, 3547-3551.
26. P. Ferreira, I. M. Fonseca, A. M. Ramos, J. Vital and J. E. Castanheiro, *Applied Catalysis B: Environmental*, 2010, **98**, 94-99.

27. P. S. Reddy, P. Sudarsanam, B. Mallesham, G. Raju and B. M. Reddy, *Journal of Industrial and Engineering Chemistry*, 2011, **17**, 377-381.
28. L. Li, T. I. Koranyi, B. F. Sels and P. P. Pescarmona, *Green Chemistry*, 2012, **14**, 1611-1619.
29. D. Nandan, P. Sreenivasulu, L. N. S. Konathala, M. Kumar and N. Viswanadham, *Microporous and Mesoporous Materials*, 2013, **179**, 182-190.
30. F. D. L. Menezes, M. D. O. Guimaraes and M. J. da Silva, *Industrial & Engineering Chemistry Research*, 2013, **52**, 16709-16713.
31. M. R. Nanda, Z. Yuan, W. Qin, H. S. Ghaziaskar, M.-A. Poirier and C. Xu, *Fuel*, 2014, **128**, 113-119.
32. M. R. Nanda, Z. Yuan, W. Qin, H. S. Ghaziaskar, M.-A. Poirier and C. Xu, *Applied Energy*, 2014, **123**, 75-81.
33. M. Shirani, H. S. Ghaziaskar and C. Xu, *Fuel Processing Technology*, 2014, **124**, 206-211.
34. M. R. Nanda, Z. Yuan, W. Qin, H. S. Ghaziaskar, M.-A. Poirier and C. C. Xu, *Fuel*, 2014, **117**, 470-477.
35. D. Royon, S. Locatelli and E. E. Gonzo, *Journal of Supercritical Fluids*, 2011, **58**, 88-92.
36. J. Tejero, E. Creus, M. Iborra, F. Cunill, J. F. Izquierdo and C. Fite, *Catal. Today*, 2001, **65**, 381-389.
37. R. V. Korzh, V. A. Bortyshevskii, T. V. Tkachenko, V. A. Evdokimenko and V. V. Boiko, *Russian Journal of Applied Chemistry*, 2007, **80**, 1335-1340.
38. H. W. Tsao. US7588690 B1, 2009.
39. M. Cadenas, R. Bringue, C. Fite, E. Ramirez and F. Cunill, *Topics in Catalysis*, 2011, **54**, 998-1008.
40. R. Bringue, E. Ramirez, M. Iborra, J. Tejero and F. Cunill, *Journal of catalysis*, 2013, **304**, 7-21.
41. C. Ramírez-López, J. Nieto-Maestre, O. Gómez-Jiménez-Aberasturi, J. R. Ochoa-Gómez, A. Arteche-Calvo, M. Belsue, J. J. Aragón, M. C. Dobarganes and M. V. Ruiz-Méndez, presented in part at the ANQUE International Congress of Chemical Engineering Seville (Spain), 2012.
42. A. Turan, M. Hrivnak, K. Klepatova, A. Kaszonyi and D. Mravec, *Applied Catalysis a-General*, 2013, **468**, 313-321.
43. X. Liao, Y. Zhu, S.-G. Wang and Y. Li, *Fuel Processing Technology*, 2009, **90**, 988-993.
44. I. Dosuna-Rodriguez and E. M. Gaigneaux, *Cata1ysis Today*, 2012, **195**, 14-21.
45. J. Dean, *Analytical Chemistry Handbook*, McGraw-Hill, New York, 1995.
46. D. F. Ewing, *Organic Magnetic Resonance*, 1979, **12**, 499-524.
47. I. Sadaba, M. Ojeda, R. Mariscal and M. Lopez Granados, *Applied Catalysis B-Environmental*, 2014, **150**, 421-431.
48. M. Lopez Granados, A. Carolina Alba-Rubio, I. Sadaba, R. Mariscal, I. Mateos-Aparicio and A. Heras, *Green Chemistry*, 2011, **13**, 3203-3212.
49. L. R. Pizzio, P. G. Vazquez, C. V. Caceres and M. N. Blanco, *Applied Catalysis A: General*, 2003, **256**, 125-139.
50. J. Esteban, A. J. Vorholt, A. Behr, M. Ladero and F. Garcia-Ochoa, *Journal of Chemical & Engineering Data*, 2014, **59**, 2850-2855.
51. R. Kunin, S. A. Fisher, E. F. Meitzner, N. Frisch and J. A. Oline, *Industrial & Engineering Chemistry Product Research and Development*, 1962, **1**, 140-144.
52. R. Tesser, L. Casale, D. Verde, M. Di Serio and E. Santacesaria, *Chemical Engineering Journal*, 2010, **157**, 539-550.
53. J.-Y. Park, D.-K. Kim and J.-S. Lee, *Bioresource Technology*, 2010, **101**, S62-S65.
54. J.-Y. Park, Z.-M. Wang, D.-K. Kim and J.-S. Lee, *Renewable Energy*, 2010, **35**, 614-618.
55. T. Popken, L. Gotze and J. Gmehling, *Industrial & Engineering Chemistry Research*, 2000, **39**, 2601-2611.
56. S. H. Ali, A. Tarakmah, S. Q. Merchant and T. Al-Sahhaf, *Chemical Engineering Science*, 2007, **62**, 3197-3217.
57. A. E. Hoerl, *Fitting curves to data. In Chemical business handbook; Perry, J. H., Ed.; McGraw-Hill: New York, 1954; pp 55-57*, McGraw-Hill, New York.

Publicación 9 / Publication 9

Autores/Authors: Jesús Esteban, Miguel Ladero and Félix García-Ochoa

Título/Title: Kinetic modeling of the of the solventless synthesis of solketal with a sulphonic ion exchange resin

Estado actual/Current status: Manuscript resubmitted to Chemical Engineering Journal after minor modifications as of January 2015

Índice de impacto / Impact factor 2013: 4.058

Resumen

El objetivo de este trabajo es profundizar en los aspectos cinéticos de la reacción catalítica heterogénea de ketalización entre la glicerina y la acetona para dar solketal, para lo cual se emplea la resina sulfónica de intercambio iónico Lewatit GF101

Al tratarse de un sistema consistente en varias fases debido a la miscibilidad limitada entre la acetona y la glicerina, además de la presencia de un sólido en el cual tiene lugar la reacción, se hace necesaria la determinación de condiciones en las cuales sea controlante de la velocidad global la reacción química. Así pues, se ha realizado un estudio de la influencia de la agitación, determinándose que a partir de 750 rpm, la transferencia externa de materia no es limitante. Además, se emplearon varios tamaños de partícula del catalizador para evaluar las limitaciones a la transferencia interna de materia: por una parte, se vio que el factor de efectividad es igual a la unidad para tamaños de partícula entre 180 y 200 μm; por otra, se observó que sometiendo el catalizador a un tratamiento de trituración, su actividad no se veía afectada.

Determinadas estas condiciones, se realizaron experimentos cinéticos variando la temperatura entre 30 y 40 ºC, la carga de catalizador entre 0.5 y 1 % en peso y excesos molares de acetona a glicerina entre 3 y 12. Se vio un efecto positivo de estas variables sobre la velocidad de reacción. Además, se comprobó que el efecto del exceso molar de acetona a glicerina sobre la posición de equilibrio era muy significativo.

Con los datos cinéticos obtenidos, se propusieron una serie de modelos cinéticos basados en modelos empleados típicamente en reacciones catalizadas por sólidos. Se plantearon cuatro modelos pseudohomogéneos, cuatro de tipo Eley-Rideal (ER) y otros cuatro basados en Langmuir-Hinshellwood-Hougen-Watson (LHHW).

Considerando el posible mecanismo de reacción dadas las condiciones de operación, así como criterios estadísticos, se discriminó entre los modelos propuestos. El que mejor se ajustó a los datos experimentales fue un modelo ER considerando la reacción inversa de orden cero respecto a las concentraciones de los reactivos y orden uno respecto a cada uno de los productos y, en el denominador, sólo la constante de adsorción del agua. Las energías de activación obtenidas fueron 124.0 ± 12.9 $kJ \cdot mol^{-1}$ y 127.3 ± 12.6 $kJ \cdot mol^{-1}$ para la reacción directa e inversa, respectivamente, y una entalpía de 128.0 ± 21.4 $kJ \cdot mol^{-1}$ para la constante de adsorción del agua.

Kinetic modeling of the of the solventless synthesis of solketal with a sulphonic ion exchange resin

Jesús Esteban, Miguel Ladero*, Félix García-Ochoa

Department of Chemical Engineering. College of Chemical Sciences. Complutense University of Madrid. 28040. Madrid. Spain.

*Corresponding author: mladero@quim.ucm.es. (Phone: +34-913944164/fax: +34-913944179)

Abstract

Synthesis of solketal from acetone and glycerol is approached in this work through a batch process in the absence of solvents. A heterogeneous catalysis approach was employed using the resin Lewatit GF101 as catalyst after selection from a few other sulphonic ion exchange resins. An initial study of the external mass transfer revealed that a stirring rate of 750 rpm sufficed for the external mass transfer not to be the rate limiting step. Similarly, a study of the internal mass transfer showed that for particle sizes of 190 μm the maximum reaction rate was achieved. Once the optimal stirring and particle size conditions were determined, a series of kinetic runs was conducted varying temperature (30-40 ºC), initial molar excess of acetone to glycerol (3-12) and catalyst load (0.5-1 % w/w) for this reaction in equilibrium. Different kinetic models based on potential laws and Eley-Rideal (ER) and Langmuir-Hinshelwood-Hougen-Watson (LHHW) equations were proposed to fit to the experimental data obtained. After physical and statistical discrimination, an ER accounting for the direct and reverse reaction was selected, with activation energies of 124.0 ± 12.9 $kJ \cdot mol^{-1}$ and 127.3 ± 12.6 $kJ \cdot mol^{-1}$ for the direct and reverse reaction, respectively, and enthalpy of adsorption of 128.0 ± 21.4 $kJ \cdot mol^{-1}$ for the adsorption constant of water.

Keywords: solketal, glycerol, solventless synthesis, kinetic model, ion exchange resin

1. Introduction

Despite glycerol (Gly) having been widely employed throughout history in multiple applications, the overproduction caused by the blooming biodiesel industry has caused a drop of its price. It is foreseen that environmental policies in the European Union will continue to spur the development of renewable sources of energy in the following years as stated in the EU 2009/28/EC Directive. As a consequence of such availability, glycerol has been widely regarded as a platform chemical from which assorted reactions can be proposed to yield valuable products. Due to its rich chemical reactivity, assorted valuable compounds through chemical routes of very distinct nature have been obtained [1-6].

Among the uses of products derived from glycerol, the utilization of oxygenate derivates as biofuel additives is receiving increasing attention. One example would be di and tritert-butyl glycerol (DTBG and TTBG) [7, 8] , which have proven to enhance the octane index of gasoline [9] as well as decrease viscosity of biodiesel, thus improving its cold-flow properties [10] while also reducing emissions of particulates, CO and certain aldehydes [11].

Ketals derived from the acetalisation of glycerol, have been more profusely studied as additives to fuels [8, 12-15]. 1,2-isopropylideneglycerol, also referred to as solketal (Sk), has received particularly high attention, for it has proven to enhance certain performance parameters and specifications. Reduced gum formation and improvement of the octane index was observed when using up to 5% volume of solketal to gasoline [16], while addition of said ketal to biodiesel not only improved its viscosity, but also complied with the flash point and oxidation stability specifications as enacted by European and American Standards (EN 14214 and ASTM D6751, respectively) [17]. Even further reactions of solketal have been explored to yield new potential additives, namely: its upgrade to benzyl alcohol ether [18] or the synthesis of solketal o-methylesters by making solketal react with dialkyl carbonates under basic conditions [19].

In addition to the mentioned applications enhancing the performance parameters of certain fuels, solketal has been put to use as a plasticizer and a green solvent and suspending agent in pharmaceutical formulations [20]. Furthermore, its chemical reactivity makes it a relevant building block in the synthesis of chemicals of

pharmaceutical interest like prostaglandins, glycerophospholipids or β-blockers like (S)-propanolol, widely used for medical treatments like hypertension or migrain [21, 22].

The synthesis of acetals mainly consists in the reaction of an alcohol with ketones or aldehydes. Specifically, cyclic ketals (like solketal) may be obtained through the reaction of polyols (like glycerol) with said carbonyl compounds through a reaction mechanism that consists of the formation of a highly unstable intermediate species and then the cyclation of said intermediate to yield the ketal [23, 24].

Assorted catalysts have been employed to such purpose. Approaches to completion of this reaction using homogeneous catalysis have been made, such as employing p-toluenesulphonic, sulphuric or hydrochloric acids [17, 25-27]. Efforts using solid catalysts appear to be the most followed trend, including the use of oxides of Group IV of the periodic table [28], zeolites [29, 30], clays [29], heteropolyacids immobilized in silica [31], sulfonic acid-functionalized mesostructured silicas [32, 33], promoted zirconia [34], various sulfonated carbon silica mesocomposite materials [35], Sn-based salts, mesoporous substituted silicates [33]. With respect to the utilization of solid catalysts, special mention must be made to the use of commercially available ion exchange resins. Table 1 compiles a brief review of the references found using such catalysts together with the conditions and operation modes used in each work to shift the equilibrium existing in this reaction towards the products [29, 30, 36-39]. Selectivity of these catalysts towards the five-membered ring isomer of solketal has been reported to be practically 100% for the vast majority of the aforementioned acid catalysts.

Operational aspects of the reaction of glycerol with acetone (Ac) to yield solketal include a wide array of temperatures from room temperature or slightly above [34] to temperatures exceeding the acetone boiling point (57 ºC), in which case removal of water is sought in order to shift the equilibrium to the products through a reactive distillation process [17, 31, 40]. Use of supercritical conditions at 250 ºC and 8 MPa has also been reported in literature, with conversions of glycerol being no greater than 29%; the absence of catalyst is ascribed to the catalytic effect of the acidic strength of the alpha hydrogen of acetone in the gas phase [41]

Moreover, molar excess of acetone with respect to glycerol (*M*) has also been used in order to shift the reaction to the products given the existing equilibrium. Typical *M* values mentioned in literature range from 2/1 to 6/1, despite sometimes being as high as 10.8/1 [41] or even 20/1 in order to reach yields of 82% of solketal under reflux

conditions [42]. More recently, excess of acetone was used together with ethanol acting as a cosolvent [36, 37, 43] for acetone and glycerol, considering the limited miscibility of these compounds at the start of the reaction [44].

Reaction kinetics is an essential tool to deepen the understanding of chemical processes. Kinetic models concerning reactions implied in the valorisation of glycerol have been found [8, 45-47] and even a kinetic model for the synthesis of solketal has recently been reported for a procedure using ethanol as a cosolvent over Amberlyst 35 [36].

The aim of this work is to describe the catalytic ketalization of glycerol with acetone under solventless conditions with sulphonic ion exchange resins. For this purpose, screening among some resins as well as a study of the operating conditions to avoid internal and external mass transfer resistance is made. Most importantly, the effect of operating variables is evaluated and suggestion and physicochemical and statistical discrimination among different kinetic models is made to propose a reaction mechanism.

2. Materials and Methods

2.1. Materials

Extra pure glycerol (99%) (Scharlau Chemie, Ltd) and acetone (HPLC grade) (Romil, Ltd) were utilized as reactants. Solketal (purity=98.1%) from Aldrich was employed for calibration purposes. Finally, the preparation of samples required methanol (HPLC grade) (Fisher Scientific UK, Ltd.) as internal standard and deuterium oxide (99.8%, NMR spectroscopy grade) (Scharlau Chemie, Ltd.) as solvent. The sulphonic ion exchange resins utilized were: Purolite CT275DR, Purolite CT276 (Purolite, Ltd.); Amberlyst 35dry, Amberlyst 36dry (Rom and Haas France SAS) and Lewatit GF101 (Lanxess Deutschland GmbH). All of them were kindly supplied by each manufacturer.

2.2. Experimental

2.2.1. Apparatus, methodology

The reactor employed to perform the ketalization runs is schematized in Figure 1. It consists of a glass vessel whose outer walls are heated by a thermal controlled by an OMRON E5CN PID controller with temperature being measured with a

thermocouple. The loads were stirred by means of a flat six-blade impeller whose speed was regulated by an IKA RW20 motor (250 to 2500 rpm). Finally, sample withdrawal was performed thanks to a syringe with a wide-bore needle piercing a Teflon lid tightly fitted to the top of the reactor.

The operational procedure started by loading the appropriate amount of both reactants into the glass reactor. Then, stirring and heating were initiated and, once the temperature reached its set value, catalyst was added through the inlet too and reaction started to take place. Prior to conducting the reactions, resin beads were crushed and sieved when necessary.

2.2.2. Analysis

Samples were analysed by ^{1}H NMR spectroscopy with a BRUKER DPX 300MHz BACS60 device. Deuterium oxide was employed as solvent for the samples and methanol as an internal standard. Solketal was the chemical species followed, with a signal of representative protons of this chemical being identified and used for quantification. This signal corresponds to chemical shifts of 1.27 and 1.33 ppm.

2.3. Mathematical methods

The data obtained from the kinetic runs were regressed following distinct kinetic models. For this purpose Aspen Custom Modeler was used, in which fitting is conducted applying the Levenberg-Marquardt algorithm together with the numerical integration of each proposed model through a fourth-order Runge-Kutta method. First, the models were individually fitted to experimental data at fixed temperature values; then, multivariable fitting of the experimental data available was completed, including temperature.

The kinetic models herein proposed have been selected on a physicochemical basis, while discrimination and final selection among them has been made following both physicochemical and statistical criteria. Among the latter, the next have been regarded: Fischer's F value (*F*), residual mean squared error (*RMSE*), variation explained (*VE*) [48] and Akaike information criterion (*AIC*) [49]. These statistical parameters and criteria are defined in detail elsewhere [50] and in the supplementary material. They have previously been used successfully for kinetic modeling discrimination purposes [51]. In statistical terms, the adequacy and quality of the

proposed models to describe the observed data improves as the value of *F* and *VE* increase and as *AIC* and *RMSE* decrease.

3. Results and discussion

3.1. Selection of a sulphonic ion exchange resin

As appointed in the Introduction section, some sulphonic resins have been studied in acetalisation reactions. For this reason, we tested the resins Lewatit GF101, Purolite CT275DR and CT276 for performance in addition to Amberlyst 35dry and 36dry. Figure 2 shows the evolution of the yield to product using the mentioned resins, in which it can be observed that Lewatit GF101 achieves the best results. Table 2 compiles some basic features of this resin, which has been selected as the catalyst for subsequent experimental work.

3.2. Effect of external mass transfer

External mass transfer could play a primary role limiting the overall rate of reaction in heterogeneously catalyzed systems. In the case studied in this work, this effect can be even higher considering that acetone and glycerol have limited miscibility prior to the generation of the reaction products [44]. The performance of the reaction was evaluated at different stirring speeds were assessed at 40 ºC, the highest temperature of the range. Figure 3 demonstrates no perceivable difference in the evolution of the yield to product using stirrer speeds above 750 rpm. For this reason, this value was selected to perform further experimentation without the limitation of external mass transfer. Despite the fact that a solventless system was used in this case contrary to the utilization of ethanol as solvent in a previous work, the mentioned stirrer speed value agrees well with that reported in such work, in which 700 rpm was used [36]. In turn, this means that the presence of two liquid phases and the high difference in viscosity between acetone (0.21 cP at 40ºC [52]) and glycerol (284 cP at 40ºC [53]) do not have an effect on external mass transfer compared to a single phase liquid system aided by the presence of a cosolvent species.

3.3. Effect of internal mass transfer

In order to assess the effect of internal mass transfer for this reaction using Lewatit GF101, the ketalization reaction was completed employing different particle sizes. Figure 4 shows the particle size obtained by sieving the catalyst as received from the supplier. Though the particle size ranges were not equal in all cases represented in the figure, it can

be seen that resin beads between 500 and 800 μm represent slightly over 50 % of the total amount of particles.

An assessment of the the internal mass transfer is displayed in Figure 5a, in which several particle sizes of Lewatit GF101 were evaluated for activity. A comparison is made using the catalyst as supplied (i.e. non-sieved), different fractions of the sieved catalyst in the range $200<d_p<1000$ μm and grinded particles below 200 μm, owing their absence in the resin as received. Additionally, to test whether grinding could potentially have an effect on the activity of the resins, Figure 5b bears witness of the evolution of the yield to solketal using two particular fractions of the resin after crushing and sieving comparing it with that of the sieved particles with no treatment. It can be observed that the difference between using the resin with or without crushing is not remarkable. This fact had already been observed

A Hoerl curve was fitted to the observed data of the concentration of solketal with respect to time. The maximum reaction rates for each assay at a different particle size were obtained from the differentiation of the mentioned curve, whose equation is defined as follows [54]:

$$C_{Sk}=A\cdot B^{t}\cdot t^{C} \tag{1}$$

in which C_{sk} is the concentration of solketal ($mol\cdot L^{-1}$), t is time and A, B and C are the fitting parameters of the equation. Figure 6 depicts the effectiveness factor, defined by equation 2:

$$\eta=\frac{r_{max}^{dp}}{r_{max}^{130}} \tag{2}$$

where r_{max}^{dp} stands for the maximum rate observed at each particle size and r_{max}^{130} corresponds to the maximum rate of solketal production observed at 130 μm (average value of the interval $80<d_p<200$ μm), diameter at which negligible internal diffusion effects can be considered to be present. Thus, from Figure 6 can be inferred that a particle size between 180 um and 200 μm can be used without internal mass transfer limitations.

3.4. Effect of temperature, catalyst load and initial molar ratio of reactants

With the stirring rate and particle size fixed at values at which no external and internal mass transfer limitations were witnessed, a series of kinetic runs were completed.

Figure 7a, 7b and 7c show the influence of varying temperature, catalyst load and the initial molar ratio of the reactants, respectively. As can be seen, the three variables show a positive effect on the kinetics of the reaction since the equilibrium position is reached more rapidly, as expected. Furthermore, Figure 7c shows the marked effect of *M* on the maximum yield to solketal, which is enhanced by a variation from 3 to 12 from 34 % to approximately 96%. This in turn evidences a significant shift of the ketalization reaction to the products. This observation agrees well with what was discussed in the introduction section regarding the large excess of acetone used for this reaction.

3.5. Kinetic modeling

Upon completion of 16 kinetic runs combining the variation of *T*, *M* and catalyst load at various levels, enough data were obtained so as to propose and fit different kinetic models.

Considering the stoichiometry of the reaction and the virtually complete selectivity towards solketal as appointed in the introduction section, this is a simple reaction whose rate is equal to the rate of generation of the products as well as that of the consumption of reactants. Furthermore, owing to the equilibrium position discussed in the previous section, the reverse reaction from the products the reactant species needs to be taken into account.

Table 3 summarizes all the kinetic models divided into three groups on which they are based, namely: potential laws (PL), Eley-Rideal (ER) and Langmuir-Hinshelwood-Hougen-Watson (LHHW). The base cases consider the dependence of the direct reaction with respect to the concentration of glycerol and acetone to a power of 1 and are designated by 1 in the three models. Models denoted as 2 and 3 are of zero order with respect to acetone and first order to glycerol and vice versa, respectively. Finally, models labeled as 4 account for zero order for both reactants. For all the models the reverse reaction was considered of first order with respect to solketal and water.

ER models are based on the assumption that only one of the molecules adsorbs onto the solid, while the other reacts with it directly from the fluid phase, without adsorbing. LHHW mechanisms, on the other hand, suggest that the two molecules adsorb and a bimolecular reaction takes place on the adjacent sites. Both mechanisms have been used to describe chemical reactions in sulphonic resins: ER for Amberlyst 15 and Relite CFS in the esterification of fatty acids [55] or other resins for the sysnthesis

of dimethyl ether [56] and LHHW for Amberlyst 15 in the dimerization and trimerization of methylbutenes [57]. PL models are pseudohomogeneous models that would consider virtually no adsorption of the species on the ion exchange resins. Thus, the reaction would take place solely in the fluid phase. In these models, the adsorption terms can be considered much lower than 1 in the denominator of the ER and LHHW models.

In the ER and LHHW models presented in Table 3, only the adsorption constant of W is included. More generalized models featuring the corresponding adsorption terms for the rest of the compounds involved were tried; nevertheless, fitting of such models to experimental data failed to converge. Suggestion of kinetic models neglecting adsorption terms other than that of water in the denominator of ER and LHHW models have previously been reported [36, 58]. In sulphonic ion exchange resins the adsorption constant for water is generally very high compared to that of other components. For instance, in methyl acetate esterification catalyzed by Amberlyst 15, a value of about four orders of magnitude higher than that of acetic acid was reported [59].

Additionally, the dependence of the kinetic constants k_1 and k_2 for the direct and reverse reactions with respect to temperature as well as the adsorption constant of water are given by the Arrhenius-based equations 3 and 4:

$$\ln k_i = \ln k_{i0} - \frac{E_{ai}}{R}\cdot\frac{1}{T} \tag{3}$$

$$\ln K_w = \ln K_{W0} - \frac{\Delta H_{aW}}{R}\cdot\frac{1}{T} \tag{4}$$

where k_{i0} and E_{ai}/R are the preexponential factor of the kinetic constants and the ratio between activation energy and the ideal gas constant and $\Delta H_{aW}/R$ is the ratio of the adsorption heat of water and the ideal gas constant.

As can be seen in Table 4, the degree of concordance between the experimental data and the predicted values together with the quality of the estimation of the model parameters, a relevant contrast exists among the models proffered.

For starters, bearing in mind the values retrieved for the models ER1, ER2, LHHW1 and LHHW2 can automatically be discarded: model ER1 gives an error in the estimation of the parameters of approximately one order of magnitude, whereas for the other three models the error amounts to various orders of magnitude. On the other hand,

the rest of the models retrieved errors around one order of magnitude less than the mean value of the parameter. Consideration of models PL3, ER3 and LHHW3 enhances notably the degree of fitting with respect to models labeled 1 and 2. Even more significantly, models PL4, ER4 and LHHW4, of zero order with respect to both reactants, show a more accurate prediction according to the statistical criteria displayed in Table 4. This in turn accounts for the concentration of acetone and glycerol in the fluid phase being much lower than that in the solid phase, and the latter being practically constant at all times. This makes sense considering that the reaction is being performed in a solventless medium, where the concentrations of acetone and glycerol are high in the fluid medium. The two reacting species enter little by little into the resin competing for the active sites with the water molecules, whose affinity for sulphonic groups is much higher and thus cover most of the sulphonic groups. Additionally, following the statistical criteria defined in Section 2.3, it becomes clear that models labeled as 4 demonstrate a much better degree of fitting regardless of whether it is based on a PL, ER or LHHW equation rate.

Statistical comparison among PL4, ER4 and LHHW4 lead to dismiss PL4. However, ER4 and LHHW4 show very similar goodness of fit, with the former performing slightly better in statistical terms. Though a LHHW model has been reported previously for this reaction [36] and represents with adequacy our data, an ER model appears more plausible. The LHHW model would involve the adsorption of glycerol onto an adjacent active site to another onto which a molecule of acetone is already adsorbed. This, in principle is much less likely to happen considering that the affinity of sulphonic groups for alcohols or glycerol would be lower due to the structure of the molecule compared to acetone. In addition, molar excess of acetone with respect to glycerol was used ranging from 3 to 12, lowering the likelihood of glycerol adsorbing right next to acetone.

The values of E_{a1}/R and E_{a2}/R retrieved from correlation give values of the activation energies of the direct and reverse reaction equal to 124.0 ± 12.9 kJ/mol and 127.3 ± 12.6 kJ/mol. These values concur with the chemical reaction being the controlling step, for activation energies are usually within the range from 40 to 200 kJ/mol for chemical reaction-controlled processes. The heat of adsorption of water deduced was 128.0 ± 21.4 kJ/mol, which is approximately twice as much as those reported on an Amberlyst 35 resin for the solvent-assisted ketalization of glycerol, 64.7

kJ/mol [36], or an Amberlyst 15 for the esterification of nonanoic acid with methanol, 60.7 kJ/mol [60].

For all of these reasons, ER4 is selected as the model that best explains the kinetics of the reaction. Finally, Figure 8 demonstrates that the model chosen is capable of predicting the vast majority of the experimental data within a margin of error of 10%.

Although ketalization of glycerol and acetone is known to be a reversible reacting system, deactivation of sulfonic acids is also well-known, mainly in esterification processes, due to a variety of mechanisms: active phase hydration, cation exchange, and catalytic site blockage [32, 61]. The use of pure reagents reduces or avoids to a certain extension the deactivation of the catalysts in one or several runs when obtaining solketal from glicerol [32]. It is more common to observe this phenomenon when working in esterification reactions or when using bio-glycerol from the biodiesel production process [32, 62]. When deactivation takes place, the inclusion of equations in the kinetic model is needed to obtain the better values for goodness-of-fit parameters (RMSE, VE, F-value, AIC) [62]. In this case, there are excellent values for VE, higher than 99%, and very low values of RMSE, with very high values for F, in the case of the chosen kinetic model. Therefore, little improvement could be obtained by including deactivation as an additional phenomenon when working in batch conditions and low reaction time values, but cation exchange could result in catalyst deactivation if using continuous operation without regeneration and technical- or lower grade glycerol (referencia de los canadienses). Regeneration of sulphonic acid resins by using cation exchange with strong acids is relatively simple and restores most of its activity, if not all [64].

4. Conclusions

The solventless synthesis of solketal has been successfully completed in batch operation making use of the sulphonic ion exchange resin Lewatit GF101. A liquid-liquid-solid system is dealt with herein, in which the study of the external and internal mass transfer becomes significant, leading to the conclusion that using an agitation speed of 750 rpm the former is negligible and that a particle size of 190 μm is sufficient so as to ignore the latter. A series of kinetic runs were performed varying temperature, molar excess of acetone to glycerol and amount of catalyst, observing that the three

variables had a positive effect in kinetic terms and that the effect of the molar excess of acetone on the equilibrium is very significant. A series of kinetic models were proposed based on potential laws to account for pseudohomogeneous models as well as Eley-Rideal and Langmuir-Hinshelwood-Hougen-Watson rate equations. After considering the plausible reaction mechanism and accounting for physical and statistical criteria, an ER model was selected. This model featured the following considerations: reverse reaction from the products, zero order with respect to the reactant species and no adsorption terms for any species other than water in the denominator. From multivariable fitting, the activation energies for the direct and reverse reaction and the adsorption constant of water were 124.0 ± 12.9 kJ/mol, 127.3 ± 12.6 kJ/mol and 128.0 ± 21.4 kJ/mol, respectively.

Acknowledgments

The authors would like to thank the labour of the NMR Research Associated Centre at the College of Chemical Sciences at the Complutense University of Madrid. Additionally, grateful appreciation goes to the Ministry of Science and Innovation (projects CTQ2007-60919 and CTQ2010-15460) for financial support.

List of abbreviations

Components

Ac	Acetone
Gly	Glycerol
Sk	Solketal
W	Water

Nomenclature

^{1}H-NMR	Proton nuclear magnetic resonance
A, B and C	Fitting parameters of the Hoerl curve (equation 1)
AIC	Akaike's information criterion
C	Concentration of the components at a given time (mol·L^{-1})
E_{ai}/R	Ratio of activation energy and the ideal gas constant (K)

ER	Eley-Rideal kinetic model
F	Fischer's F statistical parameter
$\Delta H_{aw}/R$	Ratio of the heat of adsorption of water and the ideal gas constant (K)
k	Kinetic constants of the direct and reverse reaction
K	Adsorption constant in the ER and LHHW models
LHHW	Langmuir-Hinshelwood-Hougen-Watson kinetic model
M	Initial molar ratio of acetone to glycerol
n	Total number of components
N	Total number of data to which a model is fitted
P	Number of parameters of the proposed model or potential model
PL	Kinetic model based on potential laws, i.e., pseudohomogeneous
R	Ideal gas constant ($J \cdot mol^{-1} \cdot K^{-1}$)
r	Reaction rate ($mol \cdot L \cdot min^{-1}$)
RMSE	Residual mean squared error
t	Time (min)
T	Temperature (ºC or K)
VE	Variation explained (%)
Y	Yield to product

Greek letters

η	Effectiveness factor (defined by equation 2)
ν	Stoichiometric coefficient of the component i
ω	Agitation rate (rpm)

Subscripts

0	Relative to the start of the reaction, time equals zero
i	Relative to component i
cat	Relative to the catalyst

max	Relative to the maximum rate of reaction observed using different particle sizes
w	Relative to water in the adsorption constant

Superscripts

130	Relative to the rate of reaction observed when a particle size of 130 μm was used
dp	Relative to the rate of reaction observed using a particle size of dp

References

[1] A. Behr, J. Eilting, K. Irawadi, J. Leschinski, F. Lindner. Improved utilisation of renewable resources: New important derivatives of glycerol. Green Chemistry 10 (2008) 13-30.

[2] A. Behr, J.P. Gomes. The refinement of renewable resources: New important derivatives of fatty acids and glycerol. European Journal of Lipid Science and Technology 112 (2010) 31-50.

[3] M. Pagliaro, M. Rossi. The Future of Glycerol: New Uses of a Versatile Raw Material. RSC Publishing, Cambridge, UK, 2008.

[4] C.-H. Zhou, J.N. Beltramini, Y.-X. Fan, G.Q. Lu. Chemoselective catalytic conversion of glycerol as a biorenewable source to valuable commodity chemicals. Chem. Soc. Rev. 37 (2008) 527-549.

[5] J. Kenar. Glycerol as a platform chemical: Sweet opportunities on the horizon? Lipid Technology 19 (2007) 249-253.

[6] M. Pagliaro, R. Ciriminna, H. Kimura, M. Rossi, C. Della Pina. Recent advances in the conversion of bioglycerol into value-added products. European Journal of Lipid Science and Technology 111 (2009) 788-799.

[7] J.A. Melero, G. Vicente, G. Morales, M. Paniagua, J.M. Moreno, R. Roldan, A. Ezquerro, C. Perez. Acid-catalyzed etherification of bio-glycerol and isobutylene over sulfonic mesostructured silicas. Applied Catalysis A: General 346 (2008) 44-51.

[8] K. Klepáčová, D. Mravec, A. Kaszonyi, M. Bajus. Etherification of glycerol and ethylene glycol by isobutylene. Applied Catalysis A: General 328 (2007) 1-13.

[9] R. Wessendorf. Glycerol derivatives as fuel components. Erdol & Kohle Erdgas Petrochemie 48 (1995) 138-143.

[10] H. Noureddini. Production of oxygenated biodiesel fuel of low cloud point. US6015440-A.

[11] F.J. Liotta, H.S. Kesling, L.J. Karas. Transesterifying fat with alcohol and iron oxide or alumina catalyst|comprises diesel fuel hydrocarbon(s) and particulate emission reducing amt. of di: or tri:alkyl glycerol ether. US5308365-A.

[12] R.S. Karinen, A.O.I. Krause. New biocomponents from glycerol. Applied Catalysis A: General 306 (2006) 128-133.

[13] J.A. Melero, R. van Grieken, G. Morales, M. Paniagua. Acidic mesoporous silica for the acetylation of glycerol: Synthesis of bioadditives to petrol fuel. Energy & Fuels 21 (2007) 1782-1791.

[14] N. Rahmat, A.Z. Abdullah, A.R. Mohamed. Recent progress on innovative and potential technologies for glycerol transformation into fuel additives: A critical review. Renewable & Sustainable Energy Reviews 14 (2010) 987-1000.

[15] A.L. Maksimov, A.I. Nekhaev, D.N. Ramazanov, Y.A. Arinicheva, A.A. Dzyubenko, S.N. Khadzhiev. Preparation of High-Octane Oxygenate Fuel Components from Plant-Derived Polyols. Pet. Chem. 51 (2011) 61-69.

[16] C.J.A. Mota, C.X.A. da Silva, N. Rosenbach, Jr., J. Costa, F. da Silva. Glycerin Derivatives as Fuel Additives: The Addition of Glycerol/Acetone Ketal (Solketal) in Gasolines. Energy & Fuels 24 (2010) 2733-2736.

[17] E. Garcia, M. Laca, E. Perez, A. Garrido, J. Peinado. New Class of Acetal Derived from Glycerin as a Biodiesel Fuel Component. Energy & Fuels 22 (2008) 4274-4280.

[18] N. Suriyaprapadilok, B. Kitiyanan, Synthesis of Solketal from Glycerol and Its Reaction with Benzyl Alcohol, in: 9th Eco-Energy and Materials Science and Engineering Symposium, 2011.

[19] M. Selva, V. Benedet, M. Fabris. Selective catalytic etherification of glycerol formal and solketal with dialkyl carbonates and K2CO3. Green Chemistry 14 (2012) 188-200.

[20] S. Budavari, Merck Index, 11th edition., in, Merck & Co. Inc., Rahway, New Jersey, 1989.

[21] J. Jurczak, S. Pikul, T. Bauer. Tetrahedron 42 (1986) 447-488.

[22] R.P. Hof, R.M. Kellogg. Synthesis and lipase-catalyzed resolution of 5-(hydroxymethyl)-1,3-dioxolan-4-ones: masked glycerol analogs as potential building blocks for pharmaceuticals. Journal of Organic Chemistry 61 (1996) 3423-3427.

[23] V. Calvino-Casilda, K. Stawicka, M. Trejda, M. Ziolek, M.A. Banares. Real-Time Raman Monitoring and Control of the Catalytic Acetalization of Glycerol with Acetone over Modified Mesoporous Cellular Foams. Journal of Physical Chemistry C 118 (2014) 10780-10791.

[24] M.S. Khayoon, B.H. Hameed. Solventless acetalization of glycerol with acetone to fuel oxygenates over Ni-Zr supported on mesoporous activated carbon catalyst. Applied Catalysis a-General 464 (2013) 191-199.

[25] N. Suriyaprapadilok, B. Kitiyanan. Synthesis of Solketal from Glycerol and Its Reaction with Benzyl Alcohol. Energy Procedia 9 (2011) 63-69.

[26] B. Bruchmann, K. Haeberle, H. Gruner, M. Hirn. Preparation of cyclic acetals or ketals, especially isopropylidene glycerin|comprising distilling off some of aldehyde or ketone during reaction with polyol. 1999. EP842929-A.

[27] F.D.L. Menezes, M.D.O. Guimaraes, M.J. da Silva. Highly Selective SnCl2-Catalyzed Solketal Synthesis at Room Ternperature. Industrial & Engineering Chemistry Research 52 (2013) 16709-16713.

[28] H. Matsushita, M. Shibagaki, K. Takahashi, H. Kuno. Method of preparing acetal or ketal. 1989. US Patent 4,841,075.

[29] J. Deutsch, A. Martin, H. Lieske. Investigations on heterogeneously catalysed condensations of glycerol to cyclic acetals. Journal of catalysis 245 (2007) 428-435.

[30] J.S. Clarkson, A.J. Walker, M.A. Wood. Continuous reactor technology for ketal formation: An improved synthesis of solketal. Organic Process Research & Development 5 (2001) 630-635.

[31] P. Ferreira, I.M. Fonseca, A.M. Ramos, J. Vital, J.E. Castanheiro. Valorisation of glycerol by condensation with acetone over silica-included heteropolyacids. Applied Catalysis B-Environmental 98 (2010) 94-99.

[32] G. Vicente, J.A. Melero, G. Morales, M. Paniagua, E. Martin. Acetalisation of bio-glycerol with acetone to produce solketal over sulfonic mesostructured silicas. Green Chemistry 12 (2010) 899-907.

[33] L. Li, T.I. Koranyi, B.F. Sels, P.P. Pescarmona. Highly-efficient conversion of glycerol to solketal over heterogeneous Lewis acid catalysts. Green Chemistry 14 (2012) 1611-1619.

[34] P.S. Reddy, P. Sudarsanam, B. Mallesham, G. Raju, B.M. Reddy. Acetalisation of glycerol with acetone over zirconia and promoted zirconia catalysts under mild reaction conditions. Journal of Industrial and Engineering Chemistry 17 (2011) 377-381.

[35] D. Nandan, P. Sreenivasulu, L.N.S. Konathala, M. Kumar, N. Viswanadham. Acid functionalized carbon-silica composite and its application for solketal production. Microporous and Mesoporous Materials 179 (2013) 182-190.

[36] M.R. Nanda, Z. Yuan, W. Qin, H.S. Ghaziaskar, M.-A. Poirier, C.C. Xu. Thermodynamic and kinetic studies of a catalytic process to convert glycerol into solketal as an oxygenated fuel additive. Fuel 117 (2014) 470-477.

[37] M.R. Nanda, Z. Yuan, W. Qin, H.S. Ghaziaskar, M.-A. Poirier, C. Xu. A new continuous-flow process for catalytic conversion of glycerol to oxygenated fuel additive: Catalyst screening. Applied Energy 123 (2014) 75-81.

[38] C.X.A. da Silva, V.L.C. Goncalves, C.J.A. Mota. Water-tolerant zeolite catalyst for the acetalisation of glycerol. Green Chemistry 11 (2009) 38-41.

[39] C.X.A. da Silva, C.J.A. Mota. The influence of impurities on the acid-catalyzed reaction of glycerol with acetone. Biomass & Bioenergy 35 (2011) 3547-3551.

[40] B. Bruchmann, K. Haberle, H. Gruner, M. Hirn. Preparation of cyclic acetals or ketals 1999. US Patent 5,917,059.

[41] D. Royon, S. Locatelli, E.E. Gonzo. Ketalization of glycerol to solketal in supercritical acetone. Journal of Supercritical Fluids 58 (2011) 88-92.

[42] L. Roldan, R. Mallada, J.M. Fraile, J.A. Mayoral, M. Menendez. Glycerol upgrading by ketalization in a zeolite membrane reactor. Asia-Pacific Journal of Chemical Engineering 4 (2009) 279-284.

[43] M.R. Nanda, Z. Yuan, W. Qin, H.S. Ghaziaskar, M.-A. Poirier, C. Xu. Catalytic conversion of glycerol to oxygenated fuel additive in a continuous flow reactor: Process optimization. Fuel 128 (2014) 113-119.

[44] J. Esteban, A.J. Vorholt, A. Behr, M. Ladero, F. Garcia-Ochoa. Liquid-liquid equilibria for the system acetone + solketal + glycerol at 303.2, 313.2 and 323.2 K. Journal of Chemical & Engineering Data 59 (2014) 2850-2855.

[45] J.J. Tamayo, M. Ladero, V.E. Santos, F. García-Ochoa. Esterification of benzoic acid and glycerol to α-monobenzoate glycerol in solventless media using an industrial free Candida antarctica lipase B. Process Biochemistry 47 (2012) 243-250.

[46] M. Ladero, M. de Gracia, F. Trujillo, F. Garcia-Ochoa. Phenomenological kinetic modelling of the esterification of rosin and polyols. Chemical Engineering Journal 197 (2012) 387-397.

[47] L. Zhou, T.-H. Nguyen, A.A. Adesina. The acetylation of glycerol over amberlyst-15: Kinetic and product distribution. Fuel Processing Technology 104 (2012) 310-318.

[48] R. Xu. Measuring explained variation in linear mixed effects models. Statistics in Medicine 22 (2003) 3527-3541.

[49] H. Akaike. A new look at the statistical model identification. IEEE Transactions on Automatic Control 19 (1974) 716-723.

[50] J. Esteban, E. Fuente, A. Blanco, M. Ladero, F. Garcia-Ochoa. Phenomenological kinetic model of the synthesis of glycerol carbonate assisted by focused beam reflectance measurements. Chemical Engineering Journal 260 (2015) 434-443.

[51] F. Garcia-Ochoa, A. Romero, J. Querol. Modeling of the thermal normal-octane oxidation in the liquid phase. Industrial & Engineering Chemistry Research 28 (1989) 43-48.

[52] H. Topallar, Y. Bayrak. The effect of temperature on the dynamic viscosity of acetone sunflower-seed oil mixtures. Turkish Journal of Chemistry 22 (1998) 361-366.

[53] J.B. Segur, H.E. Oberstar. Viscosity of glycerol and its aqueous solutions. Industrial and Engineering Chemistry 43 (1951) 2117-2120.

[54] A.E. Hoerl. Fitting curves to data. In Chemical business handbook; Perry, J. H., Ed.; McGraw-Hill: New York, 1954; pp 55-57. McGraw-Hill, New York.

[55] R. Tesser, L. Casale, D. Verde, M. Di Serio, E. Santacesaria. Kinetics and modeling of fatty acids esterification on acid exchange resins. Chemical Engineering Journal 157 (2010) 539-550.

[56] Z. Lei, Z. Zou, C. Dai, Q. Li, B. Chen. Synthesis of dimethyl ether (DME) by catalytic distillation. Chemical Engineering Science 66 (2011) 3195-3203.

[57] M. Granollers, J.F. Izquierdo, C. Fite, F. Cunill. Kinetic study of methyl-butenes dimerization and trimerization in liquid-phase over a macroreticular acid resin. Chemical Engineering Journal 234 (2013) 266-275.

[58] J. Lilja, D.Y. Murzin, T. Salmi, J. Aumo, P.M. Arvela, M. Sundell. Esterification of different acids over heterogeneous and homogeneous catalysts and correlation with the Taft equation. Journal of Molecular Catalysis a-Chemical 182 (2002) 555-563.

[59] W.F. Yu, K. Hidajat, A.K. Ray. Determination of adsorption and kinetic parameters for methyl acetate esterification and hydrolysis reaction catalyzed by Amberlyst 15. Applied Catalysis A: General 260 (2004) 191-205.

[60] M. Sharma, R.K. Wanchoo, A.P. Toor. Adsorption and Kinetic Parameters for Synthesis of Methyl Nonanoate over Heterogeneous Catalysts. Industrial & Engineering Chemistry Research 51 (2012) 14367-14375.

[61] J.A. Melero, L. Fernando Bautista, J. Iglesias, G. Morales, R. Sanchez-Vazquez, K. Wilson, A.F. Lee. New insights in the deactivation of sulfonic modified SBA-15 catalysts for biodiesel production from low-grade oleaginous feedstock. Applied Catalysis A: General 488 (2014) 111-118.

[62] L. Molinero, M. Ladero, J.J. Tamayo, F. Garcia-Ochoa. Homogeneous catalytic esterification of glycerol with cinnamic and methoxycinnamic acids to cinnamate glycerides in solventless medium: Kinetic modeling. Chemical Engineering Journal 247 (2014) 174-182.

[63] M.R. Nanda, Z. Yuan, W. Qin, H.S. Ghaziaskar, M.A. Poirier, C. Xu. A new continuous-flow process for catalytic conversion of glycerol to oxygenated fuel additive: Catalyst screening. Applied Energy 123 (2014) 75-81.

[64] X. Hu, C. Lievens, D. Mourant, Y. Wang, L. Wu, R. Gunawan, Y. Song, C-Z. Li. Investigation of deactivation mechanisms of a solid acid catalyst during esterification of the bio-oils from mallea biomass. Applied Energy 111 (2013) 94-103.

Table 1. References found in literature using sulphonic ion exchange resins in the synthesis of solketal.

Ref.	Ion exchange resin	T (ºC)	M	Catalyst load	Other details[a]	Y_{Sk} (%)
29	Amberlyst 36	40	2.7:1.8:1[b]	1.2% w/w	Operation with water removal using dichloromethane as solvent	88
30	Amberlyst DPT-1	70	3	5% w/w	Counter-current reaction distillation column	98
36	Amberlyst 35	50	1:2:1[b]	2% w/w	Batch operation using methanol as solvent	65
37	Amberlyst 35 and Amberlyst 36	40	1:6:1[b]	-	Operation in fixed bed using methanol as solvent. P=4,14 MPa, WHSV[c]=4 h^{-1}	88
38	Amberlyst 15	70	1.2	15% mol	Water removal by unknown method to shift equilibrium[d]	95
39	Amberlyst 15	70	2	3.18 % w/w	Water removal by unknown method to shift equilibrium[d]	95

[a]At atmospheric pressure unless otherwise specified
[b]Molar ratio solvent:acetone:glycerol
[c]WHSV: weight hourly space velocity
[d]Operation mode not explicitly stated in the reference, though it can be inferred from the yield achieved with such a low molar excess of acetone

Table 2. Properties of the ion exchange resin Lewatit GF101, used for the synthesis of solketal.

Appearance	beige opaque solid	**Pore volume ($cm^3\ g^{-1}$)[d]**	0.270
Maximum operating temperature (K)[a]	403	**Surface area ($m^2\ g^{-1}$) [d]**	48
Acid capacity (eq $H^+\ kg^{-1}$)[b]	5.11	**Bulk density (g cm^{-3}) [d]**	1.15
BET surface area ($m^2\ g^{-1}$)[c]	28	**Apparent density (g cm^{-3}) [d]**	1.67

[a]from supplier
[b]obtained from ion exchange with NaCl
[c]obtained from BET
[d]from mercury porosimetry

Table 3. Definition and nomenclature of the kinetic models proposed to correlate to experimental data.

Model name	Rate equation	Model name	Rate equation	Model name	Rate equation
PL1	$r = k_1 \cdot C_{cat} \cdot C_{Gly} \cdot C_{Ac} - k_{2.} C_{cat} \cdot C_{Sk} \cdot C_w$	ER1	$r = \frac{k_1 \cdot C_{cat} \cdot C_{Gly} \cdot C_{Ac} - k_{2.} C_{cat} \cdot C_{Sk} \cdot C_w}{1 + K_w \cdot C_w}$	LHHW1	$r = \frac{k_1 \cdot C_{cat} \cdot C_{Gly} \cdot C_{Ac} - k_{2.} C_{cat} \cdot C_{Sk} \cdot C_w}{(1 + K_w \cdot C_w)^2}$
PL2	$r = k_1 \cdot C_{cat} \cdot C_{Gly} - k_{2.} C_{cat} \cdot C_{Sk} \cdot C_w$	ER2	$r = \frac{k_1 \cdot C_{cat} \cdot C_{Gly} - k_{2.} C_{cat} \cdot C_{Sk} \cdot C_w}{1 + K_w \cdot C_w}$	LHHW 2	$r = \frac{k_1 \cdot C_{cat} \cdot C_{Gly} - k_{2.} C_{cat} \cdot C_{Sk} \cdot C_w}{(1 + K_w \cdot C_w)^2}$
PL3	$r = k_1 \cdot C_{cat} \cdot C_{Ac} - k_{2.} C_{cat} \cdot C_{Sk} \cdot C_w$	ER3	$r = \frac{k_1 \cdot C_{cat} \cdot C_{Ac} - k_{2.} C_{cat} \cdot C_{Sk} \cdot C_w}{1 + K_w \cdot C_w}$	LHHW 3	$r = \frac{k_1 \cdot C_{cat} \cdot C_{Ac} - k_{2.} C_{cat} \cdot C_{Sk} \cdot C_w}{(1 + K_w \cdot C_w)^2}$
PL4	$r = k_1 \cdot C_{cat} - k_{2.} C_{cat} \cdot C_{Sk} \cdot C_w$	ER4	$r = \frac{k_1 \cdot C_{cat} - k_{2.} C_{cat} \cdot C_{Sk} \cdot C_w}{1 + K_w \cdot C_w}$	LHHW 4	$r = \frac{k_1 \cdot C_{cat} - k_{2.} C_{cat} \cdot C_{Sk} \cdot C_w}{(1 + K_w \cdot C_w)^2}$

Table 4. Statistical comparison among the proposed kinetic models and values of the parameters retrieved with each model.

Model	Parameter	Value ± error	F	AIC	BIC	RMSE	VE (%)
PL1	$\ln k_{10}$	14.29 ± 4.01	$1.62\cdot10^{5}$	-2650	-3.15	0.204	91.08
	E_{a1}/R (K)	6879 ± 1234					
	$\ln k_{20}$	18.51 ± 7.28					
	E_{a2}/R (K)	7534 ± 2249					
PL2	$\ln k_{10}$	16.71 ± 4.58	$1.24\cdot10^{5}$	-2441	-2.90	0.231	88.53
	E_{a1}/R (K)	6883 ± 1408					
	$\ln k_{20}$	18.02 ± 7.94					
	E_{a2}/R (K)	7336 ± 2450					
PL3	$\ln k_{10}$	14.44 ± 1.39	$9.33\cdot10^{5}$	-4123	-4.92	0.084	98.48
	E_{a1}/R (K)	6775 ± 427					
	$\ln k_{20}$	18.55 ± 2.04					
	E_{a2}/R (K)	7373 ± 628					
PL4	$\ln k_{10}$	16.81 ± 1.13	$1.36\cdot10^{6}$	-4435	-5.30	0.070	98.60
	E_{a1}/R (K)	6753 ± 346					
	$\ln k_{20}$	18.45 ± 1.62					
	E_{a2}/R (K)	7321 ± 501					
ER1	$\ln k_{10}$	65.50 ± 512.51	$1.42\cdot10^{5}$	-2892	-3.43	0.176	93.33
	E_{a1}/R (K)	21579 ± 155512					
	$\ln k_{20}$	89.28 ± 509.72					
	E_{a2}/R (K)	28484 ± 154646					
	$\ln K_{w0}$	51.91 ± 519.79					
	$\Delta H_{aw}/R$ (K)	14572 ± 157736					
ER2	$\ln k_{10}$	$71.65 \pm 4.78\cdot10^{6}$	$1.13\cdot10^{5}$	-2707	-3.21	0.197	91.67
	E_{a1}/R (K)	$19824 \pm 1.45\cdot10^{9}$					
	$\ln k_{20}$	$93.21 \pm 4.78\cdot10^{6}$					
	E_{a2}/R (K)	$26743 \pm 1.45\cdot10^{9}$					
	$\ln K_{w0}$	$53.70 \pm 4.78\cdot10^{6}$					
	$\Delta H_{aw}/R$ (K)	$12186 \pm 1.45\cdot10^{9}$					
ER3	$\ln k_{10}$	43.72 ± 8.33	$1.06\cdot10^{5}$	-4576	-5.45	0.064	99.15
	E_{a1}/R (K)	15530 ± 2535					
	$\ln k_{20}$	47.04 ±8.10					
	E_{a2}/R (K)	15913 ± 2463					
	$\ln K_{w0}$	53.88 ± 13.25					
	$\Delta H_{aw}/R$ (K)	16221 ± 4063					
ER4	$\ln k_{10}$	44.14 ± 5.12	$2.12\cdot10^{6}$	-5149	-6.14	0.045	99.56
	E_{a1}/R (K)	14920 ± 1558					
	$\ln k_{20}$	45.14 ± 4.97					
	E_{a2}/R (K)	15318 ± 1513					
	$\ln K_{w0}$	51.17 ± 8.42					
	$\Delta H_{aw}/R$ (K)	15398 ± 2583					
LHHW1	$\ln k_{10}$	$527.84 \pm 9.11\cdot10^{4}$	$1.76\cdot10^{5}$	-3099	-3.43	0.157	96.64
	E_{a1}/R (K)	$1.62\cdot10^{5} \pm 2.76\cdot10^{7}$					
	$\ln k_{20}$	$971.74 \pm 3.67\cdot10^{8}$					
	E_{a2}/R (K)	$2.92\cdot10^{5} \pm 1.15\cdot10^{11}$					
	$\ln K_{w0}$	$272.34 \pm 4.56\cdot10^{4}$					
	$\Delta H_{aw}/R$ (K)	$8.21\cdot10^{5} \pm 1.38\cdot10^{7}$					
LHHW2	$\ln k_{10}$	$886.55 \pm 1.88\cdot10^{6}$	$1.49\cdot10^{5}$	-2935	-3.21	0.171	93.66
	E_{a1}/R (K)	$269931 \pm 1.27\cdot10^{21}$					
	$\ln k_{20}$	$68.79 \pm 4.19\cdot10^{18}$					
	E_{a2}/R (K)	$30400 \pm 1.27\cdot10^{21}$					
	$\ln K_{w0}$	$448.03 \pm 9.38\cdot10^{5}$					
	$\Delta H_{aw}/R$ (K)	$135302 \pm 2.84\cdot10^{8}$					
LHHW3	$\ln k_{10}$	34.21 ± 4.44	$1.7\cdot10^{5}$	-4457	-5.45	0.064	99.12
	E_{a1}/R (K)	12660 ± 1356					
	$\ln k_{20}$	37.23 ± 4.44					
	E_{a2}/R (K)	12953 ± 1281					
	$\ln K_{w0}$	34.11 ± 7.76					
	$\Delta H_{aw}/R$ (K)	10517 ± 2402					
LHHW4	$\ln k_{10}$	35.20 ± 2.84	$2.10\cdot10^{6}$	-5143	-6.14	0.046	99.55
	E_{a1}/R (K)	12222 ± 869					
	$\ln k_{20}$	35.96 ± 2.69					
	E_{a2}/R (K)	12547 ± 822					
	$\ln K_{w0}$	32.59 ± 5.16					
	$\Delta H_{aw}/R$ (K)	10058 ± 1597					

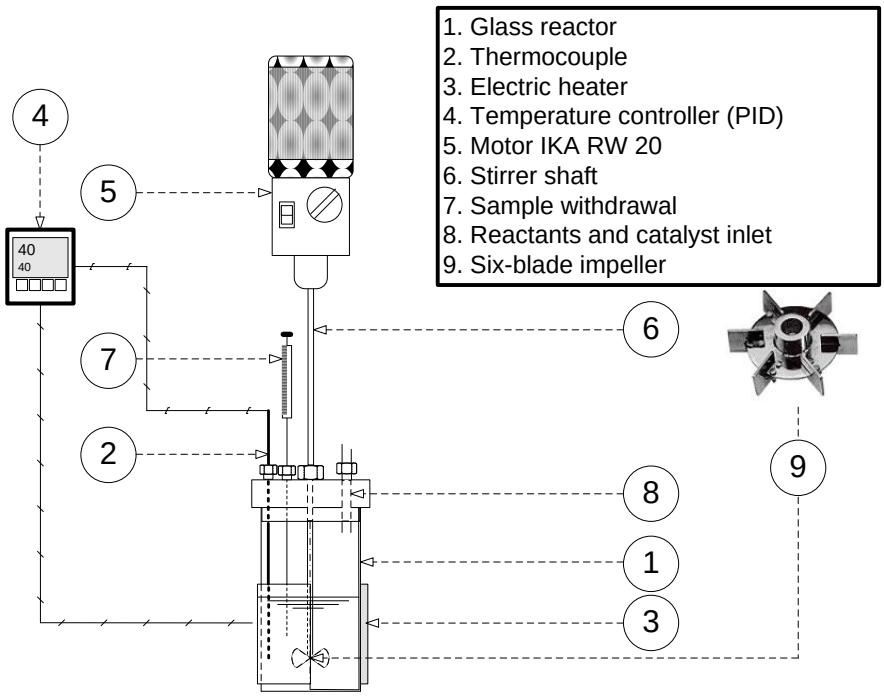

Figure 1. Experimental setup for the synthesis of solketal from glycerol and acetone.

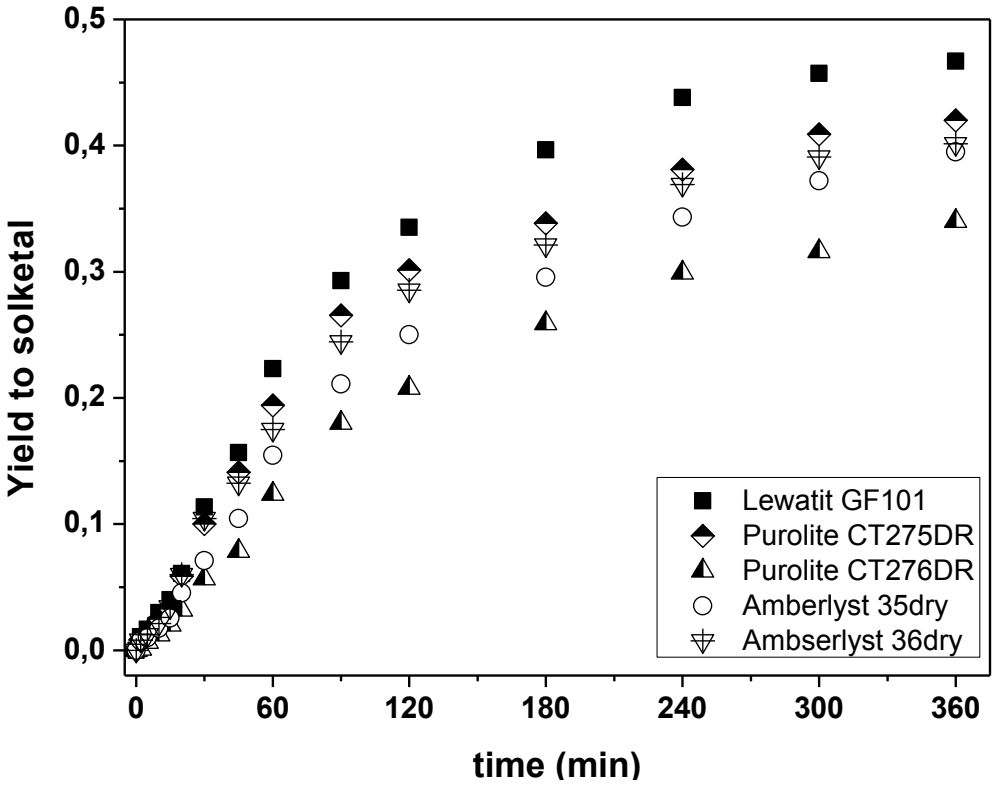

Figure 2. Comparison of the yield to product achieved among five different sulphonic ion exchange resins. Conditions: T=40 ºC, M=4.5, catalyst load=0.5 % w/v and ω=750 rpm.

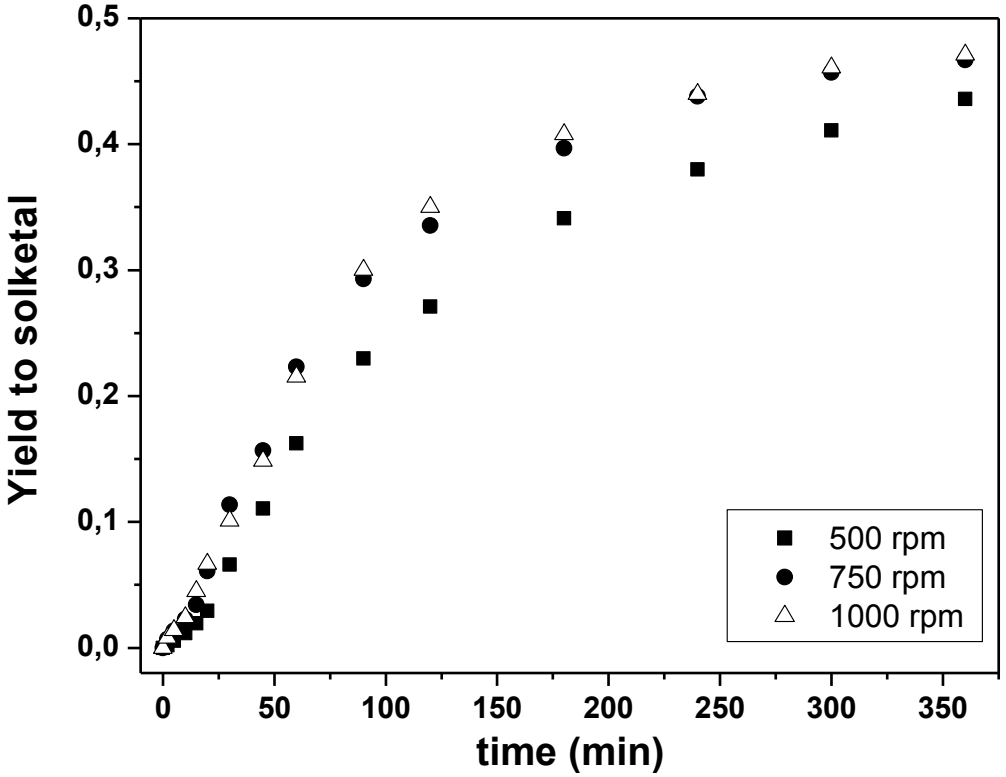

Figure 3. Effect of the agitation speed on the evolution of the reaction. Conditions: T=40 ºC, M=4.5, catalyst load=0.5 % w/v.

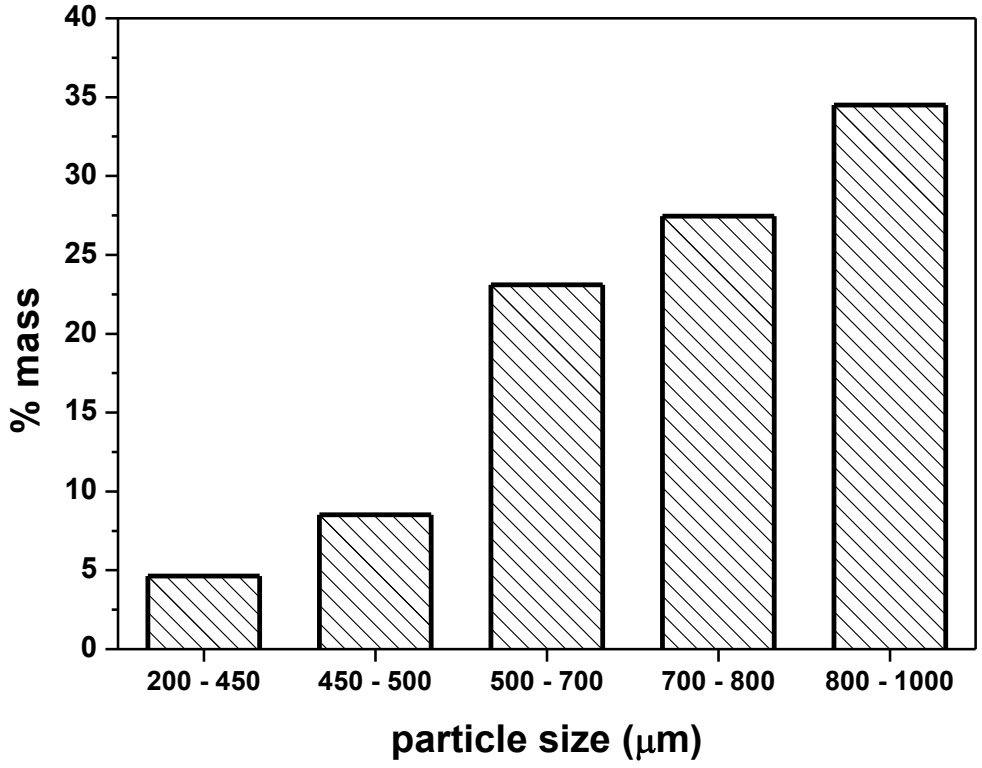

Figure 4. Particle size distribution of Lewatit GF101 obtained by sieving.

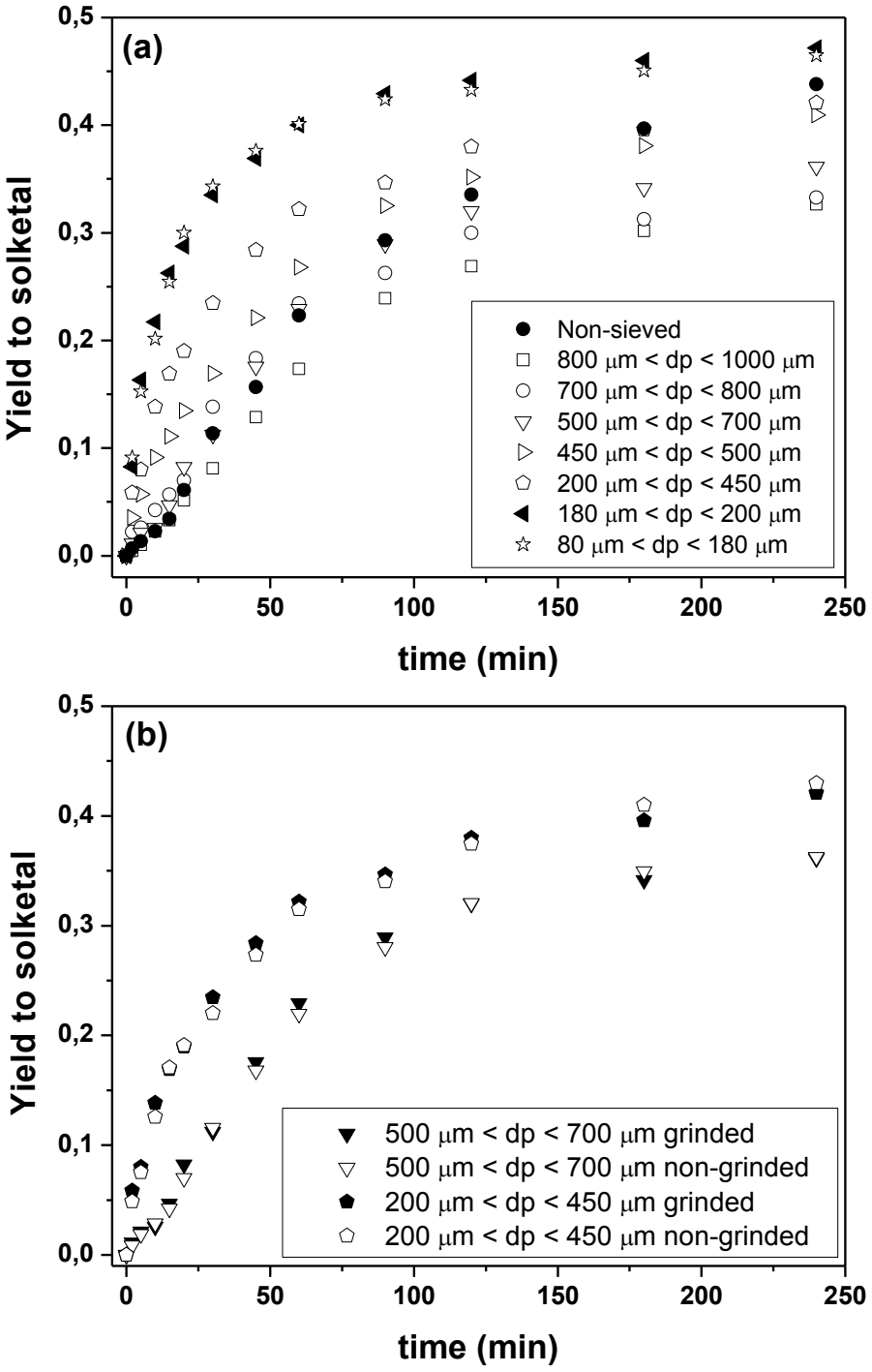

Figure 5. Comparison of the evolution of the yield to solketal using non-sieved and sieved particles of Lewatit GF101 at selected particle sizes (a) and assessment of the effect of grinding and not grinding resin beads at selected particle sizes (b). Conditions: T=40 ºC, M=4.5, catalyst load=0.5 % w/v, ω=750 rpm.

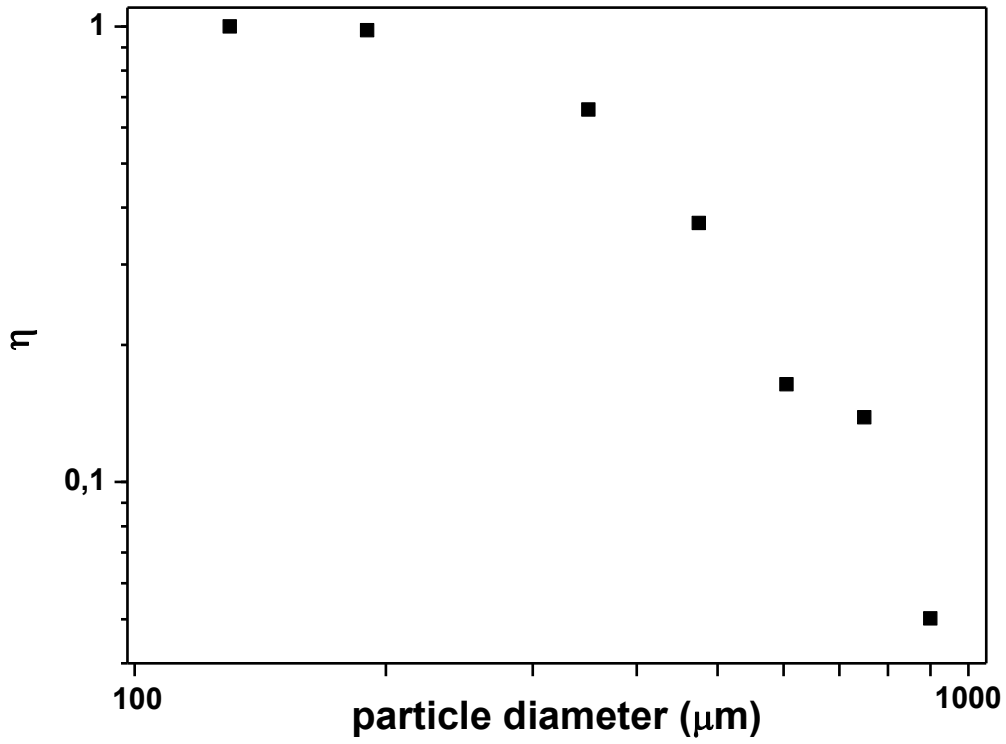

Figure 6. Influence of the particle size on the maximum reaction rates observed at each particle size. Conditions: T=40 ºC, M=4.5, catalyst load=0.5 % w/v.

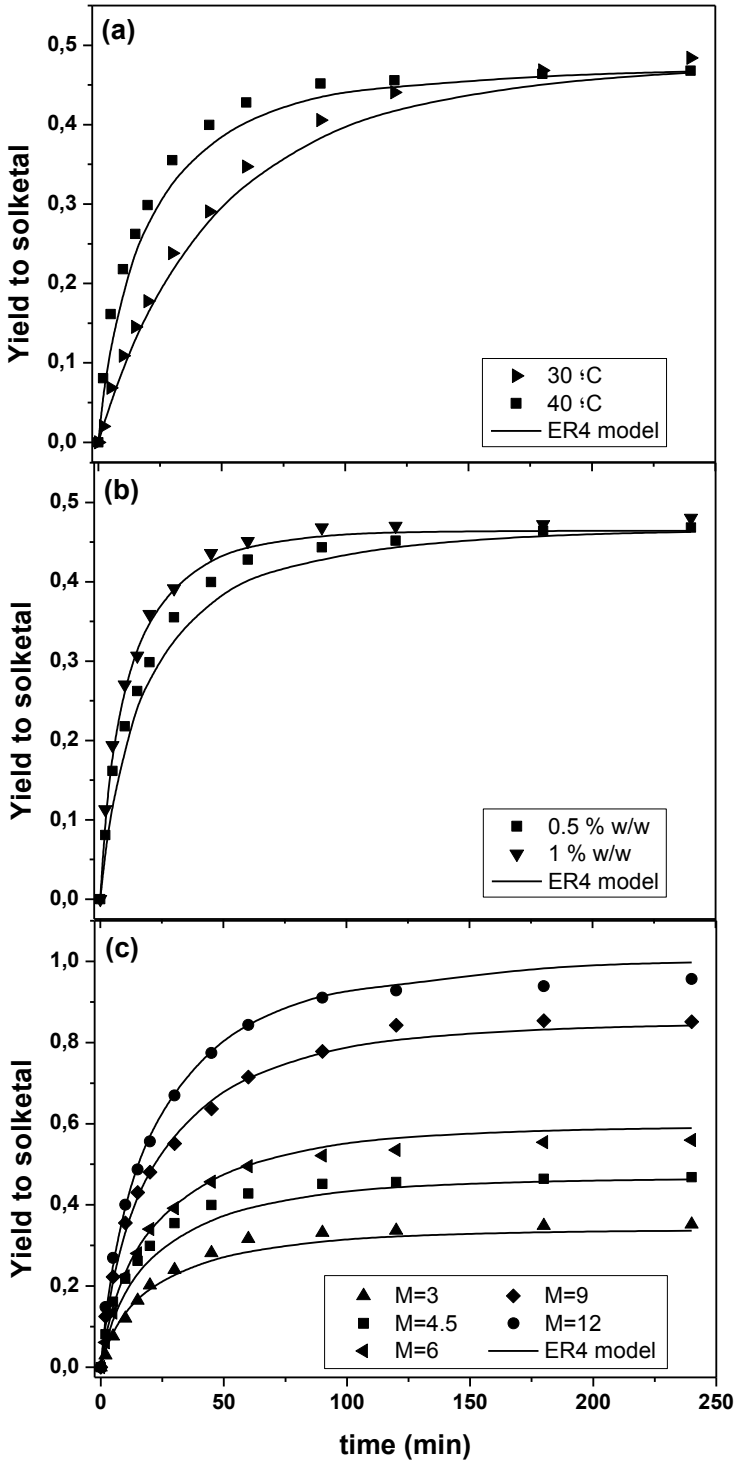

Figure 7. Influence of (a) temperature, (b) catalyst load and (c) M on the evolution of the yield to Sk. Conditions: (a) M=4.5 and catalyst load 0.5% w/w; (b) T=40 ºC and M=4.5 and (c) T=40 ºC and catalyst load 0.5% w/w. Common conditions: ω=750 rpm and d_p=190 μm.

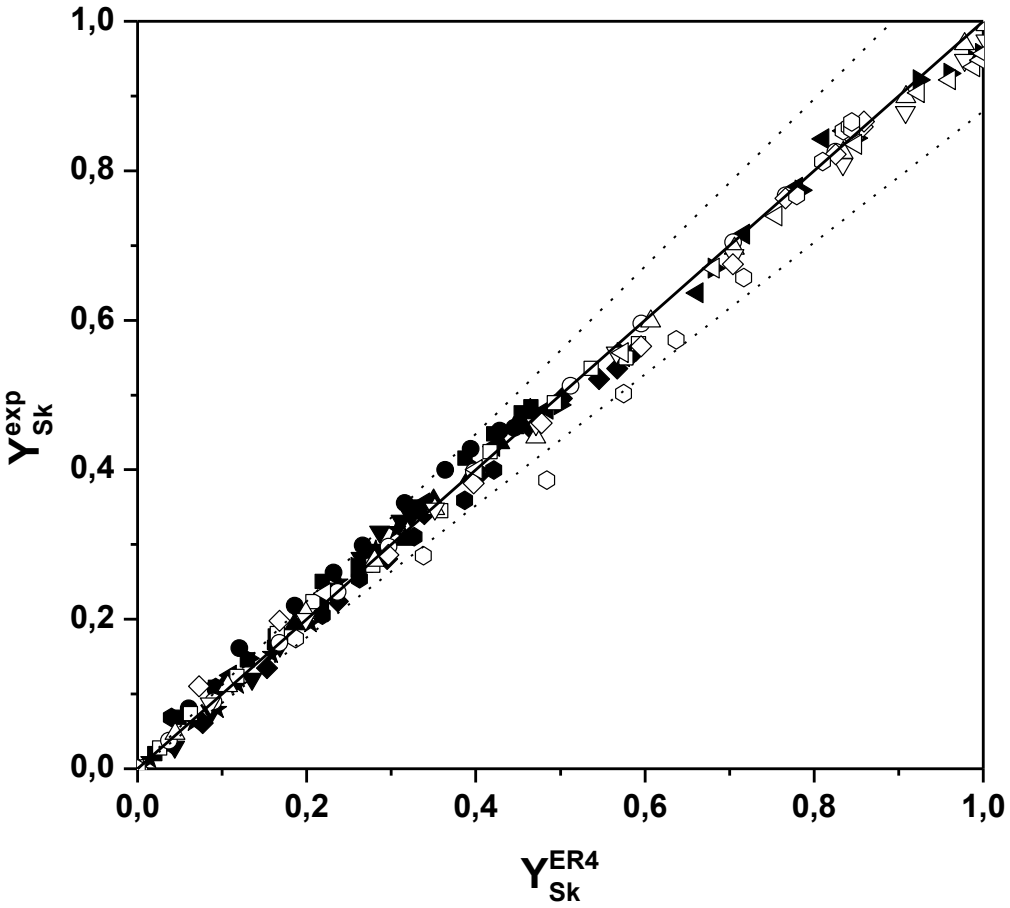

Figure 8. Validation of the LHHW4 model with all the experimental data available

Supplementary material

Statistical parameters for goodness-of-fit and information on models

F is based on a null hypothesis accounting for the adequacy of the model to the observed values of the variable. It is defined according to

$$F = \frac{\sum_{i=1}^{N} \frac{\left(y_{i,calc}\right)^2}{P}}{\sum_{i=1}^{N} \frac{SQR}{N-P}} \quad (1)$$

in which *N* refers to the total number of experimental data, *P* is the number of parameters of the model, *SQR* is the sum of quadratic residues, defined as $\left(y_{i,\exp} - y_{i,calc}\right)^2$, and $y_{i,exp}$ and $y_{i,calc}$ are the experimental and calculated values of the variable, respectively.

RMSE is regarded as a measure of the difference of the predicted values of the variable and the experimental observations. It takes into account the amount of available data and the number of parameters of the model as its definition indicates [1]:

$$RMSE = \sqrt{\frac{SQR}{N-P}} \quad (2)$$

VE also quantifies the goodness of fit as the proportion of empirical variability explained by the tested model [2]. It is defined as follows:

$$VE(\%) = 100 \cdot \left(1 - \frac{\sum_{l=1}^{L} SSQ_l}{\sum_{l=1}^{L} SSQmean_l}\right) \quad (3)$$

where SSQ_l and $SSQmean_l$ are defined as follows:

$$SSQ_l = \sum_{i=1}^{N} \frac{(y_{i,\exp} - y_{i,calc})^2}{y_{i,calc}^{\prime 1}} \quad (4)$$

$$SSQmean_l = \sum_{i=1}^{N} \frac{(y_{i,\exp} - \bar{y}_{i,\exp})^2}{y_{i,calc}^{\prime 1}} \quad (5)$$

with

$$\bar{y}_{i,\exp} = \frac{\sum_{i=1}^{N} \frac{y_{i,\exp}}{y_{i,calc}^{\gamma_j/2}}}{\sum_{i=1}^{N} \frac{1}{y_{i,calc}^{\gamma_j/2}}} \quad (6)$$

In the three previous equations, γ_j is the heteroscedasticity parameter, a measure of the type of error in the measured variable. By default, it is fixed at a value of 1 on Aspen Custom Modeler.

Finally, *AIC* relates the amount of observed data to the number of parameters in the proposed model. It gives information about the goodness of fit and penalizes model overfitting that may occur as a result of increasing the number of parameters of the model [3]. *AIC* is defined by Equation 7:

$$AIC = N \cdot \ln\left(\frac{SQR}{N}\right) + 2 \cdot P \quad (7)$$

In statistical terms, the adequacy and quality of the proposed models to describe the observed data improves as the value of *F* and *VE* increase and as *AIC* and *RMSE* decrease.

References

[1] M. Ladero, M. de Gracia, J.J. Tamayo, I.L.d. Ahumada, F. Trujillo, F. Garcia-Ochoa. Kinetic modelling of the esterification of rosin and glycerol: Application to industrial operation. Chemical Engineering Journal 169 (2011) 319-328.

[2] R. Xu. Measuring explained variation in linear mixed effects models. Statistics in Medicine 22 (2003) 3527-3541.

[3] H. Akaike. A new look at the statistical model identification. IEEE Transactions on Automatic Control 19 (1974) 716-723.